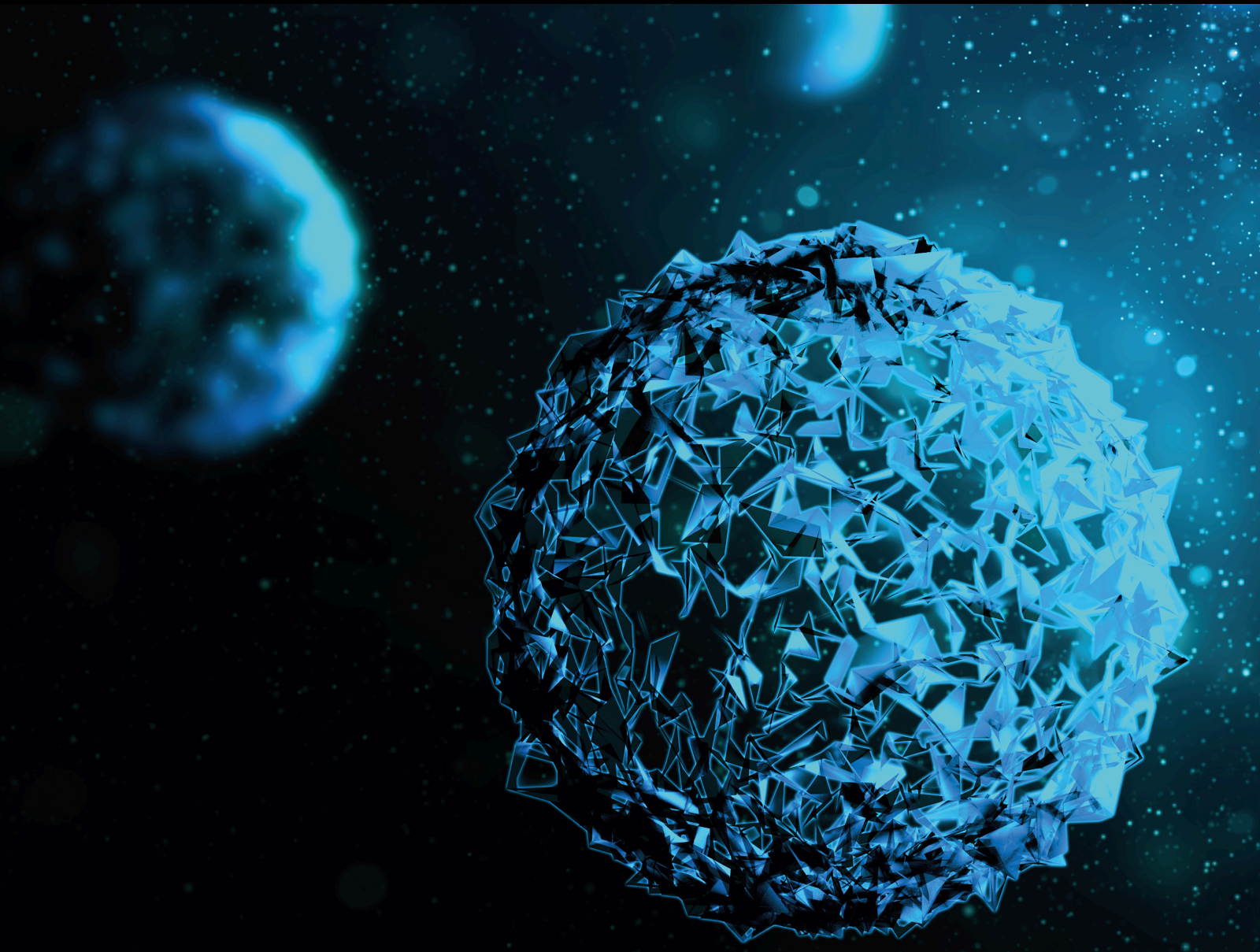


Integrative Genomics and System Biology in Domestic Animal Species

Lead Guest Editor: Hafiz Ishfaq Ahmad

Guest Editors: Muhammad Hamid, Faheem Ahmed Khan, Tesfaye Worku, and Akhtar Ali





Integrative Genomics and System Biology in Domestic Animal Species

BioMed Research International

Integrative Genomics and System Biology in Domestic Animal Species

Lead Guest Editor: Hafiz Ishfaq Ahmad

Guest Editors: Muhammad Hamid, Faheem Ahmed
Khan, Tesfaye Worku, and Akhtar Ali



Copyright © 2024 Hindawi Limited. All rights reserved.

This is a special issue published in "BioMed Research International." All articles are open access articles distributed under the Creative Commons Attribution License, which permits unrestricted use, distribution, and reproduction in any medium, provided the original work is properly cited.

Section Editors

Penny A. Asbell, USA
David Bernardo , Spain
Gerald Brandacher, USA
Kim Bridle , Australia
Laura Chronopoulou , Italy
Gerald A. Colvin , USA
Aaron S. Dumont, USA
Pierfrancesco Franco , Italy
Raj P. Kandpal , USA
Fabrizio Montecucco , Italy
Mangesh S. Pednekar , India
Letterio S. Politi , USA
Jinsong Ren , China
William B. Rodgers, USA
Harry W. Schroeder , USA
Andrea Scribante , Italy
Germán Vicente-Rodríguez , Spain
Momiao Xiong , USA
Hui Zhang , China

Academic Editors

Genomics

Contents

Retracted: The Impact of Seeding Density and Nitrogen Rates on Forage Yield and Quality of *Avena sativa* L

BioMed Research International

Retraction (1 page), Article ID 9825298, Volume 2024 (2024)

Retracted: First Record of Ichthyofauna from Gomal Zam Dam, District South Waziristan, Khyber Pakhtunkhwa, Pakistan

BioMed Research International

Retraction (1 page), Article ID 9823518, Volume 2024 (2024)

Retracted: Expression Profile of MAGE-B1 Gene and Its Hypomethylation Activation in Colon Cancer

BioMed Research International

Retraction (1 page), Article ID 9815982, Volume 2024 (2024)

Retracted: The Comparative Pharmacokinetics and Histokinetics of the Therapeutic Dose of Estradiol Valerate and Bromocriptine in Common Quails

BioMed Research International

Retraction (1 page), Article ID 9814621, Volume 2024 (2024)

Retracted: Effect of Vegetable Waste on Growth Performance and Hematology of Broiler Chicks

BioMed Research International

Retraction (1 page), Article ID 9814290, Volume 2024 (2024)

Retracted: Betamethasone Dipropionate Derivatization, Biotransformation, Molecular Docking, and ADME Analysis as Glucocorticoid Receptor

BioMed Research International

Retraction (1 page), Article ID 9810723, Volume 2024 (2024)

Retracted: Nutrigenomic Interventions to Address Metabolic Stress and Related Disorders in Transition Cows

BioMed Research International

Retraction (1 page), Article ID 9810401, Volume 2024 (2024)

Retracted: Toxicological Effects of Sewage Water on Chick Embryonic Development

BioMed Research International

Retraction (1 page), Article ID 9805397, Volume 2024 (2024)

Retracted: Pathological, Histological, and Molecular Based Investigations Confirm Novel *Mycobacterium bovis* Infection in *Boselaphus tragocamelus*

BioMed Research International

Retraction (1 page), Article ID 9893089, Volume 2024 (2024)

Retracted: Cigarette Smoke Regulates the Expression of EYA4 via Alternation of DNA Methylation Status

BioMed Research International

Retraction (1 page), Article ID 9873595, Volume 2024 (2024)

Retracted: Inter-Relationship Between a Transcriptional Regulator of Flagella Genes *cj0440c* and Thiamine Metabolic Pathway in *Campylobacter jejuni*

BioMed Research International

Retraction (1 page), Article ID 9871573, Volume 2024 (2024)

Retracted: Genomic and Therapeutic Analyses of *Staphylococcus aureus* Isolated from Cattle Reproductive Tract

BioMed Research International

Retraction (1 page), Article ID 9868047, Volume 2024 (2024)

Retracted: Biorational Control of *Callosobruchus maculatus* (Coleoptera: Bruchidae) in Stored Grains with Botanical Extracts

BioMed Research International

Retraction (1 page), Article ID 9861621, Volume 2024 (2024)

Retracted: Histopathological Investigations and Molecular Confirmation Reveal *Mycobacterium bovis* in One-Horned Rhinoceros (*Rhinoceros unicornis*)

BioMed Research International

Retraction (1 page), Article ID 9858936, Volume 2024 (2024)

Retracted: Quantifying the Soil Arthropod Diversity in Urban Forest in Dera Ghazi Khan

BioMed Research International

Retraction (1 page), Article ID 9854349, Volume 2024 (2024)

Retracted: Antioxidant and Anti-Inflammatory Activities of Coenzyme-Q10 and Piperine against Cyclophosphamide-Induced Cytotoxicity in HuH-7 Cells

BioMed Research International

Retraction (1 page), Article ID 9852678, Volume 2024 (2024)

Retracted: Evaluation of the Anticancer Potential of *Morus nigra* and *Ocimum basilicum* Mixture against Different Cancer Cell Lines: An In Vitro Evaluation

BioMed Research International

Retraction (1 page), Article ID 9847989, Volume 2024 (2024)

Retracted: Antidiabetic Effect of *Tamarindus indica* and *Momordica charantia* and Downregulation of TET-1 Gene Expression by Saroglitazar in Glucose Fed Adipocytes and Their Involvement in the Type 2 Diabetes-Associated Inflammation *In Vitro*

BioMed Research International

Retraction (1 page), Article ID 9843135, Volume 2024 (2024)

Retracted: Peelu (*Salvadora oleoides* Decne.): An Unexplored Medicinal Fruit with Minerals, Antioxidants, and Phytochemicals

BioMed Research International

Retraction (1 page), Article ID 9838421, Volume 2024 (2024)

Contents

Retracted: A Comprehensive Review of Performance of Next-Generation Sequencing Platforms

BioMed Research International

Retraction (1 page), Article ID 9837802, Volume 2024 (2024)

Retracted: Synergistic Effect of Conventional Medicinal Herbs against Different Pharmacological Activity

BioMed Research International

Retraction (1 page), Article ID 9836173, Volume 2024 (2024)

Retracted: Gut Microbiota Profiles in Dairy Cattle from Highland and Coastal Regions Using Shotgun Metagenomic Approach

BioMed Research International

Retraction (1 page), Article ID 9797325, Volume 2024 (2024)

Retracted: *Lagerstroemia speciosa* Ameliorated Blood Pressure in LNAME Induced Hypertension in Experimental Rats through NO/cGMP and Oxidative Stress Modulation

BioMed Research International

Retraction (1 page), Article ID 9792123, Volume 2024 (2024)

Retracted: Ecotoxicological Assessment of Heavy Metal and Its Biochemical Effect in Fishes

BioMed Research International

Retraction (1 page), Article ID 9791832, Volume 2024 (2024)

Retracted: Comparative Genomic Characterization of Insulin-Like Growth Factor Binding Proteins in Cattle and Buffalo

BioMed Research International

Retraction (1 page), Article ID 9784763, Volume 2024 (2024)

Retracted: The Antimicrobial Bifunctional Camel Lactoferrin: In Silico and Molecular Dynamic Perspective

BioMed Research International

Retraction (1 page), Article ID 9769316, Volume 2024 (2024)

Retracted: Apoptotic and Antioxidant Activity of Gold Nanoparticles Synthesized Using Marine Brown Seaweed: An In Vitro Study

BioMed Research International

Retraction (1 page), Article ID 9763853, Volume 2024 (2024)

Retracted: Evaluation of Hematological, Oxidative Stress, and Antioxidant Profile in Cattle Infected with Brucellosis in Southern Punjab, Pakistan

BioMed Research International

Retraction (1 page), Article ID 9756710, Volume 2024 (2024)

Retracted: In Vitro Evaluation of Cytotoxic Potential of *Caladium lindenii* Extracts on Human Hepatocarcinoma HepG2 and Normal HEK293T Cell Lines



BioMed Research International

Retraction (1 page), Article ID 9892151, Volume 2023 (2023)







[Retracted] The Antimicrobial Bifunctional Camel Lactoferrin: In Silico and Molecular Dynamic Perspective

Maathir N. Alhumam , Naser Alhumam , and Mahmoud Kandeel 
Research Article (8 pages), Article ID 2322286, Volume 2023 (2023)



[Retracted] Evaluation of the Anticancer Potential of *Morus nigra* and *Ocimum basilicum* Mixture against Different Cancer Cell Lines: An In Vitro Evaluation

Bader O. Almutairi , Ahmed I. Alsayadi, Nael Abutaha , Fahd A. AL-mekhlafi, and Mohamed A. Wadaan
Research Article (8 pages), Article ID 9337763, Volume 2023 (2023)




[Retracted] Ecotoxicological Assessment of Heavy Metal and Its Biochemical Effect in Fishes

Abdul Haseeb, Fozia , Ijaz Ahmad , Hidayat Ullah , Anwar Iqbal, Riaz Ullah , Bushra Abdulkarim Moharram , and Alicja Kowalczyk 
Research Article (11 pages), Article ID 3787838, Volume 2022 (2022)











[Retracted] First Record of Ichthyofauna from Gomal Zam Dam, District South Waziristan, Khyber Pakhtunkhwa, Pakistan

Aziz Ur Rehman, Sami Ullah, Amina Zuberi, Farman Ullah Dawar , and Muhammad Nasir Khan Khattak 
Research Article (10 pages), Article ID 7076508, Volume 2022 (2022)


[Retracted] Peelu (*Salvadora oleoides* Decne.): An Unexplored Medicinal Fruit with Minerals, Antioxidants, and Phytochemicals

Kashif Razzaq , Muhammad Muzzammal Sadiq, Hashir Ashraf, Ambreen Naz, Abid Hussain, Amir Maqbool, Muhammad Tanveer Altaf, Sami Ullah, Gulzar Akhtar, Hafiz Nazar Faried, Muhammad Amin, Ishtiaq Ahmad Rajwana, Ahmad Sattar Khan, Saleh Alfarraj, Mohammad Javed Ansari , and Ammara Saleem 
Research Article (9 pages), Article ID 5707953, Volume 2022 (2022)


***De Novo* Transcriptome Dataset Generation of the Swamp Buffalo Brain and Non-Brain Tissues**

Wang Xiaobo , Faiz-ul Hassan , Sheng Liu , Shuli Yang , Muhammad Ahmad , Ishtiaq Ahmed , Kongwei Huang, Hafiz M. N. Iqbal , Hui Yu , Qingyou Liu , and Saif ur Rehman 
Research Article (15 pages), Article ID 4472940, Volume 2022 (2022)

[Retracted] The Comparative Pharmacology and Histokinetics of the Therapeutic Dose of Estradiol Valerate and Bromocriptine in Common Quails








Muhammad Nadeem, Mehr-un Nisa, Maria Hussain Bangash, Zain Ul Abideen , Rukhsana Sattar, Huma Sattar, Muhammad Saif Ullah, Tahira Ruby, Aleem Ahmed Khan, and Aqeel Ahmad
Research Article (9 pages), Article ID 5482895, Volume 2022 (2022)

[Retracted] Effect of Vegetable Waste on Growth Performance and Hematology of Broiler Chicks




Muhammad Shahid Nisar , Anjum Zahra, Muhammad Fahad Iqbal, Muhammad Amjad Bashir, Riffat Yasin, Khizar Samiullah, Irum Aziz, Sidra Saeed, Abdulrahman Alasmari, Fahmy G. Elsaid, Ali A. Shati, Mohammed A. Al-Kahtani, Farwa Naseem, Maryam Fatima, and Faraz Ahmed
Research Article (8 pages), Article ID 4855584, Volume 2022 (2022)

Contents



[Retracted] Lagerstroemia speciosa Ameliorated Blood Pressure in LNAME Induced Hypertension in Experimental Rats through NO/cGMP and Oxidative Stress Modulation

Mohammed S. Aleissa , Mohammed Al-Zharani , Lina M. Alneghery , Md Saquib Hasnain ,
Bader Almutairi , Daoud Ali, Saud Alarifi , and Saad Alkahtani 
Research Article (8 pages), Article ID 5894416, Volume 2022 (2022)






Comparative Genomic Characterization of Relaxin Peptide Family in Cattle and Buffalo

Muhammad Saif-ur Rehman, Faiz-ul Hassan , Zia-ur Rehman, Hafiz Noubahar Hussain, Muhammad Adnan Shahid, Muhammad Mushahid , and Borhan Shokrollahi 
Research Article (11 pages), Article ID 1581714, Volume 2022 (2022)




[Retracted] A Comprehensive Review of Performance of Next-Generation Sequencing Platforms

Muhammad Tariq Pervez , Mirza Jawad ul Hasnain , Syed Hassan Abbas, Mahmoud F. Moustafa, Naeem Aslam, and Syed Shah Muhammad Shah
Review Article (12 pages), Article ID 3457806, Volume 2022 (2022)












[Retracted] Quantifying the Soil Arthropod Diversity in Urban Forest in Dera Ghazi Khan

Muhammad Mohsin, Haseeb Ahmad, Muhammad Nabeel Nasir, Zain Ul Abideen , Muhammad Nadeem, Rukhsana Sattar, Abdul Qadeer Saad , Mujahid Hussain, Syed Akbar Shah, Hanlie Cheng ,
David Sturdivant , and Syeda Amber Hameed 
Research Article (14 pages), Article ID 8125585, Volume 2022 (2022)


[Retracted] In Vitro Evaluation of Cytotoxic Potential of Caladium lindenii Extracts on Human Hepatocarcinoma HepG2 and Normal HEK293T Cell Lines

Aasia Kalsoom, Awais Altaf , Muhammad Ashraf, Muhammad Muddassir Ali , Saira Aftab, Huma Sattar, Muhammad Sajjad, Amjad Islam Aqib , and Tahir Maqbool
Research Article (11 pages), Article ID 1279961, Volume 2022 (2022)








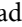




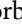
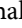

[Retracted] Genomic and Therapeutic Analyses of Staphylococcus aureus Isolated from Cattle Reproductive Tract

Laiba Shafique , Amjad Islam Aqib , Qin Liang , Chaobin Qin , Muhammad Muddassir Ali ,
Memoona Adil , Zaeem Sarwar , Arslan Saleem , Muhammad Ajmal , Alveena Khan ,
Hongping Pan , Kuiqing Cui , and Qingyou Liu 
Research Article (14 pages), Article ID 6240711, Volume 2022 (2022)






[Retracted] Gut Microbiota Profiles in Dairy Cattle from Highland and Coastal Regions Using Shotgun Metagenomic Approach

Bambang Waluyo Hadi Eko Prasetyono , Widiyanto Widiyanto, and Nuruliarizki Shinta Pandupuspitasari
Research Article (8 pages), Article ID 3659052, Volume 2022 (2022)



[Retracted] Biorational Control of *Callosobruchus maculatus* (Coleoptera: Bruchidae) in Stored Grains with Botanical Extracts

Rasheed Akbar , Imtiaz Ali Khan , Brekhna Faheem , Rashid Azad , Maid Zaman , Rubab Altaf , Amjad Usman , Muhammad Fawad , Abid Farid , Ahmad Ur Rahman Saljoqi , Asad Syed , Ali H. Bahkali , Abdallah M. Elgorban , Jawad Ali Shah , and Abdul Qayyum 
Research Article (10 pages), Article ID 3443578, Volume 2022 (2022)





[Retracted] Inter-Relationship Between a Transcriptional Regulator of Flagella Genes *cj0440c* and Thiamine Metabolic Pathway in *Campylobacter jejuni*

Muhammad Abu Bakr Shabbir , Aziz Ul-Rahman, Abdur Rauf Khalid, Nabeel Ijaz, Muhammmad Tahir Aleem, Saeed Ahmed , Abdulaziz Alouffi , Waqas Ahmed, Faiza Aslam, Muhammad Kashif Maan, Adnan Hassan Tahir, Muhammad Waqar Aziz, Mashal M. Almutairi , and Haihong Hao 
Research Article (10 pages), Article ID 4539367, Volume 2022 (2022)

[Retracted] Expression Profile of MAGE-B1 Gene and Its Hypomethylation Activation in Colon Cancer

Mikhlid H. Almutairi , Mona M. Alotaibi, Rasha Alonaizan, and Bader O. Almutairi 
Research Article (8 pages), Article ID 6066567, Volume 2022 (2022)



[Retracted] Comparative Genomic Characterization of Insulin-Like Growth Factor Binding Proteins in Cattle and Buffalo

Muhammad Saif-ur Rehman , Muqeet Mushtaq, Faiz-ul Hassan , Zia-ur Rehman , Muhammad Mushahid, and Borhan Shokrollahi 
Research Article (15 pages), Article ID 5893825, Volume 2022 (2022)







[Retracted] Evaluation of Hematological, Oxidative Stress, and Antioxidant Profile in Cattle Infected with Brucellosis in Southern Punjab, Pakistan

Riaz Hussain , Iahtasham Khan, Adil Jamal , Bahaeldeen Babiker Mohamed , and Ahrar Khan 
Research Article (10 pages), Article ID 7140909, Volume 2022 (2022)

[Retracted] Apoptotic and Antioxidant Activity of Gold Nanoparticles Synthesized Using Marine Brown Seaweed: An In Vitro Study





S. Rajeshkumar , R. P. Parameswari , J. Jayapriya, M. Tharani, Huma Ali, Nada H. Aljarba, Saad Alkahtani, and Saud Alarifi
Research Article (9 pages), Article ID 5746761, Volume 2022 (2022)

[Retracted] Antioxidant and Anti-Inflammatory Activities of Coenzyme-Q10 and Piperine against Cyclophosphamide-Induced Cytotoxicity in HuH-7 Cells




Norah S. AL-Johani , Mohammed Al-Zharani , Nada H. Aljarba , Norah M. Alhoshani , Nora Alkeraishan , and Saad Alkahtani 
Research Article (10 pages), Article ID 8495159, Volume 2022 (2022)

Contents


[Retracted] Betamethasone Dipropionate Derivatization, Biotransformation, Molecular Docking, and ADME Analysis as Glucocorticoid Receptor

Sana Rashid , Shazia Anjum , Aqeel Ahmad , Raziya Nadeem , Maqsood Ahmed , Syed Adnan Ali Shah , Muhammad Abdullah , Komal Zia , and Zaheer Ul-haq 
Research Article (9 pages), Article ID 6865472, Volume 2022 (2022)





[Retracted] Antidiabetic Effect of *Tamarindus indica* and *Momordica charantia* and Downregulation of TET-1 Gene Expression by Saroglitazar in Glucose Feed Adipocytes and Their Involvement in the Type 2 Diabetes-Associated Inflammation *In Vitro*

Madhukar Saxena , S. Venkatesa Prabhu, M. Mohseen , Amit Kumar Pal, Saud Alarifi, Neelam Gautam, and Hemalatha Palanivel 
Research Article (10 pages), Article ID 9565136, Volume 2022 (2022)

[Retracted] The Impact of Seeding Density and Nitrogen Rates on Forage Yield and Quality of *Avena sativa* L

Aroosa Kanwal, Dawood Zubair, Rao Mehboob ur Rehman, Muhammad Ibrahim, Muhammad Amjad Bashir , Muhammad Mudassar Maqbool, Muhammad Imran, Ubaid ur Rehman, Omaima Nasif, and Mohammad Javed Ansari
Research Article (9 pages), Article ID 8238634, Volume 2022 (2022)








[Retracted] Synergistic Effect of Conventional Medicinal Herbs against Different Pharmacological Activity

Huma Ali , Daoud Ali, Bader O. Almutairi, Gokhlesh Kumar, Gizachew Assefa Karga , Chandran Masi , and Venkatesa Prabhu Sundramurthy 
Research Article (7 pages), Article ID 7337261, Volume 2022 (2022)






[Retracted] Nutrigenomic Interventions to Address Metabolic Stress and Related Disorders in Transition Cows

Faiz-ul Hassan , Asif Nadeem , Maryam Javed , Muhammad Saif-ur-Rehman, Muhammad Aasif Shahzad, Jahanzaib Azhar, and Borhan Shokrollahi 
Review Article (17 pages), Article ID 2295017, Volume 2022 (2022)




[Retracted] Pathological, Histological, and Molecular Based Investigations Confirm Novel *Mycobacterium bovis* Infection in *Boselaphus tragocamelus*

Riaz Hussain , Adil Jamal , Zulfiqar Ahmed, Bahaeldeen Babiker Mohamed , Abu Baker Siddique , Iahtasham Khan , Muhammad Khalid Mansoor, Xiaoxia Du , and Ahrar Khan 
Research Article (9 pages), Article ID 7601463, Volume 2022 (2022)

[Retracted] Histopathological Investigations and Molecular Confirmation Reveal *Mycobacterium bovis* in One-Horned Rhinoceros (*Rhinoceros unicornis*)


Abu Baker Siddique , Riaz Hussain , Adil Jamal , Md. Belal Hossain , Zulfiqar Ahmad, Muhammad Khalid Mansoor, Iahtasham Khan, Kainat Zahra, and Ahrar Khan 
Research Article (7 pages), Article ID 5816986, Volume 2022 (2022)

[Retracted] Cigarette Smoke Regulates the Expression of EYA4 via Alternation of DNA Methylation Status

Bader O. Almutairi , Mikhlid H. Almutairi, Abdulwahed F. Alrefaei, Daoud Ali, Saad Alkahtani , and Saud Alarifi 

Research Article (7 pages), Article ID 5032172, Volume 2022 (2022)

[Retracted] Toxicological Effects of Sewage Water on Chick Embryonic Development

Sana Khan, Hafiz Muhammad Noman Baqa, Hamas Mahmood, Muhammad Farooq, Khizar Samiullah, Riffat Yasin, Muhammad Amjad Bashir , Abdur Rahman, Tahir Mehmood, Sagheer Atta, and Afrah Fahad Alkhuriji

Research Article (7 pages), Article ID 6859798, Volume 2022 (2022)

Retraction

Retracted: The Impact of Seeding Density and Nitrogen Rates on Forage Yield and Quality of *Avena sativa* L

BioMed Research International

Received 8 January 2024; Accepted 8 January 2024; Published 13 January 2024

Copyright © 2024 BioMed Research International. This is an open access article distributed under the Creative Commons Attribution License, which permits unrestricted use, distribution, and reproduction in any medium, provided the original work is properly cited.

This article has been retracted by Hindawi following an investigation undertaken by the publisher [1]. This investigation has uncovered evidence of one or more of the following indicators of systematic manipulation of the publication process:

- (1) Discrepancies in scope
- (2) Discrepancies in the description of the research reported
- (3) Discrepancies between the availability of data and the research described
- (4) Inappropriate citations
- (5) Incoherent, meaningless and/or irrelevant content included in the article
- (6) Manipulated or compromised peer review

The presence of these indicators undermines our confidence in the integrity of the article's content and we cannot, therefore, vouch for its reliability. Please note that this notice is intended solely to alert readers that the content of this article is unreliable. We have not investigated whether authors were aware of or involved in the systematic manipulation of the publication process.

Wiley and Hindawi regrets that the usual quality checks did not identify these issues before publication and have since put additional measures in place to safeguard research integrity.

We wish to credit our own Research Integrity and Research Publishing teams and anonymous and named external researchers and research integrity experts for contributing to this investigation.

The corresponding author, as the representative of all authors, has been given the opportunity to register their agreement or disagreement to this retraction. We have kept a record of any response received.

References

- [1] A. Kanwal, D. Zubair, R. M. u. Rehman et al., "The Impact of Seeding Density and Nitrogen Rates on Forage Yield and Quality of *Avena sativa* L," *BioMed Research International*, vol. 2022, Article ID 8238634, 9 pages, 2022.

Retraction

Retracted: First Record of Ichthyofauna from Gomal Zam Dam, District South Waziristan, Khyber Pakhtunkhwa, Pakistan

BioMed Research International

Received 8 January 2024; Accepted 8 January 2024; Published 13 January 2024

Copyright © 2024 BioMed Research International. This is an open access article distributed under the Creative Commons Attribution License, which permits unrestricted use, distribution, and reproduction in any medium, provided the original work is properly cited.

This article has been retracted by Hindawi following an investigation undertaken by the publisher [1]. This investigation has uncovered evidence of one or more of the following indicators of systematic manipulation of the publication process:

- (1) Discrepancies in scope
- (2) Discrepancies in the description of the research reported
- (3) Discrepancies between the availability of data and the research described
- (4) Inappropriate citations
- (5) Incoherent, meaningless and/or irrelevant content included in the article
- (6) Manipulated or compromised peer review

The presence of these indicators undermines our confidence in the integrity of the article's content and we cannot, therefore, vouch for its reliability. Please note that this notice is intended solely to alert readers that the content of this article is unreliable. We have not investigated whether authors were aware of or involved in the systematic manipulation of the publication process.

Wiley and Hindawi regrets that the usual quality checks did not identify these issues before publication and have since put additional measures in place to safeguard research integrity.

We wish to credit our own Research Integrity and Research Publishing teams and anonymous and named external researchers and research integrity experts for contributing to this investigation.

The corresponding author, as the representative of all authors, has been given the opportunity to register their agreement or disagreement to this retraction. We have kept a record of any response received.

References

- [1] A. U. Rehman, S. Ullah, A. Zuberi, F. U. Dawar, and M. N. K. Khattak, "First Record of Ichthyofauna from Gomal Zam Dam, District South Waziristan, Khyber Pakhtunkhwa, Pakistan," *BioMed Research International*, vol. 2022, Article ID 7076508, 10 pages, 2022.

Retraction

Retracted: Expression Profile of MAGE-B1 Gene and Its Hypomethylation Activation in Colon Cancer

BioMed Research International

Received 8 January 2024; Accepted 8 January 2024; Published 9 January 2024

Copyright © 2024 BioMed Research International. This is an open access article distributed under the Creative Commons Attribution License, which permits unrestricted use, distribution, and reproduction in any medium, provided the original work is properly cited.

This article has been retracted by Hindawi following an investigation undertaken by the publisher [1]. This investigation has uncovered evidence of one or more of the following indicators of systematic manipulation of the publication process:

- (1) Discrepancies in scope
- (2) Discrepancies in the description of the research reported
- (3) Discrepancies between the availability of data and the research described
- (4) Inappropriate citations
- (5) Incoherent, meaningless and/or irrelevant content included in the article
- (6) Manipulated or compromised peer review

The presence of these indicators undermines our confidence in the integrity of the article's content and we cannot, therefore, vouch for its reliability. Please note that this notice is intended solely to alert readers that the content of this article is unreliable. We have not investigated whether authors were aware of or involved in the systematic manipulation of the publication process.

Wiley and Hindawi regrets that the usual quality checks did not identify these issues before publication and have since put additional measures in place to safeguard research integrity.

We wish to credit our own Research Integrity and Research Publishing teams and anonymous and named external researchers and research integrity experts for contributing to this investigation.

The corresponding author, as the representative of all authors, has been given the opportunity to register their agreement or disagreement to this retraction. We have kept a record of any response received.

References

- [1] M. H. Almutairi, M. M. Alotaibi, R. Alonaizan, and B. O. Almutairi, "Expression Profile of MAGE-B1 Gene and Its Hypomethylation Activation in Colon Cancer," *BioMed Research International*, vol. 2022, Article ID 6066567, 8 pages, 2022.

Retraction

Retracted: The Comparative Pharmacokinetics and Histokinetics of the Therapeutic Dose of Estradiol Valerate and Bromocriptine in Common Quails

BioMed Research International

Received 8 January 2024; Accepted 8 January 2024; Published 9 January 2024

Copyright © 2024 BioMed Research International. This is an open access article distributed under the Creative Commons Attribution License, which permits unrestricted use, distribution, and reproduction in any medium, provided the original work is properly cited.

This article has been retracted by Hindawi following an investigation undertaken by the publisher [1]. This investigation has uncovered evidence of one or more of the following indicators of systematic manipulation of the publication process:

- (1) Discrepancies in scope
- (2) Discrepancies in the description of the research reported
- (3) Discrepancies between the availability of data and the research described
- (4) Inappropriate citations
- (5) Incoherent, meaningless and/or irrelevant content included in the article
- (6) Manipulated or compromised peer review

The presence of these indicators undermines our confidence in the integrity of the article's content and we cannot, therefore, vouch for its reliability. Please note that this notice is intended solely to alert readers that the content of this article is unreliable. We have not investigated whether authors were aware of or involved in the systematic manipulation of the publication process.

Wiley and Hindawi regrets that the usual quality checks did not identify these issues before publication and have since put additional measures in place to safeguard research integrity.

We wish to credit our own Research Integrity and Research Publishing teams and anonymous and named

external researchers and research integrity experts for contributing to this investigation.

The corresponding author, as the representative of all authors, has been given the opportunity to register their agreement or disagreement to this retraction. We have kept a record of any response received.

References

- [1] M. Nadeem, M. Nisa, M. H. Bangash et al., "The Comparative Pharmacokinetics and Histokinetics of the Therapeutic Dose of Estradiol Valerate and Bromocriptine in Common Quails," *BioMed Research International*, vol. 2022, Article ID 5482895, 9 pages, 2022.

Retraction

Retracted: Effect of Vegetable Waste on Growth Performance and Hematology of Broiler Chicks

BioMed Research International

Received 8 January 2024; Accepted 8 January 2024; Published 9 January 2024

Copyright © 2024 BioMed Research International. This is an open access article distributed under the Creative Commons Attribution License, which permits unrestricted use, distribution, and reproduction in any medium, provided the original work is properly cited.

This article has been retracted by Hindawi following an investigation undertaken by the publisher [1]. This investigation has uncovered evidence of one or more of the following indicators of systematic manipulation of the publication process:

- (1) Discrepancies in scope
- (2) Discrepancies in the description of the research reported
- (3) Discrepancies between the availability of data and the research described
- (4) Inappropriate citations
- (5) Incoherent, meaningless and/or irrelevant content included in the article
- (6) Manipulated or compromised peer review

The presence of these indicators undermines our confidence in the integrity of the article's content and we cannot, therefore, vouch for its reliability. Please note that this notice is intended solely to alert readers that the content of this article is unreliable. We have not investigated whether authors were aware of or involved in the systematic manipulation of the publication process.

Wiley and Hindawi regrets that the usual quality checks did not identify these issues before publication and have since put additional measures in place to safeguard research integrity.

We wish to credit our own Research Integrity and Research Publishing teams and anonymous and named external researchers and research integrity experts for contributing to this investigation.

The corresponding author, as the representative of all authors, has been given the opportunity to register their agreement or disagreement to this retraction. We have kept a record of any response received.

References

- [1] M. S. Nisar, A. Zahra, M. F. Iqbal et al., "Effect of Vegetable Waste on Growth Performance and Hematology of Broiler Chicks," *BioMed Research International*, vol. 2022, Article ID 4855584, 8 pages, 2022.

Retraction

Retracted: Betamethasone Dipropionate Derivatization, Biotransformation, Molecular Docking, and ADME Analysis as Glucocorticoid Receptor

BioMed Research International

Received 8 January 2024; Accepted 8 January 2024; Published 9 January 2024

Copyright © 2024 BioMed Research International. This is an open access article distributed under the Creative Commons Attribution License, which permits unrestricted use, distribution, and reproduction in any medium, provided the original work is properly cited.

This article has been retracted by Hindawi following an investigation undertaken by the publisher [1]. This investigation has uncovered evidence of one or more of the following indicators of systematic manipulation of the publication process:

- (1) Discrepancies in scope
- (2) Discrepancies in the description of the research reported
- (3) Discrepancies between the availability of data and the research described
- (4) Inappropriate citations
- (5) Incoherent, meaningless and/or irrelevant content included in the article
- (6) Manipulated or compromised peer review

The presence of these indicators undermines our confidence in the integrity of the article's content and we cannot, therefore, vouch for its reliability. Please note that this notice is intended solely to alert readers that the content of this article is unreliable. We have not investigated whether authors were aware of or involved in the systematic manipulation of the publication process.

Wiley and Hindawi regrets that the usual quality checks did not identify these issues before publication and have since put additional measures in place to safeguard research integrity.

We wish to credit our own Research Integrity and Research Publishing teams and anonymous and named external researchers and research integrity experts for contributing to this investigation.

The corresponding author, as the representative of all authors, has been given the opportunity to register their agreement or disagreement to this retraction. We have kept a record of any response received.

References

- [1] S. Rashid, S. Anjum, A. Ahmad et al., "Betamethasone Dipropionate Derivatization, Biotransformation, Molecular Docking, and ADME Analysis as Glucocorticoid Receptor," *BioMed Research International*, vol. 2022, Article ID 6865472, 9 pages, 2022.

Retraction

Retracted: Nutrigenomic Interventions to Address Metabolic Stress and Related Disorders in Transition Cows

BioMed Research International

Received 8 January 2024; Accepted 8 January 2024; Published 9 January 2024

Copyright © 2024 BioMed Research International. This is an open access article distributed under the Creative Commons Attribution License, which permits unrestricted use, distribution, and reproduction in any medium, provided the original work is properly cited.

This article has been retracted by Hindawi, as publisher, following an investigation undertaken by the publisher [1]. This investigation has uncovered evidence of systematic manipulation of the publication and peer-review process. We cannot, therefore, vouch for the reliability or integrity of this article.

Please note that this notice is intended solely to alert readers that the peer-review process of this article has been compromised.

Wiley and Hindawi regret that the usual quality checks did not identify these issues before publication and have since put additional measures in place to safeguard research integrity.

We wish to credit our Research Integrity and Research Publishing teams and anonymous and named external researchers and research integrity experts for contributing to this investigation.

The corresponding author, as the representative of all authors, has been given the opportunity to register their agreement or disagreement to this retraction. We have kept a record of any response received.

References

- [1] F.-u. Hassan, A. Nadeem, M. Javed et al., “Nutrigenomic Interventions to Address Metabolic Stress and Related Disorders in Transition Cows,” *BioMed Research International*, vol. 2022, Article ID 2295017, 17 pages, 2022.

Retraction

Retracted: Toxicological Effects of Sewage Water on Chick Embryonic Development

BioMed Research International

Received 8 January 2024; Accepted 8 January 2024; Published 9 January 2024

Copyright © 2024 BioMed Research International. This is an open access article distributed under the Creative Commons Attribution License, which permits unrestricted use, distribution, and reproduction in any medium, provided the original work is properly cited.

This article has been retracted by Hindawi following an investigation undertaken by the publisher [1]. This investigation has uncovered evidence of one or more of the following indicators of systematic manipulation of the publication process:

- (1) Discrepancies in scope
- (2) Discrepancies in the description of the research reported
- (3) Discrepancies between the availability of data and the research described
- (4) Inappropriate citations
- (5) Incoherent, meaningless and/or irrelevant content included in the article
- (6) Manipulated or compromised peer review

The presence of these indicators undermines our confidence in the integrity of the article's content and we cannot, therefore, vouch for its reliability. Please note that this notice is intended solely to alert readers that the content of this article is unreliable. We have not investigated whether authors were aware of or involved in the systematic manipulation of the publication process.

Wiley and Hindawi regrets that the usual quality checks did not identify these issues before publication and have since put additional measures in place to safeguard research integrity.

We wish to credit our own Research Integrity and Research Publishing teams and anonymous and named external researchers and research integrity experts for contributing to this investigation.

The corresponding author, as the representative of all authors, has been given the opportunity to register their agreement or disagreement to this retraction. We have kept a record of any response received.

References

- [1] S. Khan, H. M. N. Baqa, H. Mahmood et al., "Toxicological Effects of Sewage Water on Chick Embryonic Development," *BioMed Research International*, vol. 2022, Article ID 6859798, 7 pages, 2022.

Retraction

Retracted: Pathological, Histological, and Molecular Based Investigations Confirm Novel *Mycobacterium bovis* Infection in *Boselaphus tragocamelus*

BioMed Research International

Received 8 January 2024; Accepted 8 January 2024; Published 9 January 2024

Copyright © 2024 BioMed Research International. This is an open access article distributed under the Creative Commons Attribution License, which permits unrestricted use, distribution, and reproduction in any medium, provided the original work is properly cited.

This article has been retracted by Hindawi following an investigation undertaken by the publisher [1]. This investigation has uncovered evidence of one or more of the following indicators of systematic manipulation of the publication process:

- (1) Discrepancies in scope
- (2) Discrepancies in the description of the research reported
- (3) Discrepancies between the availability of data and the research described
- (4) Inappropriate citations
- (5) Incoherent, meaningless and/or irrelevant content included in the article
- (6) Manipulated or compromised peer review

The presence of these indicators undermines our confidence in the integrity of the article's content and we cannot, therefore, vouch for its reliability. Please note that this notice is intended solely to alert readers that the content of this article is unreliable. We have not investigated whether authors were aware of or involved in the systematic manipulation of the publication process.

Wiley and Hindawi regrets that the usual quality checks did not identify these issues before publication and have since put additional measures in place to safeguard research integrity.

We wish to credit our own Research Integrity and Research Publishing teams and anonymous and named external researchers and research integrity experts for contributing to this investigation.

The corresponding author, as the representative of all authors, has been given the opportunity to register their agreement or disagreement to this retraction. We have kept a record of any response received.

References

- [1] R. Hussain, A. Jamal, Z. Ahmed et al., "Pathological, Histological, and Molecular Based Investigations Confirm Novel *Mycobacterium bovis* Infection in *Boselaphus tragocamelus*," *BioMed Research International*, vol. 2022, Article ID 7601463, 9 pages, 2022.

Retraction

Retracted: Cigarette Smoke Regulates the Expression of EYA4 via Alternation of DNA Methylation Status

BioMed Research International

Received 8 January 2024; Accepted 8 January 2024; Published 9 January 2024

Copyright © 2024 BioMed Research International. This is an open access article distributed under the Creative Commons Attribution License, which permits unrestricted use, distribution, and reproduction in any medium, provided the original work is properly cited.

This article has been retracted by Hindawi following an investigation undertaken by the publisher [1]. This investigation has uncovered evidence of one or more of the following indicators of systematic manipulation of the publication process:

- (1) Discrepancies in scope
- (2) Discrepancies in the description of the research reported
- (3) Discrepancies between the availability of data and the research described
- (4) Inappropriate citations
- (5) Incoherent, meaningless and/or irrelevant content included in the article
- (6) Manipulated or compromised peer review

The presence of these indicators undermines our confidence in the integrity of the article's content and we cannot, therefore, vouch for its reliability. Please note that this notice is intended solely to alert readers that the content of this article is unreliable. We have not investigated whether authors were aware of or involved in the systematic manipulation of the publication process.

Wiley and Hindawi regrets that the usual quality checks did not identify these issues before publication and have since put additional measures in place to safeguard research integrity.

We wish to credit our own Research Integrity and Research Publishing teams and anonymous and named external researchers and research integrity experts for contributing to this investigation.

The corresponding author, as the representative of all authors, has been given the opportunity to register their agreement or disagreement to this retraction. We have kept a record of any response received.

References

- [1] B. O. Almutairi, M. H. Almutairi, A. F. Alrefaei, D. Ali, S. Alkahtani, and S. Alarifi, "Cigarette Smoke Regulates the Expression of EYA4 via Alternation of DNA Methylation Status," *BioMed Research International*, vol. 2022, Article ID 5032172, 7 pages, 2022.

Retraction

Retracted: Inter-Relationship Between a Transcriptional Regulator of Flagella Genes *cj0440c* and Thiamine Metabolic Pathway in *Campylobacter jejuni*

BioMed Research International

Received 8 January 2024; Accepted 8 January 2024; Published 9 January 2024

Copyright © 2024 BioMed Research International. This is an open access article distributed under the Creative Commons Attribution License, which permits unrestricted use, distribution, and reproduction in any medium, provided the original work is properly cited.

This article has been retracted by Hindawi following an investigation undertaken by the publisher [1]. This investigation has uncovered evidence of one or more of the following indicators of systematic manipulation of the publication process:

- (1) Discrepancies in scope
- (2) Discrepancies in the description of the research reported
- (3) Discrepancies between the availability of data and the research described
- (4) Inappropriate citations
- (5) Incoherent, meaningless and/or irrelevant content included in the article
- (6) Manipulated or compromised peer review

The presence of these indicators undermines our confidence in the integrity of the article's content and we cannot, therefore, vouch for its reliability. Please note that this notice is intended solely to alert readers that the content of this article is unreliable. We have not investigated whether authors were aware of or involved in the systematic manipulation of the publication process.

Wiley and Hindawi regrets that the usual quality checks did not identify these issues before publication and have since put additional measures in place to safeguard research integrity.

We wish to credit our own Research Integrity and Research Publishing teams and anonymous and named external researchers and research integrity experts for contributing to this investigation.

The corresponding author, as the representative of all authors, has been given the opportunity to register their agreement or disagreement to this retraction. We have kept a record of any response received.

References

- [1] M. A. B. Shabbir, A. Ul-Rahman, A. R. Khalid et al., "Inter-Relationship Between a Transcriptional Regulator of Flagella Genes *cj0440c* and Thiamine Metabolic Pathway in *Campylobacter jejuni*," *BioMed Research International*, vol. 2022, Article ID 4539367, 10 pages, 2022.

Retraction

Retracted: Genomic and Therapeutic Analyses of *Staphylococcus aureus* Isolated from Cattle Reproductive Tract

BioMed Research International

Received 8 January 2024; Accepted 8 January 2024; Published 9 January 2024

Copyright © 2024 BioMed Research International. This is an open access article distributed under the Creative Commons Attribution License, which permits unrestricted use, distribution, and reproduction in any medium, provided the original work is properly cited.

This article has been retracted by Hindawi, as publisher, following an investigation undertaken by the publisher [1]. This investigation has uncovered evidence of systematic manipulation of the publication and peer-review process. We cannot, therefore, vouch for the reliability or integrity of this article.

Please note that this notice is intended solely to alert readers that the peer-review process of this article has been compromised.

Wiley and Hindawi regret that the usual quality checks did not identify these issues before publication and have since put additional measures in place to safeguard research integrity.

We wish to credit our Research Integrity and Research Publishing teams and anonymous and named external researchers and research integrity experts for contributing to this investigation.

The corresponding author, as the representative of all authors, has been given the opportunity to register their agreement or disagreement to this retraction. We have kept a record of any response received.

References

- [1] L. Shafique, A. I. Aqib, Q. Liang et al., “Genomic and Therapeutic Analyses of *Staphylococcus aureus* Isolated from Cattle Reproductive Tract,” *BioMed Research International*, vol. 2022, Article ID 6240711, 14 pages, 2022.

Retraction

Retracted: Biorational Control of *Callosobruchus maculatus* (Coleoptera: Buchidae) in Stored Grains with Botanical Extracts

BioMed Research International

Received 8 January 2024; Accepted 8 January 2024; Published 9 January 2024

Copyright © 2024 BioMed Research International. This is an open access article distributed under the Creative Commons Attribution License, which permits unrestricted use, distribution, and reproduction in any medium, provided the original work is properly cited.

This article has been retracted by Hindawi following an investigation undertaken by the publisher [1]. This investigation has uncovered evidence of one or more of the following indicators of systematic manipulation of the publication process:

- (1) Discrepancies in scope
- (2) Discrepancies in the description of the research reported
- (3) Discrepancies between the availability of data and the research described
- (4) Inappropriate citations
- (5) Incoherent, meaningless and/or irrelevant content included in the article
- (6) Manipulated or compromised peer review

The presence of these indicators undermines our confidence in the integrity of the article's content and we cannot, therefore, vouch for its reliability. Please note that this notice is intended solely to alert readers that the content of this article is unreliable. We have not investigated whether authors were aware of or involved in the systematic manipulation of the publication process.

Wiley and Hindawi regrets that the usual quality checks did not identify these issues before publication and have since put additional measures in place to safeguard research integrity.

We wish to credit our own Research Integrity and Research Publishing teams and anonymous and named external researchers and research integrity experts for contributing to this investigation.

The corresponding author, as the representative of all authors, has been given the opportunity to register their agreement or disagreement to this retraction. We have kept a record of any response received.

References

- [1] R. Akbar, I. A. Khan, B. Faheem et al., "Biorational Control of *Callosobruchus maculatus* (Coleoptera: Buchidae) in Stored Grains with Botanical Extracts," *BioMed Research International*, vol. 2022, Article ID 3443578, 10 pages, 2022.

Retraction

Retracted: Histopathological Investigations and Molecular Confirmation Reveal *Mycobacterium bovis* in One-Horned Rhinoceros (*Rhinoceros unicornis*)

BioMed Research International

Received 8 January 2024; Accepted 8 January 2024; Published 9 January 2024

Copyright © 2024 BioMed Research International. This is an open access article distributed under the Creative Commons Attribution License, which permits unrestricted use, distribution, and reproduction in any medium, provided the original work is properly cited.

This article has been retracted by Hindawi following an investigation undertaken by the publisher [1]. This investigation has uncovered evidence of one or more of the following indicators of systematic manipulation of the publication process:

- (1) Discrepancies in scope
- (2) Discrepancies in the description of the research reported
- (3) Discrepancies between the availability of data and the research described
- (4) Inappropriate citations
- (5) Incoherent, meaningless and/or irrelevant content included in the article
- (6) Manipulated or compromised peer review

The presence of these indicators undermines our confidence in the integrity of the article's content and we cannot, therefore, vouch for its reliability. Please note that this notice is intended solely to alert readers that the content of this article is unreliable. We have not investigated whether authors were aware of or involved in the systematic manipulation of the publication process.

Wiley and Hindawi regrets that the usual quality checks did not identify these issues before publication and have since put additional measures in place to safeguard research integrity.

We wish to credit our own Research Integrity and Research Publishing teams and anonymous and named

external researchers and research integrity experts for contributing to this investigation.

The corresponding author, as the representative of all authors, has been given the opportunity to register their agreement or disagreement to this retraction. We have kept a record of any response received.

References

- [1] A. B. Siddique, R. Hussain, A. Jamal et al., "Histopathological Investigations and Molecular Confirmation Reveal *Mycobacterium bovis* in One-Horned Rhinoceros (*Rhinoceros unicornis*)," *BioMed Research International*, vol. 2022, Article ID 5816986, 7 pages, 2022.

Retraction

Retracted: Quantifying the Soil Arthropod Diversity in Urban Forest in Dera Ghazi Khan

BioMed Research International

Received 8 January 2024; Accepted 8 January 2024; Published 9 January 2024

Copyright © 2024 BioMed Research International. This is an open access article distributed under the Creative Commons Attribution License, which permits unrestricted use, distribution, and reproduction in any medium, provided the original work is properly cited.

This article has been retracted by Hindawi following an investigation undertaken by the publisher [1]. This investigation has uncovered evidence of one or more of the following indicators of systematic manipulation of the publication process:

- (1) Discrepancies in scope
- (2) Discrepancies in the description of the research reported
- (3) Discrepancies between the availability of data and the research described
- (4) Inappropriate citations
- (5) Incoherent, meaningless and/or irrelevant content included in the article
- (6) Manipulated or compromised peer review

The presence of these indicators undermines our confidence in the integrity of the article's content and we cannot, therefore, vouch for its reliability. Please note that this notice is intended solely to alert readers that the content of this article is unreliable. We have not investigated whether authors were aware of or involved in the systematic manipulation of the publication process.

Wiley and Hindawi regrets that the usual quality checks did not identify these issues before publication and have since put additional measures in place to safeguard research integrity.

We wish to credit our own Research Integrity and Research Publishing teams and anonymous and named external researchers and research integrity experts for contributing to this investigation.

The corresponding author, as the representative of all authors, has been given the opportunity to register their agreement or disagreement to this retraction. We have kept a record of any response received.

References

- [1] M. Mohsin, H. Ahmad, M. N. Nasir et al., "Quantifying the Soil Arthropod Diversity in Urban Forest in Dera Ghazi Khan," *BioMed Research International*, vol. 2022, Article ID 8125585, 14 pages, 2022.

Retraction

Retracted: Antioxidant and Anti-Inflammatory Activities of Coenzyme-Q10 and Piperine against Cyclophosphamide-Induced Cytotoxicity in HuH-7 Cells

BioMed Research International

Received 8 January 2024; Accepted 8 January 2024; Published 9 January 2024

Copyright © 2024 BioMed Research International. This is an open access article distributed under the Creative Commons Attribution License, which permits unrestricted use, distribution, and reproduction in any medium, provided the original work is properly cited.

This article has been retracted by Hindawi following an investigation undertaken by the publisher [1]. This investigation has uncovered evidence of one or more of the following indicators of systematic manipulation of the publication process:

- (1) Discrepancies in scope
- (2) Discrepancies in the description of the research reported
- (3) Discrepancies between the availability of data and the research described
- (4) Inappropriate citations
- (5) Incoherent, meaningless and/or irrelevant content included in the article
- (6) Manipulated or compromised peer review

The presence of these indicators undermines our confidence in the integrity of the article's content and we cannot, therefore, vouch for its reliability. Please note that this notice is intended solely to alert readers that the content of this article is unreliable. We have not investigated whether authors were aware of or involved in the systematic manipulation of the publication process.

Wiley and Hindawi regrets that the usual quality checks did not identify these issues before publication and have since put additional measures in place to safeguard research integrity.

We wish to credit our own Research Integrity and Research Publishing teams and anonymous and named external researchers and research integrity experts for contributing to this investigation.

The corresponding author, as the representative of all authors, has been given the opportunity to register their agreement or disagreement to this retraction. We have kept a record of any response received.

References

- [1] N. S. AL-Johani, M. Al-Zharani, N. H. Aljarba, N. M. Alhoshani, N. Alkeraishan, and S. Alkahtani, "Antioxidant and Anti-Inflammatory Activities of Coenzyme-Q10 and Piperine against Cyclophosphamide-Induced Cytotoxicity in HuH-7 Cells," *BioMed Research International*, vol. 2022, Article ID 8495159, 10 pages, 2022.

Retraction

Retracted: Evaluation of the Anticancer Potential of *Morus nigra* and *Ocimum basilicum* Mixture against Different Cancer Cell Lines: An In Vitro Evaluation

BioMed Research International

Received 8 January 2024; Accepted 8 January 2024; Published 9 January 2024

Copyright © 2024 BioMed Research International. This is an open access article distributed under the Creative Commons Attribution License, which permits unrestricted use, distribution, and reproduction in any medium, provided the original work is properly cited.

This article has been retracted by Hindawi following an investigation undertaken by the publisher [1]. This investigation has uncovered evidence of one or more of the following indicators of systematic manipulation of the publication process:

- (1) Discrepancies in scope
- (2) Discrepancies in the description of the research reported
- (3) Discrepancies between the availability of data and the research described
- (4) Inappropriate citations
- (5) Incoherent, meaningless and/or irrelevant content included in the article
- (6) Manipulated or compromised peer review

The presence of these indicators undermines our confidence in the integrity of the article's content and we cannot, therefore, vouch for its reliability. Please note that this notice is intended solely to alert readers that the content of this article is unreliable. We have not investigated whether authors were aware of or involved in the systematic manipulation of the publication process.

Wiley and Hindawi regrets that the usual quality checks did not identify these issues before publication and have since put additional measures in place to safeguard research integrity.

We wish to credit our own Research Integrity and Research Publishing teams and anonymous and named external researchers and research integrity experts for contributing to this investigation.

The corresponding author, as the representative of all authors, has been given the opportunity to register their agreement or disagreement to this retraction. We have kept a record of any response received.

References

- [1] B. O. Almutairi, A. I. Alsayadi, N. Abutaha, F. A. AL-mekhlafi, and M. A. Wadaan, "Evaluation of the Anticancer Potential of *Morus nigra* and *Ocimum basilicum* Mixture against Different Cancer Cell Lines: An In Vitro Evaluation," *BioMed Research International*, vol. 2023, Article ID 9337763, 8 pages, 2023.

Retraction

Retracted: Antidiabetic Effect of *Tamarindus indica* and *Momordica charantia* and Downregulation of TET-1 Gene Expression by Saroglitazar in Glucose Feed Adipocytes and Their Involvement in the Type 2 Diabetes-Associated Inflammation *In Vitro*

BioMed Research International

Received 8 January 2024; Accepted 8 January 2024; Published 9 January 2024

Copyright © 2024 BioMed Research International. This is an open access article distributed under the Creative Commons Attribution License, which permits unrestricted use, distribution, and reproduction in any medium, provided the original work is properly cited.

This article has been retracted by Hindawi following an investigation undertaken by the publisher [1]. This investigation has uncovered evidence of one or more of the following indicators of systematic manipulation of the publication process:

- (1) Discrepancies in scope
- (2) Discrepancies in the description of the research reported
- (3) Discrepancies between the availability of data and the research described
- (4) Inappropriate citations
- (5) Incoherent, meaningless and/or irrelevant content included in the article
- (6) Manipulated or compromised peer review

The presence of these indicators undermines our confidence in the integrity of the article's content and we cannot, therefore, vouch for its reliability. Please note that this notice is intended solely to alert readers that the content of this article is unreliable. We have not investigated whether authors were aware of or involved in the systematic manipulation of the publication process.

Wiley and Hindawi regrets that the usual quality checks did not identify these issues before publication and have since put additional measures in place to safeguard research integrity.

We wish to credit our own Research Integrity and Research Publishing teams and anonymous and named external researchers and research integrity experts for contributing to this investigation.

The corresponding author, as the representative of all authors, has been given the opportunity to register their agreement or disagreement to this retraction. We have kept a record of any response received.

References

- [1] M. Saxena, S. V. Prabhu, M. Mohseen et al., "Antidiabetic Effect of *Tamarindus indica* and *Momordica charantia* and Downregulation of TET-1 Gene Expression by Saroglitazar in Glucose Feed Adipocytes and Their Involvement in the Type 2 Diabetes-Associated Inflammation *In Vitro*," *BioMed Research International*, vol. 2022, Article ID 9565136, 10 pages, 2022.

Retraction

Retracted: Peelu (*Salvadora oleoides* Decne.): An Unexplored Medicinal Fruit with Minerals, Antioxidants, and Phytochemicals

BioMed Research International

Received 8 January 2024; Accepted 8 January 2024; Published 9 January 2024

Copyright © 2024 BioMed Research International. This is an open access article distributed under the Creative Commons Attribution License, which permits unrestricted use, distribution, and reproduction in any medium, provided the original work is properly cited.

This article has been retracted by Hindawi following an investigation undertaken by the publisher [1]. This investigation has uncovered evidence of one or more of the following indicators of systematic manipulation of the publication process:

- (1) Discrepancies in scope
- (2) Discrepancies in the description of the research reported
- (3) Discrepancies between the availability of data and the research described
- (4) Inappropriate citations
- (5) Incoherent, meaningless and/or irrelevant content included in the article
- (6) Manipulated or compromised peer review

The presence of these indicators undermines our confidence in the integrity of the article's content and we cannot, therefore, vouch for its reliability. Please note that this notice is intended solely to alert readers that the content of this article is unreliable. We have not investigated whether authors were aware of or involved in the systematic manipulation of the publication process.

Wiley and Hindawi regrets that the usual quality checks did not identify these issues before publication and have since put additional measures in place to safeguard research integrity.

We wish to credit our own Research Integrity and Research Publishing teams and anonymous and named external researchers and research integrity experts for contributing to this investigation.

The corresponding author, as the representative of all authors, has been given the opportunity to register their agreement or disagreement to this retraction. We have kept a record of any response received.

References

- [1] K. Razzaq, M. M. Sadiq, H. Ashraf et al., "Peelu (*Salvadora oleoides* Decne.): An Unexplored Medicinal Fruit with Minerals, Antioxidants, and Phytochemicals," *BioMed Research International*, vol. 2022, Article ID 5707953, 9 pages, 2022.

Retraction

Retracted: A Comprehensive Review of Performance of Next-Generation Sequencing Platforms

BioMed Research International

Received 8 January 2024; Accepted 8 January 2024; Published 9 January 2024

Copyright © 2024 BioMed Research International. This is an open access article distributed under the Creative Commons Attribution License, which permits unrestricted use, distribution, and reproduction in any medium, provided the original work is properly cited.

This article has been retracted by Hindawi following an investigation undertaken by the publisher [1]. This investigation has uncovered evidence of one or more of the following indicators of systematic manipulation of the publication process:

- (1) Discrepancies in scope
- (2) Discrepancies in the description of the research reported
- (3) Discrepancies between the availability of data and the research described
- (4) Inappropriate citations
- (5) Incoherent, meaningless and/or irrelevant content included in the article
- (6) Manipulated or compromised peer review

The presence of these indicators undermines our confidence in the integrity of the article's content and we cannot, therefore, vouch for its reliability. Please note that this notice is intended solely to alert readers that the content of this article is unreliable. We have not investigated whether authors were aware of or involved in the systematic manipulation of the publication process.

Wiley and Hindawi regrets that the usual quality checks did not identify these issues before publication and have since put additional measures in place to safeguard research integrity.

We wish to credit our own Research Integrity and Research Publishing teams and anonymous and named external researchers and research integrity experts for contributing to this investigation.

The corresponding author, as the representative of all authors, has been given the opportunity to register their agreement or disagreement to this retraction. We have kept a record of any response received.

References

- [1] M. T. Pervez, M. J. ul Hasnain, S. H. Abbas, M. F. Moustafa, N. Aslam, and S. S. M. Shah, "A Comprehensive Review of Performance of Next-Generation Sequencing Platforms," *BioMed Research International*, vol. 2022, Article ID 3457806, 12 pages, 2022.

Retraction

Retracted: Synergistic Effect of Conventional Medicinal Herbs against Different Pharmacological Activity

BioMed Research International

Received 8 January 2024; Accepted 8 January 2024; Published 9 January 2024

Copyright © 2024 BioMed Research International. This is an open access article distributed under the Creative Commons Attribution License, which permits unrestricted use, distribution, and reproduction in any medium, provided the original work is properly cited.

This article has been retracted by Hindawi following an investigation undertaken by the publisher [1]. This investigation has uncovered evidence of one or more of the following indicators of systematic manipulation of the publication process:

- (1) Discrepancies in scope
- (2) Discrepancies in the description of the research reported
- (3) Discrepancies between the availability of data and the research described
- (4) Inappropriate citations
- (5) Incoherent, meaningless and/or irrelevant content included in the article
- (6) Manipulated or compromised peer review

The presence of these indicators undermines our confidence in the integrity of the article's content and we cannot, therefore, vouch for its reliability. Please note that this notice is intended solely to alert readers that the content of this article is unreliable. We have not investigated whether authors were aware of or involved in the systematic manipulation of the publication process.

Wiley and Hindawi regrets that the usual quality checks did not identify these issues before publication and have since put additional measures in place to safeguard research integrity.

We wish to credit our own Research Integrity and Research Publishing teams and anonymous and named external researchers and research integrity experts for contributing to this investigation.

The corresponding author, as the representative of all authors, has been given the opportunity to register their agreement or disagreement to this retraction. We have kept a record of any response received.

References

- [1] H. Ali, D. Ali, B. O. Almutairi et al., "Synergistic Effect of Conventional Medicinal Herbs against Different Pharmacological Activity," *BioMed Research International*, vol. 2022, Article ID 7337261, 7 pages, 2022.

Retraction

Retracted: Gut Microbiota Profiles in Dairy Cattle from Highland and Coastal Regions Using Shotgun Metagenomic Approach

BioMed Research International

Received 8 January 2024; Accepted 8 January 2024; Published 9 January 2024

Copyright © 2024 BioMed Research International. This is an open access article distributed under the Creative Commons Attribution License, which permits unrestricted use, distribution, and reproduction in any medium, provided the original work is properly cited.

This article has been retracted by Hindawi, as publisher, following an investigation undertaken by the publisher [1]. This investigation has uncovered evidence of systematic manipulation of the publication and peer-review process. We cannot, therefore, vouch for the reliability or integrity of this article.

Please note that this notice is intended solely to alert readers that the peer-review process of this article has been compromised.

Wiley and Hindawi regret that the usual quality checks did not identify these issues before publication and have since put additional measures in place to safeguard research integrity.

We wish to credit our Research Integrity and Research Publishing teams and anonymous and named external researchers and research integrity experts for contributing to this investigation.

The corresponding author, as the representative of all authors, has been given the opportunity to register their agreement or disagreement to this retraction. We have kept a record of any response received.

References

- [1] B. W. H. E. Prasetyono, W. Widiyanto, and N. S. Pandupuspitasari, "Gut Microbiota Profiles in Dairy Cattle from Highland and Coastal Regions Using Shotgun Metagenomic Approach," *BioMed Research International*, vol. 2022, Article ID 3659052, 8 pages, 2022.

Retraction

Retracted: *Lagerstroemia speciosa* Ameliorated Blood Pressure in LNAME Induced Hypertension in Experimental Rats through NO/cGMP and Oxidative Stress Modulation

BioMed Research International

Received 8 January 2024; Accepted 8 January 2024; Published 9 January 2024

Copyright © 2024 BioMed Research International. This is an open access article distributed under the Creative Commons Attribution License, which permits unrestricted use, distribution, and reproduction in any medium, provided the original work is properly cited.

This article has been retracted by Hindawi following an investigation undertaken by the publisher [1]. This investigation has uncovered evidence of one or more of the following indicators of systematic manipulation of the publication process:

- (1) Discrepancies in scope
- (2) Discrepancies in the description of the research reported
- (3) Discrepancies between the availability of data and the research described
- (4) Inappropriate citations
- (5) Incoherent, meaningless and/or irrelevant content included in the article
- (6) Manipulated or compromised peer review

The presence of these indicators undermines our confidence in the integrity of the article's content and we cannot, therefore, vouch for its reliability. Please note that this notice is intended solely to alert readers that the content of this article is unreliable. We have not investigated whether authors were aware of or involved in the systematic manipulation of the publication process.

Wiley and Hindawi regrets that the usual quality checks did not identify these issues before publication and have since put additional measures in place to safeguard research integrity.

We wish to credit our own Research Integrity and Research Publishing teams and anonymous and named external researchers and research integrity experts for contributing to this investigation.

The corresponding author, as the representative of all authors, has been given the opportunity to register their agreement or disagreement to this retraction. We have kept a record of any response received.

References

- [1] M. S. Aleissa, M. Al-Zharani, L. M. Alneghery et al., "*Lagerstroemia speciosa* Ameliorated Blood Pressure in LNAME Induced Hypertension in Experimental Rats through NO/cGMP and Oxidative Stress Modulation," *BioMed Research International*, vol. 2022, Article ID 5894416, 8 pages, 2022.

Retraction

Retracted: Ecotoxicological Assessment of Heavy Metal and Its Biochemical Effect in Fishes

BioMed Research International

Received 8 January 2024; Accepted 8 January 2024; Published 9 January 2024

Copyright © 2024 BioMed Research International. This is an open access article distributed under the Creative Commons Attribution License, which permits unrestricted use, distribution, and reproduction in any medium, provided the original work is properly cited.

This article has been retracted by Hindawi following an investigation undertaken by the publisher [1]. This investigation has uncovered evidence of one or more of the following indicators of systematic manipulation of the publication process:

- (1) Discrepancies in scope
- (2) Discrepancies in the description of the research reported
- (3) Discrepancies between the availability of data and the research described
- (4) Inappropriate citations
- (5) Incoherent, meaningless and/or irrelevant content included in the article
- (6) Manipulated or compromised peer review

The presence of these indicators undermines our confidence in the integrity of the article's content and we cannot, therefore, vouch for its reliability. Please note that this notice is intended solely to alert readers that the content of this article is unreliable. We have not investigated whether authors were aware of or involved in the systematic manipulation of the publication process.

Wiley and Hindawi regrets that the usual quality checks did not identify these issues before publication and have since put additional measures in place to safeguard research integrity.

We wish to credit our own Research Integrity and Research Publishing teams and anonymous and named external researchers and research integrity experts for contributing to this investigation.

The corresponding author, as the representative of all authors, has been given the opportunity to register their agreement or disagreement to this retraction. We have kept a record of any response received.

References

- [1] A. Haseeb, Fozia, I. Ahmad et al., "Ecotoxicological Assessment of Heavy Metal and Its Biochemical Effect in Fishes," *BioMed Research International*, vol. 2022, Article ID 3787838, 11 pages, 2022.

Retraction

Retracted: Comparative Genomic Characterization of Insulin-Like Growth Factor Binding Proteins in Cattle and Buffalo

BioMed Research International

Received 8 January 2024; Accepted 8 January 2024; Published 9 January 2024

Copyright © 2024 BioMed Research International. This is an open access article distributed under the Creative Commons Attribution License, which permits unrestricted use, distribution, and reproduction in any medium, provided the original work is properly cited.

This article has been retracted by Hindawi, as publisher, following an investigation undertaken by the publisher [1]. This investigation has uncovered evidence of systematic manipulation of the publication and peer-review process. We cannot, therefore, vouch for the reliability or integrity of this article.

Please note that this notice is intended solely to alert readers that the peer-review process of this article has been compromised.

Wiley and Hindawi regret that the usual quality checks did not identify these issues before publication and have since put additional measures in place to safeguard research integrity.

We wish to credit our Research Integrity and Research Publishing teams and anonymous and named external researchers and research integrity experts for contributing to this investigation.

The corresponding author, as the representative of all authors, has been given the opportunity to register their agreement or disagreement to this retraction. We have kept a record of any response received.

References

- [1] M. S. Rehman, M. Mushtaq, F. U. Hassan, Z. U. Rehman, M. Mushahid, and B. Shokrollahi, "Comparative Genomic Characterization of Insulin-Like Growth Factor Binding Proteins in Cattle and Buffalo," *BioMed Research International*, vol. 2022, Article ID 5893825, 15 pages, 2022.

Retraction

Retracted: The Antimicrobial Bifunctional Camel Lactoferrin: In Silico and Molecular Dynamic Perspective

BioMed Research International

Received 8 January 2024; Accepted 8 January 2024; Published 9 January 2024

Copyright © 2024 BioMed Research International. This is an open access article distributed under the Creative Commons Attribution License, which permits unrestricted use, distribution, and reproduction in any medium, provided the original work is properly cited.

This article has been retracted by Hindawi following an investigation undertaken by the publisher [1]. This investigation has uncovered evidence of one or more of the following indicators of systematic manipulation of the publication process:

- (1) Discrepancies in scope
- (2) Discrepancies in the description of the research reported
- (3) Discrepancies between the availability of data and the research described
- (4) Inappropriate citations
- (5) Incoherent, meaningless and/or irrelevant content included in the article
- (6) Manipulated or compromised peer review

The presence of these indicators undermines our confidence in the integrity of the article's content and we cannot, therefore, vouch for its reliability. Please note that this notice is intended solely to alert readers that the content of this article is unreliable. We have not investigated whether authors were aware of or involved in the systematic manipulation of the publication process.

Wiley and Hindawi regrets that the usual quality checks did not identify these issues before publication and have since put additional measures in place to safeguard research integrity.

We wish to credit our own Research Integrity and Research Publishing teams and anonymous and named external researchers and research integrity experts for contributing to this investigation.

The corresponding author, as the representative of all authors, has been given the opportunity to register their agreement or disagreement to this retraction. We have kept a record of any response received.

References

- [1] M. N. Alhumam, N. Alhumam, and M. Kandeel, "The Antimicrobial Bifunctional Camel Lactoferrin: In Silico and Molecular Dynamic Perspective," *BioMed Research International*, vol. 2023, Article ID 2322286, 8 pages, 2023.

Retraction

Retracted: Apoptotic and Antioxidant Activity of Gold Nanoparticles Synthesized Using Marine Brown Seaweed: An In Vitro Study

BioMed Research International

Received 8 January 2024; Accepted 8 January 2024; Published 9 January 2024

Copyright © 2024 BioMed Research International. This is an open access article distributed under the Creative Commons Attribution License, which permits unrestricted use, distribution, and reproduction in any medium, provided the original work is properly cited.

This article has been retracted by Hindawi following an investigation undertaken by the publisher [1]. This investigation has uncovered evidence of one or more of the following indicators of systematic manipulation of the publication process:

- (1) Discrepancies in scope
- (2) Discrepancies in the description of the research reported
- (3) Discrepancies between the availability of data and the research described
- (4) Inappropriate citations
- (5) Incoherent, meaningless and/or irrelevant content included in the article
- (6) Manipulated or compromised peer review

The presence of these indicators undermines our confidence in the integrity of the article's content and we cannot, therefore, vouch for its reliability. Please note that this notice is intended solely to alert readers that the content of this article is unreliable. We have not investigated whether authors were aware of or involved in the systematic manipulation of the publication process.

Wiley and Hindawi regrets that the usual quality checks did not identify these issues before publication and have since put additional measures in place to safeguard research integrity.

We wish to credit our own Research Integrity and Research Publishing teams and anonymous and named

external researchers and research integrity experts for contributing to this investigation.

The corresponding author, as the representative of all authors, has been given the opportunity to register their agreement or disagreement to this retraction. We have kept a record of any response received.

References

- [1] S. Rajeshkumar, R. P. Parameswari, J. Jayapriya et al., "Apoptotic and Antioxidant Activity of Gold Nanoparticles Synthesized Using Marine Brown Seaweed: An In Vitro Study," *BioMed Research International*, vol. 2022, Article ID 5746761, 9 pages, 2022.

Retraction

Retracted: Evaluation of Hematological, Oxidative Stress, and Antioxidant Profile in Cattle Infected with Brucellosis in Southern Punjab, Pakistan

BioMed Research International

Received 8 January 2024; Accepted 8 January 2024; Published 9 January 2024

Copyright © 2024 BioMed Research International. This is an open access article distributed under the Creative Commons Attribution License, which permits unrestricted use, distribution, and reproduction in any medium, provided the original work is properly cited.

This article has been retracted by Hindawi following an investigation undertaken by the publisher [1]. This investigation has uncovered evidence of one or more of the following indicators of systematic manipulation of the publication process:

- (1) Discrepancies in scope
- (2) Discrepancies in the description of the research reported
- (3) Discrepancies between the availability of data and the research described
- (4) Inappropriate citations
- (5) Incoherent, meaningless and/or irrelevant content included in the article
- (6) Manipulated or compromised peer review

The presence of these indicators undermines our confidence in the integrity of the article's content and we cannot, therefore, vouch for its reliability. Please note that this notice is intended solely to alert readers that the content of this article is unreliable. We have not investigated whether authors were aware of or involved in the systematic manipulation of the publication process.

Wiley and Hindawi regrets that the usual quality checks did not identify these issues before publication and have since put additional measures in place to safeguard research integrity.

We wish to credit our own Research Integrity and Research Publishing teams and anonymous and named external researchers and research integrity experts for contributing to this investigation.

The corresponding author, as the representative of all authors, has been given the opportunity to register their agreement or disagreement to this retraction. We have kept a record of any response received.

References

- [1] R. Hussain, I. Khan, A. Jamal, B. B. Mohamed, and A. Khan, "Evaluation of Hematological, Oxidative Stress, and Antioxidant Profile in Cattle Infected with Brucellosis in Southern Punjab, Pakistan," *BioMed Research International*, vol. 2022, Article ID 7140909, 10 pages, 2022.

Retraction

Retracted: *In Vitro* Evaluation of Cytotoxic Potential of *Caladium lindenii* Extracts on Human Hepatocarcinoma HepG2 and Normal HEK293T Cell Lines

BioMed Research International

Received 26 September 2023; Accepted 26 September 2023; Published 27 September 2023

Copyright © 2023 BioMed Research International. This is an open access article distributed under the Creative Commons Attribution License, which permits unrestricted use, distribution, and reproduction in any medium, provided the original work is properly cited.

This article has been retracted by Hindawi following an investigation undertaken by the publisher [1]. This investigation has uncovered evidence of one or more of the following indicators of systematic manipulation of the publication process:

- (1) Discrepancies in scope
- (2) Discrepancies in the description of the research reported
- (3) Discrepancies between the availability of data and the research described
- (4) Inappropriate citations
- (5) Incoherent, meaningless and/or irrelevant content included in the article
- (6) Peer-review manipulation

The presence of these indicators undermines our confidence in the integrity of the article's content and we cannot, therefore, vouch for its reliability. Please note that this notice is intended solely to alert readers that the content of this article is unreliable. We have not investigated whether authors were aware of or involved in the systematic manipulation of the publication process.

Wiley and Hindawi regrets that the usual quality checks did not identify these issues before publication and have since put additional measures in place to safeguard research integrity.

We wish to credit our own Research Integrity and Research Publishing teams and anonymous and named external researchers and research integrity experts for contributing to this investigation.

The corresponding author, as the representative of all authors, has been given the opportunity to register their agreement or disagreement to this retraction. We have kept a record of any response received.

References

- [1] A. Kalsoom, A. Altaf, M. Ashraf et al., "*In Vitro* Evaluation of Cytotoxic Potential of *Caladium lindenii* Extracts on Human Hepatocarcinoma HepG2 and Normal HEK293T Cell Lines," *BioMed Research International*, vol. 2022, Article ID 1279961, 11 pages, 2022.

Retraction

Retracted: The Antimicrobial Bifunctional Camel Lactoferrin: In Silico and Molecular Dynamic Perspective

BioMed Research International

Received 8 January 2024; Accepted 8 January 2024; Published 9 January 2024

Copyright © 2024 BioMed Research International. This is an open access article distributed under the Creative Commons Attribution License, which permits unrestricted use, distribution, and reproduction in any medium, provided the original work is properly cited.

This article has been retracted by Hindawi following an investigation undertaken by the publisher [1]. This investigation has uncovered evidence of one or more of the following indicators of systematic manipulation of the publication process:

- (1) Discrepancies in scope
- (2) Discrepancies in the description of the research reported
- (3) Discrepancies between the availability of data and the research described
- (4) Inappropriate citations
- (5) Incoherent, meaningless and/or irrelevant content included in the article
- (6) Manipulated or compromised peer review

The presence of these indicators undermines our confidence in the integrity of the article's content and we cannot, therefore, vouch for its reliability. Please note that this notice is intended solely to alert readers that the content of this article is unreliable. We have not investigated whether authors were aware of or involved in the systematic manipulation of the publication process.

Wiley and Hindawi regrets that the usual quality checks did not identify these issues before publication and have since put additional measures in place to safeguard research integrity.

We wish to credit our own Research Integrity and Research Publishing teams and anonymous and named external researchers and research integrity experts for contributing to this investigation.

The corresponding author, as the representative of all authors, has been given the opportunity to register their agreement or disagreement to this retraction. We have kept a record of any response received.

References

- [1] M. N. Alhumam, N. Alhumam, and M. Kandeel, "The Antimicrobial Bifunctional Camel Lactoferrin: In Silico and Molecular Dynamic Perspective," *BioMed Research International*, vol. 2023, Article ID 2322286, 8 pages, 2023.

Research Article

The Antimicrobial Bifunctional Camel Lactoferrin: In Silico and Molecular Dynamic Perspective

Maathir N. Alhumam ¹, Naser Alhumam ², and Mahmoud Kandeel ^{3,4}

¹College of Medicine, King Faisal University, Al Hofuf, Al-Ahsa, Saudi Arabia

²Department of Microbiology, College of Veterinary Medicine, King Faisal University, Al Hofuf, Al-Ahsa, Saudi Arabia

³Department of Biomolecular Sciences, College of Veterinary Medicine, King Faisal University, Al Hofuf, Al-Ahsa, Saudi Arabia

⁴Department of Pharmacology, Faculty of Veterinary Medicine, Kafrelsheikh University, Kafrelsheikh, Egypt

Correspondence should be addressed to Mahmoud Kandeel; mkandeel@kfu.edu.sa

Received 9 September 2022; Revised 9 October 2022; Accepted 2 May 2023; Published 23 May 2023

Academic Editor: Hafiz Ishfaq Ahmad

Copyright © 2023 Maathir N. Alhumam et al. This is an open access article distributed under the Creative Commons Attribution License, which permits unrestricted use, distribution, and reproduction in any medium, provided the original work is properly cited.

Lactoferrin (LF) is a major natural antimicrobial agent secreted in body fluids as a natural innate immunity protein. The action and structure of LF are closely related to its iron-binding capacity with structural reporting in open and closed conformations. This study looked at how lactoferrin structures change in camel (cLF), bovine (bLF), and human (hLF) lactoferrin closed forms after iron is removed from their binding sites. Initially, the sequence comparison between cLF and the LFs of marine mammals, bats, and domestic animals was the most intriguing conclusion. Camel LF is revealed to be more closely related to marine animals (~80.36% identity) and bats (~79.3% identity) than to terrestrial mammal species (~75.5% identity). Results indicated that cLF was more dynamic in nature than bLF and hLF by showing higher RMSD values. The cLF is known to be half lactoferrin half transferrin; in this study, we show that there are different MD behavior of both iron-binding sites. While LF contains two lobes (C- and N-lobes), the C-lobe showed high fluctuations as N-lobe was more stable in the absence of ferric ions. The C-lobe and N-lobe of cLF react differently at physiological pH, revealing distinct molecular interactions between these components. In addition, cLF showed higher system flexibility derived from its larger RMSD, RMSF, lower intermolecular hydrogen bonds, and higher solvent accessible surface area (SASA).

1. Introduction

Lactoferrin (LF) is a transferrin family glycoprotein with a molecular mass of 80 kDa. The activity of essential oils and plant extracts from six medicinal plants (*Lippia citriodora*, *Ferula gummosa*, *Bunium persicum*, *Mentha piperita*, *Plantago major*, and *Salvadora persica*) against *Pseudomonas tolaasii* and *Trichoderma harzianum* as white button mushroom pathogens as well as a chimera peptide of camel lactoferrin (cLF) was established. The results revealed that when compared to other therapies, the chimeric camel lactoferrin peptide showed that the highest quantity of inhibitory zone had a substantial difference in antibacterial efficacy [1]. Milk is the primary source of LF; however, saliva, tears, bile, and pancreatic juice also contain the protein. Milk LF has been shown to have a potent inhibitory effect against pathogens

such as bacteria, fungi, and viruses. LF showed broad-spectrum antiviral activity. For instance, LF showed antiviral activity against coronaviruses [2], human enteric norovirus [3], bovine viral diarrhea virus [4], herpes simplex virus [5], human immunodeficiency virus and human cytomegalovirus [6], alphavirus [7], hantavirus [8], adenovirus [9], human papillomavirus [10], rotavirus [11], chikungunya and Zika viruses [12], hepatitis C virus [13, 14], influenza virus [15], Toscana virus [16], and enterovirus [17]. Strong antibacterial capacity for cLF was observed against *E. coli* than bovine and human lactoferrin [18]. LF exerts its antiviral activity through different mechanisms comprising inhibition of virus-host interaction or direct interaction with virus particles though the classical antibacterial activity was suggested to deprivation of bacteria from the essential iron, by trapping iron into the LF iron-binding sites.

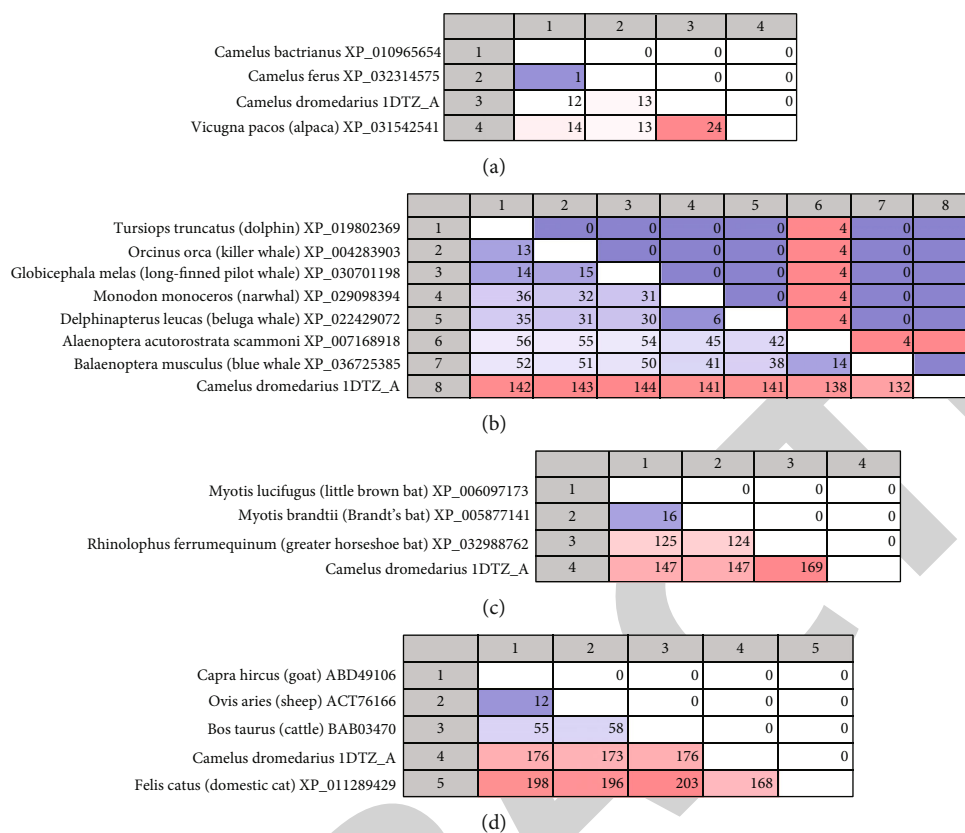


FIGURE 1: Pairwise sequence comparison matrix. The upper diagonal panel is the number of gaps. The lower diagonal panel is the percent identity. (a) Comparison of old and new world camels. (b) Comparison of dromedary camel LF with whales and other marine mammals LF. (c) Comparison of dromedary camel LF with Bats LF. (d) Comparison of dromedary camel LF with other domestic animals LF.

The cLF is a bilobal structure connected by a short peptide, with each lobe folded into two functional domains; its N-lobe is similar to that of human LF; however, the C-lobe is more akin to that of apo-ovotransferrin [19]. Both native and recombinant N- and C-lobes of camel LF showed similar high inhibitory activity against hepatitis C virus replication [20]. Each lobe is bound with one iron atom. Camel LF has 689 amino acid residues and 17 disulfide bridges, as well as four putative glycosylation sites, one in the N-lobe and three in the C-lobe. The disulfide bond pattern in cLF is identical to that discovered in human and mare LFs, but the positions of predicted glycosylation sites in cLF are completely different [19].

The purpose of this work was to evaluate the molecular dynamics of human, camel, and bovine LF after iron ions were removed from their binding sites. The structure stability, LF backbone fluctuations, and structure compactness are all compared. The findings of this investigation will provide fresh insights into the differences in LF interactions in humans, camels, and cattle.

2. Materials and Methods

2.1. Retrieval of Lactoferrin Protein Sequences. The sequences used in this study were obtained from the GenBank and protein databases, both of which are found at <https://www.ncbi.nlm.nih.gov/>.

The obtained sequences comprise LF from *Homo sapiens*, *Camelus dromedarius*, *Camelus bactrianus*, *Camelus ferus*, *Vicugna pacos*, *Balaenoptera acutorostrata scammoni*, *Tursiops truncatus*, *Orcinus orca*, *Globicephala melas*, *Monodon monoceros*, *Delphinapterus leucas*, *Balaenoptera musculus*, *Myotis lucifugus*, *Myotis brandtii*, *Rhinolophus ferrumequinum*, *Capra hircus*, *Ovis aries*, *Bos taurus*, and *Felis catus*. The sequences were imported and managed using CLC genomics software (Qiagen software, Denmark).

2.2. Multiple Sequence Alignment and Phylogenetic Tree. The sequence alignment tool in CLC genomics software was used to align the LF sequences using very accurate mode and gap extension cost of 1.00. The tree was generated using the CLC genomic software using UPMA as a tree construction method and Kimura protein distance measure. Bootstrapping was set to 100 replicates.

2.3. MD Simulations. The MD simulation setup and settings were carried out as previously reported, with minor changes [21, 22]. The retrieved proteins were 1blf, 1i6q, and 2bjj for bLF, cLF, and hLF, respectively. To run molecular dynamic simulations, the GROMACS simulation package (GROMACS 2020.4) was utilized. MD simulation of LF in water was performed for 50 ns using the CHARMM36 force field;

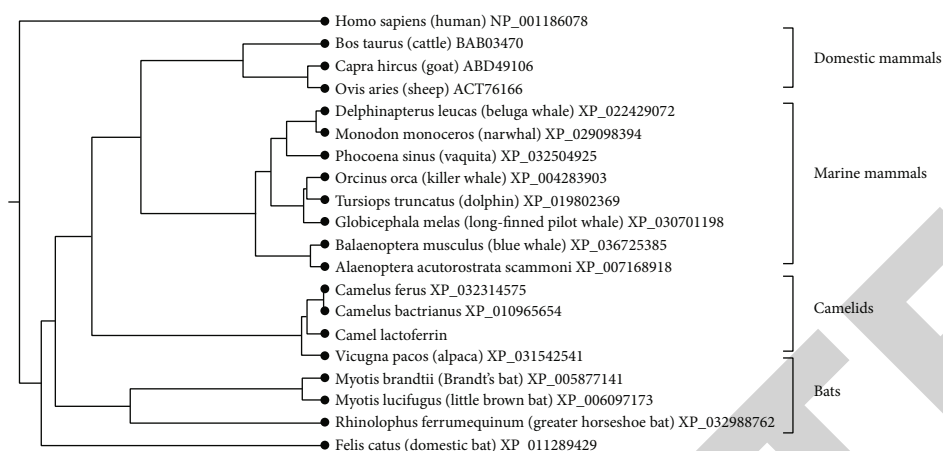


FIGURE 2: Phylogram showing the relations of camel LF.

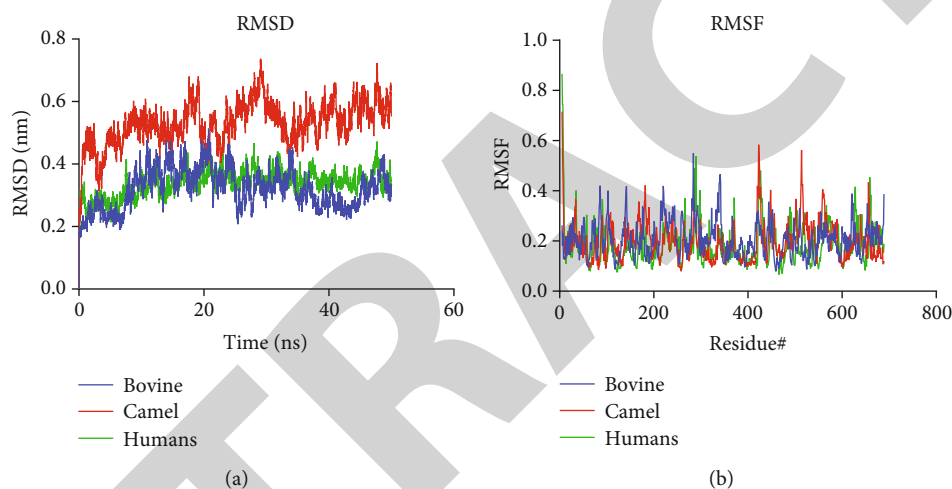


FIGURE 3: RMSD and RMSF of the bovine, camel, and human LF: (a) RMSD; (b) RMSF.

trajectory and energy files were written every 10 ps. TIP3P water molecules were used to solvate the system in a truncated octahedral box. The protein was centered in the simulation box within 1 nm of the box edge. To neutralize the entire system, potassium/chloride ions were introduced. The steepest descent method was used to minimize the system for 5000 steps, and convergence was reached within the maximum force of $1000 \text{ (kJ mol}^{-1} \text{ nm}^{-1})$ to remove any steric clashes. All systems were equilibrated at NVT and NPT ensembles for 100 ps (50,000 steps) and 1000 ps (1,000,000 steps), utilizing time steps of 0.2 and 0.1 fs, respectively, at a temperature of 300 K. The simulation runs were performed at a constant temperature of 300 K and a pressure of 1 atm or bar (NPT) using the Parrinello-Rahman and weak coupling velocity rescaling (modified Berendsen thermostat) algorithms, respectively. Using the linear constraint solver algorithm with a time step of 2 fs, all bond lengths involving the hydrogen atom were kept rigid at ideal bond lengths. Non-bonded interactions were calculated using the Verlet technique. In both x , y , and z directions, periodic boundary conditions (PBC) were applied. Each time step calculated

interactions within a 1.2 nm short-range threshold. The electrostatic interactions and forces in a homogeneous medium outside the long-range limit were calculated using particle mesh Ewald (PME). The complex's production was run for 50 ns.

3. Results and Discussion

3.1. Comparative LF Sequence Data. Multiple sequence alignment and pairwise sequence comparison matrix revealed interesting relations of camel LF with other mammal LF. Initially, LF was compared in old- and new-world camels. Dromedary, Bactrian, and feral camels shared 98.16–99.85% identity (12–14 amino acid differences). The most distant relation was between the dromedary camel and alpaca showing 96.61% identity and 24 amino acid differences (Figure 1(a)).

The most interesting result of the sequence comparison was the relationship between camel LF and the LFs of marine mammals, bats, and domestic animals (Figures 1(b)–1(d)). The results found that camel LF is more closely related to

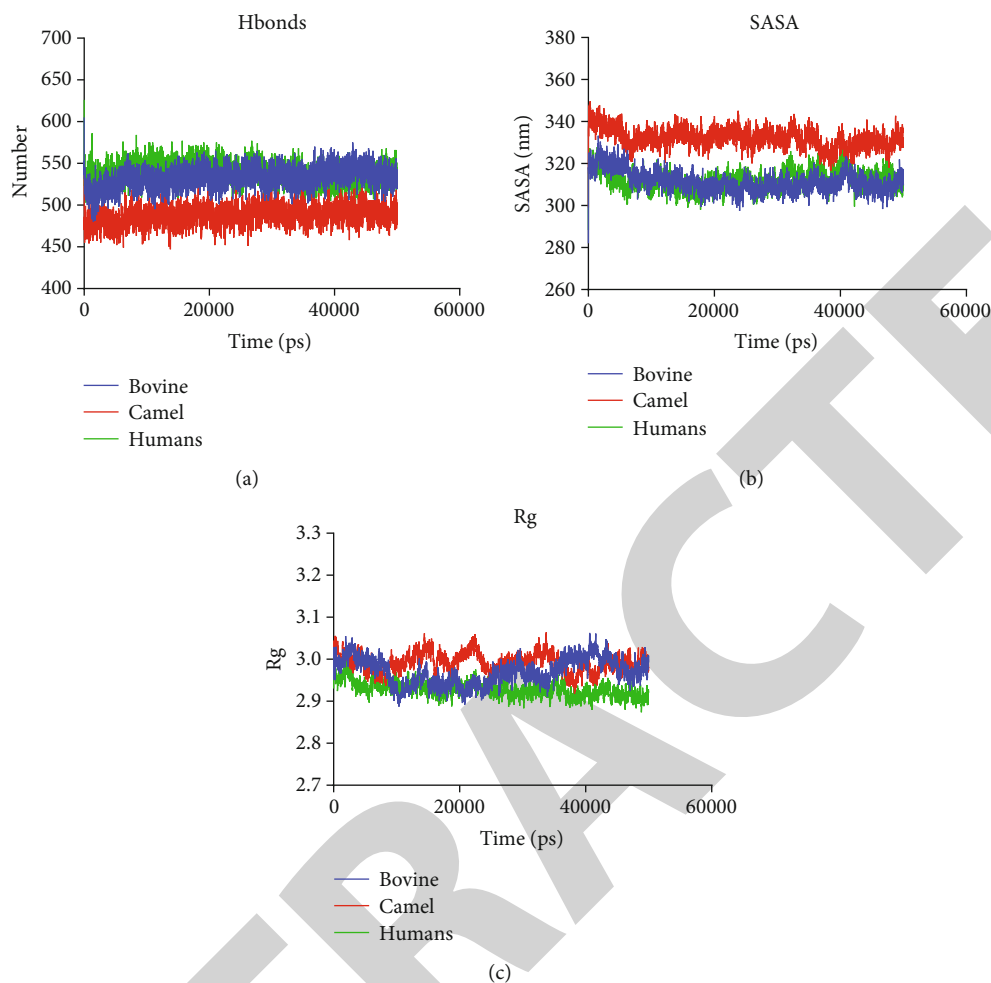


FIGURE 4: The structural characteristics of bovine, camel, and human LFs: (a) intermolecular hydrogen bonds; (b) SASA; (c) Rg.

marine mammals and bats than to terrestrial species. The functional implication of this observed relationship needs further experimental proof.

3.2. Phylogenetics. After BLAST search of protein database with camel LF, close relation with marine mammals was concluded. The marine mammals comprised of *Balaenoptera acutorostrata scammoni* (minke whale, XP_007168918), *Monodon monoceros* (narwhal, XP_029098394), *Balaenoptera musculus* (blue whale, XP_036725385), *Orcinus orca* (killer whale, XP_004283903), *Globicephala melas* (long-finned pilot whale, XP_030701198), *Delphinapterus leucas* (beluga whale, XP_022429072), and *Tursiops truncatus* (dolphin, XP_019802369). Figure 1(b) shows the pairwise comparison panel with the indicated identity rates. The % identity between the camel and these marine mammals was 79.8-80.36% with 132-144 amino acid differences.

Following marine mammals, bats come in the second rank with %identity equals 76.1-79.3%. Furthermore, lower %identity was observed with domestic animals, showing 75.1-75.5% identity with sheep, goat, cat, and bovine LF (Figure 1(d)).

TABLE 1: The intermolecular hydrogen bonds during 50 ns MD simulation for bovine, camel, and human LF.

	Bovine	Camel	Humans
Number of values	5001	5001	5001
Minimum	480	447	498
25% percentile	525	480	530
Median	533	488	539
75% percentile	542	496	548
Maximum	605	543	626
Mean \pm SD	532.8 ± 12.69	488 ± 11.49	538.8 ± 12.71

TABLE 2: The solvent accessible surface area during 50 ns MD simulation for bovine, camel, and human LF.

	Bovine	Camel	Humans
Number of values	5001	5001	5001
Median	310.9	332	312.1
Mean \pm SD	311.5 ± 5	332.1 ± 4.6	312.3 ± 4.6

TABLE 3: The frequencies of charged amino acid composition of LF. Negatively charged (D and E), positively charged (R and K), and other amino acids.

	Negatively charged (D and E)	Positively charged (R and K)	Other
<i>Camel dromedarius</i> 1DTZ	0.103	0.126	0.771
<i>Camelus bactrianus</i> XP_010965654	0.105	0.121	0.774
<i>Camelus ferus</i> XP_032314575	0.103	0.121	0.775
<i>Vicugna pacos</i> (alpaca) XP_031542541	0.104	0.117	0.779
<i>Balaenoptera acutorostrata scammoni</i> XP_007168918	0.101	0.128	0.771
<i>Monodon monoceros</i> (narwhal) XP_029098394	0.106	0.125	0.769
<i>Balaenoptera musculus</i> (blue whale) XP_036725385	0.102	0.128	0.771
<i>Tursiops truncatus</i> (dolphin) XP_019802369	0.104	0.118	0.777
<i>Orcinus orca</i> (killer whale) XP_004283903	0.103	0.127	0.770
<i>Globicephala melas</i> (long-finned pilot whale) XP_030701198	0.106	0.121	0.773
<i>Rhinolophus ferrumequinum</i> (greater horseshoe bat) XP_032988762	0.113	0.120	0.767
<i>Delphinapterus leucas</i> (beluga whale) XP_022429072	0.104	0.125	0.770
<i>Myotis lucifugus</i> (little brown bat) XP_006097173	0.107	0.119	0.774
<i>Phocoena sinus</i> (vaquita) XP_032504925	0.104	0.118	0.778
<i>Myotis brandtii</i> (Brandt's bat) XP_005877141	0.106	0.120	0.774
<i>Ovis aries</i> (sheep) ACT76166	0.105	0.119	0.777
<i>Felis catus</i> (domestic cat) XP_011289429	0.117	0.124	0.758
<i>Bos taurus</i> (cattle) BAB03470	0.107	0.131	0.761
<i>Capra hircus</i> (goat) ABD49106	0.106	0.120	0.774
<i>Homo sapiens</i> (human) NP_001186078	0.117	0.126	0.757
Average			
Camelids	0.103	0.122	0.773
Marine mammals	0.103	0.123	0.772
Domestic animals and human	0.110	0.124	0.765

The phylogenetic presentation of LF revealed that camel LF is closely related to bat and marine mammal LF but more distantly related to domestic mammals (Figure 2).

3.3. Root Mean Square Deviations (RMSD). GROMACS was used to determine RMSD for LFs based on “backbone” atoms. The RMSD graph for LF (Figure 3(a)) demonstrates that the structure remained stable during the simulation time with some fluctuation within the range of 2 Å, which is typical of globular proteins. The average RMSD was 0.32 ± 0.06 , 0.53 ± 0.06 , and 0.34 ± 0.04 for bovine, camel, and human LF, respectively. This implies that bovine and human LF is more stable than camel LF.

3.4. Root Mean Square Fluctuations (RMSF). GROMACS was used to calculate RMSF for the protein complex based on “C-alpha” atoms. Overall, the intensity of the fluctuation remains below 0.6 nm (Figure 3(b)). The maximal RMSF values were 0.55, 0.72, and 0.87 for bovine, camel, and human LF, respectively. The maximal RMSF residues in cLF were 422-425 and 513-515, while in hLF, they were 287-291 and 424-428.

3.5. Hydrogen Bonds (Intermolecular). The progress curve of the total number of hydrogen bonds formed during 50 ns of the simulation time is shown in (Figure 4(a)). The summary

statistics revealed that the cLF formed the lowest number of bonds throughout the simulation percentiles, average and mean values (Table 1).

3.6. Solvent Accessible Surface Area (SASA). The largest SASA was produced by cLF throughout the simulation (Figure 4(b)). SASA average values were 311.5 ± 5 , 332.1 ± 4 , and 312.3 ± 4.6 for bovine, camel, and human LF, respectively (Table 2). As a general rule, a lower SASA value is seen as signifying a more stable protein structure with lower values indicating more fraction is buried within the structure. Due to the fact that the cLF is made up of two lobes with distinct biological interactions, a definitive conclusion on the overall volume of protein that makes up SASA cannot be drawn.

3.7. The Radius of Gyration (Rg). The radius of gyration was calculated for the complex based on “C-alpha” atoms using GROMACS program (Figure 4(c)). The low values of Rg indicate the general compactness of the examined systems. The generally low Rg for cLF, bLF, and hLF indicates the general compactness of all protein structures during MD simulation.

3.8. Lactoferrin Composition. The amino acid composition of the used dataset was analyzed to shed light on the amino

TABLE 4: The frequencies of amino acid composition of LF. Hydrophobic residues (A, F, G, I, L, M, P, V, and W), hydrophilic residues (C, N, Q, S, T, and Y), and other amino acids.

	Hydrophobic (A, F, G, I, L, M, P, V, and W)	Hydrophilic (C, N, Q, S, T, and Y)	Other
<i>Camel dromedarius</i> 1DTZ	0.483	0.274	0.274
<i>Camelus bactrianus</i> XP_010965654	0.477	0.282	0.240
<i>Camelus ferus</i> XP_032314575	0.477	0.282	0.239
<i>Vicugna pacos</i> (alpaca) XP_031542541	0.469	0.293	0.238
<i>Balaenoptera acutorostrata scammoni</i> XP_007168918	0.480	0.279	0.241
<i>Monodon monoceros</i> (narwhal) XP_029098394	0.482	0.275	0.244
<i>Balaenoptera musculus</i> (blue whale) XP_036725385	0.483	0.276	0.241
<i>Tursiops truncatus</i> (dolphin) XP_019802369	0.482	0.285	0.234
<i>Orcinus orca</i> (killer whale) XP_004283903	0.479	0.280	0.241
<i>Globicephala melas</i> (long-finned pilot whale) XP_030701198	0.485	0.277	0.238
<i>Rhinolophus ferrumequinum</i> (greater horseshoe bat) XP_032988762	0.455	0.298	0.247
<i>Delphinapterus leucas</i> (beluga whale) XP_022429072	0.485	0.275	0.241
<i>Myotis lucifugus</i> (little brown bat) XP_006097173	0.470	0.294	0.236
<i>Phocoena sinus</i> (vaquita) XP_032504925	0.484	0.283	0.233
<i>Myotis brandtii</i> (Brandt's bat) XP_005877141	0.470	0.294	0.236
<i>Ovis aries</i> (sheep) ACT76166	0.477	0.287	0.236
<i>Felis catus</i> (domestic cat) XP_011289429	0.479	0.263	0.258
<i>Bos taurus</i> (cattle) BAB03470	0.472	0.277	0.251
<i>Capra hircus</i> (goat) ABD49106	0.476	0.287	0.237
<i>Homo sapiens</i> (human) NP_001186078	0.465	0.278	0.257
Average			
Camelids	0.479	0.27933	0.251
Marine mammals	0.48	0.28071	0.23957
Domestic animals and human	0.4738	0.2784	0.2478

acid characteristics, comprising the frequencies of hydrophobic, hydrophilic, positively charged, negatively charged, and other characteristics (Tables 3 and 4).

Camelids and marine mammals showed lower average negatively charged residue frequencies (0.103), which is lower than domestic mammals (0.11). There were a slight decrease in positive residues and a marked increase in the frequency of noncharged residues in cLF (Table 3). No major changes were observed in the frequencies of residues' hydrophilicity or hydrophobicity (Table 4).

In a previous report, the majority of positively charged residues are present in the N-terminal lobe's N-terminal region. Lactoferrins' high net positive charge at physiological pH is thought to determine their ability to bind to the different negatively charged components found on the bacterial surface, including LPS [18], DNA, and immune cells [23].

3.9. The Iron-Binding Site. About half of the iron concentrations are lost at pH 6.5, and the other half is lost in acidic circumstances (pH 4.0–2.0). The iron release mechanisms of the N-lobe and C-lobe are unique, as evidenced by the fact that the N-lobe releases iron at a lower pH (less than 4.0) while the C-lobe releases iron at a higher pH (6.5). This implies that cLF works as both transferrin (a protein that transports iron) and lactoferrin (a protein that binds iron), in contrast to other transferrins and lactoferrins,

which have distinct iron transfer or binding roles. Other transferrins and lactoferrins have a distinct iron transfer or binding activities [19, 23, 24]. Both lobes, all LFs, have the same residues for the bound Fe^{3+} ion. These residues are made up of two tyrosine residues, one aspartic acid residue, and one histidine residue, Asp 60, Tyr 92, Tyr 192, and His 253 in the LF N-lobe and Asp 395, Tyr 433, Tyr 526, and His 595 in the C-lobe. Some residues relevant to domain mobility in the protein, such as Pro418, Leu423, Lys433, Gln561, Gly629, Lys637, Arg652, and Pro592, differ in cLF from those of identified in other LFs, indicating the possibility of structural changes [19]. In the MD simulation of this study, all iron-binding site residues at the N-lobe showed low RMSF, while residues at the C-lobe showed significantly higher RMSF, indicating different behavior of LF lobes in the absence of bound iron. Since this MD simulation was performed at physiological pH, then the C-lobe and N-lobe of cLF behave differently at this pH, implying separate molecular interactions of these components.

4. Relationship of cLF and the Observed Phylogenetics

There is a surprising higher relationship between camelids' LD with marine mammals' LF, which was more distant to domestic animals' LF.

LF is present in various body fluids, comprising tears, saliva, and milk. Despite being present in water, marine mammals such as dolphins' lacrimal secretions are rich in lactoferrin for broad-spectrum bacteriostatic purposes [25].

The N-lobe of camel apolactoferrin is structurally very similar to the N-lobe of human apolactoferrin, while the C-lobe of camel apolactoferrin is structurally quite similar to that of hen and duck apo-ovotransferrin [19]. These findings show that the iron-binding and releasing behavior of camel lactoferrin's N-lobe is comparable to that of human lactoferrin's N-lobe, whereas that of the C-lobe is similar to that of duck and hen apo-ovotransferrins' C-lobes [19]. In this study, the C-lobe fluctuated more than the N-lobe, with a more variable iron-binding site. This suggests that iron is required for C-lobe stability. The reported stability of the N-lobe in camels may reflect its activity and interaction with other proteins, as well as the implementation of its functions.

Data Availability

All data is within the manuscript. Further details can be requested from the corresponding author.

Conflicts of Interest

The authors declare no conflict of interest.

Authors' Contributions

MK designed the experiment. MK, MNA, and NA performed the experiment. MK, MNA, and NA analyzed the results. MK wrote the manuscript. MNA and NA revised the manuscript. All authors revised the manuscript and approved the submission.

Acknowledgments

This work was supported by the Deanship of Scientific Research, Vice Presidency for Graduate Studies and Scientific Research, King Faisal University, Saudi Arabia (GRANT3230).

References

- [1] A. Tanhaeian, N. Nazifi, F. Shahriari Ahmadi, and M. Akhlaghi, "Comparative study of antimicrobial activity between some medicine plants and recombinant lactoferrin peptide against some pathogens of cultivated button mushroom," *Archives of Microbiology*, vol. 202, no. 9, pp. 2525–2532, 2020.
- [2] J. K. Mann and T. Ndung'u, "The potential of lactoferrin, ovotransferrin and lysozyme as antiviral and immune-modulating agents in COVID-19," *Future Virology*, vol. 15, no. 9, pp. 609–624, 2020.
- [3] H. Oda, A. O. Kolawole, C. Mirabelli et al., "Antiviral effects of bovine lactoferrin on human norovirus," *Biochemistry and Cell Biology*, vol. 99, no. 1, pp. 166–172, 2021.
- [4] J. Małaczewska, E. Kaczorek-Łukowska, R. Wójcik, and A. K. Siwicki, "Antiviral effects of nisin, lysozyme, lactoferrin and their mixtures against bovine viral diarrhoea virus," *BMC veterinary research*, vol. 15, no. 1, pp. 1–12, 2019.
- [5] M. Krzyzowska, M. Chodkowski, M. Janicka et al., "Lactoferrin-functionalized noble metal nanoparticles as new antivirals for HSV-2 infection," *Microorganisms*, vol. 10, no. 1, p. 110, 2022.
- [6] M. C. Harmsen, P. J. Swart, M.-P. Béthune et al., "Antiviral effects of plasma and milk proteins: lactoferrin shows potent activity against both human immunodeficiency virus and human cytomegalovirus replication in vitro," *Journal of Infectious Diseases*, vol. 172, no. 2, pp. 380–388, 1995.
- [7] B.-L. Waarts, O. J. Aneke, J. M. Smit et al., "Antiviral activity of human lactoferrin: inhibition of alphavirus interaction with heparan sulfate," *Virology*, vol. 333, no. 2, pp. 284–292, 2005.
- [8] M. Murphy, H. Kariwa, T. Mizutani, K. Yoshimatsu, J. Arikawa, and I. Takashima, "In vitro antiviral activity of lactoferrin and ribavirin upon hantavirus," *Archives of virology*, vol. 145, no. 8, pp. 1571–1582, 2000.
- [9] A. M. Di Biase, A. Pietrantonio, A. Tinari et al., "Heparin-interacting sites of bovine lactoferrin are involved in anti-adenovirus activity," *Journal of medical virology*, vol. 69, no. 4, pp. 495–502, 2003.
- [10] P. Drobni, J. Näslund, and M. Evander, "Lactoferrin inhibits human papillomavirus binding and uptake in vitro," *Antiviral Research*, vol. 64, no. 1, pp. 63–68, 2004.
- [11] F. Superti, M. Ammendolia, P. Valenti, and L. Seganti, "Anti-rotaviral activity of milk proteins: lactoferrin prevents rotavirus infection in the enterocyte-like cell line HT-29," *Medical Microbiology and Immunology*, vol. 186, no. 2-3, pp. 83–91, 1997.
- [12] C. A. Carvalho, S. M. Casseb, R. B. Gonçalves, E. V. Silva, A. M. Gomes, and P. F. Vasconcelos, *Bovine lactoferrin activity against chikungunya and Zika viruses*, no. article 071571, 2016bioRxiv, 2016.
- [13] E. M. El-Fakharany, L. Sánchez, H. A. Al-Mehdar, and E. M. Redwan, "Effectiveness of human, camel, bovine and sheep lactoferrin on the hepatitis C virus cellular infectivity: comparison study," *Virology journal*, vol. 10, no. 1, pp. 1–10, 2013.
- [14] M. Ikeda, A. Nozaki, K. Sugiyama et al., "Characterization of antiviral activity of lactoferrin against hepatitis C virus infection in human cultured cells," *Virus research*, vol. 66, no. 1, pp. 51–63, 2000.
- [15] K. Shin, H. Wakabayashi, K. Yamauchi et al., "Effects of orally administered bovine lactoferrin and lactoperoxidase on influenza virus infection in mice," *Journal of medical microbiology*, vol. 54, no. 8, pp. 717–723, 2005.
- [16] A. Pietrantonio, C. Fortuna, M. E. Remoli, M. G. Ciufolini, and F. Superti, "Bovine lactoferrin inhibits Toscana virus infection by binding to heparan sulphate," *Viruses*, vol. 7, no. 2, pp. 480–495, 2015.
- [17] T.-Y. Weng, L.-C. Chen, H.-W. Shyu et al., "Lactoferrin inhibits enterovirus 71 infection by binding to VP1 protein and host cells," *Antiviral Research*, vol. 67, no. 1, pp. 31–37, 2005.
- [18] H. A. Almehtar, N. A. El-Baky, A. A. Alhaider et al., "Synergistic killing of pathogenic Escherichia coli using camel lactoferrin from different Saudi camel clans and various antibiotics," *The Protein Journal*, vol. 38, no. 4, pp. 479–496, 2019.
- [19] J. A. Khan, P. Kumar, M. Paramasivam et al., "Camel lactoferrin, a transferrin-cum-lactoferrin: crystal structure of camel apolactoferrin at 2.6 Å resolution and structural basis of its dual role," *Journal of molecular biology*, vol. 309, no. 3, pp. 751–761, 2001.

Retraction

Retracted: Evaluation of the Anticancer Potential of *Morus nigra* and *Ocimum basilicum* Mixture against Different Cancer Cell Lines: An In Vitro Evaluation

BioMed Research International

Received 8 January 2024; Accepted 8 January 2024; Published 9 January 2024

Copyright © 2024 BioMed Research International. This is an open access article distributed under the Creative Commons Attribution License, which permits unrestricted use, distribution, and reproduction in any medium, provided the original work is properly cited.

This article has been retracted by Hindawi following an investigation undertaken by the publisher [1]. This investigation has uncovered evidence of one or more of the following indicators of systematic manipulation of the publication process:

- (1) Discrepancies in scope
- (2) Discrepancies in the description of the research reported
- (3) Discrepancies between the availability of data and the research described
- (4) Inappropriate citations
- (5) Incoherent, meaningless and/or irrelevant content included in the article
- (6) Manipulated or compromised peer review

The presence of these indicators undermines our confidence in the integrity of the article's content and we cannot, therefore, vouch for its reliability. Please note that this notice is intended solely to alert readers that the content of this article is unreliable. We have not investigated whether authors were aware of or involved in the systematic manipulation of the publication process.

Wiley and Hindawi regrets that the usual quality checks did not identify these issues before publication and have since put additional measures in place to safeguard research integrity.

We wish to credit our own Research Integrity and Research Publishing teams and anonymous and named external researchers and research integrity experts for contributing to this investigation.

The corresponding author, as the representative of all authors, has been given the opportunity to register their agreement or disagreement to this retraction. We have kept a record of any response received.

References

- [1] B. O. Almutairi, A. I. Alsayadi, N. Abutaha, F. A. AL-mekhlafi, and M. A. Wadaan, "Evaluation of the Anticancer Potential of *Morus nigra* and *Ocimum basilicum* Mixture against Different Cancer Cell Lines: An In Vitro Evaluation," *BioMed Research International*, vol. 2023, Article ID 9337763, 8 pages, 2023.

Research Article

Evaluation of the Anticancer Potential of *Morus nigra* and *Ocimum basilicum* Mixture against Different Cancer Cell Lines: An In Vitro Evaluation

Bader O. Almutairi , Ahmed I. Alsayadi, Nael Abutaha , Fahd A. AL-mekhlafi, and Mohamed A. Wadaan

Department of Zoology, College of Science, King Saud University, P.O. Box 2455 Riyadh 11451, Saudi Arabia

Correspondence should be addressed to Nael Abutaha; nabutaha@ksu.edu.sa

Received 20 June 2022; Revised 23 October 2022; Accepted 3 March 2023; Published 19 April 2023

Academic Editor: Akhtar Ali

Copyright © 2023 Bader O. Almutairi et al. This is an open access article distributed under the Creative Commons Attribution License, which permits unrestricted use, distribution, and reproduction in any medium, provided the original work is properly cited.

Morus nigra (M) and *Ocimum basilicum* (O) mixture (MO2) extract was extracted using hexane (MO2H), chloroform (MO2C), ethyl acetate (MO2E), and methanol (MO2M) in a Soxhlet apparatus. The cytotoxicity was evaluated using MTT (3-[4,5-dimethylthiazol-2-yl]-2,5 diphenyl tetrazolium bromide) assay. The IC_{50} values of the MO2C-treated cancer cells were 11.31 $\mu\text{g/mL}$ (MDA-MB-231), 15.45 $\mu\text{g/mL}$ (MCF-7), 18.9 $\mu\text{g/mL}$ (HepG2), 26.33 $\mu\text{g/mL}$ (Huh-7), 30.17 $\mu\text{g/mL}$ (LoVo), and 36.76 $\mu\text{g/mL}$ (HCT116). MO2C-treated cells showed cellular and nuclear morphological alterations like chromatin condensation and formation of apoptotic bodies as observed using light and fluorescent microscopy. The antioxidant and anti-inflammatory properties were investigated in vitro using 2,2'-diphenyl-1-picrylhydrazyl (DPPH) and egg albumin denaturation assays. It was evident that the MO2M extract exhibited the highest antioxidant activity (18.13%), followed by the MO2E extract (12.25%), MO2C extract (9.380%), and MO2H extract (6.31%). The highest inhibition percentage of albumin denaturation was observed in MO2H (28.54%), followed by MO2M (4.32%) at 0.2 and 0.1 mg/mL concentrations, respectively. The compounds identified using gas chromatography-mass spectrometry (GC-MS) analysis for MO2C extract were α -transbergamotene, germacrene D, selin-4,7(11)-diene, 2 tridecen-1-ol, and 2-decen-1-ol. The present study reveals that MO2C has promising anticancer activity and may serve as a potent polyherbal extract in cancer treatment.

1. Introduction

There is an increase in the incidence of cancer and death cases worldwide [1], and this could be attributed to lifestyle changes (tobacco smoking, alcohol, diet, and obesity) and environmental factors (air and water pollution) [2]. In Saudi Arabia, the estimated numbers of new cancer cases and deaths in 2020 are 27885 and 13069, respectively. Among distinct types of cancer, breast cancer is considered the leading cause of mortality and morbidity in females living in Saudi, with approximately 1095 deaths. In Saudi Arabia, the most frequently recorded cancer cases in males and females are colorectal and breast cancers, respectively. In females, breast cancer constitutes 29% of the confirmed cancer cases, followed by thyroid (14.3%) and

colorectal (9.2%) cancer. In contrast, colorectal cancer represents 19.3%, non-Hodgkin lymphoma 8%, leukemia 6.7%, and thyroid 6.2% of the total reported cases in males [3].

Surgery, chemotherapy, radiation therapy, proton therapy, and immunotherapy are cancer treatment methods that have been commonly used to treat cancer [4]. Unfortunately, these approaches can induce adverse effects on patients, causing them more discomfort. Sometimes, they are not sufficiently effective. Moreover, cells may develop resistance even to recently synthesized drugs. Despite the positive effects that pharmaceutical anticancer drugs may exert, such drugs may also cause harmful reactions, including hypertension, lung damage, menopausal symptoms, change in sexual desire, osteoporosis, cardiotoxicity, brain and spinal cord problems, nerve disorders, and hair loss

accompanied by vomiting [5]. Therefore, more studies are being conducted to explore new and safe anticancer agents from botanical sources that can prevent or suppress carcinogenesis [6, 7].

The life expectancy of cancerous cells is greatly affected by the rate of apoptosis. Therefore, modulating apoptosis may probably be helpful towards cancer treatment and prevention. In fact, natural products can markedly induce apoptotic mechanisms [8, 9]. The cytotoxic and apoptotic activities of polyherbal extracts were previously reported. An extract which was developed by mixing the root extract of *Hemidesmus indicus* (roots), *Nigella sativa* (seeds), and *Smilax glabra* rhizomes together exerted high cytotoxicity against NCI-H292 (lung cancer cells) and weaker cytotoxic effects on MRC-5 (normal lung cells) [10]. Similarly, a polyherbal medicine, “Le Pana Guliya” showed antiproliferative effects against HeLa and HepG2 cells with an IC_{50} value of 19.03 and 2.72 $\mu\text{g/mL}$, respectively. The Le Pana Guliya extract exerted anticancer effects through oxidative stress-dependent apoptosis [11]. Accordingly, this study evaluated the cytotoxicity and apoptotic potential of *Morus nigra* (black mulberry) and *Ocimum basilicum* (sweet basil) mixture against different cancer cell lines.

2. Research Methodology

2.1. Selection of Plants. Dried leaves of *Morus nigra* L. and *Ocimum basilicum* L. were purchased from a herbal store called Bin Menqash, located on Imam Saud Bin Abdulaziz Road, Riyadh, Saudi Arabia. The dried herbs were examined and identified by a taxonomist at the Botany and Microbiology Department at King Saud University.

2.2. Preparation of Polyherbal Extracts. The polyherbal extracts were prepared by mixing equal quantities of *M. nigra* (20 g) and *O. basilicum* (20 g). Then, the herbs were grinded by a coffee grinder. Subsequently, their powder was extracted via Soxhlet extractor using four solvents (450 mL each) of different polarities. The employed solvents were hexane, chloroform, ethyl acetate, and methanol (Sigma-Aldrich, France), respectively. Next, the four polyherbal extracts were evaporated using a rotary evaporator (Heidolph, Germany) at 45°C. Then, they were dissolved in DMSO (Panreac, E.U) and transferred into small tubes. Eventually, the tubes were labeled and preserved at -20°C.

2.3. Total Polyphenol Content. The total phenol content was evaluated through the Folin-Ciocalteu (Alpha Chemika, India) assay method [12]. Two microliters of each extract was mixed with twenty microliters of Folin-Ciocalteu reagent (10%) in a 96-well plate. Then, the mixture was triturated a few times and kept for ten minutes at 25°C. Subsequently, 80 μL of 7.5% sodium carbonate was pipetted into the wells and mixed for a couple of times. Then, the 96-well plate was incubated at 25°C for two hours to observe any color change. Lastly, the wells' absorbances were measured at 765 nm using a microplate reader (ChromMate, UK). The total phenolic content was recorded as mg/g gallic

acid (GAE/g) equivalent according to the standard curve ($y = 0.0042 \times +0.0489$, $R^2 = 0.97$).

2.4. Total Flavonoid Content. The total flavonoid content was evaluated using the aluminium chloride (AlCl_3) colorimetric assay [12]. In a 96-well plate, 2 μL of each plant extract was combined with 60 μL of methanol, of 10% aluminium chloride (4 μL), 1 M of potassium acetate (4 μL), and 112 μL of distilled water. After that, the mixture was triturated for a few seconds and then incubated for 30 minutes. Thereafter, the mixture was read at 420 nm via a spectrophotometer. The total flavonoid content was documented as mg/g quercetin equivalent according to the standard curve ($y = 0.0032 \times +0.0492$, $R^2 = 0.99$).

2.5. Gas Chromatography-Mass Spectrometry (GC-MS). As carried out earlier, the compounds found in MO2C extract were investigated using GC-MS (Agilent Technologies, USA) [13]. Those phytochemicals were identified by comparing their mass spectra to the library of the National Institute of Standards and Technology (NIST, 2004).

2.6. DPPH Radical Scavenging Assay. The radical scavenging activity of the MO2 extracts was evaluated *in vitro* following the method instructed by Abutaha et al. [12]. The reaction solution composed of 198 μL DPPH (0.008% in methanol) and 2 μL of various extract concentrations (4–0.125 mg/mL) of each plant, as well as standardizing gallic acid (10–90 $\mu\text{g/mL}$). The components were mixed in a 96-well plate and kept in the dark at 25°C for half an hour. Subsequently, the absorbances of the wells were measured at 517 nm using a plate reader. In addition, the percentage of the DPPH radical scavenging activity was calculated based on the standard curve.

2.7. Cell Culture. Double negative MDA-MB-231^{ER(-)/PR(-)}, double-positive MCF-7^{ER(+)/PR(+)} estrogen receptor (ER) and progesterone receptor (PR) human breast adenocarcinoma cell lines, human hepatoma (HepG2, Huh-7, and CHANG), human colorectal carcinoma (HCT116 and LoVo), and human umbilical vein endothelial cells (HUVEC) were obtained from the Leibniz-Institute DSMZ-German Collection of Microorganisms and Cell Cultures and Japanese Tissue Culture. The cells were cultured in Dulbecco's Modified Eagle Medium (DMEM) (Gibco, USA) supplemented with penicillin (100 U/mL) and streptomycin (100 $\mu\text{g/mL}$) (Gibco, USA) and 10% fetal bovine serum (Gibco, USA). Cells were grown at 37°C in a CO_2 incubator (5% CO_2) and using trypsin-EDTA solution (Gibco, USA).

2.8. Cytotoxicity Assays. Through the MTT assay, the extracts were assessed for their cytotoxic effects on eight cell lines. In 24-well plates, the cells were plated at 10^5 cells/mL density in Dulbecco's Modified Eagle Medium (DMEM) with 10% fetal bovine serum at 37°C in 5% CO_2 [14]. Additionally, the plates were kept in the incubator for 24 hours. Then, they were treated using various concentrations of the plant extracts for another 24 hours. In addition, DMSO-treated (0.5%) wells served as negative controls, and carbonyl cyanide 3-chlorophenylhydrazone was used as a positive control. After the 24-hour treatment, the MTT solution was pipetted into the wells and incubated

TABLE 1: Phytochemical profile of MO2C extract using gas chromatography-mass spectrometry.

No.	Compounds	Retention time	Area %	Formula	Molecular weight
1	α -Trans-bergamotene	10.58	8.930	C ₁₅ H ₂₄	204.35
2	Germacrene D	11.47	2.800	C ₁₅ H ₂₄	204.35
3	Selin-4,7(11)-diene	12.69	19.620	C ₁₅ H ₂₄	204.35
4	2-Decen-1-ol	14.13	62.820	C ₁₀ H ₂₀ O	156.26
5	2-Tridecen-1-ol	14.31	5.840	C ₁₃ H ₂₆ O	198.34

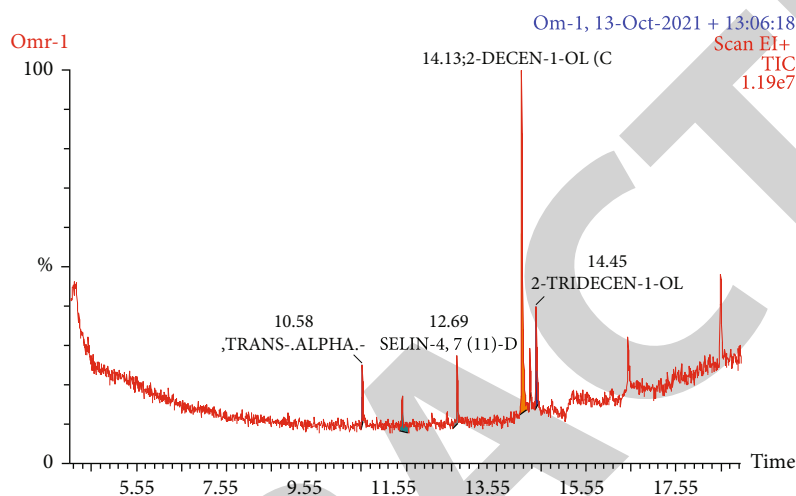


FIGURE 1: Gas chromatography-mass spectrometry chromatogram of MO2C.

for 2 hours. Subsequently, the formazan crystals were dissolved using a solubilization solution such as DMSO. The resulting-colored solution was quantified by reading the absorbances of samples at 570 nm via a spectrophotometer [12].

2.9. Morphological Changes by Light Microscopy. Cells were exposed to MO2C extract for 24 h. After the treatment period, cells were observed under light microscope (Leica, Germany) to detect apoptosis morphological changes.

2.10. DAPI (4',6-Diamidino-2-phenylindole) Staining. Initially, cells were cultured and then treated at a proper confluence (70%). Phosphate-buffered saline (1X PBS, pH 7.4) was applied to wash the treated cells. Then, the cells were fixed in 70% ethanol for five minutes. After that, they were stained with DAPI dissolved in PBS (5 μ L/mL) and incubated for half an hour at 37°C in the dark. Next, the cells were washed using PBS and examined by fluorescent microscopy.

2.11. In Vitro Anti-inflammatory Bioassay. The protein denaturation assay was carried out based on the method demonstrated by [15]. Five millilitres of the reaction mixture (0.02 mL of extract, 4.78 mL of PBS (pH 6.4), and 0.2 mL of 1% bovine albumin) was incubated for fifteen minutes at 37°C and subsequently heated at 70°C for 5 minutes. Upon cooling, the turbidity was assessed at 660 nm by a plate reader. Also, PBS solution was employed as a control. The percentage inhibition of protein denaturation was found by using the following equation:

$$\% \text{inhibition} = 100 \times \left[\frac{V_t}{V_c} - 1 \right];$$

V_t represents the absorbance of the test sample, whereas V_c refers to the absorbance of the control.

3. Result

3.1. Phenolic and Flavonoid Contents of Tested Extracts. The total phenolic content was found to be at its highest level in the ethyl acetate extract (36.69 mg gallic acid equivalent (GAE)/g dry weight), followed by methanol (33.23 mg GAE/g dry weight), chloroform (11.61 mg GAE/g dry weight), and hexane (7.510 mg GAE/g dry weight) extract. Moreover, the total flavonoid content results showed that the ethyl acetate extract had the maximum value (22.95 mg quercetin equivalent (QE)/g dry weight) followed by chloroform (7.75 mg QE/g dry weight), methanol (6.75 mg QE/g dry weight), and hexane (6.47 mg QE/g dry weight) extract.

3.2. Composition Analysis of the Extract. The chromatogram and the identified compounds are presented in Table 1 and Figure 1. A total of 5 phyto-compounds were identified in the MO2C extract. The compounds identified were α -trans-bergamotene, germacrene D, selin-4,7(11)-diene, 2-tridecen-1-ol, and 2-decen-1-ol.

3.3. In Vitro Antioxidant Activity. The *in vitro* antioxidant activity assays were performed to evaluate the capacity of herbal extracts to scavenge free radicals DPPH. Overall, it was apparent that MO2M possessed the highest antioxidant

TABLE 2: Total polyphenols and total flavonoids contents, antioxidant, and anti-inflammatory activities of different solvent extract of *M. nigra* and *O. basilicum* mixture.

No.	Sample	Total flavonoid content (1 mg/mL)	Total polyphenol content (1 mg/mL)	Antioxidant DPPH (% inhibition at 4 mg con.)	Anti-inflammatory (% inhibition of albumin denaturation at 1 mg con. except MO2H at 0.5 mg)
1	MO2H	6.47	7.510	6.31	28.54
2	MO2C	7.75	11.61	9.38	—
3	MO2E	22.95	36.69	12.25	—
4	MO2M	6.75	33.23	18.13	4.32

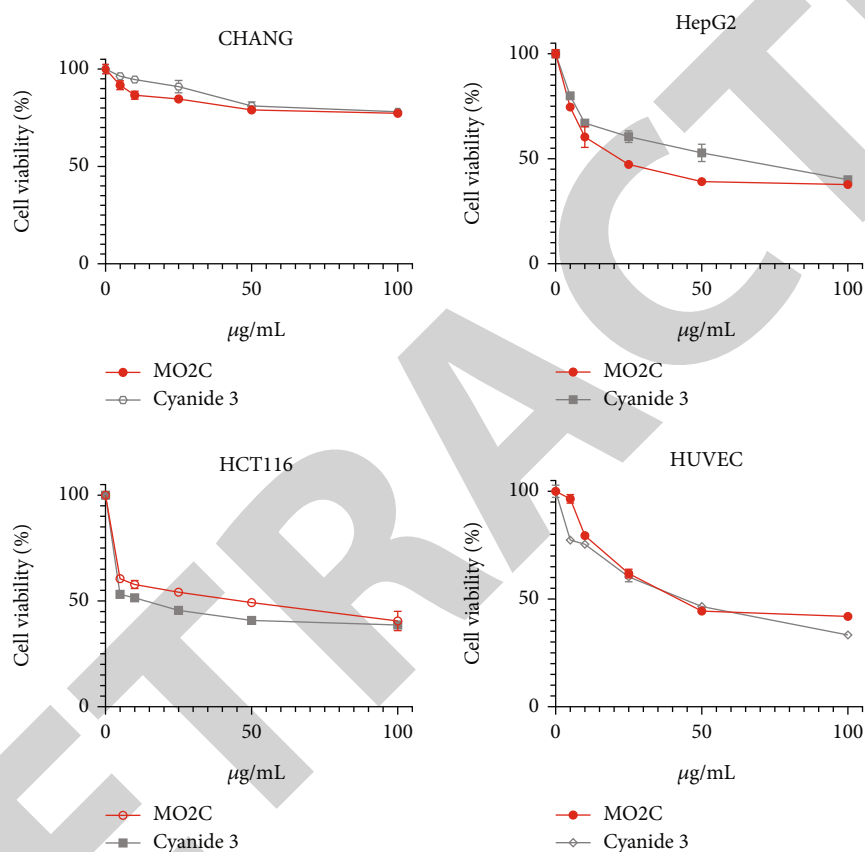


FIGURE 2: Dose-dependent cytotoxic effect of MO2C extract and cyanide 3-chlorophenylhydrazone after 24 hours of exposure on human cancer cell lines, namely, hepatocellular carcinoma (HepG2, CHANG), human colon carcinoma (HCT116), and the normal human umbilical vein endothelial cells (HUVECs).

properties (18.13%), followed by MO2E (12.25%), MO2C (9.380%), and MO2H (6.31%) (Table 2).

3.4. In Vitro Anti-inflammatory Bioassay. The anti-inflammatory properties of MO2 extracts were assessed using the egg albumin method. The highest inhibition percentage was observed in MO2H (28.54%) followed by MO2M (4.32%) at 0.2 and 0.1 mg/mL concentrations, respectively.

3.5. Cytotoxic Effects. A normal cell line and seven distinct cancer cell lines were incubated with different concentrations of solvent extracts for 24 hours to determine the effectiveness of each extract based on their corresponding cytotoxic effects. The results indicated that only the chloro-

form extract (MO2C) was toxic against all cell lines but CHANG cells at the highest concentration. (Figures 2 and 3). The IC_{50} values of the MO2C-treated cancer cells were $11.31 \mu\text{g/mL}$ (MDA-MB-231^{ER(-)/PR(-)}), $15.45 \mu\text{g/mL}$ (MCF-7^{ER(+)/PR(+)}), $18.9 \mu\text{g/mL}$ (HepG2), $26.33 \mu\text{g/mL}$ (Huh-7), $30.17 \mu\text{g/mL}$ (LoVo), and $36.76 \mu\text{g/mL}$ (HCT116). MDA-MB-231^{ER(-)/PR(-)} cells were the most sensitive cancer cell line tested with an IC_{50} value of $11.31 \mu\text{g/mL}$. In addition, HCT116 cells were the least sensitive with an IC_{50} value of $36.76 \mu\text{g/mL}$. MO2C extract displayed selective cytotoxicity because it was less toxic to the normal HUVEC cells (IC_{50} : 38.45) compared to the other cancer cell lines. Carbonyl cyanide 3-chlorophenylhydrazone was used as a positive control, and its calculated IC_{50} values were 1.36, 2.26,

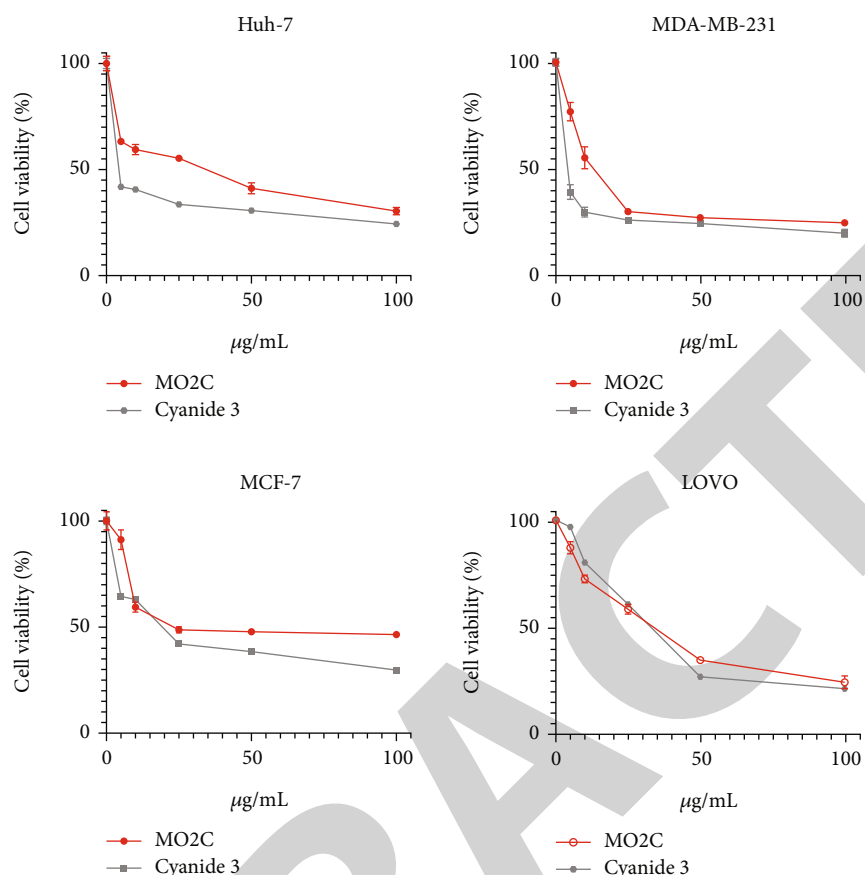


FIGURE 3: Dose-dependent cytotoxic effect of MO2C extract and cyanide 3-chlorophenylhydrazone after 24 hours of exposure on different human cancer cell lines, namely, hepatocellular carcinoma (Huh-7), human colon carcinoma (LoVo), and human breast carcinoma (MCF7 and MDA-MB-231).

10.67, 18.39, 29.06, 53.27, and 44.98 $\mu\text{g/mL}$ against Huh-7, MDA-MB-231, HCT116, MCF7, LoVo, HepG2, and HUVEC cells, respectively.

3.6. Cell Morphology and DAPI Staining. The morphology of the MCF-7 cells was affected by MO2C extract, whereas the control cells showed typical cell morphologies. Shrinkage, cell detachment, complete cellular integrity loss, and cytoplasm contraction were observed in MCF-7 cells treated with MO2C extract (Figure 4). The effect of MO2C extract on the nuclear morphology of MCF-7 cells was assessed by DAPI staining. As exhibited in Figure 4, MO2C extract-treated cells showed chromatin condensation and formation of apoptotic bodies. In contrast, the control cells were stained uniformly (Figure 4) and morphologically intact. They were adherent to the surface and tightly packed.

4. Discussion

According to the United States National Cancer Institute plant screening program, the cytotoxic activity of crude extracts is promising if the IC_{50} value is $<30 \mu\text{g/mL}$ [16]. The MO2C extract was cytotoxic at very low concentrations. Its cytotoxic activity against HepG2, MCF-7, HCT116, LoVo, MDA-MB-

231, and Huh-7 was selective compared to the normal human umbilical vein endothelial cells (HUVECs). To date, most chemotherapeutic agents attack both normal and cancer cells indiscriminately. For less damage to normal cells postcancer therapy, it is essential to develop natural product extracts with selective cytotoxicity towards cancer cells. Thus, plant extracts cytotoxic effects on cancer cells were compared to that of normal HUVEC cells. Different researchers observed similar results such as the selective cytotoxicity observed in *Artemisia absinthium* leaf and seed extract on A-549, K-562, K-562, MCF-7, and PC-3 cells compared with human bronchial epithelial cell line (BEAS-2B) [17]. Similarly, researchers claimed that the *Primula auriculata* and *Primula vulgaris* extract exhibited selective cytotoxic effects on different human cancer cell lines, including MCF-7, HepG2, HT-29, A549, PC-3, and WiDr compared with normal bovine kidney cells and human normal fibroblast cells [18, 19].

It is noted that different cancer cell lines may respond to cancer drugs differently [20, 21]. In this study, it was noticeable that there were variations in response to MO2C extract from different cell lines derived from the same organs, such as breast cancer MCF7 and MDA-MB-231, colon cancer HCT116, LoVo, and liver cancer HepG2, Huh-7, and CHANG. It has been widely acknowledged that many tumors are not

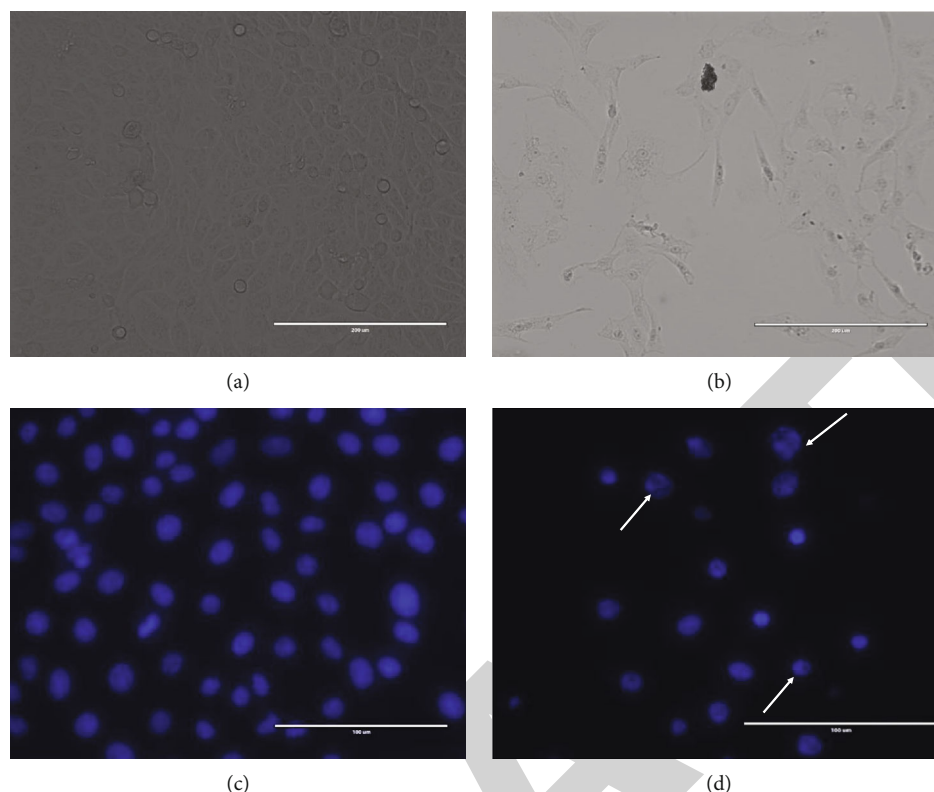


FIGURE 4: Morphological and nuclear assessment of MO2H-treated and untreated cells MCF-7ER(+)/PR(+) cells at $IC_{50} \times 2$ after 24 h. Cells were observed using light and fluorescent microscopes. (a) DMSO treated MCF-7ER(+)/PR(+) cells after 24 h. (b) Detachment of cell from culture plate (BT549) after 24 h exposure to MO2H at $IC_{50} \times 2$ value. (c) Control cells stained with DAPI appear evenly stained with no DNA fragmentation. (d) MCF7 cells treated with MO2H extract show apoptotic nuclei. Images are magnified at 40 \times . Scale bars = 100 μ m.

homogenous in nature but are comprised of cells of different characteristics. Tumoral heterogeneity occurs in many cancers causing different resistances to treatment, drug sensitivities, and relapse after treatment [22, 23]. Therefore, tumor heterogeneity is a significant obstacle in cancer treatment. Hence, cellular heterogeneity is an important factor in assessing the overall response of cells to cancer drug treatment. Therefore, drug combination and botanical extract serve as promising resources towards the mission of overcoming this obstacle.

Plant extracts are a valuable source of anticancer agents [24]. Secondary metabolites such as polyphenols, flavonoids, terpenoids, and alkaloids exhibit different biological activities, such as antioxidant, anti-inflammatory, anticancer, and anti-aging [25]. In fact, several polyphenols and flavonoids have already been reported for their anticancer activities such as hydroxycinnamates, lignins, chalcones, stilbenes, xanthones, coumarins, flavonoids, and hydroxybenzoates [26].

Anticancer agents that induce apoptosis are considered as one of the most effective strategies of chemotherapy [27]. Thus, when searching for new anticancer agents, the candidates should demonstrate apoptosis induction in cancer cells [28]. Our data showed that MO2C treatment resulted in the formation of apoptotic bodies, membrane blebbing, cell shrinkage, and other morphological changes, all of which are common features of apoptosis [29, 30]. Upon application of DAPI staining, the treated cells displayed chromatin condensation and nuclear fragmentation, which could be associated with apoptosis induc-

tion relative to normal control cells (Figure 4). Similar results have been published where polyherbal extracts showed apoptotic activity against MCF-7 and other cancer cells [31–33].

Protein denaturation causes the production of auto-antigens in different medical conditions such as diabetes, rheumatic arthritis, and cancer, which are recognized as chronic inflammatory disorders. Therefore, by inhibiting protein denaturation, inflammation is also inhibited [34]. The egg albumin method provides a cheap alternative way of testing the anti-inflammatory activity of herbal medicines. In the future, the anti-inflammatory test of MO2C should be validated by in vivo and in vitro studies such as rat paw edema, bovine serum albumin, and membrane stabilization. From phytochemical investigation, the presence of different compounds suggested that one of the constituents or their combination is responsible for producing the anti-inflammatory effects.

The compounds identified by GC-MS in the present sample (Table 1 and Figure 1), namely, germacrene D, α -trans-bergamotene, selin-4,7(11)-diene, 2-decen-1-ol, and 2-tridecen-1-ol were not individually tested. Still, they have been associated with the anticancer and anti-inflammatory activities of many plants' crude extracts [35–40]. In addition, in silico molecular docking conducted by Farooq Khan et al. showed that the possible molecular mechanism of anticancer activity is the binding of 2-Tridecen-1-ol with phase inducer phosphatases 2 with higher binding energy as compared to M-phase inducer phosphatases [37].

5. Conclusion

This study demonstrates the anticancer potential of *M. nigra* and *O. basilicum* mixture for the first time against different cancer cell lines. Further studies on combining the extract with other anticancer drugs and in vivo animal models are necessary before advancement to clinical trials.

Data Availability

All the data relevant to this study is mentioned in the manuscript. There is no supplementary data.

Conflicts of Interest

The authors have declared that they have no conflicts of interest.

Acknowledgments

This study was supported by Researchers Supporting Project number (RSP2023R414), King Saud University, Riyadh, Saudi Arabia.

References

- [1] H. Sung, J. Ferlay, R. L. Siegel et al., "Global cancer statistics 2020: GLOBOCAN estimates of incidence and mortality worldwide for 36 cancers in 185 countries," *CA: a Cancer Journal for Clinicians*, vol. 71, no. 3, pp. 209–249, 2021.
- [2] N. Parsa, "Environmental factors inducing human cancers," *Iranian Journal of Public Health*, vol. 41, no. 11, pp. 1–9, 2012.
- [3] WOH, "Saudi Arabia Fact Sheets - Global Cancer Observatory," 2021, <https://gco.iarc.fr/today/data/factsheets/populations/682-saudi-arabia-fact-sheetspdf>.
- [4] E. Bidram, Y. Esmaeili, H. Ranji-Burachaloo et al., "A concise review on cancer treatment methods and delivery systems," *Journal of Drug Delivery Science and Technology*, vol. 54, article 101350, 2019.
- [5] J. J. Tao, K. Visvanathan, and A. C. Wolff, "Long term side effects of adjuvant chemotherapy in patients with early breast cancer," *The Breast*, vol. 24, no. 2, pp. S149–S153, 2015.
- [6] R. Abalo, J. Uranga, I. Pérez-García et al., "May cannabinoids prevent the development of chemotherapy-induced diarrhea and intestinal mucositis? Experimental study in the rat," *Neurogastroenterology & Motility*, vol. 29, no. 3, article e12952, 2017.
- [7] K. Nurgali, R. T. Jagoe, and R. Abalo, "Editorial: Adverse effects of cancer chemotherapy: anything new to improve tolerance and reduce sequelae?," *Frontiers in Pharmacology*, vol. 9, p. 245, 2018.
- [8] C. Sun, H. Cui, H. Yang et al., "Anti-metastatic effect of jolkinolide B and the mechanism of activity in breast cancer MDA-MB-231 cells," *Oncology Letters*, vol. 10, no. 2, pp. 1117–1122, 2015.
- [9] G.-Y. Yang, J. Liao, K. Kim, E. J. Yurkow, and C. S. Yang, "Inhibition of growth and induction of apoptosis in human cancer cell lines by tea polyphenols," *Carcinogenesis*, vol. 19, no. 4, pp. 611–616, 1998.
- [10] V. C. Pathirana, I. Thabrew, S. R. Samarakoon, K. H. Tennekoon, U. Rajagopalan, and M. K. Ediriweera, "Evaluation of anticancer effects of a pharmaceutically viable extract of a traditional polyherbal mixture against non-small-cell lung cancer cells," *Journal of integrative medicine*, vol. 18, no. 3, pp. 242–252, 2020.
- [11] N. D. A. Wageesha, P. Soysa, K. Atthanayake, M. I. Choudhary, and M. Ekanayake, "A traditional poly herbal medicine "Le Pana Guliya" induces apoptosis in HepG 2 and HeLa cells but not in CCI cells: an in vitro assessment," *Chemistry Central Journal*, vol. 11, no. 1, pp. 1–12, 2017.
- [12] N. Abutaha, M. Al-zharani, A. A. Al-Doaiss, A. Baabbad, A. M. Al-Malki, and H. Dekhil, "Anticancer, antioxidant, and acute toxicity studies of a Saudi polyherbal formulation, PHF5," *Open Chemistry*, vol. 18, no. 1, pp. 472–481, 2020.
- [13] S. Hidayathulla, A. A. Shahat, S. R. Ahamad, A. A. N. Al Moqbil, M. S. Alsaid, and D. D. Divakar, "GC/MS analysis and characterization of 2-Hexadecen-1-ol and beta sitosterol from *Schimpera arabica* extract for its bioactive potential as antioxidant and antimicrobial," *Journal of Applied Microbiology*, vol. 124, no. 5, pp. 1082–1091, 2018.
- [14] M. Orangi, A. Pasdaran, D. Shanebandi et al., "Cytotoxic and apoptotic activities of methanolic subfractions of *Scrophularia oxyssepala* against human breast cancer cell line," *Evidence-based Complementary and Alternative Medicine*, vol. 2016, Article ID 8540640, 10 pages, 2016.
- [15] P. Dey, S. Chandra, P. Chatterjee, and S. Bhattacharya, "Neuropharmacological properties of *Mikania scandens* (L.) Willd. (Asteraceae)," *Journal of Advanced Pharmaceutical Technology & Research*, vol. 2, no. 4, pp. 255–259, 2011.
- [16] M. Suffness, "Assays related to cancer drug discovery," *Methods in plant biochemistry: assays for bioactivity*, vol. 6, pp. 71–133, 1990.
- [17] U. Deniz, H. Güneş, F. Güneş, and R. Mammadov, "Cytotoxic activities of certain medicinal plants on different cancer cell lines," *Turkish Journal of Pharmaceutical Sciences*, vol. 14, no. 3, pp. 222–230, 2017.
- [18] S. Behzad, A. Pirani, and M. Mosaddegh, "Cytotoxic activity of some medicinal plants from Hamedan district of Iran," *Iranian Journal of Pharmaceutical Research*, vol. 13, pp. 199–205, 2014.
- [19] I. Turan, S. Demir, R. Aliyazicioğlu, and Y. Aliyazicioğlu, "Evaluation of antioxidant and cytotoxic properties of *Primula vulgaris* leaf extract," *University Journal of Natural Sciences*, vol. 20, no. 4, 2017.
- [20] N. M. Mhaidat, M. Bouklihacene, and R. F. Thorne, "5-Fluorouracil-induced apoptosis in colorectal cancer cells is caspase-9-dependent and mediated by activation of protein kinase C- δ ," *Oncology Letters*, vol. 8, no. 2, pp. 699–704, 2014.
- [21] S. Nannizzi, G. J. Veal, E. Giovannetti et al., "Cellular and molecular mechanisms for the synergistic cytotoxicity elicited by oxaliplatin and pemetrexed in colon cancer cell lines," *Cancer Chemotherapy and Pharmacology*, vol. 66, no. 3, pp. 547–558, 2010.
- [22] M. Arul, A. C. Roslani, and S. H. Cheah, "Heterogeneity in cancer cells: variation in drug response in different primary and secondary colorectal cancer cell lines in vitro," *In Vitro Cellular & Developmental Biology-Animal*, vol. 53, no. 5, pp. 435–447, 2017.
- [23] R. A. Burrell, N. McGranahan, J. Bartek, and C. Swanton, "The causes and consequences of genetic heterogeneity in cancer evolution," *Nature*, vol. 501, no. 7467, pp. 338–345, 2013.

Retraction

Retracted: Ecotoxicological Assessment of Heavy Metal and Its Biochemical Effect in Fishes

BioMed Research International

Received 8 January 2024; Accepted 8 January 2024; Published 9 January 2024

Copyright © 2024 BioMed Research International. This is an open access article distributed under the Creative Commons Attribution License, which permits unrestricted use, distribution, and reproduction in any medium, provided the original work is properly cited.

This article has been retracted by Hindawi following an investigation undertaken by the publisher [1]. This investigation has uncovered evidence of one or more of the following indicators of systematic manipulation of the publication process:

- (1) Discrepancies in scope
- (2) Discrepancies in the description of the research reported
- (3) Discrepancies between the availability of data and the research described
- (4) Inappropriate citations
- (5) Incoherent, meaningless and/or irrelevant content included in the article
- (6) Manipulated or compromised peer review

The presence of these indicators undermines our confidence in the integrity of the article's content and we cannot, therefore, vouch for its reliability. Please note that this notice is intended solely to alert readers that the content of this article is unreliable. We have not investigated whether authors were aware of or involved in the systematic manipulation of the publication process.

Wiley and Hindawi regrets that the usual quality checks did not identify these issues before publication and have since put additional measures in place to safeguard research integrity.

We wish to credit our own Research Integrity and Research Publishing teams and anonymous and named external researchers and research integrity experts for contributing to this investigation.

The corresponding author, as the representative of all authors, has been given the opportunity to register their agreement or disagreement to this retraction. We have kept a record of any response received.

References

- [1] A. Haseeb, Fozia, I. Ahmad et al., "Ecotoxicological Assessment of Heavy Metal and Its Biochemical Effect in Fishes," *BioMed Research International*, vol. 2022, Article ID 3787838, 11 pages, 2022.

Research Article

Ecotoxicological Assessment of Heavy Metal and Its Biochemical Effect in Fishes

Abdul Haseeb,¹ Fozia ,² Ijaz Ahmad ,³ Hidayat Ullah ,⁴ Anwar Iqbal,⁵ Riaz Ullah ,⁶ Bushra Abdulkarim Moharram ,⁷ and Alicja Kowalczyk ⁸

¹Department of Zoology, Kohat University of Science & Technology, Kohat 26000, Pakistan

²Biochemistry Department, Khyber Medical University Institute of Medical Sciences, Kohat 26000, Pakistan

³Department of Chemistry, Kohat University of Science & Technology, Kohat 26000, Pakistan

⁴Institute of Chemical Sciences, Gomal University, Dera Ismail Khan, Pakistan

⁵Department of Chemical Sciences, University of Lakki Marwat, Lakki Marwat, Pakistan

⁶Department of Pharmacognosy, College of Pharmacy, King Saud University, Riyadh, Saudi Arabia

⁷Department of Pharmacognosy, Faculty of Pharmacy, Dhaka University, Sanaa, Bangladesh

⁸Department of Environmental Hygiene and Animal Welfare, Wrocław University of Environmental and Life Sciences, Chelmońskiego 38C, 51-630 Wrocław, Poland

Correspondence should be addressed to Bushra Abdulkarim Moharram; bushramoharam@yahoo.com

Received 4 July 2022; Accepted 19 September 2022; Published 26 November 2022

Academic Editor: Dr Muhammad Hamid

Copyright © 2022 Abdul Haseeb et al. This is an open access article distributed under the Creative Commons Attribution License, which permits unrestricted use, distribution, and reproduction in any medium, provided the original work is properly cited.

Level of toxic heavy metal concentration like lead (Pb), chromium (Cr), cadmium (Cd), iron (Fe), copper (Cu), zinc (Zn), and nickel (Ni) in thirty-six soft and hard organs and their impact on lipid profile of *Hypophthalmichthys molitrix* and *Catla catla* fish species inhabiting in Tanda Dam reservoir were investigated. The heavy metal concentrations in water, sediment, and fish of the different regions in the reservoir were determined with atomic absorption spectrophotometer. Lipid profile was carried out by AOAC official methods. The results showed that Pb was dominant among all the heavy metals in six organs, and its maximum concentration of Pb (22.5 mg kg^{-1} and 32.9 mg kg^{-1}) was observed in scales in *Hypophthalmichthys molitrix* and tail of *Catla catla*, respectively. The maximum concentrations of Cd were observed in the head, scales, fins, and gills of *Catla catla*. The bioaccumulation of heavy metals was significantly different at ($p \leq 0.01$) within the organs and between the fish species. The lipid concentration was minimum in those organs where the concentrations of heavy metals were maximum. It is clear from the findings that heavy metal accumulation reduces the lipid content of fish. It is inevitable to monitor the Tanda Dam reservoir to safeguard human health.

1. Introduction

Heavy metal toxicity on fish is multidirectional and causes physiological and chemical changes in their body. The bioaccumulation of heavy metals can cause functional disturbance of organs. Accumulation of metals in various organs of fish may cause structural lesions and functional disturbances in them. A survey of heavy metal toxicity shows that the presence of heavy metals causes alterations in condition indices (condition factor and hepatosomatic index), biochemical disorders including oxidative stress and associated genotoxicity, and histopathology on aquatic organisms.

At over 22,000 species, fish exhibited the supreme diversity of vertebrates. Although the fisheries sector in Pakistan is a subsector of agriculture and contributes 1% to the country's GDP. Pakistan is rich in fisheries in the marine and freshwater regions. In 2020, Pakistan's overall fish production was estimated at 701,726 metric tons, 474,025 metric tons of which were derived from marine fisheries and the remainder from inland freshwaters (Pakistan economic survey, 2019-20) [1]. The demands of the growing population eventually lead to an increase in food, so the fish industry can serve as a good source of healthy food, especially protein and lipids [2]. In human nutrition, the significance of fish is

primarily due to its lipids. Fish lipids are an excellent source of polyunsaturated omega-3 fatty acids (n-3PUFA), docosahexaenoic acid (DHA), and eicosatetraenoic acid (EPA). Omega-3 polyunsaturated fatty acids are important due to their involvement in several biological processes and nutritional significance. They are important for a reduction in the cholesterol levels, decreasing the risk of heart diseases and stroke incidence, and thus, the presence of n-3 PUFAs is an essential requirement in our diet [3]. Based on this evidence, the fish are regarded as an alternative cure for heart patients [4]. In recent years, the poor wastewater treatment and practices are resulting in the contamination of water resources with heavy metals, pesticides, and inorganic fertilizers in the agricultural sector, atmospheric deposition, and geomorphological weathering of the earth's crust [5, 6], and depleting aquatic and ecosystem. As part of our diet, it is not surprising that contaminated fish can be a very dangerous source of some toxic heavy metals in the diet [7, 8]. Heavy metals have acquired the soft and hard tissues of the fish via the process of bioaccumulation. The accumulation of heavy metals in fish is used as a bioindicators to detect the concentration of heavy metals in aquatic bodies. These metals are transported from fish to their predators in the food chain [9, 10].

Heavy metal accumulation causes infertility in fish populations. Their high concentration affects the physiology and biochemical parameters of fish tissues, and heavy metals disturb body biochemistry in normal metabolic processes. These heavy metals not only accumulated in fish but also in plants in the environment and cause damage to animal and plant tissues [11–14]. In aquatic animals, heavy metals cause sublethal pathology of the liver, kidneys, reproductive, respiratory, and nervous systems [15]. Furthermore, the conversions of unsaturated fatty acids into small fragments of hydrocarbon are important for membrane lipid peroxidation. This process of peroxidation results in lipid-free radical formation, extremely toxic for carbohydrates, proteins, and lipids via the process of oxidative damage. These free radicals are regarded as reactive oxygen species and play a vital role in the inhibition of antioxidant defense mechanisms. Among the most common heavy ions in wastewater are Cd (II) and Pb (II) and responsible for grave health issues and environmental problems. Cd (II) and Pb (II) ions have a sole history of an intensive bad impact on human beings and animal health [16]. For example, Cd (II) is regarded as class I human carcinogens and Pb (II) for children compared to adults due to its higher intake by ingestion [17–20]. For example, Cd (II) is regarded as class I human carcinogens and Pb (II) for children compared to adults due to its higher intake by ingestion [21]. Several environmental issues are associated with heavy metal contamination of water [20]. Literature shows the bioaccumulation of different metals in the fishes and their resultant effects on humans. Very recently, the toxic effects of heavy metals were monitored in different families and genera of fish. It was found that the consumption of heavy metals resulted in renal impairment (Pb, Cd, and Hg), decreased cognitive function (Pb and Hg), reproductive disorder (Cd and Pb), neurological abnormalities (Hg and Pb), teratogenic disorders (Hg), and

cancer (Cd) [14]. Flow sheet diagram of heavy metals in aquatic system is provided as Figure 1.

The present study explores the heavy metal concentration in two fish species *Hypophthalmichthys molitrix* and *Catla catla* and their accumulation in lipid contents in the water reservoir of Tanda Dam, a small water reservoir located in the district of Kohat, Pakistan. The reservoir is surrounded by semiarid hills of Landi Kotal and connected with river Toi in District Kohat, Khyber Pakhtunkhwa Province, Pakistan. The Tanda Dam is often used for irrigation, fishing, and picnic purposes. On July 23, 1970, it was designated as a Ramsar site for winter passage migrants stop off here as an important wetland. Local specialists in wildlife also seek to encourage cranes to use this site during migration. The area is closed off, to the captive, rare, and bred extinct animals within the province by the Khyber Pakhtunkhwa Wildlife Department. During the breeding season, the Tanda fish hatchery was established near the Tanda Dam to hatch different cyprinid species. There is rich fish fauna in the Tanda Dam, so it is a good fishing place for hunting.

2. Materials and Methods

2.1. Sample Collections. The samples of *Hypophthalmichthys molitrix* and *Catla catla* fish species, water, and sediments were collected from the Tanda Dam, Kohat, Pakistan. The water and sediment samples were collected in clear sterilized plastic bottles separately, from the inlet, outlet, and middle sides of the dam. All sediments were dried in an oven at 100°C for 24 hours. The fish specimens collected were preserved in separate bottles in a 5-percent formalin solution. To prevent deterioration, the samples were covered with sterilized polythene bags and kept at -20°C in a deep freezer until further examination. Using corrosion-resistant stainless knives, fish specimens were cut into separate sections (head, tail, abdomen, scales, fins, and gills). Each sample was placed in a separate china dish and transferred to the oven to dry at 100°C for 24 hours.

2.2. Preparation of Samples. The dried samples were crushed into small pieces. About 2.0 g of each sample was treated with 10 mL (concentrated HNO₃) and 2 mL (H₂O₂). The samples were digested by using a hot plate (Janeway, Model-1000), and 6.0 g of each sample was subjected to a protocol of total lipids extraction as per the standard method [22].

2.3. Acid Digestion of Fish and Sediment Samples. Each 2.0 g dry and crushed sample of fish was weighed and transferred to a 50 mL conical flask separately, and 10 mL concentrated HNO₃ (70%) and 2 mL H₂O₂ were added. The flask was heated gradually from 50 to 120°C for 30 minutes using a hot plate, and the process was continued for 12°C with the repeated addition of HNO₃ and H₂O₂. The process of digestion was stopped upon the appearance of a colorless solution. The solution was placed in an open container for cooling after the complete digestion of the samples. The sample was then filtered in 50 mL clean plastic bottles with

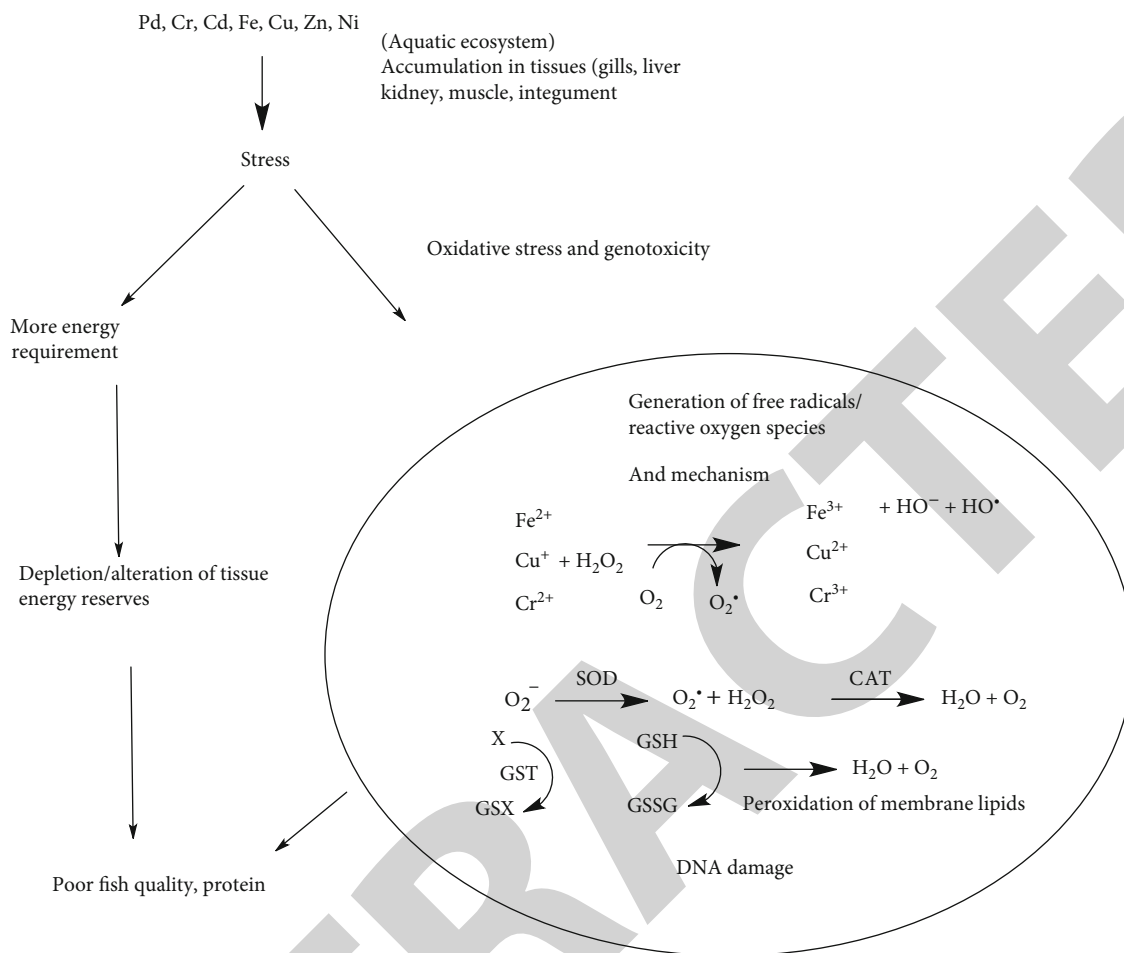


FIGURE 1: Flow sheet diagram of heavy metals in an aquatic system.

sealing plugs by Whatman Filter Paper 42. The volume of the solution was increased to 7 mL by adding 2 mL of concentrated HNO₃. The solution was then diluted by adding 25 mL of distilled water. The samples were labeled and used for heavy metal analysis. The whole procedure was repeated until all the samples were digested and prepared for the atomic absorption spectrophotometer (Model-Analyst 400) analysis. The standard calibration for each metal element was prepared from the stock solution and analyzed at regular time intervals, to check the flow of the instrument [3]. The same procedure was adopted for sediments unless otherwise mentioned.

2.4. Procedure of Lipid Extraction. A 6.0 g dried and ground sample of each organ of fish were treated with 200 mL of acetone added to the sample, separately. In the continuous extractor, lipid extraction with acetone was carried out for up to 12 hours. Using a rotary evaporator, the acetone was distilled until 10-15 mL of acetone remained in the flask and was then transferred into the beaker. Finally, to make it free of oils, the flask was washed with fresh acetone. The beaker was heated to evaporate water and lipid acetone at constant temperature in a water bath. The beaker was transferred to the oven at 80°C for 1 h for complete evaporation and then shifted to cool and weighted desiccators. The sum

of the extracted lipids is equal to the total lipid weight as mentioned in the following (Association of Official Analytical Collaboration (AOAC), official method of analysis, 948) [23, 24]:

$$\text{Formula lipid percentage} = \left(\frac{W_3 - W_1}{W_2} \right) \times 100, \quad (1)$$

where W₁, W₂, and W₃ are the weight of empty beaker, sample, and lipid, respectively.

3. Results and Discussion

This study was performed to test the concentration of heavy metals in different parts of *Hypophthalmichthys molitrix* and *Catla catla*. Table 1 presents the heavy metal Fe, Cu, Zn, Ni, Cd, Cr, and Pb concentrations in six body parts of *Hypophthalmichthys molitrix* and *Catla catla*. The metal Pb was found to be the highest (22.50 mg/kg) of all heavy metals in the scales of *Hypophthalmichthys molitrix*. The concentrations of all the metals in the head, gills, abdomen, tail, fins, and scales of the *Hypophthalmichthys molitrix* were as follows: the concentration of Pb was found to be maximum (15.60, 17.15, 20.20, 14.32, 20.10, and 22.50 mg/kg, respectively), while Cd showed the minimum concentration

TABLE 1: Heavy metals concentration (mg/kg) in different body parts of *Hypophthalmichthys molitrix* and *Catla catla* collected from the Tanda Dam (mean value \pm standard).

Heavy metals	<i>Hypophthalmichthys molitrix</i>						$p \leq$
	Head	Gills	Abdomen	Tail	Fins	Scales	
Fe	5.501 \pm 0.061	6.23 \pm 0.021	3.604 \pm 0.103	4.126 \pm 0.019	2.62 \pm 0.014	2.12 \pm 0.013	0.0016
Ni	3.26 \pm 0.039	2.70 \pm 0.013	1.648 \pm 0.027	1.728 \pm 0.011	3.12 \pm 0.033	3.13 \pm 0.011	0.0003
Cu	0.112 \pm 0.014	0.864 \pm 0.031	1.0721 \pm 0.131	3.296 \pm 0.022	3.920 \pm 0.015	2.496 \pm 0.005	0.0243
Zn	9.424 \pm 0.82	4.016 \pm 0.006	12.824 \pm 0.106	10.19 \pm 0.103	8.448 \pm 0.018	5.968 \pm 0.008	0.0012
Cd	0.032 \pm 0.005	0.112 \pm 0.003	0.112 \pm 0.002	0.096 \pm 0.001	0.064 \pm 0.005	0.016 \pm 0.010	0.0080
Cr	0.496 \pm 0.009	0.464 \pm 0.007	0.512 \pm 0.002	0.544 \pm 0.001	0.496 \pm 0.007	0.48 \pm 0.001	0.001
Pb	15.6 \pm 0.051	17.15 \pm 0.039	20.2 \pm 0.056	14.32 \pm 0.049	20.10 \pm 0.127	22.5 \pm 0.059	0.001
<i>Catla catla</i>							
Fe	2.912 \pm 0.023	5.46 \pm 0.031	9.82 \pm 0.052	1.630 \pm 0.002	2.52 \pm 0.021	2.452 \pm 0.028	0.0217
Ni	2.752 \pm 0.019	4.52 \pm 0.009	2.704 \pm 0.02	3.808 \pm 0.047	4.40 \pm 0.037	13.74 \pm 0.01	0.0267
Cu	2.512 \pm 0.006	4.656 \pm 0.096	2.96 \pm 0.035	3.152 \pm 0.047	2.752 \pm 0.02	4.432 \pm 0.112	0.0003
Zn	4.56 \pm 0.002	4.848 \pm 0.029	11.34 \pm 0.135	10 \pm 0.075	10.688 \pm 0.05	9.888 \pm 0.035	0.001
Cd	0.176 \pm 0.004	0.144 \pm 0.003	0.016 \pm 0.002	0.08 \pm 0.004	0.096 \pm 0.004	0.144 \pm 0.002	0.0056
Cr	0.528 \pm 0.001	0.496 \pm 0.001	0.528 \pm 0.001	0.496 \pm 0.002	0.352 \pm 0.003	0.480 \pm 0.002	0.001
Pb	21.2 \pm 0.041	30.0 \pm 0.094	22.24 \pm 0.110	32.9 \pm 0.141	25.6 \pm 0.056	30.8 \pm 0.095	0.001

Standard permissible limit of heavy metals in fish by WHO (FAO/WHO, 1993): Fe-0.5, Ni-0.05, Cu-3.0, Zn-30, Cd-0.5, Cr-0.6, and Pb-2.0 mg/kg.

(0.032, 0.112, 0.112, 0.096, 0.064, and 0.016 mg/kg, respectively).

In the body parts of *Catla catla*, the highest heavy metal concentration was found for Pb (32.9 mg/kg) accumulated in the tail of fish, while the concentration of multiheavy metals in six body parts of *Catla catla* is found in the head, gills, abdomen, tails, fins, and scales. The concentration of Pb were found maximum (21.2, 30.0, 22.24, 32.2, 25.6, and 30.8 mg/kg, respectively), while Cd showed the minimum concentration (0.176, 0.144, 0.016, 0.08, 0.096, and 0.144 mg/kg, respectively).

Table 2 shows the concentration of heavy metals (Fe, Ni, Cu, Zn, Cd, Cr, and Pb) in water samples collected in the inlet, medium, and outlet regions of Tanda Dam water. The concentration of Pb had the maximum concentration among all heavy metals in the outlet water sample (19.802 mg/L). The reported values of Pb in the inlet, middle, and outlet regions were 15.40, 18.10, and 19.802 mg/L, respectively, while Cd showed the lowest concentration among all metals, and their concentrations in the inlet, middle, and output regions were 0.144, 0.16, and 0.128 mg/L, respectively.

Table 3 represents the concentration of heavy metals in the sediment sample of the Tanda Dam. Out of all the metals present, Pb showed the highest concentration (12.5 mg/kg), while Cd has the lowest concentration (0.16 mg/kg).

Table 4 shows the comparison of heavy metals (Fe, Ni, Cu, Zn, Cd, Cr, and Pb) concentration for both species. The abdomen of *Catla catla* represented the highest concentration of Fe among all the organs of both species. The concentration of iron (Fe) in the head, tail, fins, and gills of *Hypophthalmichthys molitrix* was higher than that of the *Catla catla*, while the iron concentration in the scales and

TABLE 2: Heavy metal concentration (m min) in water samples of the Tanda Dam were collected from three different sides.

Heavy metals	Inlet	Middle	Outlet	Significant value
Fe	3.235 \pm 0.058	1.942 \pm 0.032	1.635 \pm 0.019	$p \leq 0.0436$
Ni	2.912 \pm 0.024	3.376 \pm 0.018	4.528 \pm 0.012	$p \leq 0.0173$
Cu	2.088 \pm 0.109	0.928 \pm 0.057	0.512 \pm 0.088	$p \leq 0.1301$
Zn	5.41 \pm 0.042	4.432 \pm 0.040	3.28 \pm 0.035	$p \leq 0.0192$
Cd	0.144 \pm 0.004	0.16 \pm 0.005	0.128 \pm 0.004	$p \leq 0.0041$
Cr	0.544 \pm 0.001	0.544 \pm 0.002	0.544 \pm 0.001	$p \leq 0.001$
Pb	15.40 \pm 0.083	18.10 \pm 0.058	19.802 \pm 0.098	$p \leq 0.0052$

The permissible limit of heavy metals in water by WHO (FAO/WHO, 1993): Fe = 0.30, Ni = 0.02, Cu = 2.00, Zn = 3.00, Cd = 0.003, Cr = 0.05, and Pb = 0.04 mg/L.

abdomen of *Catla catla* was higher than that in the *Hypophthalmichthys molitrix*. For nickel (Ni), the scales of *Catla catla* revealed the maximum concentration. Compared to the *Hypophthalmichthys molitrix*, *Catla catla* had higher concentrations of nickel in the tail, gills, fins, and scales. Only the head of the *Hypophthalmichthys molitrix* had an increased concentration of nickel than that of *Catla catla*. Copper (Cu) concentrations were higher in the scales, head, abdomen, and gills of *Catla catla* than in the *Hypophthalmichthys molitrix*. However, in the fins and tail of the *Hypophthalmichthys molitrix*, the concentration of copper was much higher than that of the *Catla catla*. The concentration of zinc in the head, tail, and abdomen of *Hypophthalmichthys molitrix* is higher than that of *Catla catla*.

TABLE 3: Heavy metal concentration (mg/kg) in sediments collected from Tanda Dam.

Heavy metal	Sediments	Significant value
Fe	5.435 ± 0.064	$p \leq 0.001$
Ni	8.272 ± 0.047	$p \leq 0.001$
Cu	5.568 ± 0.266	$p \leq 0.0008$
Zn	6.69 ± 0.078	$p \leq 0.001$
Cd	0.16 ± 0.006	$p \leq 0.0005$
Cr	0.528 ± 0.001	$p \leq 0.001$
Pb	12.5 ± 0.030	$p \leq 0.001$

Permissible limit of heavy metals in soil by WHO (FAO/WHO, 1993): Fe = 0.030, Ni = 50, Cu = 0.025, Zn = 30, Cd = 0.006, Cr = 0.8, and Pb = 0.040 mg/kg.

However, the scales, gills, and fins of the *Catla catla* have shown a greater amount of zinc than the *Hypophthalmichthys molitrix*.

In the comparison of cadmium concentration, the head, scales, gills, and fins of *Catla catla* showed higher concentration than *Hypophthalmichthys molitrix*, while the tail and abdomen of *Hypophthalmichthys molitrix* contain more cadmium concentration than *Catla catla*. The concentration of chromium in the abdomen, head, and gills of *Catla catla* was higher than that of *Hypophthalmichthys molitrix*, while the concentration of chromium in the fins and tail of *Catla catla* was lower than that of *Hypophthalmichthys molitrix*, whereas both species have an equal concentration of chromium in the scales. Lead concentration was higher in all six organs of the *Hypophthalmichthys molitrix* as compared to *Catla catla*. In *Catla catla*, the overall concentration of heavy metals, and specifically that of lead, was higher than in *Hypophthalmichthys molitrix*.

Table 5 showed the comparison of lipid percentages in both species. The highest lipid percentage (38.42 percent) was found in the head of *Hypophthalmichthys molitrix*, while scales of *Catla catla* showed the minimum lipid percentage (1.58 percent). In all six body parts, the recorded percentage of lipids was as follows: head>gills>abdomen>tail>fins>scales in both species. The overall comparison showed that the total percentage of lipids in all six organs was greater in *Hypophthalmichthys molitrix* as compared to *Catla catla*.

4. Discussion

The present study was conducted on two fish species of Tanda Dam Kohat, i.e., *Hypophthalmichthys molitrix* and *Catla catla*. The literature shows that the overconsumption of fish is sometimes toxic due to the concentration of heavy metals. Therefore, it was important to evaluate the heavy metals in the fish species *H. molitrix* and *Catla catla*.

The accumulation of heavy metal and lipid contents of these two species were screened (Tables 1–5 and Figures 1–5). Table 1 presents the concentration of multi-heavy metals (iron, nickel, copper, zinc, cadmium, and lead)

in the body parts of *Hypophthalmichthys molitrix* and *Catla catla* of Tanda Dam. Lead (Pb) has the highest concentration on the scales, i.e., 22.5 mg/kg, while cadmium (Cd) has the lowest concentration (0.016 mg/kg) on the scales, of all the heavy metals in the *Hypophthalmichthys molitrix*. In the head, gills, abdomen, tails, fins, and scales of the *Hypophthalmichthys molitrix*, the concentration of Pb was found maximum (15.60, 17.15, 20.20, 14.32, 20.10, and 22.50 mg/kg, respectively), while Cd showed the minimum concentration (0.032, 0.112, 0.112, 0.096, 0.064, and 0.016 mg/kg, respectively). The concentrations of lead, nickel, and iron, described by the WHO were above the permissible levels, while the concentrations of chromium, copper, zinc, and cadmium were below the permissible limits [25–28].

Table 1 also shows the heavy metal concentration in the body parts of the *Catla catla*. The highest concentration of lead (Pb) in the tail was 32.9 mg/kg, while the lowest concentration of cadmium (Cd) in the abdomen was found to be 0.016 mg/kg in all the metals present in *Catla catla*.

The recorded value of heavy metals in the head, gills, abdomen, tail, fins, and scales of *Catla catla* shows a higher concentration of lead in the head, gills, abdomen, tails, fins, and scales with values of 21.2, 30.0, 22.24, 32.2, 25.6, and 30.8 mg/kg, respectively, while Cd showed the minimum concentration (0.176, 0.144, 0.016, 0.08, 0.096, and 0.144 mg/kg, respectively) in these parts.

The concentration of lead in the body parts of *Catla catla* ranged from 32.9 to 21.2 mg/kg. The accumulation of lead, iron, and nickel was above the permissible limits, while cadmium, zinc, and chromium were below the permissible limits, and copper was within the permissible level of the WHO standard.

The present study showed that the organs of both species have different concentrations of metals.

Kalay et al. [29] reported that different species of fish have different concentrations of metals in their tissues. Also, Canli and Atli [30] reported that the concentration of heavy metals in fish varies according to their species and the aquatic environment. Kamaruzzaman et al. [31] reported a significant increase in the concentration of Pb and Cd in all heavy metals in *Cyprinus carpio* tissues.

Table 2 indicates the abundance of heavy metals in three water samples (i.e., inlet, middle, and outlet) of the Tanda Dam. Lead (Pb) has the highest concentration in the outlet water sample, i.e., 19.802 mg/kg among all metals.

The reported values for heavy metals in the inlet, middle, and outlet regions were as follows: Pb showed the highest concentration (15.40, 18.10, and 19.802 mg/L, respectively), while Cd showed the lowest concentration among all metals (0.144, 0.16, and 0.128 mg/L, respectively). In inlet water region, the order of concentration of metals was Pb>Zn>Fe>Ni>Cu>Cr>Cd, while in the middle water region, the order of concentration was Pb>Zn>Ni>Fe>Cu>Cr>Cd. In the outlet water region, the order of concentration of heavy metals was found as Pb>Ni>Zn>Fe>Cr>Cu>Cd. The concentration of all the metals in the water was above the WHO standard level, except for Cu.

Table 3 shows the concentration of iron, nickel, copper, zinc, cadmium, chromium, and lead in the sediment sample

TABLE 4: Comparison of Fe, Ni, Cu, Zn, Cd, Cr, and Pb concentrations (mg/kg) in the body of *Hypophthalmichthys molitrix* and *Catla catla* collected from the water of the Tanda Dam (mean value \pm standard).

Heavy metals	Parameters	<i>H. molitrix</i>	<i>Catla catla</i>	$p \leq$
		Temperature 273 K		
Fe	Head	5.50 \pm 0.06	2.91 \pm 0.02	0.1901
	Gills	6.2 \pm 0.02	5.46 \pm 0.03	0.0419
	Abdomen	3.60 \pm 0.10	9.82 \pm 0.05	0.2761
	Tail	4.13 \pm 0.02	1.63 \pm 0.01	0.2605
	Fins	2.62 \pm 0.014	2.52 \pm 0.02	0.0124
	Scales	2.12 \pm 0.013	2.45 \pm 0.03	0.0461
Ni	Head	3.26 \pm 0.04	2.75 \pm 0.02	0.0537
	Gills	2.70 \pm 0.02	4.52 \pm 0.01	0.0431
	Abdomen	1.65 \pm 0.03	2.70 \pm 0.02	0.1529
	Tail	1.728 \pm 0.01	3.80 \pm 0.05	0.2288
	Fins	3.12 \pm 0.03	4.40 \pm 0.04	0.1073
	Scales	3.13 \pm 0.01	13.74 \pm 0.01	0.3574
Cu	Head	0.11 \pm 0.01	22.51 \pm 0.01	0.4716
	Gills	0.86 \pm 0.03	4.66 \pm 0.10	0.3832
	Abdomen	1.072 \pm 0.13	2.96 \pm 0.04	0.2788
	Tail	3.30 \pm 0.02	3.15 \pm 0.05	0.0142
	Fins	3.92 \pm 0.02	2.75 \pm 0.02	0.1103
	Scales	2.50 \pm 0.01	4.43 \pm 0.11	0.1735
Zn	Head	9.42 \pm 0.82	4.56 \pm 0.01	0.2131
	Gills	4.02 \pm 0.01	4.85 \pm 0.03	0.0596
	Abdomen	12.82 \pm 0.11	11.34 \pm 0.14	0.0390
	Tail	10.19 \pm 0.10	10.00 \pm 0.08	0.0060
	Fins	8.45 \pm 0.018	10.69 \pm 0.05	0.0742
	Scales	5.97 \pm 0.01	9.89 \pm 0.04	0.1543
Cd	Head	0.03 \pm 0.01	0.18 \pm 0.01	0.3855
	Gills	0.11 \pm 0.01	0.14 \pm 0.03	0.0792
	Abdomen	0.11 \pm 0.02	0.02 \pm 0.02	0.4097
	Tail	0.10 \pm 0.01	0.08 \pm 0.02	0.0577
	Fins	0.06 \pm 0.05	0.10 \pm 0.04	0.1257
	Scales	0.02 \pm 0.01	0.14 \pm 0.02	0.4296
Cr	Head	0.50 \pm 0.01	0.53 \pm 0.01	0.0199
	Gills	0.46 \pm 0.01	0.50 \pm 0.01	0.0212
	Abdomen	0.51 \pm 0.02	0.53 \pm 0.01	0.0098
	Tail	0.54 \pm 0.02	0.50 \pm 0.02	0.0294
	Fins	0.50 \pm 0.01	0.35 \pm 0.03	0.1071
	Scales	0.48 \pm 0.01	0.48 \pm 0.02	0

TABLE 4: Continued.

Heavy metals	Parameters	<i>H. molitrix</i>	<i>Catla catla</i>	$p \leq$
		Temperature 273 K		
Pb	Head	15.60 \pm 0.05	21.20 \pm 0.04	0.0961
	Gills	17.15 \pm 0.04	30.00 \pm 0.09	0.1694
	Abdomen	20.20 \pm 0.06	22.24 \pm 0.11	0.0306
	Tail	14.32 \pm 0.05	32.90 \pm 0.14	0.2387
	Fins	20.10 \pm 0.13	25.60 \pm 0.06	0.0763
	Scales	22.50 \pm 0.06	30.80 \pm 0.10	0.0983

of the Tanda Dam, where lead has the highest concentration, i.e., 12.5 mg/kg, while cadmium has the lowest concentration, i.e., 0.16 mg/kg in all metals. The metal concentrations in the sediments were found in order of concentration (mg/kg) as lead > nickel > zinc > copper > iron > chromium > cadmium. The concentrations of iron, lead, cadmium, and copper were above the permissible limit, while the concentrations of zinc, chromium, and nickel were below the WHO limit. The correlation of heavy metal concentration is difficult, even between the same organs of the different species. This is due to variations of many factors, such as eating habits, whether carnivorous or herbivores, the fish habitat in deep water regions, whether surface feeder or bottom feeder, and age. Kamaruzzaman et al. [31] observed that there is a correlation between metal concentration and several basic fish variations such as fish size, age, and genetic makeup.

Table 4 shows a comparison of the concentrations of iron, nickel, copper, zinc, cadmium, chromium, and lead in the two species. The highest concentration of iron among all organs was recorded in the abdomen of *Catla catla*, i.e., 9.82 mg/kg. In the head, throat, tail, and wings, the concentration of *Hypophthalmichthys molitrix* was higher than that of *Catla catla*. The concentration of Fe in the abdomen and scales of *Catla catla* was higher than that of *Hypophthalmichthys molitrix*. Of all the organs, the highest concentration was recorded in the *Catla catla* scales, i.e., 13.74 mg/kg. Compared to the *Hypophthalmichthys molitrix*, the *Catla catla* had a higher concentration of nickel in the fins, tail, scales, and gills. Only the head of the *Hypophthalmichthys molitrix* showed a higher amount of nickel than the *Catla catla*. The concentration of copper in the head, abdomen, gills, and scales was higher in *Catla catla* as compared to *H. molitrix*, while fins and tail of *Hypophthalmichthys molitrix* showed a higher concentration of copper than *Catla catla*. Compared to the *Catla catla*, the concentration of zinc in the head, abdomen, and tail of the *Hypophthalmichthys molitrix* was higher, while the gills, scales, and fins of *Catla catla* had a higher concentration of zinc than *Hypophthalmichthys molitrix*.

Compared to *Hypophthalmichthys molitrix*, the *Catla catla* had a higher concentration of cadmium (Cd) in the head, scales, fins, and gills, while the tail and abdomen of the *Hypophthalmichthys molitrix* showed higher concentration than the *Catla catla*. In contrast to the *Hypophthalmichthys molitrix*, the *Catla catla* had a higher

TABLE 5: Total lipids % and age in different body parts of *Hypophthalmichthys molitrix*, *Catla catla*, and their comparison collected from the water of Tanda Dam.

Organs	Fish species		Comparison		$p \leq$
	<i>Hypophthalmichthys molitrix</i> lipids (%)	<i>Catla catla</i> lipids (%)	Lipid % of <i>H. molitrix</i>	Lipid % of <i>Catla catla</i>	
Head	38.42	32.55	38.42	32.55	0.0525
Gills	23.47	22.08	23.47	22.08	0.0194
Abdomen	19.73	16.00	19.73	16.00	0.0662
Tail	16.51	14.73	16.51	14.73	0.0362
Fins	11.75	6.37	11.75	6.37	0.1837
Scales	3.05	1.58	3.05	1.58	0.1957
p value	0.0118	0.0184	—	—	—

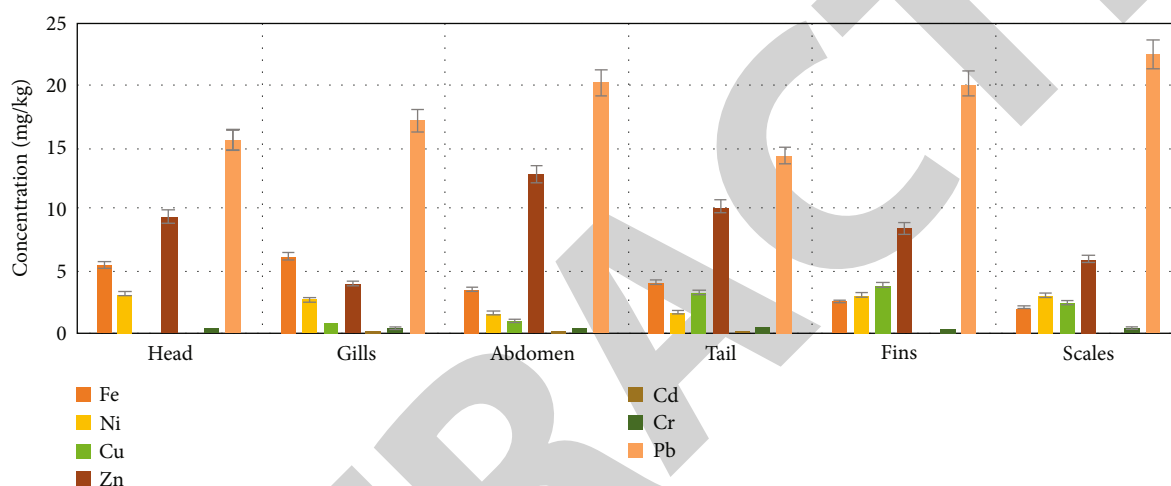


FIGURE 2: Graphical representation of heavy metal concentration in *Hypophthalmichthys molitrix*.

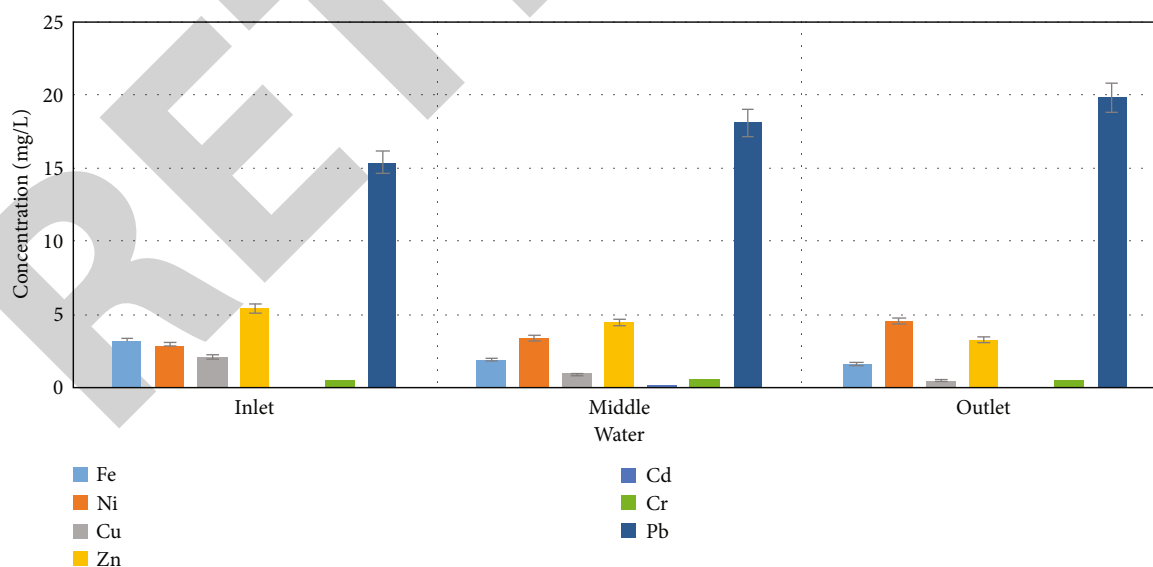


FIGURE 3: Graphical representation of heavy metal concentration in water.

concentration of chromium in the head, abdomen, and gills, but the *H. molitrix* fins and tail had a higher concentration of chromium than the *Catla catla*. The scales of both species

have an equal concentration of chromium. The concentration of lead was higher in all six organs of the *Catla catla* than in the *Hypophthalmichthys molitrix*. The overall

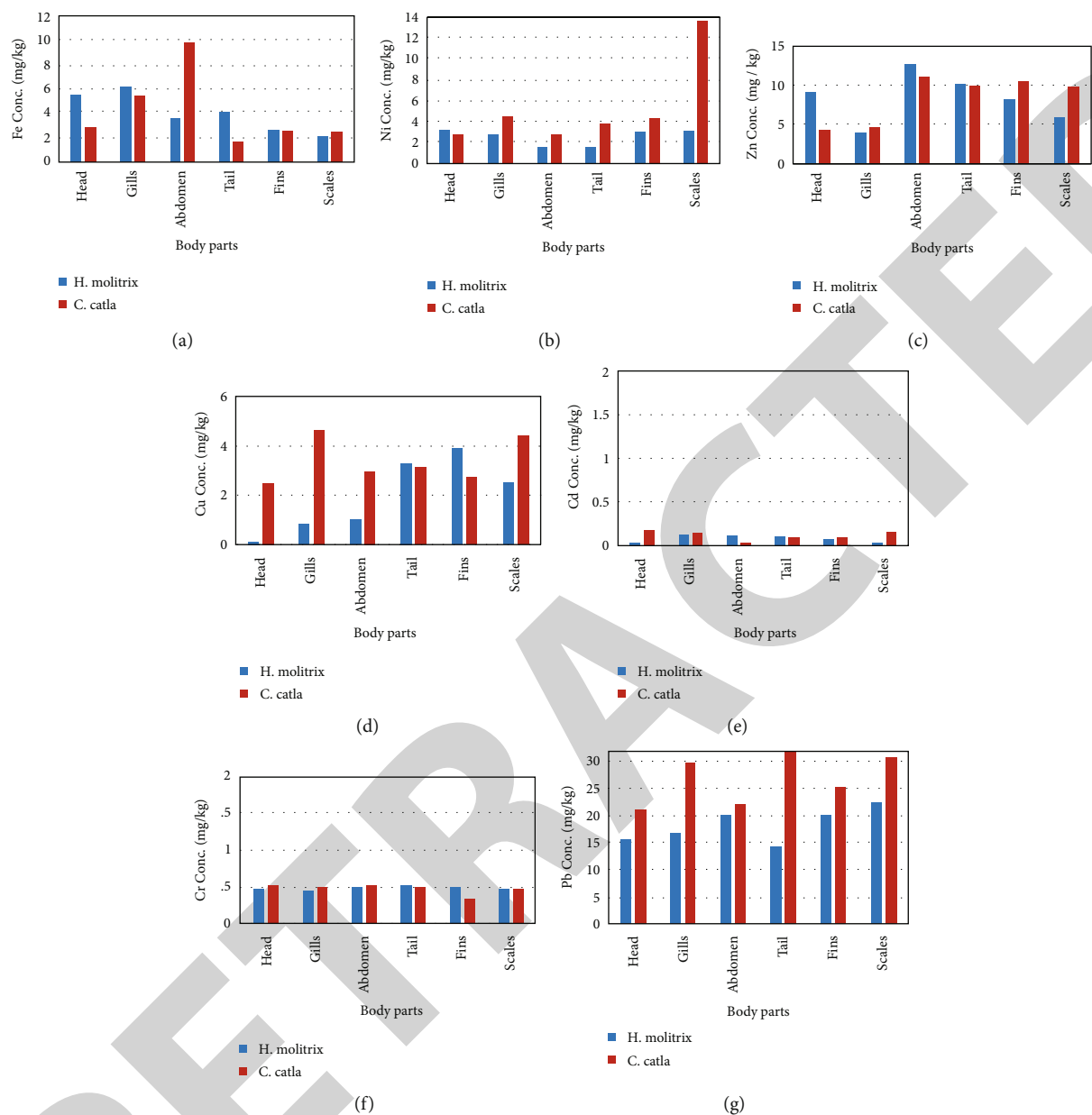
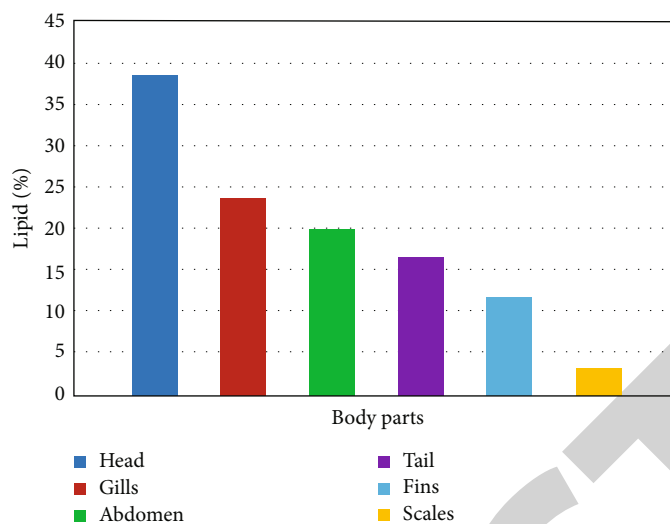


FIGURE 4: Comparison of heavy metal concentration (mg kg^{-1}) in the body of *Hypophthalmichthys molitrix* and *Catla catla*.

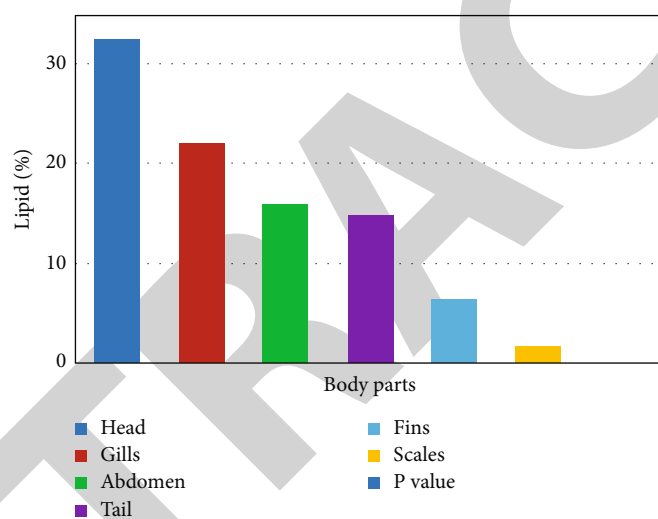
concentration of heavy metals, and especially that of lead, was higher in *Catla catla* than in *Hypophthalmichthys molitrix*. This fact may be due to the reason that the Tanda Dam is filled with floods of water from the catchment area of District Orakzai and Hangu. The erosion from unexplored mountains and valleys is the cause of the higher concentration of Pb.

Table 5 represents the comparison of the complete lipid percentage in the six body parts of both species. The data shows that the lipid concentration in the head of *Hypophthalmichthys molitrix* was higher (38.42%), while the lipid concentration in the scales was the lowest (3.05%). The *Catla catla* head has the highest lipid percentage, i.e., 32.55%, while scales have the lowest percentage

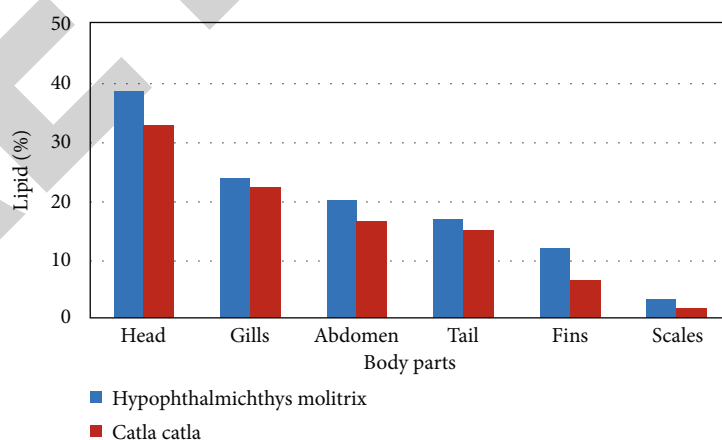
(1.58%). The recorded levels of lipid percentage in all six organs of *Catla catla* and *Hypophthalmichthys molitrix* were found in order of head>gills>abdomen>tail>fins>scales. According to the literature, the lipid content of fish varies over a wide range. [32–34] reported that lipids are found mainly in subcutaneous tissues of fish such as the belly flap, liver, head, muscles, and mesenteric tissues. The overall comparison showed that the total percentage of lipids in all six organs was greater in *Hypophthalmichthys molitrix* than in *Catla catla*. Although the concentration of heavy metals was higher in *Catla catla* than in *Hypophthalmichthys molitrix*, a heavy metal deposition allows biomolecules such as carbohydrates, proteins, and lipids to decline via oxidative damage. A decrease in lipid content in *Catla catla* tissues



(a)



(b)



(c)

FIGURE 5: Total lipids (%) in body parts of *Hypophthalmichthys molitrix* (a), *Catla catla* (b), and their comparison of total lipid (%) (c).

exposed to sublethal and lethal cadmium chloride concentration was reported by Sobha et al. [35]. The effect of heavy metals on lipid profiles has also been documented

by Levesque et al. and Defo et al. [36, 37], Dubale and Shah [38], and Nowosad et al., Bazarsadueva et al., and Pierron et al. [39–41].

5. Conclusion

It was found that heavy metal accumulation decreases the lipid quantity in fish. The heavy metal content of *Catla catla* was higher than that of *Hypophthalmichthys molitrix*, although the overall percentage of lipids in *Catla catla* was smaller than that of *Hypophthalmichthys molitrix*. In both fishes, the concentration of lead, iron, and nickel was found above the permissible range as defined by the WHO, while chromium, zinc, cadmium, and copper were found below the permissible level. The concentration of these metals was found different in different body parts of both fishes as shown in Tables 1 and 2. This fact demonstrates the level of accumulation of heavy metals in different tissues among fish species. The deposition level of heavy metals also varies with the aquatic environment. Furthermore, the presence of subcutaneous tissues and their lipid content added their effect to the accumulation of heavy metals. A higher accumulation of metals and lower lipid profile was found for *Catla catla*. The presence of heavy metals is associated with oxidative stress conditions causing a lowering of the nutritional index of fish via degrading biomolecules like lipids, proteins, and carbohydrates. In water, the concentration of all metals was above the permissible range, except for copper, which was less than the permissible range. In the case of sediments, lead, iron, copper, and cadmium were determined above the permissible level, but chromium, nickel, and zinc were below the permissible range of WHO standard. Keeping in view the above findings, another detailed study is required (data unpublished) where the factors are important for the contamination of these water resources and food (fish). Moreover, the mechanistic basis of heavy metal toxicity is important to understand for essential evaluation of health hazardous assessment.

Data Availability

All available data are incorporated in the MS.

Conflicts of Interest

The authors declared that they have no conflict of interest.

Acknowledgments

Authors wish to thank Researchers Supporting Project Number (RSP-2021/110) at King Saud University, Riyadh, Saudi Arabia, for financial support.

References

- [1] Ministry of Finance | Government of Pakistan https://www.finance.gov.pk/survey_1920.html.
- [2] M. Bahnasawy, A. A. Khidr, and N. Dheina, "Seasonal variations of heavy metals concentrations in mullet, *Mugil cephalus* and *Liza ramada* (Mugilidae) from Lake Manzala, Egypt," *Egyptian Journal of Aquatic Biology and Fisheries*, vol. 13, no. 2, pp. 81–100, 2009.
- [3] N. Al-Bader, "Heavy metal levels in most common available fish species in Saudi market," *Journal of Food Technology*, vol. 4, no. 4, pp. 173–177, 2008.
- [4] J. Pal, B. N. Shukla, A. K. Maurya, H. O. Verma, G. Pandey, and A. Amitha, "A review on role of fish in human nutrition with special emphasis to essential fatty acid," *International journal of fisheries and aquatic studies*, vol. 6, no. 2, pp. 427–430, 2018.
- [5] B. Budijono, M. Hasbi, and R. D. Sibagariang, "Heavy metals content in tissues of feather back fish (*Notopterus notopterus*) from the Sail River, Pekanbaru," *IOP Conference Series: Earth and Environmental Science*, vol. 430, no. 1, p. 12034, 2020.
- [6] F. Yilmaz, "The comparison of heavy metal concentrations (Cd, Cu, Mn, Pb, and Zn) in tissues of three economically important fish (*Anguilla anguilla*, *Mugil cephalus* and *Oreochromis niloticus*) inhabiting Koycegiz Lake-Mugla (Turkey)," *Turkish Journal of Science & Technology*, vol. 4, no. 1, pp. 7–15, 2009.
- [7] M. Cong, X. Pang, K. Zhao, Y. Song, Y. Liu, and J. Wang, "Deep-sea natural products from extreme environments: cold seeps and hydrothermal vents," *Marine Drugs*, vol. 20, no. 6, p. 404, 2022.
- [8] M. Çelik, A. Diler, and A. Küçükgülmez, "A comparison of the proximate compositions and fatty acid profiles of zander (*Sander lucioperca*) from two different regions and climatic conditions," *Food Chemistry*, vol. 92, no. 4, pp. 637–641, 2005.
- [9] A. Gupta, D. K. Rai, R. S. Pandey, and B. Sharma, "Analysis of some heavy metals in the riverine water, sediments and fish from river Ganges at Allahabad," *Environmental monitoring and assessment*, vol. 157, no. 1–4, pp. 449–458, 2009.
- [10] E. Valkova, V. Atanasov, M. Tzanova et al., "Content of Pb and Zn in sediments and hydrobionts as ecological markers for pollution assessment of freshwater objects in Bulgaria—a review," *International journal of environmental research and public health*, vol. 19, no. 15, p. 9600, 2022.
- [11] H. Ullah, M. Khaliq, N. Ullah, A. Iqbal, Fozia, and I. Ullah, "Health risk assessment and multivariate statistical analysis of heavy metals in vegetables of Khyber Pakhtunkhwa region, Pakistan," *Biological trace element research*, vol. 200, no. 6, pp. 3023–3038, 2022.
- [12] R. Ullah and A. S. Alqahtani, "GC-MS analysis, heavy metals, biological, and toxicological evaluation of *Reseda muricata* and *Marrubium vulgare* methanol extracts," *Evidence-Based Complementary and Alternative Medicine*, vol. 2022, Article ID 2284328, 9 pages, 2022.
- [13] M. Ibrahim, S. Nawaz, K. Iqbal et al., "Plant-derived smoke solution alleviates cellular oxidative stress caused by arsenic and mercury by modulating the cellular antioxidative defense system in wheat," *Plants*, vol. 11, no. 10, p. 1379, 2022.
- [14] A. S. Alqahtani, R. Ullah, and A. A. Shahat, "Bioactive constituents and toxicological evaluation of selected antidiabetic medicinal plants of Saudi Arabia," *Evidence-Based Complementary and Alternative Medicine*, vol. 2022, Article ID 7123521, 23 pages, 2022.
- [15] G. A. Engwa, P. U. Ferdinand, F. N. Nwalo, and M. N. Unachukwu, "Mechanism and health effects of heavy metal toxicity in humans," *Poisoning in the Modern World-New Tricks for an Old Dog?*, vol. 11, no. 1, pp. 853–861, 2019.
- [16] M. Balali-Mood, K. Naseri, Z. Tahergorabi, M. R. Khazdair, and M. Sadeghi, "Toxic mechanisms of five heavy metals: mercury, lead, chromium, cadmium, and arsenic," *Frontiers in Pharmacology*, vol. 12, p. 227, 2021.

Retraction

Retracted: First Record of Ichthyofauna from Gomal Zam Dam, District South Waziristan, Khyber Pakhtunkhwa, Pakistan

BioMed Research International

Received 8 January 2024; Accepted 8 January 2024; Published 13 January 2024

Copyright © 2024 BioMed Research International. This is an open access article distributed under the Creative Commons Attribution License, which permits unrestricted use, distribution, and reproduction in any medium, provided the original work is properly cited.

This article has been retracted by Hindawi following an investigation undertaken by the publisher [1]. This investigation has uncovered evidence of one or more of the following indicators of systematic manipulation of the publication process:

- (1) Discrepancies in scope
- (2) Discrepancies in the description of the research reported
- (3) Discrepancies between the availability of data and the research described
- (4) Inappropriate citations
- (5) Incoherent, meaningless and/or irrelevant content included in the article
- (6) Manipulated or compromised peer review

The presence of these indicators undermines our confidence in the integrity of the article's content and we cannot, therefore, vouch for its reliability. Please note that this notice is intended solely to alert readers that the content of this article is unreliable. We have not investigated whether authors were aware of or involved in the systematic manipulation of the publication process.

Wiley and Hindawi regrets that the usual quality checks did not identify these issues before publication and have since put additional measures in place to safeguard research integrity.

We wish to credit our own Research Integrity and Research Publishing teams and anonymous and named external researchers and research integrity experts for contributing to this investigation.

The corresponding author, as the representative of all authors, has been given the opportunity to register their agreement or disagreement to this retraction. We have kept a record of any response received.

References

- [1] A. U. Rehman, S. Ullah, A. Zuberi, F. U. Dawar, and M. N. K. Khattak, "First Record of Ichthyofauna from Gomal Zam Dam, District South Waziristan, Khyber Pakhtunkhwa, Pakistan," *BioMed Research International*, vol. 2022, Article ID 7076508, 10 pages, 2022.

Research Article

First Record of Ichthyofauna from Gomal Zam Dam, District South Waziristan, Khyber Pakhtunkhwa, Pakistan

Aziz Ur Rehman,¹ Sami Ullah,² Amina Zuberi,² Farman Ullah Dawar^{1,3} and Muhammad Nasir Khan Khattak⁴

¹Department of Zoology, Hazara University Mansehra, Khyber Pakhtunkhwa, Pakistan

²Department of Animal Sciences, Quaid E Azam University, Islamabad, Pakistan

³Department of Zoology, Kohat University of Science and Technology (KUST) Kohat, 26000 Khyber Pakhtunkhwa, Pakistan

⁴Department of Applied Biology, College of Sciences, University of Sharjah, Sharjah, UAE

Correspondence should be addressed to Farman Ullah Dawar; farmandawar@kust.edu.pk and Muhammad Nasir Khan Khattak; mnasir@sharjah.ac.ae

Received 10 August 2022; Revised 19 September 2022; Accepted 30 September 2022; Published 19 November 2022

Academic Editor: Dr Muhammad Hamid

Copyright © 2022 Aziz Ur Rehman et al. This is an open access article distributed under the Creative Commons Attribution License, which permits unrestricted use, distribution, and reproduction in any medium, provided the original work is properly cited.

The present study reports the fish fauna of Gomal Zam Dam at three different sites from October 2018 to July 2019. The total sampled fish belong to 18 species, 15 genera, 5 families, and 4 orders. Fourteen species belong to family Cyprinidae, which was the most abundant, while one species belong to each family Mastacembelidae, Channidae, Siluridae, and Sisoridae. The prominent species were *Labeo dyochielus* (18.6%), *Barilius vagra* (16.5%), and *Barilius pakistanicus* (13.8%), while the rare species were *Tor zhobensis*, *Wallago attu*, *Hyphophthalmichthys molitrix*, *Ctenophyrngodon idella*, and *Bagarius bagarius* each one forming (0.1%). Species were rich in spring with ideal temperature, followed by summer, whereas species abundance was high in summer with high temperature and minimum abundance was recorded in autumn. In conclusion, the Gomal Zam Dam is a favorable reservoir for the fish particularly for family Cyprinidae. This present study will provide useful information about the diversity of fish fauna of Gomal Zam Dam that could be used in systematic fisheries management and conservation of the country.

1. Introduction

Fish are an essential human food source, rich in protein, fats, vitamins, phosphorus, and other fundamental elements. Fish live in diverse habitats and are found from the Arctic to the Antarctic zone of the world [1, 2]. Fish are distributed in nearly all natural aquatic environments, from colder to warmer. Based on feeding habits and other ecological factors, fish that live in warmer climates with relatively stable temperatures are abundant by species count [3]. The rich taxonomic and functional diversity of freshwater fish is due to their habitat isolation [4]. Thus, the rich biodiversity of freshwater ecosystems is the freshwater fishes [5]. Glaciated regions have fewer fish fauna than temperate regions [6].

More than 27,977 species comprise 62 orders and 515 families, with 450 families of freshwater fishes identified worldwide [7].

Pakistan has diverse fish fauna due to its biogeographical location, diversified agroclimatic conditions, and diverse eco- and geodiversity. Pakistan covered a total area of 780,000 hectares with a total wetland area of 9.7%, of which 73% is covered by freshwater and 26.06% is by coastal wetlands [8, 9]. The country has 193 species of freshwater, mainly belonging to the class Actinopterygii, subclass Teleostei [10, 11]. Studies examined the biodiversity of fish species in various water bodies in Khyber Pakhtunkhwa province of Pakistan, including River Kurram at Bannu [10–12] and Baran dam of district Bannu [13]. Khan et al.

[14] recently determined the fish biodiversity of River Panjkora in both upper and lower Dir districts [14]. Ali et al. [15] studied the diversity of freshwater fishes from different locations of district Malakand including the Meherdi stream, Kharki stream, Wartier stream, Mahajar camp stream, and Dargai streams. According to Rafique and Khan [11], there are 193 freshwater fish species in Pakistan, including 5 superorders, 10 orders, 26 families, and 86 genera. The fish biodiversity from River Barandu, Pakistan was studied, and 18 species were identified [16].

The Gomal Zam Dam is constructed on river Gomal, originating from Afghanistan, and River Zhob emerging from Baluchistan, industrial-free areas; hence, the biodiversity of the Dam is conserved. Therefore, this study explored the ichthyofauna of the Gomal Zam Dam at three different sites and determined the physicochemical parameters of water. This study is the first-ever effort to record this newly constructed dam's fish fauna. Thus, the study will be attractive to Pakistan's fisheries sector and will add new understandings to the global fish industry.

2. Materials and Methods

2.1. Study Area. Gomal Zam Dam lies at 32°05'55"N and 69°52'53"E coordinates and is situated at Khajuri Katch of district South Waziristan, Khyber Pakhtunkhwa, Pakistan [17]. This dam impounds River Gomal, which emerges from Ghazni, Afghanistan and River Zhob, which emerges from Balochistan. The dam has been built for hydroelectric power generation, flood control, irrigation, and fish cultivation [18].

2.2. Study Design. The present study was carried out from October 2018 to July 2019 (10:00 am to 4:00 pm) and covered all the year's four seasons. Fish were sampled from three sites of the Dam (indicated in the map): Swai Nallah, Dotani village, and Gomal Khulla (Figure 1). Our previous protocol [16] was followed for fish and water sample collection. Sampling was carried out fortnightly from each site with the help of local fishermen where they have used gill nets with a length (10 m to 20 m), height (1.6 m), and mesh size of around 1.5 inches. Other nets like cast nets, drag nets, hand nets, and hooks were also used wherever necessary.

Similarly, water samples were collected from each site to determine its physicochemical parameters. Each catch was handled separately, and the specimens were sorted species-wise. The fish were preserved in 5-10% formalin for further identification in plastic jars. Small-sized fishes were immediately placed in the formalin solution, whereas formalin injection was given into the bodies of large-sized fishes before they were preserved in the formalin solution. The collection date, locality, and serial numbers were given to each collected and fixed fish species before they were saved in the laboratories of Fisheries and Aquaculture, Department of Animal Sciences, Quaid-I-Azam University Islamabad.

2.3. Fish Identification. The identification of the fish species was done mainly based on the color pattern, specific spots or marks on the body's surface, shape of the body, structure

of various fins, and mouth shape. Identification was made after consulting several standard keys and literature, such as fishes of Punjab [19], freshwater fishes of the Indian region [20], and Pakistan May Taza Pane Ke Machlian [21]. During identification, different materials were used, such as surgical gloves, China dish, forceps for holding fish, measuring tape, facial masks, and a digital camera for capturing fish pictures.

2.4. Indices Used to Determine the Diversity. The following diversity indices were used to find fish species diversity.

2.5. Simpson's Index of Diversity (D).

$$D = 1 - \sum(pi^2) \quad (1)$$

Here, $pi = ni/N$, where ni is the total no. of individuals of a particular species and N is the total no. of individuals of all species. $\Sigma =$ sum.

2.6. Pielou's Evenness. For calculating the evenness of species, Pielou's evenness index (E) was used [22].

$E = H/\ln S$, where H is the Shannon-Weiner diversity index and S is the total number of species in the sample.

2.7. Shannon-Weiner Index (H). The diversity of species was calculated following the Shannon-Weiner index (H), which depends on the number of species present and the abundance of each species.

$H = \sum Pi \log 2Pi$, where H is the Shannon-Wiener index, $Pi = ni/N$, $\Sigma =$ Sum, ni is the number of individuals of each species in the sample, and N is the total number of individuals of all species in the sample.

2.8. Physicochemical Parameters of Water. Water samples were collected as much as possible from the surface layer in plastic canes, avoiding unpredictable changes. The temperature, power of hydrogen ion concentration (pH), and dissolved oxygen (DO) of water were observed fortnightly on the spot. In contrast, other physicochemical parameters such as electrical conductivity (EC), turbidity, salinity, and total dissolved solids (TDS) were measured using respective digital equipment in the laboratory of Fisheries and Aquaculture, Department of Animal Sciences, Quaid-I-Azam University Islamabad.

2.9. Statistical Analysis. Statistically, SPSS version 26 was used for regression and correlation analysis and the relationship between variables was revealed.

3. Results

3.1. Fish Diversity of Gomal Zam Dam. In the present study, 703 fish specimens were collected from Gomal Zam Dam from October to July fortnightly bases. These specimens were identified as 18 species, 15 genera, 5 families, and 4 orders. Most of the species belonged to family Cyprinidae, the most abundant family with 14 species, whereas one species each belonged to families Siluridae, Sisoridae, Mastacembelidae, and Channidae. The observed/collected species with their classification up to genus are shown in (Table 1).

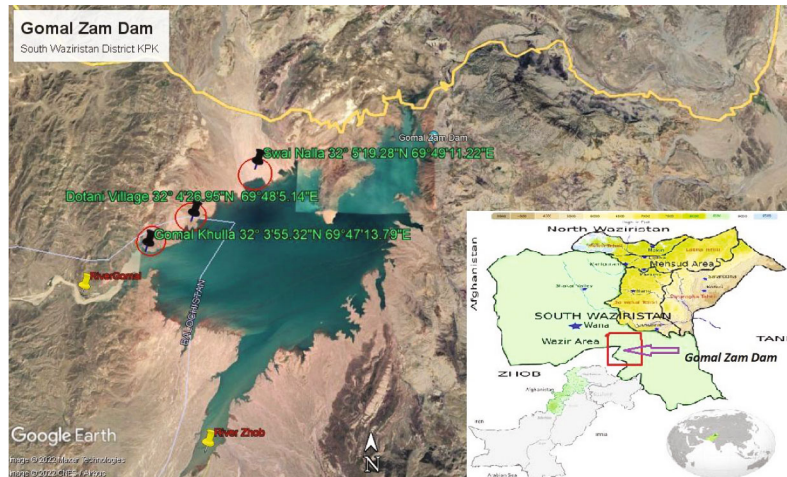


FIGURE 1: Map and location of Gomal Zam Dam and its tributaries. The three sampling sites were shown in the map. The map was cropped from Google Map and was edited accordingly.

TABLE 1: Fish species reported in this study from Gomal Zam Dam.

Family	Genus	Species
Mastacembelidae	Mastacembelus	<i>M. armatus</i>
Channidae	Channa	<i>C. marulius</i>
Siluridae	Wallago	<i>W. attu</i>
Sisoridae	Bagarius	<i>B. bagarius</i>
Cyprinidae	Tor	<i>T. zhubensis</i> ,
		<i>T. putitora</i>
//	Barilus	<i>B. pakistanicus</i> ,
		<i>B. vagra</i>
//	Labeo	<i>dyochielus</i> , <i>diplostomus</i>
		<i>L. diplostomus</i>
//	Cirrihinus	<i>C. reba</i>
//	Hypophthalmichthys	<i>H. molitrix</i>
//	Ctenophryngodon	<i>C. idella</i>
//	Puntius	<i>P. sophore</i>
//	Crossochielus	<i>C. diplochielus</i>
//	Carassius	<i>C. auratus</i>

3.2. Distribution and Abundance of the Identified Fish Species

3.2.1. *Tor putitora* (Hamilton, 1822). *Tor putitora* was found at all three sites, Swai Nallah, Gomal village, and Gomal Khula. Highest abundance of *Tor putitora* was recorded at Gomal village (36.36%), followed by both Swai Nallah and Gomal Khula (31.81%) (Table 2). The highest monthwise abundance was recorded in December (19.31%), followed by January (15.9%), March (13.63%), July (11%), June (8%), October (5.68%), November, February, and May (7.95%). The lowest value was recorded in April (2.27%) (Table 3).

3.2.2. *Cyprinion watsoni* (Day, 1872). *Cyprinion watsoni* was recorded from all three sites. The highest abundance was recorded at Swai Nallah (43.9%), followed by Dotani village (34.14%), and the lowest value was found at Gomal Khula

(21.95%) (Table 2). The highest abundance was recorded in April (26.82%), followed by May, June, and July (15%), November (12.19%), March (7.31%), and October (9.75%). However, this species was not recorded in December, January, and February (Table 3).

3.2.3. *Crossocheilus diplochilus* (Heckel, 1838). *Crossocheilus diplochilus* was recorded from all three sampling sites. The highest abundance of *Crossocheilus diplochilus* was found at Swai Nallah (36.17%), followed by Gomal Khula (34.04%), while the minimum number was recorded from Dotani village (30%) (Table 2). Similarly, monthwise highest abundance was recorded in June (34%), followed by July (21%), of March and April (12.76%), May (10.63%), and October (8.51%). In contrast, this fish was not recorded in December, January, and February (Table 3).

3.2.4. *Barilius pakistanicus* (Mirza and Sadiq 1978). *Barilius pakistanicus* was recorded from all three sites Swai Nallah, Dotani village, and Gomal Khula. The high number of *Barilius pakistanicus* was found at Dotani village (38.14%), followed by Gomal Khula (35.05%), and the lowest number was found at Swai Nallah (Table 2). The maximum number was recorded in April (27.27%), followed by July (20%), March (18%), May (12.2%), and June (10%). While the lowest value was recorded in October (6.06%), this species was utterly absent in December, January and July (Table 3).

3.2.5. *Barilius vagra* (Hamilton, 1822). *Barilius vagra* was recorded from all sites. High abundance was recorded from Dotani village (37.93%), Swai Nallah (34.48%), and Gomal Khula (27.58%). (Table 2). The highest abundance was recorded in March (23.68%), followed by April (22.8%), July (16%), June (13%), and May (10.52%), whereas in each October and November (7.01%) but no species was found in December, January, and February (Table 3).

3.2.6. *Mastacembelus armatus* (Lacpepe, 1800). *Mastacembelus armatus* was also recorded from all three sites. Its maximum number was found at Swai Nallah (57.14%), followed by Dotani village (28.57%), and the minimum number was

TABLE 2: Sitewise fish species recorded during the study from Gomal Zam Dam. The conservation status of each species was given according to Bibi et al. [23] and IUCN 2021-3 [46].

Species	Conservation status	Swai Nallah, <i>n</i> (%)	Dotani village, <i>n</i> (%)	Gomal Khula, <i>n</i> (%)	Ab	RA	%RA
<i>T. putitora</i>	Endangered	28 (31.81)	32 (36.36)	28 (31.81)	88	0.13	12.52
<i>C. watsoni</i>	Least concern	18 (43.90)	14 (34.14)	9 (21.95)	41	0.06	5.83
<i>C. diplocheilus</i>	Least concern	17 (36.17)	14 (29.78)	16 (34.04)	47	0.07	6.69
<i>B. pakistanicus</i>	Not evaluated	26 (26.80)	37 (38.14)	34 (35.05)	97	0.14	13.80
<i>B. vagra</i>	Least concern	40 (34.48)	44 (37.93)	32 (27.58)	116	0.17	16.50
<i>M. armatus</i>	Least concern	8 (57.14)	4 (28.57)	2 (14.28)	14	0.02	1.99
<i>T. zhobensis</i>	Not evaluated	0 (0)	1 (100)	0 (0)	1	0.00	0.14
<i>C. auratus</i>	Least concern	13 (31.70)	13 (31.70)	15 (36.58)	41	0.06	5.83
<i>L. dycheilus</i>	Least concern	49 (37.40)	31 (23.66)	51 (38.93)	131	0.19	18.63
<i>C. carpio</i>	Vulnerable	16 (43.24)	10 (27.02)	11 (29.72)	37	0.05	5.26
<i>W. attu</i>	Near threatened	0 (0)	1 (100)	0 (0)	1	0.00	0.14
<i>C. reba</i>	Least concern	10 (41.66)	6 (25)	8 (33.33)	24	0.03	3.41
<i>L. diplostomus</i>	Least concern	10 (35.71)	9 (32.14)	9 (32.14)	28	0.04	3.98
<i>H. molitrix</i>	Near threatened	0 (0)	1 (100)	0 (0)	1	0.00	0.14
<i>C. marulius</i>	Least concern	2 (33.33)	1 (16.66)	3 (50)	6	0.01	0.85
<i>C. idella</i>	Not evaluated	0 (0)	0 (0)	1 (100)	1	0.00	0.14
<i>P. sophore</i>	Least concern	11 (39.28)	8 (28.57)	9 (32.14)	28	0.04	3.98
<i>B. bagarius</i>	Near threatened	1 (100)	0 (0)	0 (0)	1	0.00	0.14
Total		249	226	228	703	1.00	100.0

TABLE 3: Monthwise abundance of fish species recorded during the study from Gomal Zam Dam.

Species	Oct. <i>n</i> (%)	Nov. <i>n</i> (%)	Dec. <i>n</i> (%)	Jan. <i>n</i> (%)	Feb. <i>n</i> (%)	Mar. <i>n</i> (%)	Apr. <i>n</i> (%)	May <i>n</i> (%)	June <i>n</i> (%)	July <i>n</i> (%)	Ab	RA	%RA
<i>T. putitora</i>	5 (5.7)	7 (7.2)	17 (19.3)	14 (15.9)	7 (7.)	12 (13.6)	2 (2.3)	7 (7.9)	7 (7.9)	10 (1.36)	88	0.13	12.5
<i>C. watsoni</i>	4 (9.8)	5 (12.2)	0 (0)	0 (0)	0 (0)	3 (7.3)	11 (26.8)	6 (14.6)	6 (14.6)	6 (14.6)	41	0.06	5.8
<i>C. diplocheilus</i>	4 (8.5)	0 (0)	0 (0)	0 (0)	0 (0)	6 (12.8)	6 (12.8)	5 (10.6)	16 (34.0)	10 (21.27)	47	0.07	6.7
<i>B. pakistanicus</i>	6 (6.1)	4 (4.0)	0 (0)	0 (0)	0 (0)	18 (18.2)	27 (27.3)	12 (12.1)	12 (12.1)	20 (20.2)	99	0.14	14.1
<i>Bariliusvagra</i>	8 (7.0)	8 (7.0)	0 (0)	0 (0)	0 (0)	27 (23.7)	26 (22.8)	12 (10.5)	15 (13.2)	18 (15.9)	114	0.16	16.2
<i>M. armatus</i>	1 (7.1)	0 (0)	0 (0)	1 (7.1)	0 (0)	0 (0)	0 (0)	3 (21.42)	4 (28.6)	5 (35.7)	14	0.02	1.9
<i>T. zhobensis</i>	0 (0)	1 (100)	0 (0)	0 (0)	0 (0)	0 (0)	0 (0)	0 (0)	0 (0)	0 (0)	1	0.00	0.1
<i>C. auratus</i>	0 (0)	2 (4.9)	3 (7.3)	5 (12.2)	4 (9.7)	9 (21.9)	9 (21.9)	2 (4.9)	4 (9.7)	3 (7.3)	41	0.06	5.8
<i>L. dycheilus</i>	0 (0)	14 (10.7)	13 (9.9)	20 (15.3)	16 (12.2)	8 (6.1)	11 (8.4)	6 (4.6)	25 (19.1)	18 (13.7)	131	0.19	18.63
<i>C. carpio</i>	0 (0)	1 (2.7)	5 (13.5)	1 (2.70)	2 (5.4)	3 (8.1)	4 (10.8)	4 (10.8)	3 (8.1)	14 (37.8)	37	0.05	5.26
<i>W. attu</i>	0 (0)	0 (0)	0 (0)	0 (0)	1 (100)	0 (0)	0 (0)	0 (0)	0 (0)	0 (0)	1	0.00	0.14
<i>C. reba</i>	0 (0)	0 (0)	1 (4)	2 (8)	5 (20)	3 (12)	0 (0)	4 (16)	4 (16)	6 (24)	25	0.04	3.56
<i>L. diplostomus</i>	0 (0)	0 (0)	0 (0)	2 (7.4)	2 (7.4)	4 (14.8)	3 (11.1)	1 (3.7)	8 (29.62)	7 (25.92)	27	0.04	3.84
<i>H. molitrix</i>	0 (0)	0 (0)	0 (0)	0 (0)	1 (100)	0 (0)	0 (0)	0 (0)	0 (0)	0 (0)	1	0.00	0.14
<i>C. marulius</i>	0 (0)	0 (0)	1 (16.7)	1 (16.7)	1 (16.7)	0 (0)	1 (16.7)	2 (33.3)	0 (0)	0 (0)	6	0.01	0.85
<i>C. idella</i>	0 (0)	0 (0)	0 (0)	0 (0)	1 (100)	0 (0)	0 (0)	0 (0)	0 (0)	0 (0)	1	0.00	0.14
<i>P. spore</i>	0 (0)	1 (3.6)	0 (0)	0 (0)	2 (7.1)	0 (0)	0 (0)	12 (42.8)	6 (21.4)	7 (25)	28	0.04	3.98
<i>B. bagarius</i>	0 (0)	0 (0)	0 (0)	0 (0)	0 (0)	0 (0)	0 (0)	0 (0)	0 (0)	1 (100)	1	0.00	0.14
Grand total	28	43	40	46	42	93	100	76	110	125	703	1	100

TABLE 4: Different ichthyodiversity-related parameter recorded monthwise in the study from Gomal Zam Dam.

Parameters	Months									
	Oct.	Nov.	Dec.	Jan.	Feb.	Mar.	Apr.	May	June	July
Species richness	6	6	4	7	10	6	6	9	8	9
Species abundance	28	43	40	46	42	93	100	76	110	125
S-Wiener index	1.67	1.85	1.37	1.49	1.93	1.92	1.93	2.36	2.27	2.37
S-diversity index	0.8	0.81	0.69	0.7	0.79	0.84	0.82	0.89	0.88	0.89
P-evenness index	0.5	0.49	0.37	0.39	0.52	0.49	0.42	0.52	0.48	0.49
Relative abundance	0.21	0.06	0.05	0.06	0.05	0.013	0.14	0.1	0.15	0.17
%RA	21.4	6.11	5.68	6.54	5.97	13.22	14.22	10.81	15.64	17.78

TABLE 5: Different ichthyodiversity-related parameter recorded sitewise in the study from Gomal Zam Dam.

Parameters	Study sites		
	Swai Nallah	Dotani village	Gomal Khula
Species richness	14	13	14
Species abundance	249	226	228
Shannon-Wiener index	2.37	2.32	2.29
Simpson diversity index	0.89	0.88	0.88
Pielious' evenness index	0.43	0.43	0.42
Relative abundance	0.35	0.32	0.32
%R A	35	32.14	32.43

recorded at Gomal Khula (14.28%) (Table 2), whereas the maximum number was found in July (36%), followed by June (29%) and May (21.42%), while both in October and January (7.14%). This species was absent in November, December, February, March, and April (Table 3).

3.2.7. *Tor zhobensis* (Mirza, 1967). *Tor zhobensis* was recorded merely at Dotani village and not found at Swai Nallah and Gomal Khula (Table 2). A single specimen of this species was recorded in November, utterly absent in October, December, January, February, March, April, May, June, and July (Table 3).

3.2.8. *Carassius auratus* (Linnaeus, 1758). *Carassius auratus* was recorded from all three sites. The highest abundance was found at Gomal Khula (36.58%), followed by both Swai Nallah and Dotani village (31.7%) (Table 2). The highest abundance was recorded in March and April (21.95%), followed by January (12.9%), June (10%), February (7.31%), December (7%), and July (9.75%), then in November and May (4.87%). It remained absent in October (Table 3).

3.2.9. *Labeo dyocheilus* (McClelland, 1839). *Labeo dyocheilus* was present at all three sites. The highest number was recorded from Gomal Khula (38.93%), followed by Swai Nallah (37.4%), and the lowest number was found at Dotani village (23.66%) (Table 2). Maximum abundance was found

in June (19%), followed by January (15.26%) July (14%), February (12.21%), November (10.68%), December (9.92%), April (8.39%), and March (6.1%), while the lowest number was recorded in May (4.58%). However, this species was not found during October (Table 3).

3.2.10. *Cyprinus carpio* (Linnaeus, 1758). *Cyprinus carpio* was recorded from the three selected sites, but it was most abundant at Swai Nallah (43.24%), while at Gomal Khula (29.72%) and Dotani village (27.02%) it was not that abundant (Table 2). The highest percentage was recorded in July (38%), followed by December (13.51%), both in April and May (10.81%), and in March (8.1%), June (8%), and February (5.4%). The lowest number was found in November and January (2.7%), whereas absent in October (Table 3).

3.2.11. *Wallago attu* (Bloch and Schneider, 1801). *Wallago attu* was recorded only at Dotani village, and no specimen was found at Swai Nallah and Gomal Khula (Table 2). High abundance was noted in February (100%) but remained absent in October, November, December, January, March, April, May, June, and July (Table 3).

3.2.12. *Cirrhinus reba* (Hamilton, 1822). *Cirrhinus reba* was recorded from all three sites. It was most abundant at Swai Nallah (41.66%), Gomal Khula (33.33%), and least abundant at Dotani village (25%) (Table 2). The highest number was recorded in July (24%) followed by February (20%), whereas in each May and June (1%), which was followed by March (12%), June (8%), and December (4%). However, this species was not recorded in October, November, and April (Table 3).

3.2.13. *Labeo diplostomus* (Heckel, 1838). *Labeo diplostomus* was recorded from all three sites, and their highest number was recorded at Swai Nallah (35.71%), followed by each Dotani village and Gomal Khula (32.14%) (Table 2). The largest number was recorded in the month of June (30%), followed by July (26%), March (14.81%), April (11.11%), and each January and February (7.4%). In contrast, it was not found in October, November, and December (Table 3).

3.2.14. *Hypophthalmichthys molitrix* (Valenciennes, 1844). *Hypophthalmichthys molitrix* was only found at Dotani village and not seen at Swai Nallah and Gomal Khula (Table 2). A single specimen was recorded in February but remained absent during all the months (Table 3).

TABLE 6: Mean \pm SD of physicochemical parameters from the studied sites of Gomal Zam Dam.

Variables	Units	Swai Nallah	Dotani village	Gomal Khula
Temp	$^{\circ}\text{C}$	20.81 \pm 7.78	20.13 \pm 6.99	20.49 \pm 7.42
pH	pH unit	7.97 \pm 0.26	7.73 \pm 0.27	7.73 \pm 0.27
DO	mg/L	6.53 \pm 0.53	6.65 \pm 0.98	6.78 \pm 0.82
TDS	mg/L	518.9 \pm 12.36	545.10 \pm 13.11	519.10 \pm 12.36
EC	$\mu\text{S}/\text{cm}$	1074.6 \pm 15.04	1080.60 \pm 17.73	1075.50 \pm 25.55
Salinity	mg/L	0.52 \pm 0.03	0.53 \pm 0.03	0.53 \pm 0.03
Turbidity	mg/L	2.04 \pm 0.26	2.00 \pm 0.29	2.07 \pm 0.35

3.2.15. *Channa marulius* (Hamilton, 1822). *Channa marulius* was recorded from all three sites and high abundance at Gomal Khula (50%), followed by Swai Nallah (33.33%) and the lowest number at Dotani village (16.66%) (Table 2). The maximum number was found in May (33.33%), followed by December, January, February, and April (16.66%), while this species was absent in March, June, July, October and November (Table 3).

3.2.16. *Ctenopharyngodon idella* (Valenciennes, 1844). *Ctenopharyngodon idella* was found only at Gomal Khula (100%) and was absent at the other two sites (Table 2). High abundance was found during February (100%), whereas it was lacking in October, November, December, January, March, April, May, June, and July (Table 3).

3.2.17. *Puntius sophore* (Hamilton, 1822). *Puntius sophore* was recorded from all three sites. The highest number was recorded from Swai Nallah (39.28%), followed by Gomal Khula (32.14%), while the lowest number was at Dotani village (28.57%) (Table 2). Maximum abundance was recorded in May (42.85%) followed by July (25%), June (7.14%), February (3.57%), and November (21%). This species was not recorded in December, January, March, and April (Table 3).

3.2.18. *Bagarius bagarius* (Hamilton, 1822). This species was recorded at Swai Nallah and absent at Dotani village and Gomal Khula (Table 2). It was found during July but was not recorded in October, November, December, January, February, March, April, May, and June (Table 3).

The species richness, species abundance, S-Wiener index, S-diversity index, P-evenness index, and relative abundance (%R) was given in Table 4. The highest richness was found in February (10), followed by May and July (9), June (8), January (7), March, April, October, November (6), and December (4). Species abundance was high in July (125), while minimum abundance was recorded in October (28). The Shannon-Weiner index (H) greater value (2.37) was recorded as high during July and lower in October (1.67). The value of the Simpson diversity index (D) for December was (0.69) and the highest for July (0.89). The value of Pielious' evenness (J) was found lower in December (0.37) and higher during July and March (0.49). The relative abundance was highest (21.4) in October while lowest (5.68) in December (Table 4).

The value of species richness at Swai Nallah and Gomal Khula was recorded (14), while at Dotani village, the species richness was 13. The highest value of species abundance was calculated at Swai Nallah (249), followed by Gomal Khula (228) and Dotani village (226). The value of Shannon-Weiner (H) at Swai Nallah was higher (2.37) than Gomal Khula (2.29) and (2.32) at Dotani village. Similarly, the Simpson diversity index (D) at Dotani village was (0.88) higher than Swai Nallah (0.89) and Gomal Khula (0.88). Pielious' evenness index (E) was similar both at Swai Nallah and Dotani village (0.43), followed by Gomal Khula (0.42). The relative abundance was highest at Swai Nallah (0.35), while its value at Dotani village and Gomal Khula was 0.32. The % RA was also highest (35) at Swai Nallah, while its value was 32.14 at Dotani village and was 32.43 at Gomal Khula (Table 5).

3.3. *Water Quality Parameters*. The physicochemical parameters of water are shown in Table 6. The temperature, pH, dissolved oxygen, total dissolved solids, electrical conductivity, salinity, and turbidity were recorded the same at Swai Nallah, Dotani village, and Gomal Khula (Table 6).

The correlation and regression tests were conducted for finding out the relationship between temperature, pH, DO, TDS, EC, salinity, and turbidity with fish abundance Figure 2. The correlation was positive between temperature and fish abundance ($r = 0.887$). In regression analysis, the y value was $3.955x - 12.02$ and R^2 was 0.786. The correlation between pH and fish abundance ($r = 0.887$) was also positive, and in the regression test, the y value was $11.5.7x - 852.5$ and R^2 was 0.862. The correlation between DO and fish abundance ($r = 0.967$) was negative (Table 7), whereas in the regression test, the y value was $72.48x - 414.6$ and value of R^2 was 0.934. Similarly, the negative correlation ($r = -0.0745$) was found between TDS and fish abundance (Table 7). The regression for TDS showed that the y value was $-0.047x + 97.21$ and R^2 was 0.005. The correlation between EC and fish abundance was negative ($r = -0.922$), and its regression showed that the y value was $-2.575x + 28.56$ and R^2 was 0.851. The correlation between salinity and fish abundance was negative ($r = -0.8783$), whereas its regression test showed that the y value was $-1066x + 637.4$ and R^2 was 0.771. Lastly, the correlation between turbidity and fish abundance was negative ($r = -0.909$) and its regression test

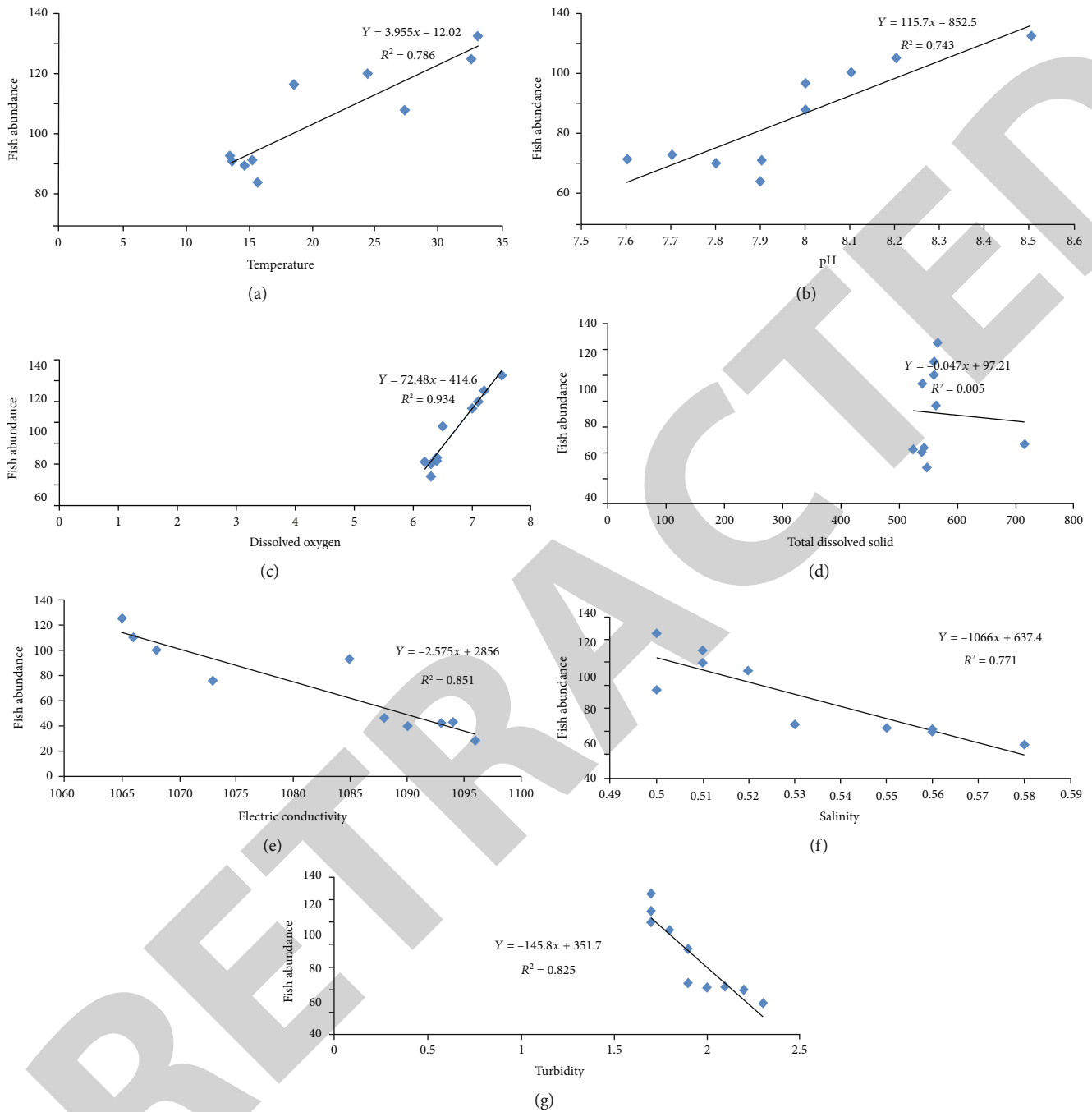


FIGURE 2: The regression between water quality parameters and fish abundance. Values for each parameter (a–g) are shown in x-axis while fish abundance is shown in y-axis, respectively.

showed that its y value was $-145.8x + 351.7$ and R^2 value was 0.825 (Table 7 and Figure 2).

4. Discussion

The study of the fish fauna of Gomal Zam Dam was carried out from October 2018 to July 2019. A total of 18 fish species belonging to 10 families, 4 orders, and 15 genera were reported from the studied sites. Based on species richness and percentage composition, order Cypriniformes was dominant with (14 species), followed by order Siluriformes (2

species), Channiformes, and Mastacembeliformes (1 species each). The ichthyodiversity of Gomal Zam Dam consists of 5 families: Cyprinidae, Siluridae, Sisoridae, Mastacembelidae, and Channidae. The fish species we report are mainly in line with the studies conducted previously in the same region on River Zhob, [24] and water bodies of Dera Ghazi Khan region [25, 26]. The shared reported species between our and previous studies were *Cyprinion watsoni*, *Labeo dyochielus*, *Cirrihins reba*, *Barilius pakistanicus*, *Tor putitora*, *Tor zhubensis*, and *Mastacembelus armatus*. However, we did not find some previously reported species such as *Labeo*

TABLE 7: Correlation analysis of water quality parameters versus fish abundance.

Variable	Correlation values (<i>r</i>)	Correlation status
Temp vs. fish abundance	0.887	Positive
PH vs. fish abundance	0.86	Positive
DO vs. fish abundance	0.96	Positive
TDS vs. fish abundance	-0.074	Negative
EC vs. fish abundance	-0.92	Negative
Salinity vs. fish abundance	-0.87	Negative
Turbidity vs. fish abundance	-0.90	Negative

rohita, *Puntius ticto*, *Crossocheilus latus*, *Aspidoparia*, *Schizocypris brucei*, *schizopygopsis stolizkae*, *Botia lohacheta*, *Glyptothorax naziri*, *Schistura kessleri*, *Schistura arifi*, and *Mastacembelus punctulus*; this may be due to anthropogenic activities, illegal fishing, and particularly environmental factors because dams cause destruction of habitats of fish species and produce negative outcomes on biodiversity [27]. Human pressure, overexploitation of resources, habitat loss, and degradation of breeding grounds led to the unrecorded extinction of the restricted range species [28]. Previously, *Barilius pakistanicus* was the least abundant species from River Zhob represented by a single specimen. At the same time, we report it as one of the most abundant species forming (14.08%) of the total collection. Similarly, *Crossocheilus diplocheilus* was reported as least diverse previously, but our study represented it by 6.69%. *Cyprinion watsoni* was reported to be the most abundant species of River Zhob by both [24, 29]. In contrast, its present status in Gomal Zam Dam is 5.83%. *Barilius vagra* is the second most abundant (16.22%) species in the present study and was also reported by [29]. However, [24] did not report it previously from the regional River Zhob. These results may indicate that the favorability of the environment is proportional to fish diversity [30]. *Garra gotyla* and *Schizothorax plagiostomus* were reported from Khanozai Dam [29]; however, it was not reported from River Zhob [24], and these two species were accordingly not reported. This may be due to global warming [31] or *S. plagiostomus*, a cold-water species living at high altitudes [32]. *Tor* was also reported previously [24], and accordingly, this species was abundant in our study (12.52%). This indicates that the warm water of Gomal Zam Dam is very suitable for *T. putitora*.

In the present study, different indices were used for finding ichthyodiversity, such as the Simpson diversity index, which is the probability of whether two individual fish taken from a huge community belong to a different species. This index has a value that ranges between 0 and 1. The larger the value, the more prominent will be the diversity sample [33]. In the present study, the values of the Simpson diversity index ranged from 0.88 to 0.89 at the three different sampling sites, with an overall value of 0.88 representing greater diversity for the entire region [34]. Shannon's index

is the diversity (species number and evenness) comparison among different sites [35, 36]. In our study, Shannon's index value ranged from 2.29 to 2.37 in all three sampling sites, with an overall value of 2.32. The usual value of Shannon's Index range between 1.5 and 3.5, whereas elevated values indicate larger diversity [37]. Evenness indices (*E*) are used for abundance standardization [38]. Its values are considered near 0 when most individuals belong to a few species, and its values are close to 1 when species are nearly equally abundant [38]. In the present study, the evenness index ranged from 0.42 to 0.43 for three sampling sites with an overall value of 0.42. This means that most individuals belong to a few species at most of the selected sampling sites.

Physicochemical analysis of water is the prime consideration to assess its fitness to be used by aquatic animals. In the present study, water temperature ranged from 13.2-33°C to air temperature (15.8-37°C). Hasan et al. [39, 40] reported a maximum water temperature (30.5°C) in July, which is less compared to the temperature (31.8°C) we reported in June. This maximum reported temperature falls entirely in the intolerable range for the identified fish species [41]. The productivity of a water body depends on hydrogen ion concentration (pH) which indicates the acidity or alkalinity of water. pH ranges from 6.4 to 8.3 are favorable for fish growth and survival [42]. The water of Gomal Zam Dam was found to be alkaline in nature, and the pH ranged 7.3 to 8.5. In the summer months, pH values were recorded higher than in other months. This may be due to increased photosynthetic activities, which increase the nutrient concentration at higher temperatures. The solubility of drinking water can be determined by TDS because it is an important physical parameter. During the present study, the values of TDS ranged between 500 and 567 ppm. Hasan et al. [39] recorded a TDS value of 111.1-139.2 ppm while working on the physicochemical parameters of River Panjkora. The increased value of TDS indicates water pollution [43]. Dissolved oxygen is essential to all aquatic organisms and is used as an index for net biomass production [44]. The present study's range varied from 5.5 to 7.9 mg/L. Its concentration in water depends mainly upon dissolved salts, temperature, pollution load, photosynthetic activity, respiration rate, and velocity of wind [45]. The composition of the particles, presence of dissolved, suspended solids, and size and shape of particles are the various factors that affect the turbidity of water. In the present study, turbidity was measured as 0.50-2.7. Water quality measurements that can help characterize turbidity include total suspended solids, volatile suspended solids, total dissolved solids, and suspended sediment concentration.

This pioneering study reported 18 fish species dominantly of the family Cyprinidae from the three new sites of Gomal Zam Dam. The species abundance was highest from May to July and lowest from December to February. Species richness was maximum at Swai Nallah and Gomal Khula, while it was minimum at Dotani village. We recommend further studies to explore other undiscovered water bodies of Pakistan for ichthyofaunal diversity. Moreover, we recommend DNA-based identification for taxonomic and evolutionary allocation of the fish.

Data Availability

The data was generated from record of the survey conducted during the field visit on hard paper; therefore, it cannot be converted into soft form to be available online.

Disclosure

This paper was prepared from the master dissertation of the principal author.

Conflicts of Interest

The authors declare that they have no conflicts of interest.

Acknowledgments

This research was partly supported by the University Research Fund of the Laboratory of Fisheries and Aquaculture, Department of Animal Sciences, Quaid-i-Azam University and was conducted in a facility developed.

References

- [1] S. C. Arya, K. S. Rao, and S. Shrivastava, "Biodiversity and fishery potential of Narmada Basin Western Zone (MP, India) with special reference to fish conservation," *Environment and Agriculture: Biodiversity, Agriculture and Pollution in South Asia*, pp. 78–83, 2001.
- [2] K. Ashok, "Studies on ichthyofaunal diversity with special reference to monthly and seasonal variations of fish landings in glacial fed mountainous Goriganga River of Kumaun Himalaya, Uttarakhand, India," *Research Journal of Animal, Veterinary and Fishery Sciences*, vol. 2, no. 4, pp. 1–12, 2014.
- [3] Q. Bone and R. Moore, *Biology of Fishes*, Taylor & Francis, 2008.
- [4] T. M. Berra, B. Gomelsky, B. A. Thompson, and D. Wedd, "Reproductive anatomy, gonad development and spawning seasonality of nurseryfish, *Kurtus gulliveri* (Perciformes: Kurtidae)," *Australian Journal of Zoology*, vol. 55, no. 4, pp. 211–217, 2007.
- [5] D. L. Saunders, J. J. Meeuwig, and A. C. J. Vincent, "Freshwater protected areas: strategies for conservation," *Conservation Biology*, vol. 16, no. 1, pp. 30–41, 2002.
- [6] C. Leveque, T. Oberdorff, D. Paugy, M. L. J. Stiassny, and P. A. Tedesco, "Global diversity of fish (Pisces) in freshwater," *Hydrobiologia*, vol. 595, no. 1, pp. 545–567, 2008.
- [7] G. Helfman, B. B. Collette, D. E. Facey, and B. W. Bowen, *The Diversity of Fishes: Biology, Evolution, and Ecology*, John Wiley & Sons, 2009.
- [8] M. Altaf, A. Javid, A. M. Khan, A. Hussain, M. Umair, and Z. Ali, "The status of fish diversity of river Chenab, Pakistan," *Journal of Animal and Plant Sciences*, vol. 25, pp. 564–569, 2014.
- [9] IUNC, *Tortoises and Freshwater Turtles: An Action Plan for their Conservation*, Tortoise Freshwater Turtle Specialist Group, 1989.
- [10] M. Rafiq, *Biosystematics and distribution of the freshwater fishes of Pakistan with special reference to the subfamilies Noemacheilinae and Schizothoracinae*, PMAS-Arid Agriculture University, Rawalpindi, 2007.
- [11] M. Rafique and N. U. H. Khan, "Distribution and status of significant freshwater fishes of Pakistan," *Record Zoological Survey of Pakistan*, vol. 21, pp. 90–95, 2012.
- [12] M. Rafique, "Fish diversity and distribution in Indus River and its drainage system," *Pakistan Journal of Zoology*, vol. 32, pp. 321–333, 2000.
- [13] U. Asmat, "The diversity of fish fauna in Baran dam of district Bannu, Khyber Pakhtunkhwa province (KPK), Pakistan," *International Journal of Advanced Research*, vol. 2, no. 9, pp. 136–145, 2014.
- [14] W. Khan, H. U. Hassan, K. Gabol et al., "Biodiversity, distributions, and isolation of microplastics pollution in finfish species in the Panjkora River at Lower and Upper Dir districts of Khyber Pakhtunkhwa province of Pakistan," *Brazilian Journal of Biology*, vol. 84, article e256817, 2024.
- [15] U. Ali, Q. Zaman, M. Farooq, J. Ali, and R. Ullah, "Identification and distribution of fishes in fresh water of district Malakand, Khyber Pakhtunkhwa Pakistan," *Pure and Applied Biology*, vol. 9, no. 4, pp. 2297–2304, 2020.
- [16] S. Mulk, A. L. Korai, A. Azizullah, and M. N. K. Khattak, "Decreased fish diversity found near marble industry effluents in River Barandu, Pakistan," *Ecotoxicology*, vol. 25, no. 1, pp. 132–140, 2016.
- [17] H. Masood, Z. Masood, N. Rafique et al., *GIS based mapping of the dams of Khyber Pakhtunkhwa (KPK) and Federally Administered Tribal Areas (FATA) For promoting fish culture in Pakistan*, 2015.
- [18] M. Zubia, S. Shagufta, W. M. Achakzai et al., "Physiochemical analysis of water and soil from Gomal Zam dam of Khajuri Kach in South Waziristan Agency of Pakistan, with special reference to their impact on fish growth and survival," *American-Eurasian Journal of Agricultural & Environmental Sciences*, vol. 15, no. 6, pp. 1182–1185, 2015.
- [19] M. R. Mirza and A. A. Sandu, *Fishes of the Punjab Pakistan, Polymer Publication, Urdu Bazar, Lahore*, National Bureau of Fish Genetic Resources (NBFGR), Lucknow (UP), India, 2007.
- [20] K. C. Jayaram, *The Freshwater Fishes of the Indian Region*, 1999.
- [21] M. R. Mirza, *Pakistan Ki Taza Pani Ki Machliyan*, Polymer Publications Lahore, 1990.
- [22] E. C. Pielou, "The measurement of diversity in different types of biological collections," *Journal of Theoretical Biology*, vol. 13, pp. 131–144, 1966.
- [23] F. Bibi, M. M. Nazir, A. N. Ahmad, and M. Akhtar, "Freshwater fish diversity and their conservation status in southern Punjab, Pakistan: a review," *Pakistan Journal of Life & Social Sciences*, vol. 16, no. 2, 2018.
- [24] A. S. Kakarabdullahzai and J. K. Kakarsulemankhel, *Additions to the fish fauna of River Zhob, Balochistan, Pakistan*, FAO of US, 2004.
- [25] M. Ali, S. Hussain, J. A. Mahmood, R. Iqbal, and A. Farooq, "Fish diversity of fresh water bodies of Suleman Mountain range, Dera Ghazi Khan region, Pakistan," *Pakistan Journal of Zoology*, vol. 42, pp. 285–289, 2010.
- [26] S. Hussain, M. Z. Hussain, R. Iqbal et al., "Diversity and status of Ichthyofauna of hill torrents of Suleman Mountain Range, Dera Ghazi Khan region Pakistan," *Pakistan Journal of Agricultural Sciences*, vol. 53, no. 4, pp. 83–842, 2016.
- [27] A. A. Agostinho, S. M. Thomaz, and L. C. Gomes, "Conservation of the biodiversity of Brazil's inland waters," *Conservation Biology*, vol. 19, no. 3, pp. 646–652, 2005.

Retraction

Retracted: Peelu (*Salvadora oleoides* Decne.): An Unexplored Medicinal Fruit with Minerals, Antioxidants, and Phytochemicals

BioMed Research International

Received 8 January 2024; Accepted 8 January 2024; Published 9 January 2024

Copyright © 2024 BioMed Research International. This is an open access article distributed under the Creative Commons Attribution License, which permits unrestricted use, distribution, and reproduction in any medium, provided the original work is properly cited.

This article has been retracted by Hindawi following an investigation undertaken by the publisher [1]. This investigation has uncovered evidence of one or more of the following indicators of systematic manipulation of the publication process:

- (1) Discrepancies in scope
- (2) Discrepancies in the description of the research reported
- (3) Discrepancies between the availability of data and the research described
- (4) Inappropriate citations
- (5) Incoherent, meaningless and/or irrelevant content included in the article
- (6) Manipulated or compromised peer review

The presence of these indicators undermines our confidence in the integrity of the article's content and we cannot, therefore, vouch for its reliability. Please note that this notice is intended solely to alert readers that the content of this article is unreliable. We have not investigated whether authors were aware of or involved in the systematic manipulation of the publication process.

Wiley and Hindawi regrets that the usual quality checks did not identify these issues before publication and have since put additional measures in place to safeguard research integrity.

We wish to credit our own Research Integrity and Research Publishing teams and anonymous and named external researchers and research integrity experts for contributing to this investigation.

The corresponding author, as the representative of all authors, has been given the opportunity to register their agreement or disagreement to this retraction. We have kept a record of any response received.

References

- [1] K. Razzaq, M. M. Sadiq, H. Ashraf et al., "Peelu (*Salvadora oleoides* Decne.): An Unexplored Medicinal Fruit with Minerals, Antioxidants, and Phytochemicals," *BioMed Research International*, vol. 2022, Article ID 5707953, 9 pages, 2022.

Research Article

Peelu (*Salvadora oleoides* Decne.): An Unexplored Medicinal Fruit with Minerals, Antioxidants, and Phytochemicals

Kashif Razzaq¹, **Muhammad Muzzammal Sadiq**², **Hashir Ashraf**³, **Ambreen Naz**⁴, **Abid Hussain**⁵, **Amir Maqbool**^{6,7}, **Muhammad Tanveer Altaf**⁸, **Sami Ullah**¹, **Gulzar Akhtar**¹, **Hafiz Nazar Faried**¹, **Muhammad Amin**⁹, **Ishtiaq Ahmad Rajwana**¹, **Ahmad Sattar Khan**¹⁰, **Saleh Alfarraj**¹¹, **Mohammad Javed Ansari**¹², and **Ammara Saleem**¹³

¹Department of Horticulture, MNS University of Agriculture, Multan 60000, Pakistan

²RHC Akhtar Abad Tehsil Renala Khurd, District Okara, Pakistan

³Medical Officer, RHC Khudian Khas, Kasur, Pakistan

⁴Department of Food Science and Technology, MNS-University of Agriculture, Multan 60000, Pakistan

⁵Department of Soil and Environmental Sciences, MNS-University of Agriculture, Multan 60000, Pakistan

⁶Department of Agricultural Genetic Engineering, Faculty of Agricultural Sciences and Technologies, Niğde Ömer Halisdemir University, Niğde, Turkey

⁷Institute for Integrative Biology of the Cell (I2BC), Université Paris-Saclay, CNRS, Gif-sur-Yvette, France

⁸Faculty of Agricultural Sciences and Technologies, Sivas University of Science and Technology, Sivas 58140, Turkey

⁹Department of Horticultural Sciences, The Islamia University Bhawalpur, 63100, Pakistan

¹⁰Institute of Horticultural Sciences, University of Agriculture, Faisalabad 38000, Pakistan

¹¹Zoology Department, College of Science, King Saud University, Riyadh 11451, Saudi Arabia

¹²Department of Botany, Hindu College Moradabad (Mahatma Jyotiba Phule Rohilkhand University Bareilly), 244001, India

¹³Faculty of Pharmaceutical Sciences, Government College University Faisalabad, Pakistan

Correspondence should be addressed to Kashif Razzaq; kashif.razzaq@mnsuam.edu.pk and Ammara Saleem; amarafurqan786@hotmail.com

Received 12 May 2022; Accepted 23 September 2022; Published 14 October 2022

Academic Editor: Hafiz Ishfaq Ahmad

Copyright © 2022 Kashif Razzaq et al. This is an open access article distributed under the Creative Commons Attribution License, which permits unrestricted use, distribution, and reproduction in any medium, provided the original work is properly cited.

The Peelu (*Salvadora oleoides* Decne.) fruit is well known for its nutritional and medicinal values. The current study analyzed the chemical composition of *Salvadora oleoides* fruit. Fresh Peelu fruits were harvested, and physicochemical properties, proximate composition, macro- and micronutrients, and phytochemical properties were determined. Moreover, ethanol and methanol fruit extract was analyzed for physicochemical properties. The Peelu fruit seemed to be a potential source of essential macro- (nitrogen (N), phosphorus (P), potassium (K), calcium (Ca), and magnesium (Mg)) and micronutrients (zinc (Zn), manganese (Mn), iron (Fe), and copper (Cu)). The fruit had significant biochemical properties (total soluble solids (TSS), total acidity (TA), and TSS : TA ratio) with appreciable moisture, crude fiber, and ash contents. The fruit extracts demonstrated significantly higher antioxidants and phenolics, ascorbic acid contents, and carotenoids. Phytochemical screening of fruit revealed the presence of coumarins, flavonoids, phlobatannins, tannins, and terpenoids. Physicochemical and sensory evaluation of extracts indicated its potential for further *in vivo* study trials. The Peelu fruit was found to be a good source of mineral nutrients, proximate contents, vitamins (ascorbic acid and carotenoid), phytochemicals (total phenolic and antioxidant contents), and pharmaceutically important metabolites that can be used as functional drink.

1. Introduction

Peelu (*Salvadora oleoides* Decne.) is a member of the Salvadoraceae family comprising of three genera, i.e., Azima, Dobera, and *Salvadora*. Ten (10) species of this family are mainly distributed in tropical and subtropical regions of Africa and Asia [1]. In Pakistan, the family is represented by a single genus *Salvadora*, with two species, i.e., *S. persica* and *S. oleoides* [2]. Recently a new species *S. alii* has also been reported and described from Sindh province of the country [3, 4]. The *Salvadora* species can grow in saline, arid, and semiarid regions [5] and serve as an excellent source of food for camels and goats. Moreover, the effective plantations can be used as shelterbelts and windbreaks [6].

It is considered a shrub or tree, 4-10 m in height with a twisted trunk. The plant had deep root system and usually known as xerophytes and facultative halophytes with high tolerance to salinity [2]. Leaves are simple, small, and high in number. It is a cross-pollinated plant [4] having greenish-white and greenish-yellow flowers born in leaves axil [6]. The fruit is a small, globose, smooth drupe with red yellow or purple color. The fruits ripen during May and June [6]. The fruit is sweet and peppery in taste with a pungent smell and eaten when fully ripe. Seed oil is pale green that is not fit for consumption [7]. Several therapeutic and industrial uses are well known about this plant which encourage the scientist in exploring more information about this medicinal plant [4]. The plant is well known for its anti-ulcer, antifungal, antiparasitic, antiviral, and antibacterial properties [8–10]. Leaves are used in the treatment of open wounds and act as a blood purifier and cooling agent. The stem is used to cure fever, asthma, cough, leprosy, rheumatism, and anthelmintic with diuretic properties [5]. Roots are effective against chest and teeth diseases [11, 12]. The oil can be used to manufacture candles, while oil cake is used as feed for animals [13].

Apart from the medicinal and nutritional importance, Peelu is a wild ignored crop with a high commercial potential for consumption and value addition. The prevalence of this plant is decreasing swiftly which may cause its extinction in the near future. Therefore, this valuable species could be conserved through exploring and promoting its commercial value. The current study examined the nutritional status of Peelu fruits. The results of the study would improve the understanding and importance of the nutritional value of the plant.

2. Materials and Methods

The Peelu fruits were harvested from a commercial field (29°06'12.64" N 70°19'30.14" E) by considering size uniformity and free from disease infestation. The characterization of nutritional composition was performed at Postharvest Laboratory, MNS-University of Agriculture, Multan, Pakistan under 30 ± 5°C temperature and 60-65% and relative humidity. Furthermore, proximate composition, mineral quantification, and phytochemical composition were explored. Hundred (100) grams of Peelu fruits were used as an experimental unit and replicated four times.

2.1. Compositional Analysis

2.1.1. Moisture (%). The moisture contents of the Peelu fruit were determined by method no. 44-15 according to AACC [14]. The sample was dried in a hot air oven at 105 ± 5°C till constant weight. The mathematical expression to compute the moisture percentage is given in

$$\text{Moisture (\%)} = \frac{\text{Fresh weight (g)} - \text{Oven dried weight (g)}}{\text{Fresh weight (g)}} \times 100. \quad (1)$$

2.1.2. Crude Fat (%). Crude fat was determined by the Soxhlet apparatus. The 2 g sample was placed in a paper thimble after removing moisture. Fat extraction was done with 75 to 100 mL diethyl ether or hexane. The extraction procedure was repeated four times with solvent. The heat was turned off after the completion of washing. The sample was placed in a hot air oven for the removal of solvent residues followed by cooling in a desiccator. The percentage of crude fat was computed according to

$$\text{Crude fat (\%)} = \frac{\text{Sample weight with fat} - \text{Sample weight without fat (g)}}{\text{Sample weight (g)}} \times 100. \quad (2)$$

2.1.3. Crude Protein (%). The crude protein was estimated by the Kjeldahl method. A 5 g sample was added in a pre-weighed digestion flask to which 3 g digestion mixture containing copper sulfate (CuSO_4), potassium sulfate (K_2SO_4), and ferrous sulfate (Fe_2SO_4) at the ratio of 5:94:1, and 25-30 mL sulfuric acid was added. The flask was placed on a burner and heated until 2-3 mL of the solution was left. The sample was then diluted up to 50 mL. Afterwards, 10 mL of the sample and 10 mL of NaOH (40%) were added in the reaction flask of the Kjeldahl apparatus. The 10 mL of boric acid (4%) was added to the receiving beaker of the Kjeldahl apparatus. The distillation continued until the volume of boric acid reached 20-22 mL and turned yellow. It was titrated with 0.1 N H_2SO_4 and N was computed according to equation (3). From the determined N percentage, crude protein was calculated according to

$$\text{N (\%)} = \frac{0.0014 \times \text{volume of 0.1 N sulfuric acid} \times \text{Volume of dilution}}{\text{Weight of sample} \times \text{Volume of sample taken}} \times 100, \\ \text{Crude protein (\%)} = \text{N (\%)} \times 6.25. \quad (3)$$

2.1.4. Crude Fiber (%). Crude fiber was determined in four steps. Primarily, a fat-free sample was added with 200 mL of boiling sulfuric acid (1.25%) till simmering (70-80°C). Afterwards, the sample was filtered with a linen cloth in the fluted funnel. In the second step, the acid-treated sample was subjected to alkaline medium of NaOH (1.25%) followed by heating, simmering, and filtration. In the third step, the treated sample was subjected to moisture removal according to the standard protocol. The weight of the sample obtained after moisture removal was denoted as W_1 . Finally, ashing was carried out. The weight of the sample after ashing was designated as W_2 . The cured fiber was calculated

TABLE 1: Compositional analysis (%) of *Salvadora oleoides* fruit.

Parameters	Minimum	Maximum	Mean*
Moisture contents	54.07	71.23	63.23 ± 6.3
Crude protein	2.53	6.04	4.23 ± 1.32
Crude fat	5.35	9.76	7.19 ± 2.09
Crude fiber	4.95	13.21	8.75 ± 3.02
Ash	5.53	12.67	8.78 ± 2.57

*Mean ± SD.

TABLE 2: Minerals (mg·100 g⁻¹·DW) composition of *Salvadora oleoides* fruit.

Parameters	Maximum	Minimum	Mean*
Nitrogen (N)	245.23	182.43	209.35 ± 22.64
Phosphorus (P)	101.56	65.78	85.08 ± 12.62
Potassium (K)	695.24	536.89	631.56 ± 60.81
Calcium (Ca)	589.78	422.76	507.56 ± 57.68
Magnesium (Mg)	127.56	100.98	113.79 ± 11.30
Iron (Fe)	9123.67	6758.34	8068.12 ± 938.53
Manganese (Mn)	678.9	645.78	656.84 ± 12.15
Zinc (Zn)	674.21	445.21	532.05 ± 97.24
Copper (Cu)	672.67	450.67	556.98 ± 88.75

*Mean ± SD.

according to

$$\text{Crude fiber (\%)} = \frac{W_1 - W_2}{\text{Weight of sample}} \times 100. \quad (4)$$

2.1.5. *Ash (%)*. The ash (%) content was estimated by Muffle Furnace (MF-1/02, PCSIR, Pakistan). The 3 g dry sample was incinerated after charring in Muffle Furnace according to Method 08-01 AACCC [14] at 550°C till grayish-white residue. The ash content was computed by using

$$\text{Ash (\%)} = \frac{\text{Weight of ash (g)}}{\text{Weight of sample (g)}} \times 100. \quad (5)$$

2.2. *Mineral Profiling*. The fresh fruits were washed with distilled water and dried in a hot air oven at 105°C till constant weight. The dried fruits were ground proceeded by acid digestion. The resultant solution was used to determine various mineral nutrients as nitrogen (N) by the micro-Kjeldahl method, phosphorus (P) by vanadomolybdo analysis, and potassium (K) by flame photometer as elaborated by Ullah et al. [15]. Additionally, other elements as Zn, Ca, Mn, and Fe were estimated by an Atomic Absorption Spectrophotometer (2-8200 Series Polarized Zeeman, Hitachi, Japan) by using a hollow cathode lamp [15].

2.3. *Phenolic and Antioxidants*. The ascorbic acid was determined by following the protocol of Kumar et al. [4] using trichloroacetic acid as reference. Moreover, ascorbic acid

contents were calculated using the standard curve of L-ascorbic acid and expressed as $\mu\text{g}\cdot 100\text{g}^{-1}\cdot\text{DW}$. Total carotenoids were determined and expressed as $\mu\text{g}\cdot\text{g}^{-1}$ of β -carotene equivalent [16]. Total phenolic contents (TPC) were estimated by following Folin-Ciocalteu (FC) method as discussed by Razzaq et al. [17]. The concentration of TPC was showed as $\text{mg GAE}\cdot 100\text{g}^{-1}$. The antioxidant activity was measured through 2,2-diphenyl-1-picrylhydrazyl radical (DPPH) by spectrophotometer in ELX800 Microplate Reader (Bio-Tek Instruments, Inc., Winooski, VT, USA) as outlined by Mimica-Dukić et al. [18] and was expressed as %. The inhibition percentage was computed according to

$$\text{Inhibition (\%)} = \frac{AB - AA}{AB} \times 100, \quad (6)$$

where AB is the absorption of a blank sample and AA is the absorbance of the tested sample.

2.4. *Tannins, Coumarins, Phlobatannins, Flavonoids, and Terpenoids*. The fruit pulp (50 mg) was boiled in distilled water (20 mL) followed by filtration. After boiling, FeCl_3 (0.1%) was added to the filtrate and a color change was noticed as blue-black or brownish-green as evidence of tannin presence. For the determination of coumarins, a fruit sample (300 g) was added to a test tube covered with a filter paper soaked in NaOH (1 N). The sample containing the test tube was placed in a hot water bath. The filter paper was removed and the sample was observed under UV light. The appearance of a yellow color indicated the presence of coumarins. In a small test tube, 300 mg of fruit was covered with filter paper moistened with 1 N NaOH. The test tube was placed in a boiling water bath for few minutes. After removing the filter paper, it was examined under UV light, yellow fluorescence indicated the presence of coumarins. The Peelu fruit was boiled in diluted hydrochloric acid (1%). The resultant deposition of red-colored precipitates indicated the occurrence of phlobatannins. The fruit sample (50 mg) was added in 100 mL of distilled water to obtain a filtrate. In the prepared filtrate, 5 mL of dilute ammonia solution plus few drops of concentrated H_2SO_4 . The flavonoids were confirmed by the appearance of the yellow color [19]. The determination of terpenoids was done by taking 5 mL of fruit pulp tissues with a dilution of 1 mg mL^{-1} , mixed with 2 mL chloroform and 3 mL of concentrated H_2SO_4 . The reddish-brown color indicated the presence of terpenoids as described by Saeed et al. [19].

2.5. *Biochemical Analysis*. The total soluble solids (TSS) were measured by a digital refractometer (ATAGO, RX5000, Atago Co. Ltd., Itabashi-ku, Tokyo, Japan) and expressed as °Brix. The total acidity (TA) was assessed via the acid-base titration method. The juice sample was titrated against NaOH (0.1 N) by using a phenolphthalein indicator. The pH of juice was estimated through a digital pH meter (Starter 3100 OHAUS Corporation, USA).

2.6. *Functional/Nutraceutical Drink*. Functional drink (Nutra-1) was developed by using various ingredients include citric acid, carboxymethylcellulose (CMC),

TABLE 3: Total phenolic, antioxidant, and ascorbic acid contents of *Salvadora oleoides* fruit.

Parameters	Minimum	Maximum	Mean*
Total phenolic contents (mg-GAE-100 g ⁻¹)	525.25	675.9	598.9 ± 100.35
Total antioxidants (% inhibition)	60.8	79.53	70.25 ± 7.33
Carotenoid (μg-100 g ⁻¹ ·DW)	4.67	8.41	6.52 ± 1.39
Ascorbic acid contents (μg-100 g ⁻¹ ·DW)	82.4	65.6	73.9 ± 1.15

*Mean ± SD.

TABLE 4: Biochemical attributes of *Salvadora oleoides* fruit.

Parameters	Minimum	Maximum	Mean*
Total soluble solids (°Brix)	7.2	10.5	8.9 ± 1.32
Titrate acidity (%)	0.325	0.62	0.5 ± 0.10
Ripening index (ratio)	11.2	32.3	19.7 ± 7.32
pH	3.8	4.1	3.9 ± 0.11

*Mean ± SD.

aspartame, sodium benzoate, flavor, and food-grade color along with propolis extract of following treatments at the dose rate of 400 mg/500 mL of the functional drink. The treatment planning of drinks was designed as T_0 (placebo), T_1 (functional drink with ethanol extract of Peelu), and T_2 (functional drink with methanol of extract of Peelu).

2.7. Functional Drink Analysis. The functional drinks were analyzed for their physicochemical attributes including TSS, TA, and pH. Sensory evaluation (color, flavor, sweetness, sourness, and overall acceptability) was done by using the 9-point hedonic scale (9 = extremely like, 1 = extremely dislike) as specified by Meilgaard et al. [20] during 10 days intervals of storage period (30 days).

2.8. Statistical Analysis. The experiment was carried out according to completely randomized design (CRD) with four replications. The data regarding different studied attributes were analyzed by descriptive statistics and presented. Statistix® statistical software was used for the data analysis [21]. The data regarding nutritional composition of functional drinks were analyzed by one-way analysis of variance (ANOVA). The normality in the data was tested indicating that the data had normal distribution. Therefore, the original data were used in the analysis. The least significant difference test at 95% probability was used to compare the means where ANOVA indicated significant differences.

3. Results and Discussion

3.1. Compositional Analysis. The compositional profiling of fruit elucidated that it contained significant moisture content (63.2%), crude fat (7.1%), crude protein (4.2%), crude fiber (8.7%), and ash (7.8%) as indicated in Table 1. The findings of the current study are closely related to the outcomes of Kumari et al. [22] who documented that ripened fruit of *Salvadora persica* had significant amounts of moisture (73.8 ± 5.0%), protein (5.9 ± 0.6%), ash (9.3 ± 0.6%),

and fiber (10.4 ± 1.9%) which was slightly higher than our results. Variation in proximate composition of the Peelu fruit may be due to different species, climatic conditions, soil type, or growing environment. The studied fruit was harvested from Southern Punjab, Pakistan, which had comparative lesser relative humidity which can be a major contributing factor in the low moisture content of fruit under investigation as compared to the results of Kumari et al. [22].

3.2. Mineral Profiling. The mineral profiling revealed the presence of a sufficient amount of macronutrients, i.e., nitrogen (N) 209.3 mg-100 g⁻¹·DW, phosphorus (P) 85.0 mg-100 g⁻¹·DW, potassium (K) 631.5 mg-100 g⁻¹·DW, calcium (Ca) 507.5 mg-100 g⁻¹·DW, and magnesium (Mg) 113.7 mg-100 g⁻¹·DW (Table 2). Our results showed that Peelu fruits contain a comparable amount of K and Ca with *Dialium guineense* [23]. The K is beneficial for cardiovascular disorders by reducing blood pressure by maintaining appropriate K⁺ and Na⁺ ratio [24]. Calcium (Ca²⁺) is a crucial mineral of the human diet that facilitates various biological functions of the body as differentiation, neuronal activities, muscles contraction, and immune responses that leads to apoptosis [25]. The Peelu fruit is rich source of Ca than common fruits, i.e., orange, apple, banana, papaya, chiku, and medicinal plants [13, 26]. The Peelu fruit was found to be a good source of Na⁺ which is important for various biological processes [27]. The Mg prevents cardiovascular diseases. It maintains bone structure by retaining Ca and vitamin D into bones which prevents osteoporosis [28]. Our results reported optimum concentrations of Mg in the Peelu fruit which are high than nonconventional fruits [29–31]. Hence, the Peelu fruit may be considered for functional foods to meet the daily requirement of minerals.

The Peelu fruits were rich in many micronutrients like Fe, Mn, Zn, and Cu as 8068.1, 656.2, 532.0, and 556.9 mg-100 g⁻¹·DW, respectively (Table 2). These micronutrients were required for the survival of human health as involved in many biochemical, physiological, and metabolic processes like DNA synthesis, mitotic division, respiration, and healthy aging [32, 33]. Moreover, micronutrient contents of Peelu in this study were at par with *Salvadora persica*, *Ziziphus jujube*, and *Capparis decidua* [29, 30]. However, these were lower than *Dialium guineense*, *Chryso-phyllum albidum*, and *Spondias mombin* [30, 31].

3.3. Phenolic and Antioxidant Contents. Phenolic substances of different origins and functions can be obtained from

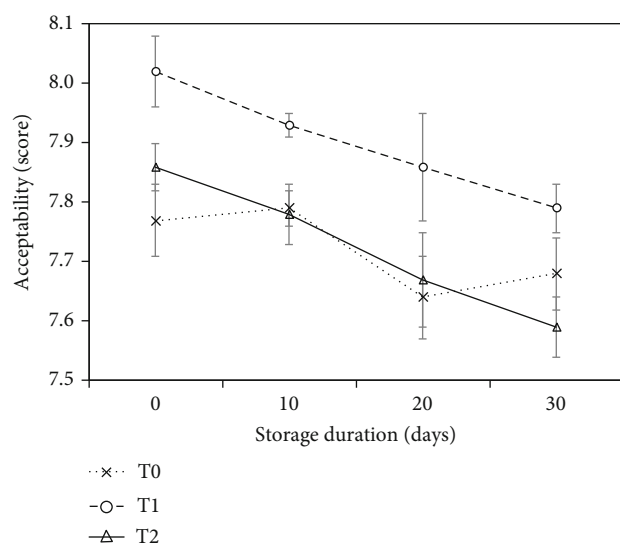


FIGURE 1: Impact of treatments (T_0 : placebo; T_1 : ethanol extract containing functional drink; T_2 : methanol extract containing functional drink) on overall acceptability of drink during storage period. Vertical bars indicate \pm standard error of means. $n = 3$, LSD ($P \leq 0.05$) for drinks.

plants. Most of these substances have antiviral, anticancerous, and antibacterial properties [34]. Phenolic contents and antioxidant activities of nontraditional fruits plants have limited description in literature [35]. The total phenolic content of the Peelu fruit extract were 598.9 ± 100.5 mg·GAE· 100 g^{-1} (Table 3). These contents are higher from *Ficus sycomorus*, *Diospyros mespiliformis*, *Parkia biglobosa*, and *Lannea microcarpa* and almost at par with *Sclerocarya birrea*, *Diospyros mespiliformis*, and *Saba senegalensis* and lower than *Tamarindus indica* and *Ziziphus mauritiana* [36]. The total phenolic content of the Peelu fruit has been found higher than the red and green peppers and at par with sour cherry and blueberry [23].

The antioxidants are becoming more important due to their role in maintaining good health and inhibiting disease through scavenging free radicals responsible for the multiplication of many diseases, including cancer, neurodegenerative, and AIDS disorder [22]. The total antioxidant capacity of the Peelu fruit was $70.2 \pm 7.3\%$ inhibition (Table 4). Antioxidant contents of the Peelu fruit were higher than banana, water apple, guava, and star fruit [37]. Among the species, the antioxidant contents of *S. oleoides* were higher than *S. persica* [22].

Carotenoids are a good source of antioxidants and considered fat-soluble pigments in plants. Moreover, color development is also dependent on carotenoids synthesis during maturity and ripening of the fruits. The carotenoid content in Peelu were $6.5 \pm 1.4\ \mu\text{g}\cdot 100\text{ g}^{-1}$ (Table 4). Carotenoids obtained from fruits and vegetables significantly reduce the risks of diseases and provide more health benefits [38, 39]; hence, Peelu could be a good choice of carotenoids for dietary intake. Ascorbic acid has antioxidant activity and maintains cellular membrane activity. Ascorbic acid inhibits the conversion of cancer-causing compound N-nitroso from nitrates and nitrides present in fruit and vegetables [40]. In

the current study, ascorbic acid contents in the Peelu fruit were $73.9 \pm 1.1\ \mu\text{g}\cdot 100\text{ g}^{-1}$ (Table 4). Higher ascorbic acid content in Peelu proved its great potential for promoting health benefits. Similarly, a higher amount of ascorbic ($67.9\text{ mg}\cdot 100\text{ g}^{-1}\cdot\text{DW}$) has been reported for *S. persica* fruit [22].

3.4. Biochemical Analysis. Data regarding biochemical profiling of the Peelu fruit indicated that TSS in fruit juice were $8.9 \pm 1.3^\circ\text{Brix}$ (Table 4). The percent TA was 0.5 ± 0.1 (%) with a pH value of 3.9 ± 0.1 . Additionally, the ripening index ratio was 19.7 ± 7.3 . These results showed that biochemical attributes of Peelu were at par with other ignored fruits like *Averrhoa carambola*, *Morus alba*, and *Syzygium cumini* [41, 42], comparable with *Grewia subinaequalis*, and lesser than *Prunus persica* and *Prunus armeniaca* [43] suggesting the usage of this rare fruit in different value-added products.

3.5. Physicochemical Analysis of Drink. Data regarding various physicochemical attributes (pH and acidity) showed a significant effect of treatments and storage duration on functional drinks prepared from Peelu. However, the interaction between treatments and storage duration was nonsignificant for pH and acidity of the functional drinks. Moreover, a nonsignificant effect of treatment and storage period, as well as their interaction, was recorded for TSS (Figure 1).

The highest concentration of TSS (1.6°Brix) was observed in functional drink with ethanol extract of Peelu as compared to placebo and functional drink with methanol extract of Peelu (1.58°Brix and 1.58°Brix). As far as the storage period was concerned, an increasing trend was observed for TSS for the storage period. The highest concentration of TA (1.67%) was obtained after 30 days of storage period as compared to 0 days (1.5%) (Figure 2(a)). An increasing trend has been observed for acidity with prolonging storage period in all treatments. This increase in acidity (%) was more in methanol extract of Peelu when compared with other treatments. After storage of 30 days drink prepared in methanol extract showed 1.03- and 1.06-fold more TA (Figure 2(b)). Among various treatments, functional drinks prepared in methanol extract exhibited the highest (3.48) value for pH. A significant linear decreasing trend (1.13 -fold) was observed for the pH of functional drinks with the increase in storage period from day-0 to day-30 (Figure 2(c)).

Previously, the average TSS documented was about 10.4°Brix in a diet drink of apple prepared with artificial sweetener. Similarly, the results of the current investigation are in corroboration with González-Molina et al. [44], who reported a nonmomentous effect of storage period on TSS of apple and pomegranate juices and their blending. The result of the present study for pH and acidity of functional drinks is similar to Ahmed [45], who observed that a negative correlation exists between acidity and pH of juice during storage. Moreover, these increase and decrease in acidity and pH are closely linked with each other as reported by Klimczak et al. [46]. Similarly, an increase in acidity and a sharp decline in pH was monitored in fruit drink during 90 days of storage [47]. The inverse relationship between pH and acidity has also been observed in yogurt-like beverages

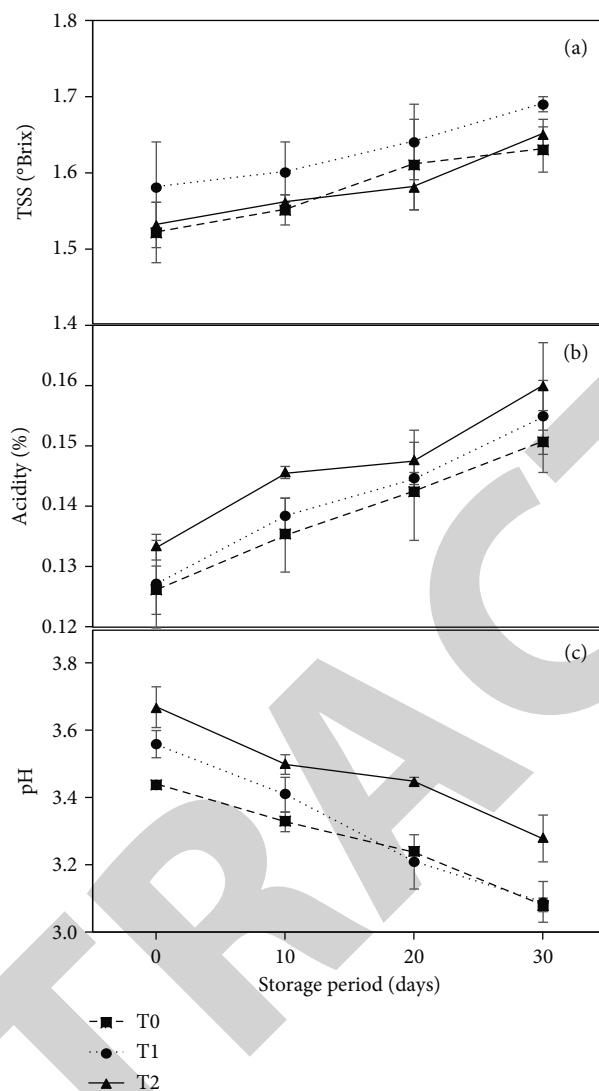


FIGURE 2: Impact of treatments (T_0 : placebo; T_1 : ethanol extract containing functional drink; T_2 : methanol extract containing functional drink) on total soluble solids (a), acidity (b), and pH (c) of functional drink during the storage period. Vertical bars indicate \pm standard error of means. $n = 3$, LSD ($P \leq 0.05$) for drinks.

including cereals [48]. This increase in acidity may be due to the breakdown of artificial sweeteners as well as citric acid in replacement of sugar for making therapeutic drinks [49]. Additionally, a decrease in pH and increase in acidity may be due to the degradation of polysaccharides and oxidation of reducing sugars that results in the production of acidic components. Furthermore, the development of uronic acid due to the breakdown of pectin may also be the reason for a change in the abovementioned parameters [50].

3.6. Sensory Evaluation. Treatments, storage period, and interaction were nonsignificant for sensory parameters of functional drinks. Color of the product/physical appearance is considered a prime factor for selection/rejection of the product by the consumer. With the increase in storage duration color score of the functional drinks was significantly reduced. The color score of the drinks was more at 0-day (6.6), while reduced to 6.1 after 30 days of storage. Among

the treatment, the highest color score was obtained from T_2 (6.51 ± 0.07) as compared to T_1 and T_0 (6.45 and 6.23, respectively) (Figure 3(a)). The flavor of drinks was found higher (7.1 ± 0.06) at 0-day, while the lowest value (6.96) was recorded after 30 days of storage (Figure 3(b)). As far as various treatments are concerned, drink prepared with ethanol extract (T_1) showed a better flavor score (7.14), as compared to drinks prepared with methanol extract (7.09) and drink without extract (6.94). Average values documented for sweetness and sourness at 0-day were 7.20 and 7.68, 7.60 and 7.79, and 7.36 and 7.5, respectively, whereas mean values for sweetness and sourness after 30 days of storage were 7.08 and 7.38, 7.22 and 7.5, and 7.18 and 7.39 for T_0 , T_1 , and T_2 treated drink accordingly. The overall acceptability means a score of functional drinks was recorded about 7.77 during storage.

Our results were in line with Ahmed [45] who reported that sensory evaluation of functional drinks prepared with

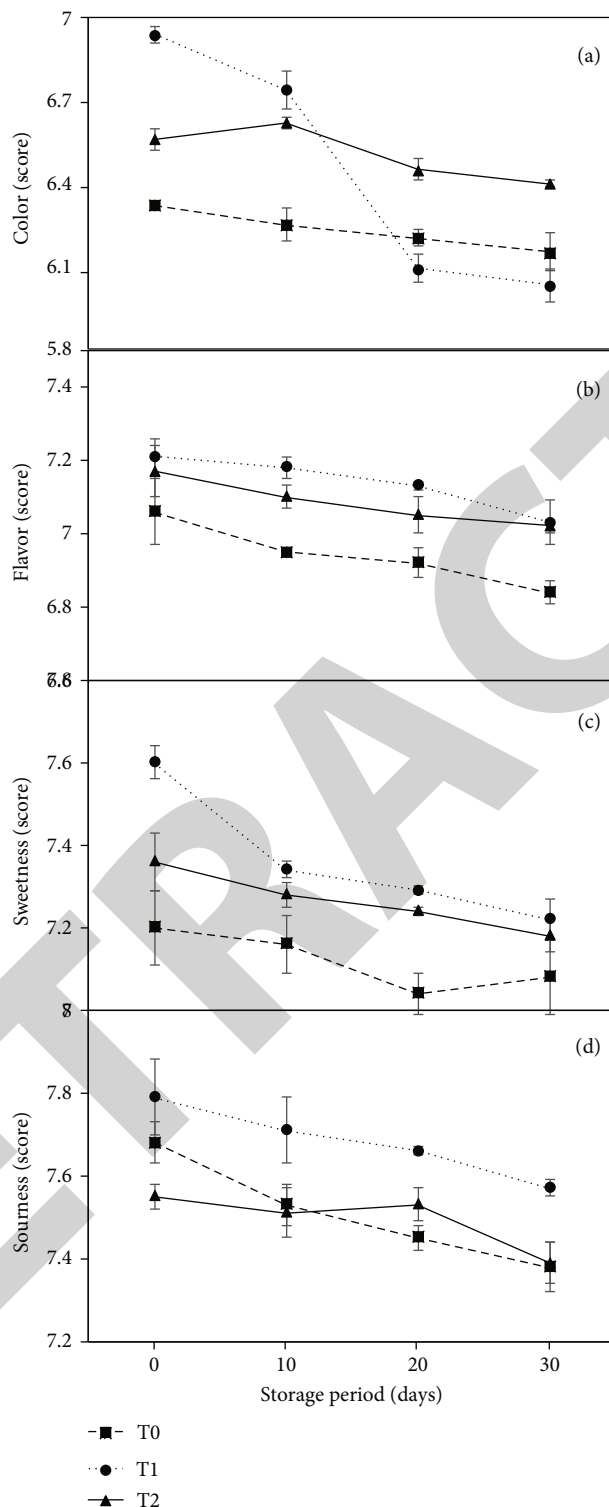


FIGURE 3: Impact of treatments (T_0 : placebo; T_1 : ethanol extract containing functional drink; T_2 : methanol extract containing functional drink) on color (a), flavor (b), sweetness (c), and sourness (d) of functional drink during storage period. Vertical bars indicate \pm standard error of means. $n = 3$, LSD ($P \leq 0.05$) for drinks.

polyphenol extracts declined in various sensory attributes including color, flavor, sweetness, sourness, and overall acceptability. This may be due to the reason that polyphenols induce color variation because of color imparting bodies linked with the plant polyphenols [51].

4. Conclusion

The Peelu fruit is a good source of macro- and micronutrients and has a sufficient quantity of biochemical contents (SSC, TA, SSC : TA ratio, and pH). Like other fruits, the

juice of the Peelu fruit is a rich source of phenolic and antioxidants, including ascorbic acid and carotenoids. However, the sensory attributes of the functional drinks were in corroboration with control representing its potential for further *in vivo* study. Conclusively, Peelu exhibit high nutritional potential and could be included in the food chain with value addition.

Data Availability

All relevant data are within the manuscript.

Conflicts of Interest

The authors have declared no conflict of interests.

Acknowledgments

The authors gratefully acknowledge the financial support from the Higher Education Commission of Pakistan for current study under SRGP Project No. 1211. This project was supported by Researchers Supporting Project Number RSP-2023R7, King Saud University, Riyadh, Saudi Arabia.

References

- [1] D. J. Mabberley, *Mabberley's Plant-Book: A Portable Dictionary of Plants, Their Classification and Uses*, Cambridge University Press, 2017.
- [2] M. A. Khan and M. Qaiser, "Halophytes of Pakistan: characteristics, distribution and potential economic usages," in *Sabkha Ecosystems*, Springer, 2006.
- [3] S. S. Tahir, M. T. Rajput, and F. Korejo, "A new species of *Salvadora* (Salvadoraceae) from Sindh, Pakistan," *Pakistan Journal of Botany*, vol. 42, pp. 63–66, 2010.
- [4] S. Kumar, C. Rani, and M. Mangal, "A critical review on *Salvadora persica*: an important medicinal plant of arid zone," *International Journal of Phytomedicine*, vol. 4, pp. 292–303, 2012.
- [5] M. Kaneria, K. Rakholiya, J. Sonagara, and S. Chanda, "Comparative assessment of antioxidant activity and phytochemical analysis of facultative halophyte *Salvadora oleoides* Decne. and *Salvadora persica* L.," *American Journal of Biochemistry and Molecular Biology*, vol. 7, no. 3, pp. 102–110, 2017.
- [6] S. N. Ghosh, *Breeding of underutilized fruit crops*, JAYA Publishing House, 2015.
- [7] F. Korejo, S. A. Ali, S. S. Tahir, M. T. Rajput, and M. T. Akhter, "Comparative morphological and biochemical studies of *Salvadora* species found in Sindh, Pakistan," *Pakistan Journal of Botany*, vol. 42, no. 3, pp. 1451–1463, 2010.
- [8] R. Sanogo, M. T. Monforte, A. D'Aquino, A. Rossitto, D. Di Mauro, and E. M. Galati, "Antiulcer activity of *Salvadora persica* L.: structural modifications," *Phytomedicine*, vol. 6, no. 5, pp. 363–366, 1999.
- [9] O. J. Hamza, C. J. van den Bout-van, M. I. Matee et al., "Antifungal activity of some Tanzanian plants used traditionally for the treatment of fungal infections," *Journal of Ethnopharmacology*, vol. 108, no. 1, pp. 124–132, 2006.
- [10] A. H. Sofrata, R. L. K. Claesson, P. K. Lingström, and A. K. Gustafsson, "Strong antibacterial effect of miswak against oral microorganisms associated with periodontitis and caries," *Journal of Periodontology*, vol. 79, no. 8, pp. 1474–1479, 2008.
- [11] N. Savithamma, C. Sulochana, and K. N. Rao, "Ethnobotanical survey of plants used to treat asthma in Andhra Pradesh, India," *Journal of Ethnopharmacology*, vol. 113, no. 1, pp. 54–61, 2007.
- [12] H. Darmani, T. Nusayr, and A. S. Al-Hiyasat, "Effects of extracts of miswak and derum on proliferation of Balb/C 3T3 fibroblasts and viability of cariogenic bacteria," *International Journal of Dental Hygiene*, vol. 4, no. 2, pp. 62–66, 2006.
- [13] M. Rathore, "Nutrient content of important fruit trees from arid zone of Rajasthan," *Journal of Horticulture and Forestry*, vol. 1, no. 7, pp. 103–108, 2009.
- [14] American Association of Cereal Chemists, *Approved Methods of the AACC 10th Edition*, American Association of Cereal Chemists, 2000.
- [15] S. Ullah, T. Alsberg, and U. Berger, "Simultaneous determination of perfluoroalkyl phosphonates, carboxylates, and sulfonates in drinking water," *Journal of Chromatography. A*, vol. 1218, no. 37, pp. 6388–6395, 2011.
- [16] H. J. D. Lalel, Z. Singh, and S. C. Tan, "Glycosidically-bound aroma volatile compounds in the skin and pulp of 'Kensington Pride' mango fruit at different stages of maturity," *Postharvest Biology and Technology*, vol. 29, no. 2, pp. 205–218, 2003.
- [17] K. Razzaq, A. S. Khan, A. U. Malik, and M. Shahid, "Ripening period influences fruit softening and antioxidative system of 'Samar Bahisht Chaunsa' mango," *Scientia Horticulturae*, vol. 160, pp. 108–114, 2013.
- [18] N. Mimica-Dukić, B. Božin, M. Soković, B. Mihajlović, and M. Matavulj, "Antimicrobial and antioxidant activities of three *Mentha* species essential oils," *Planta Medica*, vol. 69, no. 5, pp. 413–419, 2003.
- [19] N. Saeed, M. R. Khan, and M. Shabbir, "Antioxidant activity, total phenolic and total flavonoid contents of whole plant extracts *Torilis leptophylla* L.," *BMC Complementary and Alternative Medicine*, vol. 12, no. 1, p. 221, 2012.
- [20] M. C. Meilgaard, B. T. Carr, and G. V. Civille, *Sensory Evaluation Techniques*, CRC Press, 1999.
- [21] D. A. Steel, R. G. D. Torrie, and J. H. Dickey, *Principles and procedures of statistics, a biometrical approach*, McGraw Hill Book Co. Inc, New York, 1997.
- [22] A. Kumari, A. K. Parida, J. Rangani, and A. Panda, "Antioxidant activities, metabolic profiling, proximate analysis, mineral nutrient composition of *Salvadora persica* fruit unravel a potential functional food and a natural source of pharmaceuticals," *Frontiers in Pharmacology*, vol. 8, 2017.
- [23] D. Marinova, F. Ribarova, and A. Maria, "Total phenolics and flavonoid in Bulgarian fruits," *Journal of Chemical Technology and Metallurgy*, vol. 40, no. 3, pp. 255–260, 2005.
- [24] C. M. Weaver, "Potassium and health," *Advances in Nutrition*, vol. 4, no. 3, pp. 368S–377S, 2013.
- [25] F. Pu, N. Chen, and S. Xue, "Calcium intake, calcium homeostasis and health," *Food Science and Human Wellness*, vol. 5, no. 1, pp. 8–16, 2016.
- [26] M. Garcia-Alonso, "Evaluation of the antioxidant properties of fruits," *Food Chemistry*, vol. 84, no. 1, pp. 13–18, 2004.
- [27] W. B. Farquhar, D. G. Edwards, C. T. Jurkowitz, and W. S. Weintraub, "Dietary sodium and health: more than just blood pressure," *Journal of the American College of Cardiology*, vol. 65, no. 10, pp. 1042–1050, 2015.
- [28] S. Chakraborti, T. Chakraborti, M. Mandal, A. Mandal, S. Das, and S. Ghosh, "Protective role of magnesium in cardiovascular

Research Article

De Novo Transcriptome Dataset Generation of the Swamp Buffalo Brain and Non-Brain Tissues

Wang Xiaobo ^{1,2}, Faiz-ul Hassan ³, Sheng Liu ², Shuli Yang ², Muhammad Ahmad ⁴,
Ishtiaq Ahmed ⁵, Kongwei Huang,¹ Hafiz M. N. Iqbal ⁶, Hui Yu ², Qingyou Liu ^{1,2}
and Saif ur Rehman ^{1,2}

¹State Key Laboratory for Conservation and Utilization of Subtropical Agro-Bioresources, Guangxi University, Nanning 530005, China

²Guangdong Provincial Key Laboratory of Animal Molecular Design and Precise Breeding, School of Life Science and Engineering, Foshan University, Foshan 528225, China

³Institute of Animal and Dairy Sciences, Faculty of Animal Husbandry, University of Agriculture, Faisalabad 38040, Pakistan

⁴Faculty of Veterinary Sciences, Shaheed Benazir Bhutto University of Veterinary and Animal Sciences (SBBUVAS), Sakrand 67210, Pakistan

⁵Department of Regional Science Operations, La Trobe Rural Health School, Albury-Wodonga, Victoria 3690, Australia

⁶Tecnológico de Monterrey, School of Engineering and Sciences, Monterrey 64849, Mexico

Correspondence should be addressed to Hui Yu; yu71hui@aliyun.com, Qingyou Liu; qyliu-gene@gxu.edu.cn, and Saif ur Rehman; saif_ali28@yahoo.com

Received 7 June 2022; Accepted 23 September 2022; Published 12 October 2022

Academic Editor: Amjad Bashir

Copyright © 2022 Wang Xiaobo et al. This is an open access article distributed under the Creative Commons Attribution License, which permits unrestricted use, distribution, and reproduction in any medium, provided the original work is properly cited.

The sequenced data availability opened new horizons related to buffalo genetic control of economic traits and genomic diversity. The visceral organs (brain, liver, etc.) significantly involved in energy metabolism, docility, or social interactions. We performed swamp buffalo transcriptomic profiling of 24 different tissues (brain and non-brain) to identify novel transcripts and analyzed the differentially expressed genes (DEGs) of brain vs. non-brain tissues with their functional annotation. We obtained 178.57 Gb clean transcriptomic data with GC contents 52.77%, reference genome alignment 95.36%, exonic coverage 88.49%. Totally, 26363 mRNAs transcripts including 5574 novel genes were obtained. Further, 7194 transcripts were detected as DEGs by comparing brain vs. non-brain tissues group, of which 3,999 were upregulated and 3,195 downregulated. These DEGs were functionally associated with cellular metabolic activities, signal transduction, cytoprotection, and structural and binding activities. The related functional pathways included cancer pathway, PI3k-Akt signaling, axon guidance, JAK-STAT signaling, basic cellular metabolism, thermogenesis, and oxidative phosphorylation. Our study provides an in-depth understanding of swamp buffalo transcriptomic data including DEGs potentially involved in basic cellular activities and development that helped to maintain their working capacity and social interaction with humans, and also, helpful to disclose the genetic architecture of different phenotypic traits and their gene expression regulation.

1. Introduction

The buffalo belongs to the family *Bovidae* (genus *Bubalus*) and is considered a significant livestock species owing to its multiple utilities as a source of meat, milk, and draught power in agricultural fields [1–3]. Buffaloes are usually found in wet grasslands, swamps, and marshes, subtropical and tropical regions of the world. The Asian domesticated water buffalo

is generally categorized into two main subspecies including the swamp ($2n = 48$) and river buffalo ($2n = 50$) usually based on their physical appearance, body size, chromosome karyotype, and physiological features [2, 4, 5]. In China, swamp buffaloes are native animals distributed across 18 provinces in southern and central China. Based on their local regional distribution, these buffaloes have been grouped into 18 local breeds [6, 7]. Swamp buffaloes were mostly reared by small

farmers as a draught power for agricultural operations, particularly ploughing in rice paddy fields. However, owing to its economic traits like leather, horns, meat, and milk, over the last decade, extensive efforts have been made for the genetic improvement of dairy traits in buffalo through crossbreeding [2, 8, 9].

The major impediment in China's buffalo industry included poor reproductive performance and milk production of local buffalo as compared to dairy cattle, so major efforts were directed towards improving the buffalo herd size to increase reproductive efficiency through utilizing reproductive technologies [8, 10–13], to identify the genetic markers and genes, which were associated with phenotypic variations [14–16] of desirable traits [17–19]. In China, the information related to buffalo breeding is still limited regarding molecular breeding techniques. The lacking of genomic information is the key hindrance in buffalo genetic improvement programs, although several studies at the genomic level have been conducted so far by different research groups [20–22].

Even though the draft genome of the swamp and river buffalo has been released [23, 24], but genetic information on different physiological traits of buffalo is still scanty which in turn hinders the buffalo's genetic improvement [25, 26]. The transcriptomic studies are important to generate larger quantities of sequenced data for both model and non-model species [27]. In different species like sheep [28, 29], goat [30] cattle [31], and pig [32], high-throughput technologies such as RNA sequencing (RNA-seq) have efficiently been used in transcriptome analysis, molecular marker development, and gene discovery.

The swamp buffaloes have shown closer association with humans mainly because of their key utility as a draft power in agroecosystems. The genetic basis of this close social interaction of swamp buffalo has also been revealed at the genomic level in a recent study [23] that explained the selection signatures for social behavior and energy related genes in the swamp buffalo, which facilitated them to develop long-term collaboration with humans in rice paddy field work. Further, the visceral organs, like the brain, liver, heart, lungs, spleen, and kidney, etc. are the key organs that play a significant role in energy metabolism, docility, and/or social interactions. It is therefore imperative to explore the differential expression of genes associated with physiological responses and neural networks to better understand adaptive and cognitive behaviors. This study was designed with the aim to perform the transcriptomic profiling of 24 different tissues of swamp buffalo (grouped into brain and non-brain tissues), to analyze the DEGs, to evaluate the novel transcripts, and their functional annotation.

2. Materials and Methods

2.1. Sample Collection and Preparation. An adult female swamp buffalo, which was kept under uniform feeding conditions without any biotic or abiotic stress, was purchased from SIYE buffalo farm Guanxi, China, for slaughtering and sample collection. A total of 24 samples from different body parts of the swamp buffalo were collected. These samples were categorized into two groups, including the brain

and non-brain tissues. The details of the samples are given in Table 1. All these samples were used for transcriptomic sequencing analysis.

2.2. RNA Extraction, Quantification, and Quality Assessment. The total RNA of each sample was extracted by using the Trizol method [33]. Further, the purity and concentration of RNA were checked by using NanoDrop 2000 (Thermo Fisher Scientific, Wilmington, DE), and the integrity of RNA was evaluated through the RNA Nano 6000 Assay Kit of the Agilent Bioanalyzer 2100 system (Agilent Technologies, CA, USA).

2.3. Library Preparation for Transcriptomic Sequencing. To prepare the RNA sample, 1 μ g RNA from each sample was used. The NEBNext Ultra™ RNA Library Prep Kit for Illumina (NEB, USA) was used to generate the sequence libraries by following the recommendations of the manufacturer, and index codes were given to each sample feature. Briefly, the magnetic beads (poly-T oligo-attached) were used to purify the mRNA from total RNA. In NEBNext, first-strand synthesis reaction buffer (5 \times) at high temperature divalent cations was used for disintegration. The first cDNA strand was produced by using a random hexamer primer along with M-MuLV Reverse Transcriptase, while RNase H and DNA polymerase I was subsequently used to synthesize the second cDNA strand. The remaining overhangs via exonuclease/polymerase activities were changed into blunt ends. After the adenylation of DNA fragments 3' ends, the hairpin loop structure and NEBNext adaptor were ligated for hybridization purposes. The AMPure XP system (Beckman Coulter, Beverly, USA) was used to purify the library fragments to select cDNA fragments especially in the length of 240 bp. Meanwhile, before PCR, a 3 μ l of USER Enzyme (NEB, USA) was added with selected size and ligated-adaptor to cDNA at 37°C for 15 minutes and followed by 5 minutes at 95°C. Then, universal PCR primers, Index (X) primer, and Phusion High-Fidelity DNA polymerase were used to perform the PCR. At last, the AMPure XP system was used to purify the PCR products, and Agilent Bioanalyzer 2100 system was employed to access the quality of the library [34].

2.4. Clustering and Sequencing. The cBot Cluster Generation System using TruSeq PE Cluster Kit v4-cBot-HS (Illumina) was used to perform the index-coded samples clustering analysis as per the manufacturer's instructions. After the generation of the cluster, the prepared library was sequenced by using an Illumina platform (HiSeq X Ten), and reads with paired ends were produced.

2.5. Data Analysis

2.5.1. Quality Control. Firstly, the in-house Perl scripts were used to process the raw reads (raw data). The clean reads (clean data) were obtained after removing the reads having ploy-N and low-quality and adaptor sequences from the raw data. Moreover, the GC-content, Q20, Q30, and level of sequence duplication in clean reads were calculated. The high-quality clean data was used for further downstream analyses [35].

TABLE 1: Details of tissues of swamp buffalo used for sample collection.

Sr. no.	Sample tissue	Abbreviation
1	Dorsal muscles	BJ
2	Lung	F
3	Liver	GZ
4	Pain sense(24 + 32 area)	KJ24-32Q
5	Oarium (ovarium or ovary)	LC
6	Spleen	P
7	Emotional area 23 + 31	QG23-31
8	Emotional area 35	QG35Q
9	Anterior tongue muscle	QS
10	Kidney	S
11	Conarium	SGT
12	Visual sense (7-20 area)	SJ-7-20Q
13	Sense of hearing (21-22 area)	TJ21-22Q
14	Taste, language 43 area	WJYY43Q
15	Heart	X
16	Sense of smell (25 + 11 area)	XJ25-11Q
17	Opisthencephalon	XN
18	Hypothalamus	XQN
19	Sport (44-45 area, 4 + 6 area)	YD44-45Q
20	Right hind leg muscle	YHT
21	Right fore-muscle	YQZ
22	Bulbus rhachidicus	YS
23	Fattiness	ZF
24	Uterus	ZG

2.5.2. *Comparative Analysis.* Subsequently removing the low-quality and adaptor sequences from the data sets, the clean reads after data processing were transformed from raw sequences. Hisat2 tools software was used to map the clean reads to the reference genome and the sequences with exact match or single mismatch were further evaluated and annotated to the reference genome.

2.5.3. *Gene Functional Annotation.* For gene functional annotation, various databases were utilized including, Nt (NCBI nonredundant nucleotide sequences), Nr (NCBI nonredundant protein sequences), KOG/COG (Clusters of Orthologous Groups of proteins), Pfam (Protein family), GO (Gene Ontology), Swiss-Prot (A manually annotated and reviewed protein sequence database), and KO (KEGG Ortholog database) [36, 37].

2.5.4. *SNP Calling.* For each sample sorting, removing the duplicated reads and bam alignment merging was done by samtools (v0.1.18) and Picard-tools (v1.41). Moreover, SNP calling was accessed by GATK2 or samtools software. The GATK standard filter method with other parameters (including cluster Window Size: 10; MQ0 > = 4 and (MQ0/(1.0*DP) > 0.1; QUAL < 10; QUAL < 30.0 or QD <

5.0 or HRun > 5), were used to filter the raw vcf files and the SNPs with distance > 5 were retained [35, 38].

2.5.5. *Quantification of Gene Expression Levels.* The levels of gene expression were predicted in fragments per kilobase of transcript per million fragments mapped (FPKM) value by using the following formula:

$$FPKM = \frac{\text{cDNA fragments mapped}}{\text{fragments (millions)}} \times \text{transcript length (kb)}. \quad (1)$$

2.5.6. Differential Expression Analysis

(1) *For the Samples with Biological Replicates.* The DESeq2 was used to analyze the differential expression of the two tissue groups. Based on the negative binomial distribution model, DESeq2 provided practices to determine the differential expression of the digital gene expression dataset. Benjamini and Hochberg's approach were used to adjust the *P* value to control the false discovery rate (FDR). Statistically, the *P*value < 0.05 was used as the level of significance, and the genes with *P*value < 0.05 were perused as differentially expressed [39, 40].

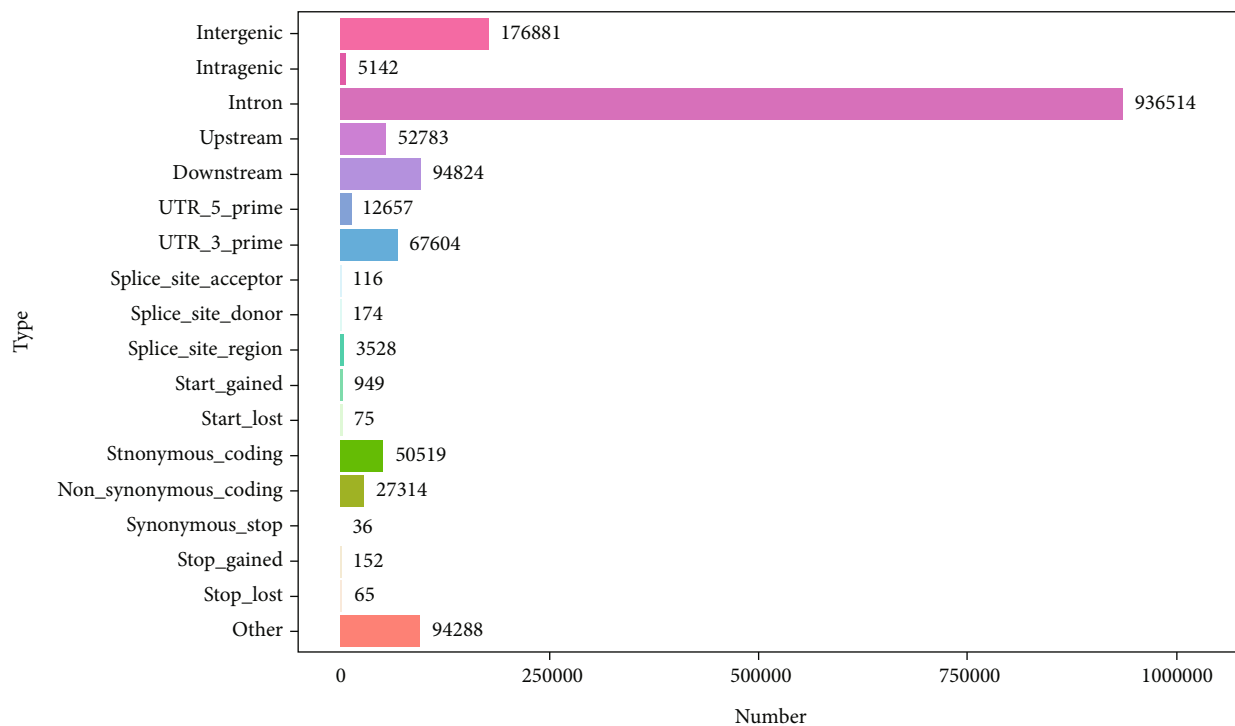
(2) *For the Samples without Biological Replicates.* For two samples, the edgeR was used to analyze the differential expression and the FDR value < 0.05 (FDR < 0.05) and fold change ≥ 2 (FC ≥ 2) was set as a criteria to categorize the significant differential expression [40, 41].

(3) *GO and KEGG Pathway Enrichment Analysis.* The Wallenius noncentral hypergeometric distribution based Goseq R packages [42] were used for GO (Gene Ontology) enrichment analysis of DEGs. The KEGG [43] is a biological system related database resource used to understand high-level utilities and functions associated with cells or organisms at the molecular level especially the large scale molecular datasets developed by high-throughput genome sequencing and experimental technologies (<http://www.genome.jp/kegg/>). The KOBAS [44] software was used to test the statistical enrichment of DEGs in KEGG pathways [43].

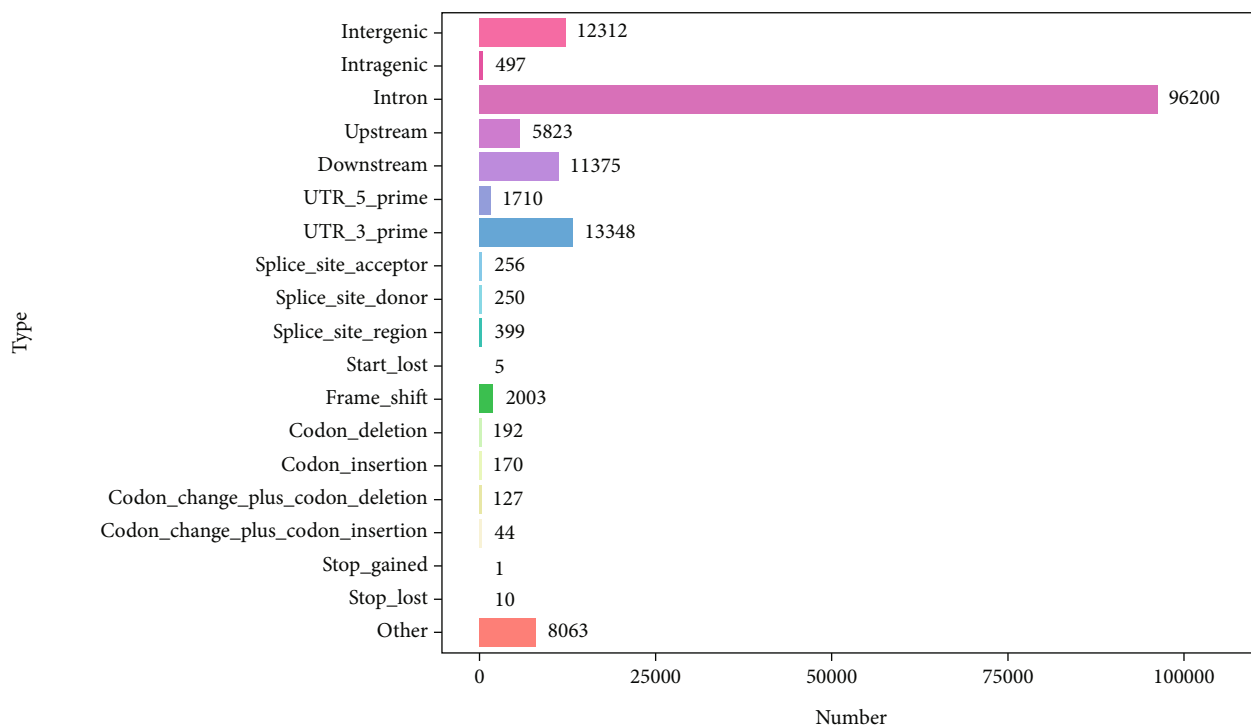
3. Results

3.1. Quality Assessment of the Data

3.1.1. *The Sequence Quality Score with Content Distribution and Data Statistics.* The quality of the data was accessed by using Phred quality scores *Q*, which is logarithmically associated with base calling error probabilities (*P*). The quality of all sample data with base error rates and ATCG content distribution is presented in Figure S1. All the samples showed an equal distribution of ATCG content revealing the accuracy of the data (Figure S1). Furthermore, after the quality control of sequenced data, a total of 178.57 Gb clean data were obtained with a minimum *Q* score as ≥ Q30 (91.27%) represented a 1/1000 probability of incorrect base call. The higher *Q* value results in lowering the false positive variants



(a)



(b)

FIGURE 1: The annotation classification of (a) SNPs and (b) InDel. [Note: The abscissa represents SNPs and InDel areas or types while ordinate is the classification numbers].

TABLE 2: The summary of novel gene number annotated in different databases.

Annotated databases	Novel gene number
GO	2,629
KEGG	1,713
KOG	541
Pfam	719
Swiss-Prot	753
Egglog	2,218
NR	3,619
COG	82
All	3,647

with the more consistent and reliable data set. The clean reads, clean bases, and GC contents were ranged between 21868067-28337044, 6560420100-8501113200, and 49.47-52.77%, respectively (Table S1).

3.1.2. The Transcriptomic Data Alignment with Reference Genome Sequence. Clean data read without paired ends were mapped to the reference genome exhibiting an alignment percentage (%) between 89.53% and 95.36% (Table S2). While the unique mapped read coverage was 84.88% to 92.48%, and the clean read percentage which multiply mapped to the reference genome was 2.13% to 4.83% (Table S2). Whereas, the percentage of clean reads marked on the sense vs. antisense chain of the reference genome was 44.58% vs. 43.79% to 47.50% vs. 47.47% (Table S2).

3.1.3. The Mapped Data Distribution on the Reference Genome with Exon, Intron, and Intergenic Regions. Additionally, the genome wide distribution of the reader's coverage was retrieved to find the location and distribution of the mapped reads on different chromosomes in terms of coverage depth, plotted on the reference genome with log₂ value ranged between -10 and 10 (Figure S2). The blue and green color represents the reads coverage on the positive and negative chain of the reference genome, respectively (Figure S2). Moreover, for each sample type the percentage of different regions including intronic, exonic, and intergenic regions based on number of mapped reads in reference to the specified reference genome were counted (Table S3). The highest exon count percentage was observed as 88.49% in the LC sample and the overall range was between 75.81% and 88.49% (Table S3). The percentage of intronic and intergenic regions for all samples was 5.05% to 16.74% and 6.04% to 7.89%, respectively (Table S3).

3.1.4. The RNA-Seq Library-Quality Evaluation. The RNA-seq library quality was accessed employing transcripts depth coverage to evaluate the randomness of the mRNA degradation and mRNA fragmentation, the distance from paired-end of read1 and read2 to judge the inserted lengths distribution extent, and the data saturation to assess the library capacity and mapped data adequacy (Figure S3(a) and (b)). All the sample RNA fragments' randomness was observed uniformly, which was simulated based on the density of mapped reads on

transcripts as shown in Figure S3(a). Further, for each sample data, the gene saturation with an interval of 15% FPKM was observed, and a gradual increase was seen, with gene saturation detected as 1 (Figure S3(b)).

3.2. Single Nucleotide Polymorphisms/InDel Analysis. Single nucleotide polymorphism (SNP) is referred to a single nucleotide variation in transcript sequence. We used GATK to identify the single base mismatch between the sample transcripts and the reference genome as a potential SNP site. The higher number of SNPs was perceived in P (495,289) and the lower number was detected in YD44-45Q4 (183,666) (Table S4). The spotted genic and intergenic SNPs were ranged between 153151 to 456941 and 29406 to 68294, respectively (Table S4). A higher ratio of transitions SNPs ($A > G$, $G > A$, $C > T$, and $T > C$) with a percentage between 71% and 73.22% as compared to the transversions ($A > C$, $C > A$, $A > T$, $T > A$, $C > G$, $G > C$, $G > T$, and $T > G$) was detected in all transcriptomic data (Table S4, Figure S4). Moreover, the SNP sites heterozygosity (more alleles) proportion was also determined which ranged from 20.31% in QS to 25.04% in KJ24-32Q (Table S4). The SNPs density for all the samples is presented in Figure S5, which showed a gradual increase of SNPs per kb of the gene length. But, the number of genes was inversely proportional to the number of SNPs per Kb (Figure S5).

Furthermore, the SnpEff tool was used to predict the SNP and InDel variability impact. In reference to the position and information on the reference genome, the location of variable sites in reference genome regions (CDS, intergenic, or genic regions, etc.) and their potential effects (nonsynonymous or synonymous mutations) were obtained (Figures 1(a) and 1(b)). A total of 936514, 176881, 94824, 67604, 52783, 12657, and 5142 SNPs were found in intronic, intergenic, downstream, 3'UTR, upstream, 5'UTR, and intragenic regions, respectively (Figure 1(a)). The synonymous coding/nonsynonymous coding SNPs ratio was 50519/27314 (Figure 1(a)). Besides, the annotated InDel retrieved on the reference genome were 96200, 13348, 12312, 11375, and 5823 in the intron, 3' UTR, intergenic, downstream, and upstream regions, respectively (Figure 1(b)).

The alternative splicing events for all samples were scanned by the ASProfile tool, which divided all these events into 12 different types. The TSS, TTS, AE, and SKIP were the most abundant mapped alternative splicing events of which the first alternative 5' exon splicing (TSS) and alternative 3' last exon splicing (TTS) were highly screened in all samples with value > 15000 (Figure S6), while XMIR was not detected in LC, P, QG23-31, QG35Q, SGT, WJYY43Q, and XN samples (Figure S6). Except for sample F, P, QS, S, YQZ, ZF, and ZG, the lower alternative splicing events XAE and XIR were also identified in all samples (Figure S6). While an equal ratio of XSKIP event was detected in all samples (Figure S6).

3.3. Novel Genes Detection and Functional Annotation. We used string tie to assemble the mapped reads based on the referenced genome and the original genome annotation was compared to discover the unique unannotated transcriptional regions, revealing novel transcripts and genes in the buffalo, and improved the existing genome annotation information.

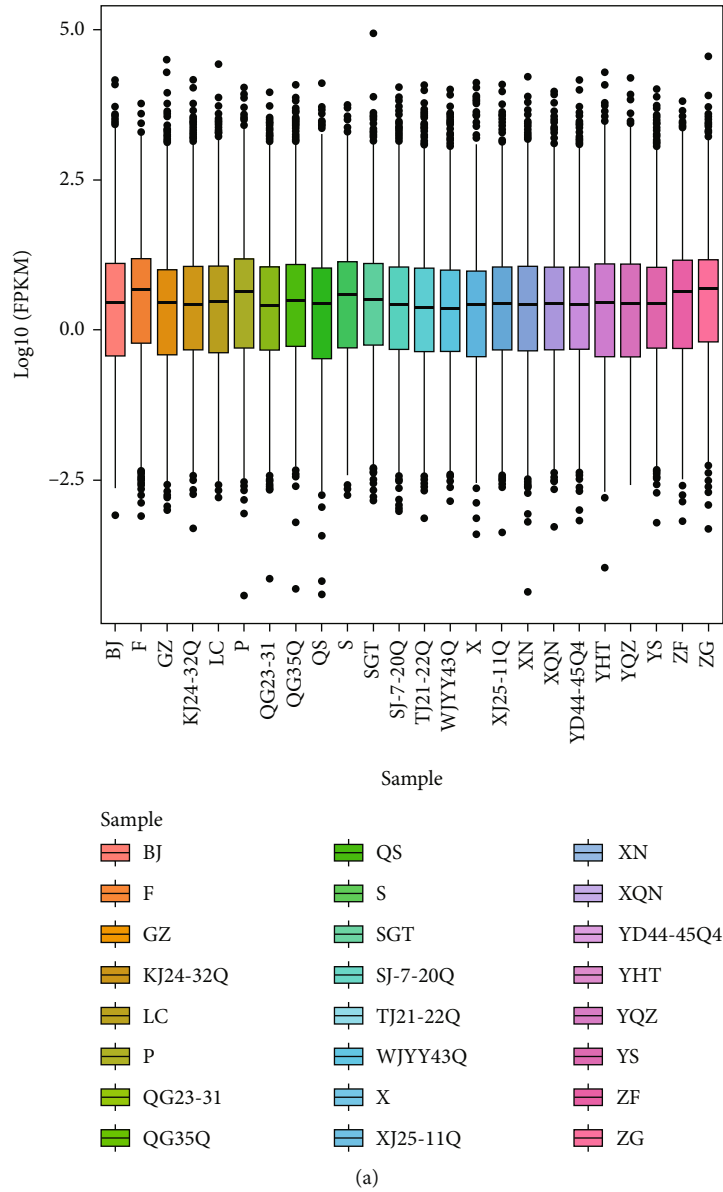


FIGURE 2: Continued.

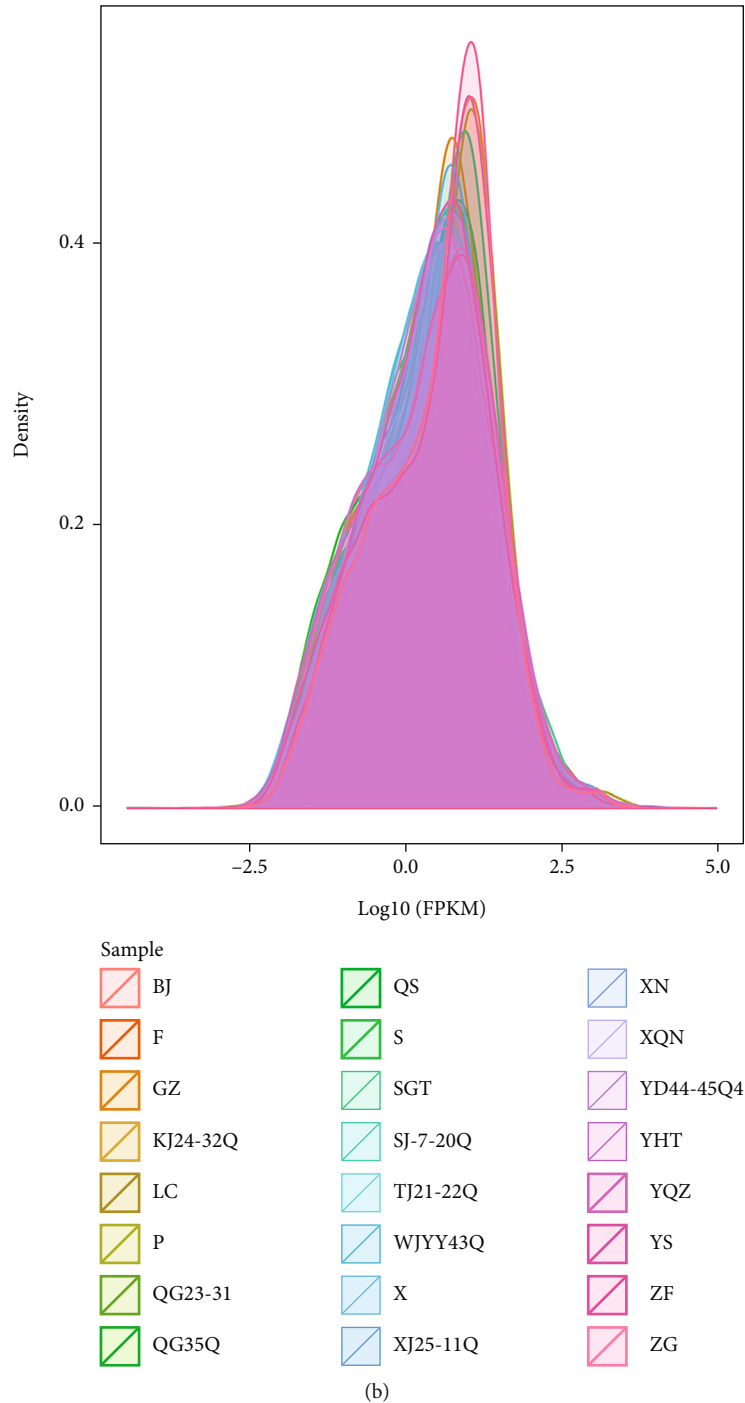


FIGURE 2: Expression levels for each sample are shown in box chart (a) and mRNAs FPKM density distribution in each sample (b).

A total of 5,574 novel genes were discovered after filtering the short peptides (<50 amino acid) and the sequence with a single exon. All the novel genes were blasted in different databases including GO, KEGG, KOG, Pfam, Swiss-Prot, eggNOG, NR, and COG to obtain the annotation information. The novel gene number annotated by different databases is summarized in Table 2.

3.4. Analysis of Genes Expression

3.4.1. Quantitation of Gene's Expression Levels. Using RNA-seq, a sum of 26363 mRNAs transcripts were detected, including 5574 novel mRNAs transcripts. The expression of transcripts was presented by FPKM value. The discrete angle of expression levels for each sample is shown in the

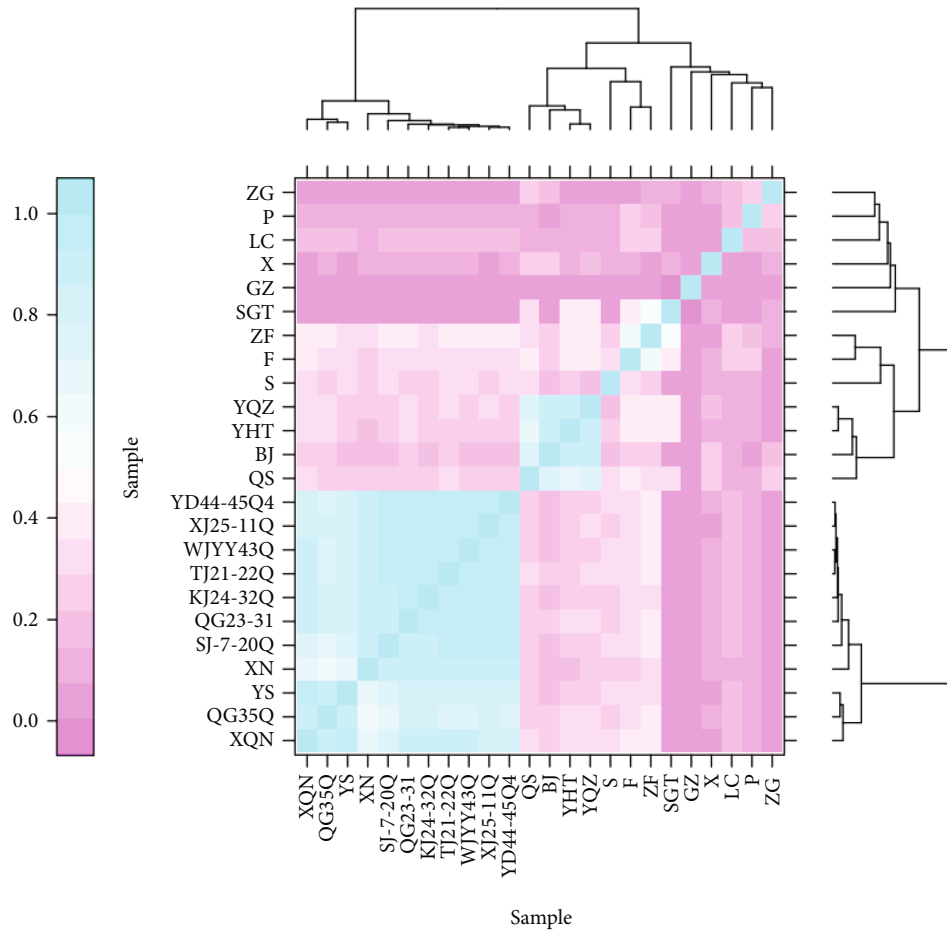


FIGURE 3: Heatmap for the correlation coefficients of samples.

box chart of Figure 2(a) and the mRNAs FPKM density distribution in all samples is shown in Figure 2(b).

3.4.2. Correlation Assessment of Biological Replicates. For transcriptomic data of biological samples, the correlation assessment is important which could provide reliable differentially expressed genes. To evaluate the index of correlation among all the samples, we used Pearson's correlation coefficient R for multiple biological samples prepared under the same conditions. The two samples are more related to each other with R^2 value close to 1 (Figure 3). So, we developed a relationship cluster diagram that reflected the relationship of the samples instinctively (Figure 3). The transcriptomic data reflected a consistent clustering effect where the samples XQN, QG35Q, YS, XN, SJ-7-20Q, QG23-31, KJ24-32Q, TJ21-22Q, WJYY43Q, XJ25-11Q, and YD44-45Q were found close to 1 and highly correlated to each other ensuring the reliability of the analysis (Figure 3).

3.4.3. Identification and Statistics of Differentially Expressed Genes. We used False Discovery Rate (FDR) < 0.05 and Fold Change (FC) ≥ 2 value as the screening criteria to identify DEGs. The FC values specified the proportion of gene expression in two groups (brain vs. non-brain tissues). The differentially expressed genes analysis was based on independent

statistical hypothesis testing, follow-on some false positives. Thus, we employed the Benjamini-Hochberg technique to correct the P value and made FDR a screening criterion. A total of 7,194 differentially expressed genes (DEGs) were identified, among which 3,999 were upregulated while 3,195 downregulated. The Volcano and MA plot was used for the presentation of gene expression level differences and the statistical significance in two groups (Figures 4(a) and 4(b)).

3.4.4. Clustering Analysis of DEGs. For hierarchical clustering analysis, the genes with differential expression were filtered and the genes with similar or same expression patterns were clustered together. The results of clustering analysis for DEGs in all the samples of both groups are shown in Figure 5.

3.4.5. Functional Annotation and Enrichment Analysis of DEGs. A total of 7,121 DEGs (brain vs. non-brain) were annotated in different functional annotation databases including GO, COG, KOG, KEGG, Pfam, Swiss-Prot, egg-nog, and NR with DEGs numbers 6267, 2152, 4781, 4744, 6431, 5493, 6929, and 7091, respectively.

3.4.6. Gene Ontology Classification of DEGs. For DEGs, the GO database was used to determine their role in biological

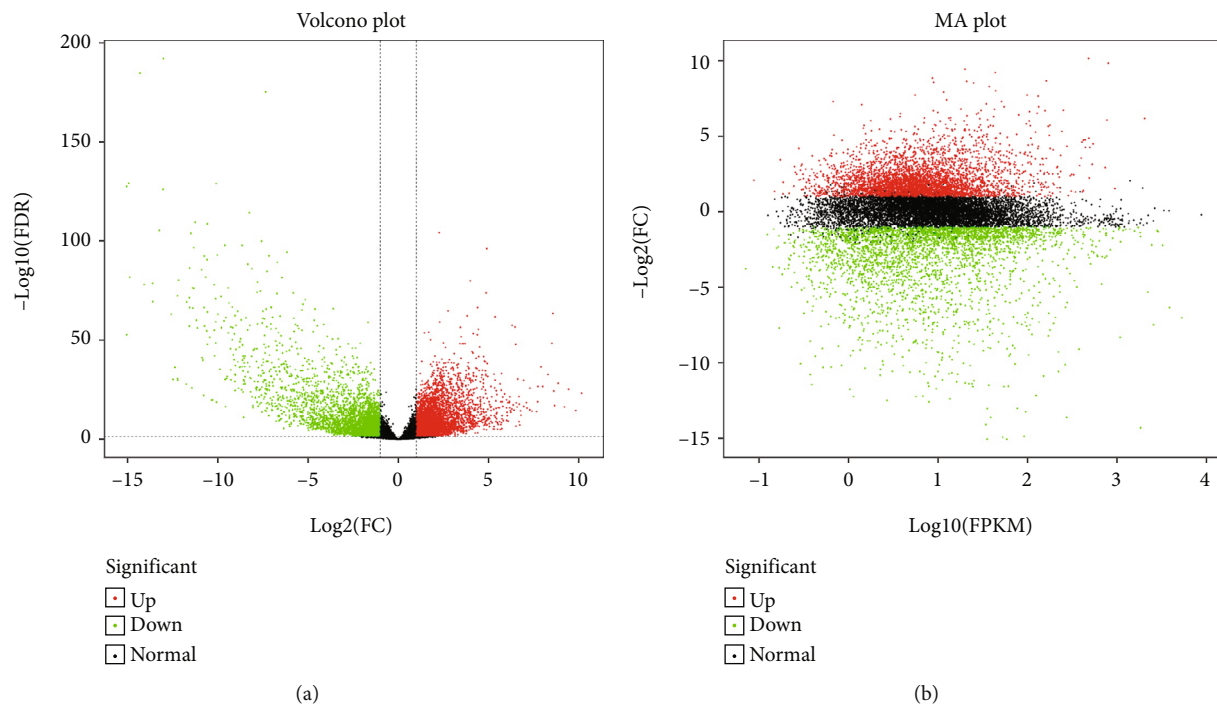


FIGURE 4: (a) Volcano plot presentation of DEGs (b) MA plot of DEGs. [Red, green, and black colors indicating the upregulated, downregulated, and normal genes, respectively].

processes, cellular components, and their molecular functions (Figure 6). The cellular component related DEGs were mainly involved in the extracellular region, membrane enclosed lumen, cell junction, synapses, supramolecular complex, virion part, nucleoid, and macromolecular complexes (Figure 6). Further, the DEGs involved in the biological process were associated with gene regulation, metabolism, development, immune system, behavior, growth, locomotion, apoptosis, rhythmic process, detoxification, reproduction, response to stimulus, signal transduction processes, and cellular response to abiotic stresses (Figure 6). The molecular functions related to DEGs included metabolic, signal transduction, transportation of molecules, antioxidant activity, transcription binding factors, protein tag, morphogen activity, electron transporter, and structural and binding activity (Figure 6).

3.4.7. Cluster of Orthologous Groups Analysis of DEGs. The COG database was also used for the annotation of DEGs (Figure 7). The products of DEGs were involved in general gene function, signal transduction mechanisms, posttranslational modification, protein turnover, chaperon activity, cell motility, metabolism, transportation, cellular and nuclear structural maintenance, transportation, defense mechanisms, etc. (Figure 7).

3.4.8. KEGG Annotation and Pathway Enrichment Analysis of DEGs. The KEGG database was used to annotate the DEGs and explore their association with different pathways. All the DEGs were classified according to their involvement in different functional pathways. About 591 DEGs were identified to be associated with pathways of cellular processes including endocytosis, regulation of actin cytoskeleton, cell cycle, apopto-

sis, phagosome, and tight junction, while 1291 DEGs were linked with different pathways of environmental information processing including various signaling pathways and molecular interactions (Figure 8(a)). Furthermore, for metabolism and genetic information processing related pathways, only 66 DEGs for each functional group were identified (Figure 8(a)). Moreover, the top 20 KEGG pathways with minimum Q values, which were analyzed by enrichment analysis for DEGs, are presented in Figure 8(b).

4. Discussion

The availability of massive DNA, RNA, and proteomic sequencing technologies has revolutionized the biological approaches which ultimately provides huge sequenced data output. For species with significant economic worth and poor genomic data resources like buffalo, it is imperative to develop improved and annotated sequenced genomic or transcriptome data, which would be helpful for understanding the genetic control of economic traits, genomic diversity, and evolutionary dynamics of available buffalo genetics resources. Transcriptomic sequencing is a cost-effective and powerful tool for producing good quality transcriptome data that might be used to explicate molecular markers and categorizing the novel genes in non-model and model organisms [45–48].

The advancement in this reverence requires both the data accuracy and reliability to decrease the error rate making the data more efficient [49]. Thus, using Phred quality scores Q with base calling error probabilities P is a crucial step to access the data quality [49]. A recent study by Singh et al. [50] isolated the RNA transcripts from buffalo liver tissues with an

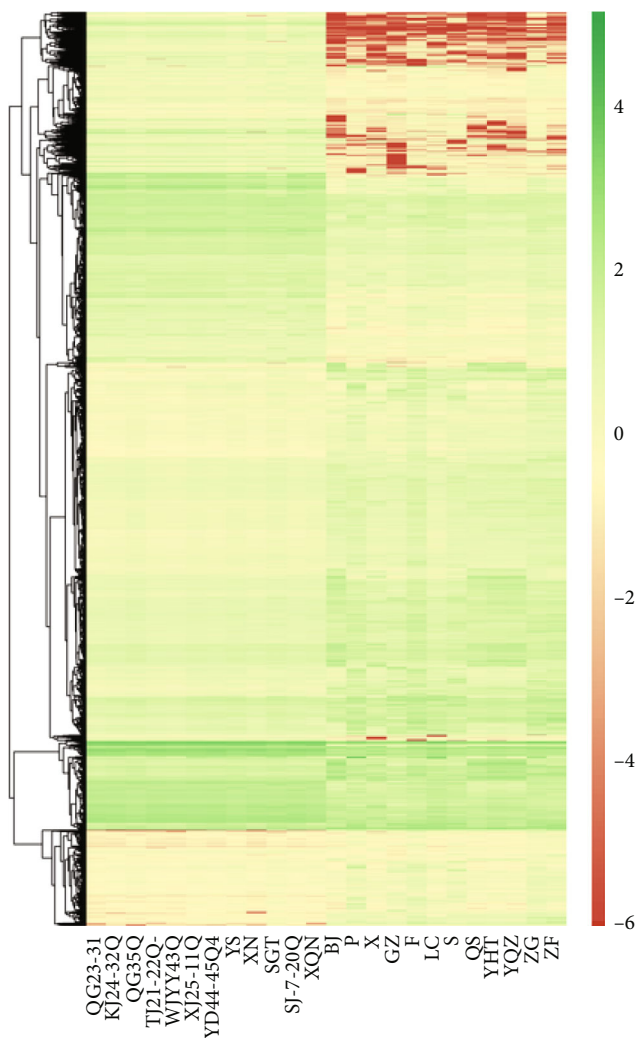


FIGURE 5: Cluster analysis of DEGs.

excellent quality of NGS data having score of FastQC quality up to 30. Further, they reported 54 million reads having an alignment percentage of $> 84\%$ with reference genome [50].

The 178.57 Gb clean transcriptomic data of our study with a minimum Q score of $\geq Q30$ revealed a 1/1000 probability of incorrect base calling and the clean reads with GC contents were 28337044 and 52.77%, respectively. Further, the clean data reads without paired ends were mapped to the reference genome with an alignment percentage of 95.36%. Earlier studies have reported that the genome wide percentage of the GC-contents in river buffalo was 42.20% and in other animals, it was 41.80%–42.30% [51–54], while our study presented a higher ratio of 52.77% GC contents. Our study is also in line with a previous study conducted on swamp buffalo having GC contents of 49.92% [55]. Moreover, a recent study on the whole genome sequence of buffalo figured out the 12.5% structural differences and 9170 structural differences were likely because of the assembly errors [56].

In comparison to the reference genome, the predicted percentage of the exonic region was 88.49% and the SNPs ratio was 456941 with a higher proportion of transition as com-

pared to the transversion with heterozygosity of 25.04%. Mostly, the detected SNPs and InDels were present in the intronic regions. This indicated the high quality transcriptome data produced from the swamp buffalo and these tissue specific unique transcripts could be utilized for designing further experiments related to transgenesis, gene cloning, and molecular genetics of the swamp buffalo [57, 58].

The alternative splicing event could produce different transcripts encoded by a single gene and can translate into protein, which varies in their sequence and function. It is an important mechanism involved in tissue specific gene expression regulation and can enhance protein diversity [59]. In this study, a total of 12 alternative splicing events were identified of which TSS, TTS, AE, and SKIP were the most abundant mapped alternative splicing events where the first alternative 5' exon splicing and alternative 3' last exon the last exon splicing were highly screened in all tissue samples.

We identified a total of 26363 mRNAs transcripts including 5574 novel mRNAs transcripts. Our study presented 34.57% novel genes whose function has not been yet identified after blasting all these novel genes in different

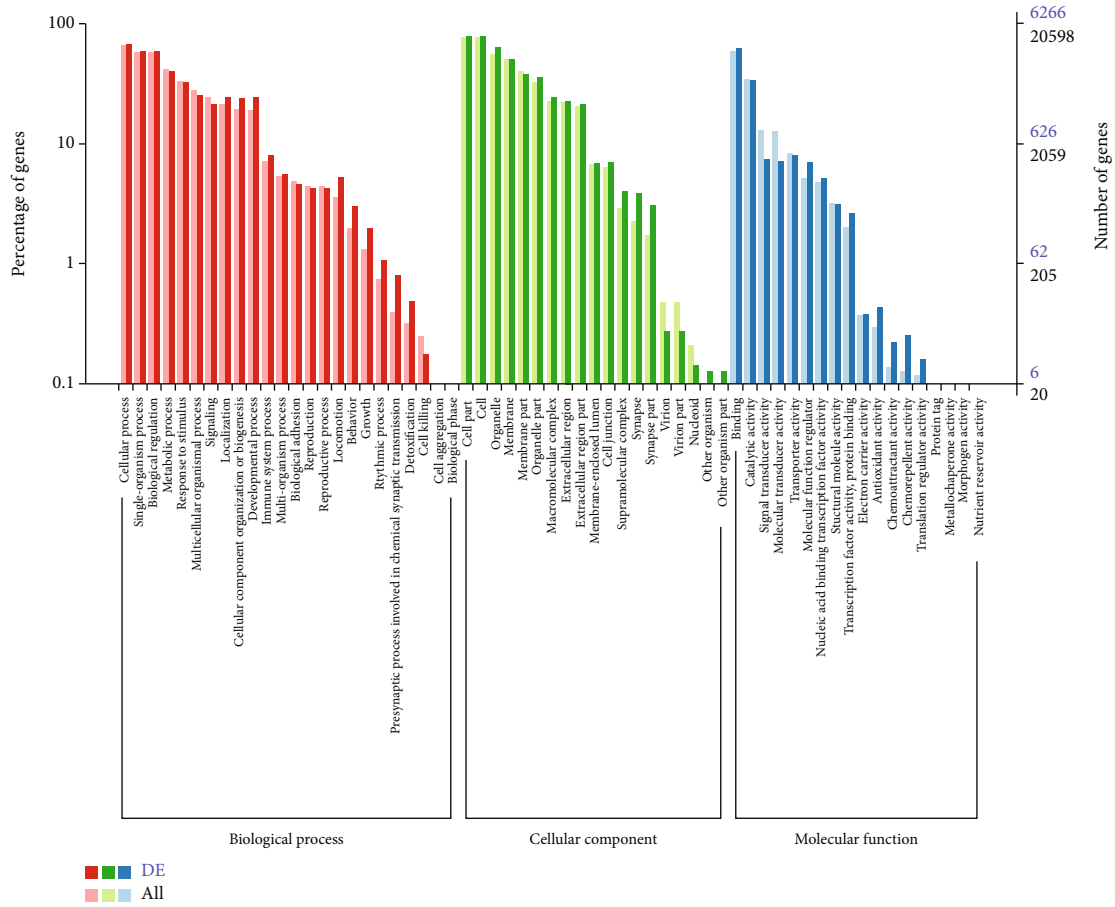


FIGURE 6: GO classification results of DEGs.

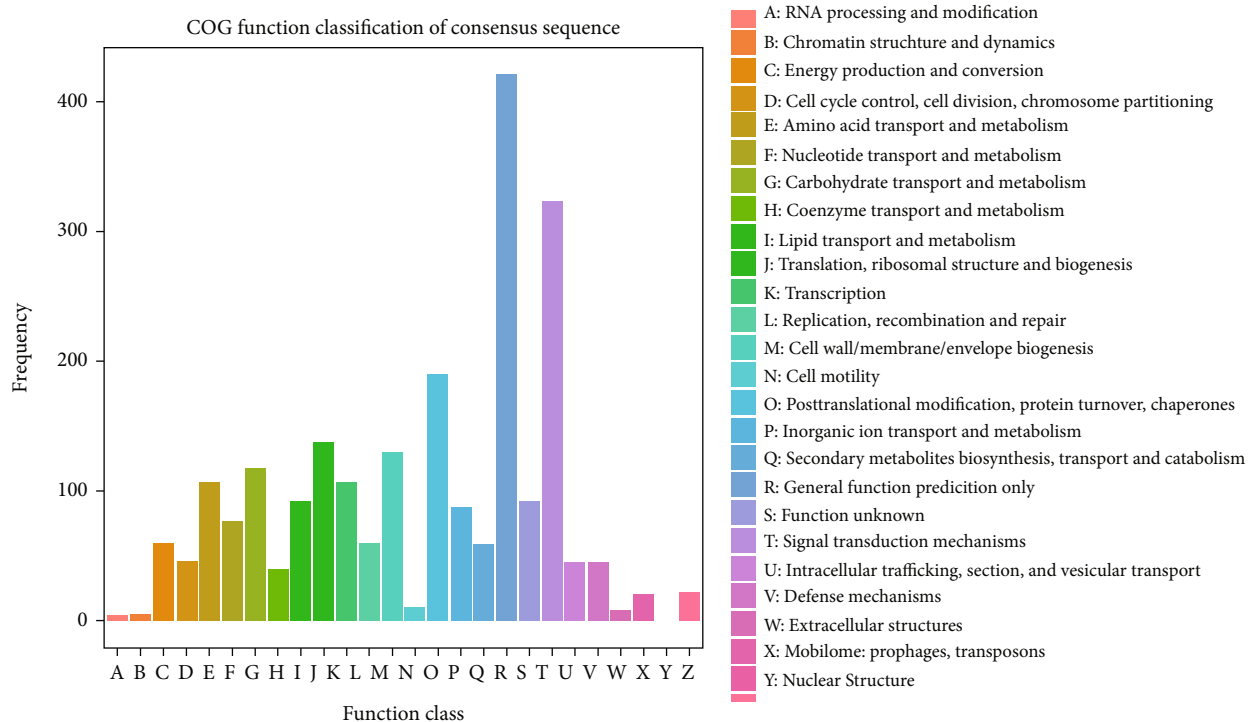
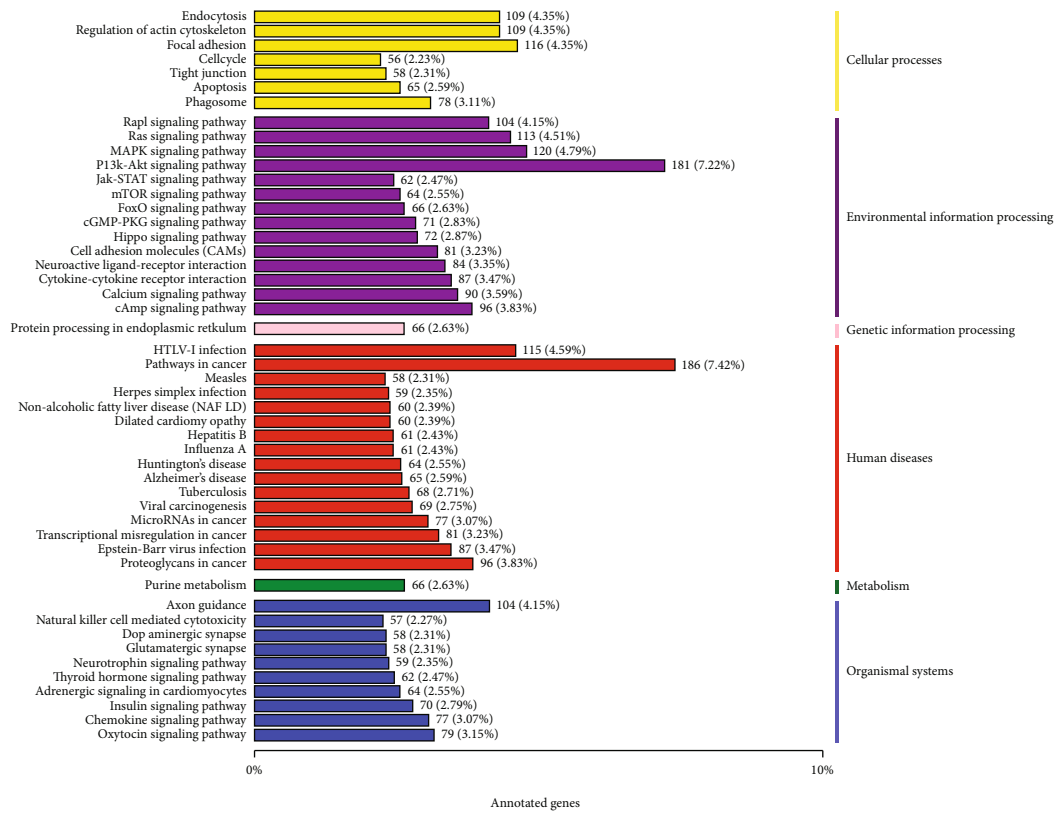
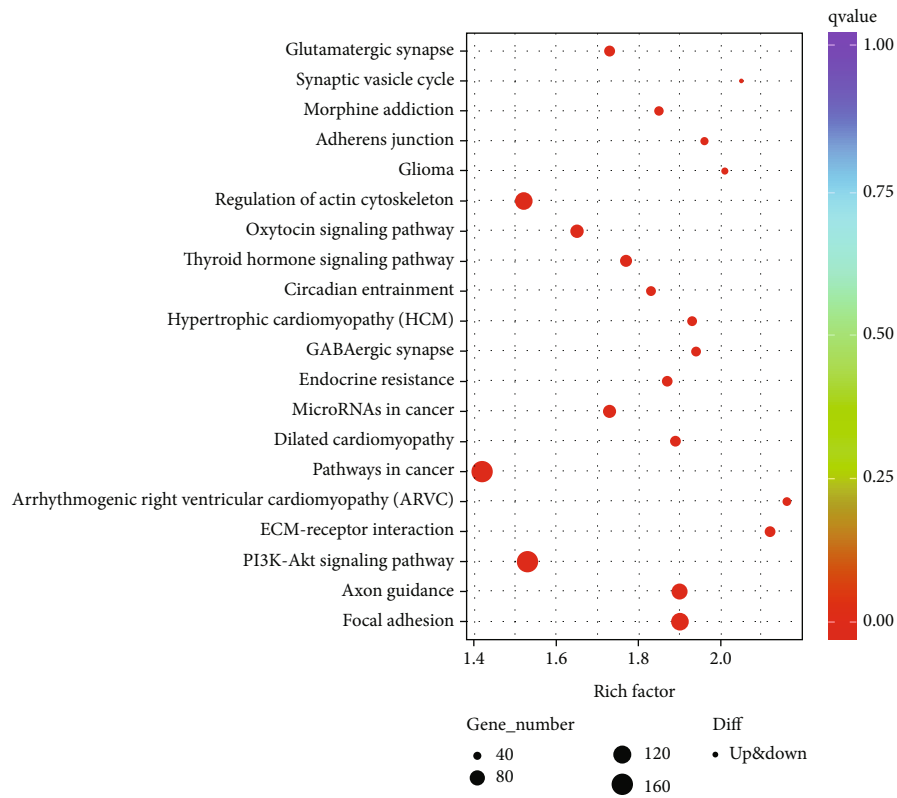


FIGURE 7: The COG annotation of DEGs.



(a)



(b)

FIGURE 8: (a) KEGG annotation of DEGs. (b) The top 20 KEGG pathway enrichment bubble diagram of DEGs.

databases including GO, KEGG, KOG, Pfam, Swiss-Prot, egg NOG, NR, and COG for annotated information, while the previous study indicated only 27.53% novel gene in swamp buffalo with unknown function [55]. For any transcriptomic analysis, the identification of DEGs is very critical [60]. Our study found variations in the expression of genes such as about 55.58% (3,999) genes were upregulated and 44.41% (3,195) were downregulated genes. In the NR database, most of the genes were annotated to *Bubalus bubalis*, *Bos taurus*, and *Bos mutus*, perhaps due to the swamp buffalo is evolutionarily more close to *Bos taurus* and *Bos mutus* than other available genetic resources [61, 62].

The GO and COG predicted molecular functioning of DEGs as metabolic, signal transduction, electron transporter, and structural and binding activity. Moreover, among the top 20 pathways, cancer pathway, PI3k-Akt signaling, axon guidance, focal adhesion, and regulation of actin cytoskeleton were abundant while the other related pathways were involved in thyroid and oxytocin hormone signaling, synaptic vesicle cycle, adhere junction, circadian entertainment, etc. These findings are in agreement with the previous study of Deng et al. [55].

5. Conclusion

The current study is one of the most comprehensive studies conducted on the swamp buffalo using 24 tissue samples, which were grouped into two main categories (brain vs. non-brain). We obtained 178.57 Gb clean transcriptome data with $Q_{score} \geq Q_{30}$ and the clean reads with GC contents were 28337044 and 52.77%, respectively. The alignment percentage of clean data reads to the reference genome was 95.36% with 88.49% exon region coverage, and the SNPs ratio was 456941 with higher transition SNPs proportion with 25.04% heterozygosity. We incur 26363 mRNAs transcripts including 5574 (34.57%) novel genes of which 55.58% (3,999) were upregulated and 44.41% (3,195) downregulated. The DEGs were mainly involved in the metabolism, signal transduction, electron transporter, structural and binding activities, among the top hit pathways, cancer pathway, PI3k-Akt signaling, axon guidance, focal adhesion, and regulation of actin cytoskeleton were abundant.

Data Availability

The transcriptome sequences data of the swamp buffalo 24 tissues (12 brain and 12 non-brain tissues) were deposited to the NCBI-GenBank BioProject under the accession number PRJNA760646.

Ethical Approval

This study was conducted according to the guidelines of Care and Use of Laboratory Animals and explicitly approved by the Guangxi University Committee on Animal Research and Bioethics (GXU-2020-290).

Conflicts of Interest

The authors declare that the research was conducted in the absence of any commercial or financial relationships that could be construed as a potential conflict of interest.

Authors' Contributions

S.R., Q.L., and H.Y. were responsible for the conceptualization. S.R. and Q.L. worked on the resources. W.X., F.H., I.A., S.L., K.H., and S.R. were assigned in data curation. H.M.N.I., S.Y. and S.R. worked on methodology. W.X., I.A., K.H., F.H., S.R., S.L., H.M.N.I., S.Y., and F.H. were assigned in the software. Q.L., S.R., and H.Y. worked on the supervision of this study. W.X., F.H., and S.R. were responsible in writing—original draft preparation. W.X., F.H., M.A., I.A., S.L., S.Y., K.H., H.Y., H.M.N.I., S.R., and Q.L. were assigned in writing—review and editing. All authors have read and agreed to the published version of the manuscript." Wang Xiabo and Faiz-ul Hassan contributed equally to this work.

Acknowledgments

This research is supported by the National Natural Science Foundation of China (U20A2051), Guangxi Innovation Driven Project (AA22361), Innovative Team Project of Guangdong Universities 2022 (KCXTD029), and Guangxi University Postdoctorate Fellowship Research Grant (A3130051019).

Supplementary Materials

Figure S1. The data quality of the samples with ATCG content distribution and base error rates. Figure S2. Position of mapped reads on the reference genome and coverage depth distribution. Figure S3. (a) The depth distributions of mapped reads on transcripts (b) the RNA-seq data saturation simulation. Figure S4. The types of SNP mutations in sequenced data (transition and transversion). Figure S5. The genes SNP density distribution. Figure S6. Statistics of alternative splicing events. Table S1. The statistics of the sequenced data. Table S2. The sequenced data mapping statistics. Table S3. Percentage of exonic, intergenic, and intronic regions of mapped reads on the reference genome. Table S4. SNP statistics detected in all samples. (*Supplementary Materials*)

References

- [1] A. S. Nanda and T. Nakao, "Role of buffalo in the socioeconomic development of rural Asia: current status and future prospectus," *Animal Science Journal*, vol. 74, no. 6, pp. 443–455, 2003.
- [2] S. U. Rehman, F. U. Hassan, X. Luo, Z. Li, and Q. Liu, "Whole-genome sequencing and characterization of buffalo genetic resources: recent advances and future challenges," *Animals*, vol. 11, no. 3, p. 904, 2021.
- [3] S. U. Rehman, A. Nadeem, M. Javed et al., "Genomic identification, evolution and sequence analysis of the heat-shock

- protein gene family in buffalo,” *Genes*, vol. 11, no. 11, p. 1388, 2020.
- [4] V. N. Michelizzi, M. V. Dodson, Z. Pan et al., “Water buffalo genome science comes of age,” *International Journal of Biological Sciences*, vol. 6, no. 4, pp. 333–349, 2010.
 - [5] S. u. Rehman, T. Feng, S. Wu et al., “Comparative genomics, evolutionary and gene regulatory regions analysis of casein gene family in *Bubalus bubalis*,” *Frontiers in Genetics*, vol. 12, no. 408, 2021.
 - [6] A. Borghese, *Buffalo livestock and products*, vol. 37 (Special Issue 1), pp. 50–74, Buffalo Bulletin, 2013.
 - [7] C. Zhang, W. Wu, L. Zou, and R. Shi, *Science and Technology in Chinese Buffaloes*, Guangxi Science and Technology Publishing House, Nanning, China, 2000.
 - [8] S. U. Rehman, L. Shafique, M. R. Yousuf, Q. Liu, J. Z. Ahmed, and H. Riaz, “Spectrophotometric calibration and comparison of different semen evaluation methods in Nili-Ravi buffalo bulls,” *Pakistan Veterinary Journal*, vol. 39, no. 4, pp. 568–572, 2019.
 - [9] B.-Z. Yang, X.-W. Liang, J. Qin, C.-J. Yang, and J.-H. Shang, “Brief introduction to the development of Chinese dairy buffalo industry,” *Buffalo Bulletin*, vol. 32, no. 1, pp. 111–120, 2013.
 - [10] M. Drost, “Advanced reproductive technology in the water buffalo,” *Theriogenology*, vol. 68, no. 3, pp. 450–453, 2007.
 - [11] W. Shi, X. Yuan, K. Cui et al., “LC-MS/MS based metabolomics reveal candidate biomarkers and metabolic changes in different buffalo species,” *Animals*, vol. 11, no. 2, p. 560, 2021.
 - [12] H. Warriach, D. McGill, R. Bush, P. Wynn, and K. Chohan, “A review of recent developments in buffalo reproduction—a review,” *Asian-Australasian Journal of Animal Sciences*, vol. 28, no. 3, pp. 451–455, 2015.
 - [13] Y. Zheng, Y. Zhang, L. Wu et al., “Generation of heritable prominent double muscle buttock rabbits via novel site editing of myostatin gene using CRISPR/Cas9 system,” *Frontiers in Veterinary Science*, vol. 9, 2022.
 - [14] C. A. Labarrere, J. R. Woods, J. W. Hardin et al., “Early prediction of cardiac allograft vasculopathy and heart transplant failure,” *American Journal of Transplantation*, vol. 11, no. 3, pp. 528–535, 2011.
 - [15] C. Lei, C. Zhang, S. Weining et al., “Genetic diversity of mitochondrial cytochrome b gene in Chinese native buffalo,” *Animal Genetics*, vol. 42, no. 4, pp. 432–436, 2011.
 - [16] X. Yuan, W. Shi, J. Jiang et al., “Comparative metabolomics analysis of milk components between Italian Mediterranean buffaloes and Chinese Holstein cows based on LC-MS/MS technology,” *PLoS One*, vol. 17, no. 1, article e0262878, 2022.
 - [17] M. A. El-Magd, H. G. Abo-Al-Ela, A. El-Nahas, A. A. Saleh, and A. A. Mansour, “Effects of a novel SNP of IGF2R gene on growth traits and expression rate of IGF2R and IGF2 genes in gluteus medius muscle of Egyptian buffalo,” *Gene*, vol. 540, no. 2, pp. 133–139, 2014.
 - [18] Z. Li, S. Lu, K. Cui et al., “Fatty acid biosynthesis and transcriptional regulation of Stearoyl-CoA desaturase 1 (SCD1) in buffalo milk,” *BMC Genetics*, vol. 21, no. 1, pp. 1–10, 2020.
 - [19] A. Pauciullo, G. Cosenza, R. Steri et al., “A single nucleotide polymorphism in the promoter region of River buffalo stearoyl CoA desaturase gene (SCD) is associated with milk yield,” *Journal of Dairy Research*, vol. 79, no. 4, pp. 429–435, 2012.
 - [20] D. Iamartino, J. L. Williams, T. Sonstegard et al., “The buffalo genome and the application of genomics in animal management and improvement,” *Buffalo Bulletin*, vol. 32, Special Issue 1, pp. 151–158, 2013.
 - [21] L. Sun, Z. Cui, S. Huang et al., “Effect of environmental temperature on semen quality and seminal plasma metabolites of Mediterranean buffalo bulls,” *Animal Biotechnology*, vol. 33, no. 5, pp. 970–980, 2022.
 - [22] S. Wu, F.-U. Hassan, Y. Luo et al., “Comparative genomic characterization of buffalo fibronectin type III domain proteins: exploring the novel role of FNDC5/Irisin as a ligand of gonadal receptors,” *Biology*, vol. 10, no. 11, p. 1207, 2021.
 - [23] X. Luo, Y. Zhou, B. Zhang et al., “Understanding divergent domestication traits from the whole-genome sequencing of swamp- and river-buffalo populations,” *National Science Review*, vol. 7, no. 3, pp. 686–701, 2020.
 - [24] A. V. Zimin and J. Williams, “*Bubalus bubalis*, whole genome shotgun sequencing project USA,” 2015, <http://www.ncbi.nlm.nih.gov/nuccore/547177826>.
 - [25] M. Javed, A. Nadeem, F.-U. Hassan, and H. Mujahid, “Genomic analysis of arginine vasopressin gene in riverine buffalo reveals its potential association with silent estrus behavior,” *Molecular Biology Reports*, vol. 49, no. 10, pp. 9315–9324, 2022.
 - [26] M. S.-U. Rehman, F. U. Hassan, Z. U. Rehman, I. Shtiaq, S. Rehman, and Q. Liu, “Molecular characterization of TGF-Beta gene family in buffalo to identify gene duplication and functional mutations,” *Genes*, vol. 13, no. 8, p. 1302, 2022.
 - [27] F. R. Finseth and R. G. Harrison, “A comparison of next generation sequencing technologies for transcriptome assembly and utility for RNA-Seq in a non-model bird,” *PLoS One*, vol. 9, no. 10, article e108550, 2014.
 - [28] F. U. Hassan, A. Nadeem, Z. Li et al., “Role of peroxisome proliferator-activated receptors (PPARs) in energy homeostasis of dairy animals: exploiting their modulation through nutrigenomic interventions,” *International Journal of Molecular Sciences*, vol. 22, no. 22, p. 12463, 2021.
 - [29] C. Zhang, G. Wang, J. Wang et al., “Characterization and comparative analyses of muscle transcriptomes in Dorper and small-tailed Han sheep using RNA-Seq technique,” *PLoS One*, vol. 8, no. 8, article e72686, 2013.
 - [30] R. Geng, C. Yuan, and Y. Chen, “Exploring differentially expressed genes by RNA-Seq in cashmere goat (*Capra hircus*) skin during hair follicle development and cycling,” *PLoS One*, vol. 8, no. 4, article e62704, 2013.
 - [31] A. Cánovas, G. Rincon, A. Islas-Trejo, S. Wickramasinghe, and J. F. Medrano, “SNP discovery in the bovine milk transcriptome using RNA-Seq technology,” *Mammalian Genome*, vol. 21, no. 11-12, pp. 592–598, 2010.
 - [32] L. Karthik, G. Kumar, T. Keswani, A. Bhattacharyya, S. S. Chandar, and K. B. Rao, “Protease inhibitors from marine actinobacteria as a potential source for antimalarial compound,” *PLoS One*, vol. 9, no. 3, article e90972, 2014.
 - [33] K. C. Pavani, E. E. Baron, M. Faheem, A. Chaveiro, and F. M. Da Silva, “Optimisation of total RNA extraction from bovine oocytes and embryos for gene expression studies and effects of cryoprotectants on total RNA extraction,” *Cytology and Genetics*, vol. 49, no. 4, pp. 232–239, 2015.
 - [34] Z. Chen, J. Zhao, J. Song et al., “Influence of graphene on the multiple metabolic pathways of *Zea mays* roots based on transcriptome analysis,” *PLoS One*, vol. 16, no. 1, article e0244856, 2021.
 - [35] A. McKenna, M. Hanna, E. Banks et al., “The genome analysis toolkit: a MapReduce framework for analyzing next-

- generation DNA sequencing data,” *Genome Research*, vol. 20, no. 9, pp. 1297–1303, 2010.
- [36] R. D. Finn, J. Tate, J. Mistry et al., “The Pfam protein families database,” *Nucleic Acids Research*, vol. 36, Supplement_1, pp. D281–D288, 2007.
- [37] S. Götz, J. M. García-Gómez, J. Terol et al., “High-throughput functional annotation and data mining with the Blast2GO suite,” *Nucleic Acids Research*, vol. 36, no. 10, pp. 3420–3435, 2008.
- [38] H. Li, B. Handsaker, A. Wysoker et al., “The sequence alignment/map format and SAMtools,” *Bioinformatics*, vol. 25, no. 16, pp. 2078–2079, 2009.
- [39] S. Anders and W. Huber, “Differential expression analysis for sequence count data,” *Nature Precedings*, p. 1, 2010.
- [40] M. I. Love, W. Huber, and S. Anders, “Moderated estimation of fold change and dispersion for RNA-seq data with DESeq2,” *Genome Biology*, vol. 15, no. 12, pp. 1–21, 2014.
- [41] M. D. Robinson, D. J. McCarthy, and G. K. Smyth, “edgeR: a bioconductor package for differential expression analysis of digital gene expression data,” *Bioinformatics*, vol. 26, no. 1, pp. 139–140, 2010.
- [42] M. D. Young, M. J. Wakefield, G. K. Smyth, and A. Oshlack, “Gene ontology analysis for RNA-seq: accounting for selection bias,” *Genome Biology*, vol. 11, no. 2, p. R14, 2010.
- [43] M. Kanehisa, M. Araki, S. Goto et al., “KEGG for linking genomes to life and the environment,” *Nucleic Acids Research*, vol. 36, Supplement_1, pp. D480–D484, 2007.
- [44] X. Mao, T. Cai, J. G. Olyarchuk, and L. Wei, “Automated genome annotation and pathway identification using the KEGG Orthology (KO) as a controlled vocabulary,” *Bioinformatics*, vol. 21, no. 19, pp. 3787–3793, 2005.
- [45] M. G. Grabherr, B. J. Haas, M. Yassour et al., “Full-length transcriptome assembly from RNA-Seq data without a reference genome,” *Nature Biotechnology*, vol. 29, no. 7, pp. 644–652, 2011.
- [46] P. G. Koringa, S. J. Jakhesara, V. D. Bhatt, A. B. Patel, D. Dash, and C. G. Joshi, “Transcriptome analysis and SNP identification in SCC of horn in (*Bos indicus*) Indian cattle,” *Gene*, vol. 530, no. 1, pp. 119–126, 2013.
- [47] K. Ropka-Molik, K. Żukowski, R. Eckert, A. Gurgul, K. Piórkowska, and M. Oczkiewicz, “Comprehensive analysis of the whole transcriptomes from two different pig breeds using RNA-Seq method,” *Animal Genetics*, vol. 45, no. 5, pp. 674–684, 2014.
- [48] Z. Wang, Y. Fan, J. Xu et al., “Transcriptome analysis of the hippocampus in novel rat model of febrile seizures,” *PLoS One*, vol. 9, no. 4, article e95237, 2014.
- [49] B. Ewing and P. Green, “Base-calling of automated sequencer traces using phred. II. Error probabilities,” *Genome Research*, vol. 8, no. 3, pp. 186–194, 1998.
- [50] S. Singh, N. Golla, D. Sharma, D. Singh, and S. K. Onteru, “Buffalo liver transcriptome analysis suggests immune tolerance as its key adaptive mechanism during early postpartum negative energy balance,” *Functional & Integrative Genomics*, vol. 19, no. 5, pp. 759–773, 2019.
- [51] Y. Dong, M. Xie, Y. U. Jiang et al., “Sequencing and automated whole-genome optical mapping of the genome of a domestic goat (*Capra hircus*),” *Nature Biotechnology*, vol. 31, no. 2, pp. 135–141, 2013.
- [52] The Bovine Genome Sequencing and Analysis Consortium, C. G. Elsik, R. L. Tellam, and K. C. Worley, “The genome sequence of taurine cattle: a window to ruminant biology and evolution,” *Science*, vol. 324, no. 5926, pp. 522–528, 2009.
- [53] M. A. Groenen, A. L. Archibald, H. Uenishi et al., “Analyses of pig genomes provide insight into porcine demography and evolution,” *Nature*, vol. 491, no. 7424, pp. 393–398, 2012.
- [54] X. Xu, W. Chen, R. Talbot et al., “Genome data from the sheep,” *GigaScience*, 2011.
- [55] T. Deng, C. Pang, X. Lu et al., “De novo transcriptome assembly of the Chinese swamp buffalo by RNA sequencing and SSR marker discovery,” *PLoS One*, vol. 11, no. 1, article e0147132, 2016.
- [56] W. Y. Low, R. Tearle, D. M. Bickhart et al., “Chromosome-level assembly of the water buffalo genome surpasses human and goat genomes in sequence contiguity,” *Nature Communications*, vol. 10, no. 1, p. 260, 2019.
- [57] K. D. Hansen, R. A. Irizarry, and Z. Wu, “Removing technical variability in RNA-seq data using conditional quantile normalization,” *Biostatistics*, vol. 13, no. 2, pp. 204–216, 2012.
- [58] D. Risso, K. Schwartz, G. Sherlock, and S. Dudoit, “GC-content normalization for RNA-Seq data,” *BMC Bioinformatics*, vol. 12, no. 1, pp. 1–17, 2011.
- [59] D. S. Greenberg and H. Soreq, “Alternative Splicing,” in *Brenner’s Encyclopedia of Genetics*, 97–98, 2013.
- [60] T. Deng, A. Liang, S. Liang et al., “Integrative analysis of transcriptome and GWAS data to identify the hub genes associated with milk yield trait in buffalo,” *Frontiers in Genetics*, vol. 10, p. 36, 2019.
- [61] Q. Qiu, G. Zhang, T. Ma et al., “The yak genome and adaptation to life at high altitude,” *Nature Genetics*, vol. 44, no. 8, pp. 946–949, 2012.
- [62] A. V. Zimin, A. L. Delcher, L. Florea et al., “A whole-genome assembly of the domestic cow, *Bos taurus*,” *Genome Biology*, vol. 10, no. 4, p. R42, 2009.

Retraction

Retracted: The Comparative Pharmacokinetics and Histokinetics of the Therapeutic Dose of Estradiol Valerate and Bromocriptine in Common Quails

BioMed Research International

Received 8 January 2024; Accepted 8 January 2024; Published 9 January 2024

Copyright © 2024 BioMed Research International. This is an open access article distributed under the Creative Commons Attribution License, which permits unrestricted use, distribution, and reproduction in any medium, provided the original work is properly cited.

This article has been retracted by Hindawi following an investigation undertaken by the publisher [1]. This investigation has uncovered evidence of one or more of the following indicators of systematic manipulation of the publication process:

- (1) Discrepancies in scope
- (2) Discrepancies in the description of the research reported
- (3) Discrepancies between the availability of data and the research described
- (4) Inappropriate citations
- (5) Incoherent, meaningless and/or irrelevant content included in the article
- (6) Manipulated or compromised peer review

The presence of these indicators undermines our confidence in the integrity of the article's content and we cannot, therefore, vouch for its reliability. Please note that this notice is intended solely to alert readers that the content of this article is unreliable. We have not investigated whether authors were aware of or involved in the systematic manipulation of the publication process.

Wiley and Hindawi regrets that the usual quality checks did not identify these issues before publication and have since put additional measures in place to safeguard research integrity.

We wish to credit our own Research Integrity and Research Publishing teams and anonymous and named

external researchers and research integrity experts for contributing to this investigation.

The corresponding author, as the representative of all authors, has been given the opportunity to register their agreement or disagreement to this retraction. We have kept a record of any response received.

References

- [1] M. Nadeem, M. Nisa, M. H. Bangash et al., "The Comparative Pharmacokinetics and Histokinetics of the Therapeutic Dose of Estradiol Valerate and Bromocriptine in Common Quails," *BioMed Research International*, vol. 2022, Article ID 5482895, 9 pages, 2022.

Research Article

The Comparative Pharmaco- and Histokinetics of the Therapeutic Dose of Estradiol Valerate and Bromocriptine in Common Quails

Muhammad Nadeem,¹ Mehr-un Nisa,² Maria Hussain Bangash,³ Zain Ul Abideen ¹, Rukhsana Sattar,¹ Huma Sattar,⁴ Muhammad Saif Ullah,¹ Tahira Ruby,⁵ Aleem Ahmed Khan,⁵ and Aqeel Ahmad⁶

¹Department of Zoology, Ghazi University, Dera Ghazi Khan, Pakistan

²Basic Health Unit, Khuda Bakhsh Mahar District Bahawalpur, Pakistan

³Basic Health Unit 14/8R, Khanewal, Pakistan

⁴Department of Biotechnology, The University of Lahore, Pakistan

⁵Department of Zoology, Bahauddin Zakariya University, Multan, Pakistan

⁶University of Chinese Academy of Science (UCAS), Beijing, China

Correspondence should be addressed to Zain Ul Abideen; zaenulabidin71@gmail.com

Received 30 June 2022; Accepted 18 August 2022; Published 11 October 2022

Academic Editor: Faheem Ahmed Khan

Copyright © 2022 Muhammad Nadeem et al. This is an open access article distributed under the Creative Commons Attribution License, which permits unrestricted use, distribution, and reproduction in any medium, provided the original work is properly cited.

The current study is aimed at examining the overall effects of steroids on the tissues of organisms and pharmacotherapeutics and pharmacokinetics of several steroids, including Bromocriptine as mesylate and estradiol valerate in common quails (*Coturnix coturnix*). A total of 100 birds were used for pharmacokinetics. The research was carried out in two separate trials, one during the fall season and the other during the spring season. Each experiment lasted for five, ten, fifteen, and twenty days. Each study group used 20 birds while basing their experiments on a control group of 5. At the stretch of five, ten, fifteen, and twenty days in each season, therapeutic dosages were administered to a sum of two groups representing two separate steroid trial groups. Each steroid was administered to each bird in a therapeutic dose, which was three drops administered twice daily. Clinical symptoms include despondency, sluggishness, and variations in weight and temperature that almost all treated birds display. However, only in trials conducted in the fall was a sizable degree of body enlargement in one treated bird noticed. The winter testing showed a mortality rate. Four birds have died in the twenty-day group. One bird died when treated with estradiol valerate, and three birds died treated with Bromocriptine as mesylate. Both the male and female birds showed signs of having lost some of their body weight. The treated birds' kidney, stomach, hearts, and livers exhibited some edema. In comparison, almost all birds show enteritis, which indicates that steroids mainly affect the intestine. There were apparent differences in the histological analysis of heart and skeletal muscle and some treated birds with the control group. The kidney, liver, and intestine show the major histopathological change in all treated birds.

1. Introduction

All the steroids are synthesised from the lanosterol in the cell. Lanosterol is the naturally occurring compound found in animals, plants, fungi, and some bacteria. The synthesis of steroids is called steroidogenesis [1]. The release of steroids and their mechanism of action are regulated by neuro-

nal and hormonal signals. The pituitary gland is stimulated by neural impulses from the hypothalamus; the pituitary gland then releases a hormone that influences the ovaries, kidneys, and testicles to regulate hormonal levels through a feedback process [1, 2]. The first steps of steroid production are performed in mitochondria. Cholesterol is converted to pregnenolone in mitochondria by the enzyme p450sec [3].

The current study reveals that steroid output is controlled by steroid metabolism, i.e., biosynthesis. In order to protect the cellular membranes against antifungal medications like amphotericin B and azol, fungus synthesise ergosterols [4]. In female humans and other animals, steroids increase sickness and the immune system's reaction [5]. Numerous physiological processes in vertebrates, including responsiveness and electrolyte balance, are influenced by corticosteroids [6]. Canada, Europe, US, and other countries throughout the world all utilise estradiol valerate. Estradiol valerate has been used by women to prevent pregnancy for more than 50 years. [7]. Estradiol valerate is a hormone that is utilised in the treatment of a variety of conditions, including transgender women, menopausal symptoms, low oestrogen levels, and hormonal birth control [8]. Estradiol valerate at large doses raises the risk of thrombosis, alters the lipid profile in the blood, and raises the level of both prolactin and insulin resistance [9]. The Control Centers for Disease claim that, between 2006 and 2008, 10.5 million persons used oral contraceptives containing estradiol valerate as a birth control method [10]. When testosterone is given to a female, the female is unable to reproduce and has fewer cloacal glands. In fact, estradiol-17 is applied to male quail to promote copulation and 5-dihydrotestosterone to promote cloacal gland development [11].

By inhibiting ovulation and using its hormone, estradiol valerate prevents conception. The endometrium and cervical mucus have changed, making it difficult for sperm to penetrate. Bromocriptine use over an extended period of time results in anxiety, agitation, suicidal thoughts, weariness, and irritability [12]. Gallstone formation and cholesterol retention are more likely to occur when the gallbladder is not completely empty in late pregnancy. Gallstone development and cholesterol retention are both increased during pregnancy [13]. During the neonatal stage and during social interactions, steroids have an impact on a mammal's body [13].

The social behaviors of mammals can be modified by altering the hormone concentration (neuropeptides) [14]. They affect the human body in a number of ways. The primary impacts on the body alter mood and raise the dangers of anxiety, sadness, and menopause [15]. The birds' immunological function is inhibited by stress, their immunity is decreased, and pathogens can easily target their system [16].

Additionally, steroids have an impact on the tarsus, badge, wing bar, size, and beak. Size, color, wings bar, crest, and visual ability of the birds are all impacted by corticosterone [17]. Regardless of dose, the CORT-administered zebra finches had fewer copulations than the control animals. As a result, pair bonds are not significantly affected by acute CORT [18]. The effects of steroids on gender, sexuality, and the immune system in general. In females, humans, and animals, steroids increase illness and the immunological response. The most important finding is that gender and sex hormones have an effect on both the innate and the adaptive immune cells, but the mechanism responsible for this effect is unknown [5]. Recent research has demonstrated that 11beta-HSD serves both physiologic and pathological functions in the skin. In the context of the skin, the functions

of 11beta-HSD include cell proliferation, the healing of wounds, inflammation, and the ageing process [19]. The goal of the current study was to explore the effects of steroids on the tissues of organisms as well as the pharmacotherapeutics and pharmaco-histokinetics of Bromocriptine as mesylate and estradiol valerate. This was accomplished through comparing the effects of Bromocriptine as mesylate and estradiol valerate on the serum and blood biochemistry of common quails that had either been subacutely or chronically stimulated with. The information was contrasted with that obtained for intact or control groups.

2. Materials and Methods

2.1. Ethical Approval. Institutional ethical approval for this study was obtained from the Ethical Committee of the Ghazi University, D G Khan, Punjab, Pakistan.

2.2. Experimental Birds. A total of 100 common quails are used during experimental periods (*Coturnix coturnix*). All of the birds are typically adult, weighing between 40 g and 150 g. These chickens are bought from D G Khan in a Pakistani chowk. The feed was manufactured at home without the use of medications and had sufficient nutrients (bajra, corn, and rice). Before beginning the treatment, all the birds had a five-day conditioning and adjustment period to the bird's condition.

2.3. Drug Formulation. Two medications were utilised over the course of the experiment. Each day, a brand-new Brotin and Pregnova solution is made and administered orally to all the birds receiving medication. The weight of the bird was used to calculate the required dosage of the medication formulation.

2.4. Dose Fixation. The dosage that was prescribed was the same as what was administered to the tiny mammals. The therapeutic dose is 2.5 mg/kg, and it is used to evaluate all of the potentially harmful effects of the whole medicine.

2.5. Therapeutic Dose. By using a syringe and a few tiny drops of steroid medication, the birds are administered their therapeutic dose.

2.6. Experimental Design. In each experiment, there were a total of 100 common quail birds, which were randomly divided into two groups of 50 birds each (summer and winter). In each experiment, there were a total of fifty birds, which were randomly assigned to one of three groups. Twenty birds were sacrificed in order to extract Brotin for drug testing. Twenty birds were sacrificed in order to collect Pregnova-treated medication samples. The remaining ten birds are split in half; five of them are utilised for the observation of clinical symptoms, while the other five are used to measure the treated birds' weights for comparison. The twenty birds are separated into four groups, each of which has five birds to make up its membership. Every trial lasts for a total of twenty days. Only five days of treatment were given to those five birds. The second group of five birds received treatment for somewhere between 1 and 10 days.

The duration of treatment for the third group ranged from one to fifteen days. The duration of treatment for the fourth group ranges from 1 to 20 days. During the course of the experiment, each of the birds became completely accustomed to the setting in which they were placed. In order to reduce the amount of stress the birds were put through, it was necessary to take their rectal temperature and record their live body weight every five days. The birds' body weight was recorded in group 1, between 1 and 5 days. Between 1 and 10 days, group 2's total body weight is recorded every day. From day 1 to day 15, group 3 members had their body weight recorded. The participants in group 4 had their body weight recorded anywhere from 1 to 20 days. It has also been observed that the birds' temperatures are identical.

2.7. Clinical and Behavioral Observation. The birds were provided with fresh water and food three times a day, and their behavior and clinical status were monitored throughout the day. The behavioral observations made included the consumption of feed, drooping of the head, unrest, jumping in cages, and a feeling of hunger. Additionally, he was observed avoiding the other cage in order to hide in it.

2.8. Sample Collection and Processing. All of the birds in group 1 were given a thorough necropsy after 1 to 5 days, birds in group 2 were examined after 1 to 10 days, birds in group 3 were examined after 1 to 15 days, and birds in group 4 were examined after 1 to 20 days. In the event that there was a pathological alteration, this information is also documented. The sample was obtained from the kidneys, liver, and heart in addition to the skeletal muscles. For the purpose of histological analysis, representative tissue specimens were preserved in formalin at a concentration of 10%. Standard paraffin processing was utilised in order to preserve and embed the tissue. A section with a thickness of 5-6 μ m was cut. Eosin and hematoxylin were then used to stain the slides that had previously been prepared.

2.9. Histopathology Grassing. A location in the laboratory where the organ is sectioned off into parts measuring one centimetre in size. When the organ fragments are more than 1 centimetre in size, the reagent does not penetrate the tissue as well. The width of the samples is 1 centimetre, while the length is 1 inch. The ability to observe everything in the specimens, including colors, figures, and tumours, is one of the benefits of using this method. Following the cutting, fragments of the organs are placed in tissue cassettes and given labels before being stored.

2.10. Tissue Fixation. There are various fixatives employed, including ethylene, picric acid, and formaldehyde. Formaldehyde is utilised quite frequently in this context as a fixative. Formaldehyde can be purchased for a low price and is readily available in most marketplaces. Additionally, advantageous is the fact that it is readily absorbed by specimens. A formaldehyde solution is created through the process of diluting 37 percent of concentrated formaldehyde with 63 percent of water. This is done in accordance with the technique. After this step, take ten percent of it, combine it with ninety percent water, and utilise it in the fixation process.

Formaldehyde should be left in contact with the tissue for a period of at least two hours and no more than sixteen.

2.11. Cutting Microtome. In cutting the tissue, a machine is used called a microtome. Different types of microtome are used, but here, a rotary microtome is used. This microtome is heavy and is fixed in place due to its weight. Parts are that holder which holds the tissue. The other is the cutter, where knives are used for cutting. Another part is the wheel which helps in cutting. After cutting the section, put it in hot water with temperature 50° to 60°C.

2.12. Staining. After removing the paraffin wax from the tissues, it was then immersed for three minutes in xylene. After that, the tissues are dipped into 100 percent alcohol for three minutes so that the xylene can be removed. The tissues are subjected to alcohol at concentrations ranging from 95 percent to 30 percent for a period of two minutes. In the five minutes that follow the alcohol, the tissues are soaked in water. For decolorization, a series of four to ten dips are performed, each using an ever higher grade of alcohol. In the subsequent 1 minute and a half to 2 minutes, eosin will be employed. The picture was then cleaned using xylene after three minutes of dehydrating the tissue to eliminate the alcohol. On the slide, a single drop of balsam from Canada was placed. On the slide, a cover slip was added before being fixed firmly.

3. Results

During the course of the trial, the clinical indications of somnolence and blindness of the eye with excessively dark speckled hues were detected in birds that had been treated with Pregnova. In the group that had been treated with Brotin, there were a few instances of diarrhoea that was bloody.

After 15 to 20 days of treatment, all clinical indications were observed in the groups who had been given medications. In comparison to the group that served as the control, the physiology of the birds' hearts and heart muscles showed no discernible signs of change (Figures 1 and 2). On the other hand, the drug-treated group's liver, kidneys, skeletal muscles, and heart showed little to no evidence of alteration. The micrographic picture of the heart in common quails during the first five days of treatment with Brotin, displays the congestion and hemorrhaging in tissues (Figure 3). When common quails were treated with Brotin in a ten-day trial, it displayed necrosis and inflammation in the heart's tissues and blood clotting in some heart tissues (Figure 4). The fifteen-day trial's common quails given Brotin displays inflamed fibroblasts and cardiac tissues (Figure 5).

The picture of the heart in common quails following a 20-day treatment with Brotin. It displays microhemorrhages and cardiac tissue irritation (Figure 6). Pregnova-treated common quail muscles in the first five days of a winter trial are depicted in a photo, with the muscles' unique areas of inflammation and fibroblast activity (Figures 7 and 8). Common quail's muscles in a photo representation from a ten-day winter study using Pregnova demonstrate the necrosis



FIGURE 1: Dissections of common quail Pregnova-treated birds. The dissection of common quail treated with Pregnova is done to compare it with controlled groups, and morphological characters have been observed keenly.



FIGURE 2: Dissections of common quail Brotin-treated birds. The dissection of common quail treated with Brotin is done to compare it with controlled groups, and morphological characters have been observed deeply.

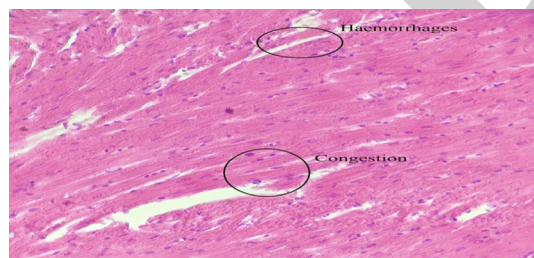


FIGURE 3: Five-day winter trial Brotin-treated heart. The photomicrographic representation of the heart in common quails treated with Brotin in the first five days of trial. It shows the congestion and hemorrhages in the tissues of the heart.

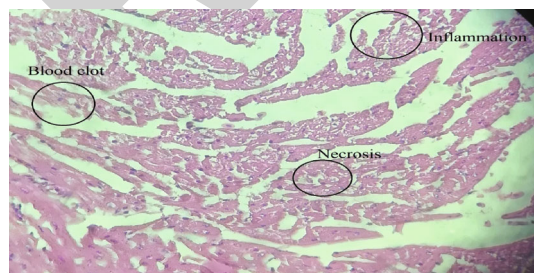


FIGURE 4: 10-day summer trial Pregnova-treated heart. The photomicrographic representation of the heart in common quails treated with Brotin in ten days' trial. It shows the inflammation in the tissues of the heart and necrosis with blood clotting at some points of the tissues of the heart.

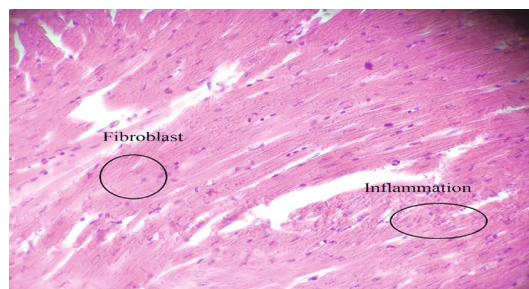


FIGURE 5: 15-day winter trial Brotin-treated heart. The photomicrographic representation of the heart in common quails treated with Brotin in fifteen days' trials. It shows the inflammation in the tissues of the heart and fibroblasts.

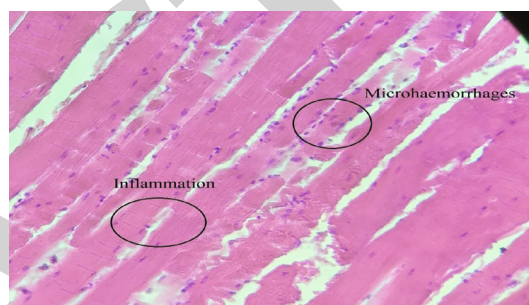


FIGURE 6: 20-day winter trial Brotin-treated heart. The photomicrographic representation of the heart in common quails treated with Brotin in twenty days' trial. It shows the inflammation in the tissues of the heart and microhemorrhages.

at certain muscle sites and fibroblast (Figures 9 and 10). Common quail muscles treated with Pregnova in a ten-day winter trial are depicted in a photo, with the muscles congested at certain locations and the vessels dilated (Figures 9 and 10). Common quail liver slices were photographed under a microscope to reveal typical histological features and characteristics (Figures 11 and 12). Common quail liver from a ten-day winter study with the drug Brotin is shown in the photo, with exudation at certain liver locations and significant hemorrhage (Figure 13). Photo representation of the common quail kidney after five days of Pregnova treatment, demonstrating inflammation and hemorrhages Figure 14). Common quail kidney was treated with Pregnova during a ten-day summer study, showing inflammation and hemorrhages (Figure 15). Common quail kidney was treated with Pregnova in a fifteen-day summer study, and the common quail kidney was treated with a photo representation of blood clotting and blood vessel break (Figure 16). Common quail kidney was treated with Brotin in a summer study for 20 days, displaying inflammation and inflammatory exudate (Figure 17).

4. Discussion

The purpose of the current study was to investigate the effect that steroids have on the histopathology of common quail. In order to accomplish this goal, data were gathered through the conduct of experiments on common quail. In this

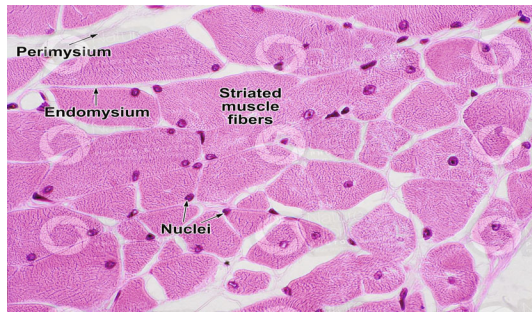


FIGURE 7: Histology of common quail normal bird's muscles (40x). Photomicrographic representation of quail's muscle sections was observed.



FIGURE 8: Five-day winter trial Pregnova-treated muscles. Photo representation of muscles of common quails treated with Pregnova in the first five days of the winter trial showed inflammation at specific muscle and fibroblast points.

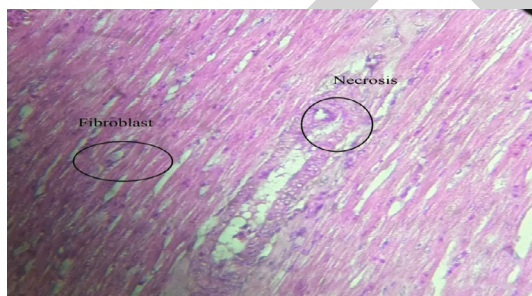


FIGURE 9: 10-day summer trial Brotin-treated muscles. Photo representation of muscles of common quails treated with Pregnova in ten days of summer trial showed necrosis at specific muscle and fibroblast points.

chapter, we addressed the findings of the most recent study, which followed the empirical research that had been done previously on the histopathology of common quail. To begin, we will talk about the histological changes that have taken place in the tissues that are the focus of our investigation. Throughout the course of the trial with the common quail, a variety of clinical symptoms were noticed. These symptoms included a drooping of the head, an increase in hunger, hemorrhaging in the liver, body inflammation, and enteritis. The administration rate of steroids was found to be 27.0 percent in obese individuals, while it was only 11.9 percent in nonobese individuals. There was a significant dis-

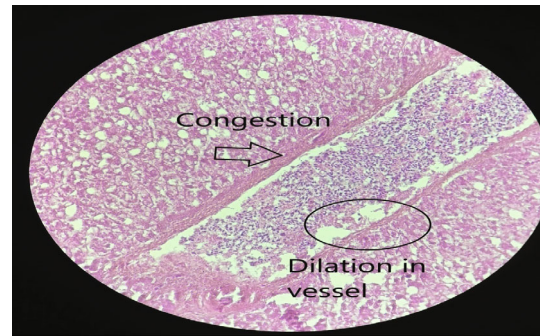


FIGURE 10: 20-day summer trial Brotin-treated muscles. Photo representation of muscles of common quails treated with Pregnova in ten days of summer trial showed congestion at specific muscle points and dilation in the vessel.

parity between the number of people who were fat and those who were not obese who used corticosteroids. It was shown that consuming corticosteroids causes a 10.5 percent rise in a person's body weight when they are already obese [13].

During the winter study, the birds that had been treated with Brotin displayed clinical signs of inflammation, including necrosis and a blood clot in the heart muscles. Throughout the course of the experiment, birds exhibit a variety of behaviors. Over the course of the test period of 10 days, there was a marginal shift in the weight of the birds. The weight of the birds in the experiment that were given Pregnova was found to be reduced, whilst the weight of the birds that were given Brotin was found to be increased. After 15 days of observation, each of the birds exhibited a distinct pattern of behavior in reference to their body weight. The experiment lasts for fifteen days, and at the end of that time, all of the birds have gained weight. The overall rise in the body weight of the birds was observed across all groups, including the control group as well as the experimental groups that received either Bromocriptine as mesylate or Pregnova. The clinical symptoms of kidney congestion, hemorrhages, and inflammatory excaudate were observed in the birds that had been treated with Brotin.

The weight of all of the different types of birds has increased. During this experiment, there was a significant shift in both the birds' outward appearance and their physical behavior. Some bird species get a dark area on their eye that appears to be tumours, and their skin develops a rough texture. There was a discernible change in the belligerent behavior of each and every bird. They are clearly agitated throughout the feeding procedures, and they attempt to break free from their stainless steel cages by making loud noises and squeezing the wire on the cages in an aggressive manner. Additionally, compared to the initial five to fifteen days of the trial, their hunger significantly increased.

Two weeks at a dose of 2 mg/kg/day, four weeks at a dose of 1 mg/kg/day, and three weeks at a dose of 0.4 mg/kg/day. The change was not particularly dramatic and did not represent a considerable departure from the baseline values. They exhibit some traces of impact despite the little amount of prednisolone that they took. The use of corticosteroids leads to an increase in mast cell degranulation as well as their

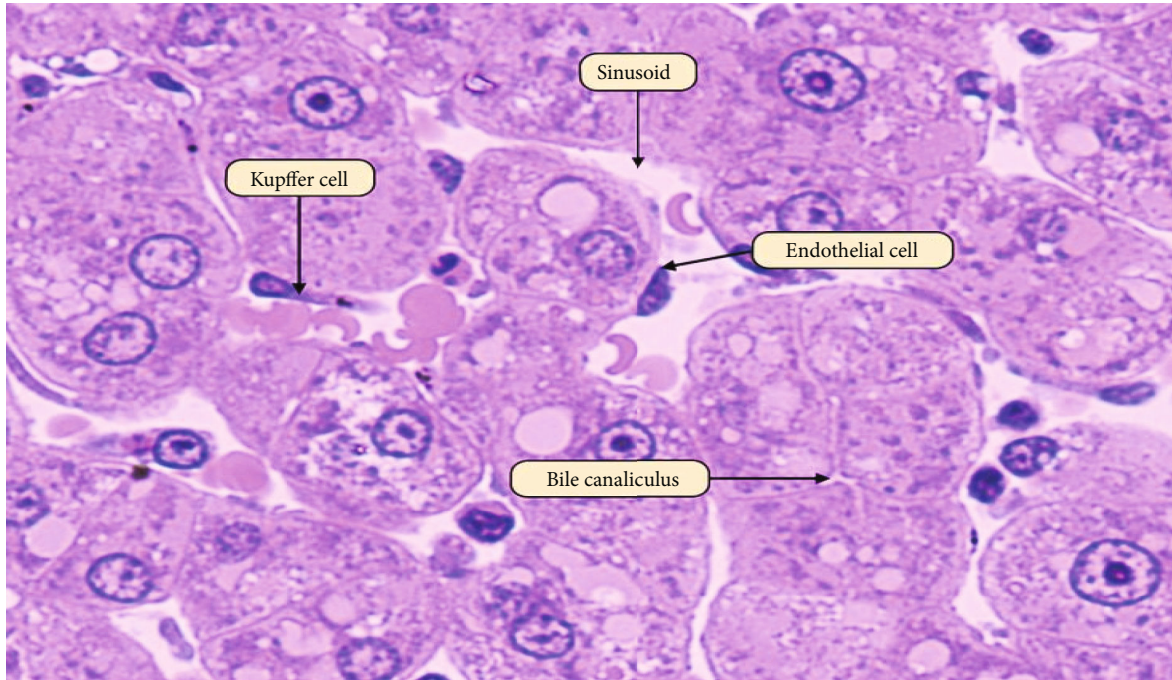


FIGURE 11: Histology of common quail normal liver (40x). Photomicrographic representation of liver sections in common quails that shows normal histological parameters and structures.

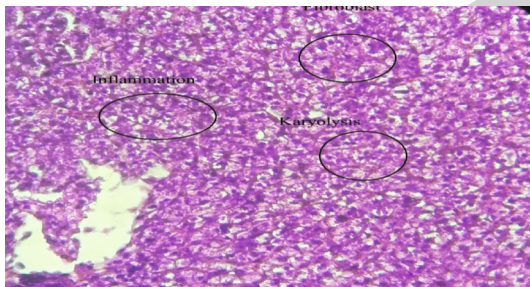


FIGURE 12: Five-day summer trial Pregnova-treated liver. Photomicrographic representation of liver sections in common quails that shows normal histological parameters and structures.

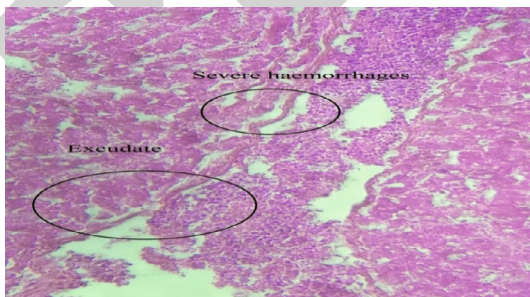


FIGURE 13: 10-day winter trial Brotin-treated liver. Photo representation of the liver of common quails treated with Brotin in ten days of winter trial showed exudation at specific liver points and severe hemorrhages.

production. Inhaled corticosteroids have also been demonstrated to induce inflammation, whereas the effects of corticosteroids mixed with those of beta-agonists have been shown to reduce the amount of inflammatory and allergic cell infiltration [20].

In the second experiment, which took place during the summertime, the actual weight of the birds exhibited varied patterns as a function of the food that they were given. During the course of the experiment, the birds' weight behavior consistently increased. When compared to Pregnova, the use of the steroid Bromocriptine as mesylate resulted in an increase in body weight that was more pronounced. During this test that lasted for 10 days, the conduct of the birds was astonishing in reference to their weight. Because we are using two separate steroids, each of these two steroids will have a unique effect. The birds that were fed Bromocriptine as mesylate consistently increased their weight, and they raised their weight day by day in comparison to the experiment that lasted five days.

The birds that were given with Brotin over the summer showed clinical symptoms of fibroblast, inflammation, and congestion. Both the winter and summer drug trials indicated relatively little changes in the organs; during the first five days of the Pregnova study, the participants gained weight; but, during the 10-day trial, they gradually lost weight. In this experiment, the birds behave less aggressively, but their medical examinations reveal that they have malignancies on the sides of their eyes. During the twenty-day winter trials of Brotin-treated birds, baldness was detected; however, during the twenty-day summer trials, baldness decrease occurred. After being observed for fifteen days, the birds behave in an unpredictable manner. The body weight of the birds that were treated with Bromocriptine

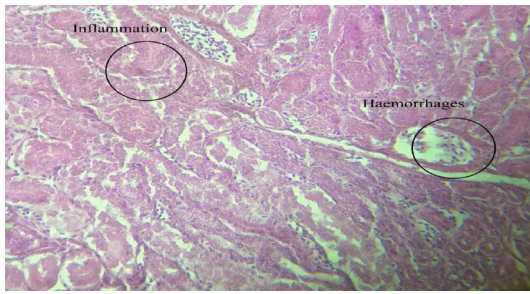


FIGURE 14: Five-day summer trial Pregnova-treated kidney. Photo representation of the kidney of common quails treated with Pregnova in five days of summer trial showing inflammation and hemorrhages.

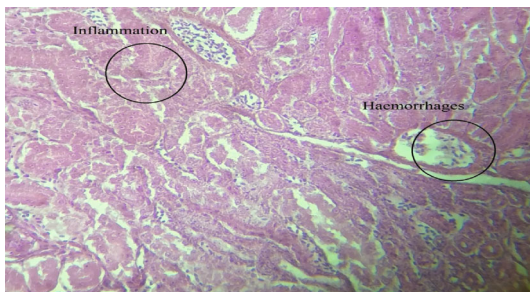


FIGURE 15: 10-day winter trial Brotin-treated kidney. Photo representation of the kidney of common quails treated with Pregnova in ten days of winter trial showing inflammation and hemorrhages.

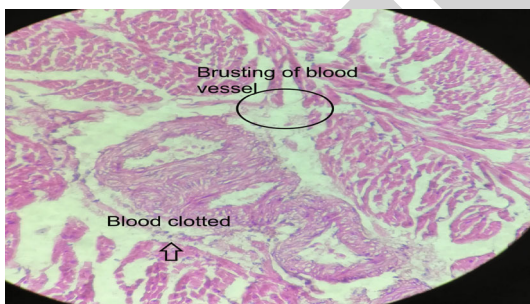


FIGURE 16: 15-day summer trial Pregnova-treated kidney. Photo representation of the kidney of common quails treated with Pregnova in fifteen days of summer trial showing blood clotting and bursting of the blood vessel.

mesylate saw an increase, while the body weight of the birds that were treated with Pregnova exhibited a reduction. The birds that were assigned to the control group saw a rise in their overall body mass. All three of these groups exhibited aggressive behavior [21], one as the control group and the other two as experimental groups.

During the summer study, birds that had been treated with Pregnova showed clinical indications consisting of modest dilatation of their kidney cells. There is a correlation between the size of a bird's body and its temperature. Because steroids alter the internal environment, this temperature varies erratically for no apparent reason. In addition to

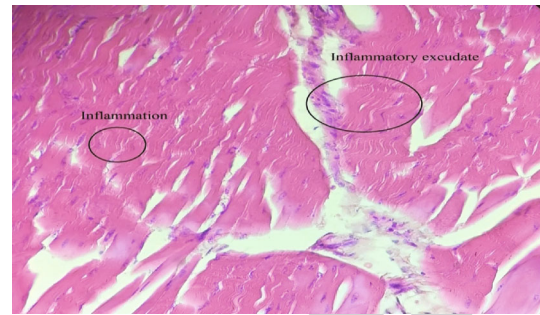


FIGURE 17: 20-day winter trial Brotin-treated kidney (40x). Photo representation of the kidney of common quails treated with Brotin in twenty days of winter trial showing inflammation and inflammatory exudate.

that, the temperature in the environment is quite hot during the summer months. During the summer trial, I discovered that the temperatures of the birds fluctuated when I administered steroid medications with brand names like Bromocriptine as mesylate and Pregnova. Every species of bird raises their body temperature, but to varying degrees. In general, the behaviors of birds were slightly altered, as evidenced by the fact that they displayed aggressive behavior, head-dropping inflammation, and particular patches on their legs. Also, birds will scratch their legs by pinching their beaks, which causes the scratching behavior. By inserting the thermometer into the anal region, the entire temperature was able to be determined with the assistance of a thermometer. A comparison of the tested member's liver with the livers of untested groups uncovered the fact that the tested member's liver displays a greater degree of change. In the course of the experimental investigation, steroids were utilised that had a considerable impact on their homeostatic function. The enzymes that are found in birds display a response to these steroids, which can also have an effect on the temperature of the birds. The temperature of the birds that were given Bromocriptine as mesylate constantly increased, and throughout the course of the trial's five days, the birds' temperature gradually declined [21].

The total effect of steroids on the temperature of birds was investigated over the course of twenty days, and during that time, the temperature did not change. There was not any discernible change in the temperature of the birds that were observed. Ovariectomized rats were used in this study to evaluate the effects of estradiol on the thermoregulatory responses brought on by methanol. For a period of two hours, the temperature was 270 or 160. When the temperature of the tail and the skin was taken at this point, it was found that the group that had been treated with methanol had a higher temperature than the rats that had not been treated with methanol. Because of this, the utilisation of methanol, which is a steroid, results in an increase in temperature [21].

The cumulative effect of consuming these steroids led to very unique and distinct manifestations of behavior. All of the birds exhibit very aggressive behaviors and vocalisations; they each pop their voices at different intervals and in varied

ways. Steroids that are anabolic and androgenic are used to increase desire in both males and females for the purpose of sexual activity. Both relieving and contributing to depression are anabolic androgenic drugs. Increasing one's testosterone level might lead to aggressive behavior as well as psychological symptoms. Some anabolic steroids are generated synthetically, and the effects of taking them might lead to hypomania. Reduced steroid usage is another factor that contributes to depression [22].

Birds had a wide variety of other characteristics as well, the most notable of which was their tendency to sleep. According to the findings of that review, the effects of steroids on social interaction and neonatal periods led to a reduction in the activity level of birds to some degree. The neonatal phase is critical for the development of the neurological system as well as the ability to interact socially. In mammals, the neonatal phases are influenced by steroid use. The neonatal phase is a particularly delicate time for all mammals. Steroids and neuropeptides (such as oxytocin, arginine, and vasopressin) influence how people connect with one another socially. Neuropeptides are known to have an effect on a wide range of behaviors, including aggression, sociosexual behavior, parental conduct, and response to stress. Altering the levels of this hormone can cause changes in the social behavior of mammals [14].

5. Conclusion

Both trials of the steroids showed the expected clinical symptoms and histological alterations, with all processed groups corresponding to varying degrees of intensity among the various drugs. Differences in pharmacokinetic potency and histological response between different steroids are uncovered in the present investigation. Pregnova exhibits less severe unfavorable histotoxic effects on birds than Brotin, according to the most recent studies.

Data Availability

Data are available on request.

Conflicts of Interest

There is no conflict of interest.

References

- [1] R. Domínguez, A. Flores, and S. E. Cruz-Morales, "Hormonal and neural mechanisms regulating hormone steroids secretion," *Steroids Basic Science*, vol. 3, p. 32, 2012.
- [2] C. S. Boon, D. J. McClements, J. Weiss, and E. A. Decker, "Factors influencing the chemical stability of carotenoids in foods," *Critical Reviews in Food Science and Nutrition*, vol. 50, no. 6, pp. 515–532, 2010.
- [3] C. R. Jefcoate, B. C. McNamara, I. Artemenko, and T. Yamazaki, "Regulation of cholesterol movement to mitochondrial cytochrome P450_{sc} in steroid hormone synthesis," *The Journal of Steroid Biochemistry and Molecular Biology*, vol. 43, no. 8, pp. 751–767, 1992.
- [4] B. L. Marrone, R. T. Gentry, and G. N. Wade, "Gonadal hormones and body temperature in rats: effects of estrous cycles, castration and steroid replacement," *Physiology & Behavior*, vol. 17, no. 3, pp. 419–425, 1976.
- [5] A. Schuur and H. Verheul, "Effects of gender and sex steroids on the immune response," *Journal of Steroid Biochemistry*, vol. 35, no. 2, pp. 157–172, 1990.
- [6] S. S. Nussey and S. A. Whitehead, *Endocrinology: An Integrated Approach*, CRC Press, Oxford: BIOS Scientific Publishers, UK, 2001.
- [7] Y. F. Sasaki, K. Sekihashi, F. Izumiya et al., "The comet assay with multiple mouse organs: comparison of comet assay results and carcinogenicity with 208 chemicals selected from the IARC monographs and U.S. NTP Carcinogenicity Database," *Critical Reviews in Toxicology*, vol. 30, no. 6, pp. 629–799, 2000.
- [8] S. Chakraborty and A. Bhattacharya, "Kaushik Ghosh," *Education*, vol. 2014, 2016.
- [9] A. Ghosh, *Mayo Clinic Internal Medicine Board Review*, Oxford university press, UK, 2010.
- [10] W. D. Mosher and J. Jones, "Use of contraception in the United States: 1982–2008," *Vital and health statistics. Series 23, Data from the National Survey of Family Growth*, vol. 1, no. 29, pp. 1–44, 2010.
- [11] M. Schumacher and J. Balthazart, "The effects of testosterone and its metabolites on sexual behavior and morphology in male and female Japanese quail," *Physiology & Behavior*, vol. 30, no. 3, pp. 335–339, 1983.
- [12] N. V. Kumar and L. Ganesh, "A simulation-based evaluation of the approximate and the exact eigenvector methods employed in AHP," *European Journal of Operational Research*, vol. 95, no. 3, pp. 656–662, 1996.
- [13] M. Savas, V. L. Wester, S. M. Staufenbiel et al., "Systematic evaluation of corticosteroid use in obese and non-obese individuals: a multi-cohort study," *International Journal of Medical Sciences*, vol. 14, no. 7, p. 615, 2017.
- [14] L. Nieman, "Making the diagnosis: laboratory testing and imaging studies," *InCushing's Disease*, vol. 1, pp. 75–90, 2017.
- [15] M. Ginecologica, "Validation of diagnostic methods for peritoneal carcinomatosis secondary to ovarian cancer. CT-scan, PET-CT or laparoscopy, what is the best?," *Minerva Ginecologica*, vol. 9, 2018.
- [16] P. O. Dunn and D. Winkler, "Changes in timing of breeding and reproductive success in birds," *Effects of climate change on birds*, vol. 10, pp. 108–119, 2019.
- [17] E. Dupont, H.-F. Zhao, E. Rheume et al., "Localization of 3 β -hydroxysteroid dehydrogenase Δ 5- Δ 4-isomerase in rat gonads and adrenal glands by immunocytochemistry and in situ hybridization," *Endocrinology*, vol. 127, no. 3, pp. 1394–1403, 1990.
- [18] D. L. Simmons, P. Lalley, and C. B. Kasper, "Chromosomal assignments of genes coding for components of the mixed-function oxidase system in mice. Genetic localization of the cytochrome P-450PCN and P-450PB gene families and the nadph-cytochrome P-450 oxidoreductase and epoxide hydratase genes," *Journal of Biological Chemistry*, vol. 260, no. 1, pp. 515–521, 1985.
- [19] M. Terao, S. Itoi, H. Murota, and I. Katayama, "Expression profiles of cortisol-inactivating enzyme, 11 β -hydroxysteroid dehydrogenase-2, in human epidermal tumors and its role in keratinocyte proliferation," *Experimental Dermatology*, vol. 22, no. 2, pp. 98–101, 2013.

Retraction

Retracted: Effect of Vegetable Waste on Growth Performance and Hematology of Broiler Chicks

BioMed Research International

Received 8 January 2024; Accepted 8 January 2024; Published 9 January 2024

Copyright © 2024 BioMed Research International. This is an open access article distributed under the Creative Commons Attribution License, which permits unrestricted use, distribution, and reproduction in any medium, provided the original work is properly cited.

This article has been retracted by Hindawi following an investigation undertaken by the publisher [1]. This investigation has uncovered evidence of one or more of the following indicators of systematic manipulation of the publication process:

- (1) Discrepancies in scope
- (2) Discrepancies in the description of the research reported
- (3) Discrepancies between the availability of data and the research described
- (4) Inappropriate citations
- (5) Incoherent, meaningless and/or irrelevant content included in the article
- (6) Manipulated or compromised peer review

The presence of these indicators undermines our confidence in the integrity of the article's content and we cannot, therefore, vouch for its reliability. Please note that this notice is intended solely to alert readers that the content of this article is unreliable. We have not investigated whether authors were aware of or involved in the systematic manipulation of the publication process.

Wiley and Hindawi regrets that the usual quality checks did not identify these issues before publication and have since put additional measures in place to safeguard research integrity.

We wish to credit our own Research Integrity and Research Publishing teams and anonymous and named external researchers and research integrity experts for contributing to this investigation.


The corresponding author, as the representative of all authors, has been given the opportunity to register their agreement or disagreement to this retraction. We have kept a record of any response received.

References

- [1] M. S. Nisar, A. Zahra, M. F. Iqbal et al., "Effect of Vegetable Waste on Growth Performance and Hematology of Broiler Chicks," *BioMed Research International*, vol. 2022, Article ID 4855584, 8 pages, 2022.

Research Article

Effect of Vegetable Waste on Growth Performance and Hematology of Broiler Chicks

Muhammad Shahid Nisar ¹, Anjum Zahra,² Muhammad Fahad Iqbal,³ Muhammad Amjad Bashir,¹ Riffat Yasin,⁴ Khizar Samiullah,⁵ Irum Aziz,⁶ Sidra Saeed,⁵ Abdulrahman Alasmari,⁷ Fahmy G. Elsaid,^{8,9} Ali A. Shati,⁸ Mohammed A. Al-Kahtani,⁸ Farwa Naseem,¹⁰ Maryam Fatima,¹¹ and Faraz Ahmed¹²

¹Department of Plant Protection, Ghazi University D. G. Khan, Pakistan

²DHQ teaching hospital Dera Ghazi Khan Punjab, Pakistan

³Avicenna medical college Lahore Punjab, Pakistan

⁴Faculty of Veterinary and Animal Sciences, MNSUA, Multan, Pakistan

⁵Department of Plant Breeding & Genetics, Ghazi University D. G. Khan, Pakistan

⁶Department of Zoology, Ghazi University D. G. Khan, Pakistan

⁷Department of Biology, Faculty of Sciences, University of Tabuk, Tabuk, Saudi Arabia

⁸Biology Department, Science College, King Khalid University, Abha, Saudi Arabia

⁹Zoology Department, Faculty of Science, Mansoura University, Mansoura, Egypt

¹⁰WMO RHD (Rural Health Dispensary), Badduke, Lahore, Punjab, Pakistan

¹¹WMO at RHD kmahan, Lahore, Punjab, Pakistan

¹²Basic Health Unit Faizabad tehsil Depalpur District Okara Punjab, Pakistan

Correspondence should be addressed to Muhammad Shahid Nisar; mnisar@gudgk.edu.pk

Received 26 May 2022; Accepted 16 September 2022; Published 10 October 2022

Academic Editor: Dr Muhammad Hamid

Copyright © 2022 Muhammad Shahid Nisar et al. This is an open access article distributed under the Creative Commons Attribution License, which permits unrestricted use, distribution, and reproduction in any medium, provided the original work is properly cited.

Vegetable waste (spinach, potato, and cauliflower) is a rich and natural source of nutrients, potentially good for supplying minerals, essential amino acids, and antioxidants to the birds. Relatively, its cost very low, easily to accessible, easily process & pose little risk of illness. The aim of present study was to evaluate the effect of vegetable waste (VW) as feed supplement on growth performance and hematology of broiler chicks. For this purpose, a total of 200 (4 days old) vaccinated chicks were acquired from a commercial hatchery Multan which was acclimated for three weeks (21 days) on basal starter feed after that 25-day-old chicks with uniform body weight were allocated according to a CRD (completely randomized design) into four dietary treatments with three replicates of each contained 15 chicks in 12 pens. In dietary treatments, chicks were feed with basal feed (BF) and supplemented feed with vegetable waste (VW) of spinach, potato, and cauliflower. For this purpose, the dietary treatments included control treatment (T_1) (100% BF+0% VW) and other dietary treatments (T_2) (75% BF+25% VW), (T_3) (50% BF+50% VW), and (T_4) (25% BF+75% VW). The body weight, feed intake, food conversion ratio (FCR), and mortality were checked on weekly and daily basis. For hematology analysis, after the 1st experimental week (25-day-old chicks) and the last 5th experimental week (56-day-old chicks), the samples of blood were gathered from the wing's veins of two birds from each treatment in random way. At the end of five weeks (35 days), birds with uniform average body weight were selected per treatment with three replicates (2 bird/replicate) and then were manually slaughtered according to the Halal method to analyze the weight of internal body organs of broilers by physical and statistical analysis (ANOVA). There was no significant effect ($P > 0.05$) on feed intake and FCR among all the dietary treatments. But in average, body weight and BWG were higher in treatment (T_2) ($P < 0.01$) than all other dietary treatments (T_3) and (T_4) and control treatment (T_1). The blood constituents in this study showed that broilers in control treatment (T_1) and other dietary treatments (T_2), (T_3), and (T_4) fed on different doses were significantly ($P < 0.01$) different from each other. The week 5 (W_5) shows higher values of blood constituents

($P < 0.01$) than week 1 (W_1). The carcass yield of the chicks fed on different doses showed that they were significantly different ($P < 0.01$) among the dietary treatments. The VW inclusion 0%, 25%, 50%, and 75% had positive effect on blood constituents and carcass yield of the broiler chicks; they were significantly ($P < 0.01$) different among the treatments.

1. Introduction

A broiler is any chicken (*Gallus gallus domesticus*) that especially for meat production is raised and bred. In comparison with beef cattle, sheep meat, and pig meat, the broiler chicks due to its less expensive and highly availability have shown an increasing trend across the world. Great flavor, tenderness, and the juiciness are the qualities of the broiler chicken due to its subcutaneous and marbling fat content in the meat and skin which makes the chicken taste more delicious when processed [1]. Broiler meats demonstrate as a functional food with more levels of natural antioxidants [2]. With the sorts of business interests, the poultry industry has become a distinct industry such as egg production, broiler production, hatchery, and poultry equipment businesses and feed mills springing up [3]. The fast growth performance of broilers supports the FCR (feed conversion ratios), but users usually accuse about bad juicy nature and aroma of poultry meat. The meat quality improved and the growth rate slows down the commercial broilers by supplementing the vegetable waste (VW). So, the VW supply only maintains their requirements [4].

Across the world, by the change in living way of the society they are becoming much serious and worried about their health performance so, that the need of the people increases for useful and pure functional feeds. So, the meat of broiler is testified as functional food due to more level of natural antioxidants ([5] & Hakim et al., 2022). Food waste (FW) can be avoided around the food supply chain. Avoidable waste food normally thrown out in the land-fills. Food waste if processed and utilized in the right way may consist of high nutrients and energy. The proper processing procedure of green vegetables produced extremely waste material or byproduct, whichever incorporate about 25-30 percent of the whole waste [6]. Consequently, appropriate and organized handlings of food waste (FW) not only produce useful and energetic products but also minimize the crush on the environment [7]. Vegetable wastes are easy to access, found everywhere, and also have high source of nutrients for the broilers to increase body weight, have good meat quality, and provide antioxidant stress to broilers [8]. The broilers which feed on vegetables produce juicy, cholesterol-free, and tenderness meat have highly demanding properties [8].

Supplemented vegetables to the commercial broilers slow down broilers' growth rate to improve and provide taste in meat quality and supply at low cost to the producers [4]. Spinach has useful constituents in a modern crop with rich nutritional and biological values. Spinach is an excellent supply of nutrients such as manganese, iron, zinc, and magnesium. Spinach also contains little amount of vitamins, like vitamin A, K, E, and C, thiamine (B1), riboflavin (B2), pyridoxine (B6), and foliate. Spinach on dry basis is an excellent source of protein, minerals, iron, and vitamins especially

vitamin A, B1, B2, and C [9]. The spinach as a leafy vegetable can dry, handle, and preserve more easily in powder form [10]. The little amount of spinach use as supplemented feed to the chicks did not enhance and better the nutritional rate of the meat but also improved the color quality and taste of the meat [11]. Potatoes are a primary food of many families and potatoes are a versatile root vegetable. Potatoes are low costly and easily grow vegetable which consist variety of nutrients. Due to their carbohydrate level and protein composition, the potatoes are considered as rich source of nutrients. Potatoes are substitute of corn [12]. As compared to the remaining apart of potato (potato tuber), the sweet potato peel contains minerals, large amount of proteins, and other noncarbohydrate compounds [13].

Cauliflower is rich in minerals and lower in calories so, that cauliflower is acceded a vigor food for the chicks. Actually, cauliflower contain approximately every minerals including calcium, iron, vitamin B-6, and vitamin C which feed to chicks as supplement feed become them healthy [14]. The inclusion of SPRM (sweet potato (*Ipomoea batata*) root meal) feed consisted of about 5 percent that was good & guide WG (weight gain), consumption of diet & had not pre contagion ability of initial broiler chickens, not interrupt with process of hematological & so that it was selected for optimum broiler starter production conducted by [15]. The average of vegetable waste used had a substantial impact ($p < 0.05$) on live weight, FCR, AMEn, and metabolic crude fiber digestibility, as well as a very massive effect ($p < 0.01$) on feed intake, nitrogen retention, and metabolic nutrient digestibility conducted by Fitasari et al. [16]. The powder of spinach impacted flesh color, but not thio-barbituric acid reaction substances or lutenin deposition conducted by [17]. Broilers fed on cauliflower waste as supplemented diets then the feed conversion efficiency increased with minimum cost. Thus, supplemented diet as cauliflower waste to broilers up to 50% level is mostly useful investigated by Kamlesh and Saraswat [18].

2. Materials and Methods

2.1. Experimental Site. To investigate the combine effect of vegetable waste like potato, spinach, and cauliflower on the growth and blood hematology of broilers, the experiment was conducted at government poultry farm (Shed) nearby circuit house D. G Khan.

2.2. Collection of Samples. Three different vegetables (potato, spinach, and cauliflower) were selected as feed supplement. For the preparation of supplemented feed, the vegetable waste was collected from the local markets, restaurants, and homes at D. G Khan.

2.3. Feed Preparation. Vegetable (potato, spinach, and cauliflower) wastes were sliced and dried under the shade to

prevent the loss of volatile nutrients. During the drying process, vegetable waste was covered by a fine mesh to keep them clean from dusts. Moreover, regular turning of vegetable waste was done to prevent the possible growth of molds. The air-dried vegetables were crushed in grinder in the form of fine granular powder or granules. The crushed vegetable waste was packed in bags of 100 kg capacity and used for further experimentation.

After that, measured amount of crushed vegetable waste and basal diet (wheat, rice, and millet) was mixed approximately for feeding purpose. So, the measured amount of feed was packed in plastic bags.

2.4. Ingredients of the Experimental Diets. The dietary ingredients used in this experiment were wheat, rice, millet, and the three selected vegetable (cauliflower, spinach, and potato) waste. The wheat, rice, and millet were used as basal diet. The vegetable wastes (spinach, cauliflower, and potato) were used as experimental diets with different percentages.

2.5. Experimental Design. The experiment was conducted in CRD (completely randomize design) composed of four (4) dietary treatments replicated thrice. Fifteen chicks were present in each treatment. Treatment (T_1) was considered as untreated controls which were fed only with basal feed (wheat, rice, and millet). The other treatments (T_2), (T_3), and (T_4) were supplemented with vegetable waste (spinach, potato, and cauliflower) along with basal feed at different percentages. Percentage of different feed supplements in all the treatments including control is given in Table 1.

2.6. Procurement and Management of Experimental Chicks. Two hundred ($n = 200$) four-day-old broiler chicks were purchased from commercial Multan hatchery. Vaccination was given against main poultry diseases as viral and bacterial diseases accordant to scale granted by Multan hatchery from where the broiler chicks were purchased. The vaccines against the diseases were received from D. G Khan veterinary institute. The broiler chicks were received with standard veterinary training and according to the completed medical care. Their initial weight was measured by weighing machine. At the experimental site, the chicks were raised for three weeks (21 days) in a brooding pen and during that time they were fed starter diets. At the completion of acclimation period (brooding period), twenty-five-day (25) old, one hundred eighty ($n = 180$) chicks with uniform body weight were randomly transferred into experimental pens. Areas given to each group were equal. Each wood mad pen had a 3*4-meter length and was designed to hold 15 chickens, as well as with drinkers and feeders. There were four treatments including one control treatment each with three replicates. Floor bedding was covered with plastic sheets. At a height of around 5 cm, the litters of wood shavings or rice husk were utilized. Those litters were dried completely.

All experimental pens, feeders, and drinkers were cleaned and formalin sterilized firstly. All of the birds were kept in the same circumstances (lighting, temperature, ventilation systems, and moisture content). The average temperature of the experimental setup was 35-37°C. Twenty-four

TABLE 1: Experimental design of feeding trials.

Dietary treatments	Inclusion rate of VW	Replications			
		R_1	R_2	R_3	Total
T_1 (control)	(0% VW+100% BF)	15	15	15	45
T_2	(25% VW+75% BF)	15	15	15	45
T_3	(50% VW+50% BF)	15	15	15	45
T_4	75% VW+25% BF)	15	15	15	45
Total broiler chicks		60	60	60	180

hour lightening system was available according to their need. The feeding trial was carried out from the 3rd to 8th week of age, and therefore, for 5 weeks, each of the four treatments of birds was fed with one of the dietary treatments. Throughout the trial, clean and fresh water was available at all times. The study was carried out for five weeks. Mortality was recorded when it occurred. The vaccination was given at 14th, 21st, and 28th day of the experimental period. Initial and weekly body weight was measured for growth performance. The FCR (feed conversion efficiency) was recorded. Blood samples were taken two times during experimental periods to check the blood status of broiler chicks. Organs' weights were measured after dissection at the end of experimental period for carcass yield.

2.7. Data Calculation and Analysis. Data were collected on daily basis and on weekly basis. On daily basis, feed consumption and feed repulsion were recorded. Each group's body weight and feed intake were monitored on a weekly basis.

The following analyses were performed to check the impact of VW (vegetable waste) on growth performance and hematology of broiler chicks.

- (i) Growth performance analysis
- (ii) Blood constituents analysis
- (iii) Statistical analysis

2.8. Growth Performance Analysis. During the experimental trail, the broiler chicks had been fed on a replica basis according to the applied feed scale, with a measured amount of diet provided each day between 8:00 am and 16:00 am. Before offering and weighing feed, the rejected feed always was gathered every next morning. The amount of feed consumed was then calculated by subtracting the repelled feed from the applied feed. The weight of body was measured at the start of the trial (called the initial weight) and subsequently on a weekly basis before feeding between 7 and 8 a.m. The ultimate body weight gain was observed by taking a weight of body at the ending of the experimental time period. After that, the total BWG (body weight gain) was determined by subtracting the starter and ended body weights. Mortality was calculated on daily bases. Total feed consumption and total BWG (body weight gain) were used to determine the FCR.

The feed conversion ratios (FCR) were measured by the following formula:

$$\text{FCR} = \text{Input of feed/Weight gained by the animal.}$$

2.9. Data on Carcass Components. Two hens per replication were chosen at the ending of the experimental period; those BWG were closest to their subgroups' mean and maintained in a separate pen with no diet. So, at the end of experiment, the chicks were starved overnight, and they were individually weighed (to determine slaughter weight) and decimated. After de-feathering and removing the feet, skull, and internal organs, the dressed carcass weight was calculated, with the skin retained. The carcass yields, drumsticks, thighs, and breast were all prepared and weighted. The wings were removed through an upper limbs incision at the distal end of the tibia. It was possible to acquire the breast part. The thighs and drumstick parts were obtained by cutting throughout the junction between the femur and the ilium bone fragments of the coccyx. An incision across the junction made by the fibula, femur, and tibia severed that the drumstick from the thigh. The dressing % was estimated by dividing the dressed carcass weight by the slaughter weight.

2.10. Blood Constituents Analysis. Analyses of proximate nutrients were performed through blood chemistry analysis by following way. For hematology constituents analysis, after the 1st experimental week (25-day-old chicks) and the last 5th experimental week (56-day-old chicks), the sample of blood were gathered from the wing's veins of two birds and were selected from each treatment in random way. Five milliliter (5 ml) blood was taken from the wing's a bird per treatment for hematology analysis. Samples of blood were taken in vials with anticoagulant two times during experimental period with each replicates. A complete blood count (CBC) test from the Kot Chutha medical lab in D. G Khan was used to calculate hematological components including RBC (red blood cell), WBC (white blood cell), HBG (hemoglobin concentration), MCHC (mean corpuscular hemoglobin concentration), MCH (mean corpuscular hemoglobin), GRA (granulocytes), PCV (pack cell volume), and MPV (mean platelet volume).

2.11. Statistical Analysis. The average feed consumption (intake) (g), average body weight and BWG (g), CBC, and output of carcass components were all analyzed using SAS software's one-way ANOVA. The means had compared by using DMR (Duncan multiple range) test. The results of the experimental trial were reported as mean \pm standard error of the mean (SEM).

3. Results and Discussion

In this current study, the initial weight of the broilers (4 days old) chicks was not significantly different from each other, which shown that all the birds had uniform body weight at the start of experiment. After the acclimation periods of 21 days, the broiler chicks show uniform body weight at the age of 25 days and agreed with work of Fitasari and Mushollaeni [19] who report that body weight and feed

intake show nonsignificant difference in commercial feeding during acclimation period until the age of 14 days which means that the impact of diet was not observed in the chicks during the commercial feedings.

3.1. Average Body Weight and Body Weight Gain (BWG). The average body weight and BWG mean body weight gain are significantly different ($P < 0.01$) among the dietary treatments described in Tables 2 and 3. The broilers of treatment (T_2) fed on (25% VW+75%) BF showed the highest final body weight and weight gain ($P < 0.01$) followed by other treatments that fed on the control treatment (T_1) (0% VW+ 100%BF) and treatments (T_3) (50% VW+ 50% BF) and (T_4) (75% VW+25%BF), respectively, but not significantly different from control treatment (T_1). In the diet of the broilers, the percentage of volume weight (VW) increased and resulted in less nutritional intake and stop the growth [20, 21]. Also the amount of the fiber increase in the diet resulted in poor nutritional value and feed efficiency [22]. The results of this study were fully agreed with the study of Oun [23] who reported that by the use of 25% VW in the diet of the broiler chicks, the FBW (final body weight) increased as compared to the diet of control treatment.

3.2. Feed Intake and Feed Conversion Ratio (FCR). In the current study, there was no significant effect ($P > 0.05$) on feed intake, but FCR was nonsignificant ($P > 0.05$) at the start and became significant at the end of experimental period ($P < 0.05$) as described in Tables 4 and 5 in accordance with Sakib et al. [24]; there was feed conversion ratio decreased at increased level of potato meal in broiler diet because the potato meal did not directly effect on the feed intake and growth performance of broiler chicks at 21, 28, 35, and 42 days of age. Maung et al. [25] observed that there was no significance difference ($P > 0.05$) at FCR and feed intake and body weight gain and live weight of broilers fed at 0 g, 34.5 g, and 69 g green vegetable (water spinach) with BF which promote the growth performance of broilers among dietary treatments agreed with current study at FCR and feed intake ($P > 0.05$) and showed controversy at live weight and body weight gain ($P < 0.01$) of broiler chicks. This study agreed with the study of Okapanchi et al. [26] who reported that there was no significant difference ($P > 0.05$) on feed intake of broilers on yam peels. He also observed that the amount of the fibers increases in the diet increases the feed intake in broiler chickens; the FCR did not show significant difference across the dietary treatments.

3.3. Carcass Components. Chicks fed on control diet (T_1) had higher weight of the liver, dress carcass, breast meat, and drum stick weight than other dietary treatments which were significantly different ($P < 0.05$) from each other. But the lungs and large intestine are nonsignificant ($P > 0.05$) among different dietary treatments described in Table 6. This study agreed with the result of Melesse et al. [27] who observed the broilers who fed on (T_2) (30 g/kg SPLM) had higher slaughter weight and things weight. The current study shows controversy with Mozafari et al.'s [28] work

TABLE 2: Average body weight for broiler chicks fed with different levels of VW (mean ± SEM).

Average body weight						
	Control: T_1	T_2	T_3	T_4	P value	Significance
Week 1	315 ± 0.86 ^b	335.5 ± 0.86 ^a	304.334 ± 0.61 ^c	286.8334 ± 0.72 ^d	.9071	NS
Week 2	567.5 ± 0.28 ^b	585.83 ± 0.88 ^a	548.167 ± 0.73 ^c	503 ± 0.764 ^d	.1939	NS
Week 3	872.67 ± 0.61 ^b	898.667 ± 0.61 ^a	863.5 ± 0.87 ^c	836.334 ± 0.88 ^d	.1233	NS
Week 4	1092.334 ± 0.44 ^b	1115.167 ± 0.44 ^a	1073.67 ± 0.601 ^c	1042.834 ± 0.73 ^d	.4274	NS
Week 5	1414 ± 0.76 ^b	1507.167 ± 0.44 ^a	1291 ± 1.041 ^c	1256.167 ± 0.73 ^d	.0184	*

abc = means with same superscripts are non significant; ** = significant.

TABLE 3: BWG for broiler chicks fed with different levels of VW (mean ± SEM) during.

Body weight gain (BWG)						
	Control: T_1	T_2	T_3	T_4	P value	Significance
Week 1	207.5 ± 0.86 ^b	226.5 ± 0.86 ^a	196.34 ± 0.61 ^c	180.834 ± 0.72 ^d	.9071	NS
Week 2	460 ± 0.288 ^b	476.83 ± 0.88 ^a	440.167 ± 0.7 ^c	397 ± 0.7637 ^d	.1939	NS
Week 3	765.167 ± 0.6 ^b	789.67 ± 0.61 ^a	755.5 ± 0.86 ^c	730.334 ± 0.88 ^d	.1233	NS
Week 4	984.83 ± 0.44 ^b	1006.167 ± 0.4 ^a	965.667 ± 0.6 ^c	936.834 ± 0.726 ^d	.4274	NS
Week 5	1306.5 ± 0.76 ^b	1398.167 ± 0.4 ^a	1183 ± 1.041 ^c	1150.167 ± 0.73 ^d	.0184	*

abc = means with different superscripts show that values are significantly different; ** = significant.

TABLE 4: Feed intake for broiler chicks fed with different levels of VW (mean ± SEM).

Feed intake						
	Control: T_1	T_2	T_3	T_4	P value	Significance
Week 1	617 ± 150.32	541 ± 4.583	450.667 ± 23.49	401.334 ± 22.06	.2751	NS
Week 2	776.67 ± 49.16	1012.334 ± 111.78	816.334 ± 20.17	869 ± 78.71	.1966	NS
Week 3	1332.34 ± 56.37	1794.67 ± 197.12	1424 ± 93.724	1923 ± 298.61	.1519	NS
Week 4	2365.34 ± 173.28	2726.334 ± 289.60	2432 ± 393.85	2857.667 ± 07.26	.5740	NS
Week 5	3980 ± 107.59	4579 ± 62.978	4287 ± 240.251	4486.667 ± 242.66	.1750	NS

NS: nonsignificant.

TABLE 5: FCR for broiler chicks fed with different levels of VW (mean ± SEM).

Feed conversion ratio (FCR)						
	Control: T_1	T_2	T_3	T_4	P value	Significance
Week 1	2.1634 ± 0.0837	2.2167 ± 0.158	2.2934 ± 0.122	2.2134 ± 0.129	.9071	NS
Week 2	1.6834 ± 0.11	2.1167 ± 0.23	1.85 ± 0.045	2.1834 ± 0.202	.1939	NS
Week 3	1.7367 ± 0.074b	2.267 ± 0.24	1.88 ± 0.123	2.63 ± 0.407	.1233	NS
Week 4	2.38 ± 0.161a	2.7067 ± 0.29	2.51 ± 0.408	3.0467 ± 0.22	.4274	NS
Week 5	3.04 ± 0.08c	3.27 ± 0.046 ^{bc}	3.59 ± 0.196 ^{ab}	3.897 ± 0.212 ^a	.0184	*

NS: nonsignificant.

who used the different level of cooked and raw potato replacing with 25 and 35% seed of maize which reported that the dietary treatments had nonsignificant effect ($P > 0.05$) on weight of thighs, breast, and liver of broiler chicks.

This study agreed with the results of Tamir and Tsega [29] who used the dried level of SPLM (sweet potato meal)

at 0, 50, 100, 150, and 200 g/kg level which showed that drumstick, breast meat, and thighs are not affected with the dietary supplements because that material did not contain any dangerous effect on the health status and performance of the broiler chickens. The giblets' weight and the slaughter weight of broilers decrease with the increase of

TABLE 6: Carcass components weight of broiler chicks fed with different levels of VW (mean \pm SEM).

Carcass components	Control: T_1	T_2	T_3	T_4	P value	Significance
Slaughter weight (g)	1413.167 \pm 0.7 ^b	1506.5 \pm 0.5 ^a	1290.167 \pm 1.01 ^c	1255.34 \pm 0.60 ^d	.9071	NS
Dress carcass (g)	901 \pm 2.08 ^a	881.34 \pm 1.8 ^b	863.67 \pm 0.8 ^c	802.334 \pm 1.45 ^d	.1939	NS
Dressed %	63.734 \pm 0.12 ^b	58.476 \pm 0.107 ^c	66.89 \pm 0.03 ^a	63.537 \pm 0.26 ^c	.1233	NS
Breast meat %	28.71 \pm 0.12 ^a	26.72 \pm 0.12 ^b	22.17 \pm 0.04 ^c	20.101 \pm 0.17 ^d	.4274	NS
Thighs %	13.23 \pm 0.036 ^d	19.51 \pm 0.04 ^a	16.92 \pm 0.109 ^b	16.4584 \pm 0.09 ^c	.0184	*
Drum stick (%)	12.54 \pm 0.089 ^a	16.561 \pm 0.09 ^b	15.821 \pm 0.14 ^b	15.4853 \pm 0.06 ^c	.9071	NS
Wings (%)	11.5203 \pm 0.16 ^d	13.002 \pm 0.136 ^b	12.33 \pm 0.09 ^c	14.68 \pm 0.165 ^a	0.011	**
Gizzard (%)	2.976 \pm 0.015 ^c	4.97 \pm 0.08 ^a	4.667 \pm 0.08 ^a	4.337 \pm 0.14 ^b	0.013	**
Liver (%)	3.4944 \pm 0.05 ^a	3.239 \pm 0.04 ^b	1.99 \pm 0.018 ^d	2.388 \pm 0.03 ^c	0.015	**
Heart (%)	0.65 \pm 0.012 ^d	0.803 \pm 0.04 ^c	0.9708 \pm 0.028 ^b	1.185b \pm 0.03 ^a	0.017	**
Lungs (%)	0.703 \pm 0.018 ^a	1.045 \pm 0.013 ^a	0.798 \pm 0.39 ^a	0.821 \pm 0.0254 ^a	0.673	NS
Kidney (%)	0.607 \pm 0.018 ^d	0.86 \pm 0.029 ^c	1.009 \pm 0.019 ^b	1.18767 \pm 0.02 ^a	0.013	**
Small intestine (%)	7.117 \pm 0.038 ^d	7.46 \pm 0.013 ^c	7.84 \pm 0.031 ^b	8.82134 \pm 0.04 ^a	0.014	**
Large intestine (%)	0.86 \pm 0.0145 ^a	0.857 \pm 0.37 ^a	0.89 \pm 0.032 ^a	0.595 \pm 0.043 ^a	0.662	NS

abc = means with different superscripts on the different rows among the different treatments are significantly different; ** = significant; NS: nonsignificant.

TABLE 7: Blood constituents for broiler chicks fed with different levels of VW (mean \pm SEM).

Blood constituents	T_1	T_2	T_3	T_4	P value	Significance
WBC ($10^3/uL$)	110.26 \pm 1.56 ^c	121.97 \pm 1.90 ^a	105.29 \pm 5.2 ^d	115.72 \pm 8.525 ^b	.9071	NS
LYM ($10^3/uL$)	99.04 \pm 0.92 ^b	109.22 \pm 0.52 ^a	92.97 \pm 1.95 ^c	98.68 \pm 3.77 ^b	.1939	NS
MID ($10^3/uL$)	7.88 \pm 0.918 ^c	8.93 \pm 0.747 ^b	7.58 \pm 1.298 ^c	13.11 \pm 3.556 ^a	.1233	NS
GRA ($10^3/uL$)	3.75 \pm 1.53 ^d	3.80 \pm 1.487 ^c	4.60 \pm 1.889 ^b	7.80 \pm 3.338 ^a	.4274	NS
RBC ($10^6/uL$)	2.17 \pm 0.023 ^b	2.30 \pm 0.008 ^a	1.95 \pm 0.090 ^c	1.46 \pm 0.174 ^d	.0184	*
HGB (g/dL)	9.15 \pm 0.086 ^a	9.08 \pm 0.048 ^a	7.85 \pm 0.45 ^c	8.65 \pm 0.52 ^b	.9071	NS
MCHC (g/dL)	33.99 \pm 0.08 ^b	34.17 \pm 0.62 ^b	34.58 \pm 0.85 ^b	50.67 \pm 6.32 ^a	.1939	NS
MCH (pg)	42.07 \pm 0.574 ^b	39.72 \pm 0.236 ^c	39.53 \pm 0.65 ^c	66.20 \pm 11.449 ^a	.1233	NS
MCV (fL)	124.48 \pm 1.38 ^b	117.68 \pm 3.09 ^d	118.67 \pm 3.73 ^c	125.43 \pm 7.08 ^a	.4274	NS
MPV (fL)	3.72 \pm 0.06 ^b	3.68 \pm 0.09 ^b	3.68 \pm 0.083 ^b	4.20 \pm 0.23 ^a	.0184	*

abc = means with different superscripts on the same rows among the different treatments are significantly different; ** = significant.

the supplemented feed as 100 g/kg dried sweet potato meal had gave higher giblets weight than 150 g/kg and 200 g/kg dried sweet potato meal.

3.4. Blood Constituents. The blood constituents in this study showed that broilers in all treatment groups fed on different doses were significantly ($P < 0.05$) different from each other. The value of RBC was lower in W_5 , and all other contents were higher in W_5 . The treatment (T_4) had higher values of WBC, MID, GRA, HGB, MCV, and MPV in W_5 than W_1 that were significantly ($P < 0.05$) different from each other as described in Table 7. This study of blood constituent's controversy with the report of waken Elle (2010), who observed that in all the treatments, the values of the hemoglobin, RBC, and MCHC obtained were within the normal range. So, the highest values can be shown in

hematocrit and mean corpuscular volume, and the mean corpuscular concentration was lower. This study show controversy with the study of [11] he used VW as 0%, 25%, 50%, 75% and 100% who reported that there was no significant difference in the immune status of broilers fed on different doses in different dietary treatments that decrease the intake of commercial by fed on more concentration of vegetable waste that not impact on the immune status of the broilers chicks. This study showed similarity at some extent with [30] who used 0%, 5%, 10%, and 15% Irish potato peel meal (IPPM) replaced with the maize in diet and observed that the blood constituents were significantly different ($P < 0.05$) from each other in different dietary treatments. The white blood cells were higher in control treatment (T_1) but also similar with (T_4) than (T_2) and (T_3) which were significantly different

($P < 0.05$). This study is in accordance with the report of [17] who reported that the concentration of HGB increased with the age of broilers.

4. Mortality

In the current study, there were no difference in the mortality of broilers during experimental periods agreed with the [19] work shown mortality on livestock experimental period experienced by illness or death in broiler chicks. The results of this study was also accordance with work of Whitemore et al. [31] and Agwunobi [32–36] who reported that the dietary treatments using potato did not show any significant effect ($P > 0.05$) on the mortality.

5. Conclusion

Spinach, potato, and cauliflowers are the vegetables that have not enhanced and bettered the nutritional rate of the meat but also improved the color quality and taste of the meat of broiler chicks. In the current research, it is concluded that the dietary supplementation of vegetable waste had good effect on growth performance at 25% concentration in dietary treatment (T_2). Consequently, appropriate and organized handlings of food waste (FW) not only produce the useful and energetic products but also minimize the crush on the environment. Processing food waste provides the valuable high nutritional organic part of food which would be reused for the animals as due to their nutritional values especially as for livestock food part.

Data Availability

All data is available within the manuscript.

Conflicts of Interest

The authors declare that they have no conflicts of interest.

Acknowledgments

The authors would like to thank the Deanship of Scientific Research at King Khilaid University, Abha, KSA for funding this work under Grant number (R. G. P. 2/113/43).

References

- [1] N. A. Mir, A. Rafiq, F. Kumar, V. Singh, and V. Shukla, "Determinants of broiler chicken meat quality and factors affecting them: a review," *Journal of Food Science and Technology*, vol. 54, no. 10, pp. 2997–3009, 2017.
- [2] M. S. Arshad, F. M. Anjum, A. Asghar et al., "Lipid stability and antioxidant profile of microsomal fraction of broiler meat enriched with α -lipoic acid and α -tocopherol acetate," *Journal of Agricultural and Food Chemistry*, vol. 59, no. 13, pp. 7346–7352, 2011.
- [3] M. K. Padhi, "Importance of indigenous breeds of chicken for rural economy and their improvements for higher production performance," *Scientifica*, vol. 2016, Article ID 2604685, 9 pages, 2016.
- [4] M. A. Hossain, A. F. Islam, and P. A. Iji, "Growth responses, excreta quality, nutrient digestibility, bone development and meat yield traits of broiler chickens fed vegetable or animal protein diets," *South African Journal of Animal Science*, vol. 43, no. 2, pp. 208–218, 2013.
- [5] B. Halliwell and J. M. C. Gutteridge, "The chemistry of free radicals and related reactive species," in *Free radicals in biology and medicine*, vol. 5pp. 1–25, Oxford University Press, Nigeria, 3rd edition, 1999.
- [6] L. Truong, D. Morash, Y. Liu, and A. King, "Food waste in animal feed with a focus on use for broilers," *International Journal of Recycling of Organic Waste in Agriculture*, vol. 8, no. 4, pp. 417–429, 2019.
- [7] A. J. Garcia, M. B. Esteban, M. C. Marquez, and P. Ramos, "Biodegradable municipal solid waste characterization and potential use as animal feed-stuffs," *Waste Management*, vol. 25, pp. 780–787, 2005.
- [8] R. O. Omenka and G. N. Anyasor, "Vegetable-based feed formulation on poultry meat quality," *African Journal of Food, Agriculture, Nutrition and Development*, vol. 10, no. 1, pp. 2001–2010, 2010.
- [9] H. C. Oomen and A. Grubben, "Tropical leaf vegetables in human nutrition," *Journal of Agriculture*, vol. 20, pp. 69–75, 1978.
- [10] P. K. Ankita and K. Prasad, "Characterization of dehydrated functional fractional radish leaf powder," *Der Pharmacia Lettre*, vol. 7, no. 1, pp. 269–279, 2015.
- [11] E. I. Sayed and M. Samah, "Use of spinach powder as functional ingredient in the manufacture of UF-soft cheese," *Helvion*, vol. 6, no. 1, article 03278, 2020.
- [12] O. Charmey, D. Nelson, and F. Zvomaya, "Nutrient cycling in the vegetable processing industry: utilization of potato by-products," *Canadian Journal of Soil Science*, vol. 86, no. 4, pp. 621–629, 2006.
- [13] B. J. Wilson, D. T. Yang, and M. R. Boyd, "Toxicity of mould-damaged sweet potatoes (*Ipomoea batatas*)," *Nature*, vol. 227, no. 5257, pp. 521–522, 1970.
- [14] R. Hetzel, "The chook and the chef," *Warm Earth*, vol. 104, pp. 36–37, 2012.
- [15] P. C. Jiwuba, E. Dauda, L. C. Ezenwaka, and C. J. Eluagu, "Replacement value of maize with sweet potato (*Ipomoea batata*) root meal on growth performance and haematological characteristics of broiler starter birds," *Archives of Current Research International*, vol. 4, pp. 1–7, 2016.
- [16] E. K. A. Fitasari, "The potential of vegetable waste-based pellets on broiler production performance and nutrient digestibility," *IOSR Journal of Agriculture and Veterinary Science*, vol. 13, no. 11, pp. 18–24, 2020.
- [17] G. H. Kang, S. H. Kim, J. H. Kim et al., "Effects of dietary radish green and spinach on meat quality and lutein accumulation in broiler tissue," *Food Science of Animal Resources*, vol. 31, no. 1, pp. 86–91, 2011.
- [18] S. Kamlesh and B. L. Saraswat, "Performance of broiler chicks fed on cauliflower waste supplemented diets," *International Journal of Animal Sciences*, vol. 15, no. 2, pp. 161–164, 2000.
- [19] E. Fitasari and W. Mushollaeni, "Similarity the potential of vegetable waste-based pellets on broiler production performance and nutrient digestibility," *IOSR Journal of Agriculture and Veterinary Science*, vol. 13, no. 11, pp. 18–24, 2020.

Retraction

Retracted: *Lagerstroemia speciosa* Ameliorated Blood Pressure in LNAME Induced Hypertension in Experimental Rats through NO/cGMP and Oxidative Stress Modulation

BioMed Research International

Received 8 January 2024; Accepted 8 January 2024; Published 9 January 2024

Copyright © 2024 BioMed Research International. This is an open access article distributed under the Creative Commons Attribution License, which permits unrestricted use, distribution, and reproduction in any medium, provided the original work is properly cited.

This article has been retracted by Hindawi following an investigation undertaken by the publisher [1]. This investigation has uncovered evidence of one or more of the following indicators of systematic manipulation of the publication process:

- (1) Discrepancies in scope
- (2) Discrepancies in the description of the research reported
- (3) Discrepancies between the availability of data and the research described
- (4) Inappropriate citations
- (5) Incoherent, meaningless and/or irrelevant content included in the article
- (6) Manipulated or compromised peer review

The presence of these indicators undermines our confidence in the integrity of the article's content and we cannot, therefore, vouch for its reliability. Please note that this notice is intended solely to alert readers that the content of this article is unreliable. We have not investigated whether authors were aware of or involved in the systematic manipulation of the publication process.

Wiley and Hindawi regrets that the usual quality checks did not identify these issues before publication and have since put additional measures in place to safeguard research integrity.

We wish to credit our own Research Integrity and Research Publishing teams and anonymous and named external researchers and research integrity experts for contributing to this investigation.



The corresponding author, as the representative of all authors, has been given the opportunity to register their agreement or disagreement to this retraction. We have kept a record of any response received.

References

- [1] M. S. Aleissa, M. Al-Zharani, L. M. Alneghery et al., "*Lagerstroemia speciosa* Ameliorated Blood Pressure in LNAME Induced Hypertension in Experimental Rats through NO/cGMP and Oxidative Stress Modulation," *BioMed Research International*, vol. 2022, Article ID 5894416, 8 pages, 2022.

Research Article

***Lagerstroemia speciosa* Ameliorated Blood Pressure in LNAME Induced Hypertension in Experimental Rats through NO/cGMP and Oxidative Stress Modulation**

Mohammed S. Aleissa ¹, **Mohammed Al-Zharani** ¹, **Lina M. Alneghery** ¹,
Md Saquib Hasnain ², **Bader Almutairi** ³, **Daoud Ali**,³ **Saud Alarifi** ³,
and **Saad Alkahtani** ³

¹Department of Biology, College of Science, Imam Mohammad Ibn Saud Islamic University, Riyadh, Saudi Arabia

²Department of Pharmacy, Palamau Institute of Pharmacy, Chianki, Daltonganj, 822102 Jharkhand, India

³Department of Zoology, College of Science, King Saud University, Riyadh, Saudi Arabia

Correspondence should be addressed to Mohammed S. Aleissa; msaleissa@imamu.edu.sa

Received 8 July
2022; Accepted 30
Academic Editor: Hafiz Ishfaq Ahmad

Copyright © 2022 Mohammed S. Aleissa et al. This is an open access article distributed under the Creative Commons Attribution License, which permits unrestricted use, distribution, and reproduction in any medium, provided the original work is properly cited.

Cardiovascular disease is the primary reason for chronic heart diseases and mortality worldwide. Hypertension (HTN) is the utmost dominant risk factor for the evolution of several diseases. Herbal medicines, traditional medicinal herbs, and their extracts are widely utilized to treat and monitor HTN. Herbal components have been shown to help relax arteries and lower oxidative stress. The current study assesses the probable role of herbal plant extract *Lagerstroemia speciosa* (LS) in the LNAME induced HTN in rats. LNAME (50 mg/100 mL) in drinkable water was given to rats for five weeks. There was a significant upsurge in LNAME-treated hypertensive rats' blood pressure (BP). On treatment with LS, it ameliorates blood pressure. Further, LS also improved body weight, reduced heart weight, and heart hypertrophy. The NO/cGMP concentration was lowered along with a substantial upsurge in the level of glutathione and a decline in MDA level. The LS extract also reduced the inflammatory cytokine markers in the systemic circulation. In conclusion, thus, the extract of LS treatment can efficiently alleviate the BP, oxidative stress markers, and inflammation and improve NO/cGMP concentration in LNAME induced HTN in rats.

1. Introduction

Hypertension (HTN) is a crucial risk element for heart attacks, heart failure, and strokes [1, 2]. HTN is a significant indicator of the potential danger of progressing cardiovascular disorder [3]. HTN is typically costly as problems arising due to it are peripheral vascular disease (PVR), coronary artery disease (CAD), chronic renal and heart failure, cerebrovascular disease, [3] and diabetic cardiomyopathy [4]. HTN has been one of the globe's most frequent manifestations linked to early disease and mortality. As per the Centres for Disease Control and Prevention, HTN is accountable for >5.8% of all deaths and greater than 45 per-

cent of all heart disease-related deaths. Antihypertensive therapy reduces the risk of severe cardiovascular risk by decreasing blood pressure (BP) and improving HTN risk factors [1, 2]. Without treatment, even a slight elevation in BP enhances the chance of attaining cardiovascular disease (CVD) and organ damage [5]. By reducing vascular resistance and increasing blood flow, vasorelaxation can help control HTN [6].

One of the factors that are supposed to involve in the progression as well as development of HTN is reactive oxygen species (ROS), which includes a number of metabolic signalling pathways. Aerobic animals continuously generate ROS, which are chief regulators of various physiological

functions. Consequently, ROS is toxic at enhanced levels and produces widespread damage to the cell and tissue and poorly marks numerous physiological activities [6]. Numerous pathways by which ROS induces HTN comprise reduced bioavailability of nitric oxide (NO) [7], enhanced expression of ACE [8], and stimulation of AT1 receptor [9]. Owing to their antioxidant potential, several natural flavonoids are demonstrated to have the effect of antihypertensive by increasing the nitric oxide bioavailability [10, 11]. Findings have shown that ROS scavenging is also essential for treating HTN and that ACEI, such as antioxidant phenols, is a preferred antihypertensive agent. Medicinal plants as well as phytopharmaceuticals have been used for the treatment of severe diseases and have least adverse effects [12–16].

Lagerstroemia speciosa (LS or LSE) is usually known by name banaba. It has antidiabetic [17], antiobesity [18], α -glucosidase inhibitors [19], and anti-inflammatory properties [20]. Additionally, it also has effects against diabetic nephropathy [21]. Since the antihypertensive activity of LS has not been reported, and no research have been done to date on the antihypertensive activity of LS. This research, therefore, explored the antihypertensive efficacy of LS in *N* ω -Nitro-L-arginine methyl ester hydrochloride (LNAME) induced HTN in rats.

2. Material and Methods

Animal experimental studies have been conducted according to Imam Mohammed Ibn Saud Islamic University's rules, Saudi Arabia-IRB. No. HAPO-01-R-0011. Throughout the duration of the trial, the animals had access to both food and water *ad libitum*. The Sprague Dawley (SD) rats were used in the present study. The rats were of the weight 150-180 g and aged 5-6 weeks old. The standard drug used was captopril (CAPT) 10 mg/kg, for six weeks [22]. The blood pressure of LNAME group was compared with extract-treated LS, and CAPT group (Supplementary Figures S1–S4).

2.1. LNAME Induced HTN in Rats. In total, four groups of 180-200 grams male SD rats were used for the experiment, containing 6 animals. The groupings of rats were as follows:

- (a) Control group: SD rats were served as control
- (b) LNAME group: LNAME (50 mg/100 ml water) in water was provided for consumption to the rats for four weeks served as a hypertensive group
- (c) LNAME+LS group: LNAME (50 mg/100 ml water) were treated with LS (400 mg/kg) for six weeks

2.2. BP Measurement. The induction of hypertension in the rats was confirmed by the use noninvasive blood pressure measurement technique (Columbus, U.S.A.) [1].

2.3. Determination of Body Weight (BW), Heart Weight and Cardiac Indices. Animals were anaesthetized with urethane at the end of the experiment, and blood was taken from the abdominal aorta. The heart was removed and cleaned, and the weights were determined. The heart weight indices

were estimated by dividing the weight of the heart by the weight of the body.

2.4. Determination of NO, cGMP and Inflammatory Cytokines Level. The plasma NO level, cGMP concentration, and inflammatory cytokines were estimated by using NO Colorimetric Assay Kit, cGMP immunoassay EIA kit (Cayman Chemical, USA) assay kit, and TNF α , IL6, and IL1 β ELISA kits (Elabscience, U.S.A.) as per the defined manufacturer's protocols.

2.5. Determination of ROS and Oxidative Enzymes. ROS was determined in heart tissue following the defined protocol [1, 3]. In tris buffer, the cardiac tissue was homogenized and then it was filtered. After that, cardiac tissue homogenate was incubated with DCFDA at 37°C for half an hour. The reading was taken at the excitation and emission wavelength of 488 nm and 530 nm. The antioxidant enzymes malondialdehyde (MDA), superoxide dismutase (SOD), and reduced glutathione (GSH) was estimated according to the methods described before [14, 15].

2.6. Hematoxylin and Eosin (H&E) Staining. After measuring the hemodynamic parameters, the hearts were subsequently removed, placed in a solution of 4% formalin, and allowed to remain there for 24 hours. The heart tissue samples were then encased in blocks made up of paraffin. The tissue samples were cut to a thickness of 5 micrometres and stained with H&E dye [3].

2.7. Real-Time PCR. The heart tissue was used for the isolation of RNA using trizol method. After the RNA isolation from the heart tissue by trizole, was then its OD was measured using nanodrop (Thermo fischer) and then it was transcribed into cDNA using reverse transcriptase kit of cDNA, and the RT qPCR was performed according to the defined protocol [1, 15]. The list of primer is given in supplementary table 1.

2.8. Data Analysis. For statistical analysis, Prism software version 8.0 (USA) have been used. To assess statistical significance, a one-way analysis of variance was performed, followed by the Newman-Keuls Multiple Comparison Test and the *t*-test. Data are represented as Mean \pm Standard error of mean (SEM), *Control vs LNAME; # LNAME vs LNAME+LSE ***P* < 0.01, ****P* < 0.001; #*P* < 0.05, ##*P* < 0.01, ###*P* < 0.001.

3. Results

3.1. Effect of LS on Hemodynamic Parameters. HTN was induced by LNAME given orally to the rats in drinking water. The BP was increased to 171.19 \pm 1.26 mmHg in LNAME group as equated to the control group 113.66 \pm 2.26 mmHg, respectively (Figure 1). On treatment with the LS for six weeks, the BP was significantly ameliorated to 126.90 \pm 1.36 mmHg compared to the diseased group rats' 171.19 \pm 1.26 mmHg (Figure 1).

3.2. Effect of LS on the Morphometric Parameters. Diseased group (LNAME) rats showed a considerable loss of BW

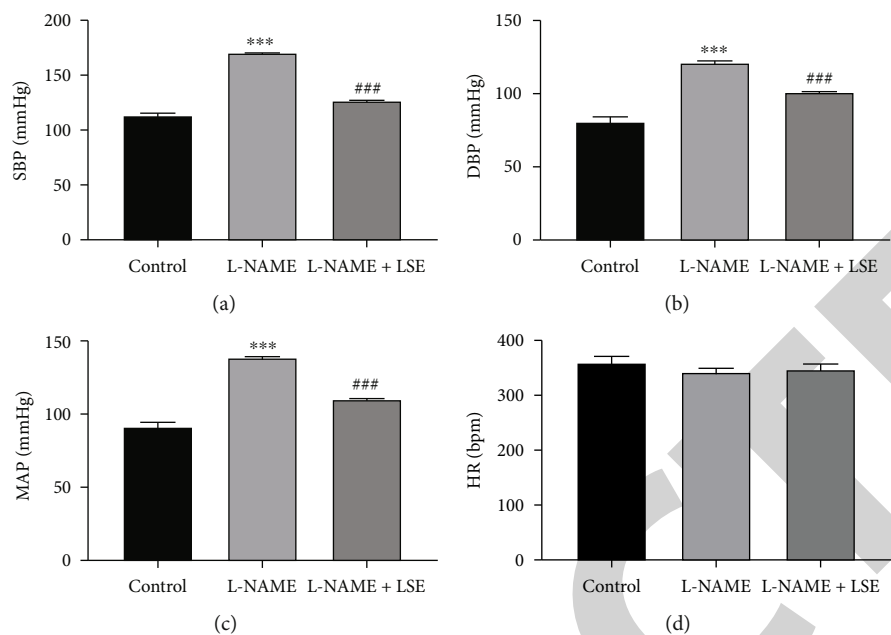


FIGURE 1: Effect of L.S.E. on BP (a) systolic blood pressure (SBP); (b) diastolic blood pressure (DBP); (c) mean arterial pressure (MAP); and (d) heart rate (HR).

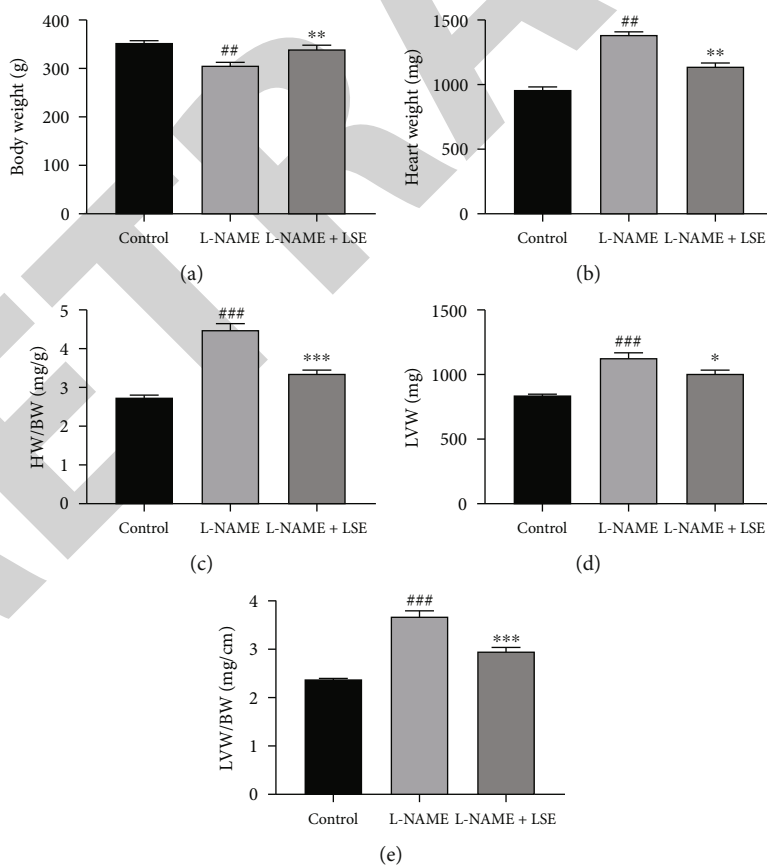


FIGURE 2: Effect of LSE on (a) body weight (BW); (b) heart weight (HW); (c) heart weight/body weight (HW/BW) (d) left ventricle weight (LVW); (e) left ventricle weight/body weight (LVW/BW).

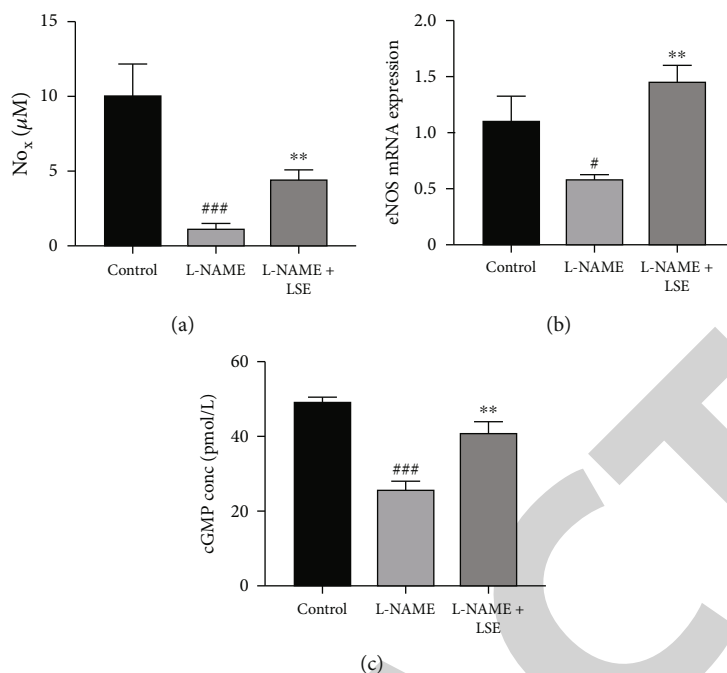


FIGURE 3: Effect of LSE on (a) total nitrate (NO_x) level (b) eNOS mRNA expression (c) cGMP concentration.

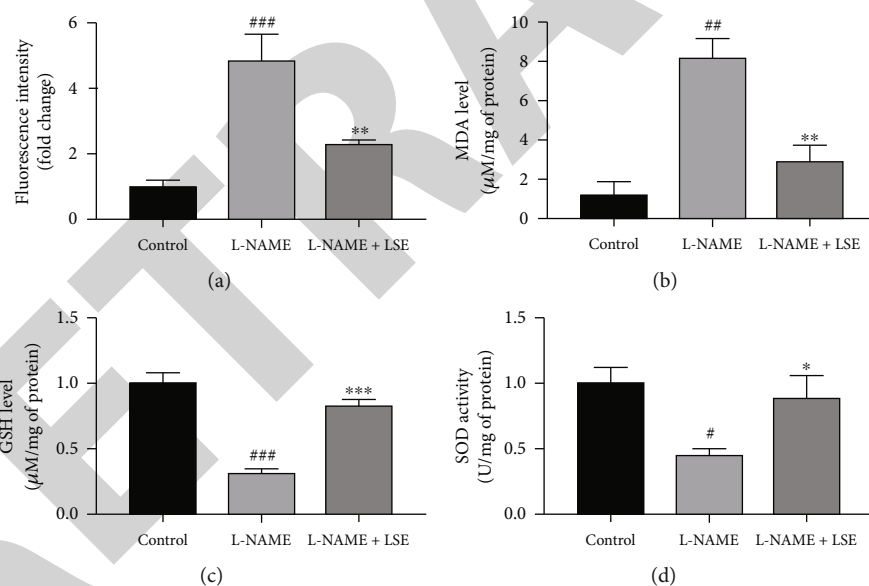


FIGURE 4: Effect of LSE on (a) fluorescence intensity, (b) MDA level, (c) GSH level, (d) SOD activity.

($P < 0.01$) equated to the normal group. LS treated for 6 weeks improves the decline in BW ($P < 0.01$) significantly as compared to the LNAME group rats. The heart weight and cardiac indices were found to upsurge substantially in the LNAME group rats. LS mitigates the heart weight and cardiac index significantly (Figure 2).

3.3. Effect of LS on NO, cGMP Level, and eNOS Expression. The plasma level of N.O., cGMP, and eNOS expression was found to be declined significantly in the LNAME group

rats (Figure 3). The NO, cGMP level, and the eNOS expression were markedly improved after the treatment.

3.4. Effect of LS on ROS Production, Oxidative Stress (OS), and Myocardial Inflammation. The ROS generation was assessed in heart tissue by fluorometry. The ROS level was increased in LNAME rats. LS treated group displayed significantly reduced level. Besides, the level of various OS markers, such as GSH, MDA, and SOD were abnormal in diseased group rats (Figure 4).

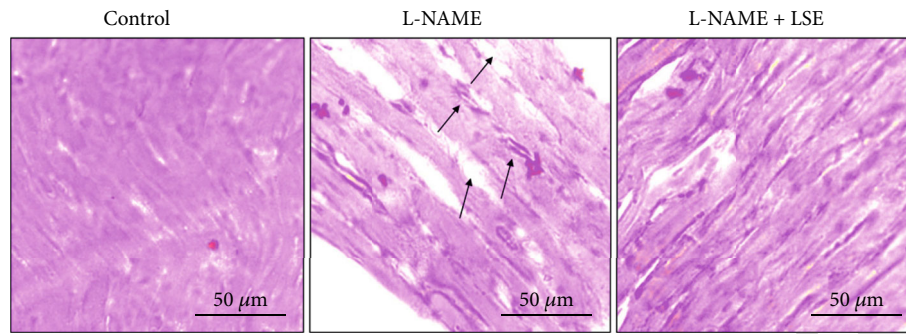


FIGURE 5: Images of the heart stained with H&E dye.

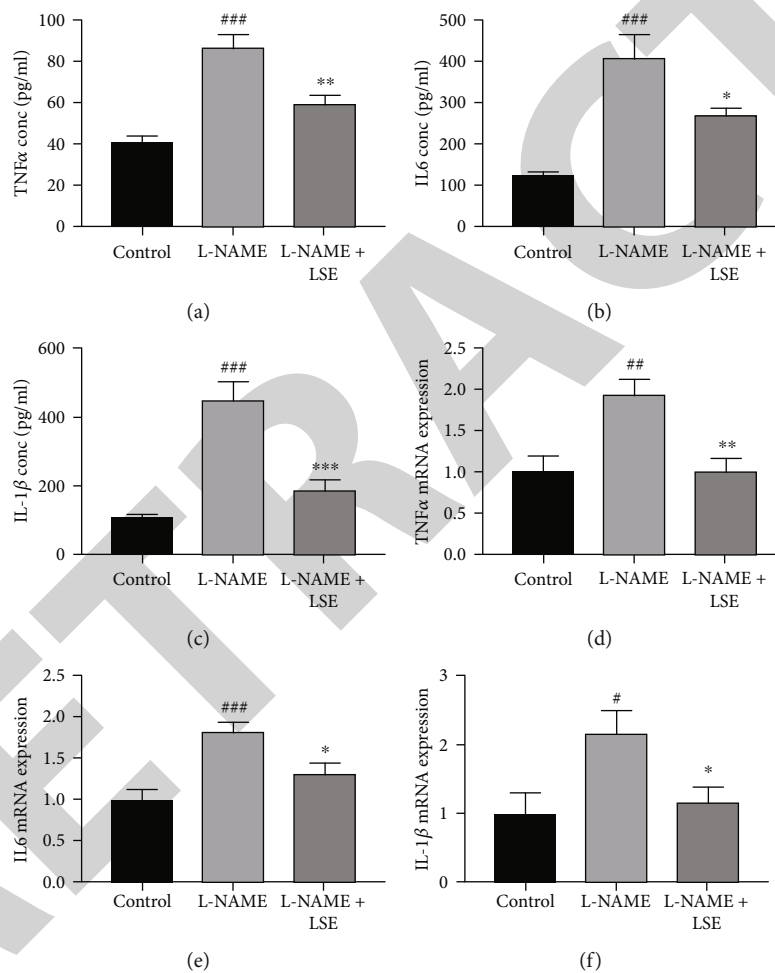


FIGURE 6: Effect of LSE on inflammatory cytokine markers (a) TNF- α level, (b) IL6 level, (c) IL-1 β level, (d) mRNA TNF- α expression, (e) mRNA IL6 expression, and (f) mRNA IL-1 β expression.

On the other hand, treatment with LS, in the above levels were improved significantly parallel to the normal group. The LNAME heart depicted hypertrophy, and the architecture was abnormal in the tissue (Figure 5).

The level of inflammatory markers, TNF α , IL1 β , and IL6 were augmented in LNAME group rats significantly, which was reduced by treatment with LS. Additionally, qPCR analysis of the gene expression of the above heart inflammatory cytokines and the mRNA level in heart tissue ascertained the

above inflammatory cytokines in hypertensive rats (Figure 6).

4. Discussion

The continuous detrimental effect of HTN on one's health, despite the availability of efficient medications, necessitates the development of new pharmacological treatments [9]. Due to their minimal side-effect profiles, complementary,

and alternative remedies may be more beneficial to many people having cardiovascular problems, and there is a demand for natural medicines. HTN and associated diseases are routinely treated using traditional medicine [1, 2].

LNAME induced HTN is due to the obstruction of enzyme nitric oxide synthase (NOS) due to which there is a deficiency of nitric oxide in the body. This leads to endothelial dysfunction and increase in BP. The blockade of NOS leads to generation of ROS [23]. Phenolics, such as flavonoids, inhibit the ROS production and have antioxidant potential, recently studied [1, 24]. Therefore, the current study shows that in vivo LS treatment to LNAME induced hypertensive rats, effectively decreases BP and enhances eNOS expression and improves NO/cGMP level. The BP decrease in the extract treatment group by the LS administration was equivalent to the group treated by standard drug captopril. The positive control drug captopril ameliorated the BP significantly in the CAPT group in line with LS treatment (Supplementary Figures S1–S4).

We found no toxicological effects in the rats during the six weeks of LS treatment, as evidenced by their demeanour. Furthermore, the BW of the LS-fed groups was similar to that of the control group, indicating that six weeks of LS administration is safe. As a result of the antihypertensive evaluation, LS revealed a considerable reduction in BP. Through the synthesis of endothelial-derived relaxing factors, such as NO/cGMP, the endothelium modulates vascular activity by modifying the effect of contractile chemicals on the vascular smooth muscle layer of the blood arteries [25, 26]. When comparing to the control group, the NO/cGMP level in the LNAME group was reduced. Vasoconstriction of the arteries occurs when NO levels are low, resulting in an augmented CO and BP. Flavonoids cause vasodilation because they have an antioxidant effect, preventing the generation of peroxynitrite and so improving the bioavailability of NO, causing vasodilation and reducing BP [27]. On further treatment with LS containing flavonoids, there was an increase in plasma NO levels compared to LNAME, hypertensive groups.

Endothelial dysfunction (ED) is delineated by reduced NO production in the aorta, which is linked to lowered eNOS [28]. The activity of p-eNOS has been observed to be ameliorated in the LNAME group rats aorta [29].

In HTN, there is an higher OS [30], leading to enhanced ROS production and inflammation in the body [31]. ROS causes inflammation in blood arteries by numerous pathways, one of which is an upsurge in inflammatory cytokines including TNF α , IL6, and IL1 β [32]. MDA is the end-product of lipid peroxidation enhanced by ROS production [33]. Injury to the different organs from enhanced ROS generation leads to development of HTN [34]. LS decreases the formation of ROS, MDA level, and recovers the level of GSH in body. MDA production is employed as a predictor of OS-induced lipid peroxidation [35, 36]. Compared to the control group, the LNAME group had lower SOD and GSH levels. The MDA level was augmented significantly in the LNAME group. On treatment with LS, it enhanced the SOD, GSH, and decreased the MDA content. LS, therefore, had some

antioxidant activities and were able to inhibit free radical production.

5. Conclusion

The antihypertensive effect of LS declined the increase in BP in LNAME induced hypertension rats. It enhanced the level of NO/cGMP, thereby enhancing the eNOS expression in the heart tissue. It also ameliorated the generation of ROS production, oxidative stress enzymes, and inflammatory cytokines. Thus, it was found that LS has antihypertensive property. Furthermore, the chemical elements from this plant need to be isolated and validated for their antihypertensive activity to be employed in the clinical trial investigation.

Data Availability

All the data used to support the findings of this study are included within the article.

Conflicts of Interest

The authors of this research affirm that they do not have any known competing economic interests or personal ties that could have given the appearance of influencing the work that is presented in this publication.

Authors' Contributions

Bader Almutairi and Mohammed Aleissa measured the BP. Lina M Alneghery and Daoud Ali performed the OS markers. Mohammed AL-Zharani, Saad Alkahtani, and Mohammed Aleissa assessed the inflammatory cytokines levels. Md Saquib Hasnain and Saud Alarifi performed the histopathological study. Saud Alarifi and Saad Alkahtani evaluated the gene expression. Lina M Alneghery and Daoud Ali performed the statistical analysis. Mohammed Aleissa, Saud Alarifi, Mohammed AL-Zharani, and Saad Alkahtani were involved in the conception and study design, interpretation of data, and critically revised the manuscript. Each contributor were responsible for reading and approving the finalized manuscript.

Acknowledgments

The authors extend their appreciation to the Deanship of Scientific Research at Imam Mohammad Ibn Saud Islamic University for funding this work through Research Group no. RG-21-09-88.

Supplementary Materials

Table 1 and Figures S1-S4 are included in supplementary file. Table 1. List of primers. Figure S1: Effect of LSE and CAPT on systolic blood pressure. Data are shown as Mean \pm S.E.M, *Control vs LNAME; #LNAME vs LNAME+LSE. ** $P < 0.01$, *** $P < 0.001$; # $P < 0.05$, ## $P < 0.01$, ### $P < 0.001$; $\delta P < 0.05$, $\delta\delta P < 0.01$, $\delta\delta\delta P < 0.001$. Figure S2: Effect of LSE and CAPT on diastolic blood pressure. Data are shown as

Mean \pm S.E.M, *Control vs LNAME; #LNAME vs LNAME+LSE. ** $P < 0.01$, *** $P < 0.001$; # $P < 0.05$, ## $P < 0.01$, ### $P < 0.001$; $\delta P < 0.05$, $\delta\delta P < 0.01$, $\delta\delta\delta P < 0.001$. Figure S3: Effect of LSE and CAPT on mean arterial blood pressure. Data are shown as Mean \pm S.E.M, *Control vs LNAME; #LNAME vs LNAME+LSE. ** $P < 0.01$, *** $P < 0.001$; # $P < 0.05$, ## $P < 0.01$, ### $P < 0.001$; $\delta P < 0.05$, $\delta\delta P < 0.01$, $\delta\delta\delta P < 0.001$. Figure S4: Effect of LSE and CAPT on systolic blood pressure. Data are shown as Mean \pm S.E.M, *Control vs LNAME; #LNAME vs LNAME+LSE. ** $P < 0.01$, *** $P < 0.001$; # $P < 0.05$, ## $P < 0.01$, ### $P < 0.001$; $\delta P < 0.05$, $\delta\delta P < 0.01$, $\delta\delta\delta P < 0.001$. (Supplementary Materials)

References

- [1] A. A. Syed, S. Lahiri, D. Mohan et al., "Evaluation of anti-hypertensive activity of *Ulmus wallichiana* extract and fraction in SHR, DOCA-salt- and L-NAME-induced hypertensive rats," *Journal of Ethnopharmacology*, vol. 193, pp. 555–565, 2016.
- [2] B. Saengnak, P. Kanla, R. Samrid et al., "Clitoria ternatea L. extract prevents kidney damage by suppressing the Ang II/Nox4/oxidative stress cascade in L-NAME-induced hypertension model of rats," *Annals of Anatomy–Anatomischer Anzeiger*, vol. 238, Article ID 151783, 2022.
- [3] A. A. Syed, S. Lahiri, D. Mohan et al., "Cardioprotective Effect of *Ulmus wallichiana* Planchon in β -Adrenergic Agonist Induced Cardiac Hypertrophy," *Frontiers in Pharmacology*, vol. 7, p. 510, 2016.
- [4] A. A. Syed, M. I. Reza, M. Shafiq et al., "*Cissus quadrangularis* extract mitigates diabetic cardiomyopathy by inhibiting RAAS activation, inflammation and oxidative stress," *Biomarkers*, pp. 1–10, 2022.
- [5] M. Aggarwal and I. A. Khan, "Hypertensive crisis: hypertensive emergencies and urgencies," *Cardiology Clinics*, vol. 24, no. 1, pp. 135–146, 2006.
- [6] R. M. Touyz, R. Alves-Lopes, F. J. Rios et al., "Vascular smooth muscle contraction in hypertension," *Cardiovascular Research*, vol. 114, no. 4, pp. 529–539, 2018.
- [7] H. Cai and D. G. Harrison, "Endothelial dysfunction in cardiovascular diseases: the role of oxidant stress," *Circulation Research*, vol. 87, no. 10, pp. 840–844, 2000.
- [8] W. Cao, Q. G. Zhou, J. Nie et al., "Albumin overload activates intrarenal renin–angiotensin system through protein kinase C and NADPH oxidase-dependent pathway," *Journal of Hypertension*, vol. 29, no. 7, pp. 1411–1421, 2011.
- [9] M. Morato, M. Reina-Couto, D. Pinho, A. Albino-Teixeira, and T. Sousa, "Regulation of the renin-angiotensin-aldosterone system by reactive oxygen species," *Renin-Angiotensin System - Past, Present and Future*, vol. 2020, pp. 119–157, 2017.
- [10] D. Maaliki, A. A. Shaito, G. Pintus, A. El-Yazbi, and A. H. Eid, "Flavonoids in hypertension: a brief review of the underlying mechanisms," *Current Opinion in Pharmacology*, vol. 45, pp. 57–65, 2019.
- [11] A. Machha, F. I. Achike, A. M. Mustafa, and M. R. Mustafa, "Quercetin, a flavonoid antioxidant, modulates endothelium-derived nitric oxide bioavailability in diabetic rat aortas," *Nitric Oxide*, vol. 16, no. 4, pp. 442–447, 2007.
- [12] A. A. Syed, M. I. Reza, P. Singh, A. Husain, S. Dadge, and J. R. Gayen, "Polyphenolic-rich *Cissus quadrangularis* extract ameliorates insulin resistance by activating AdipoR1 in *peri-/post-menopausal* rats," *Experimental Gerontology*, vol. 159, article 111681, 2022.
- [13] A. A. Syed, M. I. Reza, A. Husain, P. Singh, and J. R. Gayen, "Inhibition of NOX4 by *Cissus quadrangularis* extract protects from type 2 diabetes induced-steatohepatitis," *Phytomedicine Plus*, vol. 1, no. 1, article 100021, 2021.
- [14] A. A. Syed, M. I. Reza, R. Garg, U. K. Goand, and J. R. Gayen, "*Cissus quadrangularis* extract attenuates diabetic nephropathy by altering SIRT1/DNMT1 axis," *Journal of Pharmacy and Pharmacology*, vol. 73, no. 11, pp. 1442–1450, 2021.
- [15] A. A. Syed, M. I. Reza, M. Shafiq et al., "Naringin ameliorates type 2 diabetes mellitus-induced steatohepatitis by inhibiting RAGE/NF- κ B mediated mitochondrial apoptosis," *Life Sciences*, vol. 257, article 118118, 2020.
- [16] T. O. Omóbòwálé, A. A. Oyagbemi, B. S. Ogunpolu et al., "Antihypertensive effect of polyphenol-rich fraction of *Azadirachta indica* on *N ω* -nitro-L-arginine methyl Ester-induced hypertension and cardiorenal dysfunction," *Drug Research*, vol. 69, no. 1, pp. 12–22, 2019.
- [17] T. Kakuda, I. Sakane, T. Takihara, Y. Ozaki, H. Takeuchi, and M. Kuroyanagi, "Hypoglycemic effect of extracts from *Lagerstroemia speciosa* L. leaves in genetic diabetic KK-A Y mice," *Bioscience, Biotechnology, and Biochemistry*, vol. 60, no. 2, pp. 204–208, 1996.
- [18] G. Klein, J. Kim, K. Himmeldirk, Y. Cao, and X. Chen, "Anti-diabetes and anti-obesity activity of *Lagerstroemia speciosa*," *Evidence-Based Complementary and Alternative Medicine*, vol. 2007, Article ID 547546, 407 pages, 2007.
- [19] W. Hou, Y. Li, Q. Zhang et al., "Triterpene acids isolated from *Lagerstroemia speciosa* leaves as α -glucosidase inhibitors," *Phytotherapy Research: An International Journal Devoted to Pharmacological and Toxicological Evaluation of Natural Product Derivatives*, vol. 23, no. 5, pp. 614–618, 2009.
- [20] T. T. Priya, M. C. Sabu, and C. I. Jolly, "Free radical scavenging and anti-inflammatory properties of *Lagerstroemia speciosa* (L)," *Inflammopharmacology*, vol. 16, no. 4, pp. 182–187, 2008.
- [21] N. H. Aljarba, M. S. Hasnain, A. AlKahtane, H. Algamdy, and S. Alkahtani, "*Lagerstroemia speciosa* extract ameliorates oxidative stress in rats with diabetic nephropathy by inhibiting AGEs formation," *Journal of King Saud University-Science*, vol. 33, no. 6, article 101493, 2021.
- [22] A. A. Syed, M. Shafiq, M. I. Reza et al., "Ethanol extract of *Cissus quadrangularis* improves vasoreactivity by modulation of eNOS expression and oxidative stress in spontaneously hypertensive rats," *Clinical and Experimental Hypertension*, vol. 44, no. 1, pp. 63–71, 2022.
- [23] D. Liu, L. Gao, S. K. Roy, K. G. Cornish, and I. H. Zucker, "Role of oxidant stress on AT1 receptor expression in neurons of rabbits with heart failure and in cultured neurons," *Circulation Research*, vol. 103, no. 2, pp. 186–193, 2008.
- [24] J. M. Barbosa-Filho, V. K. M. Martins, L. A. Rabelo et al., "Natural products inhibitors of the angiotensin converting enzyme (ACE): a review between 1980 - 2000," *Revista Brasileira de Farmacognosia*, vol. 16, no. 3, pp. 421–446, 2006.
- [25] A. Sandoo, J. J. C. S. V. van Zanten, G. S. Metsios, D. Carroll, and G. D. Kitas, "The endothelium and its role in regulating vascular tone," *The Open Cardiovascular Medicine Journal*, vol. 4, p. 302, 2010.
- [26] P. M. Vanhoutte, H. Shimokawa, M. Feletou, and E. H. C. Tang, "Endothelial dysfunction and vascular disease – a 30th

Research Article

Comparative Genomic Characterization of Relaxin Peptide Family in Cattle and Buffalo

Muhammad Saif-ur Rehman,¹ Faiz-ul Hassan ,¹ Zia-ur Rehman,² Hafiz Noubahar Hussain,³ Muhammad Adnan Shahid,¹ Muhammad Mushahid ,¹ and Borhan Shokrollahi ⁴

¹Institute of Animal and Dairy Sciences, University of Agriculture, Faisalabad 38040, Pakistan

²University of Agriculture Faisalabad-Sub Campus, Toba Tek Singh 36050, Pakistan

³Animal Science Division, Nuclear Institute for Agriculture and Biology (NIAB), Faisalabad, Pakistan

⁴Department of Animal Science, Sanandaj Branch, Islamic Azad University, Sanandaj, Iran

Correspondence should be addressed to Borhan Shokrollahi; borhansh@iausdj.ac.ir

Received 30 July 2022; Accepted 9 September 2022; Published 4 October 2022

Academic Editor: Akhtar Ali

Copyright © 2022 Muhammad Saif-ur Rehman et al. This is an open access article distributed under the Creative Commons Attribution License, which permits unrestricted use, distribution, and reproduction in any medium, provided the original work is properly cited.

Relaxin family peptides significantly regulate reproduction, nutrient metabolism, and immune response in mammals. The present study aimed to identify and characterize the relaxin family peptides in cattle and buffalo at the genome level. The genomic and proteomic sequences of cattle, buffalo, goat, sheep, horse, and camel were accessed through the NCBI database, and BLAST was performed. We identified four relaxin peptides genes (*RLN3*, *INSL3*, *INSL5*, and *INSL6*) in *Bos taurus*, whereas three relaxin genes (*RLN3*, *INSL3*, and *INSL6*) in *Bubalus bubalis*. Evolutionary analysis revealed the conserved nature of relaxin family peptides in buffalo and cattle. Physicochemical properties revealed that relaxin proteins were thermostable, hydrophilic, and basic peptides except for *INSL5* which was an acidic peptide. Three nonsynonymous mutations (two in *RLN3* at positions A16>T and P29>A, and one in *INSL6* at position R32>Q) in *Bos taurus*, whereas two nonsynonymous mutations (one in *RLN3* at positions G105>w and one in *INSL3* at position G22>R) in *Bubalus bubalis*, were identified. *INSL3* had one indel (insertion) at position 55 in *Bos taurus*. Gene duplication analysis revealed predominantly segmental duplications (*INSL5/RLN3* and *INSL6/INSL3* gene pairs) that helped expand this gene family, whereas *Bubalus bubalis* showed primarily tandem duplication (*INSL3/RLN3*). Our study concluded that relaxin family peptides remained conserved during the evolution, and gene duplications might help to adapt and enrich specific functions like reproduction, nutrient metabolism, and immune response. Further, the nonsynonymous mutations identified potentially affect these functions in buffalo.

1. Introduction

The relaxin peptide family comprises seven peptides with significant structural similarities but low sequence resemblance. It includes seven genes, relaxin like *RLN1*, -2, and -3, and insulin-like *INSL3*, -4, -5, and -6 in most mammals [1], but their number varies. These peptides show a high sequence resemblance with insulin due to the presence of six cysteine residues that provide the 2 interchain and 1 intrachain disulphide linkages. Each relaxin peptide family member is constituted of two chains called A and B chains

[2]. These chains are connected by two disulfide bonds present between them and one disulfide bond within the A chain. Each chain contained the cysteine residues together with distinctive disulfide bonding, which are found conserved across all family members [2].

The *RLN1* and *RLN2* are present in humans and higher primates like apes. Both are referred to as relaxin as human *RLN2* is an orthologue to *RLN1* in other mammals [1, 3]. *RLN3* was first identified in 2002 and is considered the common ancestral gene for all relaxin peptides [2, 4]. *RLN1* and its orthologue *RLN2* play an important role in reproduction

in mammals [5], but in bovines, these genes have been lost during the evolution and have no traces in the genome [6]. *RLN3* has been shown to play a role in nutrient metabolism in cattle [7]. *INSL3* plays a crucial role in testicular descent by promoting the growth and development of the gubernaculum ligament [8]. *INSL4* is highly expressed in the placenta and might be involved in bone development [5, 9]. Its receptor is yet to be identified. *INSL5* with its cognate receptor *RXFP4* has been suggested to play important role in immune response regulation, signal transmission to CNS through the vagus nerve, and autocrine/paracrine function within the intestinal tract [10]. *INSL6* role in sperm production has been determined in buffalo [11].

Relaxin family peptides have important role in ruminant reproduction and nutrient metabolism as mentioned above. The availability of genomic data has provided opportunity to perform genome-wide characterization of protein families using the different available bioinformatics tools. Many studies have been conducted to identify the evolutionary relationships, physicochemical characteristics, comparative amino acid analysis, effects of mutations, and gene duplications in important protein families in ruminants [12–15]. The present study was conducted to characterize relaxin family peptides in cattle (*Bos taurus*) and buffalo (*Bubalus bubalis*) at genome-wide level in order to better understand their evolutionary significance, physicochemical properties, and gene duplications events.

2. Materials and Methods

2.1. Genome-Wide Identification of Relaxin Peptides. The whole genome and proteomic sequence data of buffalo (UOA WB 1), cattle (ARS-UCD1.2), sheep (Oar rambouillet v1.0), goat (ARS1), camel (CamDro3), and horse (EquCab3.0) were obtained from the National Center for Biotechnology Information (NCBI) database [16]. A genome-wide BLAST and HMM search was performed to look for all putative relaxin peptide genes in *Bos taurus*, *Bubalus bubalis*, and other targeted species [17]. The cattle (*Bos taurus*), buffalo (*Bubalus bubalis*), goat (*Capra hircus*), sheep (*Ovis aries*), horse (*Equus caballus*), and camel (*Camelus dromedarius*) relaxin peptide sequences were also validated through the UniProt database search [18]. All accession numbers of sequences used for this study are presented in Table S1. No information was available for *INSL5* gene annotation of *Bubalus bubalis* in the databases.

2.2. Phylogenetic Analysis. Relaxin peptide amino acid sequences from *Bos taurus*, *Bubalus bubalis*, *Capra hircus*, *Ovis aries*, *Equus caballus*, and *Camelus dromedarius* were aligned in ClustalW. Further, the neighbor-joining (NJ) tree was constructed through the MEGA7 software [19].

2.3. Gene Structure, Motif Patterns, and Conserved Domain Analysis of Relaxin Peptide Family. The conserved motifs in the dataset were analyzed using the MEME suite [20]. As a query, the relaxin protein sequences were submitted in Fasta format, and a site distribution with one occurrence of each site was determined for each sequence. The motifs'

minimum and maximum widths were found to be 6 and 50, respectively. The number of themes was limited to ten. The Gene Structure Display Server (GSDS) [21] was used to import all CDs and genomic sequences. The final gene structure was exhibited and illustrated using the genome annotation data in general feature format utilizing in-house scripts in the TBtools software (GFF).

2.4. Physicochemical Properties of Relaxin Proteins. The online available ProtParam tool [22] was used to evaluate the physicochemical characteristics of relaxin peptides including molecular weight (MW), amino acid count (AA), isoelectric point (pI), and aliphatic index (A.I.). Besides, it also included instability index (II) and the grand average of hydropathicity (GRAVY).

2.5. Multiple Sequence Analysis (MSA). Multiple align show [23] was used online to explore the mutations and indels in the relaxin peptides using the aligned sequences of *Bos taurus*, *Bubalus bubalis*, *Capra hircus*, and *Ovis aries*.

2.6. Mutational Analysis. Further, the mutations found in *Bos taurus* and *Bubalus bubalis* relaxin peptide sequences were subsequently examined using several online tools (PolyPhen-2, MUpro, PROVEAN, IMutant, PhD-SNP, SIFT, SNAP2, PredictSNP, Meta-SNP, and SNAP) to determine their effects on protein structure and functions.

2.7. Nuclear Hormone Receptor Sites Identification. The NHR scan [24] was employed to predict nuclear hormone receptor binding sites. Using genomic sequences in Fasta format, NHR scan was performed. The cumulative probability of entering match states was 0.01 using the NHR scan.

2.8. Synteny Analysis and Gene Duplications. To find collinear genes, the whole genomes of cattle and buffalo were blasted to each other. The dual-synteny map was constructed using the TBtools after submitting annotation files for both genomes, including information about collinear genes and chromosomal IDs.

Chromosomal locations of relaxin genes were obtained from genomic resources of respective specie. An annotated genome file was saved as a general feature format (GFF) file and was fed into the MCScanX programme [25], which was subsequently used to plot the gene locations on chromosomes and presented in TB tools. In addition, the relaxin peptide gene collinearity plots for *Bos taurus* and *Bubalus bubalis* were generated. Further, for the *Bos taurus* and *Bubalus bubalis* relaxin peptide gene family, pairwise alignment of homologous gene pairs of relaxin peptide genes using MEGA7 [19] with the MUSCLE method was utilized to analyze the frequency of duplications. DnaSP v6.0 [26] was also used to determine pairwise synonymous substitutions per synonymous site (ks) and nonsynonymous substitutions per nonsynonymous site (ka) that were corrected for multiple hits. Synonymous mutations are referred as silent mutations which can result in altered DNA sequence but does not change the encoded amino acid (evolutionary neutral mutations), whereas nonsynonymous mutations cause

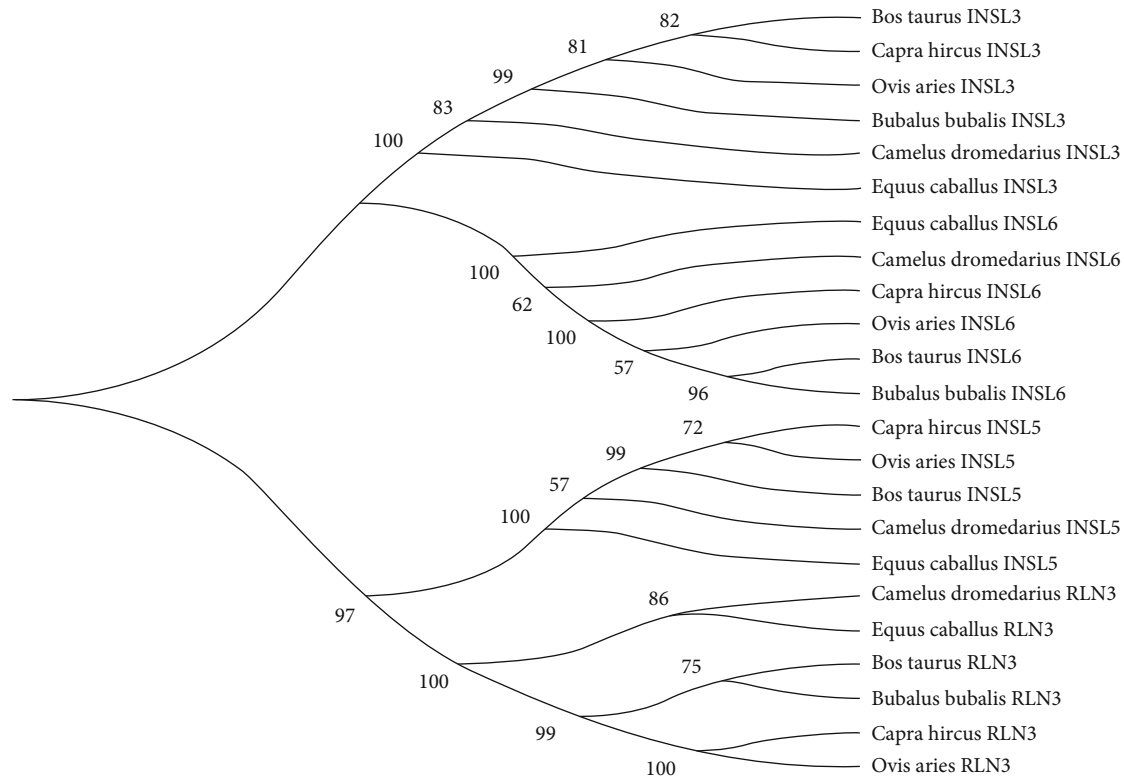


FIGURE 1: Evolutionary relationship of relaxin peptides (*RLN3*, *INSL3*, *INSL5*, *INSL6*) in six mammalian species.

change in both DNA and protein sequence (evolutionary important mutations).

3. Results

3.1. Phylogenetic Analysis. Results revealed that relaxin peptide family consisted of four genes (*RLN3*, *INSL3*, *INSL5*, and *INSL6*) in all representative species, except for *Bubalus bubalis* which had 3 of them excluding *INSL5* (Figure 1). All four genes were clustered into two sister clades. From top to downward, clade 1 included *INSL3* and *INSL6*, whereas clade 2 included *INSL5* and *RLN3*. Overall phylogenetic analysis of the relaxin peptide family revealed that the “*Bos taurus* and *Bubalus bubalis*,” “*Capra hircus* and *Ovis aries*,” and “*Camelus dromedarius* and *Equus caballus*” had close similarities between them. However, *INSL3* showed more evolutionary similarities between “*Bos taurus* and *Capra hircus*” than between “*Bos taurus* and *Bubalus bubalis*.”

3.2. Structural Categorization of the Relaxin Peptide Family. The examination of gene organization, motif patterns, and conserved domains in the relaxin peptide family of four targeted species, including *Bos taurus*, *Bubalus bubalis*, *Capra hircus*, and *Ovis aries*, were performed to carry out the structural characterization of the relaxin peptide family while taking account of their evolutionary relationships (Figures 2(a)–2(d)). The top ten MEME-conserved motifs were investigated to look for conserved domains (Table 1). No conserved domain was detected in the Pfam search for these motifs. Further, all genes were investigated to look for conserved domains across all targeted species

(Figure 3(c)). The insulin/insulin-like growth factor (IIGF) domain was found conserved across all targeted species, which was further validated through a conserved domain database (CDD) BLAST. A gene structural analysis revealed the evolutionarily conserved nature of relaxin family genes across the studied species (Figure 3(d)). The same gene across different species revealed a similar number of introns and exons.

3.3. Physico-chemical Properties of the Relaxin Proteins. The physicochemical properties like location on the chromosome, exon count, molecular weight (Da), number of amino acids (A.A) in each peptide, aliphatic index (A.I.), isoelectric point (pI), instability index (II), and grand average of hydrophobicity index (GRAVY) of the relaxin peptides were evaluated in cattle through the ProtParam tool (Table 2). The molecular weight of relaxin peptides ranged from 14 to 24 kDa. *RLN3* and *INSL3* were located on chromosomes 7, whereas *INSL5* and *INSL6* were located on chromosomes 3 and 8, respectively. All relaxin peptide genes had an exons count of 2 and a variable length of the peptides with amino acid residues. The pI values revealed all relaxin peptides were basic except for *INSL5* which was slightly acidic. The AI values suggested the thermostable nature of all peptides having AI values greater than 65. Moreover, II values greater than 40 revealed that all peptide members of the relaxin family are unstable in vitro. Negative GRAVY values suggested the hydrophilic nature of relaxin peptides.

3.4. Identification of Mutations in Relaxin Peptides. Comparative amino acid analysis was performed by aligning the

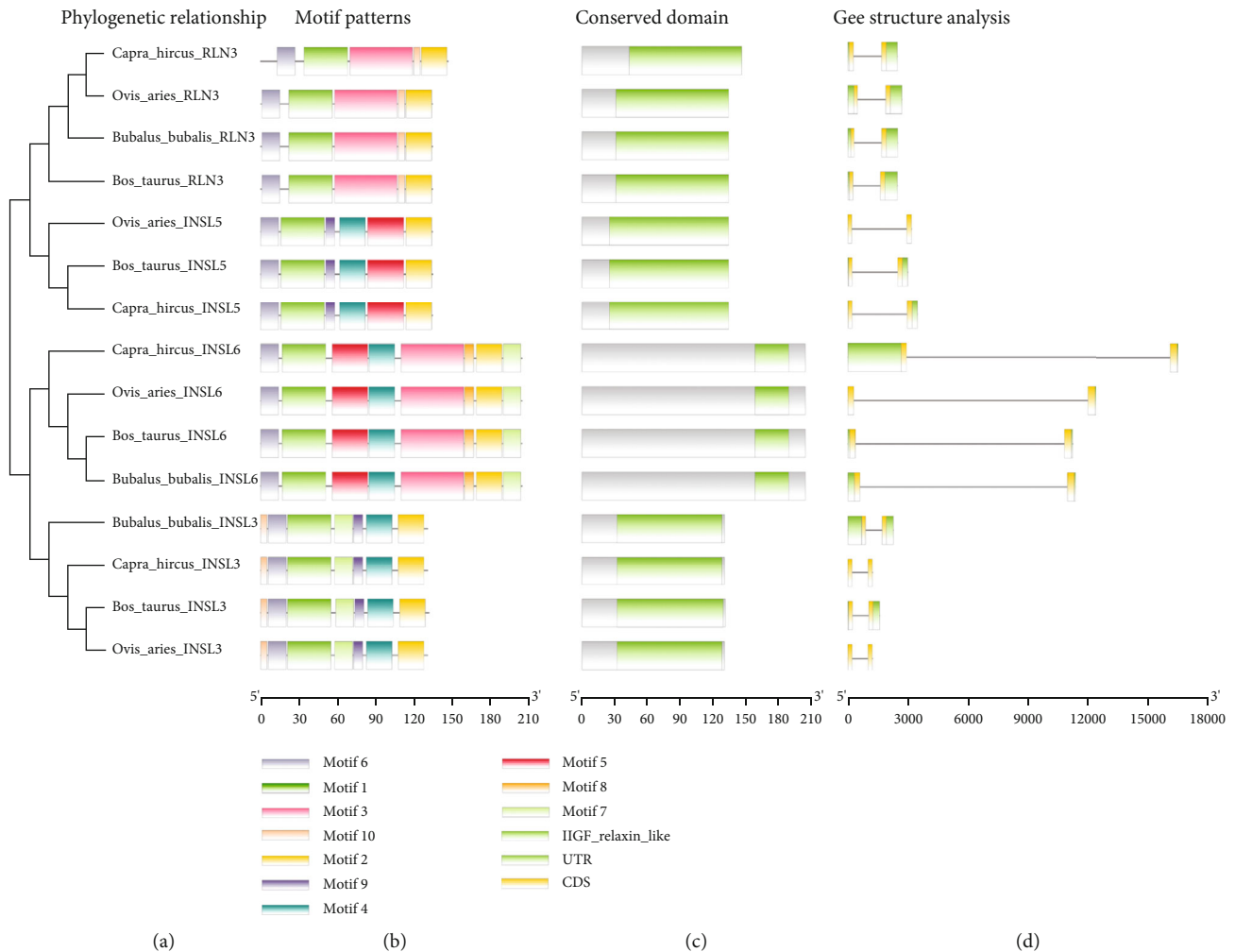


FIGURE 2: Graphical representation of motif patterns (b), conserved domains (c), and gene structure (d) of relaxin peptide family genes corresponding to their phylogenetic relationships (a) in four mammalian species.

TABLE 1: Top ten differentially conserved motifs detected in relaxin peptide family (*RLN3*, *INSL3*, *INSL5*, and *INSL6*).

Motif	Protein sequence	Length	Pfam domain
MEME-1	REAAATEAARKLCGRHFIRAVVKLCGGSRW SREEG	35	—
MEME-2	RGLSEKCKKGGCTKSELLTLC	21	—
MEME-3	PEYQYPEVBLPFESELEEAVASSEILPTKEPIEFYGNKTBKIGTSPNLF	50	—
MEME-4	DPALNPAPQPLSQEEAIHNMK	21	—
MEME-5	TQLLSZASEKVESFIPDRSESSQTTFPVW	29	—
MEME-6	MRALVLLLLALAVLL	15	—
MEME-7	LPGGDYELLRKLZGL	15	—
MEME-8	WGNHPQRK	8	—
MEME-9	HLLHGLMA	8	—
MEME-10	GDRDPL	6	—

protein sequences of the relaxin peptides of buffalo, cattle, goat, sheep, camel, and horse in multiple align show to look for indels and single amino acid variations in *Bos taurus* and *Bubalus bubalis* (Figures 3–3(d)).

In *RLN3* protein, mutations were observed in *Bos taurus* at positions A16>T, P29>A, and A62>T and *Bubalus*

bubalis at position G105>W (Figure 3). *INSL3* had one indel (insertion) at position 55 in *Bos taurus* (Figure 3(b)). In *INSL3*, mutations were observed in *Bubalus bubalis* at positions G22>R, V86>M, and V88>I, whereas no mutation was observed in *Bos taurus* (Figure 3(b)). *INSL5* sequence of *Bubalus bubalis* was not found in the database.



FIGURE 3: (a–d) Comparative amino acid analysis of the relaxin peptide family (RLN3, INSL3, INSL5, and INSL6) in *Bos taurus*, *Bubalus bubalis*, *Capra hircus*, and *Ovis aries*.

TABLE 2: Physicochemical properties of the relaxin family peptides in *Bos taurus*.

Gene	Chromosome	Exon count	MW (kDa)	A.A	pI	AI	II	GRAVY
RLN3	7	2	14.75	135	7.60	86.00	55.82	-0.162
INSL3	7	2	14.38	132	8.69	96.21	67.33	-0.145
INSL5	3	2	15.36	135	6.89	73.04	76.93	-0.389
INSL6	8	2	24.00	205	9.14	77.51	66.54	-0.717

MW: molecular weight; A.A: number of amino acids; pI: isoelectric point; AI: aliphatic index; II: instability index; GRAVY: grand average of hydrophaticity index.

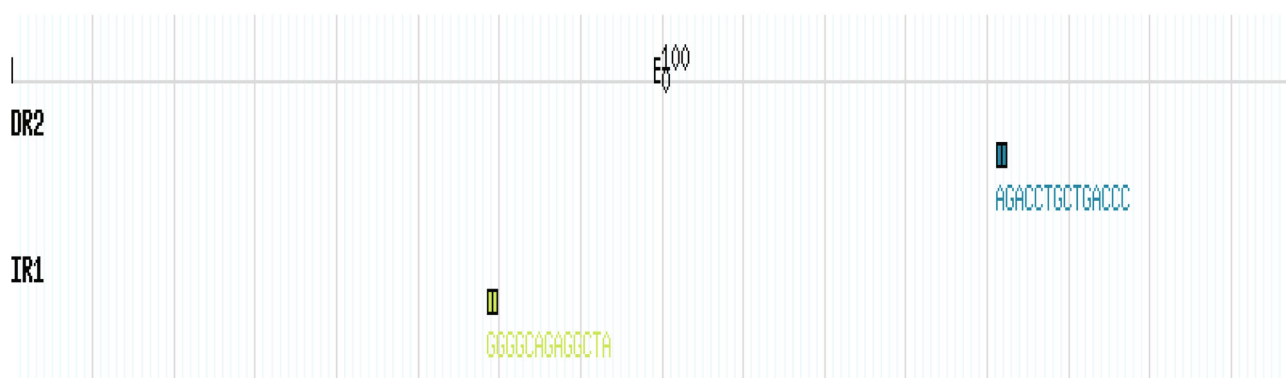
INSL6 had a mutation in *Bos taurus* at position R32 > Q, whereas no mutation was detected in *Bubalus bubalis*.

Additionally, the mutations observed in *Bos taurus* and *Bubalus bubalis* through a comparative amino acid analysis were further analyzed through different online available mutational analysis tools to predict the functional effects of these

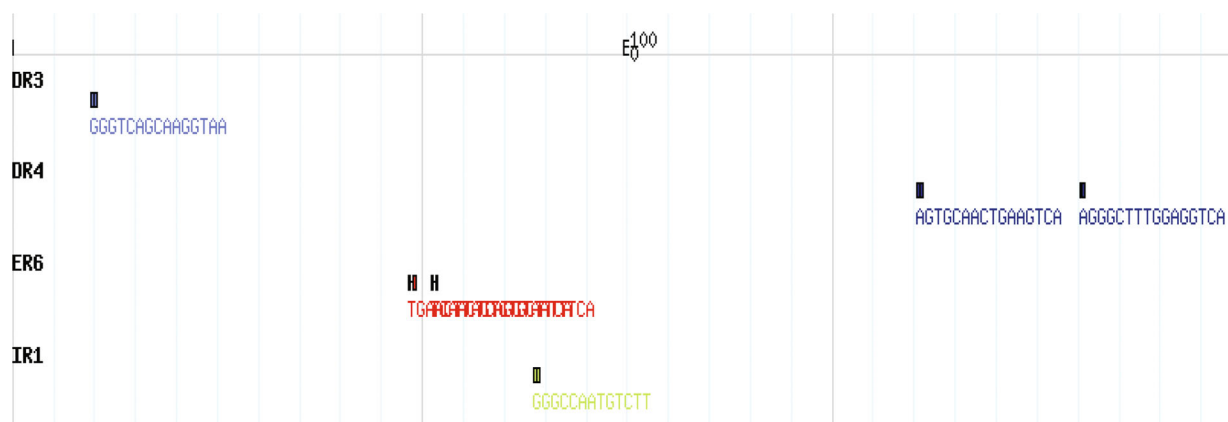
mutations (Table S2). In *Bos taurus*, a total of three nonsynonymous mutations were predicted, two in *RLN3* at positions A16 > T and P29 > A, and one in *INSL6* at position R32 > Q. In *Bubalus bubalis*, a total of two nonsynonymous mutations were predicted, one in *RLN3* at positions G105 > w, G22 > R, and one in *INSL3* at position G22 > R.



(a)

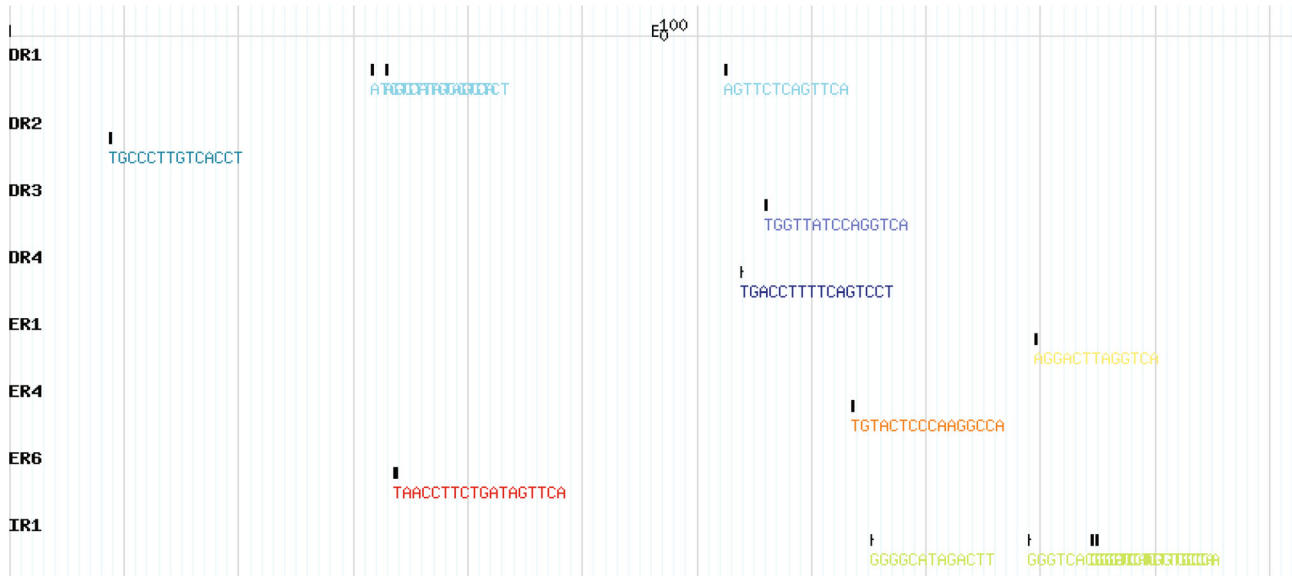


(b)



(c)

FIGURE 4: Continued.



(d)

FIGURE 4: NHR scans patterns of *RLN3* (a), *INSL3* (b), *INSL5* (c), and *INSL6* (d) in *Bos taurus*.

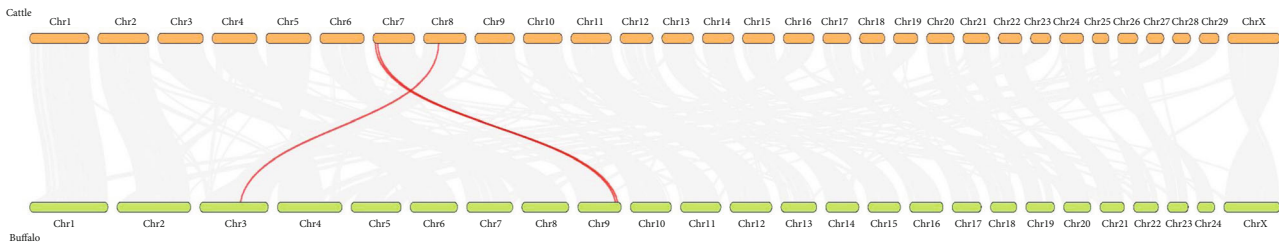


FIGURE 5: Synteny plot between *Bos taurus* and *Bubalus bubalis* genomes.

3.5. *NHR Patterns in Relaxin Peptides.* The *Bos taurus* nuclear hormone receptor sites (NHRs) were searched for all four relaxin peptides (*RLN3*, *INSL3*, *INSL5*, and *INSL6*) (Figures 4(a)–4(d)). A total of 23 NHRs were found of which *RLN3* had 3, *INSL3* had 2, *INSL5* had 6, and *INSL6* had 12. The number of direct repeats (DR) identified in *RLN3*, *INSL3*, *INSL5*, and *INSL6* were 2, 1, 3, and 6, respectively. The number of everted repeats (ER) identified in *RLN3*, *INSL3*, *INSL5*, and *INSL6* were 1, 0, 2, and 3, respectively. The number of inverted repeats (IR) identified in *RLN3*, *INSL3*, *INSL5*, and *INSL6* were 0, 1, 1, and 3, respectively.

3.6. *Synteny Analysis and Gene Duplications.* Collinearity analysis showed that relaxin family genes were randomly distributed over 2 chromosomes in both cattle and buffalo (Figure 5). In *Bos taurus*, relaxin peptide genes were present on chromosomes 7 and 8, whereas in *Bubalus bubalis*, these genes were located on chromosomes 3 and 9.

Further, the gene duplication analysis was performed to look for segmental or tandem duplication gene pairs in the relaxin peptide family of *Bos taurus* and *Bubalus bubalis* (Table 3). In *Bos taurus*, two segmental duplication events were observed between *INSL5/RLN3* and *INSL6/INSL3* gene

TABLE 3: Analysis of duplicated gene pairs and their k_a/k_s values of relaxin peptide family in *Bos taurus* and *Bubalus bubalis*.

<i>Bos taurus</i> Gene pair	Chromosome	Duplication	k_a	k_s	k_a/k_s
<i>INSL5/RLN3</i>	3/7	SD	0.32	0.47	0.68
<i>INSL6/INSL3</i>	8/7	SD	0.33	0.56	0.60
<i>Bubalus bubalis</i> Gene pair	Chromosome	Duplication	k_a	k_s	k_a/k_s
<i>INSL3/RLN3</i>	9/9	TD	0.37	0.50	0.74

k_a : number of nonsynonymous substitutions per nonsynonymous site; k_s : number of synonymous substitutions per synonymous site; SD: segmental duplication; TD: tandem duplication.

pairs, whereas in *Bubalus bubalis*, one tandem duplication was detected between *INSL3/RLN3* gene pair. The number of nonsynonymous substitutions per nonsynonymous site/number of synonymous substitutions per synonymous site (k_a/k_s) ratios was determined for this duplicated event. *Bos taurus* segmental duplicated pairs *INSL5/RLN3* and *INSL6/INSL3* showed 0.68 and 0.60 k_a/k_s ratios, respectively,

whereas *Bubalus bubalis* tandem duplication pair *INSL3/RNL3* showed 0.74 ka/ks ratio.

4. Discussion

4.1. Phylogenetic Analysis. In recent years, genomic sequencing technology, particularly next-generation sequencing, has advanced significantly, resulting in the accessibility of sequenced genomes for many important organisms, opening up a new path for understanding the genomic architecture at the molecular level of diverse animal species [27]. Comparative genomics allows for the discovery of new genes and functional components [28, 29]. Advances in bioinformatics have enabled the utilization of genomic data and look into the protein family evolutionary history, comparative amino acid analysis, gene duplications and prediction of mutations, and their functional and structural effects [12–15].

The relaxin peptide family has been found to contain seven members in most mammals, including relaxin-like genes *RLN1*, *RLN2*, and *RLN3* and insulin-like genes *INSL3*, *INSL4*, *INSL5*, and *INSL6* [30]. In our analysis, we have found four genes (*RNL3*, *INSL3*, *INSL5*, and *INSL6*) in *Bos taurus*, *Capra hircus*, *Ovis aries*, *Camelus dromedarius*, and *Equus caballus*, whereas three genes (*RNL3*, *INSL3*, and *INSL6*) in *Bubalus bubalis* from the sequenced genome of these species. Further, these genes were grouped into two sister major clades, clade 1 included *INSL3* and *INSL6*, whereas clade 2 included *INSL5* and *RLN3*. A variable number of *RLN/INSL* peptides were also observed in different vertebrates [31–33]. These variations could be explained on the basis of gene loss and fixation during the evolution and adaptation to specific niches. Overall phylogenetic analysis of the relaxin peptide family revealed that the “*Bos taurus* and *Bubalus bubalis*,” “*Capra hircus* and *Ovis aries*,” and “*Camelus dromedarius* and *Equus caballus*” had close similarities between them. Previous studies also revealed evolutionary similarities between these species [12, 13]. However, *INSL3* peptide showed more evolutionary similarity between “*Bos taurus* and *Capra hircus*” than between “*Bos taurus* and *Bubalus bubalis*”. Researchers have been fascinated by relaxin evolution for decades. Relaxins are renowned for their high sequence variability across closely related species, although unexpected parallels have been found between quite different species like pigs and whales [34].

4.2. Structural Features of Relaxin Peptides. The examination of gene organization, motif patterns, and conserved domains of the relaxin peptide family of four targeted species including *Bos taurus*, *Bubalus bubalis*, *Capra hircus*, and *Ovis aries* revealed the conserved nature of relaxin genes across the targeted species. The insulin/insulin-like growth factor (IIGF) domain was found conserved in all relaxin family genes across all targeted species. The insulin/IGF system (IIGFs) regulates a wide range of physiological processes, including development, linear growth, and aging, as well as metabolism, homeostasis, and central nervous system activities [35, 36]. This domain is important for proper function, and any dysregulation in this domain can result in abnormal

growth, increased development and progression of numerous cancers, and pathologic ailments associated with chronic inflammation and fibrosis [37, 38].

4.3. Physico-chemical Properties of Relaxin Peptides. The physicochemical properties of the relaxin peptide family proteins were evaluated in *Bos taurus* through the ProtParam tool (Table 2). The molecular weight of relaxin peptides ranged from 14 to 24 kDa. The aliphatic index (AI) tells about the thermostability of globular proteins, and values greater than 65 show greater thermostability [39]. In our study, all relaxin family peptides were found thermostable. In vitro stability of proteins can be inferred through the instability index (II), and the II value lower than 40 indicates the in vitro stability of proteins [40], as in our case, all relaxin family peptides showed in vitro instability having values greater than 40. The GRAVY values tell about the hydrophobicity of protein, the negative GRAVY values show hydrophilic nature, whereas the positive GRAVY values show hydrophobic nature of proteins [41], as in our case, all relaxin family peptides showed hydrophilic nature having negative GRAVY values.

4.4. Comparative Mutational Analysis. Comparative genomics is a large-scale, integrated technology for the comparison of two or more genomes. Comparative studies at various levels of the genomes may be conducted to obtain distinct perspectives on the organisms [35, 42]. We aligned the sequences of four species *Bos taurus*, *Bubalus bubalis*, *Capra hircus*, and *Ovis aries* in multiple align show to look for indels and single amino acid variations in *Bos taurus* and *Bubalus bubalis*. All relaxin family peptides were found well conserved with few amino acid variations in *Bos taurus* and *Bubalus bubalis*. *INSL3* had one indel (insertion) at position 55 in *Bos taurus*. Indels and mutations have all played a part in the divergence of gene family members from their progenitors [43]. Further, the mutational analysis of observed single amino acid variations predicted three nonsynonymous mutations (two in *RLN3* at positions A16 > T and P29 > A and one in *INSL6* at position R32 > Q) in *Bos taurus*, whereas two nonsynonymous mutations (one in *RLN3* at positions G105 > w, G22 > R, and one in *INSL3* at position G22 > R) in *Bubalus bubalis*. *RLN3* gene was observed to play role in feed efficiency in cattle [7]. *INSL3* is a gender-specific gene that is produced in Leydig cells of male adult and fetus and plays a key role in testicular descent [44]. Higher level of *INSL3* gene was observed in female ruminant blood with male fetus. Mutations in the *INSL3* gene resulted in failure of testicular descent (cryptorchidism) [45, 46]. *INSL6* was detected to play a role during spermatogenesis [11]. The deficiency of *INL6* in mice resulted in a decline in sperm production and immotility [47]. Mutations in these genes can interfere with functions like feed metabolism, testicular descent, and spermatogenesis in bovines.

4.5. NHR Patterns in Relaxin Peptides. Diverse biochemical mechanisms are involved in gene regulation and information flow from the DNA to the protein that is transcription and translation, and understanding of these mechanisms is

necessary to explore the cell dynamics [48]. Nuclear receptors bind to target genes at sites referred as hormone response elements (HREs) and help to regulate the transcription. These HREs are usually located in the 5-flanking region of target genes. Even though HREs are primarily found near the primary promoter, they can sometimes be found several kilobases upstream away from the start of the transcription site in enhancer regions [49]. Most of the time, a single NHR has been found to impact many genes, and sometimes, many NHRs have competition for one target gene and result in overlapping networks for the target genes [50]. This competition for the same target gene sometimes results in reduced expression of the gene. The expression of the gene can also be reduced if NHR bind with negative HREs [49]. The pattern of NHR sites in the relaxin peptide family in *Bos taurus* was investigated. A total of 23 NHR sites were detected. In total, 12 direct repeats (DR), 6 everted repeats (ER), and 5 inverted repeats (IR) were found in the *Bos taurus* relaxin genes.

4.6. Synteny Analysis and Gene Duplications. Chromosomal regions common between two genomes with the same homologous genes order as in common ancestor sites are called synteny blocks [51]. Different species originating from the common ancestor in the same tree of life can be compared using syntenic relationships, which will give an idea about the chromosomal structure and number variation between species [52, 53]. Synteny analysis revealed that relaxin peptide genes were randomly located over 2 chromosomes in both *Bos taurus* and *Bubalus bubalis*. In *Bos taurus*, relaxin genes were present on chromosomes 7 and 8, whereas in *Bubalus bubalis*, these genes were located on chromosomes 3 and 9. Further, the gene duplication events were examined for *Bos taurus* and *Bubalus bubalis*. Gene duplications have evolutionary significance as it is believed that during the evolution, whole genome duplications occurred and only 5 to 10% of duplicated genomes got fixed to perform specific functions, while others were lost in the process [54, 55]. These duplication events helped in the expansion of genome size and increased complexities to perform specific functions as indicated by two rounds of duplications hypothesis (2R hypothesis) [56, 57]. In our study, the *Bos taurus* relaxin peptide family showed predominantly segmental duplications (*INSL5/RLN3* and *INSL6/INSL3* gene pairs) that helped in the expansion of this gene family, whereas *Bubalus bubalis* showed predominantly tandem duplication (*INSL3/RLN3*). Our results are in agreement with Liu et al. [58], and they explained that segmental duplications are predominant in cattle genome and these duplications in bovine genomes are enriched with specific biological processes related to digestion, lactation, immunity, and reproduction. Further, the k_a/k_s ratios were lower than 1 for all these observed duplications, indicating the purifying pressure for these duplication events [59].

5. Conclusions

Our study revealed four relaxin peptide family genes (*RLN3*, *INSL3*, *INSL5*, and *INSL6*) in *Bos taurus*, whereas three

relaxin peptide genes (*RLN3*, *INSL3*, and *INSL6*) in *Bubalus bubalis* in contrast to seven genes in most of the mammals. The loss of genes might be the result of adaptation to specific niches during evolution. Relaxin family peptides remained conserved during evolution. Nonsynonymous mutations in *RLN3*, *INSL3*, and *INSL6* can interfere with biological functions like spermatogenesis, testicular descent, and feed metabolism in bovines. The segmental duplication in *Bos taurus* and the tandem duplication in *Bubalus bubalis* of relaxin family peptides helped in enrichment to specific functions like reproduction and feed metabolism during evolution.

Data Availability

All data are shown within the manuscript.

Conflicts of Interest

The authors declare that there is no conflict of interest regarding the publication of this paper.

Authors' Contributions

Muhammad Saif-ur Rehman and Faiz-ul Hassan contributed equally to this manuscript.

Acknowledgments

This study was funded by the "National Centre for Livestock Breeding, Genetics and Genomics (NCLBGG)", Subcentre-UAF, Pakistan.

Supplementary Materials

Table S1: Relaxin peptides gene family members' nucleotide and protein sequences accessions from NCBI database (Genbank accessions) for *Bos taurus*, *Bubalus bubalis*, *Capra hircus*, *Ovis aries*, *Camelus dromedarius* and *Equus caballus*. Table S2: Mutational effects predicted through different online software in relaxin peptides of *Bos taurus* and *Bubalus bubalis*. (*Supplementary Materials*)

References

- [1] T. N. Wilkinson, T. P. Speed, G. W. Tregear, and R. A. D. Bathgate, "Evolution of the relaxin-like peptide family," *BMC Evolutionary Biology*, vol. 5, no. 1, pp. 14–17, 2005.
- [2] L. Jiaying Chan, M. Akhter Hossain, C. S. Samuel, F. Separovic, and J. D. Wade, "The relaxin peptide family – structure, function and clinical applications," *Protein and Peptide Letters*, vol. 18, no. 3, pp. 220–229, 2011.
- [3] B. A. Evans, P. Fu, and G. W. Tregear, "Characterization of two relaxin genes in the chimpanzee," *The Journal of Endocrinology*, vol. 140, no. 3, pp. 385–392, 1994.
- [4] S. Y. T. Hsu, "New insights into the evolution of the relaxin-LGR signaling system," *Trends in Endocrinology and Metabolism*, vol. 14, no. 7, pp. 303–309, 2003.
- [5] R. A. D. Bathgate, M. L. Halls, E. T. van der Westhuizen, G. E. Callander, M. Kocan, and R. J. Summers, "Relaxin family

- peptides and their receptors," *Physiological Reviews*, vol. 93, no. 1, pp. 405–480, 2013.
- [6] L. Malone, J. C. Opazo, P. L. Ryan, and F. G. Hoffmann, "Progressive erosion of the Relaxin1 gene in bovinds," *General and Comparative Endocrinology*, vol. 252, pp. 12–17, 2017.
- [7] S. D. Perkins, C. N. Key, M. N. Marvin et al., "Effect of residual feed intake on hypothalamic gene expression and meat quality in Angus-sired cattle grown during the hot season1,2," *Journal of Animal Science*, vol. 92, no. 4, pp. 1451–1461, 2014.
- [8] R. Ivell, S. Hartung, and R. A. Anand-Ivell, "Insulin-like factor 3: where are we now?," *Annals of the New York Academy of Sciences*, vol. 1041, no. 1, pp. 486–496, 2005.
- [9] D. Chassin, A. Laurent, J.-L. Janneau, R. Berger, and D. Bellet, "Cloning of a new member of the insulin gene superfamily (INSL4) expressed in human placenta," *Genomics*, vol. 29, no. 2, pp. 465–470, 1995.
- [10] D. Hechter, B. Vahkal, T. Tiede, and S. V. Good, "Reviewing the physiological roles of the novel hormone-receptor pair INSL5-RXFP4: a protective energy sensor?," *Journal of Molecular Endocrinology*, vol. 69, no. 1, pp. R45–R62, 2022.
- [11] Y. Huang, Q. Fu, H. Pan et al., "Spermatogenesis-associated proteins at different developmental stages of buffalo testicular seminiferous tubules identified by comparative proteomic analysis," *Proteomics*, vol. 16, no. 14, pp. 2005–2018, 2016.
- [12] S. U. Rehman, T. Feng, S. Wu et al., "Comparative genomics, evolutionary and gene regulatory regions analysis of casein gene family in *Bubalus bubalis*," *Frontiers in Genetics*, vol. 12, article 662609, 2021.
- [13] M. S. Rehman, F. U. Hassan, Z. U. Rehman, I. Ishtiaq, S. U. Rehman, and Q. Liu, "Molecular characterization of TGF-beta gene family in buffalo to identify gene duplication and functional mutations," *Genes*, vol. 13, no. 8, p. 1302, 2022.
- [14] M. S. Rehman, M. Mushtaq, F. Hassan, Z. Rehman, M. Mushahid, and B. Shokrollahi, "Comparative genomic characterization of insulin-like growth factor binding proteins in cattle and Buffalo," *BioMed Research International*, vol. 2022, Article ID 5893825, 15 pages, 2022.
- [15] S. U. Rehman, A. Nadeem, M. Javed et al., "Genomic identification, evolution and sequence analysis of the heat-shock protein gene family in buffalo," *Genes*, vol. 11, no. 11, p. 1388, 2020.
- [16] NCBI: National Center for Biotechnology Information April 2022, <https://www.ncbi.nlm.nih.gov/>.
- [17] R. D. Finn, J. Clements, and S. R. Eddy, "HMMER web server: interactive sequence similarity searching," *Nucleic Acids Research*, vol. 39, pp. W29–W37, 2011.
- [18] Uniprot, "Protein databse," April 2022, <https://www.uniprot.org/>.
- [19] S. Kumar, G. Stecher, and K. Tamura, "MEGA7: molecular evolutionary genetics analysis version 7.0 for bigger datasets," *Molecular Biology and Evolution*, vol. 33, no. 7, pp. 1870–1874, 2016.
- [20] T. L. Bailey, M. Boden, F. A. Buske et al., "MEME SUITE: tools for motif discovery and searching," *Nucleic Acids Research*, vol. 37, no. Web Server, pp. W202–W208, 2009.
- [21] B. Hu, J. Jin, A.-Y. Guo, H. Zhang, J. Luo, and G. Gao, "GSDS 2.0: an upgraded gene feature visualization server," *Bioinformatics*, vol. 31, no. 8, pp. 1296–1297, 2015.
- [22] E. Gasteiger, C. Hoogland, A. Gattiker, M. R. Wilkins, R. D. Appel, and A. Bairoch, "Protein identification and analysis tools on the ExpASY server," *The proteomics protocols handbook*, pp. 571–607, Humana Totowa, NJ, 2005.
- [23] "MSA: multiple align show," April 2022, https://www.bioinformatics.org/sms/multi_align.html.
- [24] "NHR-SCAN: Nuclear hormone receptor scan," April 2022, http://nhrscan.genereg.net/cgi-bin/nhr_scan.cgi.
- [25] Y. Wang, H. Tang, J. D. DeBarry et al., "MCScanX: a toolkit for detection and evolutionary analysis of gene synteny and collinearity," *Nucleic Acids Research*, vol. 40, no. 7, pp. e49–e49, 2012.
- [26] J. Rozas, A. Ferrer-Mata, J. C. Sánchez-DelBarrio et al., "DnaSP 6: DNA sequence polymorphism analysis of large data sets," *Molecular Biology and Evolution*, vol. 34, no. 12, pp. 3299–3302, 2017.
- [27] M. S. Tantia, R. K. Vijh, V. Bhasin et al., "Whole-genome sequence assembly of the water buffalo (*Bubalus bubalis*)," *The Indian Journal of Animal Sciences*, vol. 81, no. 5, p. 38, 2011.
- [28] S. U. Rehman, F. Hassan, X. Luo, Z. Li, and Q. Liu, "Whole-genome sequencing and characterization of buffalo genetic resources: recent advances and future challenges," *Animals*, vol. 11, no. 3, p. 904, 2021.
- [29] W. Li, D. M. Bickhart, L. Ramunno, D. Iamartino, J. L. Williams, and G. E. Liu, "Genomic structural differences between cattle and river buffalo identified through comparative genomic and transcriptomic analysis," *Data in brief*, vol. 19, pp. 236–239, 2018.
- [30] F. G. Hoffmann and J. C. Opazo, "Evolution of the relaxin/insulin-like gene family in placental mammals: implications for its early evolution," *Journal of Molecular Evolution*, vol. 72, no. 1, pp. 72–79, 2011.
- [31] S. V. Good-Avila, S. Yegorov, S. Harron et al., "Relaxin gene family in teleosts: phylogeny, syntenic mapping, selective constraint, and expression analysis," *BMC Evolutionary Biology*, vol. 9, no. 293, pp. 1–19, 2009.
- [32] J.-I. Park, J. Semyonov, C. L. Chang, W. Yi, W. Warren, and S. Y. T. Hsu, "Origin of INSL3-mediated testicular descent in therian mammals," *Genome Research*, vol. 18, no. 6, pp. 974–985, 2008.
- [33] J.-I. Park, J. Semyonov, W. Yi, C. L. Chang, and S. Y. T. Hsu, "Regulation of receptor signaling by relaxin A chain motifs," *The Journal of Biological Chemistry*, vol. 283, no. 46, pp. 32099–32109, 2008.
- [34] C. Schwabe, E. E. Böllesbach, H. Heyn, and M. Yoshioka, "Cetacean relaxin," *The Journal of Biological Chemistry*, vol. 264, no. 2, pp. 940–943, 1989.
- [35] A. Belfiore, F. Frasca, G. Pandini, L. Sciacca, and R. Vigneri, "Insulin receptor isoforms and insulin receptor/insulin-like growth factor receptor hybrids in physiology and disease," *Endocrine Reviews*, vol. 30, no. 6, pp. 586–623, 2009.
- [36] A. Belfiore, R. Malaguarnera, V. Vella et al., "Insulin receptor isoforms in physiology and disease: an updated view," *Endocrine Reviews*, vol. 38, no. 5, pp. 379–431, 2017.
- [37] L. W. Bowers, E. L. Rossi, C. H. O'Flanagan, L. A. deGraffenried, and S. D. Hursting, "The role of the insulin/IGF system in cancer: lessons learned from clinical trials and the energy balance-cancer link," *Frontiers in Endocrinology*, vol. 6, p. 77, 2015.
- [38] K. I. Avgerinos, N. Spyrou, C. S. Mantzoros, and M. Dalamaga, "Obesity and cancer risk: emerging biological mechanisms and perspectives," *Metabolism*, vol. 92, pp. 121–135, 2019.

- [39] I. Atsushi, "Thermostability and aliphatic index of globular proteins," *Journal of Biochemistry*, vol. 88, no. 6, pp. 1895–1898, 1980.
- [40] K. Guruprasad, B. V. B. Reddy, and M. W. Pandit, "Correlation between stability of a protein and its dipeptide composition: a novel approach for predicting in vivo stability of a protein from its primary sequence," *Protein Engineering, Design & Selection*, vol. 4, no. 2, pp. 155–161, 1990.
- [41] J. Kyte and R. F. Doolittle, "A simple method for displaying the hydropathic character of a protein," *Journal of Molecular Biology*, vol. 157, no. 1, pp. 105–132, 1982.
- [42] L. Wei, Y. Liu, I. Dubchak, J. Shon, and J. Park, "Comparative genomics approaches to study organism similarities and differences," *Journal of Biomedical Informatics*, vol. 35, no. 2, pp. 142–150, 2002.
- [43] B. Spiller, A. Gershenson, F. H. Arnold, and R. C. Stevens, "A structural view of evolutionary divergence," *Proceedings of the National Academy of Sciences*, vol. 96, no. 22, pp. 12305–12310, 1999.
- [44] R. Anand-Ivell, S. Hiendleder, C. Viñoles et al., "INSL3 in the ruminant: a powerful indicator of Gender- and genetic-specific feto-maternal dialogue," *PLoS One*, vol. 6, no. 5, article e19821, 2011.
- [45] P. Canto, I. Escudero, D. Söderlund et al., "A novel mutation of the insulin-like 3 gene in patients with cryptorchidism," *Journal of Human Genetics*, vol. 48, no. 2, pp. 0086–0090, 2003.
- [46] S. Feng, V. K. Cortessis, A. Hwang et al., "Mutation analysis of INSL3 and GREAT/LGR8 genes in familial cryptorchidism," *Urology*, vol. 64, no. 5, pp. 1032–1036, 2004.
- [47] O. Burnicka-Turek, K. Shirneshan, I. Paprotta et al., "Inactivation of insulin-like factor 6 disrupts the progression of spermatogenesis at late meiotic prophase," *Endocrinology*, vol. 150, no. 9, pp. 4348–4357, 2009.
- [48] E. H. Davidson, *Genomic regulatory systems: in development and evolution*, Elsevier, 2001.
- [49] A. Aranda and A. Pascual, "Nuclear hormone receptors and gene expression," *Physiological Reviews*, vol. 81, no. 3, pp. 1269–1304, 2001.
- [50] D. Cotnoir-White, D. Laperrière, and S. Mader, "Evolution of the repertoire of nuclear receptor binding sites in genomes," *Molecular and Cellular Endocrinology*, vol. 334, no. 1–2, pp. 76–82, 2011.
- [51] I. A. Vergara and N. Chen, "Large synteny blocks revealed between *Caenorhabditis elegans* and *Caenorhabditis briggsae* genomes using OrthoCluster," *BMC Genomics*, vol. 11, no. 1, p. 516, 2010.
- [52] G. Zhang, B. Li, C. Li, M. T. P. Gilbert, E. D. Jarvis, and J. Wang, "Comparative genomic data of the Avian Phylogenomics Project," *Gigascience*, vol. 3, no. 1, p. 2047, 2014.
- [53] K. L. Howe, B. J. Bolt, S. Cain et al., "WormBase 2016: expanding to enable helminth genomic research," *Nucleic Acids Research*, vol. 44, no. D1, pp. D774–D780, 2016.
- [54] International Human Genome Sequencing Consortium, "Initial sequencing and analysis of the human genome," *Nature*, vol. 409, pp. 860–921, 2001.
- [55] J. C. Venter, M. D. Adams, E. W. Myers et al., "The sequence of the human genome," *Science*, vol. 291, no. 5507, pp. 1304–1351, 2001.
- [56] P. W. H. Holland, J. Garcia-Fernández, N. A. Williams, and A. Sidow, "Gene duplications and the origins of vertebrate development," *Development*, vol. 1994, pp. 125–133, 1994.
- [57] K. H. Wolfe, "Yesterday's polyploids and the mystery of diploidization," *Nature Reviews. Genetics*, vol. 2, no. 5, pp. 333–341, 2001.
- [58] G. E. Liu, M. Ventura, A. Cellamare et al., "Analysis of recent segmental duplications in the bovine genome," *BMC Genomics*, vol. 10, no. 571, pp. 1–16, 2009.
- [59] L. D. Hurst, "The Ka/Ks ratio: diagnosing the form of sequence evolution," *Trends in genetics: TIG*, vol. 18, no. 9, pp. 486–487, 2002.

Retraction

Retracted: A Comprehensive Review of Performance of Next-Generation Sequencing Platforms

BioMed Research International

Received 8 January 2024; Accepted 8 January 2024; Published 9 January 2024

Copyright © 2024 BioMed Research International. This is an open access article distributed under the Creative Commons Attribution License, which permits unrestricted use, distribution, and reproduction in any medium, provided the original work is properly cited.

This article has been retracted by Hindawi following an investigation undertaken by the publisher [1]. This investigation has uncovered evidence of one or more of the following indicators of systematic manipulation of the publication process:

- (1) Discrepancies in scope
- (2) Discrepancies in the description of the research reported
- (3) Discrepancies between the availability of data and the research described
- (4) Inappropriate citations
- (5) Incoherent, meaningless and/or irrelevant content included in the article
- (6) Manipulated or compromised peer review

The presence of these indicators undermines our confidence in the integrity of the article's content and we cannot, therefore, vouch for its reliability. Please note that this notice is intended solely to alert readers that the content of this article is unreliable. We have not investigated whether authors were aware of or involved in the systematic manipulation of the publication process.

Wiley and Hindawi regrets that the usual quality checks did not identify these issues before publication and have since put additional measures in place to safeguard research integrity.

We wish to credit our own Research Integrity and Research Publishing teams and anonymous and named external researchers and research integrity experts for contributing to this investigation.



The corresponding author, as the representative of all authors, has been given the opportunity to register their agreement or disagreement to this retraction. We have kept a record of any response received.

References

- [1] M. T. Pervez, M. J. ul Hasnain, S. H. Abbas, M. F. Moustafa, N. Aslam, and S. S. M. Shah, "A Comprehensive Review of Performance of Next-Generation Sequencing Platforms," *BioMed Research International*, vol. 2022, Article ID 3457806, 12 pages, 2022.

Review Article

A Comprehensive Review of Performance of Next-Generation Sequencing Platforms

Muhammad Tariq Pervez ¹, Mirza Jawad ul Hasnain ¹, Syed Hassan Abbas,¹
Mahmoud F. Moustafa,^{2,3} Naeem Aslam,⁴ and Syed Shah Muhammad Shah⁵

¹Department of Bioinformatics and Computational Biology, Virtual University of Pakistan, Pakistan

²Department of Biology, Faculty of Science, King Khalid University, Abha, Saudi Arabia

³Department of Botany and Microbiology, Faculty of Science, South Valley University, Qena, Egypt

⁴Department of Computer Science, NFCIET, Khanewal Road, Multan, Pakistan

⁵Department of Computer Science, Virtual University of Pakistan, Pakistan

Correspondence should be addressed to Muhammad Tariq Pervez; m.tariq@vu.edu.pk
and Mirza Jawad ul Hasnain; mirza.jawad@vu.edu.pk

Received 14 July 2022; Accepted 30 August 2022; Published 29 September 2022

Academic Editor: Dr Muhammad Hamid

Copyright © 2022 Muhammad Tariq Pervez et al. This is an open access article distributed under the Creative Commons Attribution License, which permits unrestricted use, distribution, and reproduction in any medium, provided the original work is properly cited.

Background. Next-generation sequencing methods have been developed and proposed to investigate any query in genomics or clinical activity involving DNA. Technical advancement in these sequencing methods has enhanced sequencing volume to several billion nucleotides within a very short time and low cost. During the last few years, the usage of the latest DNA sequencing platforms in a large number of research projects helped to improve the sequencing methods and technologies, thus enabling a wide variety of research/review publications and applications of sequencing technologies. **Objective.** The proposed study is aimed at highlighting the most fast and accurate NGS instruments developed by various companies by comparing output per hour, quality of the reads, maximum read length, reads per run, and their applications in various domains. This will help research institutions and biological/clinical laboratories to choose the sequencing instrument best suited to their environment. The end users will have a general overview about the history of the sequencing technologies, latest developments, and improvements made in the sequencing technologies till now. **Results.** The proposed study, based on previous studies and manufacturers' descriptions, highlighted that in terms of output per hour, Nanopore PromethION outperformed all sequencers. BGI was on the second position, and Illumina was on the third position. **Conclusion.** The proposed study investigated various sequencing instruments and highlighted that, overall, Nanopore PromethION is the fastest sequencing approach. BGI and Nanopore can beat Illumina, which is currently the most popular sequencing company. With respect to quality, Ion Torrent NGS instruments are on the top of the list, Illumina is on the second position, and BGI DNB is on the third position. Secondly, memory- and time-saving algorithms and databases need to be developed to analyze data produced by the 3rd- and 4th-generation sequencing methods. This study will help people to adopt the best suited sequencing platform for their research work, clinical or diagnostic activities.

1. Introduction

DNA sequencing methods have a history of only 60 years back, but these methods evolved very rapidly and can be said an outstanding example of progress resulting in enormous improvement and enhancement in cost reduction, high throughput, capability, and applications [1–3]. History of DNA sequencing started when two fundamental

methods, i.e., Sanger sequencing [4] and Maxam and Gilbert's approach [5], were introduced. Developments in polymerize chain reaction [6, 7], availability of good quality enzymes to modify DNA, and fluorescent automated sequencing enabled to sequence first human genome in 2001 [8, 9]. Afterwards, giant revolution in DNA sequencing methods, chemistries, and bioinformatics analysis approaches were observed.

Since 2005, several Next-generation sequencing (NGS) methods have been developed and proposed to investigate any query in genomics or clinical activity involving DNA [10, 11]. NGS proposes a novel way of sequencing constituting various approaches that depend on the amalgamation of preparing template, determining order of the bases, aligning sequences and genome assembly [12]. A major advantage of NGS over traditional mutation detection methods is the ability to sequence multiple genes and highlight millions of variants simultaneously. Other advantages include minimal DNA input, faster turnaround time; NGS has revolutionized the speed of genetic and genomic discovery and advanced our understanding of the molecular mechanisms of disease and potential treatment options. Technical advancements in these sequencing methods (replacing radiolabeling with fluorescent dyes and gel electrophoresis with capillary array electrophoresis) introduced automation in the sequencing approaches and enhanced sequencing volume to several thousand base pairs in a single run [13]. The NGS instruments can generate several billion nucleotides within a very short time and low cost [14–17]. These capabilities enabled NGS methods to use in a number of areas such as whole-genome sequencing (WGS), whole-exome sequencing (WES/ES), variant calling (VC), targeting sequencing (TS), and transcriptome sequencing (TCS) [18]. During the last few years, the usage of the latest DNA sequencing platforms in a large number of research projects helped to improve the sequencing methods and technologies, thus enabling a wide variety of research/review publications and applications of sequencing technologies. Each year, several hundreds of publications are being published, highlighting the importance of sequencing technologies.

Over the last decade, dozens of excellent studies describing advantages, disadvantages, and applications of sequencing methods [2, 12, 19, 20] including Sanger sequencing also termed as first-generation sequencing (1stGS), NGS also called as second-generation sequencing (2ndGS), third-generation sequencing (3rdGS), and fourth-generation sequencing (4thGS) have been published. History of sequencing methods reveals amazing pace of developments and improvements in these technologies that now enabled us to sequence genomes of all species at very low cost and a high speed.

The proposed study presents history, needs, and reasons of evolving the sequencing technologies. For this purpose, 120 relevant articles from PubMed and journals web sites were downloaded. The keywords such as “NGS,” “Sequencing technology,” “Sequencing chemistry,” “Comparison of NGS instruments,” and “Quality of NGS instruments” were provided to Google search engine to search these articles. At the end, 65 articles having detailed information about the history, efficiency, quality, and comparison of sequencing technologies/instruments were selected for writing this review article. It provides a detailed overview of the sequencing approaches starting from first- to fourth-generation sequencing methods. The technical features of the new and most popular sequencing instruments by various companies such as Illumina, Ion Torren, GenapSys, QIAGEN, and BGI were also summarized and compared. The proposed study contributed by highlighting the most efficient and accurate

NGS instruments and helped the researchers and clinicians to get DNA sequenced through an instrument best suited to them. This study will provide end users with the knowledge of history, background chemistries, and latest developments in the sequence technologies and help them in selecting the most suitable NGS instrument based on their needs.

2. Evolution of High-Throughput Sequencing Technologies

Initial studies which were performed before 2005 including human genome project used DNA sequencing approaches were generally called as 1stGS (1970). The most famous among them were the sequencing methods discovered by Sanger and Maxam and Gilbert [21, 22]. Slow speed and high cost of sequencing DNA by 1stGS methods raised the need of fast and cheap DNA sequencing technologies. 2ndGS methods based on the concept of massively parallel sequencing were made available in 2005. The most popular 2ndGS platforms were developed and commercialized by Roche Life Sciences, Thermo Fisher Scientific, Illumina, and Applied Biosystems. These methods are also termed as NGS platforms and have revolutionized the DNA sequencing. NGS has several advantages over 1stGS. Some more important benefits are (1) massive throughput, generating a number of short DNA sequences called as reads in parallel, (2) high speed, and (3) low cost. The reads generated by NGS methods range from 50 bp to 300 bp in length. NGS technologies are classified into two groups, sequencing by hybridization and sequencing by synthesis (SBS). Sequencing by synthesis (SBS) is actually Illumina sequencing technology and is the most popular approach generating 90% of the world’s sequence data [23]. The 3rdGS approaches (2010) include Single-Molecule Sequencing (SMS) and True Single-Molecule Sequencing (tSMS). These technologies need less starting DNA material and work without amplifying the template DNA. The 4thGS (2014) also called as nanopore sequencing include majorly the MinION by Oxford Nanopore Technology (ONT). This approach actually incorporated nanopore technology in 3rdGS. The 4thGS has capability to sequence fixed cells and tissues in real time without requiring amplification and repeated cycles in the synthesis phase [21]. Figure 1 shows evolution of sequencing methods.

3. Detailed Overview of the Sequencing Methods

3.1. First-Generation Sequencing. The first process of DNA sequencing, called as Sanger sequencing, was published in 1977. This method uses sequencing by synthesis (SBS) approach of radioactively labeled DNA strand complementary to the template strand by employing the dideoxy chain termination technique. The fragments are then investigated using polyacrylamide gel electrophoresis. This technique was then improved, automated, and made available for commercial purpose [24, 25] and is termed as 1stGS. Major improvements were the introduction of capillary electrophoresis with gel electrophoresis [26, 27]; replacement of

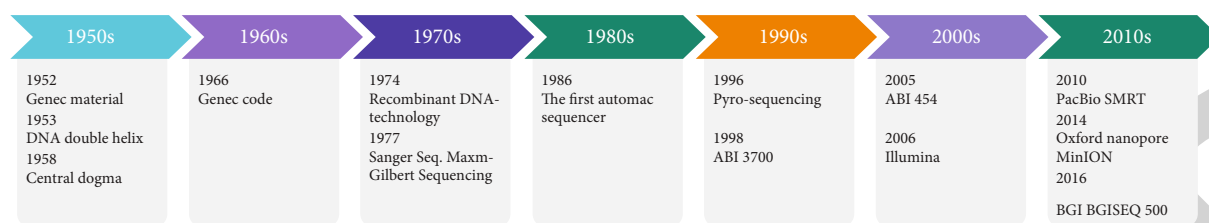


FIGURE 1: Evolution of the sequencing methods in chronological order.

TABLE 1: A comparison of Illumina benchtop sequencers [29].

Methods/applications	iSeq 100	MiniSeq	MiSeq series	NextSeq 550 series	Next Seq 1000 & 2000
Ideal for	Every size lab	TG sequencing	Long read applications	Exome and transcriptome sequencing	miRNA and sRNA analysis
Major applications	sWGS (microbes) and TGS	iSeq 100+TG EP and 16S MS	iSeq 100+16S MGS	iSeq 100+TCS	sWGS (microbes), ES, SC profiling, TS, miRNA, and sRNA analysis
Max. data quality	>85% > Q30	>85% > Q30	>90% > Q30	>80% > Q30	>90% > Q30
Run time	9.5–19 h	4–24 hours	4–55 hours	12–30 hours	11-48 hours
Maximum output	1.2 Gb	7.5 Gb	15 Gb	120 Gb	330 Gb*
Maximum reads per run	4 million	25 million	25 million	400 million	1.1 billion
Maximum read length	2 × 150 bp	2 × 150 bp	2 × 300 bp	2 × 150 bp	2 × 150 bp

radioactively labeled DNA with fluorescent labeled DNA further advancement was ensured by using recombinant DNA [28] and the PCR technologies [6]. The major drawback of 1stGS is generation/analysis of only one sequence per electrophoresis lane or capillary tube. This is the reason of dividing DNA into fragments. One thousand long read lengths were sequenced with 99.99% accuracy. Major limitations of this method were low throughput and high cost [29]. For example, this process was so costly that the human genome project consumed almost 13 years and US\$ 2.7 billion. Later on, improvement in 1stGS enabled to sequence of another human genome for US\$ 10 million. However, with the passage of time, 1stGS reached its limit and was taken as costly approach. One thing to note is that this technology is still used for validating DNA sequences and target resequencing [1].

3.2. Next/Second-Generation Sequencing. The NGS, high throughput, and massively parallel sequencing are the terms used for this type of sequencing. It is also called as 2ndGS. This approach works without separating the sequencing reactions into lanes, capillaries, or tubes. NGS allows billions of sequencing processes to be happened simultaneously in parallel on a slid surface (glass or beads), an enormous improvement in throughput and cost compared to 1stGS.

3.2.1. Illumina. Illumina, Inc. [29] is a leading manufacturer of various sequencing instruments. It was established in 1998 in San Diego, CA. Currently, it provides a number of

sequencing platforms categorized in two groups: Benchtop Sequencers (BTS) and Production Scale Sequencers (PSS). All BTSs provide support for (1) WGS for small organisms such as microbes and viruses, (2) target gene sequencing (TGS), (3) target gene expression profiling (TGEP), (4) miRNA and sRNA analysis profiling, and (5) 16S metagenomic sequencing (MS) (except iSeq100). NextSeq 550 Series and NextSeq 1000 & 2000 have extra applications such as exome sequencing (ES), s-cell profiling, chip-seq analysis, methylation sequencing, MS, and cell-free sequencing (CFS). Comparison of BTS is given in Table 1. Among PSSs, only NovaSeq 6000 supports WGS of humans, plants, and animals. Functionalities provided by other PSSs are similar to those of benchtop sequencers. Table 2 provides a summary of applications, features, and performance of the PSSs. HiSeq 2500, HiSeq 3000, HiSeq 4000, HiSeq X Ten, and HiSeq X five have been declared to discontinue (Illumina, 2021). However, their support will be provided up to March 31, 2024. So, these sequencers are not discussed here. Illumina sequencing method is based on SBS. Reaction system is a mixture of DNA polymerase, primers, and 4 dNTP with base specific fluorescent markers. The 3'-OH of dNTPs ensures addition of one base at time. On completion of the sequencing reaction, DNA polymerase and the unused dNTP are eluted. For fluorescence excitation, buffer solution is then added. The fluorescence signal is recorded by optical equipment. Optical signals, generated by optical equipment, are used for base calling. To perform next round of sequencing reaction, a chemical reagent is used for quenching

TABLE 2: A comparison of Illumina production scale sequencer sequencers [29].

Methods/applications	NextSeq 550	NextSeq 550Dx	NextSeq 1000 & 2000	NovaSeq 6000
Ideal for	Research	Research+in vitro diagnostic	Targeted sequencing	Long read applications
Major applications	sWGS (microbes), TGS, and TCS	NextSeq 550+clinical NGS applications	NextSeq 550 series+SCP	NextSeq 550 series+NextSeq 1000 & 2000+IWGS
Max. data quality	>80% > Q30	>75% > Q30	>90% > Q30	>90% > Q30
Run time	12-30 hours	35 hours	11-48 hours	13-44 hours
Maximum output	120 Gb	90 Gb	360 Gb	6000 Gb
Maximum reads per run	400 million	300 million	1.2 billion	20 billion
Maximum read length	2 × 150 bp	2 × 150 bp	2 × 150 bp	2 × 250 bp

fluorescence signal and remove the dNTP 3'-OH protective group. Sequencing data generated during the same experiment have the same length. The latest sequencing platforms can generate DNA sequence in paired-end fashion (22 × 300 bp), i.e., can read both ends of a fragment [30]. Signal decay and dephasing occurred due to incorrect cleavage of fluorescent label or terminating moieties. Average error rates of the sequencing platforms are 1-1.5% [31].

3.2.2. Ion Torrent. Ion Torrent was launched in 2011 [32]. Ion Torrent is an SBS-based approach and uses pH measurements for generating nucleotide sequences. Length of sequencing reads generated by Ion Torrent varies. Ion Torrent sequencing machines cannot generate sequencing from either ends of a fragment [30]. There are four Ion Torrent instruments; GeneXus system has ability to produce data analysis report in a single day using an automated workflow with only two touch points. This is economical for the lowest sample input and can be placed in lab or a house regardless of the level of NGS expertise. This is also termed as in-house NGS system. Ion GeneStudio S5 systems support efficient, scalable, and low-cost targeted sequencing. Based upon the Ion chips, there are five variants of this instrument with ability of generating 2M to 130M reads and 0.3 to 50 Gb data in a single run by consuming 3-21.5 hours. Table 3 describes applications, performance, and features of Ion GeneStudio S5 systems. The PGM Dx system is suitable for regulated lab environments and in vitro diagnostic. It is an integrated system of NGS instrument, reagents, consumables and software tools for sequencing and data analysis. The Ion Chef System is an improved version of Ion GeneStudio S5 systems. It is an automated approach to prepare library for Ion AmpliSeq, reproducible template and to load chip [33].

3.2.3. GenapSys. The GenapSys (founded in 2010) is a company from the Stanford Genome Technology Center. The GenapSys Sequencer enhanced SBS technique by embedding thermal detection of nucleotide incorporations [34]. It is a small (less than ten pounds), low-priced, and easy to use, even good for beginners in the genomic field. The electrical chip has several million sensors each having a single bead coated in thousands of clonal copies of a nucleotide sequence. The DNA bases are poured across the chip in a sequence, and successful incorporation is noticed by changes in impedance as the complementary DNA strand grows.

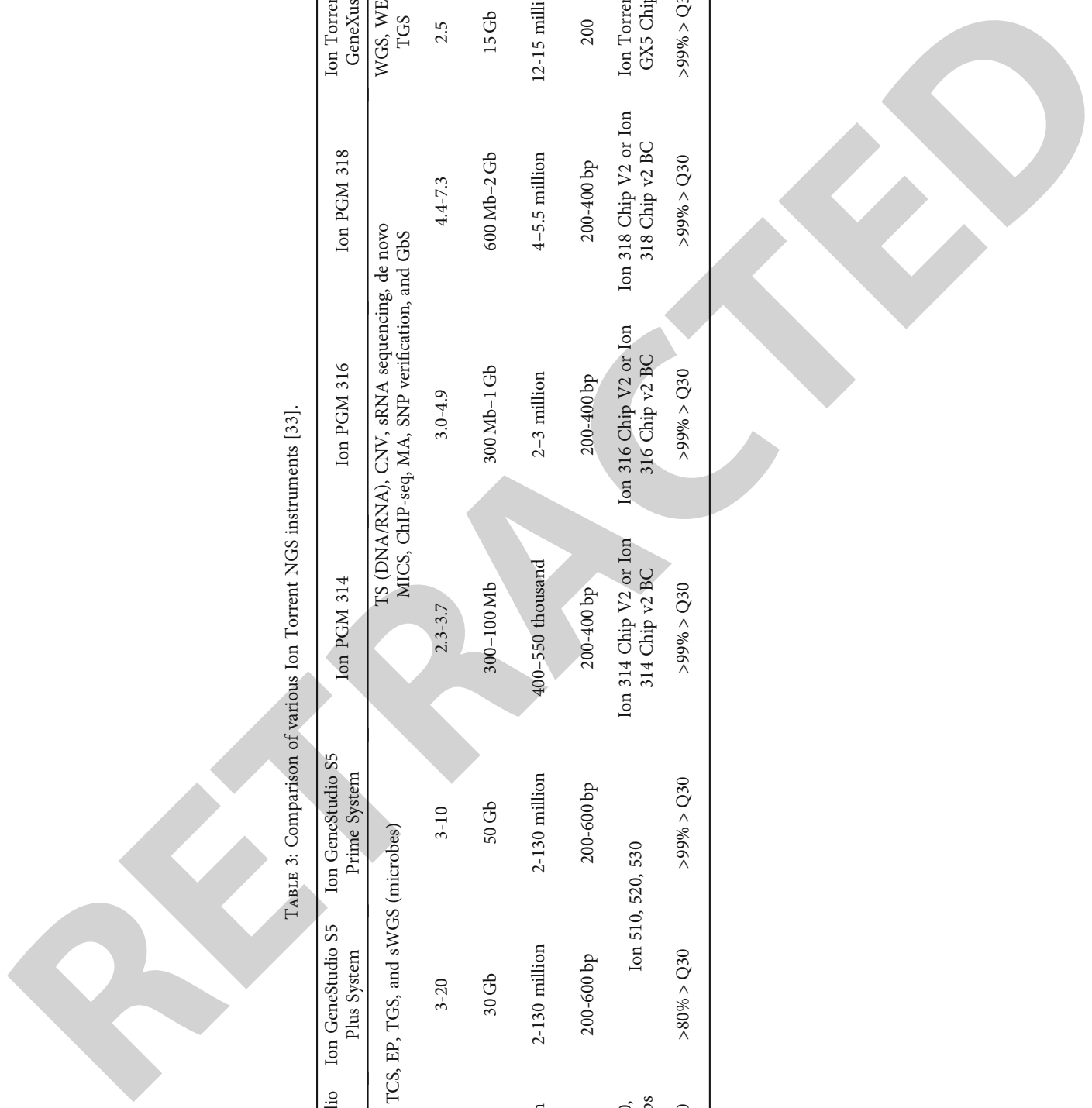
Three versions of the chip, based on varying number of sensors, are available: 1 million sensors, 16 million sensors, and 144 million sensors. This technology has enabled the sequencer to produce a massive range of data quantity. For example, the GenapSys with sixteen million sensor chips can generate thirteen million reads per day providing read length of 150bp and accuracy level of >80% > Q30 (raw accuracy 99.9%). However, its performance can be enhanced to ES, TS, and SCP by using a cluster of chips. The GenapSys can be used for identifying pathogen, sRNA, sWGS, targeted mRNA, SCP, and gene editing [35].

3.2.4. QIAGEN. QIAGEN provides GeneReader for NGS data generation. The nucleotides are detected by matching fluorescent signals templates clonally amplified by GeneRead QIACube. The GeneReader can be used only by the qualified persons trained in MB approaches and GeneReader itself. It is claimed to a complete workflow that eliminates challenges faced during sample preparation and provides very good understanding of the results. The GeneReader system helps in all sample processing and sequencing phases such as DNA extraction, library preparation, sequencing, bioinformatics data analysis, clinical implications, and evidence. It employs "QCI Analyze" and "QCI Interpret" for analyzing biological data, variant calling and their annotation, read mapping, and visualization of the alignment. Quality (>85% > Q30) is assured at run level to validate each variant for minimizing false-positive and false-negative indications [36, 37].

3.2.5. Complete Genomics Technology/BGI. Complete genomics, founded in 2006, is specialized in whole human genome sequencing. In 2013, it was purchased by BGI-Shenzhen, China, that is one of the world's leading institutions providing genomic services. The BGI provides a number of sequencing (Table 4) and data analysis tools and technologies for research, agriculture, medical, and environment applications [38]. The complete genomics developed a technology by emerging sequencing by hybridization and ligation [39], called as DNA nanoball (DNB) sequencing. Rolling circle replication is used to amplify DNA fragments consisting of 440-500bp into DNBs. This needs generation of entire circular templates before the generation of nanoballs. DNBs are poured into a flow cell, one nanoball in each well. The template bases ranging from 1 to 10 are processed

TABLE 3: Comparison of various Ion Torrent NGS instruments [33].

Methods/ applications	Ion GeneStudio S5 System	Ion GeneStudio Plus System	Ion GeneStudio S5 Prime System	Ion PGM 314	Ion PGM 316	Ion PGM 318	Ion Torrent GeneXus
Major applications	ES, TCS, EP, TGS, and sWGS (microbes)			TS (DNA/RNA), CNV, sRNA sequencing, de novo MICS, ChIP-seq, MA, SNP verification, and GBS			WGS, WES, TGS
Run time (hours)	4.5-21.5	3-20	3-10	2.3-3.7	3.0-4.9	4.4-7.3	2.5
Maximum output	15 Gb	30 Gb	50 Gb	300-100 Mb	300 Mb-1 Gb	600 Mb-2 Gb	15 Gb
Maximum reads per run	2-80 million	2-130 million	2-130 million	400-550 thousand	2-3 million	4-5.5 million	12-15 million
Maximum read length	200-600 bp	200-600 bp	200-600 bp	200-400 bp	200-400 bp	200-400 bp	200
Compatible chips	Ion 510, 520, 530, 540 chips	Ion 510, 520, 530		Ion 314 Chip V2 or Ion 314 Chip v2 BC	Ion 316 Chip V2 or Ion 316 Chip v2 BC	Ion 318 Chip V2 or Ion 318 Chip v2 BC	Ion Torrent GX5 Chip
Max. data quality	>99% > Q30	>80% > Q30	>99% > Q30	>99% > Q30	>99% > Q30	>99% > Q30	>99% > Q30



in paired-end fashion comparable to Exact Call Chemistry in SOLiD sequencing [40–42]. After eliminating ligated sequences, new probes are added, according to various interrogated positions. The process of annealing, washing, ligation, and image reading is iterated for all positions nearby to one end of one adapter. This procedure is performed for all remaining termini of the adapter. The main disadvantage of DNB sequencing is run time and short read lengths. The key advantage of this technique is the high quantity of DNBs (almost 350 million). Later on, the Retrovirology approach was incorporated for generating high quality WG and WE sequence having 50x coverage in <8 days [43]. As per their claim, more than 20,000 whole genomes of humans have been sequenced using the propriety instrument and procedures [38].

3.2.6. Roche 45. The Roche GS-FLX 454 Genome Sequencer was the first commercial system launched as the 454 Sequencer in 2004 [42, 44]. Using this platform, the second complete genome of an individual (James D. Watson) was sequenced. The upgraded 454 GS FLX Titanium system introduced by Roche in 2008 enhanced the average read length and accuracy to 700 bp and 99.997%, respectively. This platform improved an output of 0.7 Gb of data per run within 24 hours. The GS Junior bench-top sequencer system produced the average read length of 700 bp, throughput of 70 Mb, and runtime of 10 to 18 hours. However, Roche decided to reduce its focus on gene sequencing and shut down 454 Life Sciences sequencing services by the end of 2013, so Roche NGS instruments will not be discussed more in this study [45–47].

3.3. Third-Generation Sequencing. Second-generation sequencing approaches require PCR amplification of the template DNA which causes sequencing errors. This limitation can be overcome if sequencing is performed based on a single molecule without amplification. Secondly, time needed to produce results is also long because several scanning and washing cycles have to be run. Due to the addition of each nucleotide, synchronicity is also lost which may result in noisy sequencing data and short length of the reads.

The Single-Molecule Sequencing (SMS) which is 3rdGS approach is also termed as single template approach. The most famous SMS approach is Single-Molecule Real Time Sequencing (SMRT) by Pacific Biosciences (PacBio). This method uses sequencing by synthesis chemistry similar to some 2nd-generation sequencing methods but needs less starting material and PCR amplification of the template DNA which results in low error rate and produce long reads with less run time [48]. SMRT can generate tens of kilobases long reads; for examples, the latest PacBio sequencer (Sequel IIe System released on Oct. 05, 2020) can produce 4 million reads with more 99% accuracy in just 30 hours. This system was shown to have more contiguity (N50), correctness (quality score), and completeness (genome size) compared to Nanopore and Illumina (Table 5) whereas cost of PacBio HiFi Sequencing was also reported very low (Table 6) compared to its competitors [49].

The 3rd-generation sequencing has several advantages over 2nd-generation sequencing; for example, higher throughput, detecting haplotype directly, longer read lengths, better consensus accuracy to identify rare variants, whole chromosome phasing, and small amount of sample are the salient features of the 3rd-generation sequencing which had it useful in clinical diagnostic [50].

3.4. Fourth-Generation Sequencing. The fourth-generation sequencing integrated nanopore technology into SMS. This technology performs real-time sequencing without amplification and repeated cycles by eliminating synthesis and therefore is called as 4G sequencing. The 4thGS, also called in situ sequencing technology, has opened new horizons in DNA sequencing by making it possible to identify order of nucleotides in the fixed cells and tissues [21]. It differs from other sequencing generation approaches in two ways. Firstly, spatial distribution of the DNA reads over the sample can be observed which provide very useful information for highlighting tissue heterogeneity based upon the known markers. The second difference is that large number of cells can be analyzed simultaneously. For example, robust single cell RNA sequencing approaches were developed, which are cheap and are capable to sequence a number of cells with very few pictograms of the starting material [51]. Drawback of this technique is that tissue material is composed of several thousands of cells and sequencing single cells is not technically and computationally an easy job. However, it is predicted that in situ sequencing will be used to extract clinically important information from data produced by conventional NGS approaches. Targeted in situ sequencing method may be applied for filtering validated biomarkers directly on the samples whereas nontargeted technique may be useful for developing molecular profiles of the samples for classifying a disease on the molecular level or to satisfy the patients. Integrating in situ sequencing in the conventional NGS methods would expedite the development of these methods and these will eventually become essential tools for personalized medicine. Nanopore sequencing, the most popular 4thGS platform, has ability to identify molecules (proteins, DNA, RNA, etc.) while they are passed through nanoscale holes entrenched in a thin membrane [52]. In this approach, an electric field forces individual molecules to pass through a nanopore having 2 nm diameter. Due to very thin pore, single-stranded molecules are passed through the pore in a firm linear order. Distinguished electric signals are generated as DNA molecule passes through the pore. The most famous nanopore technology is the Oxford nanopore Technology. It is one of the most robust sequence technologies and can sequence whole genome with 1 million base pairs long reads and diagnose diseases very efficiently and with very low cost [53]. The MinION, which was released in 2014, is the first application of nanopore technology. Other higher throughput nanopore devices from Oxford Nanopore Technologies are GridION Mk1 and PromethION 24/48. GridION Mk1 has 1-5 flow cells with the ability of generating 250 GB data. PromethION 24/48 has 1-48 flow cells and can produce data up to 15 TB [54]. Nanopore sequencing is classified into three categories. In case of

TABLE 4: Comparison of various BGI NGS instruments [38].

Methods/applications	DNBSEQ-T7	DNBSEQ-G400 FAST	DNBSEQ-G400	DNBSEQ-G50
Major applications	WGS, DES, EGS, TS	WGS, WES, TS, MGS, RNA-seq	WGS, WES	Targeted sequencing (DNA & RNA), pathogen identification, and SPS
Max. run time (hours)	30	13	37	40
Maximum output	6 Tb	330 Gb	1440 Gb	150 Gb
Maximum reads per run	5000 million	550 million	1800 million	770 million
Maximum read length	150 PE	150 PE	200 PE/400 SE	150 PE
Data quality	>85% > Q30	>85% > Q30	>85% > Q30	>85% > Q30

1D, single-stranded DNA is sequenced. In 2D, two strands of the DNA were bounded by a hairpin-like structure. The first sequence of one strand of DNA is obtained, and then, the second strand DNA is sequenced. In this way, sequencing is repeated twice to raise base calling quality. 1D² is very close to 2D, but hairpin structure is not needed for keeping connected two strands of DNA.

4. Comparison of Sequencing Platforms

All sequencing instrument manufacturing companies offer a variety of sequencing platforms. Some produce small data and others produce huge amount of data in a single run. Reads' length and time consumed to generate data also vary among these sequencers. Table 7 provides comparison of various high-performing sequencers, and Table 8 shows analysis in terms of advantages and disadvantages of the sequencing generations. Per hour output analysis of high-performing sequencers showed that Nanopore PromethION outperformed all sequencers. BGI was on the second position and Illumina was on the third position (Figure 2).

5. Discussion

Rapid evolving approaches for genome sequencing have resulted in significant reduction in cost and time for NGS data generation and amazing increase in accuracy and throughput by using very less amount of starting material of DNA. Every day brings innovation in these technologies, and the field of genomics is progressing steadily by opening new horizons in various domains of life sciences [55–57]. Two features of NGS systems, i.e., extensive reduction in time and substantial increase in accuracy, have enabled NGS methods to be used in diagnostics, prognostics, and predicting variations [58–61] in the human genomes—leading towards the personalized medicine [62–64]. On the other hand, NGS methods have made it possible to conduct large-scale “omics” studies such as genomics, exomics, epigenomics, metagenomics, and transcriptomics [65, 66] which provided insight into the basic as well as applied research areas.

Among the SGS technologies, Illumina has been reported to offer a big variety of benchtop and production scale NGS instruments and they are the most popular [2] among the clients. The instruments are more economical [1] and are among the platforms that have the highest

TABLE 5: An overview of human genome assembly quality metrics between PacBio system, Nanopore, and Illumina [49].

	Nanopore+Illumina	PacBio HiFi sequencing
Contiguity (N50)	32.3 Mb	98.7 Mb
Correctness (quality score)	Q34	Q51
Completeness (genome size)	2.8 Gb	3.1 Gb

TABLE 6: Overall costs for sequencing a human genome [49].

	Nanopore+Illumina	PacBio HiFi sequencing (US \$)
Consumables	4800	3800
Compute	5050	3850
Data storage	5200	3900

throughput [67, 68]. The Ion Torrent instruments are more automatic in the sense that in addition to automation in NGS data generation and analysis they provide automation in library preparation as well. Some studies have shown that Ion Torrent methods are more suitable for forensic SNP investigation [69] and have better throughput than Illumina HiSeq 2000 [70, 71]. Although Roche 454 was one of the most popular instruments, now they have been discontinued [45–47]. Some studies have reported that Roche instruments are more error prone and costly and have low throughput as compared to other NGS instruments [67, 71]. The GenapSys is lightweight, low-priced, and easy to use, even good for beginners in the genomic field. This instrument has the electrical chip with different number of sensors: 1 million sensors, 16 million sensors, and 144 million sensors. This technology has enabled the sequencer to produce a massive range of data quantity. The GenapSys with sixteen million sensor chips can generate thirteen million reads per day. The GenapSys can be used for identifying pathogen, sRNA, sWGS, targeted mRNA, SCP, and gene editing [35]. The GeneReader by QIAGEN can be used only by the qualified persons trained in MB approaches and GeneReader itself. It presents a complete workflow starting from sample preparation to NGS data generation and provides very good understanding of the results. It employs “QCI Analyze”

TABLE 7: Comparison of various high-performing sequencing instruments*.

Manufacturer	Read length	Data output	Max. run time (hours)	Chemistry	Key applications**
Illumina (NovaSeq 6000)	300 PE	6 Tb (6000 Gb)	44	Sequencing by synthesis	SS-WGS and TGS, TGEP, 16sMGS, WES, SCP, LS-WGS, CA, MS, MGP, CFS, LBA
Thermo Fisher Scientific Ion Torrent (Ion GeneStudio S5 Prime)	600 SE	50 Gb	12	Sequencing by synthesis	WGS, WES, TGS
GenapSys (16 chips)	150 SE	2 Gb	24	Sequencing by synthesis	TS, SS-WGS, GEV, 16S rRNA sequencing, sRNA sequencing, TSCAS
QIAGEN (GeneReader)	100 SE	Not available	Not available	Sequencing by synthesis	Cancer research and identifying mutations
BGI/Complete Genomics	400 SE	6 Tb (6000 Gb)	40	DNA nanoball	Small and large WGS, WES and TGS
PacBio (HiFi Reads)	25 Kb	66.5 Gb	30	Real-time sequencing	DN sequencing, FT, identifying ASI, mutations, and EPM
Nanopore (PromethION)	4 Mb	14 Tb (14000 Gb)	72	Real-time sequencing	SV, GS, phasing, DNA and RNA base modifications, FT, and isoform detection

*Performance comparison is given as per manufacturer's description. **Applications by all sequencers of the respective manufacturer are listed. **Full names are given in Abbreviations.

TABLE 8: Advantages and disadvantages of sequencing generations.

Sequencing generation	Advantages	Disadvantages
First generation	High accuracy Helps in validating findings of NGS	High cost Low throughput
Second generation	High throughput Low cost Have clinical applications Short run time	Short read length Difficult sample preparation PCR amplification Long run time
Third generation	No PCR amplification Require less starting material Longer read lengths Very low cost Low error rate during library preparation Advantages of 3 rd GS+	High sequencing error rate 10–15% in the PacBio and 5–20% in the ONT Fresh DNA requires for ensuring quality of ultralong reads Database systems and algorithms/tools are rare for analyzing 3 rd and 4 th GS data
Fourth generation	Ultrafast: scan of whole genome in 15 minutes Spatial distribution of the sequencing reads over the sample can be seen	

and “QCI Interpret” for analyzing biological data and variant calling and their annotation. The GeneReader ensures quality at run level to validate each variant for minimizing false-positive and false-negative indications [36, 37]. Complete genomics, founded in 2006 and purchased by BGI-Shenzhen, China, in 2013, is one of the world's leading institutions providing genomics services. The BGI provides a number of services for research, agriculture, medical, and environment applications [38]. The BGI instruments gener-

ate high-quality WG and WE sequence with 50x coverage in <8 days [49]. As per their claim, more than 20,000 whole genomes of humans have been sequenced using the propriety instrument and procedures [38].

The third-generation sequencing technology has some advantages over SGS such as this requires less starting DNA material and does not require PCR amplification of the template DNA. This has enabled SMS to produce more accurate long reads within less time [48]. The latest PacBio

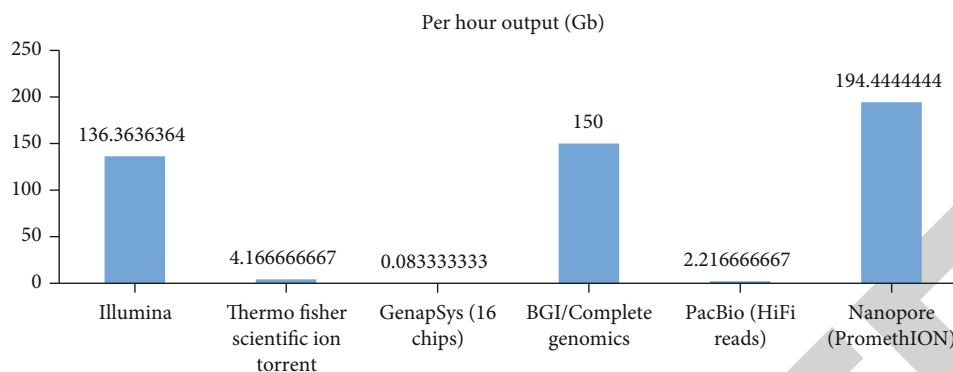


FIGURE 2: Per hour output analysis of high-performing sequencers.

sequencer (Sequel IIE System) has the ability to produce 4 million reads with more 99% accuracy in just 30 hours. This system is more accurate as compared to Nanopore and Illumina whereas the cost of PacBio HiFi Sequencing was also reported as very low [49]. The tSMS can sequence millions of individual molecules even from a picogram sample. The tSMS has an important improvement over the SGS in the sense that it can perform RNA sequencing directly [50].

Nanopore sequencing, i.e., integration of nanopore technology into the third-generation sequencing technology, falls in the category of fourth-generation sequencing. It can sequence fixed cells and tissues in real time without requiring amplification and repeated cycles in the synthesis phase [21]. The most famous nanopore technology is the ONT. It can sequence whole genome with 1 million base pair long reads and diagnose diseases very efficiently and with very low cost [53]. The MinION is the first application of nanopore technology. Others are GridION Mk1 and PromethION 24/48. GridION Mk1 can generate 250 GB data and PromethION 24/48 can produce data up to 15 TB [54].

To summarize the discussion, this may be claimed that NGS technologies are being developed with an amazing pace. In the near future, NGS technologies and instruments will be seen in action in clinical and diagnostic labs all around the world, helping us to fulfill the dream of personalized medicine. In addition, there will be very good portable and fully automatic devices for generating NGS data. So, to cater needs of the future, algorithms and databases should be developed for storing, processing, analyzing, and visualizing data of each patient, which may be useful for clinicians to make therapeutic decisions. Major challenges of NGS approaches include the lack of standardized procedures for managing quality, sequencing workflows, sequencing data handling, and analyzing [72, 73].

6. Conclusion

Sequencing platforms have reshaped the genomic era and are helping us in understanding and characterizing genomes of humans, animals, and plants. Every day brings innovation in sequencing chemistry, throughput, and nucleotide detection which enables sequencing process very easy, fast, and low-priced. The proposed study investigated various sequencing instruments and highlighted advantages, disad-

vantages, and applications based on the previous studies and the material provided by the manufacturers on their websites. Each instrument has different application, run time, and output per hour; however, overall, Nanopore PromethION is the fastest sequencing approach. It can produce 194 Gb data in an hour. BGI with an output of 150 Gb data per hour was on the second position, and Illumina with an output of 136 Gb data per hour was on the third position. The results of the proposed study showed that BGI and Nanopore can beat Illumina, which is currently the most popular sequencing company, and overcome the genomic market very soon. With respect to quality, Ion Torrent NGS instruments are on the top of the list, Illumina is on the second position, and BGI DNB is on the third position. Secondly, memory- and time-saving algorithms and databases need to be developed to analyze data produced by the 3rd- and 4th-generation sequencing methods.

7. Outcome of the Review and Recommendations

The Nanopore PromethION should be used in large-scale projects for getting maximum data in minimum time. The Ion Torrent NGS and Illumina instruments may be used for small projects where quality is an essential element. Tools and databases for storing, analyzing, and visualizing big data biology should be developed so that life science researchers may contribute in improving humans' health effectively.

Abbreviations

NGS:	Next-generation sequencing
ES:	Exome sequencing
TS:	Targeted sequencing
EP:	Expression profiling
sWGS:	Small whole-genome sequencing (bacterial and viruses)
IWGS:	Large whole-genome sequencing (animals, plants, and humans)
CNV:	Copy number variations
sRNA:	Small ribonucleic acid
MICS:	Microbial sequencing
MA:	Methylation analysis
GbS:	Genotyping by sequencing

TCS: Transcriptome sequencing
 TGS: Target gene sequencing
 SCP: Single-cell profiling
 MGS: Metagenomic sequencing
 SBS: Sequencing by synthesis
 SBH: Sequencing by hybridization
 DES: Deep exome sequencing
 EGS: Epigenome sequencing
 PE: Paired end
 SE: Single end
 SPS: Small panel sequencing
 DN: De novo
 FT: Full transcriptome
 ASI: Alternative splicing isoforms
 EPM: Epigenetic modifications
 SV: Structural variation
 GS: Genome assembly
 GEV: Gene editing validation
 TSCAS: Targeted single-cell assay sequencing

Conflicts of Interest

The authors declare that they have no conflicts of interest.

Acknowledgments

The authors acknowledge the Virtual University of Pakistan for its generous support to conduct this research work. The authors would also like to thank the Deanship of Scientific Research at King Khalid University, Abha, KSA, for funding this work under the grant number R.G.P.2/90/43.

References

- [1] Y. O. Alekseyev, R. Fazeli, S. Yang et al., "A next-generation sequencing primer—how does it work and what can it do," *Academic pathology*, vol. 5, p. 2374289518766521, 2018.
- [2] S. E. Levy and R. M. Myers, "Advancements in next-generation sequencing," *Annual Review of Genomics and Human Genetics*, vol. 17, no. 1, pp. 95–115, 2016.
- [3] M. Routbort, B. Handal, K. P. Patel et al., "Onco Seek: a versatile annotation and reporting system for next generation sequencing-based clinical mutation analysis of cancer specimens," *The Journal of Molecular Diagnostics*, vol. 14, p. 747, 2012.
- [4] F. Sanger and A. R. Coulson, "A rapid method for determining sequences in DNA by primed synthesis with DNA polymerase," *Journal of Molecular Biology*, vol. 94, no. 3, pp. 441–448, 1975.
- [5] A. M. Maxam and W. Gilbert, "A new method for sequencing DNA," *PNAS*, vol. 74, no. 2, pp. 560–564, 1977.
- [6] R. K. Saiki, D. H. Gelfand, S. Stoffel et al., "Primer-directed enzymatic amplification of DNA with a thermostable DNA polymerase," *Science*, vol. 239, no. 4839, pp. 487–491, 1988.
- [7] R. K. Saiki, S. Scharf, F. Faloona et al., "Enzymatic amplification of beta-globin genomic sequences and restriction site analysis for diagnosis of sickle cell anemia," *Science*, vol. 230, no. 4732, pp. 1350–1354, 1985.
- [8] International Human Genome Sequencing Consortium, "Initial sequencing and analysis of the human genome," *Nature*, vol. 409, no. 6822, pp. 860–921, 2001.
- [9] J. C. Venter, M. D. Adams, E. W. Myers et al., "The sequence of the human genome," *Science*, vol. 291, no. 5507, pp. 1304–1351, 2001.
- [10] K. Williams and R. W. Sobol, "Mutation research/fundamental and molecular mechanisms of mutagenesis: Special issue: DNA repair and genetic instability," *Mutation research*, vol. 743-744, pp. 1–3, 2013.
- [11] M. M. Weiss, B. van der Zwaag, J. D. H. Jongbloed et al., "Best practice guidelines for the use of next-generation sequencing applications in genome diagnostics: a national collaborative study of Dutch genome diagnostic laboratories," *Human Mutation*, vol. 34, no. 10, pp. 1313–1321, 2013.
- [12] M. L. Metzker, "Sequencing technologies – the next generation," *Nature Reviews. Genetics*, vol. 11, no. 1, pp. 31–46, 2010.
- [13] K. Lohmann and C. Klein, "Next generation sequencing and the future of genetic diagnosis," *Neurotherapeutics*, vol. 11, no. 4, pp. 699–707, 2014.
- [14] B. Rabbani, H. Nakaoka, S. Akhondzadeh, M. Tekin, and N. Mahdieh, "Next generation sequencing: implications in personalized medicine and pharmacogenomics," *Molecular Bio Systems*, vol. 12, no. 6, pp. 1818–1830, 2016.
- [15] A. Git, H. Dvinge, M. Salmon-Divon et al., "Systematic comparison of microarray profiling, real-time PCR, and next-generation sequencing technologies for measuring differential microRNA expression," *Ribonucleic Acid*, vol. 16, no. 5, pp. 991–1006, 2010.
- [16] S. W. Roh, G. C. Abell, K. H. Kim, Y. D. Nam, and J. W. Bae, "Comparing microarrays and next-generation sequencing technologies for microbial ecology research," *Trends in biotechnology*, vol. 28, no. 6, pp. 291–299, 2010.
- [17] K. V. Voelkerding, S. Dames, and J. D. Durtschi, "Next generation sequencing for clinical diagnostics—principles and application to targeted resequencing for hypertrophic cardiomyopathy: a paper from the 2009 William Beaumont Hospital Symposium on Molecular Pathology," *The Journal of molecular diagnostics*, vol. 12, no. 5, pp. 539–551, 2010.
- [18] J. Xuan, Y. Yu, T. Qing, L. Guo, and L. Shi, "Next-generation sequencing in the clinic: promises and challenges," *Cancer letters*, vol. 340, no. 2, pp. 284–295, 2013.
- [19] M. Morey, A. Fernández-Marmiesse, D. Castiñeiras, J. M. Fraga, M. L. Couce, and J. A. Cocho, "A glimpse into past, present, and future DNA sequencing," *Molecular Genetics and Metabolism*, vol. 110, no. 1-2, pp. 3–24, 2013.
- [20] J. A. Reuter, D. V. Spacek, and M. P. Snyder, "High-throughput sequencing technologies," *Molecular Cell*, vol. 58, no. 4, pp. 586–597, 2015.
- [21] M. Mignardi and M. Nilsson, "Fourth-generation sequencing in the cell and the clinic," *Genome Medicine*, vol. 6, no. 4, pp. 31–34, 2014.
- [22] B. Meera Krishna, M. A. Khan, and S. T. Khan, "Next-generation sequencing (NGS) platforms: an exciting era of genome sequence analysis," in *Microbial Genomics in Sustainable Agroecosystems*, Springer, Singapore, 2019.
- [23] M. A. Quail, M. Smith, P. Coupland et al., "A tale of three next generation sequencing platforms: comparison of Ion Torrent, Pacific Biosciences and Illumina MiSeq sequencers," *BMC Genomics*, vol. 13, p. 341, 2012.

- [24] T. Hunkapiller, R. J. Kaiser, B. F. Koop, and L. Hood, "Large-scale and automated DNA sequence determination," *Science*, vol. 254, no. 5028, pp. 59–67, 1991.
- [25] L. M. Smith, J. Z. Sanders, R. J. Kaiser et al., "Fluorescence detection in automated DNA sequence analysis," *Nature*, vol. 321, no. 6071, pp. 674–679, 1986.
- [26] J. A. Luckey, H. Drossman, A. J. Kostichka et al., "High speed DNA sequencing by capillary electrophoresis," *Nucleic Acids Research*, vol. 18, no. 15, pp. 4417–4421, 1990.
- [27] H. Swerdlow and R. Gesteland, "Capillary gel electrophoresis for rapid, high resolution DNA sequencing," *Nucleic Acids Research*, vol. 18, no. 6, pp. 1415–1419, 1990.
- [28] J. M. Prober, G. L. Trainor, R. J. Dam et al., "A system for rapid DNA sequencing with fluorescent chain-terminating dideoxynucleotides," *Science*, vol. 238, no. 4825, pp. 336–341, 1987.
- [29] Illumina Inchttps://www.illumina.com/systems/sequencing-platforms.html.2022.
- [30] N. F. Lahens, E. Ricciotti, O. Smirnova et al., "A comparison of Illumina and Ion Torrent sequencing platforms in the context of differential gene expression," *BMC Genomics*, vol. 18, no. 1, pp. 1–13, 2017.
- [31] Y. Cao, S. Fanning, S. Proos, K. Jordan, and S. Srikumar, "A review on the applications of next generation sequencing technologies as applied to food-related microbiome studies," *Frontiers in Microbiology*, vol. 8, p. 1829, 2017.
- [32] J. M. Rothberg, W. Hinze, T. M. Rearick et al., "An integrated semiconductor device enabling non-optical genome sequencing," *Nature*, vol. 475, no. 7356, pp. 348–352, 2011.
- [33] S. ThermoFisher, 2021, https://www.thermofisher.com/pk/en/home/brands/ion-torrent.html.
- [34] T. P. Niedringhaus, D. Milanova, M. B. Kerby, M. P. Snyder, and A. E. Barron, "Landscape of next-generation sequencing technologies," *Analytical Chemistry*, vol. 83, no. 12, pp. 4327–4341, 2011.
- [35] Genapsys, Inc, 2021, https://www.genapsys.com/.
- [36] A. Darwanto, A. M. Hein, S. Strauss et al., "Use of the QIAGEN GeneReader NGS system for detection of KRAS mutations, validated by the QIAGEN Therascreen PCR kit and alternative NGS platform," *BMC Cancer*, vol. 17, no. 1, pp. 1–8, 2017.
- [37] U. Koitzsch, C. Heydt, H. Attig et al., "Use of the GeneReader NGS System in a clinical pathology laboratory: a comparative study," *Journal of Clinical Pathology*, vol. 70, no. 8, pp. 725–728, 2017.
- [38] Complete Genomics Incorporated, 2022, https://www.completegenomics.com/.
- [39] R. Drmanac, A. B. Sparks, M. J. Callow et al., "Human genome sequencing using unchained base reads on self-assembling DNA nanoarrays," *Science*, vol. 327, no. 5961, pp. 78–81, 2010.
- [40] H. Shendure Jji, "Next-generation DNA sequencing," *Nature Biotechnology*, vol. 26, no. 10, pp. 1135–1145, 2008.
- [41] M. Guzvic, "The history of DNA sequencing," *Journal of Medical Biochemistry*, vol. 32, no. 4, pp. 301–312, 2013.
- [42] E. R. Mardis, "Next-generation DNA sequencing methods," *Annual Review of Genomics and Human Genetics*, vol. 9, pp. 387–402, 2008.
- [43] J. K. Kulski, "Next-generation sequencing—an overview of the history, tools, and "Omic" applications," *Next Generation Sequencing—Advances, Applications and Challenges*, vol. 10, 2016.
- [44] E. M. Mostafa, D. M. Sabri, and S. M. Aly, "Overviews of next-generation sequencing," *Research and Reports in Forensic Medical Science*, vol. 5, p. 1, 2015.
- [45] B. Fierce, 2021, https://www.fiercebiotech.com/medical-devices/roche-to-close-454-life-sciences-as-it-reduces-gene-sequencing-focus.
- [46] Genomeweb, 2021, https://www.genomeweb.com/sequencing/following-roches-decision-shut-down-454-customers-make-plans-move-other-platform#.YWDPHhpBxPY.
- [47] BioITWorld, 2021, https://www.bio-itworld.com/news/2013/04/23/roche-shuts-down-third-generation-ngs-research-programs.
- [48] W. Timp, U. M. Mirsaidov, D. Wang, J. Comer, A. Aksimentiev, and G. Timp, "Nanopore sequencing: electrical measurements of the code of life," *IEEE Transactions on Nanotechnology*, vol. 9, no. 3, pp. 281–294, 2010.
- [49] PacBio, 2022, https://www.pacb.com/.
- [50] S. Srinivasan and J. Batra, "Four generations of sequencing: is it ready for the clinic yet," *Journal of Next Generation Sequencing & Applications*, vol. 1, no. 107, 2014.
- [51] D. Ramskold, S. Luo, Y. C. Wang et al., "Full-length mRNA-Seq from single-cell levels of RNA and individual circulating tumor cells," *Nature Biotechnology*, vol. 30, no. 8, pp. 777–782, 2012.
- [52] B. Lin, J. Hui, and H. Mao, "Nanopore technology and its applications in gene sequencing," *Biosensors*, vol. 11, no. 7, p. 214, 2021.
- [53] K. H. Miga, S. Koren, A. Rhie et al., "Telomere-to-telomere assembly of a complete human X chromosome," *Nature*, vol. 585, no. 7823, pp. 79–84, 2020.
- [54] ONT, 2021, https://nanoporetech.com/products/promethion.
- [55] B. P. Portier, R. Kanagal-Shamanna, R. Luthra et al., "Quantitative assessment of mutant allele burden in solid tumors by semiconductor-based next-generation sequencing," *American Journal of Clinical Pathology*, vol. 141, no. 4, pp. 559–572, 2014.
- [56] G. M. Frampton, A. Fichtenholtz, G. A. Otto et al., "Development and validation of a clinical cancer genomic profiling test based on massively parallel DNA sequencing," *Nature Biotechnology*, vol. 31, no. 11, pp. 1023–1031, 2013.
- [57] A. L. Moreira, H. H. Won, R. McMillan et al., "Massively parallel sequencing identifies recurrent mutations in TP53 in thymic carcinoma associated with poor prognosis," *Journal of Thoracic Oncology*, vol. 10, no. 2, pp. 373–380, 2015.
- [58] R. S. Goswami, R. Luthra, R. R. Singh et al., "Identification of factors affecting the success of next-generation sequencing testing in solid tumors," *American Journal of Clinical Pathology*, vol. 145, no. 2, pp. 222–237, 2016.
- [59] D. C. Koboldt, K. M. Steinberg, D. E. Larson, R. K. Wilson, and E. R. Mardis, "The next-generation sequencing revolution and its impact on genomics," *Cell*, vol. 155, no. 1, pp. 27–38, 2013.
- [60] A. E. Siroy, G. M. Boland, D. R. Milton et al., "Beyond BRAF^{V600}: clinical mutation panel testing by next-generation sequencing in advanced melanoma," *The Journal of Investigative Dermatology*, vol. 135, no. 2, pp. 508–515, 2015.
- [61] A. Paniz-Mondolfi, R. Singh, G. Jour et al., "Cutaneous carcinosarcoma: further insights into its mutational landscape through massive parallel genome sequencing," *Virchows Archiv*, vol. 465, no. 3, pp. 339–350, 2014.
- [62] S. Morganti, P. Tarantino, E. Ferraro et al., "Role of next-generation sequencing technologies in personalized

Retraction

Retracted: Quantifying the Soil Arthropod Diversity in Urban Forest in Dera Ghazi Khan

BioMed Research International

Received 8 January 2024; Accepted 8 January 2024; Published 9 January 2024

Copyright © 2024 BioMed Research International. This is an open access article distributed under the Creative Commons Attribution License, which permits unrestricted use, distribution, and reproduction in any medium, provided the original work is properly cited.

This article has been retracted by Hindawi following an investigation undertaken by the publisher [1]. This investigation has uncovered evidence of one or more of the following indicators of systematic manipulation of the publication process:

- (1) Discrepancies in scope
- (2) Discrepancies in the description of the research reported
- (3) Discrepancies between the availability of data and the research described
- (4) Inappropriate citations
- (5) Incoherent, meaningless and/or irrelevant content included in the article
- (6) Manipulated or compromised peer review

The presence of these indicators undermines our confidence in the integrity of the article's content and we cannot, therefore, vouch for its reliability. Please note that this notice is intended solely to alert readers that the content of this article is unreliable. We have not investigated whether authors were aware of or involved in the systematic manipulation of the publication process.

Wiley and Hindawi regrets that the usual quality checks did not identify these issues before publication and have since put additional measures in place to safeguard research integrity.

We wish to credit our own Research Integrity and Research Publishing teams and anonymous and named external researchers and research integrity experts for contributing to this investigation.






The corresponding author, as the representative of all authors, has been given the opportunity to register their agreement or disagreement to this retraction. We have kept a record of any response received.

References

- [1] M. Mohsin, H. Ahmad, M. N. Nasir et al., "Quantifying the Soil Arthropod Diversity in Urban Forest in Dera Ghazi Khan," *BioMed Research International*, vol. 2022, Article ID 8125585, 14 pages, 2022.

Research Article

Quantifying the Soil Arthropod Diversity in Urban Forest in Dera Ghazi Khan

Muhammad Mohsin,¹ Haseeb Ahmad,² Muhammad Nabeel Nasir,³ Zain Ul Abideen ¹,
Muhammad Nadeem,¹ Rukhsana Sattar,¹ Abdul Qadeer Saad ⁴, Mujahid Hussain,⁴
Syed Akbar Shah,¹ Hanlie Cheng ⁵, David Sturdivant ⁶, and Syeda Amber Hameed ⁴

¹Department of Zoology, Ghazi University Dera, Ghazi Khan, Pakistan

²Rural Dispensary Chak No. 151JB, Tehsil Chiniot, District Chiniot, Pakistan

³District Headquarter Hospital, Rajanpur, Pakistan

⁴Department of Zoology, Cholistan University of Veterinary and Animal Sciences, Bahawalpur, Pakistan

⁵School of Energy Resource, China University of Geosciences (Beijing), Beijing 434000, China

⁶The King's School, BP1560, Bujumbura, Burundi

Correspondence should be addressed to David Sturdivant; davidsturdivant@ksu.edu.bi
and Syeda Amber Hameed; ahameed@gudgk.edu.pk

Received 22 July 2022; Revised 22 August 2022; Accepted 29 August 2022; Published 22 September 2022

Academic Editor: Dr Muhammad Hamid

Copyright © 2022 Muhammad Mohsin et al. This is an open access article distributed under the Creative Commons Attribution License, which permits unrestricted use, distribution, and reproduction in any medium, provided the original work is properly cited.

Arthropods can be either large or too small to be seen from the microscope. Their legs are jointed and perform a specific function in the soil. Several arthropods have been identified to date. Therefore, it is essential to identify them in a different type of soil. An experiment to quantify the soil arthropods in the urban forests of D.G. Khan was conducted at the Zoology lab of Ghazi University on four tree plants, i.e., neem (*Azadirachta indica*), mango (*Mangifera indica*), guava (*Psidium guajava*), and phalsa (*Grewia asiatica*). Soil samples were taken from different areas and on different months. The diversity of arthropods was analyzed through the Shannon index. The results were all significant. The total number of arthropods found in the experiment was 5151, with the following distributions: millipedes were 132 in neem, 133 in guava, 113 in mango, and 121 in phalsa; centipedes were 136 in neem, 142 in guava, 118 in mango, and 132 in phalsa; springtails were 138 in neem, 130 in guava, 120 in mango, and 134 in phalsa. There were a total of 12 different species of arthropods found. Neem (*Azadirachta indica*) have mites, centipede, and ants; guava (*Psidium guajava*) have centipedes and ants. Mango (*Mangifera indica*) have millipedes, centipedes, mites, springtail, and ants, and phalsa (*Grewia asiatica*) have mites, ants, and centipedes. The study reveals that millipedes, centipedes, springtails, and ants were found abundantly in the urban forest area of D.G. Khan, resulting in increased organic matter decomposition and appropriate distribution of nutrients through the soil having beneficial effects on the terrestrial ecosystem.

1. Introduction

Arthropods are soil invertebrates that can be large or quite microscopic, have jointed legs, and perform particular functions in the soil community. Due to the body, widths can be classified into two forms mesofauna and macrofauna, also termed microarthropod (0.2 mm) and macroarthropod (2 mm). Arthropod includes the class of insect. The lightest insects weigh less than 25 micrograms; the heaviest, how-

ever, weigh more than 70 grams (2.5 oz) [1]. Few of their organisms have wingless like springtails and many have wings on their body. The most abundant soil arthropods are Acari (mites and collembolans) and springtail. Springtails have segmented body and wingless, ranging from 0.2 to 6 mm, with specialized appendages used for jumping. The most conspicuous segmental specialization is in the brain. For Symphypleona in the age maturity, most of them are soil dwellers range from 50 to 100,000 individuals m⁻².

Some different species of collembolan like Protura and Diplura are also wingless insects. In 1992, a take look anticipated that in Costa Rica alone, there were 500,000 species of animals and plants, of which 365,000 had been arthropods [2].

Some other species act as predators in nature, feeding on small fauna. And few have scavengers. Soil arthropods are microscopic or big period invertebrates with jointed legs. They play big roles within the soil network. Based on body width, soil arthropods may be labeled mesofauna and macrofauna. They can be categorized additionally as microarthropods (0.2–2 mm) or macroarthropods (>2 mm). According to standard taxonomy, soil arthropods fall underneath beauty insects (e.g., Protura, Diplura, Collembola, and big insects); class Myriapoda (Symphyla and Pauropoda), class Crustacean (Tardigrada, Copepods and Isopoda), and sophistication Arachnidan (Pseudoscorpiones, Arana, and Acari). Acari (mites) and collembolans (springtails) are the most sizable soil microarthropods in terms of the range of individuals and species [3]. Springtails are wingless bugs with the segmented bodies (0.2–6 mm) and specialized appendages, in addition to a spring-like tail for jumping. Most species are dwellers of soil or litter, while few live on the floor or vegetation, particularly at the side of Entomobryidae and Symphyleona. Their abundance in mature soil is set at 50–a hundred 000 human beings m^{-2} [1]. Mites stay in litter and air-stuffed pores of the soil. Mesostigmata is one of the largest agencies of loose-living mites in soil surroundings [4]. Their density in the soil of wooded areas may be loads of masses per person m^{-2} . Oribatid mites, for instance, feeding on plant clutter, are found in an immoderate amount of approximately 25,000–500,000 people m^{-2} [5]. Yet, they continue to be undetected because of their small duration. In addition, the Formicidae dominates in agricultural areas, grasslands, and deserts [6, 7].

Protura and Diplura are also wingless insects that seem like Collembola. Protura feed on sucking the outer protecting of fungal hyphen and are generally observed in herbal soils. Campodeidae and Japygidae are the two households representing the diplomas. These species are predatory and feed on small fauna. They additionally scavenge on useless natural depend, roots, and so on. Other foremost macroarthropods are dipterans, coleopterans, and hymenopterans consisting of their juveniles. Ants, millipedes, and termites perform the herbal be counted quantity's fragmentation and transportation in deeper soil layers, thereby burrowing inner. So, they appeared as engineers of soil devices. Pauropoda is a whitish millipede-like (>1 mm) species that feed on decaying plants that rely on fungi and carrion. In contrast, some species are predatory. Symphyla is 1–8 mm in duration and determined on the entire natural loam soil feeding on living plant tissues. Tardigrada, Copepods, and terrestrial Isopoda are frequently observed in moist woodland flooring. These species perform the role in the decay of leaf litter and timber residue. Chilopoda are typically predators in soil and litter layers feeding on small arthropods. Millipedes enhance soil devices by coprophagy predominant inside the route of mineralization. Their faces are located with lots of mineral content material. Spiders and pseudoscorpions are predatory arachnids [1].

The arthropod's body is covered with a hard protective coat, and ridges are different in colors and maybe one or mixed. The specialization of body region modifies metamorphism for a specific function (stigmatization). The chitinous skeleton gives backing and assurance and is adjusted in tactile structure. The arthropod body is made from an arrangement of the fragment, and each section bears a couple of members. Their body is isolated into the fragmented structure on the outer side, yet inward cavities are not separated like this. Arthropods' exoskeleton comprises fingernail skin, a noncell material emitted by the epidermis of their skin organs [8]. Their fingernail skin shifts in each species, yet for the most part, comprised of three principle layers: the external layers are epicuticle, a dainty, and Waxy coat that dampness confirmations the alternative layer and supply them a few insurances. The exocuticle and endocuticle accommodate chitin and synthetically solidified proteins and unhardened proteins one at a time. Each body portion and appendage area is encased in solidified fingernail skin. The joints between body portions and appendages are secured by adaptable fingernail skin.

The exoskeletons of most oceanic creatures are biomineralized calcium carbonate removed from the water. Some earthbound shellfish created a calcium carbonate exoskeleton, and land creatures cannot depend on a consistent gracefully broken calcium carbonate [9]. Biomineralization typically impacts the exocuticle and the external aspect of the endocuticle [10]. Two speculations about the advancement of biomineralization in arthropods and another pack of creatures delicate that it award relentless guarded reinforcement and permits the creatures to develop in amount and more grounded by giving more inflexible skeletons [11].

The fingernail skin groups bristle developing from extraordinary cells in the epidermis. Setae (bristle) are as change fit as a fiddle and capacity as limbs. They are utilized as a tangible organ to distinguish air or water flows or product interactions. Amphibian arthropods are used as quills to extend the swimming extremities' surface area and distinguish food particles from water, and sea-going bugs are utilized as air-breathers [12]. Although all arthropods within the exoskeletons muscles are connected to show their appendages, some utilize water-driven strain to pull out. For instance, all creepy crawlies develop. Their legs are solid and can generate pressure up to their resting level often [13]. Their exoskeleton has two layers, epicuticle and procuticle. Ecdysis happens during development. The diversity of the living beings is straightforwardly related to territory, condition, and food accessibility. During this cycle, they produce the specific traits as well as the linkages (both interspecific and intraspecific) that direct the many biological system capacities that are available over the course of a developmental timeline. Soil as territory directs soil arthropod assorted variety dependent on its physical structure (porosity), supplement accessibility, water (soil dampness), state (temperature, pH), and organization of substances [14].

An arthropod plays a key part in keeping up an environment's normal assets and solidness. Predator and parasitoid arthropods offer important support by keeping up horticultural efficiency and decreasing the requirement

for agricultural pesticide contributions every year. Other than their utilization in preservation science, they are likewise significant for controlling irritations in agribusiness. Arthropods have interceded environment administrations incorporate yield fertilization and nuisance control [15]. Nearby populace elements affected the dispersal capacity and searching reach. Trophic level impacts the circulation of species.

At the upper surface of the soil, the microarthropod network is a significant part of soil biodiversity and connects with the whole framework segment. An even soil arthropod network is basic in deteriorating crop deposits to frame humus and reusing mineral supplements for progressive harvests [16]. Arthropods add to human food gracefully, legitimately, and significantly more by implication as a pollinator of yields. A few animal types are known to spread extreme malady to human animals and yields. They are the major groups of freshwater, land, air, and marine life, and they are the only two major groups that have adapted to dry environments. The other major group is the amniotes, whose live members are reptiles, birds, and warm-blooded animals [17].

Evaluations of the number of arthropod species change somewhere between 1,170,000 and 5 to 10 million and account for over 80 percent of all recognized species of living creatures. The number of species stays hard to decide. This is because the evaluation demonstrates presumptions extended to different locales. Hence, an inquiry in 1992 found that in Costa Rica alone, there were 500,000 forms of creatures and plants, of which 365,000 were arthropods [18]. The main objective of this study is to identify the soil arthropods and their level of abundance in the soil of four plant trees, Neem (*Azadirachta indica*), guava (*Psidium guajava*), mango (*Mangifera indica*), phalsa (*Grewia asiatica*), and their direct association with pH contents, organic, and inorganic contents in soil.

2. Material and Methods

2.1. Geographically Position of the Experimental Zone. The geographical location of Dera Ghazi Khan is 30°03' N and 70°38' E. The characteristic of climate is dry and little rainfall. The summer is hot, and winter is mild; the average temperature of summer is 42°C, and the winter temperature is 4°C. Windstorms are common in summer due to the barren mountains of koh-suleman and the sandy soil of the area. The highest temperature is present in summer; Fort Munro is on the edge of Punjab and has cooler weather. Scattered snowfall has been reported.

The experiment was performed in the General Zoology Laboratory of Ghazi University of Dera Ghazi Khan to quantify the soil arthropods in urban forests.

2.2. Time Duration of the Study. From Nov 2019 to March 2020 was the time duration of study. Samples were taken from four trees, including guava (*Psidium guajava*), mango (*Mangifera indica*), neem (*Azadirachta indica*), and phalsa (*Grewia asiatica*). Samples were collected from three locations: DC Garden D.G. Khan, Mustafa chowk near BISE

D.G. Khan, and Shoriya bypass near Canal City. Sampling months were January, February, and March.

2.3. Soil Sample. The soil sample was taken from the Dera Ghazi Khan District from three different areas (DC Garden, Mustafa chowk near BISE D.G. Khan, and Shoriya Bypass near Canal City). Soil samples were taken to the Government Agriculture Laboratory of D.G. Khan for further analysis of mineral composition present in the soil [19].

2.4. Sample Collection. The sample for different forest trees in different duration through the Standard Augar. Standard Augar was a 1.5" of diameter and 15" in length with a T-shaped handle. This was subjected to the forest trees where the study was conducted. Samples were collected in three different months, such as Jan, Feb, and March. Samples were taken at three different locations each month [20]. In the form of a triplet, three samples were obtained from each field for 7 days. The total samples for each month are 12, and 36 are total experimental units. The sample was wrapped in plastic bags and taken to the Department of Zoology, Ghazi University Dera Ghazi Khan laboratory, where further sample evaluation was carried out (Figure 1).

2.5. Apparatus. Apparatus used for the collection of samples and identification of collecting species were burlesque funnel, beaker, flask, microscopic slides, and liquid measurement glass.

2.6. Extraction of Arthropods. The samples were extracted through the burlesque funnel method. The sample of soils was kept in the funnel on guaz/filter paper having diminutive minuscule apertures, which sanction to pass these arthropods from apertures due to heat and light fitted at the top of the funnel. After putting soil in the funnel, we utilized light to engender heat and kept this heat light on the soil for one week. We reiterate this method with every sample of soils amassed from different plant trees and sites [21]. Beneath the funnel, a solution of ethanol (30%) and distilled water (70%) keeping, and due to the heat and light of the bulb, minuscule arthropods will move in the antithesis direction of light and heat. These arthropods will move forward to that solution which is kept beneath the funnel (Figure 2).

2.7. Chemical and Reagents

2.7.1. Solution. The solution is prepared, which consists of ethanol (30%) and distilled water (70%). Soil samples were put into a funnel, provision the light of a 100-watt bulb because arthropods are heat sensitive. Therefore, arthropods move towards the bottom. The solution can attract the soil arthropods [22].

2.8. Soil Samples Analyses. To determine the different components of soil samples, some analyses were performed in the soil testing laboratory of the agriculture department of D.G. Khan.

2.8.1. Chemical Analyses of Soil Samples from Different Tree Plants. To study the nature of the soil in terms of organic matter, pH, moisture content, electric conductivity



FIGURE 1: Standard Augar used for the sampling procedure during field survey.



FIGURE 2: Installation of berlese funnels to extract insects from soil samples. It uses a heat source (in this case, a light bulb) to dry the sample, forcing the insects through a screen and into a jar of preserving fluid.

phosphates (PO_4), and potassium (K) according to standard methods for soil analysis. The moisture content of soil samples was also determined. Details of soil sample analyses are described as follows.

2.8.2. pH. The pH of samples was determined in the laboratory using a “Digital pH meter (D-25 Horiba)”.

2.8.3. Electrical Conductivity (E.C). The EC of soil samples was determined with the help of “Conductivity meter model WTWcind330i.”

2.8.4. Phosphates. The 4500-P standard method was used to determine the sample’s level of phosphates (APHA, 2005).

2.8.5. Potassium. Soil potassium extraction with ammonium-acetate (NH_4OAc) from oven-dried samples was used to determine potassium. To determine the potassium content of the filtered extracted, we can use Jenway PFP7 Flame Photometer.



FIGURE 3: Stereoscope was used to visualize the respective arthropods for their examination during this study.

2.8.6. Moisture Content. The moisture content of the soil was determined using a simple Memmert incubator (oven) (Model INB 300).

2.9. Identification of Arthropods. The arrangement with the arthropods was moved for the minute investigation to distinguish the arthropods and gauge the insects’ thickness. The identification of the insects was accomplished by using a stereoscope (Bresser GmbH’s Science ETD-201, Art No. 58-06200, Lot No. 5806200-1617) in conjunction with a high-definition camera and a personal computer screen, both of which were located in the laboratory of the Zoology Department at Ghazi College in Dera Ghazi Khan (Figure 3). We took photographs of various soil arthropods available in this isopropyl arrangement. The arrangement was put onto the slides, and with a high-goal camera associated with a stereoscope and screen, we took the photographs of various soil arthropods and spared them in PC. Later, ID was finished [23].

2.10. Diversity Analyses. Some of the following diversity indices were employed to calculate the diversity in observed soil arthropods: *T*-test, Shannon Weiner, cluster analysis, species abundance, species richness and similarity index, evenness, dominance, and maximum diversity.

2.10.1. Species Richness. The presence of species in a specific region was calculated with the help of samples.

2.10.2. Species Diversity. The accumulation of a different type of species in a given community was calculated.

2.10.3. Relative Species Abundance. The proportion of any specific species as compared to other species was measured. The percentage of any particular species compared to the total species in the area was also measured.

2.10.4. Dominance. The dominance of arthropods was studied by calculating the relative abundance of arthropods

TABLE 1: Soil analysis was done for the different sites of experimental areas. For this purpose, several soil parameters (EC, pH, organic matter percentage, available P and K, soil saturation, and texture) were considered.

Parameter	DC Garden			Soil sample sites Mustafa Chowk						Canal City		
	Neem	Guava	Mango	Phalsa	Neem	Guava	Mango	Phalsa	Neem	Guava	Mango	Phalsa
E _c (ms/cm)	1.88	1.71	4.85	3.12	1.56	1.98	4.92	2.94	1.6	1.75	4.32	3.23
Soil pH	7.61	7.59	7.52	7.02	7.65	7.78	7.58	7.28	7.69	7.58	7.32	7.33
Organic matter (%)	0.79	0.66	0.88	0.56	0.66	0.77	0.92	0.42	0.72	0.62	0.77	0.67
Available phosphorous (ppm)	8.26	7.67	8.32	7.92	7.72	8.72	8.42	7.96	8.56	8.52	8.18	7.32
Available potassium (ppm)	226	182	186	182	195	195	196	184	190	175	192	176
Saturation (%)	38	38	36	36	38	38	36	36	38	38	36	36
Texture	Loam	Loam	Loam	Loam	Loam	Loam	Loam	Loam	Loam	Loam	Loam	Loam
Remarks	Normal soil	Normal soil	Normal soil	Normal soil	Normal soil	Normal soil	Normal soil	Normal soil	Normal soil	Normal soil	Normal soil	Normal soil



identified from each soil sample. The species is present in more numbers than other species in a given community.

2.10.5. Evenness, Species Abundance, and Diversity Index. To compare the similarity of all species in a given population. The number of individuals per species was calculated. The diversity index was used to calculate the species in a given community.

2.11. Statistical Analysis. *T*-test was used to analyze the *p* values.

Shannon index was used to find out the species diversity in the sample.

$$\text{Shannon Index } (H) = -\sum p_i \ln p_i = 1.$$

Shannon index tells us about the diversity of species in the sample.

p is the proportion of particular species in the total number of individual species, *n/N* is the no. of species in the natural log, and Σ is the sum of the calculations.

3. Results

3.1. Soil Sample Analysis Report. In this study, we have discussed the findings of our experiment. The experiment was laid out to check the biodiversity of arthropods in different soil samples under different types of trees, i.e., *Psidium guajava*, *Azadirachta indica*, *Grewia asiatica*, and *Mangifera indica*. The discussion of the findings of the results is given below (Table 1).

3.2. Estimation of Arthropods in Neem (*Azadirachta indica*). There were total 12 numbers of species of arthropods that were found in the soil. The maximum number of species found in *Azadirachta indica* during January was mites (50), followed by millipedes (41) and centipedes (40). The minimum number of arthropods found in the soil was termites (8). During February, the maximum number of species found was mites (51), followed by springtail and ants (47) and millipedes (43), while the minimum numbers of arthropods were wolf spider, which was counted at 21 in February. During March, the maximum number of species of arthropods was a centipede, and ants counted 54, followed by mites, 53, and millipede, 48, while the minimum number of species was a wolf spider, 30. The maximum number of 12 species of arthropods was highest in March 535, followed by February 453 and January 361. (Table 2).

3.3. Relative Abundance of Arthropods in *Azadirachta indica*. Relative abundance % during January and February was found to be highest for mites, and during March, it was found to be highest for ants, springtail, and centipedes.

3.4. Estimation of Arthropods in *Psidium guajava*. There were a total of 12 numbers of species of arthropods that were found in the soil. The maximum number of species found in *Psidium guajava* during January was centipedes (39), followed by ants (37) and millipedes, springtail, and oribatid mites (36). The minimum number of arthropods found in the soil was termites (16). During February, the maximum number of species found were centipedes (49), followed by

TABLE 2: The total numbers of arthropods in *Azadirachta indica* were counted during all three sampling months.

Arthropods species	<i>Azadirachta indica</i> (Jan)	<i>Azadirachta indica</i> (Feb)	<i>Azadirachta indica</i> (March)
Millipedes	41	43	48
Sow bug	21	32	36
Spider	34	42	47
Pseudoscorpion	27	32	34
Wolf spiders	16	21	30
Centipedes	40	42	54
Mites	50	51	53
Tiger beetle	26	38	43
Springtail	37	47	54
Oribatid mites	22	37	47
Termites	8	21	35
Ants	39	47	54
	361	453	535

TABLE 3: The total numbers of arthropods in *Psidium guajava* were counted during all three sampling months.

Arthropods species	<i>Psidium guajava</i> (Jan)	<i>Psidium guajava</i> (Feb)	<i>Psidium guajava</i> (March)
Millipedes	36	43	54
Sow bug	17	29	38
Spider	34	41	45
Pseudoscorpion	29	30	31
Wolf spiders	29	35	29
Centipedes	39	49	54
Mites	29	40	50
Tiger beetle	18	34	41
Springtail	36	42	52
Oribatid mites	36	26	35
Termites	16	25	34
Ants	37	46	55
Total	356	440	518

ants (46) and millipedes (43), while the minimum number of arthropods was termites, which were counted at 25 in February. During March, the maximum number of species of arthropods were ants counted at 55, followed by millipedes and centipedes, 54, while the minimum number of species were wolf spiders at 29. The maximum number of a total of 12 species of arthropods was found highest during March 518, followed by February 440 and January 356. (Table 3).

3.5. Relative Abundance of Arthropods in *Psidium guajava*. Relative abundance % during January and February was found to be highest for centipedes, and during March, it was highest for ants.

3.6. Estimation of Arthropods in *Mangifera indica*. There were total 12 numbers of species of arthropods that were

TABLE 4: The total numbers of arthropods in *Mangifera indica* were counted during all three sampling months.

Arthropods species	<i>Mangifera indica</i> (Jan)	<i>Mangifera indica</i> (Feb)	<i>Mangifera indica</i> (March)
Millipedes	32	34	47
Sow bug	24	29	39
Spider	28	38	43
Pseudoscorpion	26	23	30
Wolf spiders	20	23	22
Centipedes	32	37	49
Mites	32	42	50
Tiger beetle	24	24	34
Springtail	32	38	50
Oribatid mites	28	39	46
Termites	18	24	34
Ants	29	39	50
Total	325	390	494

TABLE 5: The total numbers of arthropods in *Grewia asiatica* were counted during all three sampling months.

	<i>Grewia asiatica</i> (Jan)	<i>Grewia asiatica</i> (Feb)	<i>Grewia asiatica</i> (March)
Millipedes	29	41	51
Sow bug	19	31	38
Spider	28	39	49
Pseudoscorpion	31	29	35
Wolf spiders	32	38	54
Centipedes	29	42	61
Mites	33	42	54
Tiger beetle	30	25	28
Springtail	31	44	59
Oribatid mites	26	14	16
Termites	14	25	31
Ants	30	46	55
	332	416	531

found in the soil. The maximum number of species found in *Mangifera indica* during January was millipedes, centipedes, mites, and springtail (32), while the minimum number of arthropods found was termites (18). During February, the maximum number of species found was mites (42), followed by ants and oribatid mites (39). The minimum number of arthropods was a pseudoscorpion, and wolf spider counted 23 each in February. During March, the maximum number of species of arthropods was mites, springtail, and ants counted at 50, while the minimum number of species was wolf spider 22. The maximum number of a total of 12 species of arthropods was found highest during March 494, followed by February 390 and January 325 (Table 4).

3.7. *Estimation of Arthropods in Grewia asiatica.* There were total 12 numbers of species of arthropods that were found in

TABLE 6: Statistical analyses of all four respective tree samples were done. Three samples from each tree were taken under consideration. Following results showed that the entire samples have a significant level of arthropods.

Name and sample	T test	p value
<i>Azadirachta indica</i> 1	8.60	0.000***
<i>Azadirachta indica</i> 2	13.46	0.000***
<i>Azadirachta indica</i> 3	17.54	0.000***
<i>Psidium guajava</i> 1	12.33	0.000***
<i>Psidium guajava</i> 2	15.91	0.000***
<i>Psidium guajava</i> 3	15.43	0.000***
<i>Mangifera indica</i> 1	19.49	0.000***
<i>Mangifera indica</i> 2	15.31	0.000***
<i>Mangifera indica</i> 3	15.30	0.000***
<i>Grewia asiatica</i> 1	17.02	0.000***
<i>Grewia asiatica</i> 2	12.28	0.000***
<i>Grewia asiatica</i> 3	10.76	0.000***

the soil. The maximum number of species found in *Grewia asiatica* during January was mites (33), while the minimum number of arthropods found was termites (14). During February, the maximum number of species found were ants (46), followed by springtail (44), while the minimum number of arthropods was oribatid mites, which were counted 14 in February. During March, the maximum number of species of arthropods was centipedes that counted 61, while the minimum number of species was oribatid mites, 16. A maximum number of total of 12 species of arthropods was found highest during March 531, followed by February 416 and January 332 (Tables 5 and 6).

3.8. *Shannon-Weiner Index.* The Shannon diversity index measured the difference in the diversity of trees. Table 7 below presents the diversity indices of arthropods among selected tree species i.e., *Azadirachta indica*, *Mangifera indica*, *Grewia asiatica*, and *Psidium guajava*. Accordingly, the diversity of arthropods was significantly different among all selected tree species. The highest diversity was observed in samples 1 of *Mangifera indica* and 3 of *Azadirachta indica* ($H' = 2.47$) followed by samples 2 and 3 of *Psidium guajava* and *Mangifera indica* ($H' = 2.46$).

3.9. *Cluster Analysis.* In this dendrogram, it is evident that in *Psidium guajava* and *Grewia asiatica*, population of millipede is more similar to other trees. *Mangifera indica* has the highest number of millipedes and is more different than any other tree. Similarly, the population of sow bugs in *Azadirachta indica* and *Grewia asiatica* is similar, and *Psidium guajava* and *Mangifera indica* are similar. Still, the highest number of sow bugs was found in the *Grewia asiatica* and *Psidium guajava*. Cluster analysis showed that the number of spiders in *Azadirachta indica* and *Psidium guajava* was similar, while the highest number of spiders was found in *Mangifera indica*. As far as the pseudoscorpion is concerned,

TABLE 7: Shannon-Wiener index (Shannon-Weiner index) describes the disorder and uncertainty of individual species. Higher uncertainty means the higher the diversity.

Trees	No. of species	Sample 1 (H')	No. of species	Sample 2 (H')	No. of species	Sample 3 (H')
<i>Azadirachta indica</i>	361	2.40	416	2.45	535	2.47
<i>Psidium guajava</i>	356	2.45	390	2.46	518	2.46
<i>Mangifera indica</i>	325	2.47	440	2.46	494	2.46
<i>Grewia asiatica</i>	332	2.46	453	2.44	531	2.43

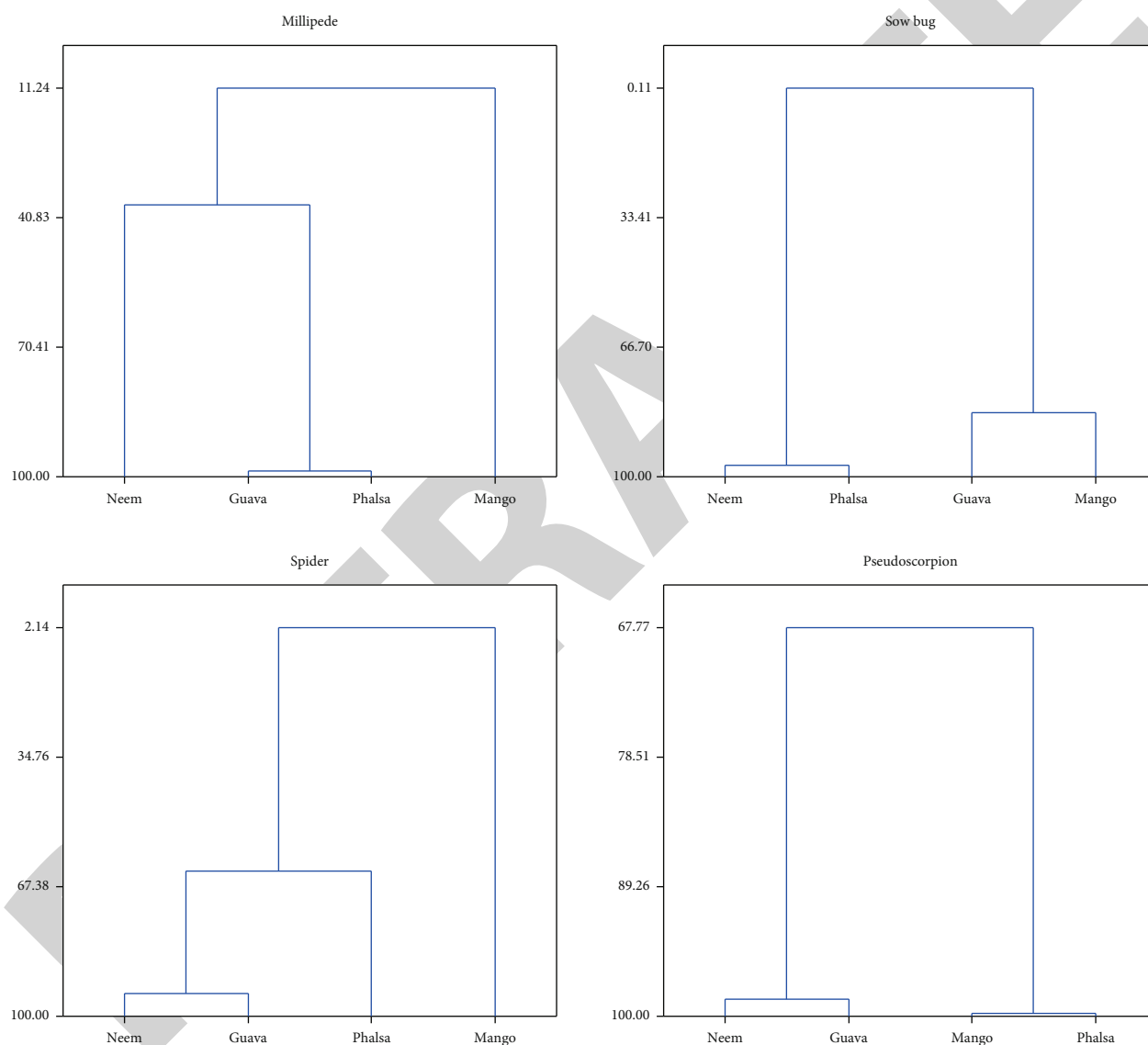


FIGURE 4: Cluster analysis of millipedes, sow bug, spider, and pseudoscorpion species in all observed trees to construct groups, or clusters, while ensuring that within a group, the observations are as similar as possible. In contrast, observations belonging to different groups are as different as possible.

cluster analysis showed that *Mangifera indica* and *Grewia asiatica* have similar numbers. In contrast, *Psidium guajava* and *Azadirachta indica* have a similar number of pseudoscorpions, while the highest number of pseudoscorpions was found in the soil taken from *Psidium guajava* and *Mangifera indica* (Figure 4).

Cluster analysis for wolf spiders showed that *Psidium guajava* and *Mangifera indica* have a similar number, and *Azadirachta indica* and *Grewia asiatica* have the same number of wolf spiders. It can be seen from the graphs that *Grewia asiatica* and *Psidium guajava* had the highest number of wolf spiders. For centipedes, it is evident that

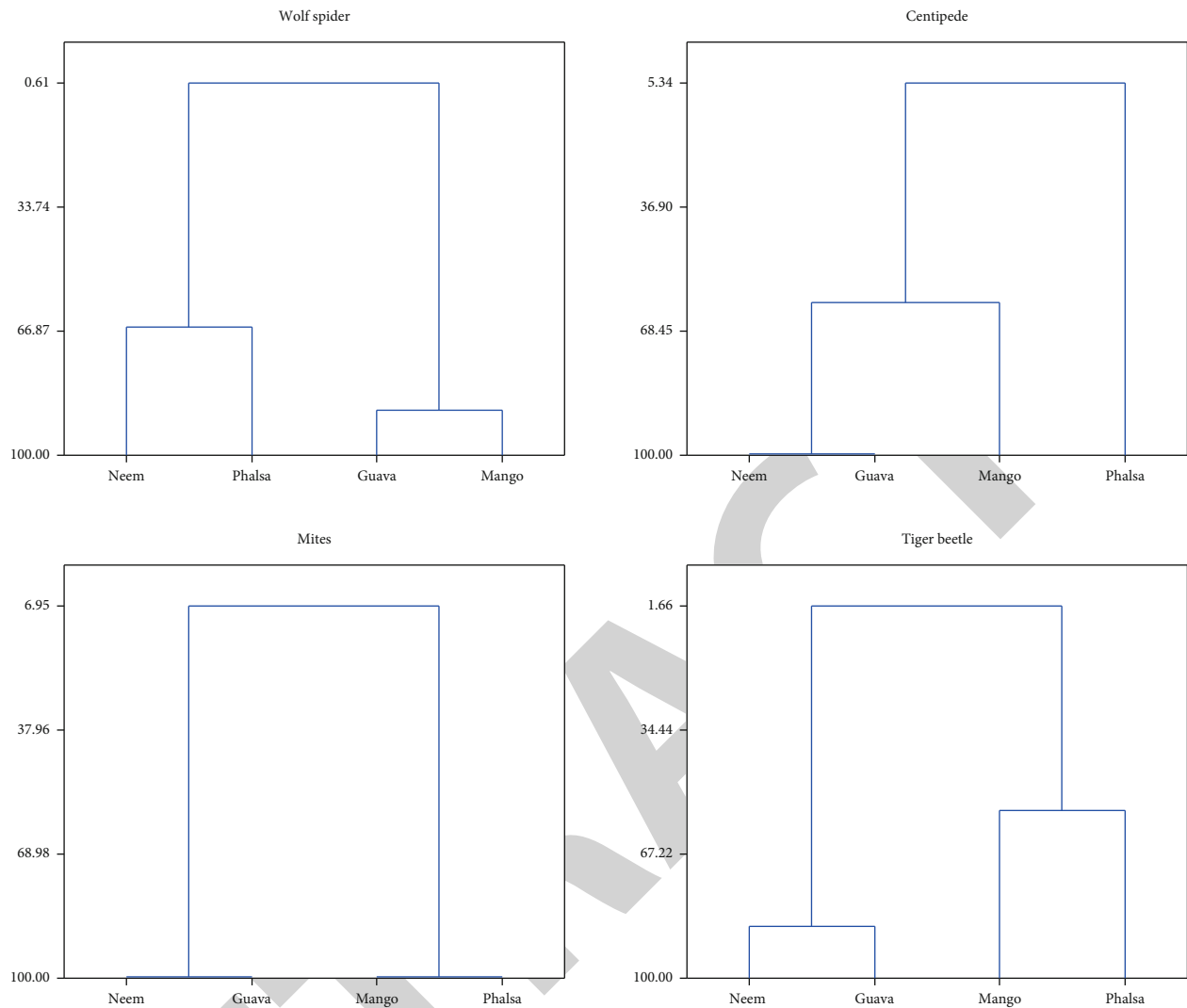


FIGURE 5: Cluster analysis of wolf spider, centipede, mites, and tiger beetle species in all observed trees to construct groups, or clusters, while ensuring that within a group, the observations are as similar as possible, while observations belonging to different groups are as different as possible.

Azadirachta indica and *Psidium guajava* had a similar number of centipedes, while the maximum number of centipedes was present in *Grewia asiatica* as compared in the cluster analysis. The maximum number of mites was present in the soil taken from the *Psidium guajava* and *Mangifera indica*. In contrast, the maximum number of tiger beetles was also present in the same tree species as in mites (Figure 5).

There was less or no difference in the presence of spider tail numbers in *Mangifera indica* and *Azadirachta indica*. In contrast, the maximum number of spider tails were present in *Psidium guajava*. As far as oribatid mites are concerned, the maximum number of these arthropods was present in *Psidium guajava* and *Mangifera indica*. The maximum number of termites and ants was also present in *Psidium guajava*, as indicated by the cluster analysis dendrograms (Figure 6).

3.10. Arthropod Diversity. The graph below represents the total number of arthropods in the sample collected in the experiment. The results are given in the number of each arthropod species and the percentage. The total number of arthropods in the experiment was 5151, millipedes contributed 10% (499) of the total population, and the sow bug represented 7% of the total population which was 353. The number of spiders accounted for 9% (468), the number of pseudoscorpions accounted for around 7% (357), and the number of wolf spiders accounted for 7% (349). There were 528 centipedes (ten percent), but there was only a difference of two mites (526, ten percent). Tiger beetles were found in 365 (7%) of the overall population, springtails numbered 522 (10%), and oribatid mites made up 7% (372) of the whole population (Figure 7). In the samples taken for the trials, the number of termites was the lowest, contributing just 6%, and there were only

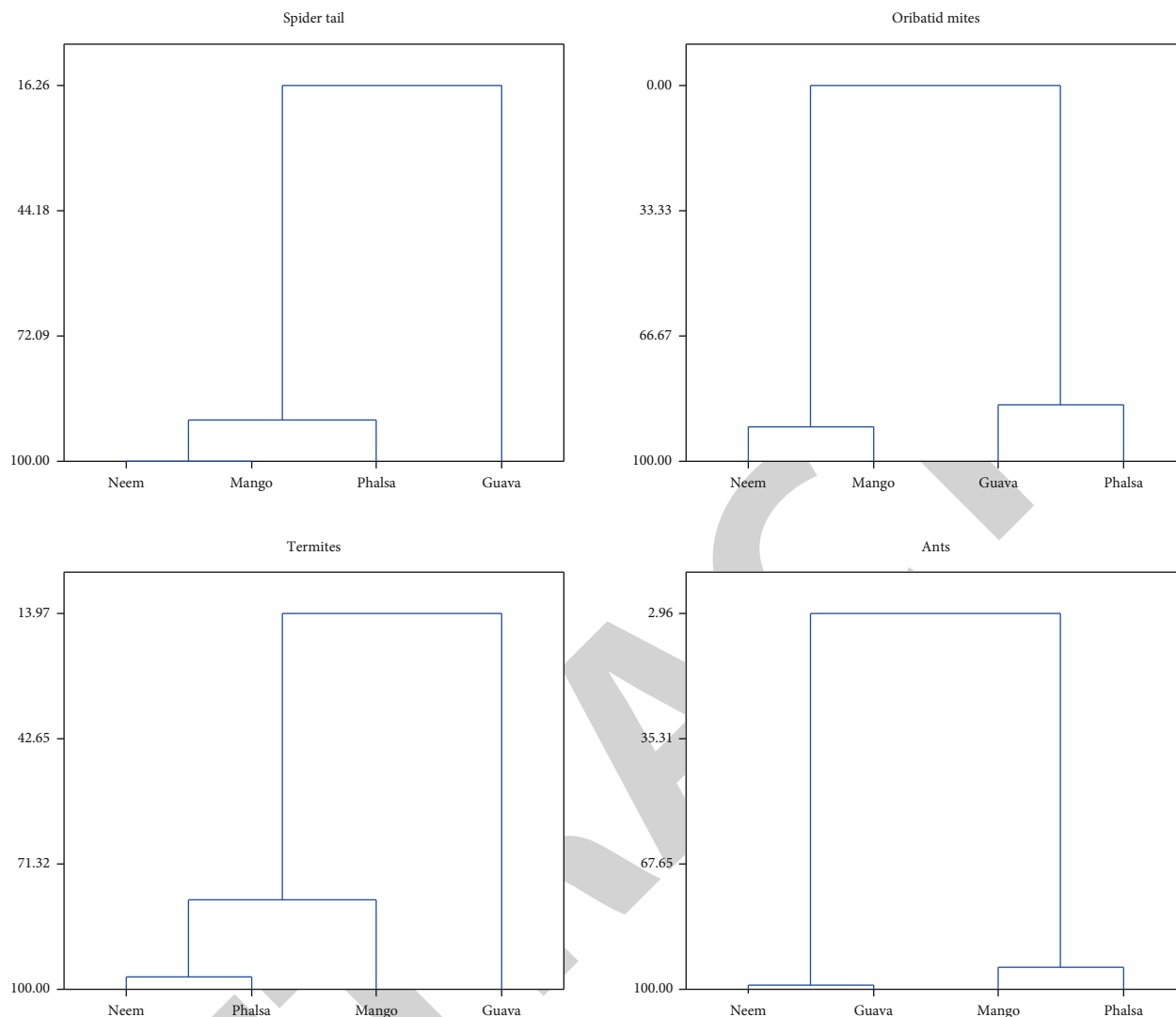


FIGURE 6: Cluster analysis of spider tail, oribatid mites, termites, and ants species in all observed trees to construct groups, or clusters, while ensuring that within a group, the observations are as similar as possible. In contrast, observations belonging to different groups are as different as possible.

285. In contrast, the percentage of ants was 10%, with 522 of them (Table 8).

4. Discussion

For the analysis of the soil characteristics, samples from the experiment sites were taken and sent for analysis. The analysis report is given in Table 1. It is evident from the report that the soil was normal and needed no amendments, i.e., the addition of gypsum etc., to overcome the problem of salts depletion or salt deposition on the surface of the soil. From the results, it is concluded that EC of the soil lies in between 2.94 and 4.92 ms/cm. Soil pH in Pakistan fall in very optimum range so as our sample does, pH of the samples fall in the range of 7.02–7.58. Organic matter in the soil is the main characteristic that defines the fertility of the soil. The maximum organic matter % of the sampled soil was 0.92, and the minimum % was 0.42. Available phosphorus and

potassium of the soil lies in between 7.32 and 8.42 and 176 and 196, respectively. Saturation % of the sampled soil was the same for the entire sample, 36, while the soil texture was loam, according to the soil analysis report.

In our study, more arthropods are captured compared to those that report arthropods in the agronomic crops. According to previous studies, the near-natural habitat offers arable land, stable protection, a food source, and a microclimate for various arthropods [23]. Therefore, more arthropods can be caught near the orchard.

For a long time, people have believed that plant diversity is an important factor in determining nutrient-rich biodiversity [24]. The close relationship between the composition of plants and arthropods is complex and beyond the scope of this study. However, this study has shown that “habitat complexity” significantly impacts the abundant arthropods in the soil. Therefore, our results agree with those of [25] observed that the frequency of arthropods generally decreases with

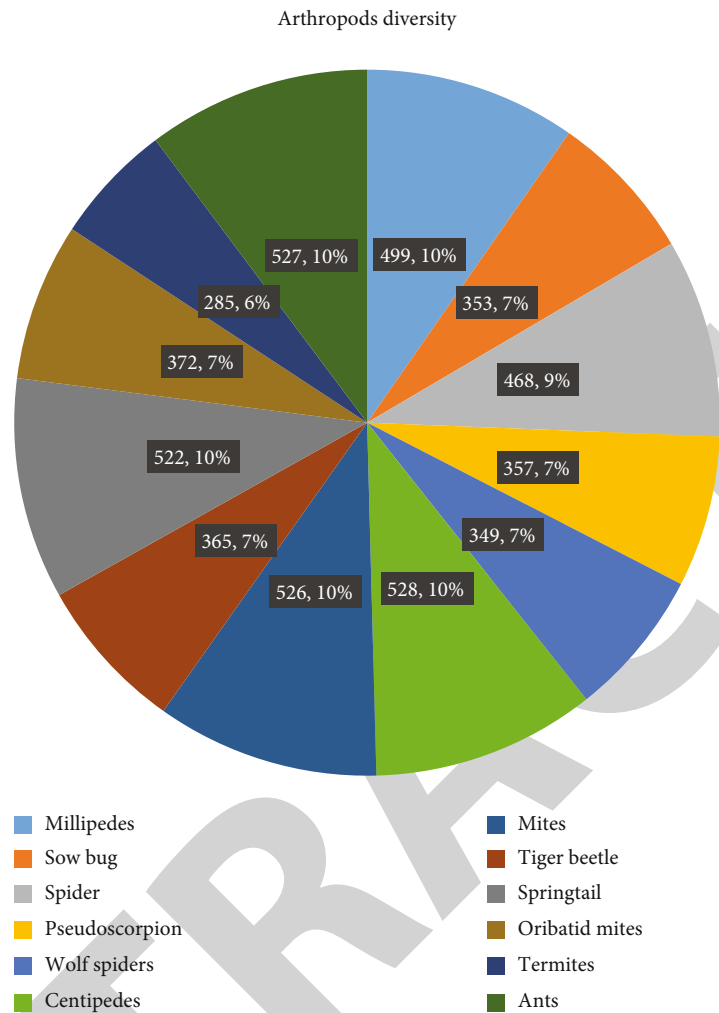


FIGURE 7: Arthropod diversity in the sampled tree soil during January, February, and March. The diversity has been shown in terms of numbers as well as percentage.

increasing land use and management intensity. These authors believe that the entire process of agriculture intensification, from full local vegetation associations to fragmented mixed agricultural landscapes to high-intensity farming or pasture systems, can create a range of impacts and threats that lead to biodiversity reduce. Many possible explanations exist for the abundance of arthropods in less land-intensive systems [26]. Areas with little to moderate improvement/intensification (such as indigenous vegetation and pastures) may have greater habitat complexity because the risk of intensification and uniform management is lower than that of many agricultural systems. Therefore, there can be many niche opportunities with complex land use, while fewer niches are available for systems with less complex structure and composition. Therefore, in a simplified system, the possibility of coexistence by resource allocation can be reduced, reducing species abundance.

The habitat's more complex composition and structure may offer humans more opportunities to obtain a wider range of alternative food resources [27], which helps classify omnivorous and nonspecific predatory organisms. Another

possible explanation for the increase in wealth in less disturbed habitats is that in environments with frequent or severe disturbance, the composition of the community cannot go beyond the initial pioneering stage. Frequent "resetting of the continuous clock" in areas of high disturbance results in an environment conducive to the first continuous species but not to the later continuous species [28]. If the disorder is severe and common (e.g., in intensive farming), all but the most diverse group can be excluded, reducing the total number of species.

Soil arthropods react differently to light. One explanation is that light can speed up the sample drying rate to reflect it compared to extraction without light. On the contrary, soil arthropods are more sensitive to an increase in temperature or a decrease in humidity. In this case, the use of light during the extraction process inactivates the arthropod before exiting the sample, so its apparent abundance decreases. In addition, soil arthropods live in relatively cool and dark (soil) habitats [14]. They can therefore react sensitively to increased temperature and incidence of light, so that the use of light in the extraction process can lead to

TABLE 8: Total numbers of arthropod species found in all experimental sites on four respective trees.

Arthropods species	Experimental sites												Total
	DC Garden				Mustafa Chowk				Canal City				
	Neem	Guava	Mango	Phalsa	Neem	Guava	Mango	Phalsa	Neem	Guava	Mango	Phalsa	
Millipedes	41	36	32	29	43	43	34	41	48	54	47	51	499
Sow bug	21	17	24	19	32	29	29	31	36	38	39	38	353
Spiders	34	34	28	28	42	41	38	39	47	45	43	49	468
Pseudoscorpion	27	29	26	31	32	30	23	29	34	31	30	35	357
Wolf spiders	16	29	20	32	21	35	23	38	30	29	22	54	349
Centipedes	40	39	32	29	42	49	37	42	54	54	49	61	528
Mites	50	29	32	33	51	40	42	42	53	50	50	54	526
Tiger beetle	26	18	24	30	38	34	24	25	43	41	34	28	365
Springtails	37	36	32	31	47	42	38	44	54	52	50	59	522
Oribatid mites	22	36	28	26	37	26	39	14	47	35	46	16	372
Termites	08	16	18	14	21	25	24	25	35	34	34	31	285
Ants	39	37	29	30	47	46	39	46	54	55	50	55	527

an underestimation of soil arthropods. The immature soft epidermis makes it more susceptible to moisture droplets in the suction cup. Organisms such as mites (the vast majority of young animals in this study) are inactive during moulting and, therefore, cannot leave the sample [29]. As a result, another extraction method, such as flotation, should be more suitable for the immature form.

In March, soil arthropods left the sample faster. Similarly, the March samples had the highest frequency, while the January samples had the low frequency. One explanation is that the loose structure of the sample stores less moisture and dries faster, so the temperature/moisture gradient can be established more quickly than with compact samples, which can store more moisture [30].

This has a double effect: over a month, the gradient created by drying the sample at room temperature slowly moves down, forcing the arthropods to leave the sample, but their size is not large enough to kill them, translating into a greater abundance of arthropods. In March, the gradient created by drying the sample at room temperature reached a higher critical level. It became larger, forcing the arthropods to move outward, resulting in a higher estimate of the frequency of arthropods in the sample. This can also be elaborated by the fact that during January the richness of the soil in terms of fertility or organic matter is enhanced during March due to moderate temperature and humidity.

Compared to traditional methods, organic farming can also increase the abundance of many species and biota. For example, the use of herbicides in conventional agricultural systems will reduce the incidence of weeds in nature. Depending on the species of these plants, this can have harmful effects on insects and birds [31]. Similarly, the use of insecticides will reduce not only pests but also predatory insects.

Common methods of plant management such as deep ploughing, the application of agrochemicals, and mechanical harvesting can increase the frequency and severity of interference systems [32]. We have not analyzed the effects of these factors in our research. However, we are studying agri-

cultural and nonagricultural systems [33] which showed that agriculture in the vineyard system destroyed the numbers of invertebrates, including ants, pennies, and millipedes. Agriculture in particular destroys the combination of ants [34] which found a similar conclusion in the olive tree ecosystem: if olive trees are frequently disturbed, sensitive ant species are gradually eliminated.

Many arthropods now become serious pests due to excessive use of pesticides without any proper recommendations on all types of fruit plants especially. These pesticides may also cause the reduction of arthropods which are the common source of soil reclamation by decomposing with the help of bacteria in their bodies. Mango, guava, and falsa trees are susceptible to various insects and mites. It is known that there are 400 pests on these trees reported in different parts of the world [35]. According to the precise classification of the infestation parts of the pests, the main (about 45% of total species) is branch and leaf food, followed by fruit food (32%), and the rest feed on inflorescences, branches, and trunks. Secondary pests can become serious due to cultural customs or climatic and/or species changes or the indiscriminate use of pesticides on the main pests. [36] reported that large-scale insects became serious pests due to the ruthless use of insecticides on fruit flies. Similarly, mites, considered minor pests, can become serious due to human interference. Occasional or sporadic pests can cause economic losses in local areas even at a specific time.

Our results suggest that agricultural orchards affect soil arthropods in all areas. Arthropods are important drivers of ecosystem functions as nutrient cycling, pest control, pollination, and maintenance of soil structure. So, strategies for addressing the conservation of arthropods in agricultural orchards must be promoted.

5. Conclusion

Different kinds of trees were selected to check the diversity of arthropods. The total number of arthropods in the experiment was 5151, in millipedes 10%, spiders accounted for

9%, sow bug, pseudoscorpion, wolf spider, and tiger beetles were present in 7% of the total population. *T*-test and statistical analysis showed that the results were significant. The Shannon diversity index of the arthropods is also developed. Similarly, the highest dissimilarity in the number of sow bugs was found in the phalsa and guava, for spiders in mango, pseudoscorpion and mites in guava and mango, centipedes in phalsa, oribatid mites, and for termites, ants and spider tails were present in guava.

Data Availability

All data relevant to this paper will be available to readers upon request from the corresponding authors.

Conflicts of Interest

The authors declare that there is no conflict of interest.

References

- [1] S. Roy, M. Roy, A. Jaiswal, and A. Baitha, "Soil arthropods in maintaining soil health: thrust areas for sugarcane production systems," *Sugar Tech*, vol. 20, no. 4, pp. 376–391, 2018.
- [2] G. Giribet and G. D. Edgecombe, "The phylogeny and evolutionary history of arthropods," *Current Biology*, vol. 29, no. 12, pp. R592–R602, 2019.
- [3] P. Brahmam, C. Sravanthy, P. Laxman, C. Samatha, and C. Sammaiah, "Biodiversity of soil arthropods in Bt-cotton fields of Warangal, Andhra Pradesh, India," *Bioscan*, vol. 5, no. 1, pp. 159–160, 2010.
- [4] A. Bagheri Kordeshami, J. Khajehali, and A. Nemati, "Some edaphic mesostigmatic mites from Lordegan, Chaharmahal Bakhtiari province with their world distribution," *Journal of Crop Protection*, vol. 4, no. 4, pp. 589–604, 2015.
- [5] R. Mahalakshmi and S. Jayaparvathi, "Diversity of spider fauna in the cotton field of Thailakulam, Virudhunagar district, Tamil Nadu, India," *Journal of Zoology Studies*, vol. 1, no. 1, pp. 12–18, 2014.
- [6] G. H. Cheli, J. Corley, O. Bruzzone et al., "The ground-dwelling arthropod community of Península Valdés in Patagonia, Argentina," *Journal of Insect Science*, vol. 10, no. 1, p. 50, 2010.
- [7] J. Pérez-Bote and A. Romero, "Epigeic soil arthropod abundance under different agricultural land uses," *Spanish Journal of Agricultural Research*, vol. 10, no. 1, pp. 55–61, 2012.
- [8] A. Minelli and G. Fusco, "Arthropod post-embryonic development," in *Arthropod Biology and Evolution*, pp. 91–122, Springer, Berlin, Heidelberg, 2013.
- [9] J. Dzik and T. Sulej, "A review of the early Late Triassic Krasiejów biota from Silesia, Poland," *Phytopatologia Polonica*, vol. 64, pp. 3–27, 2007.
- [10] G. Luquet, "Biomineralizations: insights and prospects from crustaceans," *Zookeys*, vol. 176, p. 103, 2012.
- [11] Y. Chen, Y. Feng, J. G. Deveaux et al., "Biomineralization forming process and bio-inspired nanomaterials for biomedical application: a review," *Minerals*, vol. 9, no. 2, p. 68, 2019.
- [12] C. E. Bowman, "Feeding design in free-living mesostigmatid chelicerae (Acari: Anactinotrichida)," *Experimental and Applied Acarology*, vol. 84, no. 1, pp. 1–119, 2021.
- [13] J. Michels, E. Appel, and S. N. Gorb, "Functional diversity of resilin in Arthropoda," *Beilstein Journal of Nanotechnology*, vol. 7, no. 1, pp. 1241–1259, 2016.
- [14] M. M. Shakir and S. Ahmed, "Seasonal abundance of soil arthropods in relation to meteorological and edaphic factors in the agroecosystems of Faisalabad, Punjab, Pakistan," *International Journal of Biometeorology*, vol. 59, no. 5, pp. 605–616, 2015.
- [15] A. Khadijah, A. Azidah, and S. Meor, "Diversity and abundance of insect species at Kota Damansara community forest reserve, Selangor," *Scientific Research and Essays*, vol. 8, no. 9, pp. 359–374, 2013.
- [16] D. A. Neher and M. E. Barbercheck, "Soil microarthropods and soil health: Intersection of decomposition and pest suppression in agroecosystems," *Insects*, vol. 10, no. 12, p. 414, 2019.
- [17] S. Meiri, G. Murali, A. Zimin et al., "Different solutions lead to similar life history traits across the great divides of the amniote tree of life," *Journal of Biological Research-Thessaloniki*, vol. 28, no. 1, pp. 1–17, 2021.
- [18] N. Amber, I. Ashraf, T. Hussain, and I. Ahmad, *Studies on the diversity and relative abundance of Orthoptera and Lepidoptera species in urban and crop land areas of Dera Ghazi Khan*, Research Gate, 2015.
- [19] M. Abudulai, A. B. Salifu, D. Opere-Atakora et al., "Field efficacy of neem (*Azadirachta indica* a. Juss) for managing soil arthropods and *Cercospora* leaf spots damage for increased yield in peanut," *Plant Protection Science*, vol. 49, no. 2, pp. 65–72, 2013.
- [20] M. F. Barberena-Arias, G. González, and E. Cuevas, "Quantifying variation of soil arthropods using different sampling protocols: is diversity affected," in *Tropical Forest*, pp. 51–70, InTech Online Publisher, 2012.
- [21] R. Bano and S. Roy, "Extraction of soil microarthropods: a low cost Berlese-Tullgren funnels extractor," *International Journal of Fauna and Biological Studies*, vol. 2, pp. 14–17, 2016.
- [22] A. K. Khan, M. H. Bashir, B. S. Khan, and N. Javed, "Biodiversity of soil inhabiting Mesostigmata (Arachnida: Acari) from different agro-ecological zones of Punjab, Pakistan," *Pakistan Journal of Zoology*, vol. 49, no. 2, 2017.
- [23] F.-f. Li, G.-y. Ye, Q. Wu, Y.-f. Peng, and X.-x. Chen, "Arthropod abundance and diversity in Bt and non-Bt rice fields," *Environmental Entomology*, vol. 36, no. 3, pp. 646–654, 2014.
- [24] M. S. Hashmi, "Agrochemical and agricultural sustainability: a case study of Pakistan," *Journal of Environmental and Agricultural Sciences*, vol. 9, pp. 1–9, 2016.
- [25] M. A. Bashir, S. Saeed, A. Sajjad et al., "Insect pollinator diversity in four forested ecosystems of southern Punjab, Pakistan," *Saudi Journal of Biological Sciences*, vol. 26, no. 7, pp. 1835–1842, 2019.
- [26] T. P. Inayat, S. A. Rana, and H. A. Khan, "Diversity of insect fauna in croplands of district Faisalabad," *Pakistan Journal of Agricultural Sciences*, vol. 47, no. 3, pp. 245–250, 2010.
- [27] C. Menta, F. D. Conti, C. Lozano Fondón, F. Staffilani, and S. Remelli, "Soil arthropod responses in agroecosystem: implications of different management and cropping systems," *Agronomy*, vol. 10, no. 7, p. 982, 2020.
- [28] I. Munir, A. Ghaffar, A. Aslam, M. K. Shahzad, and M. Jafir, "Impact of weeds on diversity of soil arthropods in Bt cotton field in Faisalabad Pakistan," *Pakistan Journal of Weed Science Research*, vol. 26, no. 1, p. 117, 2020.

Retraction

Retracted: *In Vitro* Evaluation of Cytotoxic Potential of *Caladium lindenii* Extracts on Human Hepatocarcinoma HepG2 and Normal HEK293T Cell Lines

BioMed Research International

Received 26 September 2023; Accepted 26 September 2023; Published 27 September 2023

Copyright © 2023 BioMed Research International. This is an open access article distributed under the Creative Commons Attribution License, which permits unrestricted use, distribution, and reproduction in any medium, provided the original work is properly cited.

This article has been retracted by Hindawi following an investigation undertaken by the publisher [1]. This investigation has uncovered evidence of one or more of the following indicators of systematic manipulation of the publication process:

- (1) Discrepancies in scope
- (2) Discrepancies in the description of the research reported
- (3) Discrepancies between the availability of data and the research described
- (4) Inappropriate citations
- (5) Incoherent, meaningless and/or irrelevant content included in the article
- (6) Peer-review manipulation

The presence of these indicators undermines our confidence in the integrity of the article's content and we cannot, therefore, vouch for its reliability. Please note that this notice is intended solely to alert readers that the content of this article is unreliable. We have not investigated whether authors were aware of or involved in the systematic manipulation of the publication process.

Wiley and Hindawi regrets that the usual quality checks did not identify these issues before publication and have since put additional measures in place to safeguard research integrity.

We wish to credit our own Research Integrity and Research Publishing teams and anonymous and named external researchers and research integrity experts for contributing to this investigation.

The corresponding author, as the representative of all authors, has been given the opportunity to register their agreement or disagreement to this retraction. We have kept a record of any response received.

References

- [1] A. Kalsoom, A. Altaf, M. Ashraf et al., "*In Vitro* Evaluation of Cytotoxic Potential of *Caladium lindenii* Extracts on Human Hepatocarcinoma HepG2 and Normal HEK293T Cell Lines," *BioMed Research International*, vol. 2022, Article ID 1279961, 11 pages, 2022.

Research Article

***In Vitro* Evaluation of Cytotoxic Potential of *Caladium lindenii* Extracts on Human Hepatocarcinoma HepG2 and Normal HEK293T Cell Lines**

Aasia Kalsoom,¹ Awais Altaf ,¹ Muhammad Ashraf,¹ Muhammad Muddassir Ali ,² Saira Aftab,³ Huma Sattar,¹ Muhammad Sajjad,⁴ Amjad Islam Aqib ,⁵ and Tahir Maqbool¹

¹Institute of Molecular Biology and Biotechnology, The University of Lahore, Lahore 54000, Pakistan

²Institute of Biochemistry and Biotechnology, University of Veterinary and Animal Sciences, Lahore 54000, Pakistan

³Postdoctoral Fellow Department of Biochemistry and Biophysics, Stockholm University, Stockholm A 425-B16, Sweden

⁴School of Biological Sciences, University of the Punjab, Lahore 54000, Pakistan

⁵Department of Medicine, Cholistan University of Veterinary and Animal Sciences, Bahawalpur 63100, Pakistan

Correspondence should be addressed to Awais Altaf; a.altaf.uaf@gmail.com and Muhammad Muddassir Ali; muddassir.ali@uvas.edu.pk

Received 28 July 2022; Accepted 9 September 2022; Published 22 September 2022

Academic Editor: Faheem Ahmed Khan

Copyright © 2022 Aasia Kalsoom et al. This is an open access article distributed under the Creative Commons Attribution License, which permits unrestricted use, distribution, and reproduction in any medium, provided the original work is properly cited.

Data regarding the therapeutic potential of *Caladium lindenii* (*C. lindenii*) are insufficient. It becomes more important to explore plants as an alternative or palliative therapeutics in deadly diseases around the globe. The current study was planned to explore *C. lindenii* for its anticancer activity of ethanolic and hexane extracts of *C. lindenii* leaves against hepatic carcinoma (HepG2) and human embryonic kidney (HEK293T) cell lines. HepG2 and HEK293T cells were treated with 10, 50, 100, 200, and 400 $\mu\text{g}/\text{mL}$ of ethanolic and hexane extracts of *C. lindenii* and were incubated for 72 h. Antiproliferative activity was measured by 3-(4,5-dimethylthiazol-2-yl)-2,5-biphenyl tetrazolium bromide (MTT) assay, and percentage viability were calculated through crystal violet staining and cellular morphology by Fluid Cell Imaging Station. The study showed ethanolic extract exhibiting a significantly higher antiproliferative effect on HepG2 ($\text{IC}_{50} = 31 \mu\text{g}/\text{mL}$) in a concentration-dependent manner, while HEK293T ($\text{IC}_{50} = 241 \mu\text{g}/\text{mL}$) cells showed no toxicity. Hexane extract exhibited lower cytotoxicity ($\text{IC}_{50} = 150 \mu\text{g}/\text{mL}$) on HepG2 cells with no effect on HEK293T ($\text{IC}_{50} = 550 \mu\text{g}/\text{mL}$). On the other hand, the percentage viability of HepG2 cells was recorded as 78%, 67%, 50%, 37%, and 28% by ethanolic extracts, and 88%, 80%, 69%, 59%, and 50% by hexane extracts at tested concentrations of both extracts. Toxicity assay showed significantly safer ranges of percentage viabilities in normal cells (HEK293T), i.e., 95%, 90%, 88%, 76%, and 61% with ethanolic extract and 97%, 95%, 88%, 75%, and 62% with hexane extract. The assay validity revealed 100% viability in the control negative (dimethyl sulfoxide treated) and less than 45% in the control positive (cisplatin) on both HepG2 and HEK293T cells. Morphological studies showed alterations in HepG2 cells upon exposure to $>50 \mu\text{g}/\text{mL}$ of ethanolic extracts and $\geq 400 \mu\text{g}/\text{mL}$ of hexane extracts. HEK293T on the other hand did not change its morphology against any of the extracts compared to the aggressive changes on the HepG2 cell line by both extracts and positive control (cisplatin). In conclusion, extracts of *C. lindenii* are proved to have significant potential for cytotoxicity-induced apoptosis in human cancer HepG2 cells and are less toxic to normal HEK293T cells. Hence *C. lindenii* extracts are proposed to be used against hepatocellular carcinoma (HCC) after further validations.

1. Introduction

Due to the critical premise of epidemiology, cancer assures the most complex pathological state among the health of

the population [1]. In 2018, 18 million people were affected by cancer including 8.5 million females and 9.5 million males from which 9.5 million deaths were reported. Approximately, 19.3 million new cancer cases and 10.0 million

deaths have been reported in 2020. The estimation of cancer incidence is expected to be 28.4 million cases by the year 2040 [2]. Conventional medicines stimulate apoptosis and exploit the cascade of intracellular events in cancer cells. In the earliest times, various natural remedies had been used to manage diseases counting cancer, as these products have diversified mechanisms comprising the onset of apoptosis to inhibit signaling [3]. Morphological, biochemical, and gene-based characterization of cell lines come up with new intuitions regarding the diversity of polygenic traits, chemotherapy resistance, and the understanding of targeted cancer therapies [4].

Plant-based phytochemicals and antioxidants are known for anticancer treatment because of their anti-proliferative, antioxidative, and apoptotic values in recent times [5]. Polyphenols are a large family of naturally occurring compounds with antioxidant properties. Volatile organic compounds (VOC) are responsible for aromatic characteristics in medicinal and aromatic plants (MAPs). These polyphenols can combat various diseases including neurodegenerative diseases, cardiovascular diseases, inflammations, and different types of cancers. The two existing biosynthetic pathways of secondary metabolites which lead to the formation of phenolic compounds are the shikimic acid pathway gives rise to phenylpropanoids, tannins, lignin, and many others, while the acetate-mevalonate pathway produces phenols [6]. Vegetables and MAPs are enriched with phenolic compounds (isoflavonoids, anthocyanins, lignans, and phenols). Their therapeutic effects on human health have been studied more efficiently in recent years. Flavonoids belong to the group of polyphenolic secondary metabolites found in plants and vegetables are responsible for health benefits through signaling pathways and antioxidant effects [7].

The enormous therapeutic nature of medicinal plants are phytochemicals that provide a revolutionary advantage everywhere on the globe due to their hidden epitome [8]. A lot of analgesics, narcotics, and other drugs have been used since ancient times including opium, aspirin, quinine, and digitalis. Identified phytochemicals recommended for cancer treatment are vinca alkaloids, podophyllotoxin, taxanes, and roscovitine, and their derivatives have considerable effects on cancer development and proliferation. Because of diverse ethnomedicinal and ethnopharmacological comparisons of various species, many scientific works have been assembled over the past decade. Many phytochemicals including gingerol, curcumin, kaempferol, resveratrol, and nutritional phenolic compounds revealed anticancer activity both *in vivo* and *in vitro* experimentation [9]. Many *in vivo* as well as *in vitro* studies have reported the anticancerous properties of plant-derived natural compounds through the inhibition of enzymatic activity, stimulating DNA repair pathways, bringing antioxidant mechanism, and the release of protective enzymes [10].

C. lindenii is a flowering plant native to South America and belongs to the family Araceae. Many species of *Caladium* grow in wild areas of Nigeria. Authors reported that the plant parts of *Caladium* species have been used to manage various disease conditions including various kinds of tumors and infections in traditional medicine system [11].

The leaves, tubers, and other parts of *C. lindenii* were used therapeutically for stingray lesions in the regions of Brazil. However, no sufficient data has been found to reveal the presence of phytochemicals and pharmacological effects of *C. lindenii* in literature [12]. The underlying principle of the current research work is to explore the efficacy of organic extracts of *C. lindenii* with antiproliferative activity in response to the HepG2 (liver cancer) and normal HEK293T (human embryonic kidney 293T) cell lines.

2. Materials and Methods

2.1. Plant Collection and Identification. The leaves of *C. lindenii* were collected in the summer season from the botanical garden of Quaid-e-Azam University, Islamabad, Pakistan. The identification of leaves was confirmed by taxonomist Dr. Zaheer-ud-Din Khan (GC. Herb. Bot. 3854) working as a legendary professor in the Department of Botany, Government College University Lahore, and the samples were also submitted at the University Herbarium bank.

2.2. Plant Extract Preparation. The leaves of *C. lindenii* were shade dried for 10 days and then crushed into the powdered form using a laboratory grinding mill (Thomas Scientific). Powdered leaves (300 g) were macerated into 1.0 L of ethanol (Sigma-Aldrich, 90%) and *n*-hexane (Sigma-Aldrich, 95%) separately and incubated for 2 weeks at 37°C. Filtration was done by using Whatman No.1 filter paper in reagent bottles. A rotary evaporator (Heidolph Hei-Vap, Germany) was used to concentrate the filtrates separately under a vacuum at 40°C, and the lyophilization or freeze-drying method was used to achieve dry extracts, and then samples were stored at 4°C [13].

2.3. Cancer Cell Cultivation. Hepatocellular carcinoma (HepG2) cell line and the human embryonic kidney (HEK293T) cell line were arranged from the UOL cell line BioBank (IMBB/CRiMM), The University of Lahore, Lahore, Pakistan. The cancer cells were successfully cultured in Dulbecco's Modified Eagle's Medium (DMEM) (Caisson Lot#02160032), 10% heat-inactivated fetal bovine serum (FBS) (Sigma-Aldrich Lot#BCBS3184V), and 100 U/mL of *Penicillin-Streptomycin* (Caisson Lot#10201011). The normal human kidney cells (HEK293T) were grown in Minimum Essential Media (MEM) (Gibco) with 15% FBS and incubated at 37°C with 5% CO₂. Once the cells reach 80% confluent, the passage was carried out with minor changes. The medium was then removed and the cells were washed with PBS (Inovatiqa Lot#153595). Trypsinization was done by adding 3 mL of trypsin (Gibco Lot#1297823) until cells detach from the surface of the flask. A complete medium (5 mL) was added to end up the reaction, centrifuged the cells at 1500 rpm for 5 minutes, and then aspirated the supernatant. The passage was carried out by adding 10 mL of fresh growth medium and every 5 mL of cell suspension was shifted to a T75 cm² cell culture flask [14].

2.4. Cell Counting and MTT Assay for Cytotoxicity Analysis. Trypsin was applied to cells to detach from the surface. Centrifugation was carried out and the cells were resuspended in

3 mL of the active medium. The hemocytometer was used for cell counting. The cell suspension was then placed into 96-well microtitre plastic plates and incubated at 37°C for 24h with 5% CO₂. The MTT assay was performed with slight modifications following the protocol described by Riaz [15]. The ethanolic and hexane crude extracts of *C. lindenii* were dissolved in dimethyl sulfoxide (DMSO) (Invitrogen Inc., USA) at a concentration of 160 mg/mL. HepG2 cells were seeded in 96-well microtitre plate (1 × 10⁴ cells/well) in 200 μL of the complete medium in the microtitre plate, and the prepared concentrations (400, 200, 100, 50, and, 10 μg/mL) were administered to cells. The last step was to incubate under the temperature mentioned previously with 5% CO₂. The same protocol was used for HEK293T cells with MEM medium and 15% of FBS. Cisplatin drug (Patients Welfare Society Inmol Receipt No, 651278) (10 μg/mL) was used as a positive control, DMSO (0.1%) as a negative control, and untreated cells containing plan DMEM medium (2% FBS) were used for the comparison, before and after treatment. The normal HEK293T and cancer HepG2 cell lines were used to assess the toxicity of plant extracts on healthy and cancer cells. After 72 h of incubation, the medium aspirated and the degree of cellular proliferation was observed under the microscope. MTT assay was performed by adding 20 μL of MTT reagent (Invitrogen Inc., USA) into each well and continued with incubation for 2 h. After removing the supernatant, 150 μL of DMSO was mixed and then placed on a plate shaker to dissolve formazan crystals. After incubation for 15 minutes, the absorption spectra across the wells were determined by using a microplate reader (BIO-RAD) at a specified wavelength of 570 nm. Reactions in triplicate were performed for all samples. Half-maximal inhibitory concentration IC₅₀ was calculated using a linear regression method.

2.5. Cell Viability/Adhesion Assay. Crystal violet solution (0.1% wv) (Sigma-Aldrich) was prepared in 9 mL of PBS. Crystal violet (CV) assay was performed by following the protocol of Nawaz et al. with slight changes [16]. HepG2 and HEK293T cells were seeded in a 96-well microtitre plate (1 × 10⁴ cells/well) in 200 μL of complete medium. Incubation was carried out for 72 h under a specified temperature (37°C) with humidity and 5% CO₂. The treated (with plant extract) and untreated media were removed, and the cells were fixed with 70% ethanol for 10 min. CV solution was added for cell staining and stayed for 30 min. The plate was washed with PBS and then destained the cells with 200 μL of triton X-100 solution (Sigma-Aldrich CAS#9036-19-5) used to de-stain cells. The cells were incubated at room temperature for 30 min and the optical density (OD) of samples was measured in triplicate at 570 nm using a spectrophotometer.

2.6. Percentage Calculation of Cell Viability. The percentage of viable cells was calculated by using the formula equation:

$$\% \text{Cell viability} = \frac{\text{Mean absorbance of treated cells}}{\text{Mean absorbance of control}} * 100. \quad (1)$$

2.7. Morphological Examination. To inspect the effect of plant extracts on cancer cell proliferation, the morphological variations were visualized and compared with the control group by applying different treatment concentrations on HepG2 and HEK293T cells using Fluid Cell Imaging Station.

2.8. Data Analysis. The experiments were carried out in three corresponding or identical parts and the data were expressed as mean ± standard deviation (SD). One-way analysis of variance (ANOVA) and Tukey's test were used to determine the interaction among three variables through Graph pad prism 5.0. IC₅₀ values were calculated by linear regression method using AA Bioquest calculator. *p* < 0.05 was considered statistically significant with a confidence interval (CI) of 95%.

3. Results

3.1. Cytotoxic Effects of Plant Extracts on HepG2 and HEK-293T Cells. Cell proliferation inhibition activity of ethanol and hexane extracts of *C. lindenii* leaves on HepG2 and HEK-293 cell lines are represented in Figure 1 and Table 1. Depending on the results, the MTT test on the ethanolic extract showed a high antiproliferative effect against HepG2 (IC₅₀ = 31 μg/mL) in comparison with HEK293T (IC₅₀ = 241 μg/mL) at 72 h. It confounds that ethanolic extract concentrations (400, 200, 100, 50, 10 μg/mL) become more toxic to cancer cells as compared to cisplatin (10 μg/mL) which was taken as positive control and DMSO as negative control (Figure 1). Hence, the ethanolic extract enhanced the mortality of cancer cells even at the lowest concentration (50 μg/mL). The wells treated with hexane extract exhibited lower cytotoxicity (IC₅₀ = 150 μg/mL) on HepG2 cells, however, HEK293T (IC₅₀ = 550 μg/mL) cells displayed very less or no effect at the same time. The aggressive effect of cisplatin on both cell lines was also examined. Plant extracts showed more cytotoxic effects on the viability of HepG2 cells at 400, 200, and 100 μg/mL, whereas minimal effects were observed on normal cells (HEK293T). Results demonstrated that alcoholic extract had strong antiproliferative activity on cancer cells with a partial effect on HEK293T at 72 h, whereas, hexane extract showed negligible effects in all *in vitro* tested concentrations (10-400 μg/mL).

3.2. Morphological Observation of Ethanolic Concentrations. Morphological assessment of ethanolic concentrations was observed in HepG2 and HEK293T cells shown in Figure 2. Alterations in cell structure, shape, and size were observed in a concentration-dependent manner. Cells at 50 μg/mL and higher concentrations reduced the survival rate of cancer cells by losing their normal morphology and the capacity to attach to the surface. The lower concentration (10 μg/mL) did not show any alteration in shape or reduced viability in HepG2 cells as observed by the MTT assay. In the case of cisplatin (positive control), a round-shaped image and less viability were observed in HepG2 treated cells. The morphological features and cytotoxicity of HEK293T cells were also assessed after treatment. Antiproliferative effects of ethanolic extract concentrations of *C. lindenii* stop the proliferation of

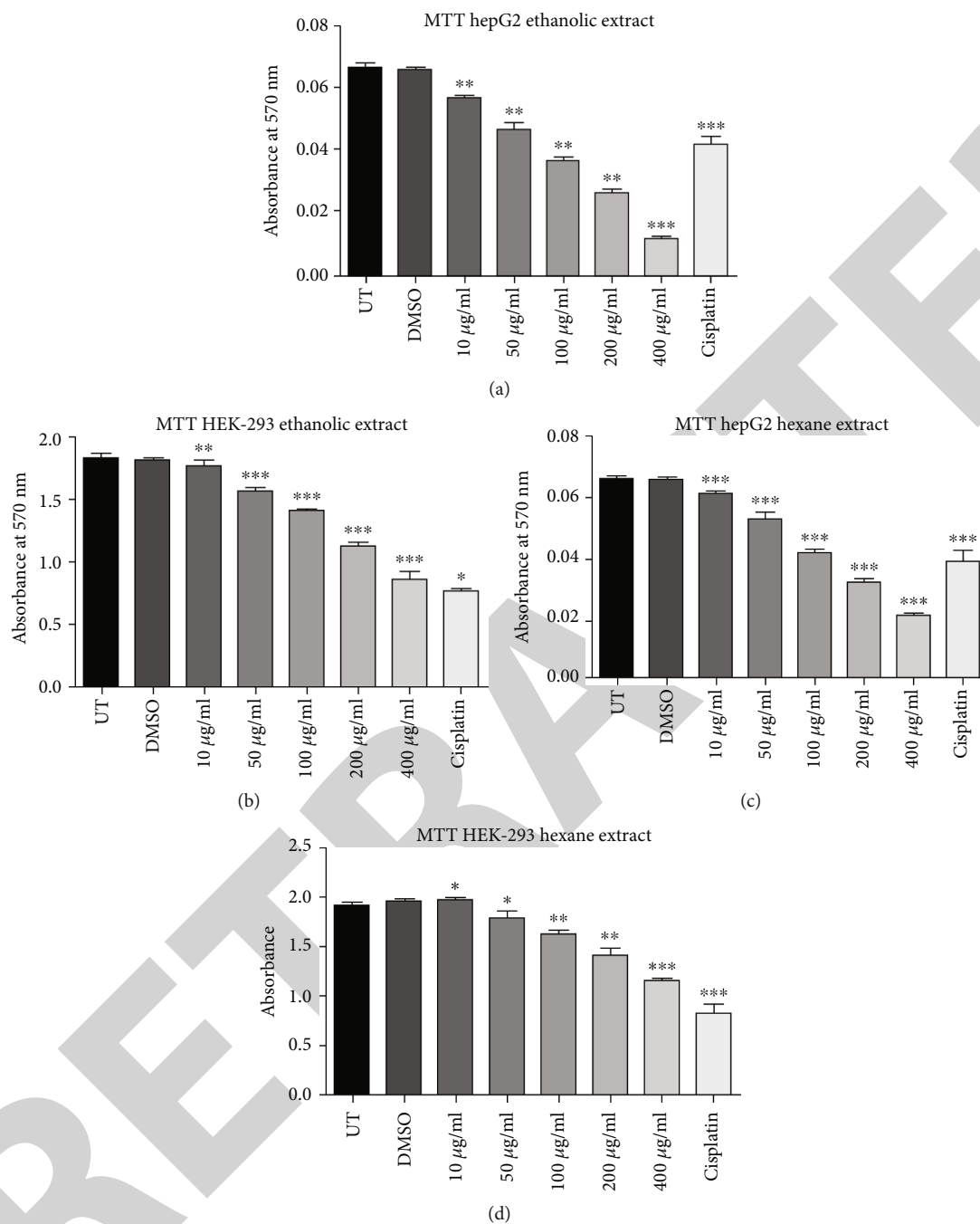


FIGURE 1: Graphical representation: *In vitro* assessment of ethanolic and hexane extracts of *C. lindenii* on HepG2 and HEK293T cell lines. (a) MTT assay results showed a significantly increased mortality rate of HepG2 cells after treatment with higher concentrations at 72 h. (b) HEK293T being a normal cell line revealed less toxicity of ethanolic extract only at the highest concentrations (400, 200 $\mu\text{g/ml}$) as compared to hexane extract. (c) Hexane concentration on HepG2 cells showed less effect. (d) HEK293T cell line revealed less or no activity of hexane extract. Cisplatin was used as positive control and showed more negative effects against normal cell line, however, DMSO was taken as a negative control. * $p \leq 0.05$, ** $p \leq 0.001$, and *** $p \leq 0.0001$ referred as statistically significant. Error bars showed error or standard deviation as mean \pm SD of each group. MTT: 3-(4, 5-dimethylthiazol-2-yl)-2, 5-biphenyl tetrazolium bromide; DMSO: dimethyl sulfoxide; SD: standard deviation.

cancerous cells, whereas healthy (HEK293T) cells were stable even at the highest concentration.

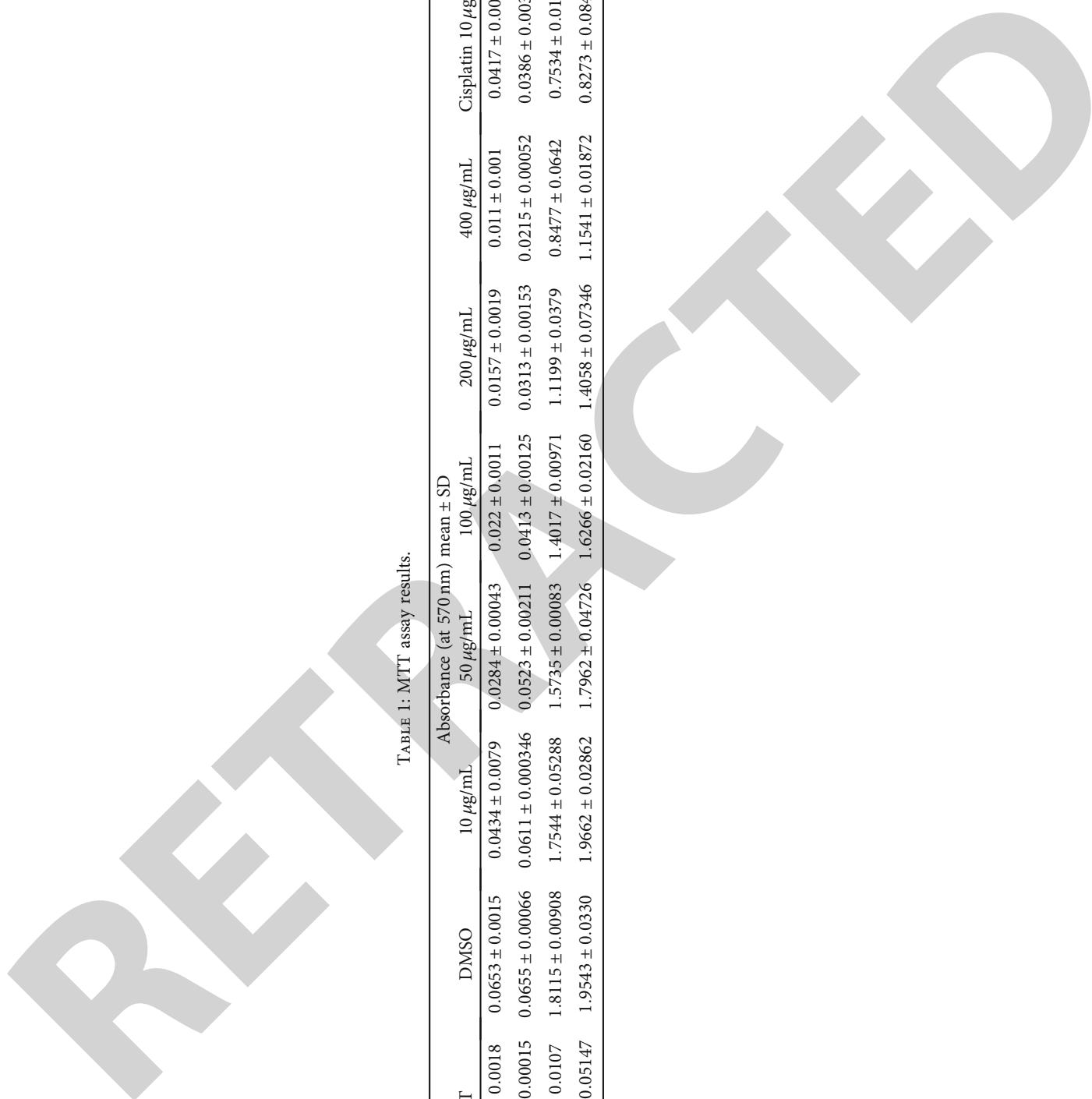
3.3. *Cell Viability Assay*. Crystal violet staining is another way to assess the percentage viability of cells after treatment.

The number of cells alive or adherent to the surface was estimated by using crystal violet staining of HepG2 and HEK293T cells as shown in Figure 3.

Effects of ethanolic and hexane extracts of *C. lindenii* on HepG2 cells with different concentrations starting from 10-

TABLE 1: MTT assay results.

Cell lines	Solvents	UT	DMSO	Absorbance (at 570 nm) mean \pm SD					
				10 μ g/mL	50 μ g/mL	100 μ g/mL	200 μ g/mL	400 μ g/mL	Cisplatin 10 μ g/mL
HepG2	Ethanol	0.0661 \pm 0.0018	0.0653 \pm 0.0015	0.0434 \pm 0.0079	0.0284 \pm 0.00043	0.022 \pm 0.0011	0.0157 \pm 0.0019	0.011 \pm 0.001	0.0417 \pm 0.0042
	Hexane	0.0662 \pm 0.00015	0.0655 \pm 0.00066	0.0611 \pm 0.000346	0.0523 \pm 0.00211	0.0413 \pm 0.00125	0.0313 \pm 0.00153	0.0215 \pm 0.00052	0.0386 \pm 0.00390
HEK293T	Ethanol	1.8313 \pm 0.0107	1.8115 \pm 0.00908	1.7544 \pm 0.05288	1.5735 \pm 0.00083	1.4017 \pm 0.00971	1.1199 \pm 0.0379	0.8477 \pm 0.0642	0.7534 \pm 0.0146
	Hexane	1.8937 \pm 0.05147	1.9543 \pm 0.0330	1.9662 \pm 0.02862	1.7962 \pm 0.04726	1.6266 \pm 0.02160	1.4058 \pm 0.07346	1.1541 \pm 0.01872	0.8273 \pm 0.08484



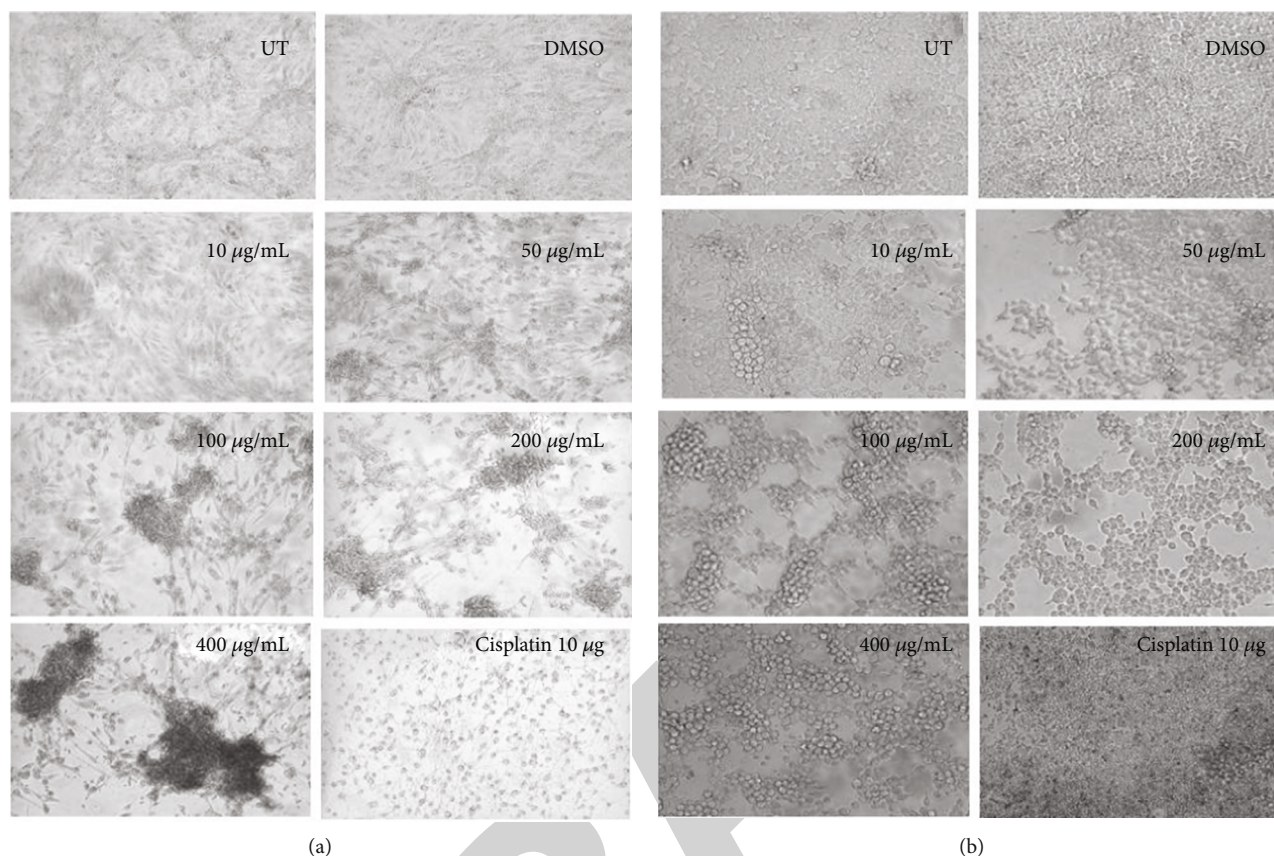


FIGURE 2: Morphological representation of HepG2 cells following the exposure of increasing concentrations of ethanolic extract of *C. lindenii* at 72 h observed by Floid cell imaging station. Changes in the morphology of hepatocellular carcinoma (HepG2) cells are very obvious when exposed to ethanolic concentrations. (a) The concentration of 50 $\mu\text{g/mL}$ and higher changed the normal morphology and the cell adhesion capability to the surface as compared to the control. Higher cellular concentrations give the impression of clusters. The lower concentration (10 $\mu\text{g/mL}$) did not show altered shape or reduced viability in HepG2 cells as observed by the MTT assay. Application of cisplatin (positive control) changed the morphology of both cancerous and healthy cells round-shaped with less viability. (b) The morphological features and cytotoxicity of *C. lindenii* on normal cells (HEK293T) did not show a negative effect even at the highest concentration. However, the drug (cisplatin) response elaborated altered cellular morphology. MTT: 3-(4,5-dimethylthiazol-2-yl)-2,5-biphenyl tetrazolium bromide; DMSO: dimethyl sulfoxide.

400 $\mu\text{g/mL}$ showed different responses. Ethanolic concentrations showed a dose-dependent decrease in percentage viability. HepG2 cells were exposed to ethanolic concentrations at 10, 50, 100, 200, and 400 $\mu\text{g/mL}$ found to be more toxic by measuring the absorbance at 570 nm. Staining facilitates the visualization of cell morphology by giving 100% of viability. Measurements were recorded as 78%, 67%, 50%, 37%, and 28% when treated with ethanolic concentrations exhibited a statistically significant decrease in HepG2 cells in comparison with negative control (99.5%). At higher concentrations of 200 and 400 $\mu\text{g/mL}$, cell viability decreased to 37% and 28%, respectively. However, the viability assessment in healthy (HEK293T) cells were observed to be 95%, 90%, 88%, 76%, and 61% of ethanolic extract and 99% of DMSO. Upon treatment with hexane extracts showed 88%, 80%, 69%, 59%, 50% and 97% of DMSO cell viability. On the other hand, the nontumor HEK293T cells exhibited negligible effects on cell inhibition at 72 h with all concentrations of hexane extract. The observed cell viability of HEK293 treated cells was 97%, 95%, 88%, 75%, and 62%,

and DMSO was 99.48%. Cisplatin concentration (10 $\mu\text{g/mL}$) was administered to both cancer and healthy cells for the comparison of chemotherapeutic and natural antioxidants containing plant extracts. Percentage cell viability on HepG2 cells was 42%, while HEK293T exhibited 45% (Figure 3). R^2 represents the coefficient of determination. Higher R -squared values demonstrate smaller differences between observed data and fitted values. Our results revealed a significant positive correlation ($R^2 = 0.9578, 0.9992, 0.9903, \text{ and } 0.9885, p \text{ value} < 0.05$) for both *C. lindenii* extracts.

3.4. Morphological Observation of Hexane Concentrations.

The morphological observation showed the effect of hexane extract of *C. lindenii* on both HepG2 and HEK293T cells in Figure 4. *In vitro* treatment of hexane extract on HepG2 cells demonstrated mild alteration in cell morphology at all concentrations except the higher concentrations (200 and 400 $\mu\text{g/mL}$). Cells treated with high concentrations of 200 and 400 $\mu\text{g/mL}$ became degraded and shrunken, while the

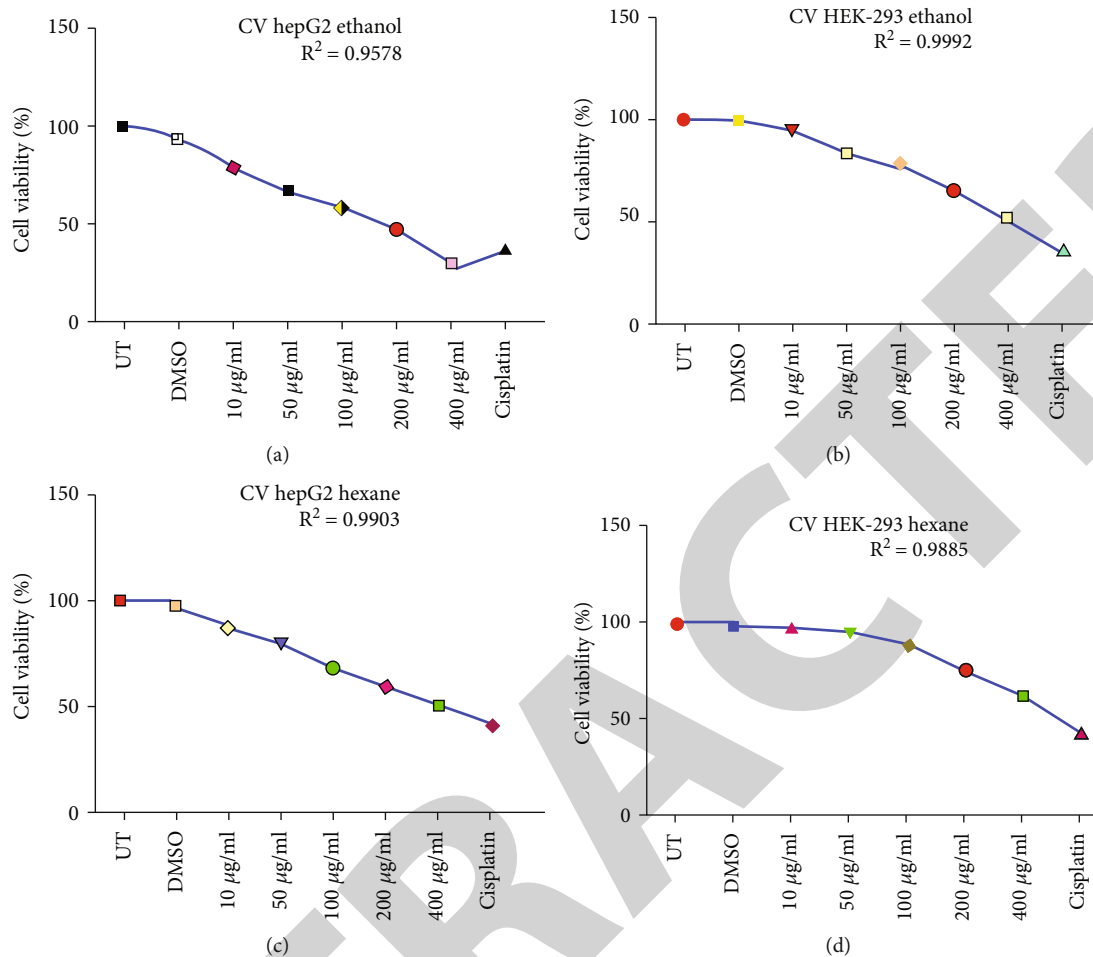


FIGURE 3: The growth rate of cells was calculated by the crystal violet staining protocol. Optical density (OD) at 570 nm was measured and plotted to obtain the percentage viability of untreated, treated, and control cells. In cell viability assay, a drug response is driven by cell density. A trend-line slope showed the number of cells/well certified to be significant. (a) The calculated percentage elaborated a clear dose-dependent decrease in HepG2 cells with significant R^2 (coefficient of determination) values. (b) HEK293T plotted slope remained constant with a slight fall and showed good viability. (c) Hexane extract showed 59% and 50% viability on HepG2 cells at higher (200 and 400 µg/mL) concentrations. (d) Nontumor cells did not show the activity of hexane extract at any concentration. Statistical analysis described as * $p < 0.05$, ** $p < 0.001$, and *** $p < 0.0001$. DMSO: Dimethyl sulfoxide; SD: standard deviation; CV: crystal violet; MTT: 3-(4, 5-dimethylthiazol-2-yl)-2, 5-biphenyl tetrazolium bromide.

lower concentrations of 10, 50, and 100 µg/mL did not show satisfactory results. About 50% of cell reduction was calculated by percentage viability assay at 400 µg/mL. The nontumor HEK293T cells showed normal morphology at all concentrations and did not show any sign of toxicity. Cisplatin (positive control) applied on healthy as well as cancer cells was observed with 45% and 42% of cell viability, respectively.

4. Discussion

Modern technologies have underlined bioactive compounds and their importance in the world of drug discovery. A strong affiliation between flavonoids and anticancer activity has been reported in many studies [17]. Numerous active drugs are the byproduct of natural sources and are designed by the summation of synthetic polymers to overcome the burden of diseases [18]. Earlier researchers have demon-

strated the phytochemical composition, antiproliferative, and antimicrobial potential of various *Caladium* species. Numerous studies have reported the antiangiogenic activity of methanolic extract of *C. bicolor* by inhibiting vascular endothelial growth factor (VEGF) signaling, a glycoprotein that promotes angiogenesis and vascular permeability. By this means, certain properties displayed are observed for the reduction of cancer growth and metastasis [19]. In Brazil, *C. lindenii* was used for the treatment of stingray wounds and other pathogenic infections. There is no pharmacological or phytochemical research has been reported on *C. lindenii*¹².

Cell-based assays are used to determine the effect of compounds on cell growth or to monitor cytotoxic effects that ultimately lead to cell death. Despite prevailing circumstances of the cell-based assay, it is much more important to understand the remaining population of cells at the end of the reaction. MTT assay is the simplest and most effective

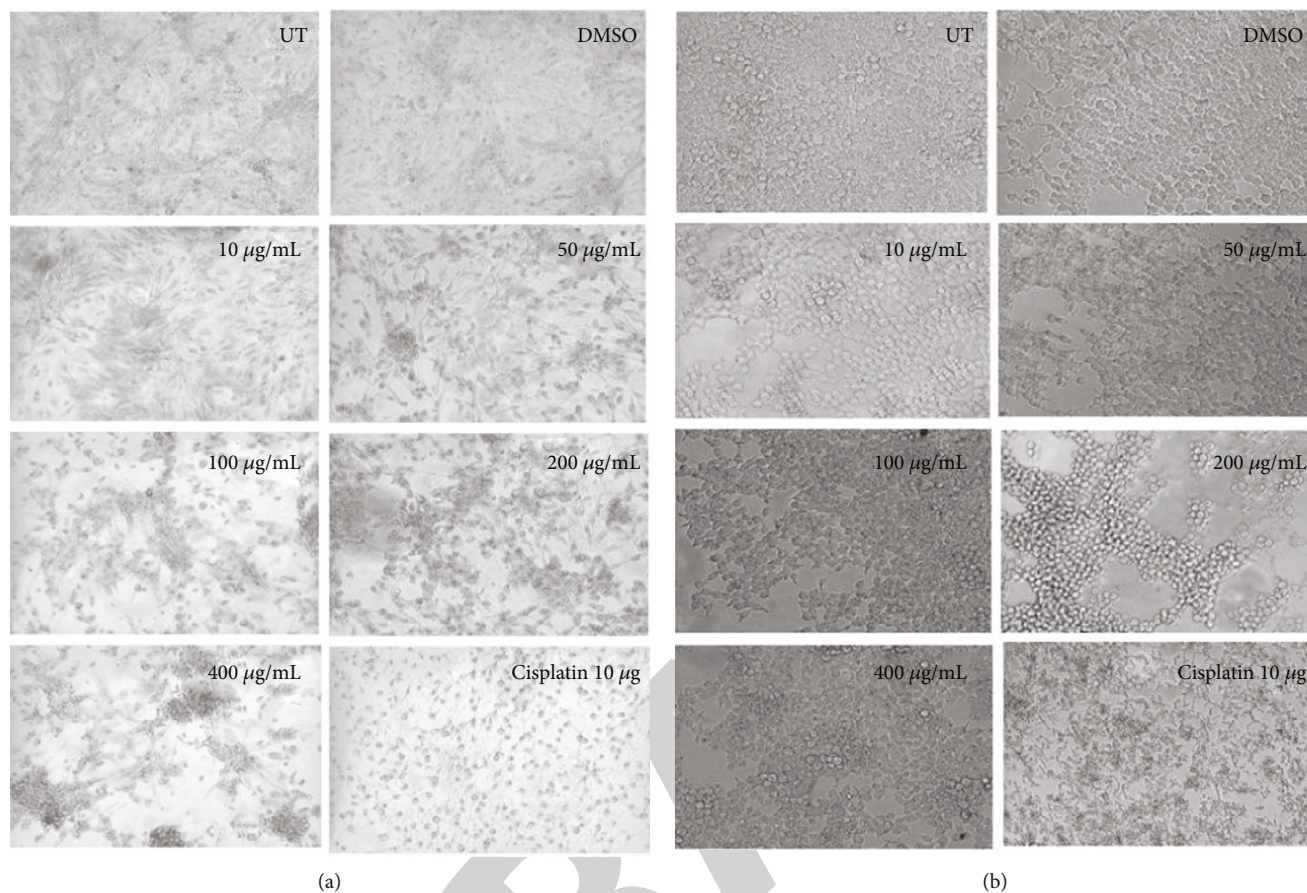


FIGURE 4: The morphological features showed the effect of hexane extract of *C. lindenii* on both HepG2 and HEK293T cells. (a) *In vitro* treatment of hexane extract on HepG2 cells demonstrated mild alteration in cell morphology at all concentrations except the higher (200 and 400 $\mu\text{g/mL}$) concentrations. The lower concentrations 10, 50, and 100 $\mu\text{g/mL}$ did not show satisfactory results. Cells treated with high concentrations became degraded and shrunken. 50% of cell reduction was calculated by percentage viability assay at 400 $\mu\text{g/mL}$. (b) The nontumor HEK293T cells showed normal morphology at all concentrations and did not reveal any sign of toxicity in comparison with UT and DMSO (negative control). Cisplatin (10 $\mu\text{g/mL}$) was the positive control applied on healthy (HEK293T) as well as cancer (HepG2) cells showed 45% and 42% of cell viability, respectively.

method developed by Mosmann for quantifying *in vitro* chemo-sensitivity of applied drugs on human cancer cell lines. The principle of MTT assay is determined by the tetrazolium salt reduced into formazan crystals by the action of mitochondrial dehydrogenase enzyme that assists this function in living cells [20]. In this study, both extracts showed remarkably significant antiproliferative effects on the HepG2 cancer cell line, however, any sign of toxicity has not been observed in HEK293T cells. Calculated IC₅₀ values for ethanolic and hexane extracts were assessed by MTT assay using different concentrations, i.e., 10, 50, 100, 200, and 400 $\mu\text{g/mL}$ showed that the ethanolic concentrations have high antiproliferative activity against HepG2 cells with IC₅₀ = 31 $\mu\text{g/mL}$, while HEK293T cells exhibited minimal cytotoxicity even at the highest concentration with IC₅₀ = 241 $\mu\text{g/mL}$. Hexane extract showed less cytotoxic effects on HepG2 (IC₅₀ = 150 $\mu\text{g/mL}$) and statistically insignificant effects were found on normal human embryonic kidney cells with calculated IC₅₀ = 550 $\mu\text{g/mL}$ (Figure 1). The present study also demonstrated the sensitivity of liver cancer (HepG2) and normal (HEK293T) cells against an apoptosis-inducing agent (cis-

platin). Cisplatin is an inorganic compound used for the treatment of various malignancies including gastric, bladder, and prostate cancer by inhibiting the DNA replication and transcription events. The severe side effects of cisplatin as an anticancer drug also triggered drug resistance and the termination of normal cell proliferation by damaging DNA [21]. However, the potential organic extracts were more effective against HepG2 cells as compared to HEK293T cells with favorable IC₅₀ values. In this study, cisplatin showed an anticancer effect on HepG2 and an adverse effect on the normal morphology of HEK293T cells when compared with UT (untreated) and DMSO (negative control) (Figures 2, 4). Cancer cells are categorized and recognized from normal cells due to their high proliferative and colony-forming potential. Drug discovery involves a complex mechanism that demands the assessment of the cell viability of living cells on cultured cancer and normal cells. Crystal violet is the simple method to calculate the sustained cells with crystal violet staining dye that binds to DNA and proteins. During the assay, the dead cells were detached from the surface and vanished from the cell population. This practice

TABLE 2: Crystal violet assay results.

Cell lines	Solvents	UT	DMSO	Absorbance (at 570 nm) mean \pm SD					
				10 μ g/mL	50 μ g/mL	100 μ g/mL	200 μ g/mL	400 μ g/mL	Cisplatin 10 μ g/mL
HepG2	Ethanol	0.0647 \pm 0.00062	0.0613 \pm 0.00055	0.0518 \pm 0.0013	0.0403 \pm 0.0029	0.0304 \pm 0.00043	0.0217 \pm 0.00078	0.0127 \pm 0.0011	0.0333 \pm 0.00179
	Hexane	0.0659 \pm 0.0021	0.0652 \pm 0.00198	0.0554 \pm 0.00671	0.0522 \pm 0.000141	0.0450 \pm 0.00091	0.0382 \pm 0.00021	0.0320 \pm 0.0044	0.0321 \pm 0.00023
HEK293T	Ethanol	1.8457 \pm 0.0128	1.8362 \pm 0.00513	1.7355 \pm 0.01655	1.5355 \pm 0.01022	1.4368 \pm 0.00804	1.2061 \pm 0.05218	0.9512 \pm 0.00438	0.6628 \pm 0.02832
	Hexane	1.9427 \pm 0.01682	1.8898 \pm 0.05844	1.8996 \pm 0.06039	1.7944 \pm 0.05833	1.6735 \pm 0.05427	1.4245 \pm 0.02889	1.1615 \pm 0.01011	0.8154 \pm 0.1153

describes a standard outline for the analysis of plant extracts on cell survival and growth inhibition [22]. In this study, cell viability was calculated using crystal violet staining of HepG2 and HEK293T cells as described in Figure 3 and Table 2 as mean \pm SD. The cell population was measured for two cell lines by obtaining optical densities and plotting a curve and slope. It has been observed that drug response is directly proportional to cell density in a time-dependent manner. The decreased percentage signifies strong cytotoxicity of plant extracts against hepatocellular carcinoma, whereas an increased value showed less effect on dose concentration. The percentage viability of ethanolic concentrations (10, 50, 100, 200, and 400 $\mu\text{g}/\text{mL}$) decreases with the increase in dose. The higher concentrations of 200 and 400 $\mu\text{g}/\text{mL}$ showed reduced percentage viability on calculation. While evaluating hexane extract, the cell viability displayed more viable cells indicating less cytotoxicity on HepG2 cells, otherwise, HEK293T cells showed increased cell viability with minimal or no effects. The microscopic assessment revealed a clear dose-dependent decrease in cell density and altered morphology of HepG2 cells with ethanolic and *n*-hexane extract concentrations.

5. Conclusion

The crude organic extracts of *C. lindenii* showed remarkable cytotoxicity against the HepG2 cell line by inducing apoptosis and significantly reducing viability percentage and transforming morphology in a dose-dependent manner. The activity exhibited by ethanolic extract showed the most favorable results for HepG2 cells as compared to hexane extract. However, these extracts show minimal or no effects on the healthy HEK293 cell line. These findings justify the antiproliferative activity of *C. lindenii* that may be used for the specific treatment of cancer after further validations.

Data Availability

All datasets used and analyzed during the current study are available from the corresponding author on reasonable request.

Ethical Approval

This work does not contain any studies on animals or threatened species performed by any of the authors.

Conflicts of Interest

The authors declare no competing interests.

Authors' Contributions

A.K and A.A conceptualize and design the project, analyze the in-vitro experiments, and draft the manuscript. M.A supervise and facilitate in conducting of the research. M.M.A was responsible for data analysis, manuscript proof-reading, and financial contribution. S.A was responsible for data analysis and review of the manuscript. H.S conceptualize and supervise the research project. M.S review the man-

uscript and facilitate the research. A.I.A was responsible for data analysis and results interpretation. T.M facilitates in conducting the research. All authors agreed and approved the final manuscript.

Acknowledgments

This research work was supported by the Institute of Molecular Biology and Biotechnology (IMBB/CRiMM), the University of Lahore, Lahore, Pakistan.

References

- [1] P. Garcia-Oliveira, P. Otero, A. G. Pereira et al., "Status and challenges of plant-anticancer compounds in cancer treatment," *Pharmaceuticals*, vol. 14, no. 2, p. 157, 2021.
- [2] H. Sung, J. Ferlay, R. L. Siegel et al., "Global cancer statistics 2020: GLOBOCAN estimates of incidence and mortality worldwide for 36 cancers in 185 countries," *CA: a Cancer Journal for Clinicians*, vol. 71, no. 3, pp. 209–249, 2021.
- [3] M. A. Emam, H. I. Khattab, and M. G. Hegazy, "Assessment of anticancer activity of *Pulicaria undulata* on hepatocellular carcinoma HepG2 cell line," *Tumor Biology*, vol. 41, no. 10, p. 101042831988008, 2019.
- [4] P. Mirabelli, L. Coppola, and M. Salvatore, "Cancer cell lines are useful model systems for medical research," *Cancers*, vol. 11, no. 8, p. 1098, 2019.
- [5] I. Dagogo-Jack and A. T. Shaw, "Tumour heterogeneity and resistance to cancer therapies," *Nature Reviews Clinical Oncology*, vol. 15, no. 2, pp. 81–94, 2018.
- [6] N. F. Santos-Sánchez, R. Salas-Coronado, B. Hernández-Carlos, and C. Villanueva-Cañongo, "Shikimic acid pathway in biosynthesis of phenolic compounds," *Plant physiological aspects of phenolic compounds*, vol. 1, pp. 1–5, 2019.
- [7] T. Pinto, A. Aires, F. Cosme et al., "Bioactive (poly) phenols, volatile compounds from vegetables, medicinal and aromatic plants," *Food*, vol. 10, no. 1, p. 106, 2021.
- [8] R. Bisht, A. Bhattacharyya, A. Shrivastava, and P. Saxena, "An overview of the medicinally important plant type III PKS derived polyketides," *Frontiers in Plant Science*, vol. 12, p. 2155, 2021.
- [9] D. J. Newman and G. M. Cragg, "Natural products as sources of new drugs from 1981 to 2014," *Journal of Natural Products*, vol. 79, no. 3, pp. 629–661, 2016.
- [10] A. Roy and N. Bharadwaja, "Medicinal plants in the management of cancer: a review," *Int J Complement Alt Med.*, vol. 9, article 00291, 2017.
- [11] F. I. Uche, D. Onuchukwu, C. N. E. Ibezim, and H. I. Ogbu, "Methanolic extract of *Caladium bicolor* leaves against selected clinical isolates," *GSC biol. pharm. sci.*, vol. 6, no. 2, pp. 098–107, 2019.
- [12] D. Zhang, K. Arunachalam, Y. Wang et al., "Evaluation on antidiabetic properties of medicinal plants from Myanmar," *Scientific World Journal*, vol. 2021, pp. 1–10, 2021.
- [13] J. W. Mukavi, P. W. Mayeku, J. M. Nyaga, and S. N. Kituyi, "In vitro anti-cancer efficacy and phyto-chemical screening of solvent extracts of *Kigelia africana* (Lam.) Benth," *Heliyon*, vol. 6, no. 7, article e04481, 2020.
- [14] N. P. Masuku and S. L. Lebelo, "Investigation of the effects of *Kigelia africana* (Lam.) Benth. Extracts on TM3 Leydig cells,"

Retraction

Retracted: Genomic and Therapeutic Analyses of *Staphylococcus aureus* Isolated from Cattle Reproductive Tract

BioMed Research International

Received 8 January 2024; Accepted 8 January 2024; Published 9 January 2024

Copyright © 2024 BioMed Research International. This is an open access article distributed under the Creative Commons Attribution License, which permits unrestricted use, distribution, and reproduction in any medium, provided the original work is properly cited.

This article has been retracted by Hindawi, as publisher, following an investigation undertaken by the publisher [1]. This investigation has uncovered evidence of systematic manipulation of the publication and peer-review process. We cannot, therefore, vouch for the reliability or integrity of this article.

Please note that this notice is intended solely to alert readers that the peer-review process of this article has been compromised.

Wiley and Hindawi regret that the usual quality checks did not identify these issues before publication and have since put additional measures in place to safeguard research integrity.

We wish to credit our Research Integrity and Research Publishing teams and anonymous and named external researchers and research integrity experts for contributing to this investigation.

The corresponding author, as the representative of all authors, has been given the opportunity to register their agreement or disagreement to this retraction. We have kept a record of any response received.

References

- [1] L. Shafique, A. I. Aqib, Q. Liang et al., “Genomic and Therapeutic Analyses of *Staphylococcus aureus* Isolated from Cattle Reproductive Tract,” *BioMed Research International*, vol. 2022, Article ID 6240711, 14 pages, 2022.

Research Article

Genomic and Therapeutic Analyses of *Staphylococcus aureus* Isolated from Cattle Reproductive Tract

Laiba Shafique ^{1,2}, **Amjad Islam Aqib** ³, **Qin Liang** ⁴, **Chaobin Qin** ²,
Muhammad Muddassir Ali ⁵, **Memoona Adil** ⁵, **Zaeem Sarwar** ⁶, **Arslan Saleem** ⁷,
Muhammad Ajmal ⁸, **Alveena Khan** ⁹, **Hongping Pan** ², **Kuiqing Cui** ^{1,2},
and **Qingyou Liu** ^{1,2}

¹Guangdong Provincial Key Laboratory of Animal Molecular Design and Precise Breeding School of Life Science and Engineering, Foshan University, Foshan 528225, China

²State Key Laboratory for Conservation and Utilization of Subtropical Agro-Bioresources, Guangxi University, Nanning, Guangxi 530005, China

³Department of Medicine, Cholistan University of Veterinary and Animal Sciences, Bahawalpur 63100, Pakistan

⁴Jinan City Zhangqiu District Animal Husbandry and Veterinary Development Center, China

⁵Institute of Biochemistry and Biotechnology, University of Veterinary and Animal Sciences, Lahore 54000, Pakistan

⁶Department of Theriogenology, Cholistan University of Veterinary and Animal Sciences, Bahawalpur-63100, Pakistan

⁷Department of Aerospace and Geodesy, Technical University of Munich, Arcisstra. 21, 80333 Munich, Germany

⁸Department of Veterinary Medicine, Sindh Agriculture University, Tandojam 70060, Pakistan

⁹Allama Iqbal Medical College Lahore (University of Health Sciences), 54770, Pakistan

Correspondence should be addressed to Kuiqing Cui; 923000612@qq.com and Qingyou Liu; qyliu-gene@fosu.edu.cn

Laiba Shafique and Amjad Islam Aqib contributed equally to this work.

Received 29 April 2022; Accepted 9 August 2022; Published 13 September 2022

Academic Editor: Faheem Ahmed Khan

Copyright © 2022 Laiba Shafique et al. This is an open access article distributed under the Creative Commons Attribution License, which permits unrestricted use, distribution, and reproduction in any medium, provided the original work is properly cited.

Staphylococcus aureus is emerging as a ubiquitous multidrug-resistant pathogen circulating among animals, humans, and their environment. The current study focused on molecular epidemiology and evidence-based treatment against *S. aureus* from bovine endometritis. For this study, $n = 304$ cattle were screened for endometritis using ultrasonography while presenting case history, and clinical signs were also considered. *S. aureus* was isolated from endometritis-positive uterine samples which were further put to molecular identification, phylogenetic analysis, susceptibility to antibiotics, and testing of novel drug combinations in both *in vitro* and field trials. The findings of the study revealed 78.20% of bovine endometritis samples positive for *S. aureus*, while *nuc* gene-based genotyping of *S. aureus* thermal nuclease (SA-1, SA-2, and SA-3) showed close relatedness with *S. aureus* thermal nuclease of *Bos taurus*. Drug combinations showed 5.00 to 188.88% rise in zones of inhibitions (ZOI) for drugs used in combination compared to the drugs used alone. Gentamicin in combination with amoxicillin and enrofloxacin with metronidazol showed synergistic interactions in an *in vitro* trial. Co-amoxiclav with gentamicin, gentamicin with enrofloxacin, and metronidazole with enrofloxacin showed 100%, 80%, and 60% efficacy in treating clinical cases in field trials, respectively. As a result, the study came to the conclusion the higher prevalence of endometritis-based *S. aureus*, genetic host shifts, narrow options for single drugs, and need for novel drug combinations to treat clinical cases.

1. Introduction

Endometritis is among the leading causes of morbidity in animals thus significantly compromising the farm economy [1, 2]. Reproductive manipulations around parturition are the principal source of bacterial invasions, resulting in severe uterine infections associated with huge economic losses compromising herd health and production [1]. Economic losses in terms of decreased reproductive efficiency, treatment costs, premature culling, increased services per conception, and pathogen transmission risks proclaim endometritis as one of the prime challenges in the dairy industry [2, 3]. Inflammatory expressions of the endometrium depict the fate of animals, as compromised fertility leads to premature culling [4]. *S. aureus* transfers at an animal-human-environment interface, thus making it a major threat to optimum reproductive efficiency in farm animals too [5–7]. Authentic diagnosis of various strains demands genome analyses because conventional microbiological methods are no longer enough [8]. It is noted that among several major challenges to the dairy farming industry is the drug resistance which presents itself as an invariably significant risk factor [9]. Resistance to commonly used antibiotics in animal-originated *S. aureus* isolates poses a threat to global public health [3, 10]. These strains commonly colonize mucosal surfaces and sustain their colonies by producing biofilm [7]. Drug resistance, localization in epithelium, longer attachment duration, bypassing immunity, and enhancement of pathogenesis make *S. aureus* a specific pathogen [11–13]. Some strains are also emerging as multi-drug-resistant, even depicting reduced susceptibility to vancomycin [14]. MRSA is a salient contagious pathogen which is equally found in humans and animals [15]. According to the literature, the prevalence of MRSA varies from 0.4 percent in Hungary to 47.6 percent in China [16, 17].

To ensure optimum reproductive performance, it is necessary to combat *S. aureus*-based endometritis in dairy animals. Non-judicious exposure to antibiotics results in the development of resistance to pathogens. Certain antibiotics can act as antimicrobial signaling molecules, homeostatic modulators, and induce the transcription of virulent genes at sublethal levels [18]. Subminimal inhibitory concentration (sub-MIC) of drugs is unable to kill resistant bacteria but leads to modification of chemical and physical characteristics of the cell surface, adhesion mechanisms, and expressions of some of the virulent genes leading to biofilm formation, toxin production, motility, and 68 hydrophobicity [19, 20]. Approaches such as double antibiotic combination therapy has been suggested for the treatment of resistant *S. aureus* strains [21, 22]. Moreover, more efficacious antimicrobials are being sought to reduce the use of unnecessary medication. Thus, the hypothesis of the study reads “*Staphylococcus aureus* endometritis is prevalent in dairy animals, host shifts exist, and novel antibiotic combinations are effective against multidrug-resistant *S. aureus* isolates.”

2. Materials and Methods

2.1. Ethics Statement. This study was approved by the Experimental Animal Care and Use Committee of Guangxi University (No. GXU-2021-128 and dated 30-6-2020).

2.2. Tracking Endometritis Cases from Bovines. The study was conducted in selected dairy farms of the district of Khanewal, Punjab, Pakistan (Figure 1). District Khanewal is located at 71°55'0" E and 30°18'0" N with an altitude of 128 meters and a human population of 2.922 million. Clinical reproductive complaints were defined as any kind of reproductive problem, e.g., repeat breeding, abortion, misconceptions, and signs associated with these issues. The inclusion criteria for the current study were commercial dairy farms having ≥ 50 lactating cattle/farm, farm accessibility, reproductive complaints, and ultrasonographic findings. Supplementary information included calving history, milk yield/day, days in milk, parity, feeding regime, and treatment approach. Random sampling was done to check for endometritis in $n = 304$ cattle using ultrasonography (7.5 MHz with probe linear array transrectal; B mode) [23]. Endometritis was defined as a swollen lumen partly filled with snowy echogenic patches and black nonechogenic fluid [24, 25]. It was found that if all rays were reflected after striking any structure, the area looked whitish [26]. Clinical identification of animals having endometritis through ultrasonography is represented in Figure 2.

Aseptically, the uterine flushing was done by an artificial insemination gun whereas the fluid was taken out and stored by a syringe. The samples were shifted to the laboratory (central diagnostic laboratory) of CUVAS, Bahawalpur, Pakistan, in a container having 4°C temperature.

2.3. Isolation of Pathogenic *S. aureus*. The samples were put to incubation in sterile nutrient broth overnight at 37°C to retrieve the maximum yield of those bacteria which were present in a low quantity. The incubated nutrient broth was centrifuged, and the sediments were put to blood agar for the same incubation [27]. The colonies obtained were further put on Mannitol salt agar with the same incubation and preceded further to several biochemical tests as per set protocols [28].

2.4. Molecular Identification of Pathogenic *S. aureus*. Isolates biochemically characterized were further put to genomic analysis. PCR amplification was done with *Nuc* gene (Figure 3). Primers were formulated using Primer-BLAST (<https://www.ncbi.nlm.nih.gov/tools/primer-blast/>) software (Nuc forward 5'AAGGGCAATACGCAAAGAG3' and Nuc reverse 5'AAACATAAGCAACTTTAGCCAAG3') (figure reaction mixture consists of PCR 2X master mix = 10 μ L (Thermo Scientific Catalog #K0171), forward primer = 1 μ L (10 pmoL), reverse primer = 1 μ L (10 pmoL), DNA = 2 μ L (50 ng/L), deionized water = 6 μ L, and reaction volume = 20 μ L). The detailed protocol has been described in Aziz et al. [7].

2.5. Sequence Analysis of the Local *S. aureus* Isolate. A phylogenetic analysis of nucleotides was carried out with MEGA X software. Highly similar sequences acquired via Primer-BLAST were combined in a phylogenetic analysis of nucleotides of the *Nuc* gene in *S. aureus*. The phylogenetic tree was made to find lengths of branches in similar units like those of the evolutionary distances utilized to conclude the

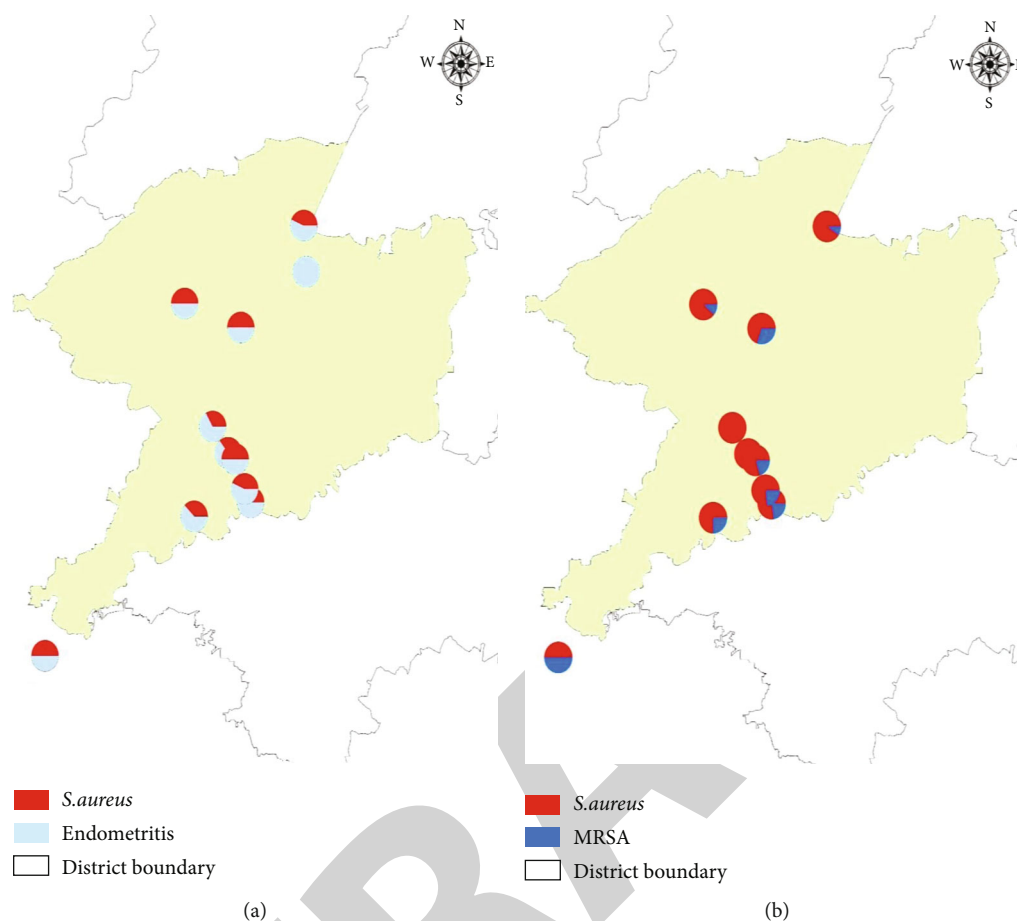


FIGURE 1: Tracking burden of (a) *S. aureus* from endometritis and (b) MRSA from different dairy farms (each circle is showing one dairy farm). In the second map (b) there are 9 farms as one farm in the first map (a) did not show *S. aureus*.

phylogenetic tree. Further, the maximum composite likelihood method was applied to find distances in the evolutionary tree, and the similar was calculated in unit numbers of substitutions of base pairs at each site. The rest of the protocol was done the same as described in the author's previous study (doi:10.3390/antibiotics10080997). Moreover, motifs were found through the MEME (Multiple EM for Motif Elicitation) Suite and STRING was used to find the protein-protein interaction.

2.6. Confirmation of Pathogenic Nature of *Staphylococcus aureus*. Using the cefoxitin disc diffusion assay [29], methicillin resistance in *S. aureus* was determined as per standards provided in clinical and laboratory standard institute [30]. Antibiotic discs were placed on Mueller Hinton agar on which *S. aureus* was already swabbed. Plates were incubated for 24 hours while zones of inhibition were measured and compared as per guidelines of the clinical and laboratory standard institute [30].

2.7. Molecular Confirmation of Methicillin-Resistant *Staphylococcus aureus*. The molecular confirmation of methicillin resistant *S. aureus* was done by targeting the *mecA* gene. DNA extraction was done by WizPrep™ gDNA Mini extraction kit. Amplification was done utiliz-

ing *mecA* forward P1: 59-TGGCATTTCGTGTCACA ATCG-39 and reverse primers P2: 59-CTGGAAGTTGT TGAGCAGAG-3' with amplified product size 310 bp as described by Shoaib et al. [31]. Further specification of PCR was followed by previously established protocol for identification of MRSA by targeting *mecA* in *S. aureus*. Bands examined at a 310 bp level were taken into consideration as positive (Figure 4).

2.8. Assessment of Antibiotic Resistance Profile of Methicillin-Resistant *Staphylococcus aureus*. Using the disc diffusion method, commonly used antibiotics were tested against drug-resistant *S. aureus* isolates according to the guidelines of clinical and laboratory standard institute [30]. The antibiotics tested were enrofloxacin (10 µg), gentamicin (10 µg), linezolid (30 µg), vancomycin (30 µg), trimethoprim-sulphamethoxazole (25 µg), fusidic acid (10 µg), ciprofloxacin (5 µg), chloramphenicol (30 µg), and levofloxacin (5 µg). Antibiotics were aseptically placed on Mueller Hinton agar having swabbed with *S. aureus* and put to incubation for 24 hours at 37°C. The zone of inhibition of each antibiotic was measured and compared as per guidelines of the clinical laboratory and standard institute [30].

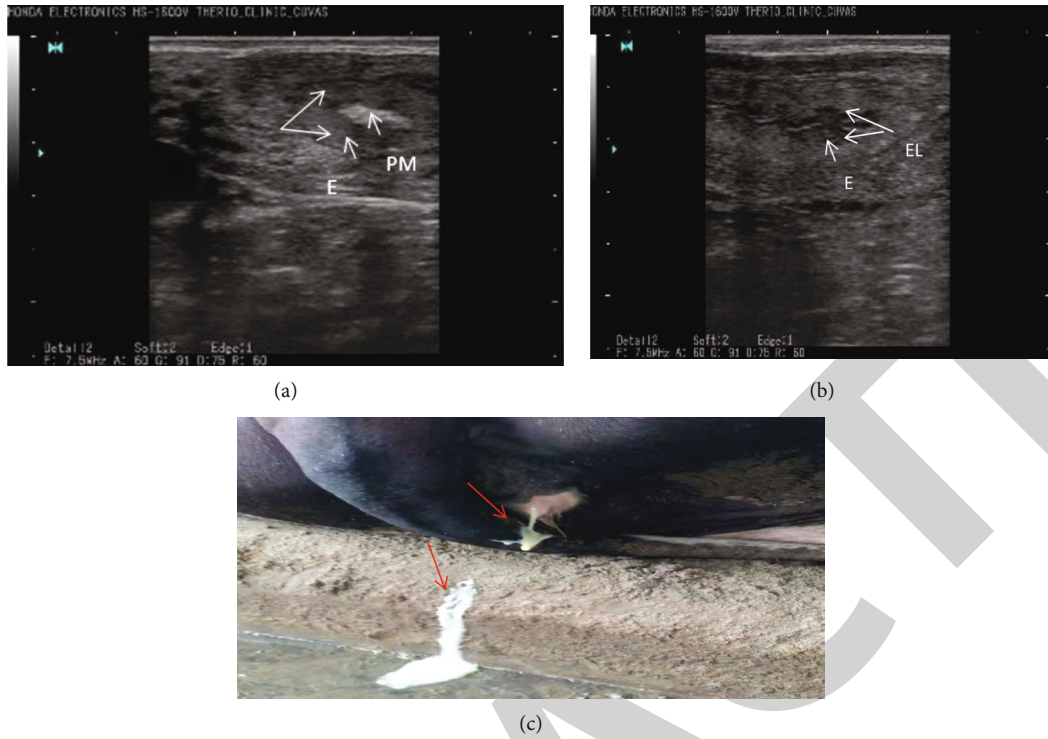


FIGURE 2: Clinical identification of animals having endometritis through (a, b) ultrasonography and (c) abnormal secretions. (a) EL=endometrial lining; E=endometritis in the form of swelling of the lining; PM=pus material; (b) EL=endometrial lining; E=endometritis in the form of an inflamed wall; (c) red arrows point out pus material from uterine material.

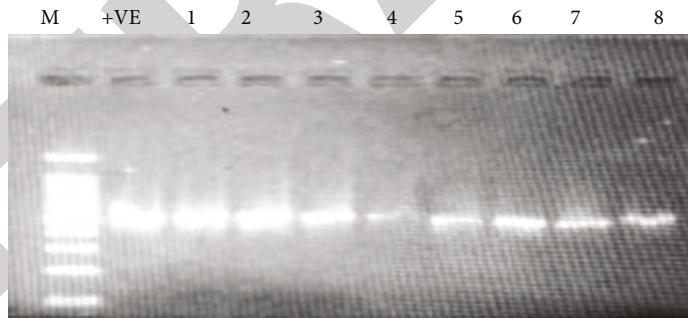


FIGURE 3: Molecular identification of *S. aureus*. M = marker 1000 bp; +VE = positive control wells 1-8 samples.

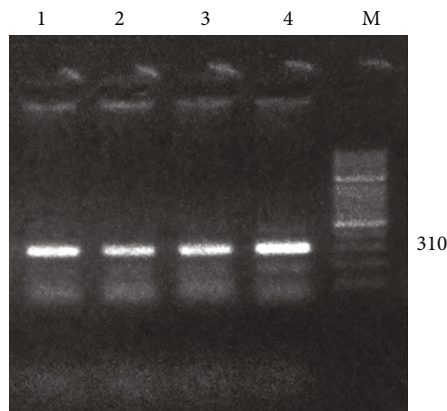


FIGURE 4: Molecular identification of methicillin-resistant *S. aureus*. M = marker leader 1000 bp, 1-9 wells were samples at 310 bp; positive control = +ve; negative control = -ve.

TABLE 1: The prevalence of *Staphylococcus aureus* and methicillin-resistant *Staphylococcus aureus*.

Farm name	No. of animals screened (A)	Prevalence of endometritis			S. aureus positive (C)	S. aureus (%)		MRSA (%)		
		Endometritis positive (B)	Prevalence (B/A × 100)	Confidence interval -95%		S. aureus% (C/B × 100)	Confidence interval -95%	MRSA positive (D)	MRSA (D/C × 100)	Confidence interval -95%
(A)	27	9	33.33	18.64-52.17	5	55.55	26.67-81.13	2	40	11.76-76.93
(B)	27	8	29.63	15.85-48.48	8	100	67.56-100	1	12.5	2.24-47.09
(C)	18	8	44.44	24.56-66.28	4	50	21.52-78.48	0	0	—
(D)	34	14	41.18	26.37-57.78	14	100	78.47-100	6	42.86	21.38-67.41
(E)	54	26	48.15	35.4-61.15	24	92.31	75.86-97.87	7	29.17	14.92-49.17
(F)	12	5	41.67	19.33-68.05	3	60	23.07-88.24	1	33.33	6.15-79.23
(G)	28	13	46.43	29.53-64.19	10	76.92	49.74-91.82	1	10	1.79-40.41
(H)	48	26	54.17	40.29-67.43	20	76.92	57.95-88.96	6	30	14.55-5.19
(I)	38	16	42.10	27.86-57.81	16	100	80.64-100	4	25	10.98-4.15
(J)	18	8	44.44	24.56-66.28	0	0	0.00-32.44	0	0	—
Total	304	133	43.75		104	78.20		28	26.92	

TABLE 2: Risk factors associated with methicillin-resistant *S. aureus* isolated from bovine endometritis.

Parameter	Categories	Total	Positive	% age	p value
Calving history	Dystocia	81	18	22.22	0.879
	Abortion	4	1	25	
	Eutocia	48	9	18.75	
Milk yield/day	10-20	38	8	21.05	0.956
	21-30	56	12	21.42	
	31-40	26	6	23.07	
	41-50	13	2	15.38	
Days in milk	1-100	86	19	22.09	0.919
	101-200	32	6	18.75	
	201-300	15	3	20	
Parity	1-3	76	21	27.63	0.032
	4-6	57	7	12.28	
Feeding regime	Silage+concentrate	43	10	23.25	0.832
	Silage+hay+concentrate	56	12	21.42	
	Silage+concentrate+fresh fodder	34	6	17.64	
Treatment approach	Single antibiotic	85	18	21.17	0.835
	Combination	48	10	20.83	

2.9. Synergy Testing of Novel Drug Combinations against MRSA. To validate the synergism of novel drug combinations, various drug combinations were tested using the agar and broth dilution methods [32]. To conduct well diffusion assay, 6-8 mm diameter wells were made through good borer on Mueller Hinton which was later swabbed with activated growth of bacteria [32]. To evaluate the antibacterial potential of the antibiotics, following drugs were used alone and in combination against *S. aureus*: amoxicillin, oxytetracycline, gentamicin, streptomycin, metronidazole, enrofloxacin, and co-amoxiclav. Zones formed around antibiotics were measured post-incubation. The checkerboard method was applied to find synergism

between different combinations of drugs using broth microdilution protocol. An activated growth of *S. aureus* adjusted at $1 - 1.5 \times 10^5$ CFU/mL was used in this trial. Optical density was calculated at 570 nm following incubation at 37°C/24 hours. Fractional inhibitory concentration indices (FICI) were calculated as per the following formula. Experiment was executed in triplicate [32].

$$\text{Fractional inhibitory concentration index} = \text{FIC product A} + \text{FIC product B},$$

$$\text{FIC of Product B} = \frac{\text{MIC of Product B in combination with Product A}}{\text{MIC of Product B alone}}, \quad (1)$$

$$\text{FIC of Product A} = \frac{\text{MIC of Product A in combination with Product B}}{\text{MIC of Product A alone}}.$$

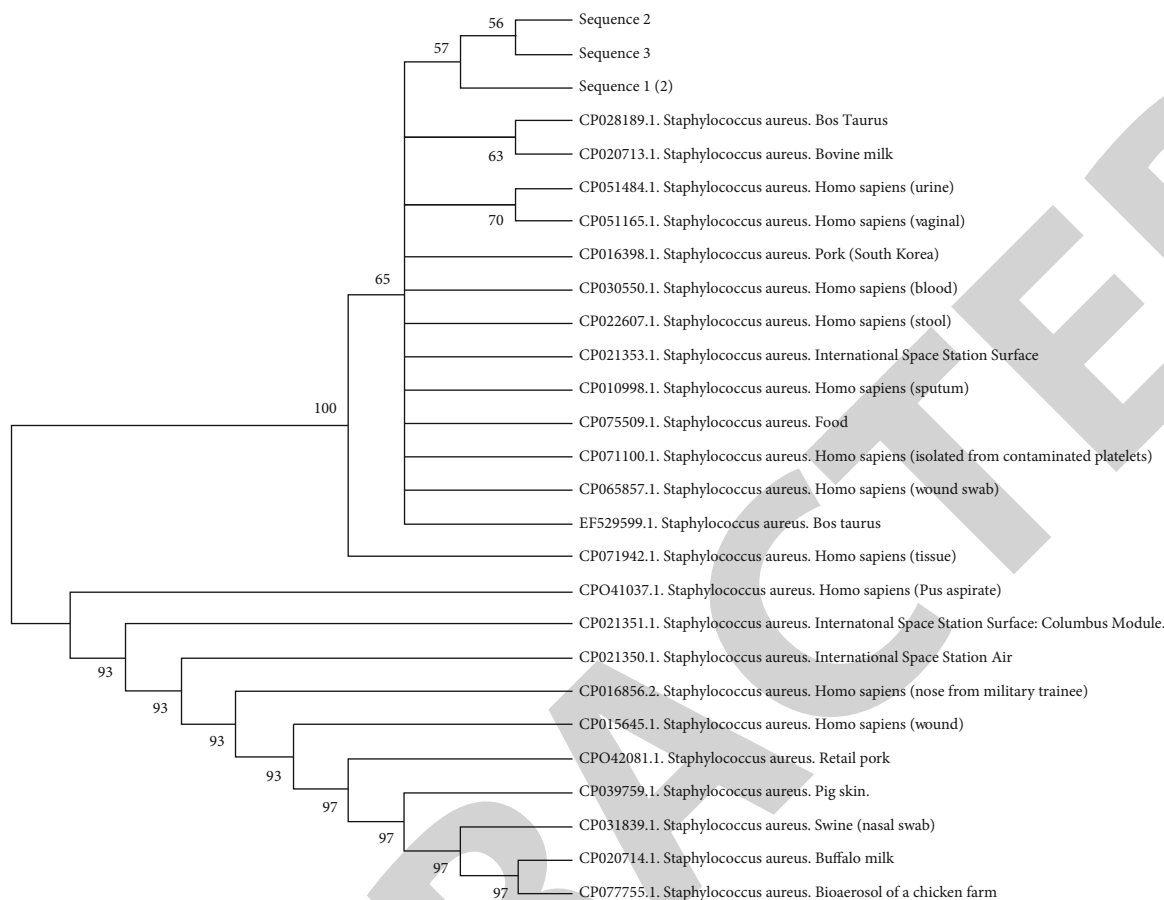


FIGURE 5: Phylogenetic tree of *S. aureus* Nuc gene (nucleotide sequences). An analysis has been performed among different source samples of *S. aureus* Nuc gene from different countries with our isolated sequenced samples. The branch length (numbers) is representing the nucleotide substitutions per 100 nucleotide sites.

The fractional inhibitory concentration indices (FICI) ≤ 0.5 were considered as synergistic, FICI > 0.5 but ≤ 1.0 as additive, FICI > 1.0 but < 4.0 as indifferent, and FICI > 4.0 considered as antagonistic [33].

2.10. Field Trial to Treat Endometritis. Methicillin resistant *S. aureus* positive endometritis cases were included in a field trial of drugs. Drugs selected for the trials were gentamicin, oxytetracycline, co-amoxiclav, amoxicillin, streptomycin, metronidazole, and enrofloxacin. The dosage regimen and drug combinations were as follows (Supplementary Table 1). The rate of success was calculated using the following criteria: (i) ultrasonography determined normal uterine walls, (ii) absence of bacterial load from vaginal/uterine discharge, and/or (iii) successful conception [34, 35]. The first two points were considered necessary while the third was kept optional because there might be other reasons for no conception.

2.11. Statistical Analysis. A univariate analysis was applied to the prevalence and antibiotic susceptibility [23]. An increase of percentage (%) in inhibition zones as well as in fractional inhibitory indices was computed by using formulae described previously [32, 33]. Parametric tests (ANOVA and *t*-tests) were applied for quantitative data. Tukey test

was applied as post hoc test, a succession to ANOVA, to decide significant difference among groups at a 5% level of probability. SPSS version 22 of statistical computer software program was used for data analysis.

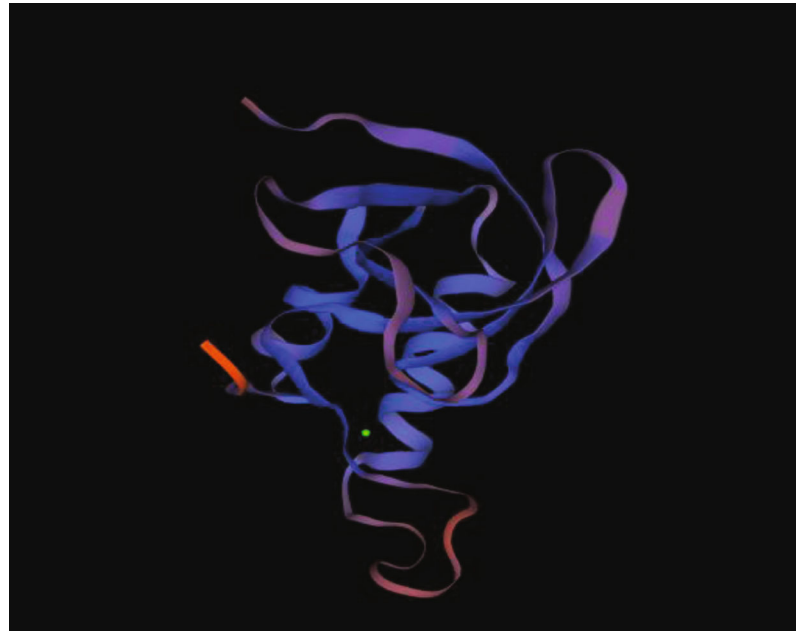
3. Results

3.1. Prevalence and Risk Factors Associated with *S. aureus*. The study showed 78.20% of endometritis samples positive for *S. aureus*, while 26.92% of these were MRSA (Table 1). Calving history, milk yield, days in milk, treatment approach, and feeding regimen were non-significant while parity showed significant ($p < 0.05$) association (Table 2).

3.2. Sequencing of *Staphylococcus aureus*

3.2.1. Nucleotide Output. Nucleic acid alignment revealed that reference sequence and local isolate *S. aureus* thermal nuclease (SA-1, SA-2, and SA-3) sequences were found 99.8% identical (Supplementary Figure 1).

3.2.2. Phylogenetic Analysis. According to constructed phylogenetic tree of *S. aureus* thermal nuclease, it was found that local isolate (SA-1, SA-2, and SA-3) gene sequence was closely linked to the *S. aureus* thermal nuclease of *Bos taurus* and from other bovine milk (Figure 5).



(a)

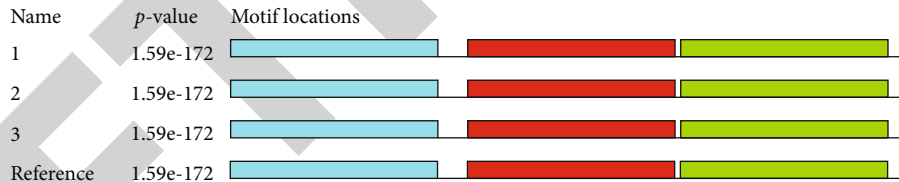
```

Reference  GQYAKRFFYFATSCVLVTLVVVSSLSSANASQTDNGVNRSGSEDPVYSATSTKLLHKE  60
1          GQYAKRFFYFATSCVLVTLVVVSSLSSANASQTDNGVNRSGSEDPVYSATSTKLLHKE  60
2          GQYAKRFFYFATSCVLVTLVVVSSLSSANASQTDNGVNRSGSEDPVYSATSTKLLHKE  60
3          GQYAKRFFYFATSCVLVTLVVVSSLSSANASQTDNGVNRSGSEDPVYSATSTKLLHKE  60
*****

Reference  PATLIKAIDGDTVKLMYKGQPMFRLLLVDTPETKHPKKGVEKYGPEASFTKKPMENAK  120
1          PATLIKAIDGDTVKLMYKGQPMFRLLLVDTPETKHPKKGVEKYGPEASFTKKPMENAK  120
2          PATLIKAIDGDTVKLMYKGQPMFRLLLVDTPETKHPKKGVEKYGPEASFTKKPMENAK  120
3          PATLIKAIDGDTVKLMYKGQPMFRLLLVDTPETKHPKKGVEKYGPEASFTKKPMENAK  120
*****

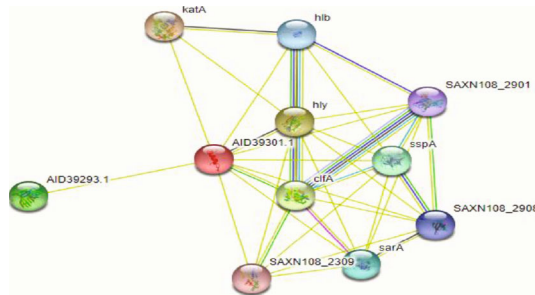
Reference  KIEVEFDKGQRTDKYGRGLAYIYADGKMVNEALVRQGLAKVAYV  164
1          KIEVEFDKGQRTDKYGRGLAYIYADGKMVNEALVRQGLAKVAYV  164
2          KIEVEFDKGQRTDKYGRGLAYIYADGKMVNEALVRQGLAKVAYV  164
3          KIEVEFDKGQRTDKYGRGLAYIYADGKMVNEALVRQGLAKVAYV  164
*****
    
```

(b)



Motif	Symbol	Motif consensus
1.		HKEPATLIKAIDGDTVKLMYKGQPMFRLLLVDTPETKHPKKGVEKYGPE
2.		GQYAKRFFYFATSCVLVTLVVVSSLSSANASQTDNGVNRSGSEDPVYS
3.		SAFTKKMVENAKKIEVEFDKGQRTDKYGRGLAYIYADGKMVNEALVRQGL

(c)



(d)

FIGURE 6: (a) Protein structure (exonic region) of *S. aureus*. (b) Alignment of *S. aureus* thermal nuclease protein (*S. aureus*-1, *S. aureus*-2, *S. aureus*-3, and reference sequence). (c) Protein motifs of *S. aureus*. (d) Protein-protein interaction of *S. aureus* protein (*S. aureus*-1 protein, *S. aureus*-2 protein, and *S. aureus*-3 protein).

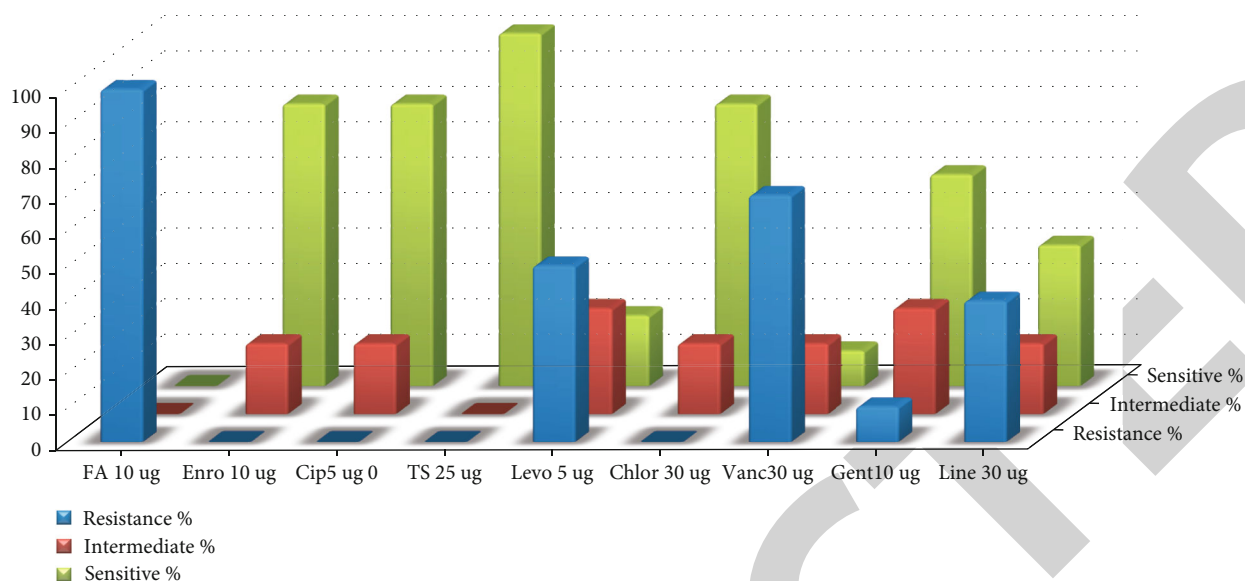


FIGURE 7: Antibiogram of *S. aureus* isolates. FA = fusidic acid; Enro = enrofloxacin; Cip = ciprofloxacin; TS = trimethoprim-sulphamethoxazole; Levo = levofloxacin; Chlor = chloramphenicol; Van = vancomycin; Gent = gentamicin; Line = linezolid.

3.2.3. Assessment of Motif and Structure of Gene. The nucleic acid motif of the reference sequence and all local isolates was found 1.13e-126. The differences in motifs were shown in different colors (Supplementary Figure 2). It was found that the coding region was only associated with nucleotide structure (Supplementary Figure 3). Protein motif of reference sequence and all local isolates was found 1.59e-172 (Figure 6(a)). Protein structure of reference protein and local isolate (SA-1, SA-2, and SA-3) proteins was found identical (Figure 6(b)). Protein motif p value of reference sequence and all local isolates was found (Figure 6(c)). Protein-protein interaction (Figure 6(d)) was noted in SA-1, SA-2, and SA-3 proteins. Conserved domain of the *Staphylococcal* nuclease was found in reference, Sample-1, Sample-2, and Sample-3 protein sequences (Supplementary Table 2).

3.3. Antibiogram against MRSA. An antibiogram of tested isolates showed trimethoprim-sulphamethoxazole and ciprofloxacin as highly effective antibiotics, while fusidic acid remained the least effective. The susceptibility profile of *S. aureus* against different antibiotics with “increasing number of resistant isolates” was observed as follows: trimethoprim-sulphamethoxazole > ciprofloxacin ≥ enrofloxacin ≥ chloramphenicol > gentamicin > levofloxacin > linezolid > vancomycin > fusidic acid (Figure 7). The antibacterial activity of different antibiotics represented by ZOI can be seen in Supplementary Figure 4(i).

3.4. In Vitro Drug Synergy Testing

3.4.1. Zone of Inhibition Expressed by Tested Drugs. The study revealed that metronidazole+gentamicin when compared with other drugs showed a significant difference ($p < 0.05$) of ZOIs (Table 3, Supplementary Figure 4ii). Drug combination analysis of well diffusion zones showed

that there was a maximum increase in inhibitory zone for the combination of oxytetracycline with streptomycin when compared to oxytetracycline alone. The highest combination of drugs favored oxytetracycline in that there was more than a 100% increase in its ZOIs when combined with other drugs. Amoxicillin and enrofloxacin gave greater percentage increase when combined with gentamicin and chloramphenicol, respectively.

3.4.2. Fractional Inhibitory Concentration Indices. The minimum inhibitory concentrations of all tested drugs varied significantly from each other. The lowest MIC was noted in the case of enrofloxacin which was followed by gentamicin, co-amoxiclav, amoxicillin, oxytetracycline, streptomycin, and metronidazole. Synergy testing of all the tested drug combinations against MRSA isolates showed synergistic behavior of amoxicillin+gentamicin and metronidazole +enrofloxacin, while antagonism was observed in oxytetracycline+amoxicillin and co-amoxiclav+oxytetracycline. An additive effect was found when amoxicillin was combined with enrofloxacin and streptomycin; co-amoxiclav with enrofloxacin and gentamicin; and enrofloxacin with gentamicin. All other remaining combinations remained indifferent (Table 4).

3.5. Field Trial Outcomes. The study noted the highest percentage recovery in case of co-amoxiclav+gentamicin, oxytetracycline alone, gentamicin+enrofloxacin, gentamicin alone, and metronidazole+enrofloxacin combinations presenting 100%, 100%, 80%, 80%, and 60% success rate, respectively. The uterine wall exhibiting normalization is shown in Figure 8. Amoxicillin+gentamicin, amoxicillin +streptomycin, and metronidazole+amoxicillin, on the other hand, showed success rates of 30%, 20%, and 10% against MRSA, respectively.

TABLE 3: Comparison of zones of inhibition against methicillin-resistant *Staphylococcus aureus* isolates using the well diffusion method for antimicrobial drugs alone and/or in combination.

Drugs	Patterns used (alone/combination)	Mean \pm Std. (mm)	% variation [(combination-alone)/(alone \times 100)]	p value
Co-amoxiclav	Alone	15 \pm 1.414		0.299
	C+E	12.5 \pm 4.949	-16.67	
	C+M	11.5 \pm 0.707	-23.33	
	C+G	10.5 \pm 2.121	-30	
	C+O	9.5 \pm 0.707	-36.67	
	C+A	10.5 \pm 2.121	-30	
	C+S	9.0 \pm 1.414	-40	
Enrofloxacin	Alone	6.0 \pm 0		0.082
	E+M	5.5 \pm 0.707	-8.33	
	E+G	4.5 \pm 0.707	-25	
	E+O	7.5 \pm 0.707	25	
	C+E	12.5 \pm 4.949	108.33	
	E+A	10.0 \pm 2.828	66.66	
	E+S	9.0 \pm 1.414	33.33	
Metronidazole	Alone	6.0 \pm 1.414		0.025
	M+G	8.5 \pm 0.707	41.67	
	M+O	8.5 \pm 0.707	41.67	
	C+M	11.5 \pm 0.707	91.67	
	E+M	5.5 \pm 0.707	-8.33	
	M+A	8.0 \pm 1.414	33.33	
	M+S	7.5 \pm 2.121	25	
Oxytetracycline	Alone	4.5 \pm 0.707		0.093
	C+O	9.5 \pm 0.707	111.11	
	M+O	8.5 \pm 0.707	88.89	
	E+O	7.5 \pm 0.707	66.67	
	G+O	9.5 \pm 0.707	111.11	
	O+A	10.5 \pm 3.535	133.33	
	O+S	13.0 \pm 4.242	188.88	
Gentamicin	Alone	10 \pm 2.828		0.034
	G+O	9.5 \pm 0.707	-5	
	C+G	10.5 \pm 2.121	5	
	E+G	4.5 \pm 0.707	-55	
	M+G	8.5 \pm 0.707	-15	
	G+A	16.0 \pm 2.828	60	
	G+S	13.0 \pm 4.242	30	
Amoxicillin	Alone	7.5 \pm 2.121		0.199
	A+S	13.5 \pm 4.949	80	
	C+A	10.52 \pm 2.12	40.27	
	M+A	8.0 \pm 1.414	6.67	
	O+A	10.5 \pm 3.535	40	
	E+A	10.0 \pm 2.828	33.33	
	G+A	16.0 \pm 2.828	113.33	

TABLE 3: Continued.

Drugs	Patterns used (alone/combination)	Mean \pm Std. (mm)	% variation [(combination-alone)/(alone \times 100)]	p value
Streptomycin	Alone	9.5 \pm 0.707		0.402
	A+S	13.5 \pm 4.949	42.10	
	C+S	9.0 \pm 1.414	-5.26	
	M+S	7.5 \pm 2.121	-21.05	
	O+S	13.0 \pm 4.242	36.84	
	E+S	9.0 \pm 1.414	-5.26	
	G+S	13.0 \pm 4.242	36.84	

M = metronidazole; O = oxytetracycline; A = amoxicillin; S = streptomycin; G = gentamicin; C = co-amoxiclav; E = enrofloxacin.

TABLE 4: Synergy testing of drugs against methicillin-resistant *Staphylococcus aureus*.

Combinations	MIC AB	MIC A	FIC A	MIC BA	MIC B	FIC B	FICI	Results
amoxi+co-amoxiclav	5.86	11.72	0.5	1.95	5.86	0.33	0.83	Additive
amoxi+metro	15.62	11.72	1.33	250	375	0.67	2	Indifferent
amoxi+enro	4.56	11.72	0.39	0.98	1.95	0.5	0.89	Additive
amoxi+strepto	3.91	11.72	0.33	7.81	15.62	0.5	0.83	Additive
amoxi+genta	2.93	11.72	0.25	0.98	3.91	0.25	0.5	Synergistic
amoxi+oxy	23.44	11.72	2	31.25	15.62	2	4	Antagonistic
co-amoxiclav+metro	4.56	5.86	0.78	125	375	0.33	1.11	Indifferent
co-amoxiclav+enro	2.93	5.86	0.5	0.49	1.95	0.25	0.75	Additive
co-amoxiclav+strepto	3.91	5.86	0.67	7.81	15.62	0.5	1.17	Indifferent
co-amoxiclav+genta	2.93	5.86	0.5	1.95	3.91	0.5	1	Additive
co-amoxiclav+oxy	15.62	5.86	2.67	62.5	15.62	4	6.67	Antagonistic
metro+enro	31.25	375	0.08	0.49	1.95	0.25	0.33	Synergistic
metro+strepto	125	375	0.33	15.62	15.62	1	1.33	Indifferent
metro+genta	187.5	375	0.5	1.95	3.91	0.5	1	Indifferent
metro+oxy	500	375	1.33	62.5	15.62	4	5.33	Antagonistic
enro+strepto	3.91	1.95	2	7.81	15.62	0.5	2.5	Indifferent
enro+genta	0.49	1.95	0.25	1.95	3.91	0.5	0.75	Additive
enro+oxy	7.81	1.95	4	7.81	15.62	0.5	4.5	Antagonistic
strepto+genta	5.86	15.62	0.37	4.56	3.91	1.17	1.55	Indifferent
strepto+oxy	20.51	15.62	1.31	18.23	15.62	1.17	2.48	Indifferent
genta+oxy	7.81	3.91	2	20.51	15.62	1.31	3.31	Indifferent

co-amoxiclav = co-amoxiclav; enro = enrofloxacin; metro = metronidazole; genta = gentamicin; oxy = oxytetracycline; amoxi = amoxicillin; strepto = streptomycin.

4. Discussion

The prevalence of *S. aureus* in this study was in line with previous studies in that aborted cattle revealed 17.2% endometritis and 88.3% *S. aureus* [36]. Different studies have also found that the number of people with MRSA seems to be lower (16.7% in Germany, 13.1% in India, and 4% in the USA), and the low expression of the *mecA* gene could be the cause of the varying outcomes for MRSA. The risk factors' association in our study was in agreement with results of a previous study [37]. Favorable climatic conditions and the presence of predisposing risk factors trigger the process of acquired resistance.

After the confirmation of phenotypical methods, the genomic confirmation of *S. aureus* with PCR is a reliable tool for the identification of species [8]. Other scientists also used the *nuc* gene to identify *S. aureus* [38, 39]. The MEME Suite web server is used for sequence analysis that provides information on protein interaction domains and DNA binding sites [40]. Gene structure servers provide gene images that describe gene structure and features. These, in turn, are required to further investigate evolution and functional attributes [41]. Different softwares are used for the identification of structural similarities that to some extent can be used to find functional attributes [42].

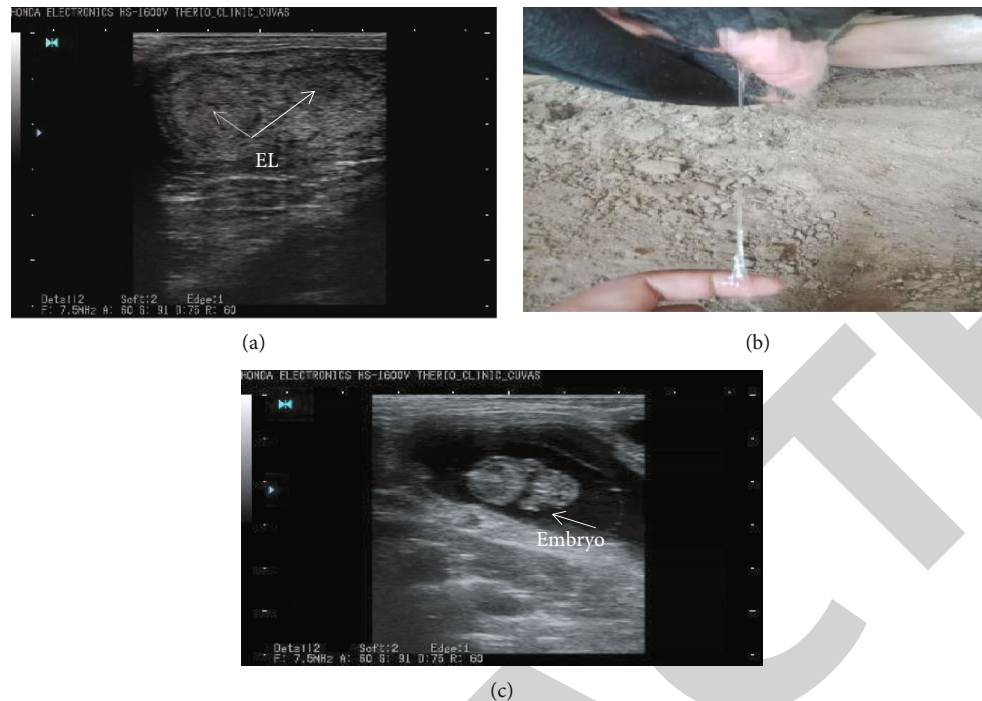


FIGURE 8: Parameters of successful treatment and post treatment successful pregnancy: (a) normal endometrial lining (EL), (b) normal uterine secretions—clear string formed without any pus material, and (c) pregnancy established in animals as evident by developing.

The vancomycin resistance reported in the present study resemble with the previous studies. This may be because of acquired resistance, as reported in the methicillin case [43]. Vancomycin resistance in *S. aureus* may also be because of acquired transposon Tn1546, via vancomycin-resistant *Enterococcus faecalis*, resulting from variations in the structure of the cell wall and cellular metabolism of isolates [44]. The study showed downward receptivity trends to enhanced penicillin that could be because of genetic variation in penicillin-binding proteins. Mutation in penicillin-binding proteins is proposed to change the capacity of antibiotics to the receptor proteins, resulting in an increasing MIC of penicillin group [29–31] and thus supports the findings of the current study. A similar pattern of MIC for commonly used drugs was reported in previous studies [45–48] against animal and human associated *S. aureus*. Sanganyado and Gwenzi [49] found that *tet* (A, B, C, G, O) and *tet* (W) genes which code for tetracycline resistance may be linked to higher MIC values for oxytetracycline. Streptomycin's MIC in the current study was in line with results reported by Zhang et al. [50], which showed that microbes have acquired resistant genes against streptomycin resulting in higher MIC values. Studies that evaluated milk samples have shown that *S. aureus* is resistant to multiple antibiotics in the same way [51].

Drug combination therapy for the treatment of MRSA infections is highly regarded in literature to avoid further resistance and to immediately clear the infection. Previous studies [32, 33, 52] found antimicrobial resistance to be tackled by combination of antibiotics with non-steroidal anti-inflammatory drugs. Similarly, plant extracts [53, 54] and nanoparticles [55, 56] were well documented with promising antimicrobial results. Changes in the results of the response

to the drugs tested *in vivo* and *in vitro* agreed with previous studies [57–60]. The differences in the results could be attributed to binding pathways at cellular level, temperature changes, the effect of cellular matrix on drug activity [57], response of the immune system, enzymatic degradation [59], and pharmacokinetic and pharmacodynamic specifications of the living being [58]. These associated attributes make it hard to get reproducibility and similarity in results [61]. Rise in antimicrobial resistance with respect to novel strains like vancomycin resistant *S. aureus* [62] and presence of MRSA not only in dairy udder [63] but also in companion livestock e.g poultry [64, 65] adds additional burden to the economy and health of animals as well as public.

5. Conclusion

The study confers hiked percentages of *S. aureus* in endometritis and found a clue of pathogen transfer from other animals. *In vitro* drug combinations showed many folds of antibacterial activity with very limited antagonism. In the field trials, novel drug combinations provided a wider range of treatment options which encouraged the use of evidence-based therapeutics instead of conventional treatment. It is therefore suggested that molecular epidemiology and evidence-based drug combinations should be regularly observed to culminate drug resistance and to save one's health.

Data Availability

Supplementary file is attached for some of the data related to this article.

Conflicts of Interest

All authors declare that they have no conflict of interest.

Authors' Contributions

Hongping Pan was responsible for funding acquisition; Zaeem Sarwar and Muhammad Ajmal were responsible for the resources; Muhammad Muddassir Ali, Memmona Adil, and Arslan Saleem were responsible for the software; Amjad Islam Aqib was responsible for supervision; Chaobin Qin, Qin Liang, and Alveena Khan were responsible for visualization; Laiba Shafique was responsible for writing the original draft; Qingyou Liu and Kuiqing Cui were responsible for writing—review and editing. Laiba Shafique and Amjad Islam Aqib equally contributed.

Acknowledgments

The present study was granted and supported by the National Natural Science Fund (U20A2051) and the Guangxi Science and Technology Major Project (AA22068099). We are thankful to the Department of Medicine, Central Diagnostic Laboratory of Cholistan University of Veterinary and Animal Sciences Bahawalpur, and field veterinarians from Pakistan for their support in this study. We are also thankful to the State Key Laboratory for Conservation and Utilization of Agrobioresources China for their technical support.

Supplementary Materials

Supplementary Table 1: drug combinations and dosage regimens. Supplementary Table 2: *S. aureus* thermal nuclease protein conserved domain structure (reference sequence, Staph-1, Staph-2, and Staph-3). Supplementary Figure 1: multiple sequence alignment of *S. aureus* Nuc gene (reference and local isolate PK nucleotide sequences). Supplementary Figure 2: motif locations in gene sequences (1 to 5), sequence of individual motif and *p* value of motifs in sequences 1 to 5. Supplementary Figure 3: structural analysis of *S. aureus* Nuc gene from Pakistan. Supplementary Figure 4: antibacterial activity of different antibiotics/drugs against *S. aureus* (i) disc diffusion assay (1 = chloramphenicol; 2 = linezolid; 3 = levofloxacin; 4 = gentamicin; 5 = vancomycin), (ii) well diffusion assay (1 = metronidazole; 2 = co-amoxiclav; 3 = enrofloxacin; 4 = co-amoxiclav+metronidazole; 5 = enrofloxacin+metronidazole; 6 = co-amoxiclav+enrofloxacin; 7 = gentamicin). (*Supplementary Materials*)

References

- [1] A. E. M. Megahed, K. Basal, and A. Almilaibary, "Preoperative vaginal preparation with chlorhexidine gluconate to reduce post-cesarean delivery infectious morbidity," *International Journal of Medical Arts*, vol. 4, no. 2, pp. 2118–2123, 2022.
- [2] M. Taylor and L. S. Pillarisetty, "Endometritis," 2020.
- [3] L. Chen, Z. Y. Tang, S. Y. Cui et al., "Biofilm production ability, virulence and antimicrobial resistance genes in *Staphylococcus aureus* from various veterinary hospitals," *Pathogens*, vol. 9, no. 4, p. 264, 2020.
- [4] R. B. Paiano, D. B. Birgel, J. Bonilla, and E. H. Birgel Junior, "Alterations in biochemical profiles and reproduction performance in postpartum dairy cows with metritis," *Reproduction in Domestic Animals*, vol. 55, no. 11, pp. 1599–1606, 2020.
- [5] A. Kumar and K. S. Prasad, "Role of nano-selenium in health and environment," *Journal of Biotechnology*, vol. 325, pp. 152–163, 2021.
- [6] I. Muzammil, M. I. Saleem, A. I. Aqib et al., "Emergence of pathogenic strains of *Staphylococcus aureus* in goat milk and their comparative response to antibiotics," *Pakistan Journal of Zoology*, pp. 1–9, 2021.
- [7] S. Aziz, N. M. Saeed, H. O. Dyary et al., "Divergent analyses of genetic relatedness and evidence-based assessment of therapeutics of *Staphylococcus aureus* from semi-intensive dairy systems," *BioMed Research International*, vol. 2022, Article ID 5313654, 13 pages, 2022.
- [8] S. McDougall, J. Williamson, and J. Lacy-Hulbert, "Bacteriological outcomes following random allocation to quarter-level selection based on California Mastitis Test score or cow-level allocation based on somatic cell count for dry cow therapy," *Journal of Dairy Science*, vol. 105, no. 3, pp. 2453–2472, 2022.
- [9] W. P. Silvada, J. A. Silva, M. R. P. Macedode, M. R. Araújo, M. M. Mata, and E. A. Gandra, "Identification of *Staphylococcus aureus*, *S. intermedius* and *S. hyicus* by PCR amplification of *coa* and *nuc* genes," *Brazilian Journal of Microbiology*, vol. 34, pp. 125–127, 2003.
- [10] T. Umar, X. Ma, B. Yin et al., "miR-424-5p overexpression inhibits LPS-stimulated inflammatory response in bovine endometrial epithelial cells by targeting IRAK2," *Journal of Reproductive Immunology*, vol. 150, article 103471, 2022.
- [11] Á. Stegger, P. S. Andersen, A. Kearns et al., "Rapid detection, differentiation and typing of methicillin-resistant *Staphylococcus aureus* harbouring either *_mecA_* or the new *_mecA_* homologue *_mecA_{LGA251}_*," *Clinical Microbiology and Infection*, vol. 18, no. 4, pp. 395–400, 2012.
- [12] W. Walana, B. P. Bobzah, E. D. Kuugbee et al., "Staphylococcus aureus nasal carriage among healthcare workers, inpatients and caretakers in the Tamale Teaching Hospital, Ghana," *Scientific African*, vol. 8, article e00325, 2020.
- [13] C. K. Kim, C. Milheiriço, H. de Lencastre, and A. Tomasz, "Antibiotic resistance as a stress response: recovery of high-level oxacillin resistance in methicillin-resistant *Staphylococcus aureus* "auxiliary"(fem) mutants by induction of the stringent stress response," *Antimicrobial Agents and Chemotherapy*, vol. 61, no. 8, article e00313-17, 2017.
- [14] N. Velázquez-Guadarrama, A. L. Olivares-Cervantes, E. Salinas et al., "Presencia de estafilococos coagulasa positiva ambientales, su relacion clonal, factores de resistencia y habilidad para formar biopelícula," *Revista Argentina de Microbiología*, vol. 49, no. 1, pp. 15–23, 2017.
- [15] M. Verheghe, F. Crombé, K. Luyckx et al., "Prevalence and genetic diversity of livestock-associated methicillin-resistant *Staphylococcus aureus* on Belgian pork," *Journal of Food Protection*, vol. 79, no. 1, pp. 82–89, 2016.
- [16] É. Juhász-Kaszanyitzky, S. Jánosi, P. Somogyi et al., "MRSA transmission between cows and humans," *Emerging Infectious Diseases*, vol. 13, article 630, 2007.
- [17] M. N. Hoque, Z. C. Das, A. N. M. A. Rahman, M. G. Haider, and M. A. Islam, "Molecular characterization of *Staphylococcus aureus* strains in bovine mastitis milk in Bangladesh," *International journal of veterinary science and medicine*, vol. 6, no. 1, pp. 53–60, 2018.

- [18] W. L. D. C. Bernardo, J. J. D. Silva, J. F. Höfling, E. A. R. Rosa, and M. F. G. Boriollo, "Dynamics of the seasonal airborne propagation of *Staphylococcus aureus* in academic dental clinics," *Journal of Applied Oral Science*, vol. 26, 2018.
- [19] A. Pompilio, V. Crocetta, P. Confalone et al., "Adhesion to and biofilm formation on IB3-1 bronchial cells by *Stenotrophomonas maltophilia* isolates from cystic fibrosis patients," *BMC Microbiology*, vol. 10, no. 1, article 102, 2010.
- [20] D. Wojnicz, D. Tichaczek-Goska, K. Korzekwa, M. Kicia, and A. B. Hendrich, "Study of the impact of cranberry extract on the virulence factors and biofilm formation by *Enterococcus faecalis* strains isolated from urinary tract infections," *International Journal of Food Sciences and Nutrition*, vol. 67, no. 8, pp. 1005–1016, 2016.
- [21] M. J. Cheesman, A. Ilanko, B. Blonk, and I. E. Cock, "Developing new antimicrobial therapies: are synergistic combinations of plant extracts/compounds with conventional antibiotics the solution?," *Pharmacognosy Reviews*, vol. 11, no. 22, pp. 57–72, 2017.
- [22] Y. Guo, G. Song, M. Sun, J. Wang, and Y. Wang, "Prevalence and therapies of antibiotic-resistance in *Staphylococcus aureus*," *Frontiers in Cellular and Infection Microbiology*, vol. 10, article 107, 2020.
- [23] M. Thrusfield, *Sampling in veterinary epidemiology*, London Black well Sci. Ltd, London, 2007.
- [24] R. A. Pierson and O. J. Ginther, "Ultrasonic imaging of the ovaries and uterus in cattle," *Theriogenology*, vol. 29, no. 1, pp. 21–37, 1988.
- [25] P. Racewicz, M. Sickinger, J. Włodarek, and J. M. Jaśkowski, "Ultrasonographic diagnosis of early pregnancy in cattle using different ultrasound systems," *Tierärztliche Praxis Ausgabe G: Großtiere/Nutztiere*, vol. 44, no. 3, pp. 151–156, 2016.
- [26] B. Ihnatsenka and A. P. Boezaart, "Ultrasound: basic understanding and learning the language," *International Journal of Shoulder Surgery*, vol. 4, no. 3, article 55, 2010.
- [27] I. Sarwar, A. Ashar, A. Mahfooz et al., "Evaluation of antibacterial potential of raw turmeric, nano-turmeric, and NSAIDs against multiple drug resistant *Staphylococcus aureus* and *E. coli* isolated from animal wounds," *Pakistan Veterinary Journal*, vol. 41, pp. 209–214, 2021.
- [28] J. G. Holt, N. R. Krieg, and P. H. A. Sneath, "Bergey's Manual of Determinative Bacterology," 1994.
- [29] N. Zaatout and D. Hezil, "A meta-analysis of the global prevalence of methicillin-resistant *Staphylococcus aureus* (MRSA) isolated from clinical and subclinical bovine mastitis," *Journal of Applied Microbiology*, vol. 132, no. 1, pp. 140–154, 2022.
- [30] Clinical Institute, L S, "Performance Standards for Antimicrobial Susceptibility Testing of Anaerobic Bacteria: Informational Supplement; Clinical and Laboratory Standards Institute (CLSI)," 2009.
- [31] M. Shoaib, S. U. Rahman, A. I. Aqib et al., "Diversified epidemiological pattern and antibiogram of *mecA* gene in *Staphylococcus aureus* isolates of pets, pet owners and environment," *Pakistan Veterinary Journal*, vol. 40, 2020.
- [32] M. A. Anwar, A. I. Aqib, K. Ashfaq et al., "Antimicrobial resistance modulation of MDR *E. coli* by antibiotic coated ZnO nanoparticles," *Microbial Pathogenesis*, vol. 148, article 104450, 2020.
- [33] A. I. Aqib, M. Saqib, S. R. Khan et al., "Non-steroidal anti-inflammatory drugs, plant extracts, and characterized micro-particles to modulate antimicrobial resistance of epidemic *mecA* positive *S. aureus* of dairy origin," *Applied Nanoscience*, vol. 11, pp. 553–563, 2021.
- [34] D. Eshghi, M. Kafi, H. Sharifyazdi et al., "Intrauterine infusion of blood serum of dromedary camel improves the uterine health and fertility in high producing dairy cows with subclinical endometritis," *Animal Reproduction Science*, vol. 240, p. 106973, 2022.
- [35] E.-K. Shin, J.-K. Jeong, I.-S. Choi et al., "Relationships among ketosis, serum metabolites, body condition, and reproductive outcomes in dairy cows," *Theriogenology*, vol. 84, no. 2, pp. 252–260, 2015.
- [36] T. Petit, J. Spersger, R. Rosengarten, and J. Aurich, "Prevalence of potentially pathogenic bacteria as genital pathogens in dairy cattle," *Reproduction in Domestic Animals*, vol. 44, no. 1, pp. 88–91, 2009.
- [37] D. R. MacFadden, S. F. McGough, D. Fisman, M. Santillana, and J. S. Brownstein, "Antibiotic resistance increases with local temperature," *Nature Climate Change*, vol. 8, no. 6, pp. 510–514, 2018.
- [38] R. Moretti, D. Soglia, S. Chessa et al., "Identification of SNPs associated with somatic cell score in candidate genes in Italian Holstein Friesian bulls," *Animals*, vol. 11, no. 2, p. 366, 2021.
- [39] D. O. Morris, A. Loeffler, M. F. Davis, L. Guardabassi, and J. S. Weese, "Recommendations for approaches to methicillin-resistant staphylococcal infections of small animals: diagnosis, therapeutic considerations and preventative measures. Clinical Consensus Guidelines of the World Association for Veterinary Dermatology," *Veterinary Dermatology*, vol. 28, no. 3, 2017.
- [40] T. L. Bailey, M. Boden, F. A. Buske et al., "MEME SUITE: tools for motif discovery and searching," *Nucleic Acids Research*, vol. 37, no. Web Server, pp. W202–W208, 2009.
- [41] B. Hu, J. Jin, A.-Y. Guo, H. Zhang, J. Luo, and G. Gao, "GSDS 2.0: an upgraded gene feature visualization server," *Bioinformatics*, vol. 31, no. 8, pp. 1296–1297, 2015.
- [42] C. A. Orengo, A. E. Todd, and J. M. Thornton, "From protein structure to function," *Current Opinion in Structural Biology*, vol. 9, no. 3, pp. 374–382, 1999.
- [43] J. O. Veloso, J. Lamarco-Cardoso, L. S. Neves et al., "Methicillin-resistant and vancomycin-intermediate *Staphylococcus aureus* colonizing patients and intensive care unit environment: virulence profile and genetic variability," *APMIS*, vol. 127, no. 11, pp. 717–726, 2019.
- [44] S. Gardete and A. Tomasz, "Mechanisms of vancomycin resistance in *Staphylococcus aureus*," *The Journal of Clinical Investigation*, vol. 124, no. 7, pp. 2836–2840, 2014.
- [45] A. Tomasz, H. B. Drugeon, H. M. de Lencastre, D. Jabes, L. McDougall, and J. Bille, "New mechanism for methicillin resistance in *Staphylococcus aureus*: clinical isolates that lack the PBP 2a gene and contain normal penicillin-binding proteins with modified penicillin-binding capacity," *Antimicrobial Agents and Chemotherapy*, vol. 33, no. 11, pp. 1869–1874, 1989.
- [46] C. Rağbetli, M. Parlak, Y. Bayram, H. Guducuoglu, and N. Ceylan, "Evaluation of antimicrobial resistance in *Staphylococcus aureus* isolates by years," *Interdisciplinary Perspectives on Infectious Diseases*, vol. 2016, Article ID 9171395, 4 pages, 2016.

Retraction

Retracted: Gut Microbiota Profiles in Dairy Cattle from Highland and Coastal Regions Using Shotgun Metagenomic Approach

BioMed Research International

Received 8 January 2024; Accepted 8 January 2024; Published 9 January 2024

Copyright © 2024 BioMed Research International. This is an open access article distributed under the Creative Commons Attribution License, which permits unrestricted use, distribution, and reproduction in any medium, provided the original work is properly cited.

This article has been retracted by Hindawi, as publisher, following an investigation undertaken by the publisher [1]. This investigation has uncovered evidence of systematic manipulation of the publication and peer-review process. We cannot, therefore, vouch for the reliability or integrity of this article.

Please note that this notice is intended solely to alert readers that the peer-review process of this article has been compromised.

Wiley and Hindawi regret that the usual quality checks did not identify these issues before publication and have since put additional measures in place to safeguard research integrity.

We wish to credit our Research Integrity and Research Publishing teams and anonymous and named external researchers and research integrity experts for contributing to this investigation.

The corresponding author, as the representative of all authors, has been given the opportunity to register their agreement or disagreement to this retraction. We have kept a record of any response received.

References

- [1] B. W. H. E. Prasetyono, W. Widiyanto, and N. S. Pandupuspitasari, "Gut Microbiota Profiles in Dairy Cattle from Highland and Coastal Regions Using Shotgun Metagenomic Approach," *BioMed Research International*, vol. 2022, Article ID 3659052, 8 pages, 2022.

Research Article

Gut Microbiota Profiles in Dairy Cattle from Highland and Coastal Regions Using Shotgun Metagenomic Approach

Bambang Waluyo Hadi Eko Prasetyono ¹, **Widiyanto Widiyanto**,²
and **Nuruliarzki Shinta Panduspitasari**²

¹Laboratory of Feed Technology, Animal Science Department, Faculty of Animal and Agricultural Sciences, Universitas Diponegoro, Indonesia

²Laboratory of Animal Nutrition and Feed Science, Animal Science Department, Faculty of Animal and Agricultural Sciences, Universitas Diponegoro, Indonesia

Correspondence should be addressed to Bambang Waluyo Hadi Eko Prasetyono; bambangwhep@gmail.com

Received 26 July 2022; Accepted 11 August 2022; Published 9 September 2022

Academic Editor: Dr Muhammad Hamid

Copyright © 2022 Bambang Waluyo Hadi Eko Prasetyono et al. This is an open access article distributed under the Creative Commons Attribution License, which permits unrestricted use, distribution, and reproduction in any medium, provided the original work is properly cited.

There is significant difference in milk production of highland and coastal regions in Indonesia of which the latter is critically low. The recent studies indicate a possibility of improving the milk yield and quality by manipulating the gut microbiota, for which profiling and abundance of gut microbiota in these divergent regions need to be addressed. The present study was the first of its kind to explore the dairy cattle gut microbiota diversity, abundance, and functional annotation of the two divergent Indonesian regions, the highland and coastal regions, by shotgun metagenomic approach. Unfavorable environmental conditions such as type of forage grass in coastal regions and high temperature remain a limiting factor; however, the improvement through manipulating the gut microbiota was not considered until recently to improve the quality and quantity of coastal region dairy cattle. The application of recent advance technologies can help achieve this goal on sustainable basis. The results show Bacteroidetes in higher abundance in coastal region (FPP) than in highland (Salatiga) while Firmicutes were higher in Salatiga. Furthermore, a collective physiology of the community was found by annotating the sequences against KEGG, eggNOG, and CAZy databases. To identify the role in pathways, an mPATH analysis was performed to have insight into the microbiota community in different metabolic pathways. The identified targets can be used as prebiotic and/or probiotic to improve the average milk yield of coastal region dairy cattle by manipulating the dairy feed with desired microbes.

1. Introduction

Indonesian dairy industry production remains at 1,800 tonnes of milk a day in 2022 which only provides 5% of the country demand [1]. The average daily production by local farmers in Indonesia ranges from 4 to 6 litters a day while the Holstein cow production varies 16-20 litters a day which is much lower than its potential [2]. However, it was observed that highland dairy cattle produced 45 litters of milk on average in comparison to coastal region dairy cows.

The gut microbiota of cow and its abundance are associated with a wide range of activities and functions such as fermentation of feed, fatty acid formation, methane production,

nitrogen emissions, and cellulose digestion [3]. The cow's rumen houses ancestrally diverse community of anaerobic bacteria, viruses, ciliated protozoa, fungi, and methanogenic archaea. These microbiota are capable of degrading indigestible plant fibre of the host [4, 5]. The rumen microbiome is critical for the host animal's nutrition, by providing essential nutrients by fermentation of feed, which on ruminant growth in number of ways. The ruminants especially dairy cows are dependent on the microbial metabolites for the production of economically important products such as milk.

The most convoluted microbial communities which inhabit the rumen have triggered the microbiologists' curiosity. Physiologists and nutritionists are also aware of the rumen's critical role in the digestion of fibrous feed and

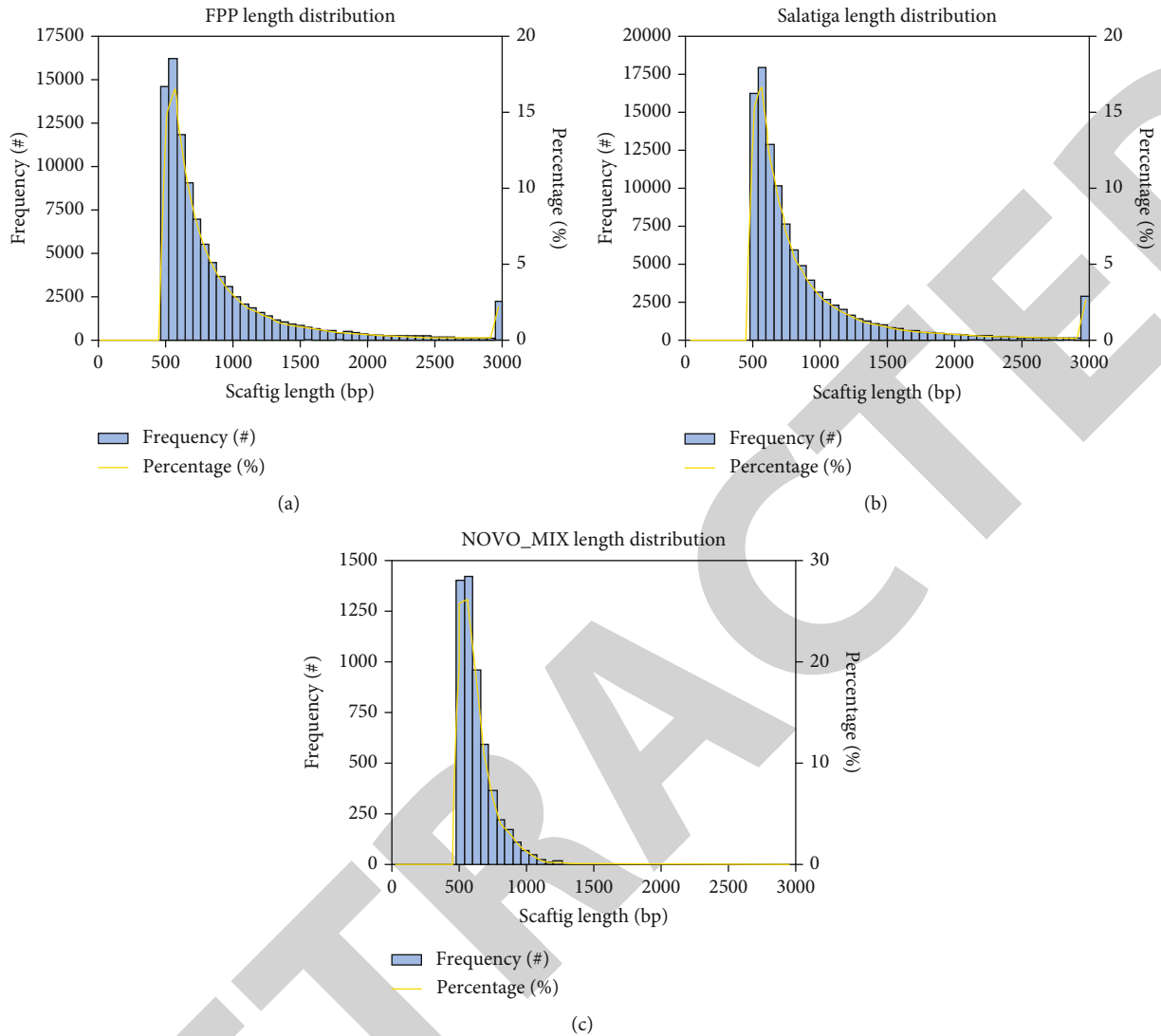


FIGURE 1: Length distribution of scaftigs of different samples. The distribution of scaftigs length is calculated and plotted in each sample; frequency(#) is shown at the longitudinal axis; the number of scaftigs and the percentage of scaftigs number percentage (%) are represented in yellow curve. The scaftigs length is shown horizontally. (a) Sample coastal region (FPP). (b) Sample highland region (Salatiga). (c) NOVO-MIX.

the provision of the host animals' nutritional requirements. They enable the ruminants to provide food to people [6]. Furthermore, as previously demonstrated by a relationship between microbiome components and residual feed intake, the composition of these various types of microbes influences the productive efficiency [7, 8].

The composition of the rumen microbiota has been widely studied previously across various regions of the globe for various reasons [9]. Microbes work alongside the host to provide them with their metabolic products [10]. Ciliate protozoa account for 50% of microbial community of the cow gut [11]. The protozoa also vary greatly in ruminants in terms of abundance or diversity, but their presence or absence is not greatly impactful to the host as a great amount of their products can also be synthesized by other groups of the gut microbiota [9, 12].

Anaerobic fungi break down plant's toughest structure for efficient usage of feed [13]. In CH₄, the Archaea are

important contributors [14, 15]. Several studies have been done on dairy cow's gut microbiota for their roles in various pathways and metabolic activities [16–19], where recently heritable component of the gut microbiota are reported [20]. Microbiota are composed mainly of bacterial families along with Archaea and fungi, each of them working to produce various important compounds for the host [21, 22]. It is also extensively studied that the type and colony size of these microbiota are effected by factors such as temperature, pH, feed, water quality, age, genetics, region, and health [23–25].

Several factors including age, diet, genetics, and feed efficiency and environmental stimuli affect the rumen microbiota composition which directly influence the productivity of host [26]. The present study was an effort to explore the fecal gut microbiota of the highland and coastal region dairy cattle in Indonesia to explore its abundance and to figure out the potential prebiotic and probiotic candidates to enhance

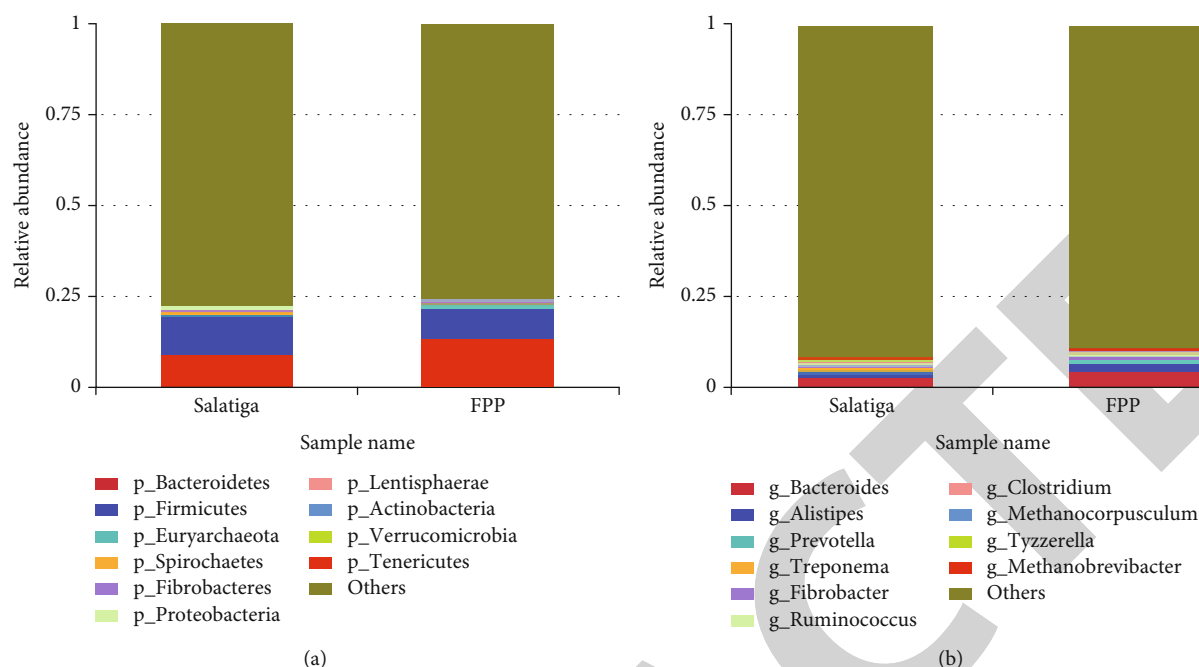


FIGURE 2: Relative abundance in phylum and genus level in highland (Salatiga) and coastal regions (FPP): (a) phylum level; (b) genus level.

quantity and quality of the coastal region dairy cattle in Indonesia.

2. Material and Methods

2.1. Farm and Animal Selection. The well managed farms which keep the organized record of dairy cattle in highland and coastal areas of Indonesia were selected for the study. The fecal samples of healthy cows were collected in DNA/RNA shield tubes. The DNA/RNA shield tubes were brought back to laboratory for further processing. DNA was extracted from the fecal samples utilizing 1 gram of the collected sample [27]. The quality test for the extracted DNA sample was performed before constructing libraries for the samples.

For library construction, genomic DNA was sheared randomly into short fragments. The fragments obtained were A-tailed and end repaired and then ligated to Illumina adapter. The adapter-ligated fragments were amplified using PCR, selected for size, and then purified. Qubit was used to check library for quantification by real-time PCR, and the bioanalyzer was used to detect size distribution. The libraries that were quantified were pooled, and Illumina platforms were used to sequence, as per the requirements of the effective library concentration and the amount of data required.

2.2. Bioinformatic Analysis. The certain percentage of low-quality data reads obtained in raw data after sequencing was host filtered to establish the accuracy and reliability of the subsequent information analysis to obtain effective data termed as clean data; clean data was used to assemble metagenome after quality control of each sample, and mixed assembly was made from unutilized reads to explore the information regarding low abundant species from each sam-

ple. MetaGeneMark was used for the gene prediction utilizing scaffigs which were assembled by single and mixed samples. Gene catalogue was constructed by pooling the predicted genes for dereplication. The abundance information of each sample was obtained from the gene catalogue. Metagenomic reads were compared to NR database, i.e., the database of taxonomically informative gene families for annotation of each metagenomic homolog. Gene abundance table was obtained from the abundance tables of different taxonomic ranks. The coding sequence function was obtained from its similarity to sequences in three databases, i.e., KEGG, eggNOG, and CAZy. Doing this for all metagenomic sequences, we produced a profile of distinct types of functions and their relative abundance in the studied metagenome.

3. Results and Discussion

The next generation sequencing (NGS) was used to obtain the sequencing reads from metagenomic DNA isolated from fecal samples of coastal region (FPP) and highland (Salatiga) dairy cattle. The sequencing was done on NovoSeq6000. The sample coastal region (FPP) and highland (Salatiga) produced 7.15 GB and 7.33 GB of raw base data, respectively. The clean bases for coastal region (FPP) and highland (Salatiga) were 7.14 GB and 7.33 GB of raw bases, respectively. The data with less than 0.001 sequencing error rate in coastal region (FPP) and highland (Salatiga), i.e., Clean_Q30, were 94.72% and 94.02%, respectively. In all the assembled results, all scaffigs were counted and the distribution of scaffigs length in each sample. A mixed assembly was conducted on the reads that were unutilized keeping the same assemble parameter. The results are presented in Figure 1.

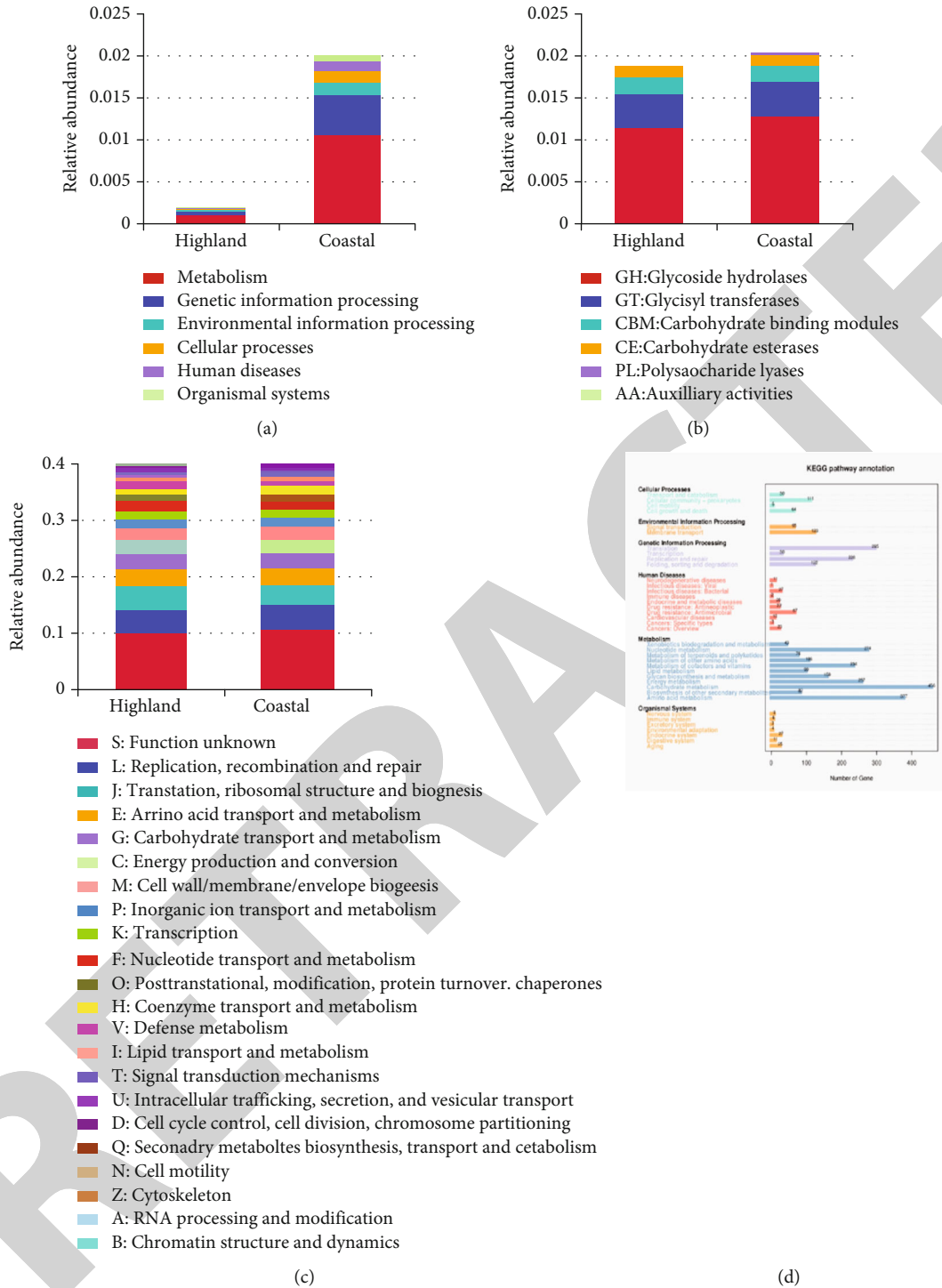


FIGURE 3: Continued.

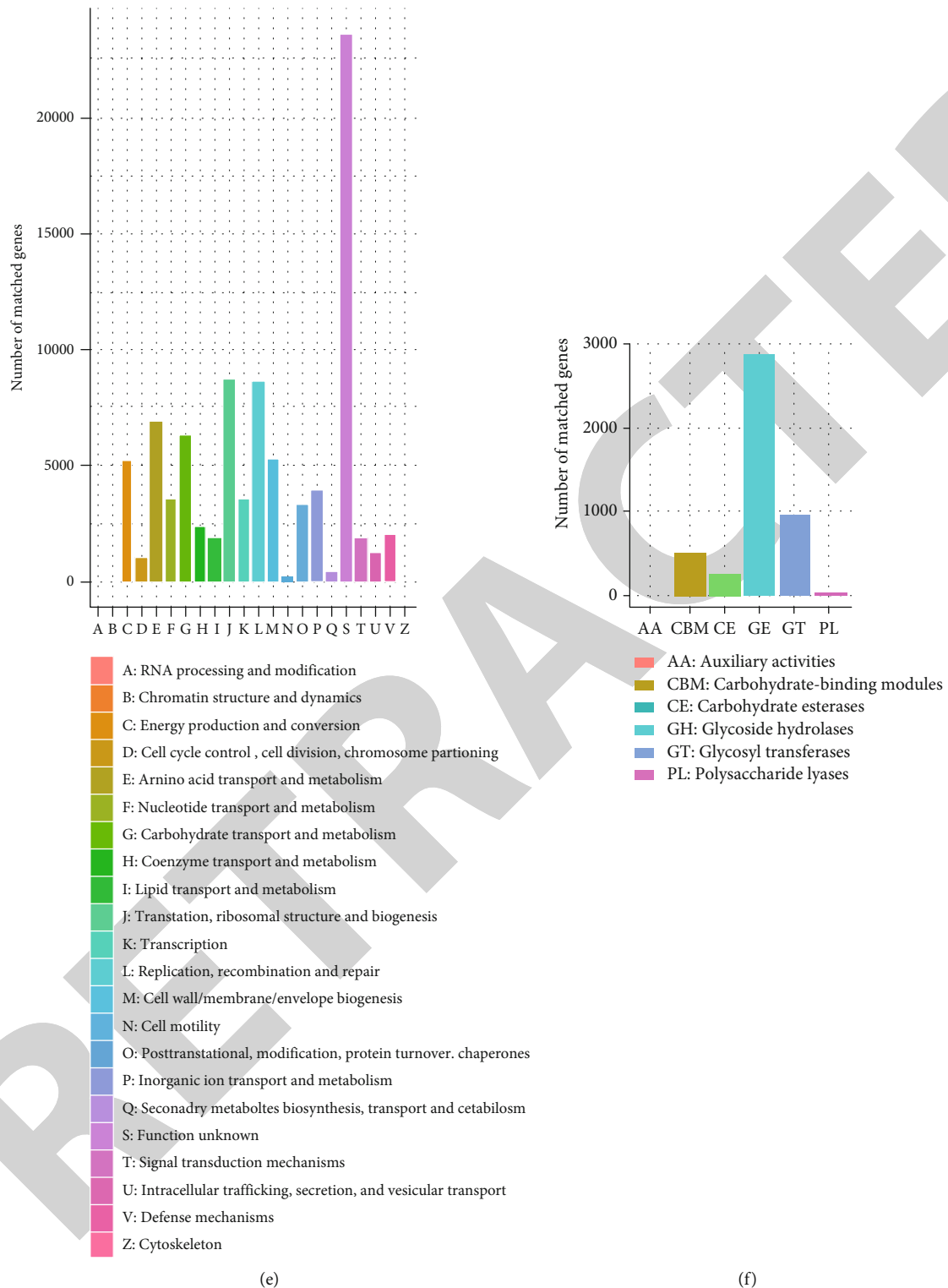


FIGURE 3: Relative abundance of each database. (a) KEGG unique gene level 1. (b) eggNOG unique gene level 1. (c) CAZy unique gene level 1. Summarized chart for the gene number annotated by every database: (d) KEGG pathway annotation; (e) eggNOG database; (f) CAZy database.

3.1. Taxonomic Analysis of Highland and Coastal Region Dairy Cattle. The question of communities' similarity needs to be ascertained by identifying reads that serves as the marker gene homologs to a taxonomically informative gene

families by phylogenetic and sequence similarity to NR database [28] and to annotate taxonomically each metagenomic homolog (MEGAN [29]). Several analyses were performed according to abundance table at each taxonomic level.

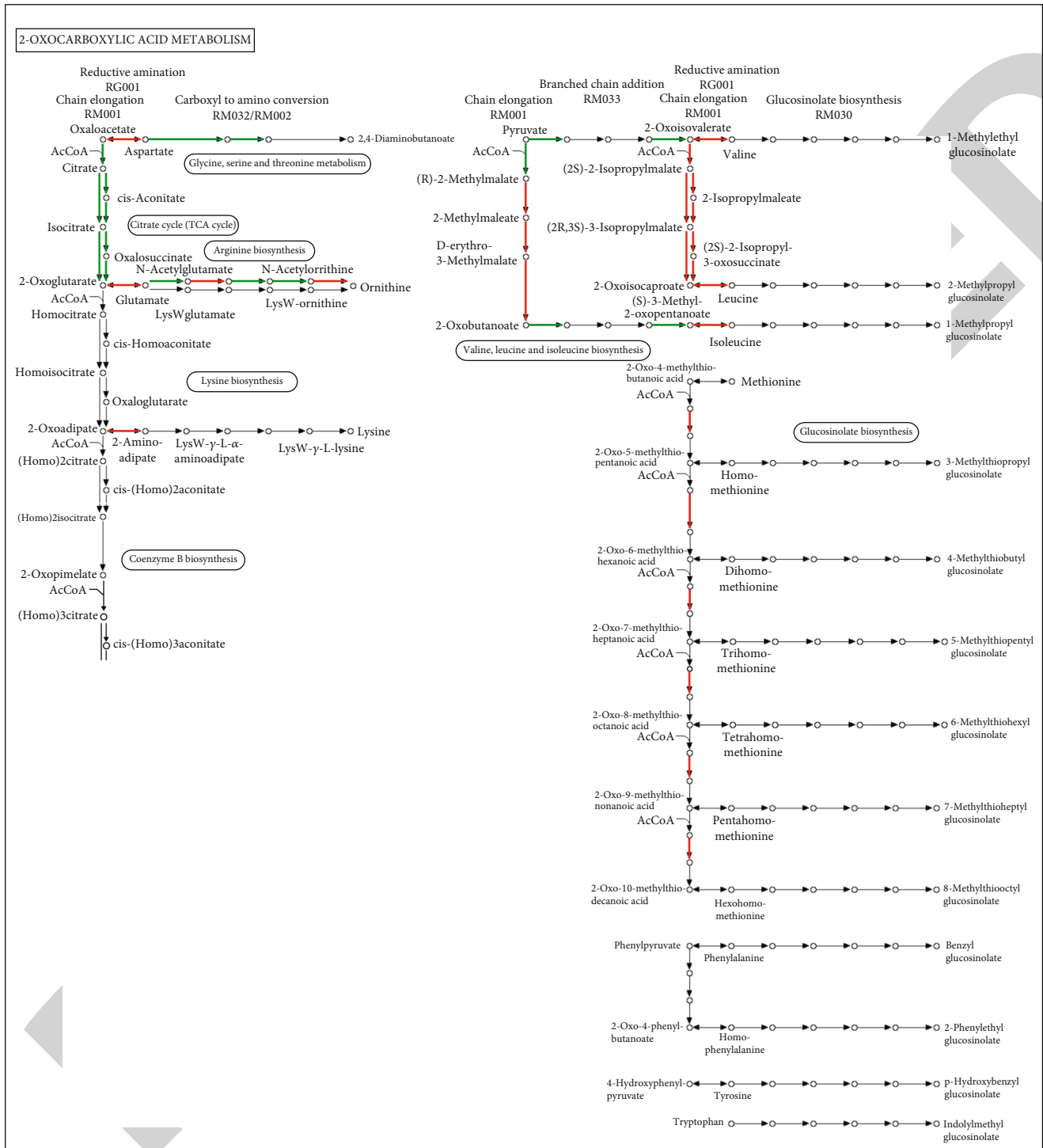


FIGURE 4: The compare analysis for oxocarboxylic metabolic pathway.

3.2. Relative Abundance of Bacteria in Highland (Salatiga) and Coastal (FPP) Farms. As reviewed earlier, the milk yield in coastal regions is critically low. To identify the reasons behind this low milk yield, we compare the gut microbiota of highland to coastal region dairy cattle. We found that Bacteroidetes were at higher abundance, i.e., 52% in coastal region to that of 37% in highland. Bacteroidetes is a phyla that is mostly producing metabolites that are responsible

for hormones that causes satiety and weight loss [30, 31]. As we observed, the dysbiosis of Bacteroidetes in coastal region indicates that it might be one of the reasons for lower milk yield in coastal region.

Furthermore, the data indicate that the *Prevotella* sp. MGM2 was highly abundant in coastal region, i.e., 19% to 2% in highland region. It has been identified that *Prevotella* sp. MGM2 is involved in enhancing Treg cells which is an

indication of poor health of host [32]. The *Prevotella* sp. CAG:891 shows 11% in coastal region and 3% in highland region. *Prevotella* sp. CAG:891 is responsible producing L-pipecolic acid of which higher concentrations are associated with metabolic disorders [33].

It is noteworthy that the abundance of *Prevotella* sp. CAG:485 shows lower abundance, i.e., 0.6% in coastal region to that of 5% in highland region. *Prevotella* sp. CAG:485 produces metabolite grpE which participates in active response to hyperosmotic pressure and heat stress [34]. It prevents the accumulation of unfolded proteins in the cytoplasm and hence provide protection against death. The lower abundance in coastal region (FPP) is indicating the lesser ability coastal dairy cattle of lesser ability to resist heat and higher temperature which negatively affects milk yield and quality (Figure 2).

3.3. Functional Annotation of Coastal and Highland Dairy Cattle Fecal Gut Microbiota. The identified unigene functional annotation was performed against the CAZy [35], eggNOG [36], and KEGG [37] databases, and the results obtained are shown in Figures 3(a)–3(c). We observed that coastal region (FPP) dairy cattle showed statistically significant higher number of pathway genes for metabolism, environmental information processing, cellular processes, and genetic information processing. Scientifically, dairy cattle shows that higher metabolic rate produces lower quantity of milk.

The eggNOG database revealed several pathway genes related to metabolism including nucleotide transport and metabolism, amino acid transport and metabolism, coenzyme transport and metabolism, carbohydrate transport and metabolism, inorganic ion transport and metabolism, and lipid transport and metabolism (Figure 3(c)). The significant unigene number involved with metabolism is 2163, cellular processes is 210, and environmental information processing is 188 as shown in Figure 3(d). The CAZy database shows a large number of glycoside hydrolases and glycosyl hydrolases (Figure 3(b)).

3.4. Metabolic Pathway. To further elaborate metabolic pathways among samples, we apply mPATH analysis. We created a web version pathway report which demonstrates variances of pathway patterns. We obtained shared and unique pathway information.

We identified that genes involved in uric acid cycle that may cause citrullinemia; i.e., disturbance in urea cycle was found to be unique for its expression in coastal region (FPP) dairy cattle. Figure 4 shows the shared and unique pathway information for 2-oxycarboxylic acid metabolism. The data suggests if the dysbiosis in the gut microbiota of coastal region dairy cattle can be corrected will be way forward for high yielding and sustainable milk productions in future.

4. Conclusion

The high quality and quantity of milk yield are the desirable traits for dairy farming. The achievement of these traits is

challenged by several factors including environmental stresses, diseases, and parasites. The animals do develop strategies to cope with such conditions; however, interventions to improve it accelerate the process. The use of advanced next generation sequencing technologies has brought an immense and targeted improvements in desired traits. The present study has explored the gut microbiota of coastal region (FPP) and highland (Salatiga) dairy cattle and found interesting targeted microbial species which after further validation can be developed as novel prebiotic and/or probiotic to improve milk quality and quantity specifically in coastal regions which can bring huge benefit to local farms of the coastal region in Indonesia.

Data Availability

Data can be requested to the corresponding author with a reasonable request.

Conflicts of Interest

The authors declare no conflict of interest.

Authors' Contributions

B.W.H.E.P, W., and N.S.P. conceptualized the idea. N.S.P. performed the analysis. B.W.H.E.P, W., and N.S.P. wrote and reviewed the draft.

Acknowledgments

This study was supported by the *Riset Publikasi Internasional*, Institute for Research and Community Services, Universitas Diponegoro.

References

- [1] Statistics I, *Statistics of milk cow establishment 2013. Statistics Indonesia*, Government of Indonesia, 2014.
- [2] N. Widyas, F. Y. Putra, T. Nugroho, A. Pramono, A. Susilowati, and S. P. Sutarno, "Persistency of milk yield in Indonesian Holstein cows," *IOP Conference Series: Earth and Environmental Science*, vol. 142, p. 012005, 2018.
- [3] C. J. Newbold and E. Ramos-Morales, "Review: ruminal microbiome and microbial metabolome: effects of diet and ruminant host," *Animal*, vol. 14, Supplement 1, pp. s78–s86, 2020.
- [4] C. Milani, S. Duranti, S. Napoli et al., "Colonization of the human gut by bovine bacteria present in parmesan cheese," *Nature Communications*, vol. 10, no. 1, p. 1286, 2019.
- [5] E. J. Contijoch, G. J. Britton, C. Yang et al., "Gut microbiota density influences host physiology and is shaped by host and microbial factors," *eLife*, vol. 8, article e40553, 2019.
- [6] H. Steinfeld, P. Gerber, T. Wassenaar, V. Caste, M. Rosales, and C. de Haan, *Livestock's Long Shadow*, FAO, 2006.
- [7] P. R. Myer, T. P. L. Smith, J. E. Wells, L. A. Kuehn, and H. C. Freetly, "Rumen microbiome from steers differing in feed efficiency," *PLoS One*, vol. 10, no. 6, article e0129174, 2015.
- [8] S. K. B. Shabat, G. Sasson, A. Doron-Faigenboim et al., "Specific microbiome-dependent mechanisms underlie the energy

Retraction

Retracted: Biorational Control of *Callosobruchus maculatus* (Coleoptera: Buchidae) in Stored Grains with Botanical Extracts

BioMed Research International

Received 8 January 2024; Accepted 8 January 2024; Published 9 January 2024

Copyright © 2024 BioMed Research International. This is an open access article distributed under the Creative Commons Attribution License, which permits unrestricted use, distribution, and reproduction in any medium, provided the original work is properly cited.

This article has been retracted by Hindawi following an investigation undertaken by the publisher [1]. This investigation has uncovered evidence of one or more of the following indicators of systematic manipulation of the publication process:

- (1) Discrepancies in scope
- (2) Discrepancies in the description of the research reported
- (3) Discrepancies between the availability of data and the research described
- (4) Inappropriate citations
- (5) Incoherent, meaningless and/or irrelevant content included in the article
- (6) Manipulated or compromised peer review

The presence of these indicators undermines our confidence in the integrity of the article's content and we cannot, therefore, vouch for its reliability. Please note that this notice is intended solely to alert readers that the content of this article is unreliable. We have not investigated whether authors were aware of or involved in the systematic manipulation of the publication process.

Wiley and Hindawi regrets that the usual quality checks did not identify these issues before publication and have since put additional measures in place to safeguard research integrity.

We wish to credit our own Research Integrity and Research Publishing teams and anonymous and named external researchers and research integrity experts for contributing to this investigation.
















The corresponding author, as the representative of all authors, has been given the opportunity to register their agreement or disagreement to this retraction. We have kept a record of any response received.

References

- [1] R. Akbar, I. A. Khan, B. Faheem et al., "Biorational Control of *Callosobruchus maculatus* (Coleoptera: Buchidae) in Stored Grains with Botanical Extracts," *BioMed Research International*, vol. 2022, Article ID 3443578, 10 pages, 2022.

Research Article

Biorational Control of *Callosobruchus maculatus* (Coleoptera: Buchidae) in Stored Grains with Botanical Extracts

Rasheed Akbar ¹, Imtiaz Ali Khan ², Brekhna Faheem ³, Rashid Azad ¹,
Maid Zaman ¹, Rubab Altaf ¹, Amjad Usman ², Muhammad Fawad ⁴, Abid Farid ¹,
Ahmad Ur Rahman Saljoqi ⁵, Asad Syed ⁶, Ali H. Bahkali ⁶, Abdallah M. Elgorban ⁶,
Jawad Ali Shah ⁷ and Abdul Qayyum ⁸

¹Department of Entomology, The University of Haripur, Haripur 22620, Pakistan

²Department of Entomology, The University of Agriculture, Peshawar, Pakistan

³Department of Zoology, Abdul Wali Khan University, Mardan, Pakistan

⁴Department of Environmental Sciences, The University of Haripur, Haripur 22620, Pakistan

⁵Department of Plant Protection, The University of Agriculture, Peshawar, Pakistan

⁶Department of Botany and Microbiology, College of Science, King Saud University, P.O. 2455, Riyadh 11451, Saudi Arabia

⁷Department of Plant Protection, Faculty of Agrobiological Food & Natural Resources, Czech University of Life Sciences, Prague, Czech Republic

⁸Department of Agronomy, The University of Haripur, Haripur 22620, Pakistan

Correspondence should be addressed to Rasheed Akbar; rasheed.akbar@uoh.edu.pk

Received 14 June 2022; Accepted 16 August 2022; Published 29 August 2022

Academic Editor: Hafiz Ishfaq Ahmad

Copyright © 2022 Rasheed Akbar et al. This is an open access article distributed under the Creative Commons Attribution License, which permits unrestricted use, distribution, and reproduction in any medium, provided the original work is properly cited.

Globally, around 2000 plant species are used against pest control. The utilization of botanicals is considered the most economic and biodegradable methods for the control of stored grains pests. Therefore, the current study was carried out to investigate the repellency potential of five botanicals against *Callosobruchus maculatus* F. in Haripur, Pakistan. The concentrations of *Azadirachta indica* L., *Nicotiana tabacum* L., *Melia azedarach* L., *Nicotiana rustica* L., and *Thuja orientalis* L. were, i.e., 0.5, 1.0, 1.5, 2.0, 2.5, and 3.0% in four replicates to establish contact effects. The data were recorded after 1, 2, 3, 6, 24, 48, 72, and 96 hours. The repellency effect of these plant species against *C. maculatus* were increased in both the time- and dose-dependent manner, and highest effect was observed at 72 h. In addition, the repellency effect was 91% for *A. indica* (class: V), 86% *M. azedarach*, 82%, *N. tabacum* (class: V), 79% *N. rustica* (class: IV), and 75% *T. orientalis* (class: IV) at 3% concentration against *C. maculatus*. Furthermore, following 96 hours' exposure to treatment the sensitivity response of insects decreases as the time interval increases, i.e., 86% *A. indica* (class: V) was followed by 71% *M. azedarach* (class: IV), 65% *N. tabacum* (class: IV), 61% *N. rustica* (class: IV), and *T. orientalis* 57% (class: III) repellency at highest concentration of 3%. The current study concluded that *A. indica* and *M. azedarach* can be incorporated for the management of *C. maculatus* and these plant species might be helpful in the productions of new biopesticides.

1. Introduction

The practice of using plant extracts as biopesticides or medicines is well known [1]. As many as 2000 plant species are in use globally in the control of insect pests. Local people adopt more economic and biodegradable method

used as different plant part extracts as pesticides against stored products [2]. However, the effectiveness or use of biopesticide increases as pest management in field and stored product pests [3].

Among the stored products, insect pests, the Genus *Callosobruchus* causes annual losses to different stored

products including 30% in Mung bean, 20% in pigeon pea and 15% in chick pea [4]. About 2.5-3 million tons of stored grains are lost annually due to *C. maculatus* [5]. The Bruchid beetle, *C. maculatus* F. (Coleoptera: Bruchidae), is a cosmopolitan pest attack on economically important legumes such as mung bean, lentil, black gram, and cow peas [6].

This beetle damages the pulses both quantitatively and qualitatively which then become unfit for consumption [7]. *C. maculatus* breed from March to November and maximum damage is caused from February to August when all the developmental stages are present [8]. It is reported that farmer uses highly toxic insecticides to protect their stored commodities including mung bean. The use of chemical insecticides which have known side effects including handling hazards, toxic residues, and development of insecticide resistance [9]. Therefore, insecticides having toxic residues should be discouraged for the control of insect pests [10]. Due to injudicious use of insecticides, most of the stored product pests showed resistance against synthetic insecticides [11].

It is necessary to investigate alternative sources for the management of stored insect pests [12]. For the control of insect pests in storage, there is limited information regarding the utilization of plant products. Overuse of insecticides creates resistance in pest and has a harmful impact on the environment. Therefore, alternative strategies for the management of pests should be adopted [13]. The plant extracts not only environmental friendly but also social acceptable and easily available for local store keeper, farmers, and the people whose business is related with stored commodities. Keeping in view the importance of botanicals pesticides, the present studies were conducted with the aims to find out repellency response of *C. maculatus* against different plant extracts.

2. Material and Methods

The experiment was laid out in completely randomized design (CRD) with factorial arrangement having five treatments each with four replications. The leaves and fruits of five selected plants viz. *A. indica*, *M. azedarach*, *N. rustica*, *N. tabacum*, and *T. orientalis* were collected from different locations of district Swabi, Khyber-Pakhtunkhwa Pakistan (as shown in Table 1 and Figure 1).

2.1. Collection and Establishment of Stock Culture Insects. *C. maculatus* were collected from infested godowns at District Swabi. The collected *C. maculatus* were then brought to Entomological Laboratory, Department of Entomology, the University of Haripur, and released in a glass jar having mung bean as favorite food medium; the jars were covered with muslin cloth and kept in the lab at 30°C and 60 ± 5% RH [9].

2.2. Preparation of Plant Aqueous Extract. Six concentrations of all the selected 5 botanicals were prepared according to the methods adopted by [14]. Leaves and fruits were placed in distilled water for the duration of 48 hr. 0.25, 0.50, 0.75, 1.00, 1.25, and 1.50 g of each botanicals (different

parts) were directly diluted in 50 ml of distilled water to make 0.5, 1, 1.5, 2, 2.5 and 3% (*w/v*) solution. Each concentration was prepared separately [9].

2.3. Phytochemical Screening of Selected Plant Aqueous Extracts. The standard solution of 200 ml extracts was prepared by mixture of selected plant extract and distilled water [15]. The extracts were subjected for phytochemical for the following standard methods.

2.3.1. Extraction Procedure. Maceration: For maceration (for fluid extract), whole or coarsely powdered plant drug was kept in contact with the solvent in a stopper container for a defined period with frequent agitation until soluble matter is dissolved [16].

2.3.2. Tests for Alkaloid Wegener's tests. Extracts of the test plants were dissolved individually in dilute hydrochloric acid 1.5% and filtered with Whatman No. 1 filter paper by the treatment filtrates with few drops of iodine in 2 to 3 drops of potassium iodide. The presence of brown reddish precipitates that pointed out the presence of alkaloids in the samples [17].

2.3.3. Tests for Phenols. In ferric chloride test, for the screening of phenol plant aqueous extracts, the phenol plant aqueous extracts were treated with 3-4 drops of ferric chloride solution. The appearance of bluish black color indicated the presence of phenols [18].

2.3.4. Tests for Phytosterols: Salkowski's Test. The test plant aqueous extracts were treated with chloroform and filtered with Whatman no. 1 filter paper. Few drops of concentrated sulphuric acid were added and then vortexed it and allowed to stand for some time. The golden yellow color indicated the presence of phytosterol [18].

2.3.5. Tests for Diterpenes. To observe the presence of diterpenes, the plant aqueous extracts were treated with 3-4 drops of copper acetate solution. Formation of emerald green color indicated the presence of diterpenes [18].

2.3.6. Tests for Saponins. For dilution about 2 ml of plant aqueous extracts were taken in test tube, in distilled water and vortexed it for 5 minutes. Foam produced and persisted for ten minutes indicated the presence of saponins [17].

2.3.7. Tests for Flavonoids. In the alkaline reagent test, for the presence of flavonoids, the plant aqueous extracts were treated with 2-3 drops of lead acetate solutions. The formation of intense yellow color, which becomes colorless on addition of dilute acid, indicated the presence of flavonoids [19].

2.4. Bioassay of *C. maculatus* Adults. The repellency effect of tested botanicals used against the beetles was assessed by using the area preference method [9]. In bioassays, 6 concentrations viz. 0.5, 1, 1.5, 2, 2.5, and 3% of aqueous extracts were used. Whatman No.1 filter paper was equally divided into 2 halves (about 7.2 cm diameter). First half portion of each filter paper was treated with the extract by using

TABLE 1: List of plant species and plant parts used in the experiment with *C. maculatus* during 2021.

Sr. no.	Common name	Botanical name	Family	Part used
1	Neem	<i>Azadirachta indica</i>	Meliaceae	Seed
2	Bakion	<i>Melia azedarach</i>	Meliaceae	Fruit
3	White Patta	<i>Nicotiana rustica</i>	Solanaceae	Leaf
4	Virginia tobacco	<i>Nicotiana tabacum</i>	Solanaceae	Leaf
5	Chinese arborvitae	<i>Thuja orientalis</i>	Cupressaceae	Fruit

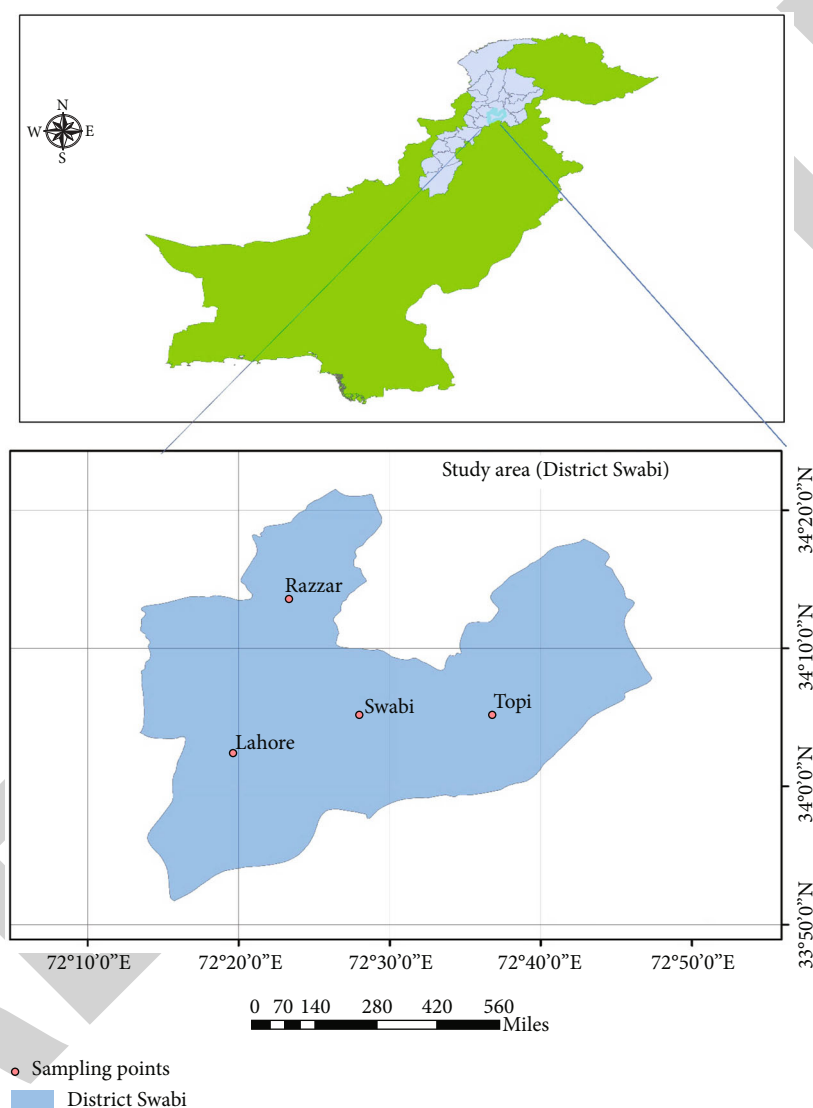


FIGURE 1: Location from which plant species collected during 2021.

micropipette, and the 2nd half portion of filter paper was treated with distilled water as a control. Each filter paper was air dried for about 30 minutes, till complete evaporation of solvent. The filter paper was then pasted length wise, edge wise with the help of masking tape and kept at the bottom of 16 cm diameter Petri dishes. Ten pairs of freshly emerged adult beetles (total of 20 per dish) were released at the center of the test arena in the Petri dishes and covered with muslin cloth and kept in an incubator at $27 \pm 2^\circ\text{C}$ and $65 \pm 5\%$ relative humidity. Total numbers of insects residing on treated

and untreated portions of filter paper were counted after 1, 2, 3, 6, 24, 48, 72, and 96 hours, and percent repellency (PR) was calculated by using the formula adopted by [20]

$$PR = \left[\frac{N_c - N_t}{N_c} \right] \times 100, \tag{1}$$

where N_c is the no. of insects counted in control and N_t is the no. of insects counted in treated.

TABLE 2: Repellency classes according to McDonald et al. [21].

Sr. no.	Class	&R1
1	0	>0.01-0.1
2	I	0.1-20
3	II	20.1-40
3	III	40.1-60
4	IV	60.1-80
5	V	80.1-100

1%R: percentage of repellency rate.

The botanicals were then categorized into different classes (as shown in Table 2), [21].

2.5. Statistical Analysis. The recorded data were subjected to analysis of variance (ANOVA) with two factors CRD (complete randomized design), and means were separated by using the least significant difference (LSD) test at 5% level of probability. Statistical analyses were carried out using STATISTIX 8.1 [22].

3. Results

3.1. Screening of Aqueous Extracts of Plants for Phytochemical Constituents. In this experiment, phytochemical constituents of five plant species were determined from their crude extracts (as shown in Table 3). It was clear from the results that all the phytochemical constituents were present in *M. azedarach*, with both phytosterol and phenol in moderate amount while the rest of phytochemicals were present in lower quantities. *A. indica* also exhibited all the phytochemicals in high quantities. Moreover, in *N. tabacum* all the phytochemicals were present, whereas diterpenes and phenols were present in high amount and the others in moderate quantities. In *N. rustica*, saponins were not present while, rest in low quantities. In *T. orientalis*, all the phytochemicals were present in low quantities.

3.2. Repellency. The settling response of *C. maculatus* was significantly ($P < 0.05$) affected by concentration. The adults of *C. maculatus* preferred the untreated arena (control) as compared with treated arena. The preference response of tested insects significantly declined with the increases in concentrations of extracts. The repellency of five different botanicals against *C. maculatus* were studied under controlled laboratory conditions, and result revealed different trends in different parameters which are explained as follows.

3.2.1. Mean Percent Repellency of *C. maculatus* after 1h Exposure Period. After one hour of exposure, highest repellency of *C. maculatus* was observed with *A. indica* (53.75 ± 4.26) ($df = 5$, $P < 0.05$, $F = 34.38$) which show class III repellency, while the lowest was recorded with *T. orientalis* (32.25 ± 0.75) which show class II repellency. An increasing trend in repellency was observed with the increase in concentration of botanicals (Figure 2).

3.2.2. Mean Percent Repellency of *C. maculatus* after 2h Exposure Period. The repellency of tested botanical against *C. maculatus* after two hours of exposure. *A. indica* showed

the highest repellency (57.5 ± 3.22) against *C. maculatus*, and the lowest repellency was observed with *T. orientalis* (41.25 ± 3.75) ($df = 5$; $P < 0.05$; $F = 34.38$) (Figure 3).

3.2.3. Mean Percent Repellency of *C. maculatus* after 3h Exposure Period. Result showed the highest repellency of *C. maculatus* against *A. indica* (60 ± 2.04) at 3% concentration, while the lowest repellency was observed against *T. orientalis* (51.5 ± 3.09) ($df = 5$; $P < 0.05$; $F = 49.98$) after the exposure period of 3 hours (Figure 4).

3.2.4. Mean Percent Repellency of *C. maculatus* after 6h Exposure Period. Results described the repellency of tested botanical insecticides against *C. maculatus* ($df = 5$; $P < 0.05$; $F = 49.33$). At 3% concentration after 6 hours of exposure, highest repellency (class IV repellency) was recorded in *A. indica* (66 ± 3.7). In comparison, the lowest repellency (class III repellency) was observed in *T. orientalis* (51.25 ± 2.39) (Figure 5).

3.2.5. Mean Percent Repellency of *C. maculatus* after 24h Exposure Period. After 24 hours of exposure at 3% concentration ($df = 5$; $P < 0.05$; $F = 54.07$), highest repellency was observed in *A. indica* (72.5 ± 2.5) and the lowest repellency was observed in *T. orientalis* (60.25 ± 2.25) (Figure 6).

3.2.6. Mean Percent Repellency of *C. maculatus* after 48h Exposure Period. After 48 hours of exposure, the repellency effect of different concentration of selected plant extract presented (Figure 7) ($df = 5$; $P < 0.05$; $F = 109.38$). Results revealed the highest repellency (class V repellency) at 3% concentration in *A. indica* (85 ± 2.04) while the lowest repellency was observed in *T. orientalis* (70 ± 2.04) (class IV repellency).

3.2.7. Mean Percent Repellency of *C. maculatus* after 72h Exposure Period. After 72 hours of exposure ($df = 5$; $P < 0.05$; $F = 104.80$), *A. indica* (91.25 ± 1.49) showed the highest repellency (class V repellency), while the lowest repellency (class III repellency) was recorded in *T. orientalis* (75 ± 3.53) at 3% concentration (Figure 8).

3.2.8. Mean Percent Repellency of *C. maculatus* after 96h Exposure Period. After 96 hours ($df = 5$; $P < 0.05$; $F = 123.10$), the repellency effect of tested plant extract against *C. maculatus* was significantly presented. Decreasing trend in repellency was observed after 72 hours of exposures; however, the highest repellency (class V repellency) was observed in *A. indica* (86.25 ± 1.75) and lowest repellency (class III repellency) was observed in *T. orientalis* (57.5 ± 1.44) at 3% concentration (Figure 9).

4. Discussion

Entomologists and pest controllers around the world are using plant-based insecticides increasingly frequently, most likely as a result of public awareness of the risks connected with many chemical pesticides. However, the method of extraction, the section of the plant used, and the type of solvent employed for their extraction all directly or indirectly affect the efficiency of many botanical insecticides [23].

TABLE 3: Phytochemical composition of crude extracts of five plant species during 2021.

Plant species	Phytochemical constituents of five plant species					
	Alkaloids	Flavonoids	Saponins	Diterpenes	Phytosterol	Phenols
<i>A. indica</i>	+++	+++	++	++	+++	+++
<i>N. tabacum</i>	++	++	++	+++	++	+++
<i>M. azedarach</i>	+	+	+	+	++	++
<i>N. rustica</i>	+	+	—	+	+	+
<i>T. orientalis</i>	+	+	+	+	+	+

+++; highly present; ++: moderately present; +: low present; -: not present.

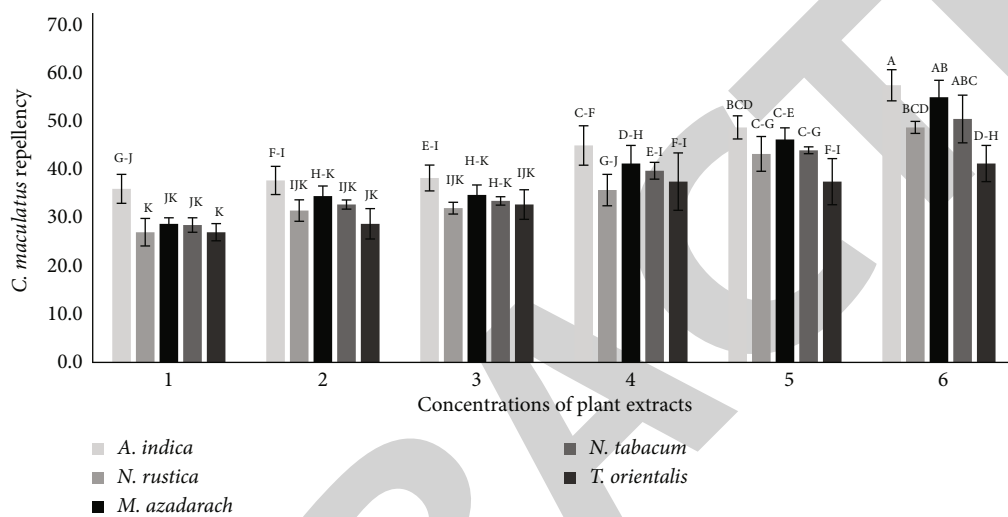


FIGURE 2: Mean percent repellency of *C. maculatus* after 1-hour exposure period treated with six different concentrations of crude extracts of five plant species.

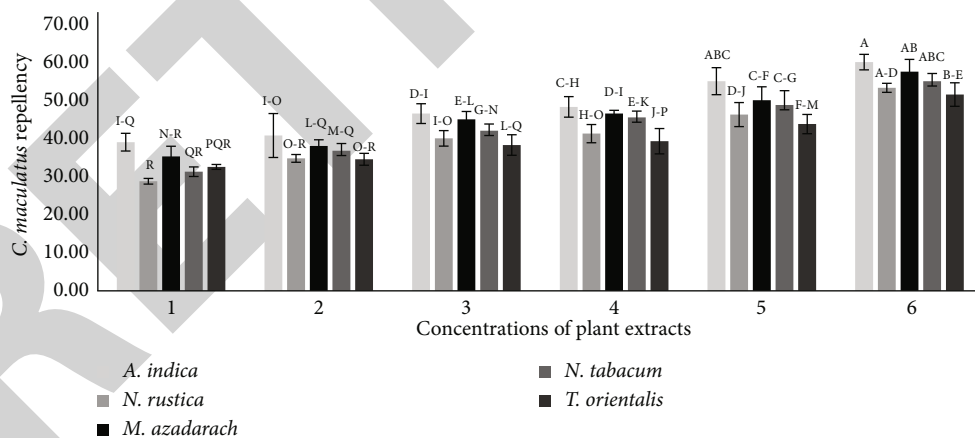


FIGURE 3: Mean percent repellency of *C. maculatus* after 2-hour exposure period treated with six different concentrations of crude extracts of five plant species.

Different solvents' polarities may result in variations in how well they extract the active ingredient found in botanicals. Present experiments based on phytochemicals in five plants species yielded variable results. All the phytochemicals were found in all the five plant species. Some earlier researchers have reported results similar to the current study, such as [24] reported that the aqueous extract of *N. tabacum* leaves tested positive for alkaloids, tannins, flavonoids, steroids, car-

diac glycosides, essential oils, resins, and polypeptides. [25] stated that tobacco leaves contain nicotine, as we know that nicotine is an alkaloid which is the most biologically active component of tobacco. Alkaloids, being one of the largest group of phytochemicals in plants have pronounced effect on humans which have led to development of pain killer medication [26]. Moreover, these alkaloids have also been act as insect repellents as mentioned by [27]. According to [28], A.

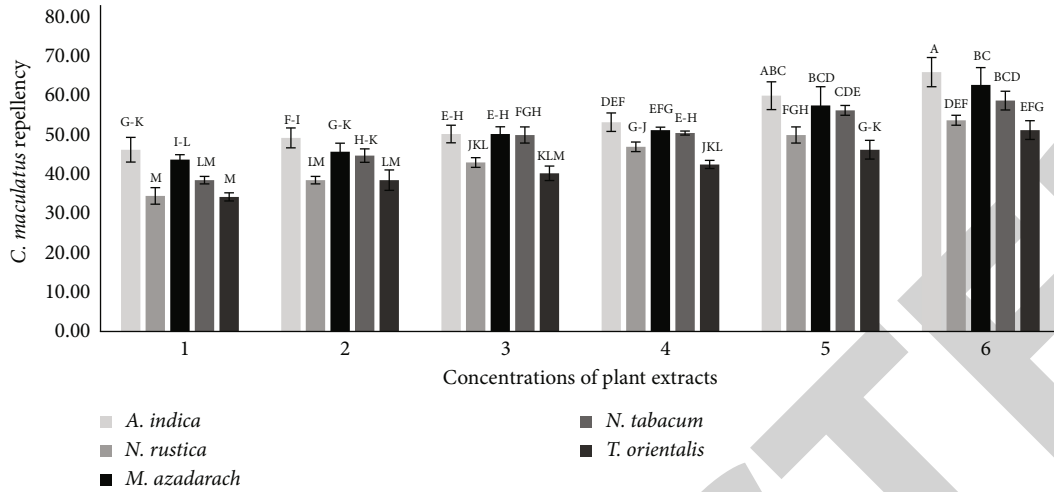


FIGURE 4: Mean percent repellency of *C. maculatus* after 3-hour exposure period treated with six different concentrations of crude extracts of five plant species.

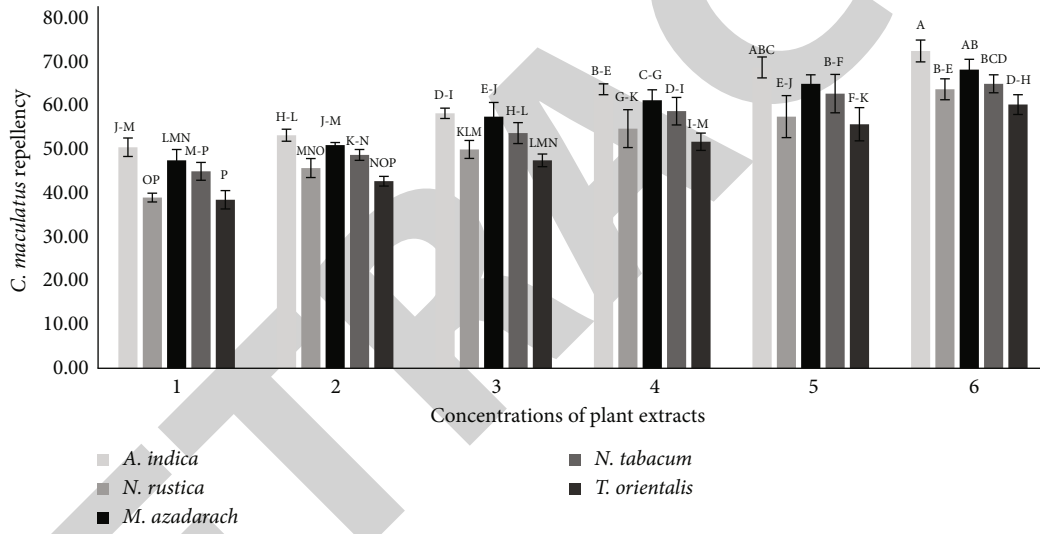


FIGURE 5: Mean percent repellency of *C. maculatus* after 6-hour exposure period treated with six different concentrations of crude extracts of five plant species.

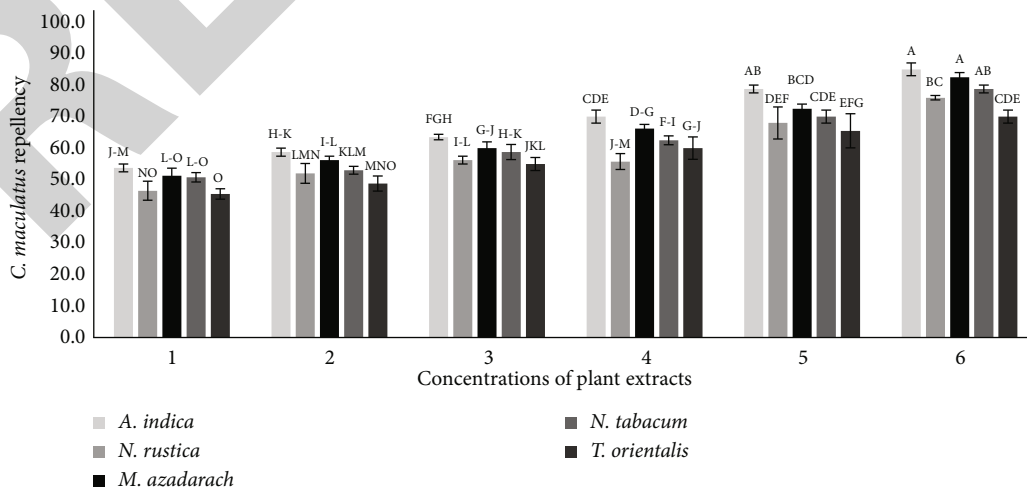


FIGURE 6: Mean percent repellency of *C. maculatus* after 24-hour exposure period treated with six different concentrations of crude extracts of five plant species.

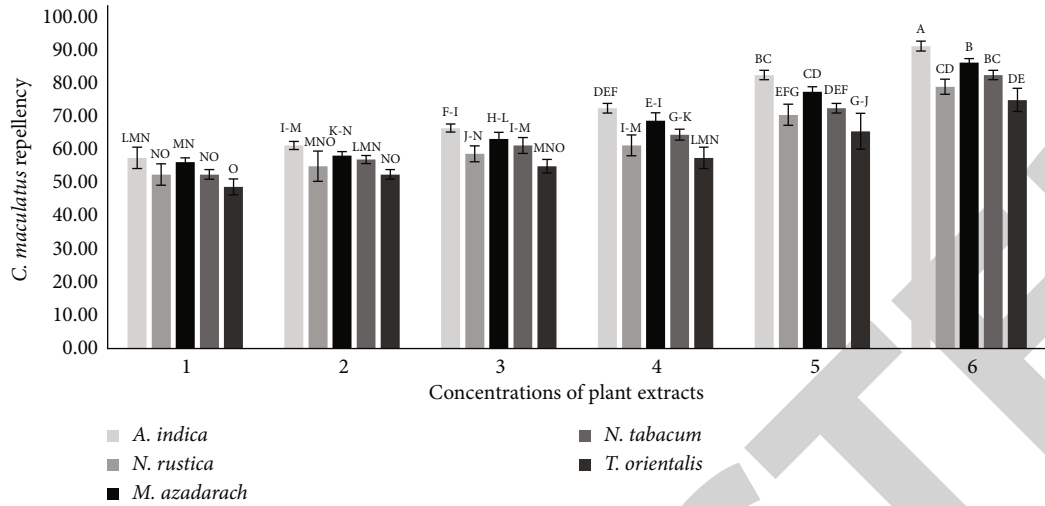


FIGURE 7: Mean percent repellency of *C. maculatus* after 48-hour exposure period treated with six different concentrations of crude extracts of five plant species.

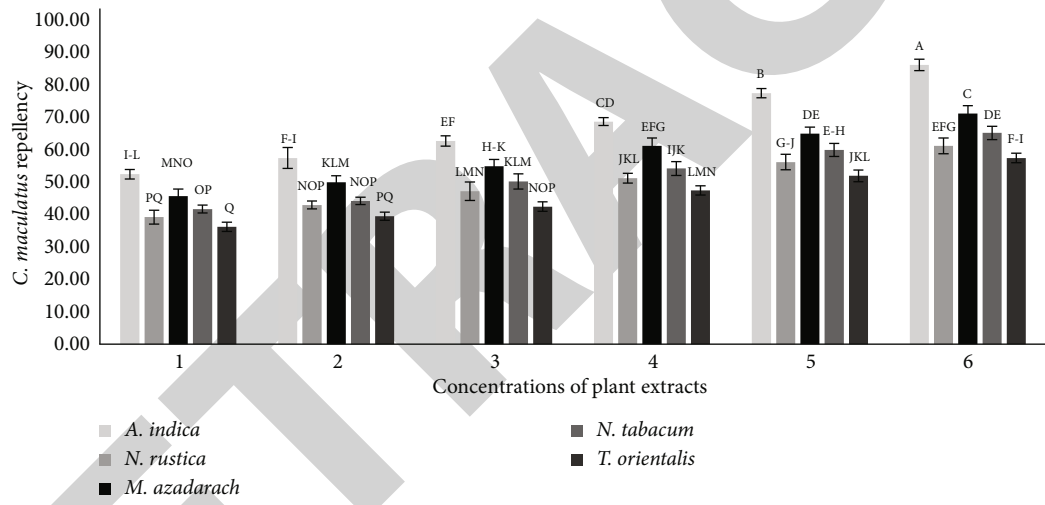


FIGURE 8: Mean percent repellency of *C. maculatus* after 72-hour exposure period treated with six different concentrations of crude extracts of five plant species.

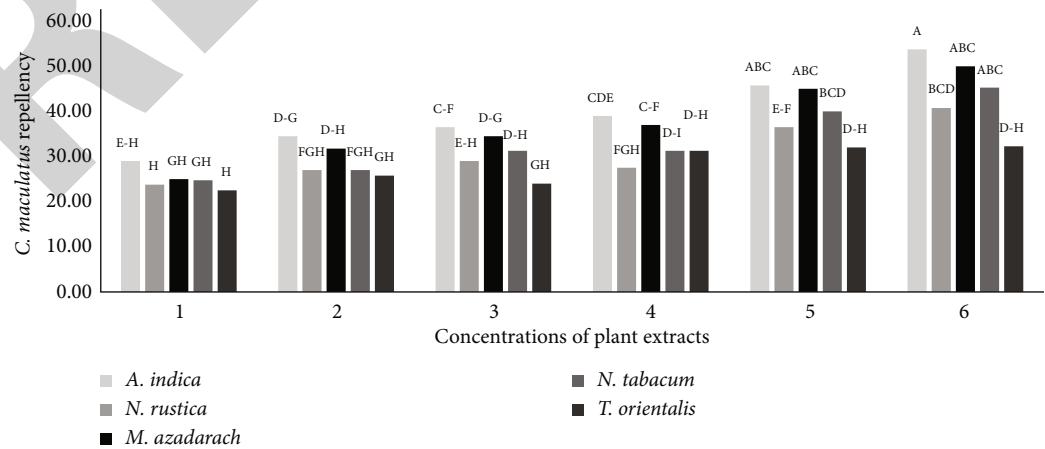


FIGURE 9: Mean percent repellency of *C. maculatus* after 96-hour exposure period treated with six different concentrations of crude extracts of five plant species.

indica crude extracts showed the presence of alkaloids, glycosides, flavonoids, saponins, tanins, and phenolic compounds. In the present research, crude extracts of *M. azedarach* indicated high presence of terpenoids, saponins, flavonoids, and phenols. [29] yielded results similar to our findings. According to [30], crude extracts of *M. azedarach* gave phenols, flavonoids, tannins, alkaloids, terpenoids, and saponins.

Outcomes of the present studies are consistent with [31] who also reported the highest repellency of *A. indica* against *T. castaneum*, with decreasing trend with the passage of time. Our results also agreed with some earlier researcher [32, 33] that *A. indica* repels insect and causes them to stop their feeding. Neem extracts contain azadirachtin and salannin that function as insect feeding deterrent. [34, 35] also reported the use of *A. indica* for the control different foliage pests. In case of *M. azedarach*, our results are in agreement with [36] who also reported that the repellency effect of *M. azedarach* decreases after the 72-hour exposure period. Research carried out worldwide during the last three decades have also shown significant repellency effect of the *M. azedarach* for the management of stored product pests [30]. Tobacco (*N. tabacum* and *N. rustica*) is traditionally known as a natural insecticide [37]. In our studies, we observed 82% repellency in *N. tabacum* and 76% in *N. rustica* against *C. maculatus* at 3% concentration. Our results are agreed with [38] who recorded similar repellency trend as in our study (increases repellency at increased concentration of plant extracts. This result also coincides with the findings of [39] who also reported the maximum repellency in *N. tabacum* at high concentration against *T. castaneum*. Nicotiana species contain nicotine which is an alkaloid act as a potent insecticide that bind the acetylcholine receptor and affect the nerve transmission that act as a feeding deterrent. In our study, among the tested botanicals, the lowest repellency was observed in *T. orientalis* against *C. maculatus*. Our results are in contradiction with the findings of [40] who observed high repellency (92%) in *T. orientalis* against *Tribolium confusum*. Difference in results might be due to the different plant parts used for the extraction that have different percentage compositions of the ingredients [41]. The insecticidal constituents of many plant extracts and essential oils are mainly monoterpenoids [42]. Monoterpenoids are typically volatile and rather lipophilic compounds that can penetrate into insects rapidly and interfere with their physiological functions [43]. Due to their high volatility, they have fumigant activity that might be of importance for controlling stored product insects [44]. Studies carried out worldwide during last the three decades have significantly extended our knowledge on botanical pesticides. Many plant-derived natural products active against insect could be produced from locally available raw materials, perhaps in many cases right at the site of usage, so as to be relatively inexpensive [43]. In this study, pure liquid extract of *A. indica* and *M. azedarach* was effective at managing the population of *C. maculatus*. It may therefore be one of the alternative control options in our immediate environment. The natural phytochemicals from Plants have potential being ecofriendly can replace synthetic pesticides for the insect pests [45]. Nevertheless, despite their efficiency, the extracts have no negative

impact on the stored pulses. Consequently, these plant extracts may be utilized to help reduce the number of *C. maculatus*.

5. Conclusion

It is reported that the utilization of phytochemicals is eco-friendly, socially acceptable, and economically feasible approach for the management and biocontrol of *C. maculatus*. Based on our result, it can be concluded that *A. indica* and *M. azedarach* at all concentration might serves as alternative to insecticides in rural areas of tropic and subtropic region. The promising and effective repellency of these botanicals suggesting that these botanicals as a potential candidate agent against the *C. maculatus* and can be recommended for their integration with other control strategies that will reduced environmental pollution and health hazards problems. Moreover, use of these plant extracts can open new avenue for the management of *C. maculatus*.

Data Availability

Data is included in the article.

Additional Points

Novelty of the Study. This laboratory work evaluated the anti-insect potential of local plant species from District Swabi and Haripur, Khyber Pakhtunkhwa of Pakistan, against destructive insect pest of stored grain, i.e., *Callosobruchus maculatus*. Bioassays revealed that water extracts of *A. indica*, *M. azedarach*, *N. rustica*, *N. tabacum*, and *T. orientalis* at various concentrations particularly at 3% and exhibited considerable repellency of insect pest individuals suggesting their biocidal potential against this insect pest.

Conflicts of Interest

The authors declare no conflict of interest.

Acknowledgments

The authors extend their appreciation to the Researchers supporting project number (RSP-2021/367), King Saud University, Riyadh, Saudi Arabia.

References

- [1] W. R. Tavares, M. D. C. Barreto, and A. M. L. Seca, "Aqueous and ethanolic plant extracts as bio-insecticides— establishing a bridge between raw scientific data and practical reality," *Plants*, vol. 10, no. 5, pp. 920–929, 2021.
- [2] K. D. Singh, A. J. Mobolade, R. Bharali, D. Sahoo, and Y. Rajashekar, "Main plant volatiles as stored grain pest management approach: a review," *Journal of Agriculture and Food Research*, vol. 4, article 100127, 2021.
- [3] U. C. Arakere, S. Jagannath, S. Krishnamurthy, S. Chowdappa, and N. Konappa, "Microbial bio-pesticide as sustainable solution for management of pests: achievements and prospects," *Biopesticides*, vol. 2, pp. 183–200, 2022.
- [4] S. Sekender, S. Sultana, T. Akter, and S. Begum, "Susceptibility of different stored pulses infested by pulse beetle,

- Callosobruchus chinensis (Lin.),” *Dhaka University Journal of Biological Sciences*, vol. 29, no. 1, pp. 19–25, 2020.
- [5] S. Gupta, S. D. Apte, G. Post, G. College, and M. P. Khargone, “Influence of storage containers on *Callosobruchus maculatus* (Fab.) infesting green gram,” *Archives of Applied Science Research*, vol. 8, no. 8, pp. 21–23, 2016.
- [6] W. Demis and E. Yenewa, “Review on major storage insect pests of cereals and pulses,” *Asian Journal of Advances in Research*, vol. 1, no. 1, pp. 41–56, 2022.
- [7] U. Zafar, D. I. Khan, M. Mamoon-Ur-Rashid, and M. Shah, “Entomotoxicity of plant powders against pulse beetle (*Callosobruchus chinensis*) on stored mung bean (*Vigna radiata*),” *Journal of Entomology and Zoology Studies*, vol. 6, no. 1, pp. 1637–1641, 2018.
- [8] L. A. Tapondjou, C. Adler, H. Bouda, and D. A. Fontem, “Efficacy of powder and essential oil from *Chenopodium ambrosioides* leaves as post-harvest grain protectants against six-stored product beetles,” *Journal of Stored Products Research*, vol. 38, no. 4, pp. 395–402, 2002.
- [9] R. Akbar and I. A. Khan, “Toxicity of five plant extracts against *Fallosobruchus maculatus* Fab. (Coleoptera Bruchidae) a major insect pest of stored pulses,” *Fresenius Environmental Bulletin*, vol. 30, no. 5, pp. 5098–5107, 2021.
- [10] G. M. W. Lengai, J. W. Muthomi, and E. R. Mbega, “Phytochemical activity and role of botanical pesticides in pest management for sustainable agricultural crop production,” *Scientific African*, vol. 7, article e00239, 2020.
- [11] M. Özkara, D. Akyil, and M. Konuk, “Pesticides, environmental pollution, and health,” in *Environmental health risk-hazardous factors to living species*, p. 27, IntechOpen, 2016.
- [12] F. Jian, “Influences of stored product insect movements on integrated pest management decisions,” *Insects*, vol. 10, no. 4, p. 100, 2019.
- [13] H. A. Raza, R. M. Amir, M. A. Idrees et al., “Residual impact of pesticides on environment and health of sugarcane farmers in Punjab with special reference to integrated pest management,” *Journal Global Innovation Agriculture Social Science*, vol. 7, no. 2, pp. 79–84, 2019.
- [14] G. Vijayalakshmi, K. Elango, E. A. P. Vasanthi et al., “Insecticidal, oviposition deterrent and antifeedant property of certain plant extracts against pulse beetle, *Callosobruchus chinensis* Linn. (Coleoptera: Bruchidae),” *Legume Research*, vol. 44, no. 11, pp. 1386–1391, 2021.
- [15] M. Suleman, S. Nouren, S. M. Hassan et al., “Vitality and implication of natural products from *viburnum grandiflorum*: an eco-friendly approach,” *Polish Journal of Environmental Studies*, vol. 27, no. 3, pp. 1407–1411, 2018.
- [16] C. Y. Hamany Djandé, L. A. Piater, P. A. Steenkamp, N. E. Madala, and I. A. Dubery, “Differential extraction of phytochemicals from the multipurpose tree, *Moringa oleifera*, using green extraction solvents,” *South African Journal of Botany*, vol. 115, pp. 81–89, 2018.
- [17] S. Snigdha, M. Ravish, G. Narayan, N. Manisha, K. Nilotpol, and D. Kishore, “Phytochemical analysis of papaya leaf extract: screening test,” *EC Dental Science*, vol. 18, no. 3, pp. 485–490, 2019.
- [18] R. P. Senthilkumar, V. Bhuvaneshwari, V. Malayaman, R. Ranjithkumar, and S. Sathiyavimal, “Phytochemical screening of aqueous leaf extract of *Sida acuta* Burm. F. and its antibacterial activity,” *Journal of Emerging Technologies and Innovative Research*, vol. 5, no. 8, pp. 474–478, 2018.
- [19] S. Nathenial, A. Fatima, R. Fatima et al., “Phytochemical study of acetone solvent extract of *Coriander sativum*,” *Journal of Pharmacognosy and Phytochemistry*, vol. 8, no. 6, pp. 136–140, 2019.
- [20] D. Obeng-Ofori, “Plant oils as grain protectants against infestations of *Cryptolestes pusillus* and *Rhyzopertha dominica* in stored grain,” *Entomologia Experimentalis et Applicata*, vol. 77, no. 2, pp. 133–139, 1995.
- [21] L. McDonald, R. Guy, and R. Speirs, “Preliminary evaluation of new candidate materials as toxicants, repellents and attractants against stored product insects,” in *Marketing Research Repertory*, vol. 882, p. 183, Agriculture Reserve Service, US Department of Agriculture, Washington, 1970.
- [22] R. G. D. Steel, J. H. Torrie, and D. A. Dickey, “Principles and Procedures of Statistics,” in *Principles and Procedures of Statistics*, McGraw-Hill, New York, 2nd edition, 1980.
- [23] O. M. Obembe and O. C. Ogungbite, “Entomotoxic effect of tobacco seed extracted with different solvents against *Callosobruchus maculatus* infesting stored cowpea,” *International Journal of Entomology Research*, vol. 1, no. 1, pp. 22–26, 2016.
- [24] Y. Sharma, A. Kaur, R. Bhardwaj et al., “Preclinical assessment of stem of *Nicotiana tabacum* on excision wound model,” *Bioorganic Chemistry*, vol. 109, article 104731, 2021.
- [25] S. P. Kernodle, S. Webb, T. M. Steede, and R. S. Lewis, “Combined reduced expression of two gene families lowers nicotine content to ultra-low levels in cultivated tobacco,” in *Plant Cell Reports*, Springer, 2022.
- [26] T. Behl, G. Rocchetti, S. Chadha et al., “Phytochemicals from plant foods as potential source of antiviral agents: an overview,” *Pharmaceuticals*, vol. 14, no. 4, 2021.
- [27] R. Nirola, M. Megharaj, A. Subramanian et al., “Analysis of chromium status in the revegetated flora of a tannery waste site and microcosm studies using earthworm *E. fetida*,” *Environmental Science and Pollution Research*, vol. 25, no. 6, pp. 5063–5070, 2018.
- [28] R. Kumar, S. Sharma, and L. Devi, “Investigation of total phenolic, flavonoid contents and antioxidant activity from extracts of *Azadirachta indica* of Bundelkhand region,” *International Journal of Life-Sciences Scientific Research*, vol. 4, no. 4, pp. 1925–1933, 2018.
- [29] J. Iqbal, A. Qayyum, and S. Z. Mustafa, “Repellent effect of ethanol extracts of plant materials on *Tribolium castaneum* (Herbst) (Tenebrionidae: Coleoptera),” *Pakistan Journal of Zoology*, vol. 42, no. 1, pp. 81–86, 2010.
- [30] I. Naimi, M. Zefzoufi, H. Bouamama, and T. B. M’hamed, “Chemical composition and repellent effects of powders and essential oils of *Artemisia absinthium*, *Melia azedarach*, *Trigonella foenum-graecum*, and *Peganum harmala* on *Tribolium castaneum* (Herbst) (Coleoptera: Tenebrionidae),” *Industrial Crops and Products*, vol. 182, article 114817, 2022.
- [31] M. Berhe, S. Dugassa, S. Shimelis, and H. Tekie, “Repellence and larvicidal effects of some selected plant extracts against adult *Anopheles arabiensis* and *Aedes aegypti* larvae under laboratory conditions,” *International Journal of Tropical Insect Science*, vol. 41, no. 4, pp. 2649–2656, 2021.
- [32] R. C. Lima, M. F. Almeida, A. de Sousa Freitas et al., “Effect of the aqueous extract of neem leaves (*Azadirachta indica* A. Juss.) on the control of *Costalimaita ferruginea* (Fabricius, 1801),” *Annual Research & Review in Biology*, vol. 36, no. 9, pp. 31–37, 2021.
- [33] S. E. Atawodi and J. C. Atawodi, “*Azadirachta indica* (neem): a plant of multiple biological and pharmacological activities,” *Phytochemistry Reviews*, vol. 8, no. 3, pp. 601–620, 2009.

Retraction

Retracted: Inter-Relationship Between a Transcriptional Regulator of Flagella Genes *cj0440c* and Thiamine Metabolic Pathway in *Campylobacter jejuni*

BioMed Research International

Received 8 January 2024; Accepted 8 January 2024; Published 9 January 2024

Copyright © 2024 BioMed Research International. This is an open access article distributed under the Creative Commons Attribution License, which permits unrestricted use, distribution, and reproduction in any medium, provided the original work is properly cited.

This article has been retracted by Hindawi following an investigation undertaken by the publisher [1]. This investigation has uncovered evidence of one or more of the following indicators of systematic manipulation of the publication process:

- (1) Discrepancies in scope
- (2) Discrepancies in the description of the research reported
- (3) Discrepancies between the availability of data and the research described
- (4) Inappropriate citations
- (5) Incoherent, meaningless and/or irrelevant content included in the article
- (6) Manipulated or compromised peer review

The presence of these indicators undermines our confidence in the integrity of the article's content and we cannot, therefore, vouch for its reliability. Please note that this notice is intended solely to alert readers that the content of this article is unreliable. We have not investigated whether authors were aware of or involved in the systematic manipulation of the publication process.

Wiley and Hindawi regrets that the usual quality checks did not identify these issues before publication and have since put additional measures in place to safeguard research integrity.

We wish to credit our own Research Integrity and Research Publishing teams and anonymous and named external researchers and research integrity experts for contributing to this investigation.






The corresponding author, as the representative of all authors, has been given the opportunity to register their agreement or disagreement to this retraction. We have kept a record of any response received.

References

- [1] M. A. B. Shabbir, A. Ul-Rahman, A. R. Khalid et al., "Inter-Relationship Between a Transcriptional Regulator of Flagella Genes *cj0440c* and Thiamine Metabolic Pathway in *Campylobacter jejuni*," *BioMed Research International*, vol. 2022, Article ID 4539367, 10 pages, 2022.

Research Article

Inter-Relationship Between a Transcriptional Regulator of Flagella Genes *cj0440c* and Thiamine Metabolic Pathway in *Campylobacter jejuni*

Muhammad Abu Bakr Shabbir ¹, Aziz Ul-Rahman,² Abdur Rauf Khalid,³ Nabeel Ijaz,⁴ Muhammad Tahir Aleem,⁵ Saeed Ahmed ⁶, Abdulaziz Alouffi ⁷, Waqas Ahmed,⁸ Faiza Aslam,⁹ Muhammad Kashif Maan,¹⁰ Adnan Hassan Tahir,¹¹ Muhammad Waqar Aziz,¹ Mashal M. Almutairi ¹² and Haihong Hao ¹³

¹Institute of Microbiology, University of Veterinary and Animal Sciences Lahore, 54600, Pakistan

²Department of Pathobiology, Faculty of Veterinary and Animal Sciences, MNS University of Agriculture, Multan 66000, Pakistan

³Department of Livestock and Poultry Production, Faculty of Veterinary Sciences, Bahauddin Zakariya University, Multan, Pakistan

⁴Department of Clinical Sciences, Faculty of Veterinary Sciences, Bahauddin Zakariya University, Multan, Pakistan

⁵MOE Joint International Research Laboratory of Animal Health and Food Safety, College of Veterinary Medicine, Nanjing Agricultural University, Nanjing 210095, China

⁶Department of Biological Sciences, National University of Medical Sciences (NUMS), Islamabad, Pakistan

⁷King Abdulaziz City for Science and Technology, Riyadh 12354, Saudi Arabia

⁸Department of Biomedical and Diagnostic Science, University of Tennessee Knoxville, USA

⁹Livestock and Dairy Development Department, Lahore 54000, Pakistan

¹⁰Department of Veterinary Surgery and Pet Sciences, Faculty of Veterinary Science, University of Veterinary and Animal Sciences, Lahore, Pakistan

¹¹Department of Clinical Sciences, Faculty of Veterinary and Animal Sciences, PMAS-Arid Agriculture University Rawalpindi, Pakistan

¹²Department of Pharmacology and Toxicology, College of Pharmacy, King Saud University, Riyadh 11451, Saudi Arabia

¹³MOA Laboratory for Risk Assessment of Quality & Safety of Livestock & Poultry Products, Huazhong Agricultural University, Wuhan 430070, China

Correspondence should be addressed to Mashal M. Almutairi; mmalmutairi@ksu.edu.sa and Haihong Hao; haohaihong@mail.hzau.edu.cn

Received 9 June 2022; Accepted 20 July 2022; Published 21 August 2022

Academic Editor: Fu-Ming Tsai

Copyright © 2022 Muhammad Abu Bakr Shabbir et al. This is an open access article distributed under the Creative Commons Attribution License, which permits unrestricted use, distribution, and reproduction in any medium, provided the original work is properly cited.

Campylobacter jejuni is a major cause of gastroenteritis in humans. It has been reported that the pathogenesis of *C. jejuni* is closely related to the formation, adhesion, and invasion of flagella toxin in host epithelial cells. A putative transcriptional regulator, known as *cj0440c*, is thought to be involved in the regulation of flagellar synthesis. However, confirmation of this hypothesis requires deep insight into the regulation mechanism of *cj0440c* and its possible relationship with different antibiotics. Therefore, the study explained here was designed to determine the relationship and function (phenotypically and genotypically) of *cj0440c* in the flagellar synthesis of *C. jejuni* NCTC11168. The study determined the mode of expression of *cj0440c* and flagella-related genes under exposure to various drugs. To verify the involvement of *cj0440c* protein in the metabolic pathway of thiamine, an enzymatic hydrolysis experiment was performed and analyzed through the application of mass spectrometry. The overexpression vector of *C. jejuni* NCTC11168 was also constructed to find out whether or not target genes were regulated by *cj0440c*. The findings of the study showed that *cj0440c* and other flagella-related genes were expressed

differentially under the influence of various antibiotics including erythromycin, tylosin, azithromycin, gentamicin, etimicin, enrofloxacin, gatifloxacin, tetracycline, and tigecycline. The analysis showed that the *cj0440c* protein did not catalyze the degradation of thiamine. In conclusion, the study aids in the understanding of the inter-relationship between the regulatory mechanism of flagella genes and the thiamine metabolic pathway.

1. Introduction

Campylobacter jejuni (*C. jejuni*) is a pathogenic bacterium that is considered a major cause of food-borne diarrhea around the globe [1]. It is estimated that more than 400 million people each year are exposed to these bacteria and, as a consequence, develop gastroenteritis [2]. Humans may be infected via the consumption of contaminated poultry meat, milk, or water [3, 4]. Outbreaks of *C. jejuni* infection in humans are relatively rare. However, *Campylobacter* infection has serious consequences in those with autoimmune-mediated diseases such as Guillain-Barre syndrome and Miller-Fisher syndrome [5]. It has been found that the pathogenesis of *Campylobacter* is closely related to the formation, adhesion, and invasion of the toxin of the flagella in the host epithelial cells [6]. The motility of the flagella helps the bacteria to cross the membrane of intestinal epithelial cells [7]. Therefore, the role of flagella in *C. jejuni* virulence should not be underestimated.

The synthesis of *C. jejuni* flagella is a complex process; more than 50 genes such as *flgS* (*Cj0793*), *flgR* (*Cj1024*), and *fliA* (*Cj0061*) are involved in their synthesis and regulation [8]. Three sigma factors (σ^{70} , σ^{54} , and σ^{28}) are involved in the regulation of flagellar synthesis in *C. jejuni*. However, research on the regulatory mechanism of flagella has focused on the deletion mutation of known genes, and information is scarce regarding the *cj0440c* gene. Bioinformatic analysis reveals that *cj0440c* is a putative transcriptional regulator that encodes a TEN/THI-4 protein family, but the molecular function of this family has not been determined. This gene (*cj0440c*) is present upstream of *cj0441* (which creates an acyl carrier protein, *acpP*) [9] and downstream of the *cj0437-cj0439* operon, which plays a pivotal role in the susceptibility of *Campylobacter* to hydrogen peroxide (H_2O_2) [10, 11]. Hence, genes that lie both upstream and downstream of *cj0440c* are essential for *Campylobacter's* survival, growth, colonization, and pathogenesis. Although the *cj0440c* gene is present at opposite ends of the DNA coding strand, it can be divergently transcribed with its up-and-downstream genes and probably acts as a transcriptional regulator for several genes that are involved in the biosynthesis of flagella. However, the biological functions of *cj0440c* in *C. jejuni* are mostly unknown.

Due to the involvement of the *cj0440c* gene in the regulation of flagellar synthesis and the lack of information on the possible influence of antibiotic resistance, the study explained here was designed to determine the relationship and function (phenotypically and genotypically) of *cj0440c* in the flagellar synthesis of *C. jejuni* NCTC11168. To achieve that, the expression of *cj0440c* and other flagella genes during exposure to eight different kinds of antibiotics was detected through the use of reverse-transcription polymerase chain reaction (RT-PCR) preliminarily to detect the rela-

tionship between *cj0440c* and flagella genes. The *cj0440c* protein was expressed and purified, and a digestion experiment was designed that employed thiamine as the substrate to determine whether or not *cj0440c* was a thiaminase and can regulate directly the expression of flagella genes.

2. Materials and Methods

2.1. Bacterial Strains, Plasmids, and Culture Conditions. The *C. jejuni* NCTC11168 strain that was designated as sensitive (S) was obtained from the Chinese Centre for Disease Control and Prevention. The *Escherichia coli* strains and plasmids that were used in this study and their sources are listed in Table 1. *Campylobacter* strains were grown on plates that contained Skirrow *Campylobacter* selective agar (Hopebio, Qingdao, China) and were supplemented with 5% sterile defibrinated sheep blood at 42 °C under a micro-aerobic environment (85% N_2 , 10% CO_2 , and 5% O_2). The *C. jejuni* NCTC11168 strain that was designated as resistant (R), which was resistant to different kinds of antibiotics, was procured from our laboratory (the China Ministry of Agriculture Laboratory for Risk Assessment of Quality and Safety of Livestock and Poultry Products, Huazhong Agricultural University, Wuhan, China). *E. coli* cells were grown at 37 °C in a shaking incubator (200 rpm) in Luria-Bertani (LB) medium. When necessary, LB media were supplemented with kanamycin (30 $\mu g/ml$) or ampicillin (100 $\mu g/ml$).

2.2. Antimicrobial Susceptibility Assessment. The minimal inhibitory concentrations (MICs) of S and R against nine commercially available and frequently practiced antimicrobials, which were erythromycin (Ery), tylosin (Tyl), azithromycin (Azi), gentamicin (Gen), etimicin (Eti), enrofloxacin (Enr), gatifloxacin (Gati), tetracycline (Tet), and tigecycline (Tige), were determined by use of the broth microdilution susceptibility method, as described previously by the Clinical and Laboratory Standards Institute [12]. *C. jejuni* ATCC33560 was used as the quality control strain. The experiment was performed in triplicate.

The mutant prevention concentration (MPC) was defined as the lowest concentration of drug that prevented bacterial colony formation in a culture that contained $>10^{10}$ bacteria. The determination was similar to that for the MIC, except that $>10^{10}$ cells were tested at high drug concentrations (from 1 MIC to 128 MIC) and agar plates were used. Inoculated plates were incubated for 72 h. The minimum drug concentration that led to nonbacterial growth was the provisional MPC (MPC_{pr}). The mutant selection window (MSW) was the drug concentration range between the MIC and the MPC.

2.3. Detection of Expression of Flagella Genes in *C. jejuni* by RT-PCR. Both strains (S and R) were induced by the

TABLE 1: Bacterial strain and plasmid used in the present study.

Name	Description
Bacterial strain	
NCTC 11168	<i>Campylobacter jejuni</i> NCTC 11168 (S)
NCTC 11168	<i>Campylobacter jejuni</i> NCTC 11168 (R)
ATCC 33560	<i>Campylobacter jejuni</i> ATCC 33560
DH5 α	<i>E. coli</i> strain for DNA manipulation
BL21	<i>E. coli</i> strain for DNA manipulation
Plasmid	
pRY112	Cm-resistant <i>C. jejuni</i> / <i>E. coli</i> vector
pMD19-T simple	Amp-resistant <i>E. coli</i> vector
pET28-a	Km-resistant <i>E. coli</i> vector

addition of 0.5MPC of each of the eight antibiotics. The total RNA from each sample was extracted using the RNAPrep pure cell/bacteria kit (Tiangen Biotech, Beijing, China). The quality and quantity of the RNA were determined by the application of formaldehyde denaturing gel electrophoresis and the use of a Nanodrop TM 2000 Spectrophotometer (Thermo Fisher Scientific, Waltham, MA, USA). The cDNA was synthesized from the extracted RNA using a HiScript II one-step RT-PCR kit (Nanjing Vazyme Biotech Co, Nanjing, China).

The batches of cDNA of nine antibiotic-resistant bacteria and standard bacteria were subjected to RT-PCR to determine the expression of the flagellar genes, according to a previously described study [13]. Briefly, the PCR amplification was performed in the IQ5 Multicolor Real-time PCR Detection System (Bio-Rad Laboratories, Hercules, CA, USA). The cycling conditions were as follows: 3 min of pre-incubation at 95°C, followed by 45 cycles of 10s at 95°C and 40s at 52°C. The primer sets used for specific genes (*cj0440c*, *cj1339c*, *cj1338c*, *cj0043*, *cj0697*, and 16S) are listed in Table 2. It was decided to use 16S rDNA as an internal control for normalization. The experiment was performed in triplicate to obtain an average value for the fold change. A *t*-test was performed to analyze the significant difference between resistant bacteria and standard bacteria.

2.4. Construction of *cj0440c* Overexpression Mutants in *C. jejuni* NCTC11168. The DNA fragment of the *cj0440c* gene and promoter *CmeABC* was amplified from the *C. jejuni* NCTC11168 genome using Taq polymerase (Takara, Kusatsu, Shiga, Japan) with primers of *cj0440c*-F/R and *CmeABC*-F/R (Table 2). The *cj0440c*-F/R carried endonuclease restriction sites of *Sac* I and *Sac* II, while *CmeABC*-F/R carried endonuclease restriction sites of *Sac* I and *Spe* I. PCRs were performed in a total volume of 20 μ l using 0.5 μ l of each primer (10 μ M), 2 μ l of Taq polymerase buffer (10 \times), 1.6 μ l of deoxynucleoside triphosphates (2.5 mM), 0.2 μ l of Taq polymerase, and 200 ng of DNA template. The amplification program was as follows: initial denaturation at 95°C for 5 min, denaturation at 95°C for 30s, and annealing at 52°C for 30s, followed by 35 cycles of extension at 72°C for 1 min and an additional final extension at 72°C

for 5 min. PCR products were evaluated on a 1% agarose gel under ultraviolet light in the presence of ethidium bromide. After the reaction, the PCR products were analyzed on agarose gel, and the desired gene fragments were excised and purified through the use of a gel extraction kit (Omega Bio-tek Inc. Georgia, USA).

T4 DNA ligase enzyme (Takara, Kusatsu, Shiga, Japan) was used to connect *cj0440c* and *CmeABC* fragments by the same restriction sites (*Sac* I) to gain a new fragment *Cme440*. This new fragment was then cloned into a pMD19-T sample vector (Takara, Kusatsu, Shiga, Japan) to generate plasmid *T-Cme440*. Enzymatic double digestion (which involves cutting DNA with two restriction enzymes simultaneously) was used for *Spe* I and *Sac* II. A similar action was replicated on the vector pRY112. Insertion was performed at 16°C using the T4 DNA ligase enzyme. The ligation product was transformed into DH5 α by heat shock (at 4°C for 30 min, 42°C for 90s, and 4°C for 2 min). Afterward, the transformed cells were restored through the addition of LB liquid medium to the transformants, and the mixture was incubated for 2 h. Bacteria were collected through the use of low-speed centrifugation. Finally, bacterial pellets were added to an LB medium that contained chloramphenicol to produce the recombinant clones that contained the vector. The clones were sent to the company for sequencing and the right plasmid was named *pRY-Cme440*.

2.5. Cloning, Expression, and Purification of *cj0440c* in *E. coli*. The size of the target gene *cj0440c* (Gene ID: 904765) was 666 bp. The DNA fragment of the *cj0440c* gene was amplified from the *C. jejuni* NCTC11168 genome through the use of Taq polymerase (Takara, Kusatsu, Shiga, Japan) with primers of *cj0440c*-F1/R1 (Table 2) that carried endonuclease restriction sites of *Bam*H I and *Xho* I. The vector (*pET28a*) was of size 5369 bp and carried a kanamycin resistance gene and different restriction sites for various enzymes. The expression vector was constructed through the use of the method described above and was named the expression vector *P-440*.

2.6. Inducible Expression and Purification of *cj0440c* Protein. The expression host *E. coli* BL21 was used for the expression of recombinant protein *cj0440c*. Induction of the bacteria that contained *P-440* was performed by overnight culture in the presence of 50 μ g/ml kanamycin. Bacterial culture (200 μ l) was grown in broth media and transferred to 20 ml of fresh liquid medium. The growth of bacterial culture was monitored by an optical density (OD) spectrophotometer at 600 nm. Isopropyl- β -d-thiogalactoside (IPTG) was added when the OD₆₀₀ value reached 0.6 to induce the protein expression. The best conditions for expression of *cj0440c* protein were found to be 0.1 mM IPTG at 25°C for 20 h with the use of *E. coli* BL21 (DE3) cells.

The recombinant protein contained N-terminal 6 \times His tags and C-terminal 6 \times His tags. It was purified from the cell lysate through the use of nickel-nitriloacetic acid (Ni-NTA) affinity chromatography. The *E. coli* BL21 cells, which contained *P-440* after induction, were harvested by centrifugation at 4000 rpm for 20 min. The cells were resuspended in

TABLE 2: Primers used for qRT-PCR in the current study.

Gene	Sequence (5'-3')
Cj0440c-F	CGAGCTCATGcaccaccaccaccacATGCTTTTCTCTAATTTAATCA
Cj0440c-R	TCCCCGCGGTTAAAGATTTAATTCCATTCTTAAAGAA
CmeABC-F	GGACTAGTTAAATGGAATCAATAGCTCCAAAGC
CmeABC-R	CGAGCTCCAGGGTAAGTAAAACTAAGTGGTAA
Cj0440c-F1	CGGGATCCATGATGCTTTTCTCTAATTTAATCA
Cj0440c-R1	CCCTCGAGAAGATTTAATTCCATTCTTAAAGAA
Cj0440cF	AGTTGCTCTTAGTGCTTGCG
Cj0440cR	TGCTCCAAAAAGCCACTTC
Cj1339cF	TCCATTAAACGGTTGATATCTGCTT
Cj1339cR	AAGGCTATGGATGAGCAACTTAAAT
Cj0043F	GGGTCTCTGTTGCAAGTGA
Cj0043R	GCCCTAAAAACCCCAAAAAAT
Cj1338cF	TTACCATTGTTGATAGCTTGACCTAAA
Cj1338cR	TGCTTCAGGGATGGCGATA
Cj0697F	TGGTTCAGACCAAAGATGGA
Cj0697R	TGCCAGCATTCTGAGGATTA
16SF	GCTCGTGTCTGAGATGTTG
16SR	GCGGTATTGCGTCTCATTGTAT

ice-cold phosphate-buffered saline (PBS) and sonicated at 50% power for 30 min. The cell lysates were centrifuged at 12000 rpm for 30 min at 4°C. The supernatant was incubated with 100 µl Ni-NTA Sepharose (GE Healthcare, Chicago, IL, USA) in 1.5 ml tubes at 4°C for 2 h in a shaking incubator. The supernatant was washed with 1 ml of Ni-NTA wash buffer (50 mM NaH₂PO₄, pH 8.0, 300 mM NaCl, and 300 mM imidazole). Next, the bound proteins were eluted in 1 ml of Ni-NTA elution buffer (50 mM NaH₂PO₄, pH 8.0, 300 mM NaCl, and 500 mM imidazole). The eluted protein was run through a 12% sodium dodecyl sulfate-polyacrylamide gel electrophoresis (SDS-PAGE) system and then transferred to a polyvinylidene difluoride (PVDF) membrane and immunoblotted with anti-His antibody.

2.7. Detection of the Role of cj0440c in Thiamine Metabolism. TenA can catalyze thiamine degradation to 4-methyl-5-(2-hydroxyethyl) thiazole (THZ) and 4-amino-5-hydroxymethyl-2-methylpyrimidine (HMP) (Figure 1).

For qualitative assessment, thiaminase activity of *cj0440c* was identified by incubating different concentrations (15 µM, 20 µM, 25 µM, or 30 µM) of *cj0440c* and thiamine (2.5 mM) at room temperature in 50 mM tris(hydroxymethyl)aminomethane (tris buffer) (pH 8.0). A 100 µl aliquot of this reaction mixture was removed after 5 h and quenched by heating at 95°C for 2 min. The reaction was repeated without *cj0440c* to produce the control, and then the compounds were analyzed by mass spectrometry (MS).

3. Results

3.1. Antimicrobial Susceptibility of *C. jejuni* NCTC11168 (S and R Strains). The susceptibility of *C. jejuni* NCTC11168 (S and R strains) to each of nine antibiotics was determined. As expected, the *C. jejuni* NCTC11168 (R) showed higher resistance to the nine tested antibiotics than the S strain, as shown in Table 3. Likewise, high MPC and MSW were observed in the *C. jejuni* NCTC11168 (R) strain when compared with the S strain.

3.2. Expression of *cj0440c* and Other Flagella-Related Genes in *C. jejuni* NCTC11168 (S and R Strains) Exposed to Antibiotics. The expression of flagella-related genes was measured through the use of real-time quantitative RT-PCR (qRT-PCR) during exposure to the macrolide, aminoglycoside, quinolone, and tetracycline groups of antibiotics. Among these genes, 16S rDNA was used as an internal control, *cj1338c* and *cj1339c* were those that transcribed the filament proteins, *cj0043* was the gene for the flagellar hook protein, and *cj0697* was the gene for the flagellar basal body protein. It is of note that these four genes are distributed in every part of the flagella. A trend toward increased expression of all genes including *cj0440c* in the presence of macrolides (Ery and Azi), aminoglycosides (Gen and Eti), quinolones (Enr and Gati), and tetracyclines (Tet and Tige) was observed in the study (Figures 2(a)–2(d)).

3.3. The Western Blot Analysis of *cj0440c* Protein. A western blot analysis revealed the increased expression of protein

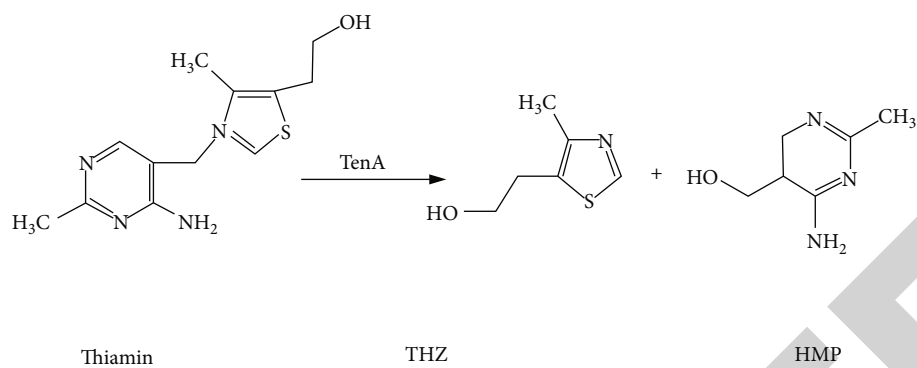


FIGURE 1: The degradation of thiamine into THZ and HMP catalyzing by *TenA*.

TABLE 3: The MIC, MPC, and MSW results of *C. jejuni* NCTC11168 (S) and *C. jejuni* NCTC11168 (R) for nine antibiotic drugs.

Name	NCTC11168 (S)			NCTC11168 (R)		
	MIC ($\mu\text{g/mL}$)	MPC	MSW	MIC ($\mu\text{g/mL}$)	MPC	MSW
Erythromycin	0.125	2MIC	1-2MIC	0.5	2MIC	1-4MIC
Tylosin	0.5	2MIC	1-2MIC	2.0	4MIC	1-4MIC
Azithromycin	<0.125	2MIC	1-2MIC	0.5	4MIC	1-4MIC
Gentamicin	0.25	4MIC	1-4MIC	0.5	8MIC	1-8MIC
Etimicin	1.0	4MIC	1-4MIC	2.0	8MIC	1-8MIC
Enrofloxacin	0.125	8MIC	1-8MIC	4.0	32MIC	1-32MIC
Gatifloxacin	0.25	4MIC	1-4MIC	4.0	8MIC	1-8MIC
Tetracycline	0.125	32MIC	1-32MIC	16.0	128MIC	1-128MIC
Tigecycline	<0.125	8MIC	1-8MIC	0.25	64MIC	1-64MIC

under the influence of IPTG (Figure 3). The best conditions for induction of *cj0440c* protein were 20 h in 0.1 mM IPTG at 25 °C; the best purification conditions for this protein were its elution in 500 mM imidazole.

3.4. Reaction of *cj0440c* with Thiamine. MS was used to determine the products of the reaction of catalyzed thiamine with different concentrations of *cj0440c* protein (Figures 4(a)–4(e)). Figure 4(a) represents the blank group that is without *cj0440c*. The molecular weight of thiamine is 337 kDa, that of THZ is 143 kDa and that of HMP is 139 kDa. There was no difference between the results for the experimental group and those for the blank group. MS analysis showed that the *cj0440c* protein did not catalyze the degradation of thiamine.

4. Discussion

Over the last decade, *C. jejuni* has become considered one of the leading causes of food poisoning in many countries including those in Europe [14]. Because of its public health significance, it is important to study the pathogenic mechanisms that are adopted by this bacterium. Among pathogenic mechanisms, the formation of flagella is key, as they aid bacterium motility, biofilm formation, adherence, and invasion into the host cell [15]. The *cj0440c* gene, a putative transcriptional regulator of several flagella-related genes, and its role in the biosynthesis of flagella is not fully understood.

Therefore, the study described here was conducted to determine the association of this transcriptional regulator with other flagella-related genes. The determination was performed with the use of RT-PCR. It was observed through the use of MS analysis that *cj0440c* had no role in thiamine hydrolysis. It was also found that *cj0440c* was not involved directly in the regulation of flagella genes. Increased expression of *cj0440c* and other flagellar genes (*cj1338c*, *cj1339c*, *cj0697*, and *cj0043*) was found in *C. jejuni* NCTC11168 (S and R strains) upon exposure of the bacterium to eight different kinds of antibiotics. Flagella-related genes such as *cj1338c*, *cj1339c*, *cj0697*, and *cj0043* are distributed in every part of the flagella, including the basal body, the hook, and the filament. These genes along with a putative transcriptional regulator (*cj0440c*) were upregulated upon exposure to antibiotics.

The outcomes of this study are in agreement with previous observations on the upregulation of the *cj0440c* gene in the Ery^r *C. jejuni* [16]. It is known that bacteria suffer a fitness cost during antibiotic resistance; however, numerous other factors are involved in the compensation for the adaptation weakness [14–18]. In this study, increased expression of flagella-related genes and *cj0440c* suggest that the putative transcriptional regulator may affect morphological changes of the flagella by taking part in the regulation of filament. One possible explanation is that *cj0440c* may be involved in compensating for the fitness cost of various antibiotics via a positive relationship with flagella-related genes. These findings are in agreement with those of a previous study [19].

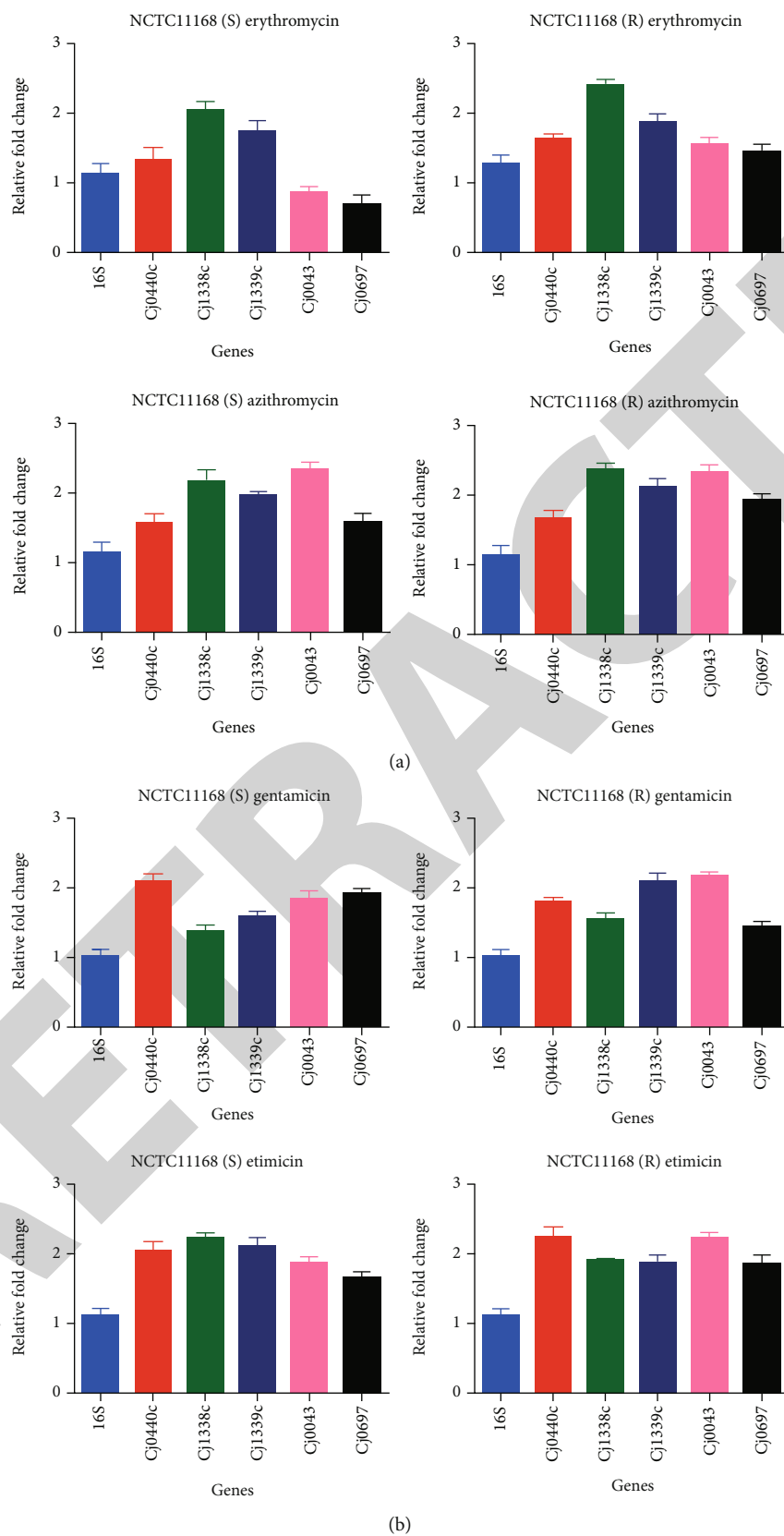


FIGURE 2: Continued.

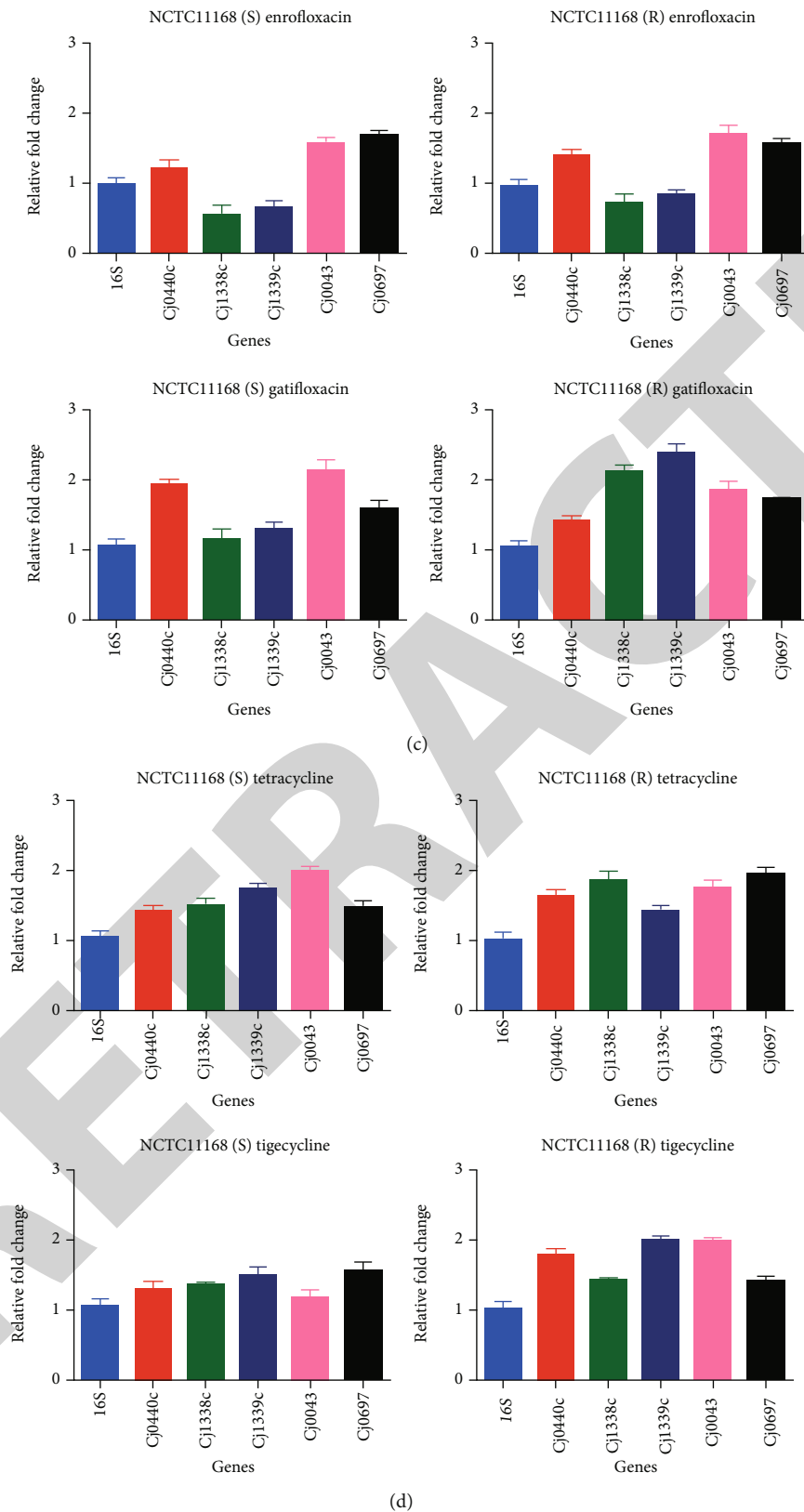


FIGURE 2: (a)–(d) The increased expression of Flagella-related genes by qRT-PCR under the exposure of different antibiotics in *C. jejuni* NCTC11168 (S & R) strains. (a) shows the increased expression of flagella-related genes under the exposure of macrolide antibiotics; (b) shows the increased expression of flagellar-related genes under the exposure of aminoglycoside antibiotics; (c) shows the increased expression of flagella-related genes under the exposure of quinolone antibiotics, and (d) shows the increased expression of flagella-related genes under the exposure of tetracycline antibiotics in *C. jejuni* NCTC11168 (S & R) strains.

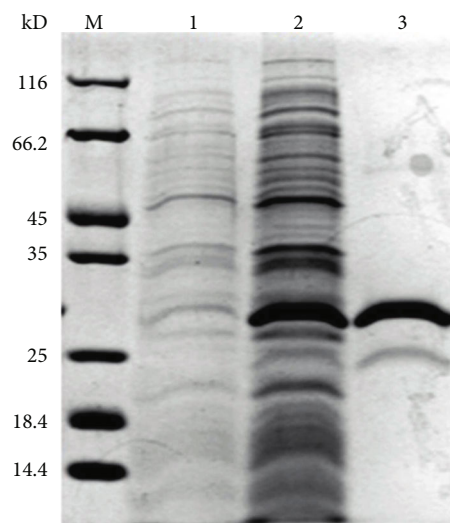


FIGURE 3: The expression of protein *Cj0440c* through western blot. Lane M is protein molecular weight 116 Marker; lane 1 is *C. jejuni* NCTC1118 control before induction; lane 2 is overexpression protein after induction by IPTG, and lane 3 is a purified protein.

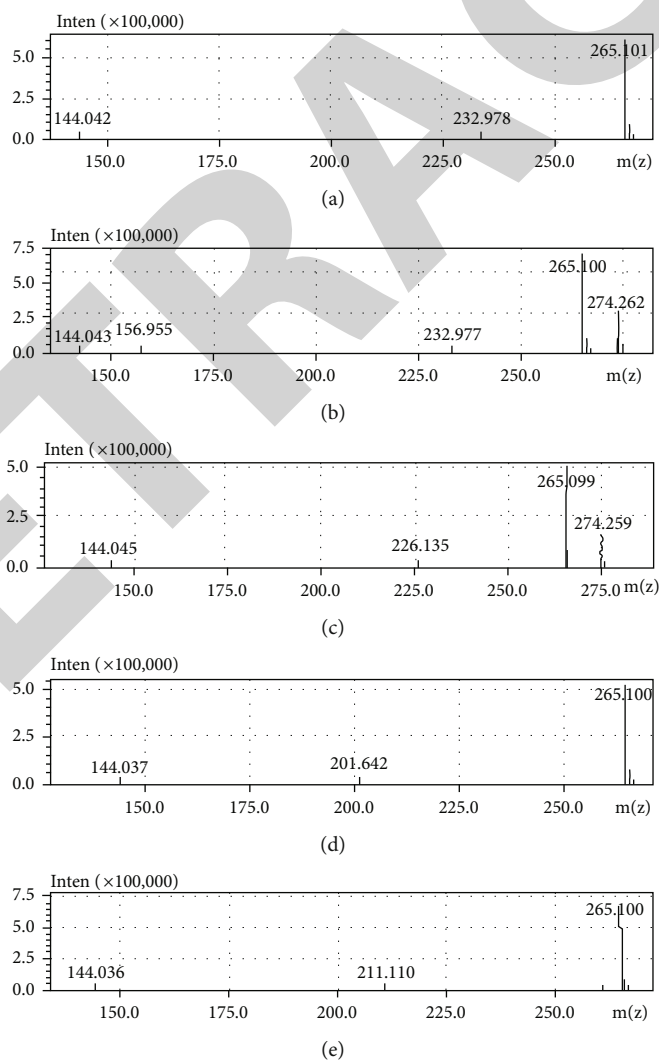


FIGURE 4: (a)–(e) The mass spectrogram of the product of *cj0440c* protein enzymatic hydrolysis. (a) The blank group (without *cj0440c* protein); (b) contains 15 μM *cj0440c* protein; (c) contains 20 μM *cj0440c* protein; (d) contains 25 μM *cj0440c* protein; (e) contains 30 μM *cj0440c* protein.

It has been reported that the *cj0440c* gene may have a role in encoding the TenA/PQQC/THI-4 family of proteins. TenA proteins enhance the expression of extracellular enzymes such as alkaline proteases, levansucrases, and neutral proteases [20]. TenA is a thiaminase II [21], and it can catalyze the degradation of thiamine [22, 23]. This family also includes pyrroloquinoline quinone synthesis protein C (PQQC). This PQQC is a prosthetic group of numerous bacterial enzymes such as methanol dehydrogenase of methylotrophs and glucose dehydrogenase [24, 25]. Biosynthesis of PQQC in *E. coli* can be affected by the actions of the *tldD* gene, which is involved in the processing of small peptides [26]. This gene removes repression of the *cdtB* and *lgeR* genes, which may regulate some flagella genes [27]. However, the findings of the present study show that *cj0440c* is not an enzyme, and it cannot take part in the metabolic pathways of thiamine.

This study preliminarily explored the function of *cj0440c*; it contributed to the improvement of the genome informatics of *Campylobacter*, and it provided the theoretical basis for the study of the mechanism in *Campylobacter*. The limitation of the current study was that all the experiments were performed *in vitro*, and research methods on the regulatory mechanisms of prokaryotes are limited. Therefore, further study is required to understand the signaling pathway.

5. Conclusion

Owing to the potential of *Campylobacter jejuni* to cause health issues among public communities with the involvement of antibiotic resistance, the current study revealed that the transcriptional regulator known as *cj0440c* does not transcribe an enzyme; therefore, this gene may not be involved in the synthesis of thiamine. The outcome also revealed that *C. jejuni* NCTC11168 (R) showed higher resistance to the nine tested antibiotics than the S strain with increased expression of the *cj0440c* gene in the presence of macrolides, aminoglycosides, quinolones, and tetracyclines. The study aids in the understanding of the inter-relationship between the regulatory mechanism of flagella genes and the thiamine metabolic pathway.

Data Availability

All the data are available in the manuscript.

Conflicts of Interest

The authors declare no conflict of interest.

Acknowledgments

This study was supported with the researchers' supporting project number (RSP2022R494), in King Saud University, Riyadh, Saudi Arabia.

References

- [1] J. E. Moore, D. Corcoran, J. S. G. Dooley et al., "Campylobacter," *Veterinary Research*, vol. 36, no. 3, pp. 351–382, 2005.
- [2] D. Acheson and B. M. Allos, "Campylobacter jejuni infections: update on emerging issues and trends," *Clinical Infectious Diseases*, vol. 32, no. 8, pp. 1201–1206, 2001.
- [3] T. Pitkänen, "Review of Campylobacter_ spp. in drinking and environmental waters," *Journal of Microbiological Methods*, vol. 95, no. 1, pp. 39–47, 2013.
- [4] H. Huang, B. W. Brooks, R. Lowman, and C. D. Carrillo, "Campylobacter species in animal, food, and environmental sources, and relevant testing programs in Canada," vol. 721, pp. 701–721, 2015.
- [5] K. Han, S. S. Jang, E. Choo, S. Heu, and S. Ryu, "Prevalence, genetic diversity, and antibiotic resistance patterns of *Campylobacter jejuni* from retail raw chickens in Korea," *International Journal of Food Microbiology*, vol. 114, no. 1, pp. 50–59, 2007.
- [6] E. Scanlan, L. Yu, D. Maskell, J. Choudhary, and A. Grant, "A quantitative proteomic screen of the *Campylobacter jejuni* flagellar-dependent secretome," *Journal of Proteomics*, vol. 152, pp. 181–187, 2017.
- [7] D. T. Akahoshi and C. L. Bevins, "Flagella at the host-microbe interface: key functions intersect with redundant responses," *Frontiers in Immunology*, vol. 13, 2022.
- [8] M. M. S. M. Wösten, J. A. Wagenaar, and J. P. M. van Putten, "The FlgS/FlgR two-component signal transduction system regulates the *fla* Regulon in *Campylobacter jejuni*," *The Journal of Biological Chemistry*, vol. 279, no. 16, pp. 16214–16222, 2004.
- [9] D. M. Byers and H. Gong, "Acyl carrier protein: structure--function relationships in a conserved multifunctional protein family," *Biochemistry and Cell Biology*, vol. 85, no. 6, pp. 649–662, 2007.
- [10] I. I. Kassem, M. Khatri, M. A. Esseili et al., "Respiratory proteins contribute differentially to campylobacter jejuni's survival and in vitro interaction with hosts' intestinal cells," *BMC Microbiology*, vol. 12, no. 1, pp. 1–10, 2012.
- [11] R. A. Weingarten, M. E. Taveirne, and J. W. Olson, "The dual-functioning fumarate reductase is the sole succinate: quinone reductase in *Campylobacter jejuni* and is required for full host colonization," *Journal of Bacteriology*, vol. 191, no. 16, pp. 5293–5300, 2009.
- [12] J. B. Patel, F. R. Cockerill, and P. A. Bradford, "Performance standards for antimicrobial susceptibility testing: Twenty-Fifth Informational Supplement," *Clinical and Laboratory Standards Institute*, vol. 35, no. 3, pp. 29–50, 2015.
- [13] M. A. B. Shabbir, Q. Wu, M. Z. Shabbir et al., "The CRISPR-cas system promotes antimicrobial resistance in *Campylobacter jejuni*," *Future Microbiology*, vol. 13, no. 16, pp. 1757–1774, 2018.
- [14] V. Bronnec, H. Turoňová, A. Bouju et al., "Adhesion, biofilm formation, and genomic features of campylobacter jejuni Bf, an atypical strain able to grow under aerobic conditions," *Frontiers in Microbiology*, vol. 7, p. 1002, 2016.
- [15] P. Guerry, "Campylobacter flagella: not just for motility," *Trends in Microbiology*, vol. 15, no. 10, pp. 456–461, 2007.
- [16] H. Hao, Z. Yuan, Z. Shen et al., "Mutational and transcriptomic changes involved in the development of macrolide resistance in campylobacter jejuni," *Antimicrobial Agents and Chemotherapy*, vol. 57, no. 3, pp. 1369–1378, 2013.

Retraction

Retracted: Expression Profile of MAGE-B1 Gene and Its Hypomethylation Activation in Colon Cancer

BioMed Research International

Received 8 January 2024; Accepted 8 January 2024; Published 9 January 2024

Copyright © 2024 BioMed Research International. This is an open access article distributed under the Creative Commons Attribution License, which permits unrestricted use, distribution, and reproduction in any medium, provided the original work is properly cited.

This article has been retracted by Hindawi following an investigation undertaken by the publisher [1]. This investigation has uncovered evidence of one or more of the following indicators of systematic manipulation of the publication process:

- (1) Discrepancies in scope
- (2) Discrepancies in the description of the research reported
- (3) Discrepancies between the availability of data and the research described
- (4) Inappropriate citations
- (5) Incoherent, meaningless and/or irrelevant content included in the article
- (6) Manipulated or compromised peer review

The presence of these indicators undermines our confidence in the integrity of the article's content and we cannot, therefore, vouch for its reliability. Please note that this notice is intended solely to alert readers that the content of this article is unreliable. We have not investigated whether authors were aware of or involved in the systematic manipulation of the publication process.

Wiley and Hindawi regrets that the usual quality checks did not identify these issues before publication and have since put additional measures in place to safeguard research integrity.

We wish to credit our own Research Integrity and Research Publishing teams and anonymous and named external researchers and research integrity experts for contributing to this investigation.

The corresponding author, as the representative of all authors, has been given the opportunity to register their agreement or disagreement to this retraction. We have kept a record of any response received.

References

- [1] M. H. Almutairi, M. M. Alotaibi, R. Alonaizan, and B. O. Almutairi, "Expression Profile of MAGE-B1 Gene and Its Hypomethylation Activation in Colon Cancer," *BioMed Research International*, vol. 2022, Article ID 6066567, 8 pages, 2022.

Research Article

Expression Profile of MAGE-B1 Gene and Its Hypomethylation Activation in Colon Cancer

Mikhlid H. Almutairi , Mona M. Alotaibi, Rasha Alonaizan, and Bader O. Almutairi 

Zoology Department, College of Science, King Saud University, P.O. Box: 2455, 11451 Riyadh, Saudi Arabia

Correspondence should be addressed to Mikhlid H. Almutairi; malmutari@ksu.edu.sa

Received 20 June 2022; Revised 4 July 2022; Accepted 7 July 2022; Published 27 July 2022

Academic Editor: Hafiz Ishfaq Ahmad

Copyright © 2022 Mikhlid H. Almutairi et al. This is an open access article distributed under the Creative Commons Attribution License, which permits unrestricted use, distribution, and reproduction in any medium, provided the original work is properly cited.

Cancer-testis (CT) genes are typically expressed in the testes; however, they have been linked to aberrant expression in a variety of malignancies. *MAGE-B* family genes are an example of CT genes. Therefore, the overarching objective of this study was to examine the expressions of *MAGE-B* family genes in several patients with colon cancer (CC) to see if they might be employed as cancer biomarkers in the early phases of cancer detection and to improve treatment. In this investigation, RT-PCR was used to analyze *MAGE-B* family genes in neighboring normal colon (NC) tissue from 10 CC patients. In addition, the effect of DNA demethylation on the expression status of the *MAGE-B1* gene was evaluated by RT-PCR in HCT116 and Caco-2 cells and by qRT-PCR for HCT116 only after treating both CC cell lines with varying concentrations of 5-aza-2'-deoxycytidine (1.0, 5.0, and 10.0 μ M) for 48 or 72 hours. All *MAGE-B* family genes except for *MAGE-B1* showed weak bands in several samples of NC tissues: *MAGE-B2*, *MAGE-B3*, *MAGE-B4*, *MAGE-B5*, and *MAGE-B6* genes were observed in 40%, 50%, 40%, 30%, and 60% of the NC samples, respectively. Nonetheless, they had strong bands in multiple samples of CC tissues, with 70%, 90%, 60%, 50%, and 90% of the CC samples, respectively. Interestingly, *MAGE-B1* was detected in 60% of CC tissues but not in NC tissues, suggesting that it is a potential biomarker for early CC detection. *MAGE-B1* expression was not observed in either untreated or DMSO-treated HCT116 cells after 48 or 72 hours of treatment. However, according to the RT-PCR and qRT-PCR results, the *MAGE-B1* gene was overexpressed in the HCT116 cells treated with three different concentrations of 5-aza-2'-deoxycytidine. This shows that demethylation plays a crucial role in *MAGE-B1* expression activation.

1. Introduction

Colon cancer (CC) is a leading cause of mortality globally, and its incidence is anticipated to double by 2030 [1]. Between nations, CC incidence and death rates vary around tenfold, with the highest rates reported in wealthy countries, where they have remained relatively stable. However, rates are rapidly increasing in developing nations [1]; despite the fact that CC screening programs have reduced incidence rates around the globe, mortality rates continue to rise in certain locations [2, 3]. In Saudi Arabia, CC is the most prevalent type of cancer in men and the third most common in women [4–6]. The majority of CC instances in Saudi Arabia are detected during clinical exams rather than through screening initiatives. Screening for CC can help reduce the incidence of death and mortality associated with this condi-

tion, as CC is a slow-progressing disease that can be treated if detected early. Therefore, the development of a noninvasive biomarker for early disease detection could be advantageous [7]. CC carcinogenesis is a multistep process involving oncogene and tumor suppressor gene alterations that results in the gradual transformation of the normal colorectal epithelium into adenoma, invasive tumor, and metastatic tumor [8]. CC has been associated with a variety of risk variables, including ethnic origin, environment, and genetics [9].

Early identification and successful cancer therapy continue to be substantial clinical hurdles. Thus, there is an urgent need to identify novel tumor-associated chemicals that can be exploited to develop novel clinical diagnostics and therapeutic targets for a variety of cancers [10]. Numerous studies on diverse antigen classes as potential novel

cancer-specific biomarkers for early detection of malignancy have been conducted. Cancer-testis (CT) antigens are a type of cancer-specific antigen that express proteins only in human germ line cells of the testis and cancer cells [11]. Due to their particular, cancer-specific expression pattern, CT antigens could be useful as cancer biomarkers and treatments [11, 12].

CT expression is seen in a variety of tumor types, including ovarian, colon, and melanoma [13]. In cancer tissue, aberrant expression of these CTs could play a critical role in tumor growth, proliferation, and antiapoptotic processes [14]. van der Bruggen et al. discovered the first CT gene in a patient with malignant melanoma and designated it a part of the melanoma antigen family (MAGE-1) [15]. Most CT genes are situated on the X chromosome [16]; are classified as member of multicopy, paralogous gene families; and express splice variants, including the *MAGE-A*, *GAGE*, *PAGE*, *XAGE1*, and *SSX* families.

MAGEs are encoded by a paralogous gene family consisting of about 60 genes [17]. Although their function in testis germ cells is unknown, their oncogenic activity is widely documented [18]. The first member of the human MAGE family that was identified is a member of a cluster of 12 MAGE-A genes found on the Xq28 [19]. Following that, a second cluster, dubbed MAGE-B, was discovered in human Xp21 [20], and, lastly, another cluster, dubbed MAGE-C, was located in Xq26–27 [21]. They are completely inactive in normal tissues, as they are a component of male germ cells. Unexpectedly, MAGEs have been found to be frequently expressed in a range of cancers [22], including colorectal, melanoma, breast, and esophageal [22–25].

The MAGE-B family, including MAGE-B1, MAGE-B2, MAGE-B3, and MAGE-B4 genes, is strongly homologous with the MAGE-A gene family. *MAGE-B* gene expression was not detected in normal tissues except the testis. However, *MAGE-B1* and *MAGE-B2* genes were significantly expressed among various types of cancer, such as esophageal, gastric, and colorectal carcinoma [25]. *MAGE-B2* and *MAGE-B3* genes were overexpressed in hepatocellular carcinoma and colorectal cancer patients [22, 26]. Additionally, they are often exhibited in cancer patients from a variety of ethnic backgrounds, including German, Chinese, Taiwanese, Italian, and Japanese [22, 25–28].

DNA methylation regulates the expression of numerous CT genes and is mostly carried out in the gene promoter region by DNA methyltransferase enzymes (DNMTs) [29]. The expression of certain CT genes, such as *MAGE-A1* in oral carcinoma and *MAGE-A4* in thyroid cancer, is apparently enhanced by DNA hypomethylation [30, 31]. Treatment of colon and ovarian cancer cell lines with a DNA methyltransferase 1 inhibitor (DNMTi), 5-aza-2'-deoxycytidine, can stimulate the expression of many CT genes [32, 33].

The expression patterns of *MAGE-B* family genes have not been examined in Saudi populations with CC. Thus, the overall purpose of this study was to analyze the expression of *MAGE-B* genes in Saudi patients with CC to identify potential cancer biomarkers that might aid in the early identification and treatment of CC.

2. Materials and Methods

2.1. Collecting Samples and Obtaining Ethical Approval. In this study, CC and normal colon (NC) tissues were taken from 10 Saudi male patients who had not received any treatment, including chemotherapy, physiotherapy, or radiation. Stabilization solution for *RNAlater* was stored in an Eppendorf tube (Thermo Fisher Scientific; 76106). Ethical approval was provided by the Al-Imam Muhammad Ibn Saud Islamic University with IRB number HAPO-01-R-011 and project number 214/2022 [34]. Patients were asked to sign a permission form and complete a survey as well as a self-administered questionnaire that inquired about their age, social behaviors, family history of cancer, and personal medical history.

2.2. Primer Design for the Selected Genes. The National Center for Biotechnology Information's (<http://www.ncbi.nlm.nih.gov/>) database was used to generate primers for each gene. Then, using the Primer-BLAST program (<https://www.ncbi.nlm.nih.gov/tools/primer-blast/>), individual primers for each gene were constructed. MacroGen Company (Seoul, South Korea) synthesized the designed primers at a final concentration of 10 μ M for use in studies (<https://dna.macrogen.com>). The primer sequences and predicted sizes of each gene are listed in Table 1.

2.3. Human CC Cell Line, HCT116, and Caco-2: Source and Culture. The HCT116 and Caco-2 cells were obtained from the American Type Culture Collection (ATCC, Manassas, VA, USA), and the cells were cultured in DMEM (Thermo Fisher Scientific; 61965026) supplemented with 10% fetal bovine serum (FBS) (Thermo Fisher Scientific; A3160801) and penicillin-streptomycin (Thermo Fisher Scientific; 15140122) and then kept in the incubator with 5% CO₂ at 37°C.

2.4. 5-Aza-2'-Deoxycytidine Treatment of HCT116 and Caco-2 Cell Lines at Various Concentrations. For 48 or 72 hours, the HCT116 and Caco-2 cell lines were treated with various concentrations of demethylating agent (5-aza-2'-deoxycytidine) 1.0, 5.0, and 10.0 μ M, whereas the control cells received the same concentration of drug solvent DMSO. Every 24 hours, the media was refreshed.

2.5. Extraction of Total RNA and Production of Complementary DNA (cDNA). Fifty milligrams of tissues and about 3×10^6 cells of cultivated cells were used to extract the total RNA using the All Prep DNA/RNA Mini Kit (Qiagen; 80204), according to the manufacturer's guidelines. The Nano-Drop8000 spectrophotometer was then used to determine the RNA concentration. To convert 1 μ g of RNA to cDNA, the High-Capacity cDNA Reverse Transcription Kit (Applied Biosystems; 4368814) was used, according to the manufacturer's instructions. After dilution to a 1:10 concentration, the cDNA was kept at -20°C until needed.

2.6. RT-PCR with Gel Electrophoresis. The PCR reaction, which comprised 100 ng of cDNA, 0.25 μ M of reverse and forward primers, and 1X of BioMix Red (BioLine; BIO-25006), was left in the PCR machine for 5 minutes, followed

TABLE 1: Primer sequences and their expected product sizes for *ACTB*, *MAGE-B* family, and *SSX2* genes.

Symbol	Official gene Full name	Primer direction and sequence (from 5' → 3')	Ta	Product size (bp)
<i>ACTB</i>	Actin beta	Forward: AGAAAATCTGGCACCACACC Reverse: AGGAAGGAAGGCTGGAAGAG		553
<i>MAGE-B1</i>	MAGE family member B1	Forward: CAGGAATGCTGATGCACTTC Reverse: GAGGACTTTCATCTTGGTGG		524
<i>MAGE-B2</i>	MAGE family member B2	Forward: CACTGAAGCAGAGGAAGAAG Reverse: GGTCTACCTTGTCGATGAAG		467
<i>MAGE-B3</i>	MAGE family member B3	Forward: GACTCCTATGTCCTTGTCAG Reverse: GCACTACTGCCATCATTGAG		464
<i>MAGE-B4</i>	MAGE family member B4	Forward: TCTTTGGCCTTGCCCTGAAG Reverse: GGAATACGCACTAGTCATGG	58	524
<i>MAGE-B5</i>	MAGE family member B5	Forward: CAGTAGAGATGAGGAGTACC Reverse: GGGCTCTCCATAGATGTAGT		472
<i>MAGE-B6</i>	MAGE family member B6	Forward: GCGCTTAAGCAAAGATGCTG Reverse: GCCGGTAAACCACGTACTTA		473
<i>SSX2</i>	SSX family member 2	Forward: CAGAGAAGATCCAAAAGGCC Reverse: CTCGTGAATCTTCTCAGAGG		407

Abbreviations: Ta: temperature of annealing for each gene; bp: base pair.

by 35 cycles at 96°C for 30 seconds, 58°C for 30 seconds, and 72°C for 30 seconds, respectively. The run was concluded with a 5-minute warm-up at 72°C. Finally, the PCR results were examined in a 1% agarose gel containing 0.5 g/mL of ethidium bromide. A total of 3 µL of 100 bp DNA marker (New England Biolabs; N0467) was added to determine the size of the PCR result.

2.7. Purification and Sequencing of RT-PCR Products. 15 µL of cDNA (15 ng/µL) and 20 µL of forward and/or reverse primers (5 pmol/µL) were inserted into two clean, separate Eppendorf tubes (1.5 mL). Then, the Microgen Company received both tubes for DNA sequencing. The resultant sequencing of each product was uploaded to the BLAST website (<https://blast.ncbi.nlm.nih.gov/Blast.cgi>) for comparison with the NCBI database.

2.8. Real-Time Quantitative Polymerase Chain Reaction (qRT-PCR) Primer Design. All primers were designed manually and had an amplicon size below 175 bp to facilitate qRT-PCR amplification. Each primer was 20 nucleotides in length and included 50% G/C to prevent the internal secondary structure that was expected. To avoid the creation of primer dimers, the forward and reverse primers lacked significant complementarity at their 3' ends and melted at the same temperature. To guarantee primer specificity, a BLAST search was performed on them. Commercially available primers were produced (Macrogen Inc., South Korea), and their sequences are presented in Table 2. The stock primers were diluted to a final concentration of 10 pmol using sterile distilled water.

2.9. The qRT-PCR Setup. The qRT-PCR tests were performed according to the manufacturer's instructions using the iTaq Universal SYBR Green Supermix (Bio-Rad;

1725120, Hercules, CA, USA). The volume was then adjusted to 10 µL on a 96-well plate by adding 5 µL of SYBR Green Supermix, 2 µL of cDNA (200 ng), 0.25 µL of each primer, and lastly water. Three duplicate samples were amplified utilizing a 30-second predenaturation step at 95°C, followed by 40 cycles of 15-second denaturation at 95°C, 30-second primer annealing at 58°C, and 15-second extension at 95°C. Following the completion of the 40 cycles, a melting curve study was conducted. *GAPDH* was utilized as a positive control to normalize the qRT-PCR results. qRT-PCR was performed using a QuantStudio 7 Flex Real-time PCR System (Applied Biosystems, Hercules, CA, USA).

2.10. Statistical Analyses. Statistical analysis was conducted using SPSS version 22 (SPSS Inc., Chicago, USA). The comparisons between the expressions of *MAGE-B* genes in NC and CC groups and *MAGE-B1* gene in the untreated and treated of HCT116 cell lines were analyzed using an unpaired Student's *t*-test. The findings were provided as average ± SD. All *P* values were statistically significant (**P* < 0.05 and ***P* < 0.01).

3. Results

3.1. Clinical Data on the Studied Subjects. Table 3 summarizes the demographic and clinical features of the study participants. The mean age of the 10 CC patients on diagnosis was 57 years (range: 24 to 83 years). Fifty percent of CC patients were under the age of 57, and 50% were over the age of 57.

3.2. Expression Profile of *MAGE-B* Genes in CC and Matched Adjacent NC Tissues. In this paper, the expressions of six members of the *MAGE-B* family (*MAGE-B1*, *MAGE-B2*,

TABLE 2: Primer sequences and their expected product size for qRT-PCR.

Symbol	Official gene Full name	Primer direction and sequence (from 5' → 3')	Ta*	Product size
<i>GAPDH</i>	Glyceraldehyde-3-phosphate dehydrogenase	Forward: GGGAAGCTTGTCATCAATGG Reverse: GAGATGATGACCCTTTTGGC	58	173 bp
<i>MAGE-B1</i>	MAGE family member B1	Forward: GAAGGCAGATATGCTGAAGG Reverse: CACTAGGGTTGTCTTCCTTC		

Abbreviations: Ta: temperature of annealing for each gene; bp: base pair.

TABLE 3: Clinical characteristics of the research participants.

Clinical parameters	CC	NC
	N (%)	N (%)
Participants	10 (100%)	10 (100%)
Mean of age (min-max)	57 (24-83)	
Below 57	5 (50%)	5 (50%)
Above 57	5 (50%)	5 (50%)

Abbreviations: CC: colon cancer; NC: normal colon; N: number of samples.

MAGE-B3, *MAGE-B4*, *MAGE-B5*, and *MAGE-B6*) were investigated in different samples of CC and their matching NC samples. The RT-PCR validation process began with the identification of *MAGE-B* family genes in various RNAs extracted from 10 NC tissues to determine their testis specificity. Testis cDNA was synthesized from total RNA of human testis and used to verify the primers for each *MAGE-B* gene (Thermo Fisher Scientific; AM7972). The *ACTB* gene expression was utilized as a positive control to determine that the cDNA was of acceptable quality.

In this study, no expression of *MAGE-B1* was detected in NC (Figure 1, left side), whereas 60% of CC displayed its expression (Figure 1, right side). The transcriptional level of *MAGE-B2*, *MAGE-B3*, *MAGE-B4*, *MAGE-B5*, and *MAGE-B6* was faintly seen in 40%, 50%, 40%, 30%, and 60% of NC, respectively (Figure 1, left side). However, 70%, 90%, 60%, 50%, and 90% of CC, respectively, showed strong induction of *MAGE-B2*, *MAGE-B3*, *MAGE-B4*, *MAGE-B5*, and *MAGE-B6* expression consecutively (Figure 1, right side). Furthermore, this study analyzed the positive (the case was designated as positive if a band was found) expressions for genes from *MAGE-B2* to *MAGE-B6* in NC and CC tissues. Only *MAGE-B3* showed a statistically significant positive expression in CC compared with NC tissues ($P = 0.0543$, Table 4). Intriguingly, because *MAGE-B1* was not expressed in any of the matched NC tissues but was expressed in 60% of CC tissues ($P = 0.0017$, Table 4), it might be regarded a potential CT gene marker and could be used for early CC diagnosis. A total of three CC samples selected at random from *MAGE-B1* that had positive findings were sequenced to confirm the RT-PCR results.

3.3. Epigenetic Modification of *MAGE-B1* Expression in HCT116 and Caco-2 Cell Lines. The DNA methylation status controls and regulates the expression of many CT genes at the promoter level [29]. Thus, HCT116 and Caco-2 cell lines were subjected to a methylation-modifying agent, 5-aza-2'

-deoxycytidine, to investigate the effect of DNA demethylation on the *MAGE-B1* gene expression status. For 48 or 72 hours, three different doses of 5-aza-2'-deoxycytidine (1.0, 5.0, and 10.0 μM) were employed. Because the drug was dissolved in DMSO, both cell lines were treated with DMSO to compare gene expression. Additionally, untreated HCT116 and Caco-2 cells were employed as negative controls to evaluate *MAGE-B1* gene expression in treated and untreated cells. The normal testis was used as a positive control for primer efficacy, whereas the *ACTB* gene was used to determine the quality of cDNA. *SSX2* is a well-characterized CT gene that was utilized as a positive control to assess its expression. The expression of the *MAGE-B1* gene was determined first by RT-PCR and then by qRT-PCR, as shown in Figures 2 and 3.

RT-PCR results shows that *MAGE-B1* expression was not observed in untreated or DMSO-treated HCT116 cells after 48 or 72 hours of treatment. However, the band intensities of this gene were significantly greater in HCT116 and Caco-2 cells treated with three different doses of 5-aza-2'-deoxycytidine than in untreated cells after 48 and 72 hours of treatment.

qRT-PCR was also performed to determine whether RT-PCR results correlates with qRT-PCR results for *MAGE-B1* expression in HCT116 cells following treatment with 1.0, 5.0, and 10.0 μM of 5-aza-2'-deoxycytidine. Notably, the expression of *MAGE-B1* was significantly increased after 48 and 72 hours of exposure to the three doses of 5-aza-2'-deoxycytidine in comparison to cells treated with DMSO (Figure 3). The highest expression of *MAGE-B1* mRNA was detected after treating HCT116 cells with 10.0 μM 5-aza-2'-deoxycytidine for 48 and 72 hour. Taken together, these findings indicated that the *MAGE-B1* expression can be upregulated by the demethylating agent.

4. Discussion

CC is a leading cause of mortality in Saudi Arabia, affecting predominantly elderly persons. Nonetheless, it now affects people of all ages [6, 35]. As a result, biomarkers for the early stages of CC must be found to reduce death and mortality rates [6, 7]. The MAGE gene produces CT antigens, which are expressed preferentially in a variety of human malignancies but not in normal tissues [36]. However, the *MAGE-B* gene expression profiles in Saudi populations with CC are unclear. As a result, this research sought to obtain a better understanding of the *MAGE-B* gene expression patterns and their epigenetic regulation.

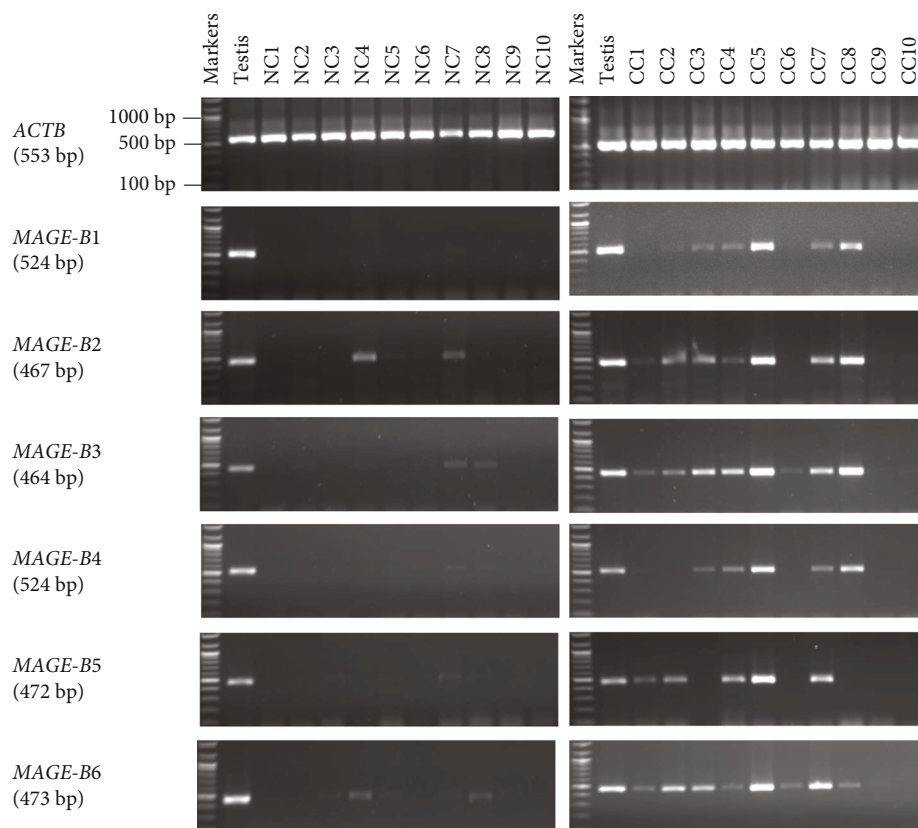


FIGURE 1: Expression profile of *MAGE-B* genes in CC and matched adjacent NC tissues. The *MAGE-B1*, *MAGE-B2*, *MAGE-B3*, *MAGE-B4*, *MAGE-B5*, and *MAGE-B6* genes were examined on 1% agarose gels. Total RNA from 10 NC tissues (left side) and 10 CC tissues (right side) was used to make cDNAs. Testis cDNA was used to validate the primers for each gene. As a positive control for the cDNA samples, *ACTB* expression was used. The expected size of each gene's product is indicated on the left between brackets.

TABLE 4: Positive expression of *MAGE-B* genes in NC and CC tissues.

<i>MAGE-B</i> genes	Number of positive expression in NC (%)	Number of positive expression in CC (%)	<i>P</i> value
<i>MAGE-B1</i>	0 (0)	6 (60)	0.0017**
<i>MAGE-B2</i>	4 (40)	7 (70)	0.1963
<i>MAGE-B3</i>	5 (50)	9 (90)	0.0543*
<i>MAGE-B4</i>	4 (40)	6 (60)	0.3978
<i>MAGE-B5</i>	3 (30)	5 (50)	0.3880
<i>MAGE-B6</i>	6 (60)	9 (90)	0.1345

Abbreviations: NC: normal colon cancer; CC: colon cancer. Note: values in bold represent a significant result as **P* < 0.05 and ***P* < 0.01.

In this study, RT-PCR was used to analyze *MAGE-B* family genes in CC tissues and neighboring NC tissues. Any genes that were expressed in CC tissues but not in NC tissues might serve as a biomarker for early diagnosis and treatment (such as immunotherapy) of CC in the Saudi population. Immunotherapy for cancer has demonstrated long-term outcomes in individuals with advanced illness, which are not observed with the conventional treatment of chemotherapy [37].

In this work, RT-PCR was used to validate *MAGE-B* family genes in various Saudi CC tissues compared with their neighboring NC tissues. For the first time, this paper demonstrated that the *MAGE-B2*, *MAGE-B3*, *MAGE-B4*, *MAGE-B5*, and *MAGE-B6* genes exhibited PCR products

that were distinct from those seen in NC tissues. However, the band intensities in CC tissues were stronger than in NC tissues. Additionally, the positive *MAGE-B3* expression in CC tissues was more statistically significant than in NC tissues. This pattern was also found in prior studies on *MAGE-B2* and *MAGE-B3* gene expressions in esophageal cancer cell lines [25] and in Taiwanese patients with colorectal cancer [22], consistent with findings in this study. In comparison, *MAGE-B1* was found as a viable candidate for CC markers in the Saudi population because it was expressed in a variety of 60% CC samples but not in NC samples. However, because the sample size was small in that study, more research is required to elucidate the expression of *MAGE-B* genes in different types of malignancies. In a

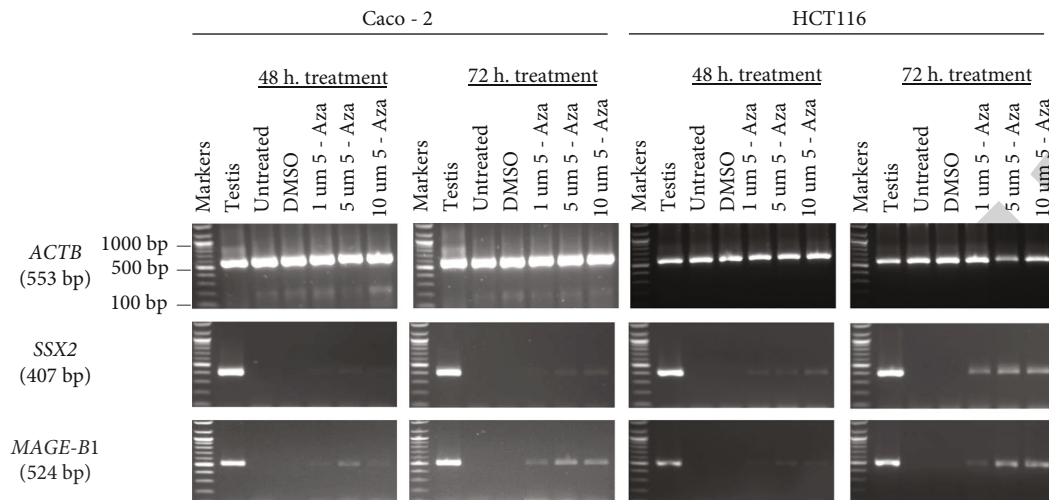


FIGURE 2: The effects of 5-aza-2'-deoxycytidine on *MAGE-B1* gene expression in the CC cell lines. *MAGE-B1* gene expression was exhibited in 1% agarose gels following treatment with a variety of 5-aza-2'-deoxycytidine doses (1.0, 5.0, and 10.0 μM) for 48 h (left side) or 72 hours (right side). Untreated HCT116 and Caco-2 cells were used for comparison with treated cells. Testis cDNA was used to validate the primer efficiency of the *MAGE-B1* gene. HCT116 and Caco-2 cells were treated with DMSO as a control, as DMSO was utilized to prepare the 5-aza-2'-deoxycytidine solution. As a positive control for the cDNA samples, *ACTB* expression was used. The expected size of each gene's product is indicated on the left between brackets.

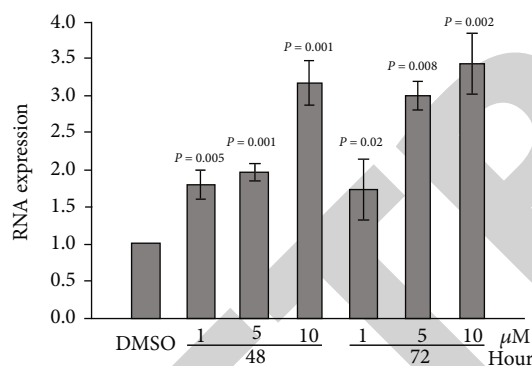


FIGURE 3: qRT-PCR analysis of *MAGE-B1* expression in the HCT116 cell line. The gene expression data for *MAGE-B1* in the HCT116 cell line is shown in the bar chart. The *GAPDH* reference gene was used to normalize the expression data. The error bars indicate the standard error of the mean for three repeats (* $P < 0.05$ and ** $P < 0.01$). N denotes the number of samples.

previous work, a similar result was detected for *MAGE-B1* mRNA in approximately 45% of hepatocellular carcinoma, whereas it was not detected in the neighboring normal liver tissues [26]. This is most likely related to the activation of CT genes in cancer. Demethylation, for example, can result in the activation of previously identified CT genes in cancer [33].

In malignancies, the regulatory mechanisms that control expression of *MAGE-B* genes remain unclear. However, DNA methylation has been found to regulate in *MAGE-A* gene expressions [36]. De Smet et al. demonstrated that demethylation of the CpG sites in promoter of *MAGE-A1* gene is correlated with high levels of gene transcription [38]. To determine whether DNA methyla-

tion inhibition induces *MAGE-B1* expression, HCT116 cells were treated for 48 or 72 hours with various concentrations of 5-aza-2'-deoxycytidine. In this study, it was demonstrated that 5-aza-2'-deoxycytidine treatment of HCT116 cells induces *MAGE-B1* expression, indicating that DNA methylation plays a role in the regulation of this gene. Although there are no previous studies on the correlation between genetic hypomethylation and *MAGE-B1* expression, these findings will be interesting and are in accordance with those found in other reports on *MAGE-A* family genes [31, 39, 40].

In this study, *MAGE-B1* was identified as a gene biomarker for the early detection of CC, which might help in the screening of potential CC candidates. However, the present study includes weaknesses. First, only ten samples from CC patients were used, and the results must be replicated with larger number of samples. Second, it was unable to determine the protein levels of the putative *MAGE-B1* genes in CC due to a shortage of samples.

5. Conclusions

The expression patterns of *MAGE-B* family genes in CC and NC tissues were examined to determine whether any *MAGE-B* gene biomarkers might assist in the early detection of the disease. The mRNA expression of the *MAGE-B1* gene was found in 60% of individuals with CC but not in nearby NC tissues. The pattern of expression of this gene in CC samples implies that it might be employed as a biomarker for malignancy. Additional studies at the protein level and with a bigger cohort of patients are required to validate this finding. Furthermore, it was identified that hypomethylation has a fundamental role in activating *MAGE-B1* gene

expression. This observation indicates that its expression is upregulated and could play a crucial role in the genesis and progression of CC.

Data Availability

All the data relevant to this study is mentioned in the manuscript. There is no supplementary data.

Ethical Approval

The study was conducted according to the guidelines of the Declaration of Helsinki and was approved by the Institutional Review Board (or Ethics Committee) of the Al-Imam Muhammad Ibn Saud Islamic University (project number: 214/2022, IRB-HAPO-01-R-011).

Conflicts of Interest

The authors declare that there is no conflict of interest regarding the publication of this article.

Authors' Contributions

Mikhliid Almutairi was responsible for project management, supervision, validation, sample collection, primer design, and writing of the original draft of the manuscript; Mona Alotaibi was responsible for the RT-PCR and epigenetic studies; Rasha Alonaizan was responsible for data analysis; and Bader Almutairi was responsible for the epigenetic and qRT-PCR experiments.

Acknowledgments

The authors extend their appreciation to the Researchers Supporting Project number (RSP-2021/191), King Saud University, Riyadh, Saudi Arabia.

References

- [1] M. Arnold, M. S. Sierra, M. Laversanne, I. Soerjomataram, A. Jemal, and F. Bray, "Global patterns and trends in colorectal cancer incidence and mortality," *Gut*, vol. 66, no. 4, pp. 683–691, 2017.
- [2] E. Dekker, P. J. Tanis, J. L. A. Vleugels, P. M. Kasi, and M. B. Wallace, "Colorectal cancer," *Lancet*, vol. 394, no. 10207, pp. 1467–1480, 2019.
- [3] I. A. Issa and M. Noureddine, "Colorectal cancer screening: an updated review of the available options," *World Journal of Gastroenterology*, vol. 23, no. 28, pp. 5086–5096, 2017.
- [4] M. A. Althubiti and M. M. Nour Eldein, "Trends in the incidence and mortality of cancer in Saudi Arabia," *Saudi Medical Journal*, vol. 39, no. 12, pp. 1259–1262, 2018.
- [5] H. K. Herzallah, B. R. Antonisamy, M. H. Shafee, and S. T. al-Otaibi, "Temporal trends in the incidence and demographics of cancers, communicable diseases, and non-communicable diseases in Saudi Arabia over the last decade," *Saudi Medical Journal*, vol. 40, no. 3, pp. 277–286, 2019.
- [6] M. H. Almutairi, T. M. Alrubie, A. M. Alamri et al., "Cancer-testis gene biomarkers discovered in colon cancer patients," *Genes*, vol. 13, no. 5, p. 807, 2022.
- [7] D. Kanojia, M. Garg, S. Gupta, A. Gupta, and A. Suri, "Sperm-associated antigen 9 is a novel biomarker for colorectal cancer and is involved in tumor growth and tumorigenicity," *The American Journal of Pathology*, vol. 178, no. 3, pp. 1009–1020, 2011.
- [8] E. R. Fearon and B. Vogelstein, "A genetic model for colorectal tumorigenesis," *Cell*, vol. 61, no. 5, pp. 759–767, 1990.
- [9] A. S. Sameer, "Colorectal cancer: molecular mutations and polymorphisms," *Frontiers in Oncology*, vol. 3, p. 114, 2013.
- [10] A. Suri, N. Jagadish, S. Saini, and N. Gupta, "Targeting cancer testis antigens for biomarkers and immunotherapy in colorectal cancer: current status and challenges," *World journal of gastrointestinal oncology*, vol. 7, no. 12, pp. 492–502, 2015.
- [11] A. W. Whitehurst, "Cause and consequence of cancer/testis antigen activation in cancer," *Annual Review of Pharmacology and Toxicology*, vol. 54, no. 1, pp. 251–272, 2014.
- [12] D. K. Krishnadas, F. Bai, and K. G. Lucas, "Cancer testis antigen and immunotherapy," *ImmunoTargets and therapy*, vol. 2, pp. 11–19, 2013.
- [13] O. Hofmann, O. L. Caballero, B. J. Stevenson et al., "Genome-wide analysis of cancer/testis gene expression," *Proceedings of the National Academy of Sciences of the United States of America*, vol. 105, no. 51, pp. 20422–20427, 2008.
- [14] Z. A. Gibbs and A. W. Whitehurst, "Emerging contributions of cancer/testis antigens to neoplastic behaviors," *Trends Cancer*, vol. 4, no. 10, pp. 701–712, 2018.
- [15] P. van der Bruggen, C. Traversari, P. Chomez et al., "A gene encoding an antigen recognized by cytolytic T lymphocytes on a human melanoma," *Science*, vol. 254, no. 5038, pp. 1643–1647, 1991.
- [16] M. Kalejs and J. Erenpreisa, "Cancer/testis antigens and gametogenesis: a review and "brain-storming" session," *Cancer Cell International*, vol. 5, no. 1, p. 4, 2005.
- [17] P. Chomez, O. de Backer, M. Bertrand, E. de Plaen, T. Boon, and S. Lucas, "An overview of the MAGE gene family with the identification of all human members of the family," *Cancer Research*, vol. 61, no. 14, pp. 5544–5551, 2001.
- [18] M. F. Ladelfa, L. Y. Peche, M. F. Toledo, J. E. Laiseca, C. Schneider, and M. Monte, "Tumor-specific MAGE proteins as regulators of p53 function," *Cancer Letters*, vol. 325, no. 1, pp. 11–17, 2012.
- [19] E. De Plaen, C. Traversari, J. J. Gaforio et al., "Structure, chromosomal localization, and expression of 12 genes of the MAGE family," *Immunogenetics*, vol. 40, no. 5, pp. 360–369, 1994.
- [20] B. Dabovic, E. Zanaria, B. Bardoni et al., "A family of rapidly evolving genes from the sex reversal critical region in Xp21," *Mammalian Genome*, vol. 6, no. 9, pp. 571–580, 1995.
- [21] S. Lucas, C. De Smet, K. C. Arden et al., "Identification of a new MAGE gene with tumor-specific expression by representational difference analysis," *Cancer Research*, vol. 58, no. 4, pp. 743–752, 1998.
- [22] F. Y. Chung, T. L. Cheng, H. J. Chang et al., "Differential gene expression profile of MAGE family in Taiwanese patients with colorectal cancer," *Journal of Surgical Oncology*, vol. 102, no. 2, pp. 148–153, 2010.
- [23] C. Barrow, J. Browning, D. MacGregor et al., "Tumor antigen expression in melanoma varies according to antigen and stage," *Clinical Cancer Research*, vol. 12, no. 3, pp. 764–771, 2006.

Retraction

Retracted: Comparative Genomic Characterization of Insulin-Like Growth Factor Binding Proteins in Cattle and Buffalo

BioMed Research International

Received 8 January 2024; Accepted 8 January 2024; Published 9 January 2024

Copyright © 2024 BioMed Research International. This is an open access article distributed under the Creative Commons Attribution License, which permits unrestricted use, distribution, and reproduction in any medium, provided the original work is properly cited.

This article has been retracted by Hindawi, as publisher, following an investigation undertaken by the publisher [1]. This investigation has uncovered evidence of systematic manipulation of the publication and peer-review process. We cannot, therefore, vouch for the reliability or integrity of this article.

Please note that this notice is intended solely to alert readers that the peer-review process of this article has been compromised.

Wiley and Hindawi regret that the usual quality checks did not identify these issues before publication and have since put additional measures in place to safeguard research integrity.

We wish to credit our Research Integrity and Research Publishing teams and anonymous and named external researchers and research integrity experts for contributing to this investigation.

The corresponding author, as the representative of all authors, has been given the opportunity to register their agreement or disagreement to this retraction. We have kept a record of any response received.

References

- [1] M. S. Rehman, M. Mushtaq, F. U. Hassan, Z. U. Rehman, M. Mushahid, and B. Shokrollahi, "Comparative Genomic Characterization of Insulin-Like Growth Factor Binding Proteins in Cattle and Buffalo," *BioMed Research International*, vol. 2022, Article ID 5893825, 15 pages, 2022.

Research Article

Comparative Genomic Characterization of Insulin-Like Growth Factor Binding Proteins in Cattle and Buffalo

Muhammad Saif-ur Rehman ¹, Muqees Mushtaq,¹ Faiz-ul Hassan ¹, Zia-ur Rehman ²,
Muhammad Mushahid,¹ and Borhan Shokrollahi ³

¹Institute of Animal and Dairy Sciences, University of Agriculture, Faisalabad 38040, Pakistan

²University of Agriculture, Faisalabad–Subcampus Toba Tek Singh, Pakistan

³Department of Animal Science, Sanandaj Branch, Islamic Azad University, Sanandaj, Iran

Correspondence should be addressed to Borhan Shokrollahi; borhansh@iausdj.ac.ir

Received 31 May 2022; Revised 30 June 2022; Accepted 6 July 2022; Published 25 July 2022

Academic Editor: Dr Muhammad Hamid

Copyright © 2022 Muhammad Saif-ur Rehman et al. This is an open access article distributed under the Creative Commons Attribution License, which permits unrestricted use, distribution, and reproduction in any medium, provided the original work is properly cited.

The somatotrophic axis consists of genes associated with economic traits like muscle growth and carcass traits in livestock. Insulin-like growth factor binding proteins (IGFBPs) are the major proteins that play a vital role in the somatotrophic axis. The present study performed a genome-wide characterization of IGFBP genes in cattle. Genomic sequences of the IGFBP gene family for different mammals (cattle, buffalo, goat, and sheep) were recovered from the NCBI database. Sequence analyses were performed to investigate cattle's genomic variations in the IGFBP gene family. Phylogenetic analysis, gene structure, motif patterns, and conserved domain analysis (CDA) of the IGFBP family revealed the evolutionarily conserved nature of the IGFBP genes in cattle and other studied species. Physicochemical properties of IGFBP proteins in cattle revealed that most of these proteins are unstable, hydrophilic, thermostable, and acidic. Comparative amino acid analysis revealed variations in all protein sequences with single indels in IGFBP3 and IGFBP6. Mutation analysis revealed only one nonsynonymous mutation D212 > E in the IGFBP6 protein of cattle. A total of 245 nuclear hormone receptor (NHRs) sites were detected, including 139 direct repeats (DR), 65 everted repeats (ER), and 41 inverted repeats (IR). Out of 133 transcription factors (TFs), 10 TFs (AHR, AHRARNT, AP4, CMYB, E47, EGR2, GATA, SPI, and SRF) had differential distribution (P value < 0.05) of putative transcriptional binding sites (TFBS) in cattle compared to buffalo. Synteny analysis revealed the conserved nature of genes between cattle and buffalo. Two gene pairs (IGFBP1/IGFBP3 and IGFBP2/IGFBP5) showed tandem duplication events in cattle and buffalo. This study highlights the functional importance of genomic variation in IGFBP genes and necessitates further investigations better to understand the role and mechanisms of IGFBPs in bovines.

1. Introduction

IGFBPs are cysteine-rich proteins with high essential amino acid sequence similarity. Almost six mammalian types of IGFBPs commonly exist, ranging from IGFBP1 to 6. They can bind insulin-like growth factor (IGF) growth with a very high affinity [1]. IGF-independent activities of IGFBPs significantly affect biological procedures, including angiogenesis or cell proliferation [1, 2]. The expression of IGFBP is controlled by various physiological conditions such as exercise, nutrition, and pregnancy. IGFBPs are used as a bio-

marker for improving husbandry conditions, health status, phenotype selection, or disease analysis in farm animals [3].

IGFs are the most important polypeptides in mammals that control body growth, metabolism, mitosis, and cell differentiation [4, 5]. IGFs have a galactopoietic role and stimulate the development and growth of the mammary glands [6]. IGFBPs are a member of a family of six homologous proteins that always bind with IGFs. They control most of the biological activities (metabolism and growth). Based on amino acid similarity analysis, IGFBP1 is more closely related to IGFBP2 than to IGFBP3, which in turn is more

closely associated with *IGFBP5* [1]. *IGFBP3* induces cell proliferation or apoptosis (programmed cell death) in various cells [7]. Lower levels of *IGFBP2* in estrogen-dominant bovine follicles are not attributable to enhanced proteolysis; lower levels of *IGFBP4* and 5 are most likely to exhibit protease activity [8]. *IGFBP4* protease plays a significant role in developing dominant ovarian follicles [9]. *IGFBP6* levels, on the other hand, were shown to rise with age [10].

The *IGFBP3* is a direct growth inhibitor and a regulator of *IGF* bioactivity in extravascular tissues [11]. *IGFBP3* was the primary component of six *IGFBPs* in mammalian circulation [12]. In plasma, it is associated with more than 90% of *IGFs* [13]. The *IGFBP3* gene is present on chromosome 4 in cattle [14] and is 8.9 kb in length, having five exons [15]. The *IGFBP3* is involved in various body functions, including metabolism, immunity, growth, energy balance, and reproduction. Due to the primary role of *IGFBP3* in animal growth and maturity, the *IGFBP3* gene is considered a candidate gene and a good marker for production and growth traits [16].

The development of the *IGFBP* gene family has been attributed to repetitive chromosomal duplications. According to thorough sequence analysis, sequence-based phylogenies, and chromosomal information, the ancestral chordate *IGFBP* gene experienced a localized gene duplication, forming a gene pair close to a *HOX* cluster [17]. The *IGFBP* gene family follows the six *IGFBP* types in today's placental mammals due to 2 basal vertebrate tetraploidization. Many *IGFBP* genes have survived despite that the gene family's ancient expansion strongly implies that each gene gained different and significant functions early in mammal evolution [17].

The genomic characterization of the *IGFBP* gene family is necessary to provide insights into genetic variation in different *IGFBP* genes and their comparative physiological role in production performance in cattle. Moreover, identifying transcription binding sites and nuclear receptors can help better comprehend the regulation of *IGFBP* genes in cattle. Therefore, the present study was planned for the genomic characterization of the *IGFBPs* in cattle to elucidate nucleotide sequence variations.

2. Materials and Methods

2.1. Identification of *IGFBP* Genes in Cattle. The cattle (ARS-UCD1.2), buffalo (UOA_WB_1), sheep (Oar Rambouillet_v1.0), and goat (ARS1) genomes, proteomes, and annotation data were retrieved from the National Center for Biotechnology Information (NCBI) genome database [18] aiming at identifying *IGFBP* genes in cattle. The GenBank accession number of each member of the *IGFBP* gene family of every species is listed in supplementary Table S1. To validate all potential *IGFBP* genes in cattle at a genome-wide level, both the basic local alignment search tool (BLAST) and the hidden Markov model (HMM) searches were carried out. The buffalo (*Bubalus bubalis*), goat (*Capra hircus*), and sheep (*Ovis aries*) *IGFBP* (insulin-like growth factor binding protein) sequences were also validated from the UniProt database [19].

The sequences were submitted to BLASTp, with a threshold of e value = 10^{-5} , using the BLOSUM62 matrix, which had a word size of six, a gap cost of eleven, an extension of one, and an adjustment for the conditional compositional score matrix. The cattle dataset was also searched with the HMMER [20] program using the HMM profile of the *IGFBP* domain (PF00219) from the Pfam database with an e value threshold of 1.0×10^{-5} . Duplicated sequences were excised after retrieving the necessary protein sequences to avoid ambiguity. These nonredundant sequences were examined using the Simple Modular Architecture Research Tool (SMART) to validate the presence of domains in the *IGFBP* protein sequences [21]. The conserved protein domains in the cattle *IGFBP* family were compared with the NCBI's conserved domain database (CDD).

2.2. Phylogenetic Analysis. ClustalW (protein sequence alignment tool) was used to align the amino acid sequences of *IGFBP* from cattle, buffalo, goats, and sheep. The aligned sequences were utilized to create a neighbour-joining (NJ) phylogenetic tree of the *IGFBP* gene family by the MEGA7 program, using a Poisson model with pairwise deletion and a bootstrap value of 1000 replicates.

2.3. Structural Feature Analysis. The MEME suite [22] was used to analyze the conserved motifs in the dataset. The *IGFBP* protein sequences were provided in FASTA format as a query, and a site distribution was chosen for each sequence with one occurrence of each site. The minimum and maximum widths of motifs were 6 and 50, respectively. The number of motifs was set as 10. All CDs and genomic sequences were imported into the Gene Structure Display Server 2.0. (GSDS) [23]. Then, the final gene structure was displayed and visualized using the cattle genome annotation file in general feature format (GFF) using in-house scripts in the TBtools software.

2.4. Characterization of Physicochemical Properties of *IGFBP* Proteins. The ProtParam was used to describe physical and chemical characteristics of *IGFBP* proteins, such as molecular weight (MW), amino acid number, isoelectric point (pI), aliphatic index (AI), instability index (II), and grand average of hydropathicity (GRAVY) as described, previously [24, 25].

2.5. Multiple Sequence Alignment. In order to identify indels and illustrate sequence variations in the *IGFBP* protein sequence, the Multiple Align Show [26] tool was used to perform multiple sequence alignment of the *IGFBP* protein sequences.

2.6. Mutation Analysis. The mutations observed in the protein sequences of four species were further analyzed through different online tools (PolyPhen-2, MUpro, PROVEAN, I-Mutant, PhD-SNP, SIFT, SNAP2, PredictSNP, Meta-SNP, and SNAP) to look for their impacts on protein structure and functions. Further, the 3-dimension structures of *IGFBP6* genes of cattle, buffalo, goat, and sheep were predicted through MODELLER and the quality of the structures was checked in SAVES server through ERRAT, Verify 3D,

PROVE, PROCHECK, and Whatcheck. The Ramachandran plot showed mostly residues in allowed regions. No residue was present in the disallowed region. To calculate the RMSD value, the mutated cattle *IGFBP6* protein structure was aligned against protein structures of *IGFBP6* genes of buffalo, goat, and sheep in Moe 2021 (<https://www.chemcomp.com/Products.htm>) software to know the structural similarities and deviations.

2.7. Detection of TF Binding Sites. Detection of possible signals for a putative transcription binding factor was accomplished using the Promoter 2.0 prediction server [27]. As input, cattle and buffalo genomic sequences were provided in FASTA format. The site with a higher score (>1.0) is a probable predicted site. TFBIND [28] was used to find the sequence of 100 bp upstream from the increased likelihood predicted location, which was obtained and entered into the program. The weight matrix of the transcription factor database TRANSFAC R.3.4 was used to identify transcription factor binding sites.

2.8. Nuclear Hormone Receptor Site Identification. Further, for the prediction of nuclear hormone receptor binding sites, the NHR scan [29] was employed using genomic sequences in FASTA format. The cumulative probability of entering match states was 0.01 using the NHR scan.

2.9. Synteny Analysis. The whole genomes of cattle and buffalo were blasted to each other to identify collinear genes. TBtools was used to construct the dual-synteny plot, which was created by providing annotation files for both genomes, including information about collinear genes and chromosomal IDs.

Chromosomal locations of buffalo *IGFBP* genes were acquired from their genome resources. A genome annotation file with a general feature format (GFF) was given as an input to the MCScanX program [30] to map the physical locations of genes on chromosomes and then visualized in TB tools. Furthermore, the buffalo and cattle dual-synteny plots were plotted for *IGFBP* gene collinearity. Additionally, pairwise alignment of homologous gene pairs of *IGFBP* genes using MEGA7 [31] with the MUSCLE algorithm was used to assess the occurrences of duplications for the buffalo *IGFBP* gene family. The DnaSP v6.0 [32] software was also used to calculate pairwise synonymous substitutions per synonymous site (Ks) and nonsynonymous substitutions per nonsynonymous site (Ka) adjusted for multiple hits.

3. Results

3.1. Phylogenetic Analysis. The molecular phylogenetic study of representative species indicated that all of the *IGFBP* gene sequences were classified into seven types: *IGFBP1*, *IGFBP2*, *IGFBP3*, *IGFBP4*, *IGFBP5*, *IGFBP6*, and *IGFBP7* (Figure 1). All seven genes were grouped into three sister clades. From top to bottom, clade 1 included *IGFBP2*, -4, and -1; clade 2 included *IGFBP6*, -3, and -5; and clade 3 included *IGFBP7*. Overall, phylogenetic analysis of the *IGFBP* gene family revealed that the *Bos taurus* is more closely related to *Bubalus bubalis* in all *IGFBP* gene family groups except *IGFBP7*

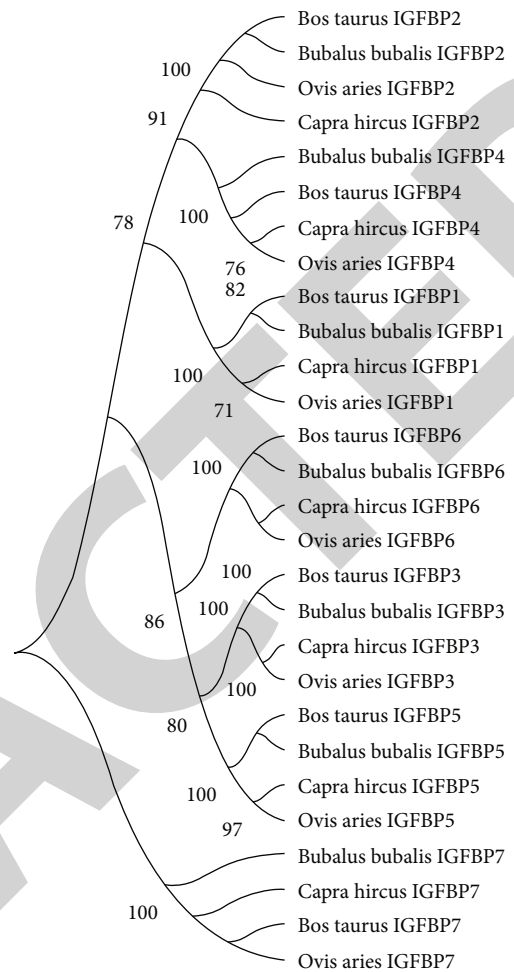


FIGURE 1: Molecular phylogenetic analysis of the *IGFBP* gene family (*IGFBP1* to *IGFBP7*) in *Bos taurus*, *Bubalus bubalis*, *Capra hircus*, and *Ovis aries*.

where it was distantly related. Similarly, *Capra hircus* is more closely associated with *Ovis aries* except for *IGFBP2* and *IGFBP7* where it was distantly related (Figure 1).

3.2. Structural Categorization of the *IGFBP* Gene Family. The investigation of gene organization, motif patterns, and conserved domains in the *IGFBP* gene family in four studied species was also carried out to undertake structural characterization of the *IGFBP* gene family while considering their evolutionary connections (Figures 2(a)–2(d)). The top ten MEME-conserved motifs in the *IGFBP* genes were analyzed (Table 1). The MEME1 motif with a 41 amino acid sequence length was annotated as the Thyroglobulin_1 domain, while the MEME2 motif with a 50 amino acid sequence length was annotated as the IB (insulin growth factor-binding protein homologs) domain after Pfam search. Further, conserved domain analysis for all genes revealed Ig superfamily and Kazal domains (Figure 2(c)). Identified conserved domains were further confirmed using the CDD BLAST in NCBI. A gene structural analysis revealed that cattle *IGFBP* genes in the same group had a similar number of introns and exons, even though the untranslated regions (UTRs) upstream and

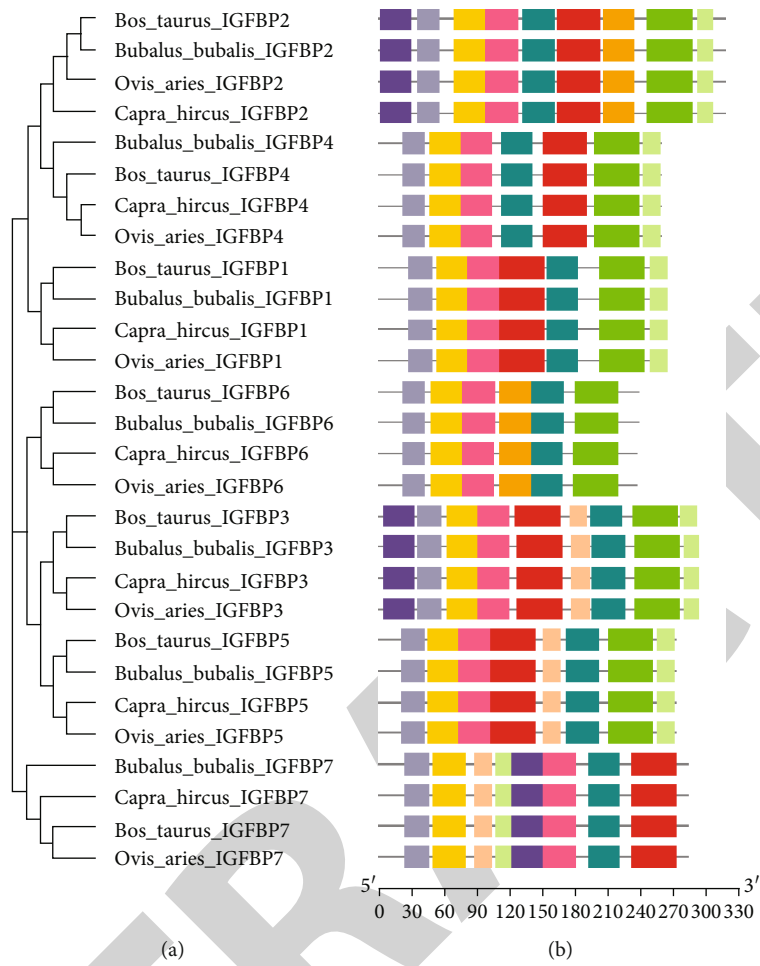


FIGURE 2: Continued.



(c)
FIGURE 2: Continued.

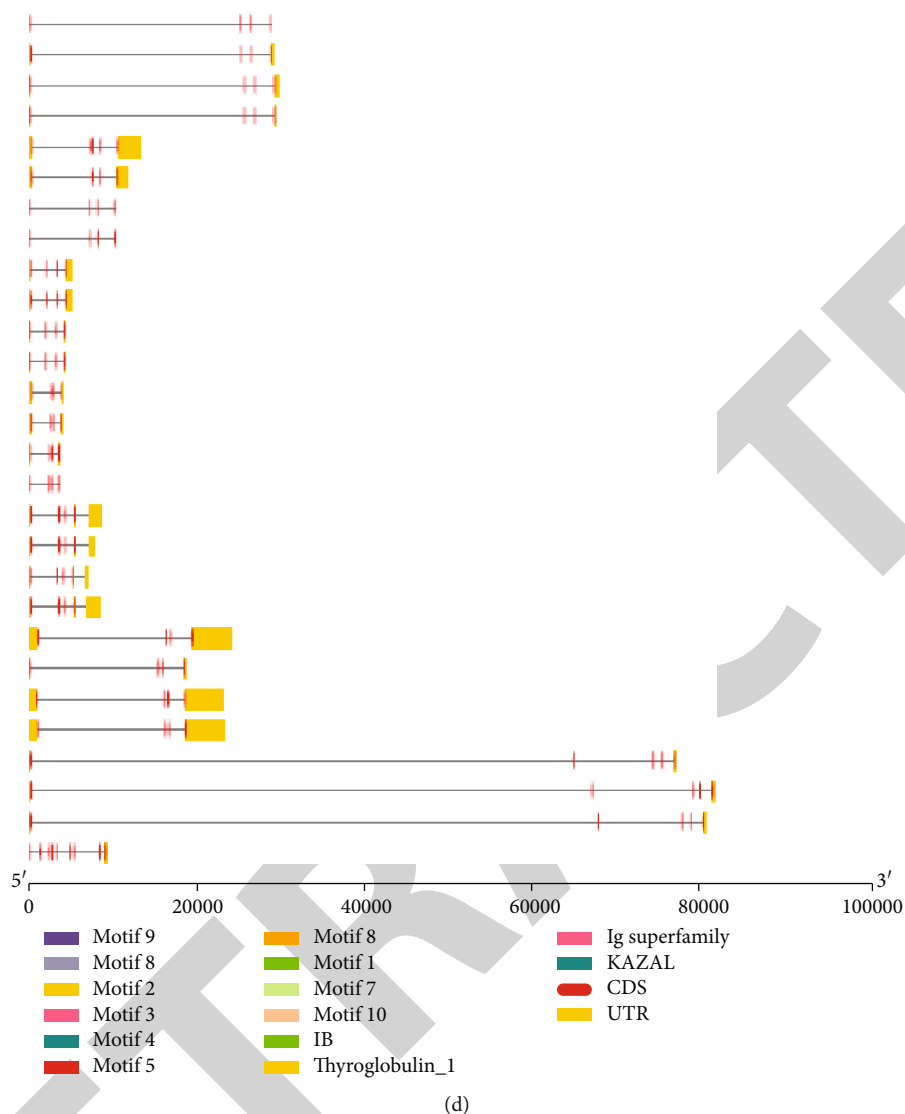


FIGURE 2: Phylogenetic relationships, gene structure, motif patterns, and conserved domain regions of the *IGFBP* gene family in *Bos taurus*, *Bubalus bubalis*, *Capra hircus*, and *Ovis aries*. (a) Phylogenetic relationship of 7 *IGFBPs*. (b) Motif pattern. (c) Conserved domain regions of the *IGFBP* gene family. (d) Gene structure of *IGFBPs*. Ten putative motifs are indicated in different colored boxes.

TABLE 1: Top ten differentially conserved motifs detected in the *IGFBP* (*IGFBP1*, *IGFBP2*, *IGFBP3*, *IGFBP4*, *IGFBP5*, *IGFBP6*, and *IGFBP7*) gene family.

Motif	Protein sequence	Length	Pfam domain
MEME1	YALYJPNCDKKGFYKKKQCKPSLGGKRGLCWCVDKYGGKLP	41	Thyroglobulin_1
MEME2	PGCGCCATCALREGQPCGVYTPRCAQGLRCYPPPGEEKPLHALLHGRGVC	50	IB
MEME3	SESRQETEQGPCRRELEKVLZRLKAEQLR	29	—
MEME4	TAGAGEVVRCEPCDEEALARCPPPPGSP	29	—
MEME5	SEKIDGDPZCHTFDN	15	—
MEME6	PLLLLALLAA	11	—
MEME7	KVFREKVTPIHVSMGSGGKKH	21	—
MEME8	ESTESGEIEEN	11	—
MEME9	RASADYVLLAEQLAA	15	—
MEME10	VERGSDEH	8	—

TABLE 2: Physicochemical characteristics of the *IGFBP* gene family in cattle.

Gene	Chromosome	Exon count	MW (Da)	A.A	pI	AI	II	GRAVY
<i>IGFBP1</i>	4	4	28794.05	263	6.33	75.02	54.07	-0.295
<i>IGFBP2</i>	2	4	34014.92	317	7.13	72.02	36.20	-0.521
<i>IGFBP3</i>	4	5	31570.09	291	9.03	56.05	47.67	-0.636
<i>IGFBP4</i>	19	4	27890.00	258	7.10	70.00	46.51	-0.483
<i>IGFBP5</i>	2	4	30313.96	271	8.72	61.22	51.81	-0.632
<i>IGFBP6</i>	5	5	24966.92	237	8.73	51.10	63.20	-0.781
<i>IGFBP7</i>	6	5	29078.28	282	8.25	77.84	46.77	-0.193

MW: molecular weight in Daltons; A.A: number of amino acids; pI: isoelectric point; AI: aliphatic index; II: instability index; GRAVY: grand average of hydropathicity index.

downstream of the gene structure differed significantly between them (Figure 2(d)). However, different *IGFBP* genes displayed a differential distribution of introns and exons in their coding regions.

3.3. Physicochemical Properties of the *IGFBPs*. The physicochemical characteristics of the *IGFBP* gene in cattle were evaluated in terms of their location on the chromosome, exon count, molecular weight (Da), number of amino acids (A.A) in each peptide, aliphatic index (AI), isoelectric point (pI), instability index (II), and grand average of hydropathicity index (GRAVY) (Table 2). *IGFBP1* and *IGFBP3* were discovered on chromosome 4, *IGFBP2* and *IGFBP5* on chromosome 2, *IGFBP4* on chromosome 19, *IGFBP6* on chromosome 5, and *IGFBP7* on chromosome 6 in the region between 250 kb, which contains a variable number of exons and a variable number of length of the gene with amino acid residues. The *IGFBPs* had a molecular weight ranging from 24 to 34 kDa. The *IGFBPs* in cattle were unstable but thermostable proteins, as shown by the presence of values greater than 60 for the aliphatic index of all *IGFBPs*. The pI values also indicated that the *IGFBP1* protein is a slightly acidic peptide but the other *IGFBP* proteins (*IGFBP2*, *IGFBP3*, *IGFBP4*, *IGFBP5*, *IGFBP6*, and *IGFBP7*) are basic peptides in nature. The *IGFBPs* in cattle were unstable except for *IGFBP2*, which showed an instability index value smaller than 40. All proteins were thermostable due to higher values of the aliphatic index. Lower GRAVY values suggested cattle's hydrophilic nature of *IGFBP* proteins (Table 2).

3.4. Comparative Amino Acid Analysis of *IGFBP*. Comparative amino acid analysis of targeted species revealed 2 short indels in the *IGFBP* gene family, including a single indel in *IGFBP3* and a single indel in *IGFBP6* (Figure S1A–S1G).

In the *IGFBP1*, a single amino acid variation was observed at positions L40>M and I249>V in *Bos taurus*, Q19>H in *Bubalus bubalis*, and L14>P and E226>D in *Ovis aries*. Comparatively, amino acids A, R, and K were observed at positions 146, 166, and 254, respectively, in *Bos taurus* and *Bubalus bubalis*, while amino acids T, K, and Q were observed at the same positions, respectively, in *Capra hircus* and *Ovis aries* (Figure S1A).

In the *IGFBP2*, a single amino acid variation was observed at positions A58>S and H145>Q in *Bubalus bubalis*, E130>V, M233>V, and E304>G in *Capra hircus*,

and L150>Q, S175>F, and G176>R in *Ovis aries* (Figure S1B).

Only one indel was observed in *IGFBP3* in *Bos taurus*, at position 132>133. A single amino acid variation was observed at position A17>T in *Bos taurus*, A34>T in *Bubalus bubalis*, A61>T in *Capra hircus*, and E79>V and L232>P in *Ovis aries*. Comparatively, amino acids Q, R, S, S, S, H, V, F, P, R, H, M, G, G, D, Y, and M were observed at positions 107, 126, 134, 136, 158, 160, 164, 167, 169, 208, 225, 231, 236, 276, 278, 288, and 290, respectively, in *Bos taurus* and *Bubalus bubalis*, while amino acids H, S, P, P, T, R, D, S, L, H, D, T, A, F, S, L, and T were observed at the same positions in *Capra hircus* and *Ovis aries*. Additionally, amino acid M was observed at position 32 in *Bos taurus* and *Bubalus bubalis*, while amino acids A and V were observed at the same position in *Capra hircus* and *Ovis aries*, respectively. Similarly, amino acids L and A were observed at positions 156 and 170, respectively, in *Capra hircus* and *Ovis aries*. In contrast, amino acids G and V were observed at position 156 in *Bos taurus* and *Capra hircus*, respectively, and amino acids I and V were regarded at position 170 in *Bos taurus* and *Bubalus bubalis*, respectively (Figure S1C).

In *IGFBP4*, single amino acid variation was observed at positions V7>M in *Bos taurus*, A161>C and P162>T in *Bubalus bubalis*, and A8>T in *Ovis aries*. Two amino acid variations were seen at position 166 in the targeted species. Comparatively, amino acid A was observed at position 166 in *Bos taurus* and *Bubalus bubalis*, while amino acid V was regarded at the same position in *Capra hircus* and *Ovis aries* (Figure S1D).

In *IGFBP5*, single amino acid variation was observed at positions P16>S and E185>K in *Bos taurus* and G258>R in *Capra hircus*. Comparatively, amino acid M was observed at position 182 in *Bos taurus* and *Bubalus bubalis*, while amino acid L was observed at the same position in *Capra hircus* and *Ovis aries* (Figure S1E).

In *IGFBP6*, one indel was observed at position 46 in *Capra hircus* and *Ovis aries*. Single amino acid variation was observed at positions D212>E in *Bos taurus*, N147>S in *Bubalus bubalis*, G103>V in *Capra hircus*, and Q97>R, G190>D, and S235>G in *Ovis aries*. Comparatively, amino acid S was observed at positions 144 and 146 in *Bos taurus* and *Bubalus bubalis*, while amino acid V and P were observed at the same positions in *Capra hircus* and *Ovis aries*, respectively (Figure S1F).

TABLE 3: Effects of mutations on the *IGFBP6* protein structure of cattle aligned against buffalo, goat, and sheep *IGFBP6* protein structures.

Structure A	Structure B	RMSD value
IGFBP6 cow (blue)	IGFBP6 buffalo (yellow)	0.073
IGFBP6 cow (blue)	IGFBP6 goat (cyan)	0.000
IGFBP6 cow (blue)	IGFBP6 sheep (green)	0.171

In *IGFBP7*, single amino acid variation was observed at positions P5 > L, L21 > P, R78 > G, V229 > A, and Q256 > R in *Ovis aries*. Comparatively, amino acid R was observed at position 95 in *Bos taurus* and *Ovis aries*, while amino acid K was observed at the same position in *Bubalus bubalis* and *Capra hircus* (Figure S1G).

3.5. Mutation Analysis. After the comparative amino acid analysis, the mutations observed were further analyzed using online tools to predict their effects on protein structures and functions. The results differed for different tools (Table S2). For all the mutations, the overall impact was neutral (synonymous mutations) except for position D212E in *IGFBP6* protein in cattle, which was found damaging (nonsynonymous).

Further, the mutated cattle *IGFBP6* protein structure was superimposed against *IGFBP6* protein structures of buffalo, goat, and sheep to know the structural similarities and differences (Figure S2A-S2C) and the root means square deviation (RMSD) values were calculated (Table 3). The RMSD values were less than 2 Å for all superimposed structures. “Cattle and goat” had zero RMSD values showing the identical structure, following the “cattle and buffalo” (0.073) and “cattle and sheep” (0.171) (Table 3).

3.6. Transcription Factor Binding Sites. The putative transcription factor binding sites (TFBS) were observed for *IGFBP* genes in cattle and buffalo. 133 transcriptional factors (TFs) were screened for differential distribution of TFBS, out of which only 10 TFs (*AHR*, *AHRARNT*, *AP4*, *CMYB*, *E47*, *EGR2*, *GATA*, *SPI1*, and *SRF*) were found to have the high differential distribution of TFBS. Both cattle and buffalo had a variable number of binding sites for most TFs (Table S3).

3.7. NHR Sites in *IGFBP*. The pattern of NHR (nuclear hormone receptor) sites in the *IGFBP* gene family in cattle was investigated using the genomic sequence of the *Bos taurus*. 245 NHR sites were identified in the cattle *IGFBP* gene family (Figure S3). Moreover, the identified NHRs in *IGFBP1*, *IGFBP2*, *IGFBP3*, *IGFBP4*, *IGFBP5*, *IGFBP6*, and *IGFBP7* were 6, 50, 12, 26, 28, 6, and 117, respectively. In total, 139 direct repeats (DR) and 65 everted repeats (ER) were found in the cattle *IGFBP* genes which are prominently used by type II receptors (RXR) and some type III receptors (orphan receptors) can also use DR. The DR distributed in *IGFBP1*, *IGFBP2*, *IGFBP3*, *IGFBP4*, *IGFBP5*, *IGFBP6*, and *IGFBP7* were 3, 31, 8, 15, 17, 4, respectively, and 61 and ER were 3, 13, 2, 3, 6, 0, and 38, respectively.

A total of 41 inverted repeats (IR) were observed in different *IGFBP* genes primarily used as the hormonal response element (HRE) important for steroid receptors. The IR distributed in *IGFBP1*, *IGFBP2*, *IGFBP3*, *IGFBP4*, *IGFBP5*, *IGFBP6*, and *IGFBP7* were 0, 6, 2, 8, 5, 2, and 18, respectively.

3.8. Synteny Analysis. Collinearity analysis showed that *IGFBP* genes were randomly distributed over 5 chromosomes in cattle and buffalo (Figure 3). In cattle, *IGFBP* genes were present on chromosomes 2, 4, 5, 6, and 19, whereas these genes were located on chromosomes 2, 3, 4, 7, and 8 in buffalo. Most genes were present close to the centromere of chromosomes in cattle.

Gene duplication events were observed in *IGFBP* family members of cattle and buffalo using Tb tools (Figures 4(a) and 4(b)). No segmental duplication was observed in both species. Tandem duplication was observed between homologous gene pairs *IGFBP1/IGFBP3* and *IGFBP2/IGFBP5* for both species at chromosome positions 4 and 2 for cattle and 8 and 2 for buffalo, respectively. Further, the ratios of nonsynonymous substitutions per nonsynonymous site (Ka) to synonymous substitutions per synonymous site (Ks) were calculated for these duplication events. The results indicated that duplicated gene pairs *IGFBP1/IGFBP3* and *IGFBP2/IGFBP5* had 0.81 and 0.86 Ka/Ks ratios in cattle and 0.79 and 0.73 in buffalo, respectively (Table 4).

4. Discussion

Recent developments in genomic sequencing technology, particularly next-generation sequencing, resulted in the availability of sequenced genomes for many animal species, opening new avenues for understanding the genomic architecture at the molecular level [33]. Comparative genomics allows for identifying novel genes and the functional components underlying the unique traits of different species [34].

4.1. Evolutionary and Phylogenetic Analysis. Understanding the genetics and evolutionary processes of physiologically crucial genes, such as the *IGFBP* gene family in mammals, is necessary for understanding the regulatory mechanisms of these genes. Previously, the *IGFBP* gene family has been reported to contain six members (*IGFBP1-IGFBP6*) in vertebrates [1, 17]. Our molecular phylogenetic analysis of the *IGFBP* gene family revealed that all the four representative species contained seven genes (*IGFBP1-IGFBP7*) (Figure 1). The *Bos taurus* was closely related to *Bubalus bubalis*, whereas *Capra hircus* and *Ovis aries* shared higher sequence similarities. Our results are also supported by the study performed in *Capra hircus*, where *Ovis aries* and *Capra hircus* were closely related evolutionary, whereas *Bos taurus* was distantly related [35].

4.2. Structure of the *IGFBP* Gene Family. The top ten MEME-conserved motifs were observed in the *IGFBP* genes in the present study. The six human *IGFBPs* ranged in size between 240 and 328 residues and shared a common structural organization with two conserved domains separated by a variable central region. The N-terminal domain

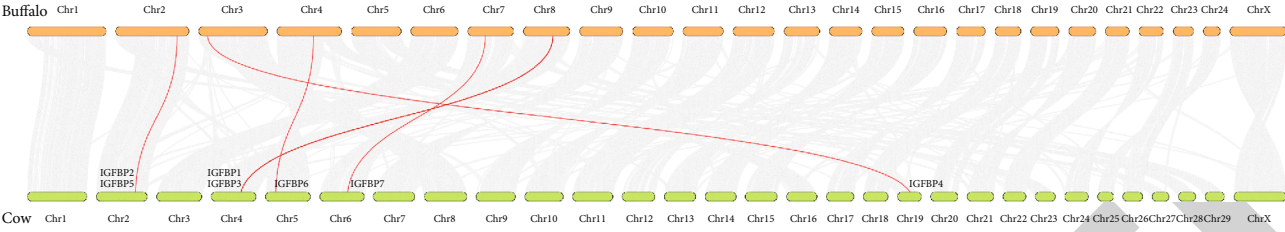


FIGURE 3: Synteny plot between cattle and buffalo genomes.

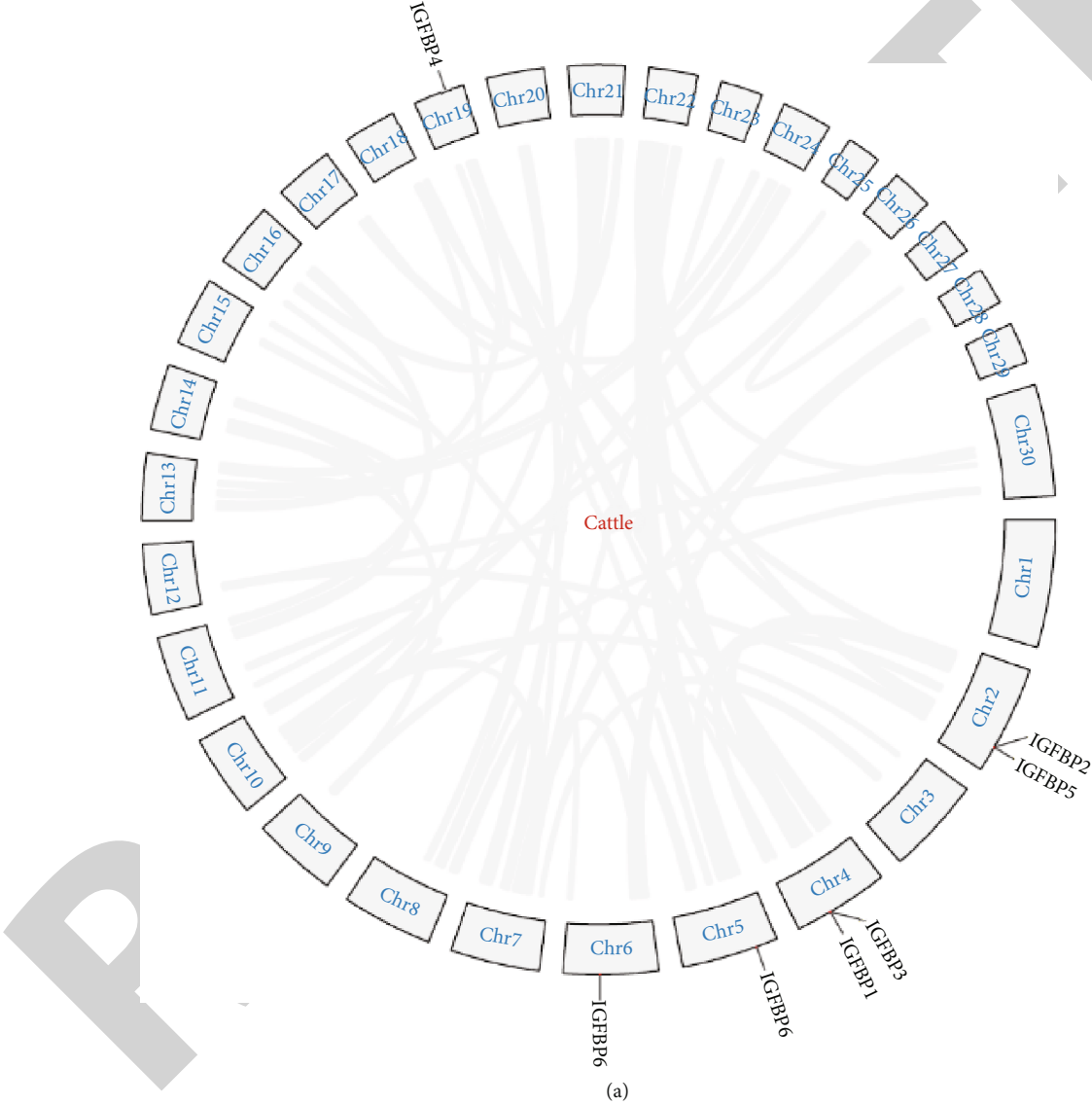


FIGURE 4: Continued.

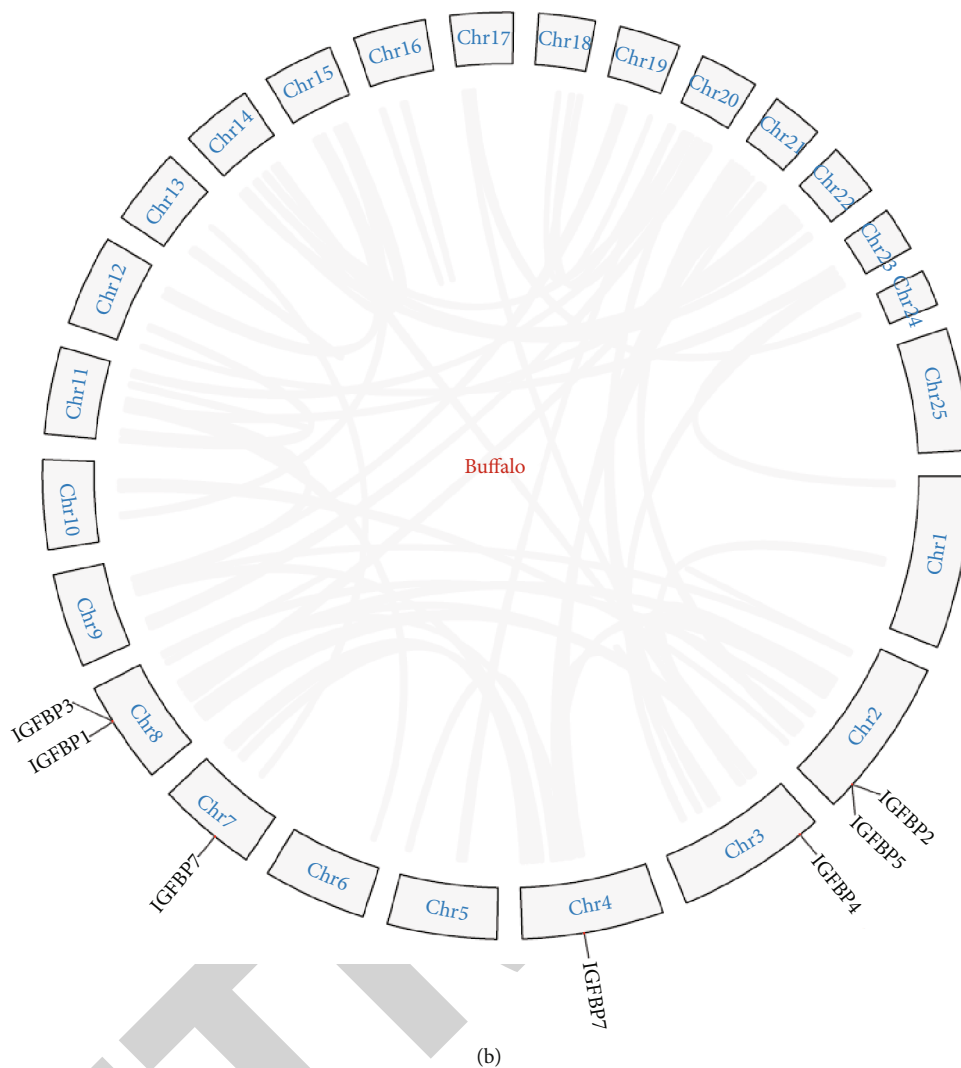


FIGURE 4: Gene duplication events in the *IGFBP* gene family of (a) cattle and (b) buffalo.

TABLE 4: Analysis of the Ka/Ks ratios for each pair of the duplicated *IGFBP* gene pair in cattle and buffalo.

Cow					
Gene pairs	Chr	Duplication	Ka	Ks	Ka/Ks
IGFBP1/IGFBP3	4/4	TD	0.7143	0.8809	0.81
IGFBP2/IGFBP5	2/2	TD	0.6230	0.7288	0.86
Buffalo					
Gene pairs	Chr	Duplication	Ka	Ks	Ka/Ks
IGFBP1/IGFBP3	8/8	TD	0.6848	0.8641	0.79
IGFBP2/IGFBP5	2/2	TD	0.6021	0.8202	0.73

contains the primary IGF-binding (IB) site, and the C-terminal domain is a thyroglobulin type-1 domain [11, 17]. Our study annotated the MEME1 motif with a 41 amino acid sequence length as the thyroglobulin_1 domain. Previously, the thyroglobulin_1 domain is present in several protein families, including IGFBP6, a member of IGFBPs [36]. Thyroglobulin-1 repeats exhibit inhibitory activity against cysteine proteases and show greater selectivity in their inter-

actions with target proteases. The MEME2 motif with a 50 amino acid sequence length was annotated as IB (insulin growth factor-binding protein homologs) domain after Pfam search (Table 1). The presence of thyroglobulin_1 and IB domains in C-terminal and N-terminal regions, respectively, suggested that the *IGFBPs* across all the studied species remained conserved throughout the evolution. Further, similar intron and exon structures of *IGFBP* genes across all studied species supported the conserved structural organization of *IGFBPs*. The upstream and downstream UTR structure considerably varied in different *IGFBP* genes mainly attributed to the absence or presence of retroposon elements.

4.3. *IGFBP* Physicochemical Properties. The physicochemical properties of the *IGFBP* gene family in cattle revealed that their molecular weight ranged from 24 to 34kDa. The pI values indicated that all proteins are basic except *IGFBP1*, slightly acidic. The instability index (II) reflects the stability of proteins within the test tube. The II values lower than 40 indicate stable proteins [37]. The *IGFBP* peptides in cattle were unstable except for *IGFBP2*, which showed an

instability index value smaller than 40. Higher values of AI reveal the thermostability of globular proteins [38]. The AI values of *IGFBP1*, *IGFBP2*, and *IGFBP4* were more than 65, indicating their higher thermostability than *IGFBP3*, *IGFBP5*, and *IGFBP6*. All proteins were found thermostable due to higher values of the aliphatic index. GRAVY values tell about the hydrophobic character of proteins [39]. In our study, negative GRAVY values suggested that cattle's IGFBP proteins are hydrophilic.

4.4. Comparative Amino Acid Sequence Analysis. Comparative genomics is a large-scale, integrative method that analyzes two or more genomes to determine their similarities and differences and investigate the biology of the individual genomes. To acquire diverse views on the organisms, comparative studies may be carried out at different levels of the genomes [40].

Comparative amino acid analysis of cattle with buffalo, goat, and sheep revealed amino acid variations in all *IGFBP* protein sequences (Figure S1). Overall, all six proteins were well conserved in all four analyzed species with a size range of 263 to 317 amino acid residues. The *IGFBP* superfamily was also found conserved in humans with a size range of 240 to 328 amino acid residues [17]. Deletions were observed in *IGFBP3* in cattle at position 132 > 133 and in *IGFBP6* in goats and sheep at position 46. Insertions, deletions, and mutations have played an important role in *IGFBP* family members' divergence from their progenitor [41]. Most of the variations were observed in the *IGFBP3* gene. *IGFBP3* is the most common *IGF* carrier protein in bovine serum, binding more than 95 percent of the *IGF-I* and *II* in circulation [42]. The nucleotide sequencing study revealed similarity percentages of 88.54, 89.63, and 95.0 in *IGFBP3* gene sequences between "sheep and cattle," "sheep and buffalo," and "cattle and buffalo," respectively [43]. In another study, sheep's *IGFBP3* gene nucleotide and amino acid sequence were compared with cattle and buffalo and 90 and 93 percent similarities were observed, respectively [44].

4.5. Mutation Analysis. Mutations can improve the overall fitness or can damage the structural conformation resulting in altered functions or being neutral without any change [45]. Synonymous mutations are those where no change in amino acid sequence occurs due to nucleotide change, while nonsynonymous mutations change the protein sequence by altering the amino acid. In our study, single amino acid variations observed by aligning the sequences of all target species were further analyzed to check for their effects on the protein structure and functions. Only one nonsynonymous mutation was observed at position D212E in *IGFBP6* protein in cattle using different online tools (Table S1). *IGFBP6* protein sequence alignment comparison of human with rat, mouse bovine, pig, and zebrafish revealed 70–85% sequence identity [46]. The same amino acid variation was also recognized in that comparison only for cattle. Mutations in the protein structure can cause problems in protein catalytic activity, stability, and interaction with other molecules [45]. The *IGFBP6* role has been

determined in folliculogenesis [47], carcass traits [48], and 305 days in milk yield [49] in cattle. So, a nonsynonymous mutation in *IGFBP6* protein may affect these functions. The altered expression of the *IGFBP6* gene in different tissues of abnormal cloned cattle was linked with increased birth weight and other abnormalities [50].

RMSD values quantify the structural similarities between two or more proteins. The present study showed lower RMSD values < 2 Å, which indicated high structural similarity in the *IGFBP6* protein of cattle with buffalo and sheep, and a zero RMSD value for "cattle and goat" indicated that the structures are identical in conformation [51]. RMSD is also one of the methods to quantify the sequence alignment and evolutionary similarities between the two proteins [52, 53].

4.6. Putative Transcription Factor Binding Sites. A total of 133 TFs were screened for differential distribution of putative TFBS, out of which 10 TFs were found to have a differential distribution of binding sites in cattle and buffalo (Table S3). Aryl hydrocarbon receptor (AhRs) binding factor sites were found variable in cattle and buffalo. A study indicated that AhR can suppress the IGF pathway via upregulation of *IGFBP1*, resulting in decreased IGFs' bioavailability [54]. Activator protein 4 (AP4) is also an important TF and plays an important role in cell proliferation, cell growth, apoptosis, and metabolism [55]. AP4 binds to the E-box motifs at the *IGFBP-2* promoter in luciferase reporter assays and serves as a transactivator [56]. C-myb is a member of the myb protein family involved in cell growth, differentiation, and apoptosis and acts as a transcriptional transactivator [57]. C-myb is highly expressed in immature hematopoietic cells and is known as an oncogene. C-myb was found to regulate the function of the *IGFBP3* gene in leukaemia cells and the *IGFBP5* gene in neuroblastoma cells [58, 59]. Transcription factor E47 is involved in gene regulation of muscle tissue differentiation by interacting with MyoD [60]. Specificity protein 1 (Sp1) is an important binding factor and is observed to control cell growth and its overexpression leads to tumour formation [61]. In rats, the TATA-less promoter for the *IGFBP2* gene requires three clustered Sp1 sites for effective transcription [62]. The serum response factor (SRF) is related to the MADS (MCM1, Agamous, Deficiens, and SRF) family of proteins and plays an important role in skeletal muscle growth in adult mammals [63].

4.7. NHR Patterns in IGFBP. Understanding the complex biochemical systems that regulate gene transcription is essential for understanding the information flow from gene to protein and, as a result, the cell's dynamics [64]. Nuclear receptors regulate transcription by attaching DNA sequences in target genes to hormone response elements (HREs). These elements are found in regulatory sequences usually found in the target gene's 5-flanking region. Although HREs are frequently located near the main promoter, many kilobases upstream of the transcriptional start point can also be found in enhancer regions [65]. A single

NHR frequently affects many genes, and various NHRs may compete for the same target sites, resulting in target gene networks that overlap [66]. NHR can also suppress the gene expression due to competition for the same target site or binding with negative HREs [65]. The pattern of NHR sites in the *IGFBP* gene family in cattle was investigated using the genomic sequence of the *Bos taurus*. 245 NHR sites were found in the cattle *IGFBP* gene family (Figure S2). In a total of 139 direct repeats (DR), 65 everted repeats (ER) and 41 inverted repeats (IR) were identified in the cattle *IGFBP* genes.

4.8. Synteny Analysis. Synteny blocks are chromosomal segments shared by two genomes with the same order of homologous genes originating from a common ancestor site [67]. The capability to examine evolutionary mechanisms that lead to diversification of a chromosomal number and shape in numerous lineages throughout the tree of life has been made possible by comparing genomic synteny between and within species [68, 69]. Collinearity analysis showed that *IGFBP* genes were randomly distributed over 5 chromosomes in cattle and buffalo showing the collinear relationship (Figure 3). Comparative genomic studies between cattle and buffalo revealed up to 97% similarities [70, 71]. Expansion of the genome happened during evolution through gene duplication events, leading to the increased genome size of organisms as indicated by the “2R hypothesis” [72, 73]. All the duplicated genomes did not get fixed, only 5 to 10% got fixed, and others were lost in the evolutionary process [74, 75]. In cattle and buffalo, predominantly tandem duplication events were observed, revealing the role of tandem duplication in the expansion of the *IGFBP* gene family. Our results are also supported by Liu et al. [76], who suggested that 75–90% of segmental duplications are organized into local tandem duplication clusters in the cattle genome. These genomic duplication events that happened during evolution helped in adaption and speciation. The duplicated genes under positive selection pressure show >1 Ka/Ks ratios, whereas duplicated genes under purifying pressure show <1 Ka/Ks ratios [77]. In our results, duplicated gene pairs in cattle and buffalo showed <1 Ka/Ks ratios, indicating purifying pressure for these genomic duplications. Due to two basic vertebrate tetraploidization, the *IGFBP* gene family follows the six *IGFBP* types found in today's placental animals. The fact that numerous *IGFBP* genes have survived despite the gene family's ancient expansion clearly suggested that each gene acquired distinct and important tasks early in mammalian evolution [17].

5. Conclusion

The present study concluded that the *IGFBP* gene family remained well conserved throughout its evolution in cattle and buffalo. Mutation analysis revealed one nonsynonymous mutation at position D212>E in *IGFBP6* in cattle which may affect important functions like folliculogenesis, growth and development, and lactation. Differential distribution of NHRs and TFBS in cattle and buffalo indicated the variation of putative regulation of these genes. Gene duplications

revealed the role of tandem duplication in the expansion of the *IGFBP* gene family in bovines, and these genome duplication events helped in adaption and speciation.

Data Availability

All data are shown within the manuscript.

Conflicts of Interest

The authors declare that there is no conflict of interest regarding the publication of this paper.

Authors' Contributions

Muhammad Saif-ur Rehman and Muqet Mushtaq contributed equally to this manuscript.

Acknowledgments

This study was funded by the “National Centre for Livestock Breeding, Genetics and Genomics (NCLBGG)”, subcentre, UAF, Pakistan.

Supplementary Materials

Figure S1 (S1A–S1G): comparative amino acid analysis of the *IGFBP* gene family (TGFBP1–IGFBP7) in *Bos taurus*, *Bubalus bubalis*, *Capra hircus*, and *Ovis aries*. Figure S2 (S2A–S2C): superimposed structures of the *IGFBP6* protein (cattle vs buffalo, cattle vs goat, and cattle vs sheep). Figure S3 (S3A–S3G): NHR scan patterns of the *IGFBP* gene family (IGFBP1–IGFBP7). Table S1: GenBank accession numbers of all *IGFBP* genes for all study species. Table S2: mutational analysis of the *IGFBP* gene family (IGFBP1–IGFBP7) in cattle and buffalo. Table S3: transcription factor binding sites observed in cattle and buffalo. (*Supplementary Materials*)

References

- [1] R. G. Rosenfeld, V. Hwa, E. Wilson, S. R. Plymate, and Y. Oh, “The insulin-like growth factor-binding protein superfamily,” *Growth Hormone and IGF Research*, vol. 10, pp. S16–S17, 2000.
- [2] M. J. Moreno, M. Ball, M. Rukhlova et al., “IGFBP-4 Anti-Angiogenic and Anti-Tumorigenic Effects Are Associated with Anti-Cathepsin B Activity,” *Neoplasia*, vol. 15, no. 5, pp. 554–567, 2013.
- [3] S. Rajaram, D. J. Baylink, and S. Mohan, “Insulin-like growth factor-binding proteins in serum and other biological fluids: regulation and functions,” *Endocrine Reviews*, vol. 18, no. 6, pp. 801–831, 1997.
- [4] L. A. Bach, “The insulin-like growth factor system: towards clinical applications,” *The Clinical Biochemist. Reviews*, vol. 25, no. 3, pp. 155–164, 2004.
- [5] K. L. Hossner, R. H. McCusker, and M. V. Dodson, “Insulin-like growth factors and their binding proteins in domestic animals,” *Animal Science*, vol. 64, no. 1, pp. 1–15, 1997.
- [6] D. L. Kleinberg, T. L. Wood, P. A. Furth, and A. V. Lee, “Growth hormone and insulin-like growth factor-I in the transition from normal mammary development to preneoplastic

- mammary lesions,” *Endocrine Reviews*, vol. 30, no. 1, pp. 51–74, 2009.
- [7] B. J. Leibowitz and W. S. Cohick, “Endogenous IGFBP-3 is required for both growth factor-stimulated cell proliferation and cytokine-induced apoptosis in mammary epithelial cells,” *Journal of Cellular Physiology*, vol. 220, no. 1, pp. 182–188, 2009.
- [8] L. J. Spicer, C. S. Chamberlain, and G. L. Morgan, “Proteolysis of insulin-like growth factor binding proteins during preovulatory follicular development in cattle¹,” *Domestic Animal Endocrinology*, vol. 21, no. 1, pp. 1–15, 2001.
- [9] G. M. Rivera, Y. A. Chandrasekher, A. C. O. Evans, L. C. Giudice, and J. E. Fortune, “A potential role for insulin-like growth factor binding protein-4 proteolysis in the establishment of ovarian follicular dominance in cattle 1,” vol. 111, pp. 102–111, 2001.
- [10] H. Yu, J. Mistry, M. J. Nisar et al., “Insulin-like growth factors (IGF-I, free IGF-I, and IGF-II) and insulin-like growth factor binding proteins (IGFBP-2, IGFBP-3, IGFBP-6, and ALS) in blood circulation,” *Journal of Clinical Laboratory Analysis*, vol. 13, no. 4, pp. 166–172, 1999.
- [11] D. R. Clemmons, “Insulin-like growth factor binding proteins,” *Growth Factors and Cytokines in Health and Disease*, vol. 3, no. C, pp. 191–222, 1997.
- [12] J. I. Jones and D. R. Clemmons, “Insulin-like growth factors and their binding proteins: biological actions,” *Endocrine Reviews*, vol. 16, no. 1, pp. 3–34, 1995.
- [13] F. M. Rodríguez, N. R. Salvetti, C. G. Panzani, C. G. Barbeito, H. H. Ortega, and F. Rey, “Influence of insulin-like growth factor-binding proteins-2 and -3 in the pathogenesis of cystic ovarian disease in cattle,” *Animal Reproduction Science*, vol. 128, no. 1–4, pp. 1–10, 2011.
- [14] S. M. Kappes, J. W. Keele, R. T. Stone et al., “A second-generation linkage map of the bovine genome,” *Genome Research*, vol. 7, no. 3, pp. 235–249, 1997.
- [15] J. Y. Kim, D. H. Yoon, B. L. Park et al., “Identification of novel SNPs in bovine insulin-like growth factor binding protein-3 (IGFBP3) gene,” *Asian-Australasian Journal of Animal Sciences*, vol. 18, no. 1, pp. 3–7, 2005.
- [16] V. Choudhary, P. Kumar, V. K. Saxena et al., “Effect of leptin and IGFBP-3 gene polymorphisms on serum IgG level of cattle calves,” *Asian-Australasian Journal of Animal Sciences*, vol. 19, no. 8, pp. 1095–1099, 2006.
- [17] D. Ocampo Daza, G. Sundström, C. A. Bergqvist, C. Duan, and D. Larhammar, “Evolution of the insulin-like growth factor binding protein (IGFBP) family,” *Endocrinology*, vol. 152, no. 6, pp. 2278–2289, 2011.
- [18] NCBI, *National Center for Biotechnology Information* April 2022 Available online: <https://www.ncbi.nlm.nih.gov/>.
- [19] Uniprot, *Protein database* April 2022 Available online: <https://www.uniprot.org/>.
- [20] R. D. Finn, J. Clements, and S. R. Eddy, “HMMER web server: interactive sequence similarity searching,” *Nucleic Acids Research*, vol. 39, pp. W29–W37, 2011.
- [21] SMART, *Simple Modular Architecture Research Tool* April 2022 Available online: <http://smart.embl-heidelberg.de/>.
- [22] T. L. Bailey, M. Boden, F. A. Buske et al., “MEME SUITE: tools for motif discovery and searching,” *Nucleic Acids Research*, vol. 37, pp. W202–W208, 2009.
- [23] B. Hu, J. Jin, A.-Y. Guo, H. Zhang, J. Luo, and G. Gao, “GSDS 2.0: an upgraded gene feature visualization server,” *Bioinformatics*, vol. 31, no. 8, pp. 1296–1297, 2015.
- [24] S. U. Rehman, T. Feng, S. Wu et al., “Comparative genomics, evolutionary and gene regulatory regions analysis of casein gene family in *Bubalus bubalis*,” *Frontiers in Genetics*, vol. 12, p. 662609, 2021.
- [25] E. Gasteiger, C. Hoogland, A. Gattiker, M. R. Wilkins, R. D. Appel, and A. Bairoch, “Protein identification and analysis tools on the ExPASy server,” in *The Proteomics Protocols Handbook*, pp. 571–607, Humana Press, 2005.
- [26] MSA, *Multiple Align Show* April 2022 Available online: https://www.bioinformatics.org/sms/multi_align.html.
- [27] Promoter, *Prediction Server* April 2022 Available online: <http://www.cbs.dtu.dk/services/Promoter/>.
- [28] TFBIND, *Transcription factor binding sites input* April 2022 Available online: <https://tfbind.hgc.jp/>.
- [29] NHR-SCAN, *Nuclear hormone receptor scan* April 2022 Available online: http://nhscan.genereg.net/cgi-bin/nhr_scan.cgi.
- [30] Y. Wang, H. Tang, J. D. DeBarry et al., “MCScanX: a toolkit for detection and evolutionary analysis of gene synteny and collinearity,” *Nucleic Acids Research*, vol. 40, no. 7, pp. e49–e49, 2012.
- [31] S. Kumar, G. Stecher, and K. Tamura, “MEGA7: molecular evolutionary genetics analysis version 7.0 for bigger datasets,” *Molecular Biology and Evolution*, vol. 33, no. 7, pp. 1870–1874, 2016.
- [32] J. Rozas, A. Ferrer-Mata, J. C. Sánchez-DelBarrio et al., “DnaSP 6: DNA sequence polymorphism analysis of large data sets,” *Molecular Biology and Evolution*, vol. 34, no. 12, pp. 3299–3302, 2017.
- [33] X. Luo, Y. Zhou, B. Zhang et al., “Understanding divergent domestication traits from the whole-genome sequencing of swamp- And river-buffalo populations,” *National Science Review*, vol. 7, no. 3, pp. 686–701, 2020.
- [34] M. Rijnkels, L. Elnitski, W. Miller, and J. M. Rosen, “Multispecies comparative analysis of a mammalian-specific genomic domain encoding secretory proteins,” *Genomics*, vol. 82, no. 4, pp. 417–432, 2003.
- [35] S. Y. Zhan, L. Chen, L. Li, L. J. Wang, T. Zhong, and H. P. Zhang, “Molecular characterization and expression patterns of insulin-like growth factor-binding protein genes in postnatal Nanjiang brown goats,” *Genetics and Molecular Research*, vol. 14, no. 4, pp. 12547–12560, 2015.
- [36] M. Mihelič and D. Turk, “Two Decades of Thyroglobulin Type-1 Domain Research,” *bchm*, vol. 388, no. 11, pp. 1123–1130, 2007.
- [37] K. Guruprasad, B. V. B. Reddy, and M. W. Pandit, “Correlation between stability of a protein and its dipeptide composition: a novel approach for predicting in vivo stability of a protein from its primary sequence,” *Protein Engineering, Design and Selection*, vol. 4, no. 2, pp. 155–161, 1990.
- [38] I. Atsushi, “Thermostability and aliphatic index of globular proteins,” *Journal of Biochemistry*, vol. 88, no. 6, pp. 1895–1898, 1980.
- [39] J. Kyte and R. F. Doolittle, “A simple method for displaying the hydrophobic character of a protein,” *Journal of Molecular Biology*, vol. 157, no. 1, pp. 105–132, 1982.
- [40] L. Wei, Y. Liu, I. Dubchak, J. Shon, and J. Park, “Comparative genomics approaches to study organism similarities and differences,” *Journal of Biomedical Informatics*, vol. 35, no. 2, pp. 142–150, 2002.
- [41] P. V. Gordon and M. Marcinkiewicz, “An analysis of IGFBP evolution,” *Growth Hormone and IGF Research*, vol. 18, no. 4, pp. 284–290, 2008.

- [42] L. A. Wetterau, M. G. Moore, K. W. Lee, M. L. Shim, and P. Cohen, "Novel aspects of the insulin-like growth factor binding proteins," *Molecular Genetics and Metabolism*, vol. 68, no. 2, pp. 161–181, 1999.
- [43] A. A. Saleh, A. M. A. Rashad, N. N. A. M. Hassanine, M. A. Sharaby, and Y. Zhao, "Comparative analysis of IGFBP-3 gene sequence in Egyptian sheep, cattle, and buffalo," *BMC Research Notes*, vol. 12, no. 1, pp. 1–7, 2019.
- [44] P. Kumar, V. Choudhary, K. G. Kumar et al., "Nucleotide sequencing and DNA polymorphism studies on IGFBP-3 gene in sheep and its comparison with cattle and buffalo," *Small Ruminant Research*, vol. 64, no. 3, pp. 285–292, 2006.
- [45] R. A. Studer, B. H. Dessailly, and C. A. Orenge, "Residue mutations and their impact on protein structure and function: detecting beneficial and pathogenic changes," *Biochemical Journal*, vol. 449, no. 3, pp. 581–594, 2013.
- [46] L. A. Bach, "Recent insights into the actions of IGFBP-6," *Journal of Cell Communication and Signaling*, vol. 9, no. 2, pp. 189–200, 2015.
- [47] S. Llewellyn, R. Fitzpatrick, D. A. Kenny, J. J. Murphy, R. J. Scaramuzzi, and D. C. Wathes, "Effect of negative energy balance on the insulin-like growth factor system in pre-recruitment ovarian follicles of post partum dairy cows," *Reproduction*, vol. 133, no. 3, pp. 627–639, 2007.
- [48] M. C. Baeza, P. M. Corva, L. A. Soria et al., "Genetic markers of body composition and carcass quality in grazing Brangus steers," *Genetics and Molecular Research*, vol. 10, no. 4, pp. 3146–3156, 2011.
- [49] R. Zamorano-Alg, P. Luna-NevÁ, G. RincÁn et al., "Research Article Genotypes within the prolactin and growth hormone insulin-like growth factor-I pathways associated with milk production in heat stressed Holstein cattle: genotypes and milk yield in heat stressed Holstein cows," *Genetics and Molecular Research*, vol. 16, no. 4, 2017.
- [50] Z.-J. Gong, Y.-Y. Zhou, M. Xu et al., "Aberrant expression of imprinted genes and their regulatory network in cloned cattle," *Theriogenology*, vol. 78, no. 4, pp. 858–866, 2012.
- [51] O. Carugo, "Statistical validation of the root-mean-square-distance, a measure of protein structural proximity," *Protein Engineering, Design & Selection*, vol. 20, no. 1, pp. 33–37, 2007.
- [52] A. I. Jewett, C. C. Huang, and T. E. Ferrin, "MINRMS: an efficient algorithm for determining protein structure similarity using root-mean-squared-distance," *Bioinformatics*, vol. 19, no. 5, pp. 625–634, 2003.
- [53] F. Armougom, S. Moretti, V. Keduas, and C. Notredame, "The iRMSD: a local measure of sequence alignment accuracy using structural information," *Bioinformatics*, vol. 22, no. 14, pp. e35–e39, 2006.
- [54] C. Talia, L. Connolly, and P. A. Fowler, "The insulin-like growth factor system: a target for endocrine disruptors?," *Environment International*, vol. 147, p. 106311, 2021.
- [55] M. M. K. Wong, S. M. Joyson, H. Hermeking, and S. K. Chiu, "Transcription factor AP4 mediates cell fate decisions: to divide, age, or die," *Cancers*, vol. 13, no. 4, p. 676, 2021.
- [56] L. Badinga, S. Song, R. C. M. Simmen, and F. A. Simmen, "A distal regulatory region of the insulin-like growth factor binding protein-2 (IGFBP-2) gene interacts with the basic helix-loop-helix transcription factor, AP-4," *Endocrine*, vol. 8, no. 3, pp. 281–290, 1998.
- [57] I. H. Oh and E. P. Reddy, "The myb gene family in cell growth, differentiation and apoptosis," *Oncogene*, vol. 18, no. 19, pp. 3017–3033, 1999.
- [58] M. S. Kim, S. Y. Kim, S. Arunachalam et al., "C-myb stimulates cell growth by regulation of insulin-like growth factor (IGF) and IGF-binding protein-3 in K562 leukemia cells," *Biochemical and Biophysical Research Communications*, vol. 385, no. 1, pp. 38–43, 2009.
- [59] B. Tanno, A. Negroni, R. Vitali et al., "Expression of insulin-like growth factor-binding protein 5 in neuroblastoma cells is regulated at the transcriptional level by c-Myb and B-Myb via direct and indirect mechanisms," *Journal of Biological Chemistry*, vol. 277, no. 26, pp. 23172–23180, 2002.
- [60] J. M. Lingbeck, J. S. Trausch-Azar, A. Ciechanover, and A. L. Schwartz, "E12 and E47 modulate cellular localization and proteasome-mediated degradation of MyoD and Id1," *Oncogene*, vol. 24, no. 42, pp. 6376–6384, 2005.
- [61] L. Li and J. R. Davie, "The role of Sp1 and Sp3 in normal and cancer cell biology," *Annals of Anatomy*, vol. 192, no. 5, pp. 275–283, 2010.
- [62] Y. R. Boisclair, A. L. Brown, S. Casola, and M. M. Rechler, "Three clustered Sp1 sites are required for efficient transcription of the TATA-less promoter of the gene for insulin-like growth factor-binding protein-2 from the rat," *Journal of Biological Chemistry*, vol. 268, no. 33, pp. 24892–24901, 1993.
- [63] S. Li, M. P. Czubryt, J. McAnally et al., "Requirement for serum response factor for skeletal muscle growth and maturation revealed by tissue-specific gene deletion in mice," *Proceedings of the National Academy of Sciences of the United States of America*, vol. 102, no. 4, pp. 1082–1087, 2005.
- [64] E. H. Davidson, *Genomic Regulatory Systems: In Development and Evolution*, Elsevier, 2001.
- [65] A. Aranda and A. Pascual, "Nuclear hormone receptors and gene expression," *Physiological Reviews*, vol. 81, no. 3, pp. 1269–1304, 2001.
- [66] D. Cotnoir-White, D. Laperrière, and S. Mader, "Evolution of the repertoire of nuclear receptor binding sites in genomes," *Molecular and Cellular Endocrinology*, vol. 334, no. 1–2, pp. 76–82, 2011.
- [67] I. A. Vergara and N. Chen, "Large synteny blocks revealed between *Caenorhabditis elegans* and *Caenorhabditis briggsae* genomes using OrthoCluster," *BMC Genomics*, vol. 11, no. 1, p. 516, 2010.
- [68] G. Zhang, B. Li, C. Li, M. T. P. Gilbert, E. D. Jarvis, and J. Wang, "Comparative genomic data of the avian phylogenomics project," *GigaScience*, vol. 3, no. 1, pp. 1–8, 2014.
- [69] K. L. Howe, B. J. Bolt, S. Cain et al., "WormBase 2016: expanding to enable helminth genomic research," *Nucleic Acids Research*, vol. 44, no. D1, pp. D774–D780, 2016.
- [70] W. Li, D. M. Bickhart, L. Ramunno, D. Iamartino, J. L. Williams, and G. E. Liu, "Genomic structural differences between cattle and river buffalo identified through comparative genomic and transcriptomic analysis," *Data in Brief*, vol. 19, pp. 236–239, 2018.
- [71] P. Dutta, A. Talenti, R. Young et al., "Whole genome analysis of water buffalo and global cattle breeds highlights convergent signatures of domestication," *Nature Communications*, vol. 11, no. 1, pp. 1–13, 2020.
- [72] P. W. H. Holland, J. Garcia-Fernández, N. A. Williams, and A. Sidow, "Gene duplications and the origins of vertebrate development," *Development*, vol. 1994, pp. 125–133, 1994.

Retraction

Retracted: Evaluation of Hematological, Oxidative Stress, and Antioxidant Profile in Cattle Infected with Brucellosis in Southern Punjab, Pakistan

BioMed Research International

Received 8 January 2024; Accepted 8 January 2024; Published 9 January 2024

Copyright © 2024 BioMed Research International. This is an open access article distributed under the Creative Commons Attribution License, which permits unrestricted use, distribution, and reproduction in any medium, provided the original work is properly cited.

This article has been retracted by Hindawi following an investigation undertaken by the publisher [1]. This investigation has uncovered evidence of one or more of the following indicators of systematic manipulation of the publication process:

- (1) Discrepancies in scope
- (2) Discrepancies in the description of the research reported
- (3) Discrepancies between the availability of data and the research described
- (4) Inappropriate citations
- (5) Incoherent, meaningless and/or irrelevant content included in the article
- (6) Manipulated or compromised peer review

The presence of these indicators undermines our confidence in the integrity of the article's content and we cannot, therefore, vouch for its reliability. Please note that this notice is intended solely to alert readers that the content of this article is unreliable. We have not investigated whether authors were aware of or involved in the systematic manipulation of the publication process.

Wiley and Hindawi regrets that the usual quality checks did not identify these issues before publication and have since put additional measures in place to safeguard research integrity.

We wish to credit our own Research Integrity and Research Publishing teams and anonymous and named external researchers and research integrity experts for contributing to this investigation.

The corresponding author, as the representative of all authors, has been given the opportunity to register their agreement or disagreement to this retraction. We have kept a record of any response received.

References

- [1] R. Hussain, I. Khan, A. Jamal, B. B. Mohamed, and A. Khan, "Evaluation of Hematological, Oxidative Stress, and Antioxidant Profile in Cattle Infected with Brucellosis in Southern Punjab, Pakistan," *BioMed Research International*, vol. 2022, Article ID 7140909, 10 pages, 2022.

Research Article

Evaluation of Hematological, Oxidative Stress, and Antioxidant Profile in Cattle Infected with Brucellosis in Southern Punjab, Pakistan

Riaz Hussain ¹, Iaftasham Khan,² Adil Jamal ³, Bahaeldeen Babiker Mohamed ⁴,
and Ahrar Khan ^{5,6}

¹Department of Pathology, Faculty of Veterinary and Animal Sciences, The Islamia University of Bahawalpur, Bahawalpur 63100, Pakistan

²Section of Epidemiology and Public Health, Department of Clinical Sciences, University of Veterinary and Animal Sciences, Lahore Sub-Campus Jhang 12-Km Chiniot Road, Jhang 35200, Pakistan

³Sciences and Research, College of Nursing, Umm Al Qura University-715, Makkah, Saudi Arabia

⁴Institute of Environment Natural Resources, The National Centre of Research, Khartoum, Sudan

⁵Shandong Vocational Animal Science and Veterinary College, Weifang 261061, China

⁶Faculty of Veterinary Science, University of Agriculture, Faisalabad, Pakistan

Correspondence should be addressed to Riaz Hussain; dr.riaz.hussain@iub.edu.pk and Bahaeldeen Babiker Mohamed; bahaeldeen.elhag@ncr.gov.sd

Received 26 May 2022; Accepted 5 July 2022; Published 18 July 2022

Academic Editor: Faheem Ahmed Khan

Copyright © 2022 Riaz Hussain et al. This is an open access article distributed under the Creative Commons Attribution License, which permits unrestricted use, distribution, and reproduction in any medium, provided the original work is properly cited.

Brucellosis is a well-known and harmful zoonotic disease that poses a severe threat to public health and wild and dairy animals. Due to a lack of monitoring and awareness, disease incidence has increased. Therefore, this study was conducted for the first time to ascertain the status of seroprevalence of brucellosis, hematological, oxidative stress, and antioxidant enzymes in different breeds of cattle reared under tropical-desert conditions in Pakistan. This study comprised 570 cattle of different breeds. We recorded some epidemiological traits, including age and gender. The blood samples were obtained from all the cattle, screened with RBPT, and then confirmed by ELISA and PCR. The results recorded an overall 11.75%, 10.7%, and 9.64% prevalence of brucellosis based on RBPT, ELISA, and PCR. We obtained nonsignificant results in different age and sex groups of cattle. The results showed significantly ($P \leq 0.05$) lower values of erythrocyte counts, hemoglobin quantity, hematocrit, lymphocytes, and monocytes in infected cases. The results showed that the total leukocyte and neutrophil cells significantly ($P \leq 0.05$) increased. The lipid peroxidation parameters (MDA- and NO-scavenging activity of erythrocyte) increased significantly ($P \leq 0.05$) in infected cattle, whereas significantly reduced antioxidant enzymes like SOD, RGS, and CAT were. Similarly, significantly lower serum albumin levels and total serum proteins were recorded in infected cattle.

1. Introduction

Brucellosis is a zoonotic and contagious disease of wild and domestic animals and affects public health resulting in substantial economic losses. In livestock, it results in reduced productivity (20-25%), decreased milk production, abortion, and weak offspring and is a significant impediment to the trade [1, 2]. A high incidence of temporary and permanent infertility could result in the culling of animals. The disease

has worldwide distribution and affects animals and humans in developed and developing countries [3, 4]. In developing countries, the disease burden is more profound due to inadequate public health measures, domestic animal health programs, and appropriate diagnostic facilities [5].

Brucellosis caused by *Brucella* poses severe threats to public health worldwide [6]. However, its prevalence worldwide is highly prevalent in Mediterranean countries [7]. *Brucella* is an intracellular gram-negative bacterium and

species-specific. The disease is caused by different species of Brucellae (nonmotile, anaerobic coccobacilli, and gram-negative), including two marine and six terrestrial species. Brucellosis is commonly transmitted via aborted fetuses, semen, uterine exudates, and fetal contents. In the male, brucellosis manifests permanent sterility, epididymitis, seminal vesiculitis, and orchitis [8]. In females, the disease causes death due to severe metritis, damage to fetal membranes, and retained placental contents. The exact mechanisms of pathogenesis of disease in animals are still under debate. Still, various studies have indicated that the causative agent enters the body via the digestive tract, mucosal layers, respiratory tract, and intact skin and spreads through the blood and lymphatic system to multiple tissues where it establishes the disease [9]. The infectious agent escapes from the phagocytizing and killing cells by inhibiting the phagosome-lysosome fusion and multiplication inside the macrophages [10].

In Pakistan, the prevalence of brucellosis increased over time, both in dairy animals and Equidae [11–13]. *Brucella* is commonly transmitted to humans by consuming raw milk and its products (milk cream, butter, and fresh cheese) or through contact with contaminated material. In Pakistan, work has been reported on the seroprevalence of brucellosis in cattle [14, 15], buffaloes [16], camels [17], dogs [18], equines [19–23], humans [13, 24, 25], and sheep and goats [26].

The maximum incidence of brucellosis in bovines ranged from 0.85% to 76% globally [27–30]. There are four provinces in Pakistan, i.e., Punjab, Balochistan, Sindh, and Khyber Pakhtunkhwa. In all livestock species in Pakistan, the seroprevalence of brucellosis is reported from zero to 76% [16, 30–37]. The highest (76%) seroprevalence of brucellosis was reported in goats, followed by bulk tank milk samples (42%) from Punjab, Pakistan [38]. During the preliminary assessment, it was reported that seroprevalence of brucellosis in different species was 0.00%, 0.23%, 3.41%, 26.19%, and 38.88% in sheep, goats, camels, cattle, and buffaloes, respectively [39]. Between KPK and Sindh, 11% and 21% of brucellosis prevalence have been reported [37, 38]. The overall prevalence of brucellosis in Baluchistan in small ruminants was 3.40% [40] and in large ruminants was 20% [25]. Many factors affect the prevalence of brucellosis, such as age, sex, species, different climatic conditions, geography, and diagnostic tests [3, 32, 41].

It is an alarming situation that needs immediate attention. Most seroprevalence studies are based on RBPT and SAT; however, few studies are based on ELISA [1, 24, 25]. RBPT is based on the agglutination of serum antibodies with a stained whole cell preparation of killed *Brucella*. For confirmation of RBPT results, the serum agglutination test (SAT) or in more sophisticated equipped laboratories, ELISA may be used [42].

Monitoring oxidative stress, blood biochemistry, and defense system profile (antioxidant enzymes) are important tools to lower the adverse impacts of oxidative stress in animals. Studies have indicated that free radicals affect steroidogenesis, apoptosis, lipid peroxidation, and folliculogenesis leading to disorders in embryo preimplantation and infertility in animals [43–45]. Therefore, estimation of blood bio-

chemistry, oxidative stress, and endogenous antioxidants are considered critical factors in initiating different molecular mechanisms during infectious diseases [46]. Scanty information is available in the published literature regarding the hematological, oxidative stress, and antioxidant profile in brucellosis-infected cattle. There is no information regarding brucellosis seroprevalence in cattle mainly kept in desert conditions, particularly in southern Punjab, Pakistan. Therefore, the present study has been planned to investigate the seroprevalence of brucellosis in food animals through serological and molecular-biological techniques.

2. Materials and Methods

2.1. Study Area and Animals. This study was conducted in three districts, including Lodhran, Bahawalpur, and Bahawalnagar of the Southern Punjab province. In Pakistan, about 52% of the agroecological area of Punjab province belongs to Southern Punjab and is inhabited by 32% of the total human population of the province. In southern Punjab, the desert area (Cholistani) lies between longitudes 69° 52' to 75° 24'E and latitudes 27° 42' 29'45'N and is comprised of three districts (Bahawalpur, Rahim Yar Khan, and Bahawalnagar).

The present study comprised 571 cattle of various breeds, including Cholistani ($n = 163$), Friesian ($n = 148$), Jersey ($n = 123$), and cross-bred ($n = 137$) cattle reared at three districts for the estimation of the burden of brucellosis.

2.2. Blood Sampling and Screening of Brucellosis. We drew 5 mL of blood from the jugular vein of all the study animals separately. According to previous procedures, all the serum samples were subjected to RBPT and ELISA to detect brucellosis [23, 47]. We used an automated hematology analyzer for hematology. Take about 1 mL of collected blood to estimate various blood parameters like counting red blood cells, white blood cells, neutrophils, monocytes, lymphocytes, hemoglobin, and hematocrit. A total of 10 blood samples of each breed of healthy as control and brucellosis-positive cattle were used for hematological investigation.

2.3. Estimation of Oxidative Stress and Antioxidant Enzymes in Erythrocyte of Animals. Lipid peroxidation in the RBC hemolysate was identified as thiobarbituric acid reactive substance (TBARS) according to Grewal et al. [48]. The procedure depends on creating a color complex between thiobarbituric acid and the byproducts of lipid peroxidation (TBA). In a brief, 0.2 mL of RBC hemolysate was added to 1.3 mL of 0.2 M Tris-KCl buffer (pH 7.4), and the solution was then incubated at 37°C for 30 min before being heated in a boiling water bath for 10 min. After cooling, 3 mL of pyridine/n-butanol (3:1 v/v) and 1 mL of 1 N NaOH were added and mixed by continuous shaking. At 532 nm, the absorbance was measured using bidistilled water as a blank. 1,1,3,3-Tetramethoxypropane was utilized as a reference in this experiment. Lipid peroxidation in the RBC hemolysate was expressed as MDA nanomoles per grams of hemoglobin (nmol/gHb).

The activity of superoxide dismutase (SOD EC 1.15.1.1) was measured by the Misra and Fridovich method [49]. At 560 nm, the sample absorption was measured. Half of the rate of nitro blue tetrazolium (NBT) reduction is inhibited by one SOD activity unit. In a 1 cm cuvette, the NBT decrease rate is measured at 0.0165 absorbance units per minute. SOD activity was expressed as IU·mg⁻¹ hemoglobin. Ransod (superoxide dismutase) control SD 126 from RAN-DOX Laboratories Ltd. was used to evaluate the method's accuracy.

By using a two-step colorimetric approach that was described by Asri-Rezaei and Dalir-Naghadeh [50], the activity of catalase was assessed. The samples were initially incubated with a known quantity of hydrogen peroxide since the rate of hydrogen peroxide dismutation to water and oxygen is proportional to the concentration of catalase. After a predetermined incubation time, the amount of hydrogen peroxide left was subsequently calculated by an oxidative coupling reaction involving 3,5-dichloro-2-hydroxybenzenesulfonic acid (DHBS) and 4-aminoantipyrene (4-AAP), which was accompanied by horseradish peroxidase. The resulted quinoneimine dye was detected at 520 nm (Catalase Assay Kit, Oxford Biochemical Research, Inc., USA). The enzyme activities were measured in IU/mgHb.

At physiological pH, nitric oxide produced from an aqueous sodium nitroprusside (SNP) solution reacts with oxygen to form nitrite ions, which can be measured and identified using the Griess Illosvoy reaction [51]. 10 mM SNP in 0.5 M phosphate buffer (pH 7.4) and different quantities (100-1000 g/mL) of MPE were included in the reaction mixture with final volume of 3 mL. Griess reagent (0.1 percent α -naphthyl-ethylenediamine in water and 1 percent sulphanic acid in 5 percent H₃PO₄) was added following a 60-minute incubation period at 37°C. At 540 nm, spectrophotometric values were measured of the pink chromophore produced after the diazotization of nitrite ions with sulfanilamide and subsequent coupling with α -naphthyl-ethylenediamine. Ascorbic acid was used as a positive control. Nitric oxide scavenging ability (%) was calculated by using above percent inhibition (I%) formula for DPPH assay.

The method of Asri-Rezaei and Dalir-Naghadeh [50], which is based on the production of a stable yellow hue when 2-nitrobenzoic acid is added to sulfhydryl compounds, was used to evaluate the activity of GSH-Px in the RBC hemolysate. The amounts of reduced product, thionitrobenzene, were measured by commercially available kits (Ransel test kit, Randox laboratories Ltd. GB) at 412 nm and express as IU/mgHb.

2.4. PCR-Based Confirmation of *Brucella abortus*. For confirmation of *Brucella abortus*, we extracted DNA. We performed PCR using specific primers (F=GAC GAA CGG AAT TTT TCC AAT CCC and R=TGC CGATCA CTT AAG GGC CTT CAT) as reported in a previous study [21]. Briefly, PCR reactions contained a total of 25 μ L reaction mixture having 1 μ L (dNTP), 1.2 μ L forward and reverse primers, and 1 μ L DNA template. The PCR amplification was carried out (35 cycles) with initial denaturation at 93°C for 5 min followed by denaturation at 90°C for 1 min,

annealing at 58°C for 1 min, and elongation at 72°C for 1 min with final elongation at 72°C for 1 min.

2.5. Statistical Analysis. Data collected in this study were subjected to statistical software [52]. Data on some epidemiological traits, including age, species, and gender, were analyzed by chi-square. Data on blood, oxidative stress, and antioxidant parameters were subjected to by *t*-test.

3. Results

3.1. Brucellosis Prevalence in Cattle. The overall prevalence of brucellosis disease in dairy cattle has been shown in Table 1. The results showed an 11.75% disease prevalence based on RBPT, while the disease prevalence based on the ELISA test was 10.7%. Based on PCR techniques, the results recorded an overall 9.64% disease prevalence in dairy cattle. The results showed nonsignificantly occurring diseases in dairy cattle based on gender and age groups (Table 1).

3.2. Hematological Parameters. The results of different hematological parameters of different dairy cattle breeds are presented in Table 2. The results revealed that the erythrocyte counts, hemoglobin quantity, hematocrit, lymphocytes, and monocytes decreased significantly ($P \leq 0.05$) in all cattle breeds infected with brucellosis compared to healthy animals. The results showed that the total leukocyte and neutrophil cells significantly ($P \leq 0.05$) increased in all cattle breeds infected with brucellosis compared to healthy animals.

3.3. Oxidative Stress Parameters and Antioxidant Enzymes. The results of different oxidative stress parameters and antioxidant enzymes in erythrocytes of brucellosis-infected and healthy cattle are presented in Table 3. The results on different oxidative stress parameters recorded in brucellosis-infected cattle indicated a substantial increase ($P \leq 0.05$) in values of lipid peroxidation product (MDA) and nitric oxide scavenging activity in brucellosis-positive cattle as compared to healthy animals. The results on different antioxidant enzymes showed significantly ($P \leq 0.05$) lower values of SOD, reduced glutathione, and CAT enzymes in erythrocytes of infected cattle as compared to healthy cattle. The results indicated significantly ($P \leq 0.05$) lower serum albumin levels and total serum proteins in infected cattle compared to noninfected animals (Figure 1).

4. Discussion

Previously, 21.4% prevalence by RBPT of brucellosis and 3.56% by ELISA in equine animals kept in different districts of Punjab province, Pakistan, have been recorded [23]. In our study, no significant difference was recorded in the prevalence of disease based on different age groups of cattle. Previously, studies have recorded that the prevalence of brucellosis decreases due to advancement in the age of equines [23, 53, 54]. In contrast to our results, different earlier studies have found a significant association between the prevalence of brucellosis with age [8, 40, 55, 56]. The results

TABLE 1: RBPT-, ELISA-, and PCR-based prevalence of brucellosis in cattle kept at the Cholistan.

Species/sex/age	No. of animals	Positive		95% CI	Odd ratio/P value
		N	%		
RBPT test					
Sex					
Male	31	03	9.67	2.52-24.12	0.80 (reciprocal = 1.26)
Female	539	64	11.87	9.34-14.81	
Overall	570	67	11.75		
Age groups (years)					
3-4	167	13	7.78	4.40-12.63	Mantel-Haenszel chi-sq. $P = 0.817$
5-6	305	39	12.78	9.38-16.90	
>7	98	15	15.30	9.17-23.47	
ELISA					
Sex					
Male	31	02	6.45	1.10-19.72	0.56 (reciprocal = 1.78)
Female	539	59	10.94	8.51-13.80	
Overall	570	61	10.70		
Age groups (years)					
3-4	167	11	6.58	3.51-11.16	Mantel-Haenszel chi-sq. $P = 0.611$
5-6	305	36	11.80	8.53-15.80	
>7	98	14	14.28	8.37-22.29	
Polymerase chain reaction					
Sex					
Male	31	02	6.45	1.10-19.72	0.63 (reciprocal = 1.58)
Female	539	53	9.83	7.53-12.57	
Overall	570	55	9.64	7.42-12.28	
Age groups (years)					
3-4	167	09	5.38	2.66-9.66	Mantel-Haenszel chi-sq. $P = 0.067$
5-6	305	35	11.47	8.25-15.43	
>7	98	11	11.22	6.05-18.67	

showed a nonsignificant association of sex of animals regarding the presence of brucellosis in our study.

Similarly, no significant difference in the prevalence of brucellosis has also been recorded in animals [23]. An overall 12.7% prevalence of brucellosis in cattle kept in a periurban condition in Pakistan has also been reported [57]. At different livestock farms in Pakistan, up to 16.19% seroprevalence of brucellosis has been recorded in the cattle [3]. Compared to brucellosis in animals, a significantly increased prevalence of the disease has been recorded in females [14, 57, 58]. Variable prevalence of brucellosis includes 4.97% in goats and 5.6% in buffaloes using MRT, while 1.9% in buffaloes and 16.1% in goats with ELISA have been reported [47].

Our study's hematological findings showed that the values of red blood cell count, hemoglobin quantity, and hematocrit significantly decreased in cattle of different breeds infected with brucellosis. Previously, scanty information was available regarding hematological changes in brucellosis-infected cattle [59]. Due to brucellosis in horses, lower erythrocyte sedimentation rate, basophils, and neutrophil counts have been reported [22]. Significantly reduced

values of neutrophils, monocytes, and lymphocytes in brucellosis-infected cattle were seen. The increased neutrophil count in the present study could be related to oxidative stress leading to tissue damage. The lower values of lymphocytes and monocytes could be due to the poor immunological response of brucellosis-infected cattle. Few studies have reported that monocytosis mainly occurs due to damaged tissue debris in brucellosis animals' reproductive and urinary tract [60–62]. However, no report is available on the induction mechanisms of various hematological disorders in brucellosis-positive animals in published data. The changes in hematological parameters might be due to oxidative stress on bone marrow induction.

In the present study, the quantity of different antioxidant enzymes in erythrocytes of positive brucellosis cattle like RGS, SOD, and CAT was significantly reduced ($P \leq 0.05$). Previously, no information was available about the concentrations of different antioxidant enzymes in erythrocytes in brucellosis-positive animals. The lower concentrations of these antioxidant biomarkers in erythrocytes of brucellosis-positive cattle can be related to increased turnover of free radicals and depletion of antioxidants during

TABLE 2: Blood profile (mean \pm SD) of different breeds of cattle infected with brucellosis.

Cattle breed/parameters	Healthy	Infected	P value
Cholistani			
Erythrocyte counts ($10^6/\mu\text{L}$)	5.01 \pm 0.15	3.69 \pm 0.09	<0.01
Hemoglobin quantity (g/dL)	11.97 \pm 1.12	8.19 \pm 0.13	<0.01
Hematocrit (%)	34.50 \pm 1.30	28.9 \pm 2.3	<0.01
Leukocyte counts ($10^3/\mu\text{L}$)	9.11 \pm 0.89	13.83 \pm 0.71	<0.01
Neutrophil (%)	19.70 \pm 1.90	25.9 \pm 1.7	<0.01
Lymphocyte (%)	49.80 \pm 3.70	31.5 \pm 1.83	<0.01
Monocyte (%)	6.33 \pm 0.15	4.01 \pm 0.07	<0.01
Jersey			
Erythrocyte counts ($10^6/\mu\text{L}$)	5.17 \pm 0.13	3.81 \pm 0.05	<0.01
Hemoglobin quantity (g/dL)	12.09 \pm 0.93	7.97 \pm 0.41	<0.01
Hematocrit (%)	36.77 \pm 2.05	28.24 \pm 2.75	<0.01
Leukocyte counts ($10^3/\mu\text{L}$)	10.07 \pm 1.03	16.19 \pm 1.07	<0.01
Neutrophil (%)	21.23 \pm 2.19	31.29 \pm 2.13	<0.01
Lymphocyte (%)	53.40 \pm 2.40	37.3 \pm 2.3	<0.01
Monocyte (%)	5.59 \pm 0.31	3.97 \pm 0.23	<0.01
Cross-bred			
Erythrocyte counts ($10^6/\mu\text{L}$)	5.33 \pm 0.19	3.92 \pm 0.11	<0.01
Hemoglobin quantity (g/dL)	13.01 \pm 1.03	8.55 \pm 0.33	<0.01
Hematocrit (%)	37.13 \pm 3.11	26.39 \pm 3.03	<0.01
Leukocyte counts ($10^3/\mu\text{L}$)	12.13 \pm 0.91	17.03 \pm 0.03	<0.01
Neutrophil (%)	23.49 \pm 3.33	39.01 \pm 4.51	<0.01
Lymphocyte (%)	46.91 \pm 3.70	34.90 \pm 3.25	<0.01
Monocyte (%)	5.73 \pm 0.19	3.99 \pm 0.03	<0.01
Friesian			
Erythrocyte counts ($10^6/\mu\text{L}$)	4.99 \pm 0.07	3.59 \pm 0.11	<0.01
Hemoglobin quantity (g/dL)	13.01 \pm 0.03	9.05 \pm 0.29	<0.01
Hematocrit (%)	35.03 \pm 1.19	27.03 \pm 1.07	<0.01
Leukocyte counts ($10^3/\mu\text{L}$)	11.07 \pm 0.07	17.01 \pm 0.87	<0.01
Neutrophil (%)	24.11 \pm 1.15	39.01 \pm 1.01	<0.01
Lymphocyte (%)	55.11 \pm 3.13	39.1 \pm 3.02	<0.01
Monocyte (%)	4.93 \pm 0.57	3.63 \pm 0.29	<0.01

TABLE 3: Oxidative stress and antioxidant parameters (mean \pm SD) of brucellosis-positive and brucellosis-negative cattle.

Parameters	Noninfected	Infected	P value
Oxidative stress biomarkers			
MDA (nmol/gHb)	1.54 \pm 0.11	2.030 \pm 0.08	<0.01
NO scavenging activity (%)	21.36 \pm 0.40	28.71 \pm 3.50	<0.001
Antioxidant biomarkers			
SOD (IU/mgHb)	142.40 \pm 9.80	121.50 \pm 2.10	<0.01
RGSH (IU/mgHb)	171.40 \pm 7.10	151.70 \pm 2.60	<0.001
CAT (IU/mgHb)	131.30 \pm 6.70	105.40 \pm 2.20	<0.01

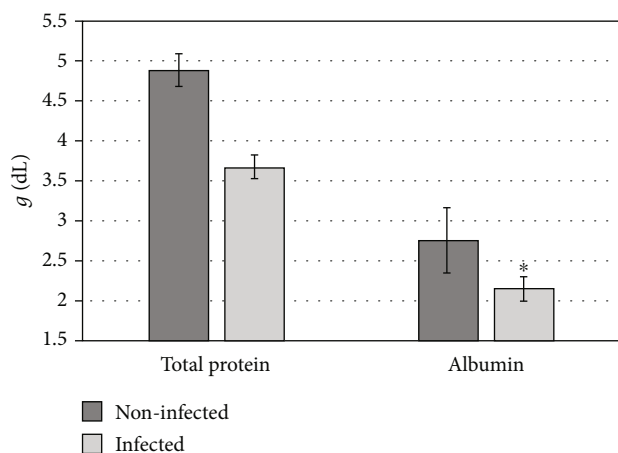


FIGURE 1: Total proteins and albumin in brucellosis-negative and brucellosis-positive cattle. Note: the reading (mean \pm SD) of total proteins and albumin is significantly ($P \leq 0.05$) reduced in brucellosis-infected cows as compared to noninfected cows.

disease prevention [63]. The lower values of various antioxidant enzymes in erythrocytes of brucellosis-positive cattle might be due to disorders in the physiological state and integrity of erythrocytic membranes due to low-grade inflammatory response resulting in inhibition of release of IL-1 and TNF- α [64].

Oxidative stress performs a vital role in the development of clinical disease and also leads to DNA damage, enzymic deactivation, lipid peroxidation, apoptosis, and cell necrosis [64–70]. With the declining body's antioxidant-based defense mechanism, oxidative stress concentration gets enhanced in brucellosis [71–73]. Before entrance in the macrophages, *Brucella* are opsonized inside the host with Brucella-specific immunoglobulin G (IgG), and the entrance into the macrophages is mainly because of phagocytosis initiated by Fc receptor. SOD, CAT, and glutathione peroxidase are vital antioxidant enzymes for the intracellular protection [65, 74]. The *Brucella* existence depends on the concentration of CAT and SOD in the *Brucella*. Of these, SOD performs a significant role in the pathophysiology of the *Brucella* [73].

SOD catalyzes the transformation of superoxide radical to hydrogen peroxide [75] serving as the primary line of defense in response to oxidative stress [70], explaining why this enzyme showed high activity. SOD keeps the O_2^- levels under control in the cellular components and plays a crucial part in the death of phagocytosed bacteria intracellularly [72]. CAT is removed for the inhibition of OH^- production that leads to formation of hydrogen peroxide in the cells. The hydrogen peroxide formed by SOD is degraded by the action of CAT, and it is able to cross the nuclear membrane and induce damage through enzymatic reactions [70, 75]. Thus, SOD and CAT are vital in the removal of nitrogen radicals and free oxygen produced by the *Brucella*, while glutathione peroxidase (GPx) handles the diminution hydroperoxides intracellularly [76, 77]. Glutathione peroxidase is another important antioxidant enzyme present intracellularly and is present within the cell in reduced form (GSH)

as oxidants counter to endogenously formed peroxides. GPx catalyzes this reaction. To be able to effectively protect the cell, it is necessary that major part of glutathione has to be kept in reduced form [64, 78].

Brucella owns two SODs, SodA and SodC [73, 79], those directly cleanse radicals of superoxide. Superoxide cannot easily pass through with cellular membranes as being a charged molecule, and consequently, each SOD usually cleanses superoxide radical produced intracellularly in the bacterial components where they are present [80]. The lessening of *Brucella* in macrophages is also controlled by the acid-sensitive kind of the SodA transformed, thus are able to lower the oxygen readiness, and the reduced growth rate [81] may prevent endogenous superoxide concentration achieving an optimum level at which a cytoplasmic SOD cleanse in *Brucella* strains after setting up intracellularly in the host [65, 72].

The hydrogen peroxide generated during the process is deactivated by CAT. The CAT action is primarily limited to the *Brucella*'s periplasm [82] and responsible to supply safety against H_2O_2 produced during immune reaction provoked against brucellosis. Control of CAT is necessary for the adjustment procedure of *Brucella* to endure and preserve under frightening circumstances. As CAT and Cu-Zn SOD are present at periplasmic location, thus are engaged in safeguarding the *Brucella* from peripheral oxidative complexes [82, 83]. In addition to this, a set of specific proteins are more sensitive to superoxide and activate signaling pathways and promote adaptation of elevated SODs or, alternatively, may initiate cellular death [84].

Previous studies have investigated those lower concentrations of SOD, CAT, and RGS in the erythrocytes of infected cattle, suggesting increased exposure of erythrocytes to oxidative stress and protecting effects of erythrocytes against oxidative damage [83]. Furthermore, a lower quantity of reduced glutathione might also be due to depletion of these enzymes during decomposition of lipid peroxidase and prevention of oxidative damage to membranes of red blood cells. The changes in host tissue and cells take place with increased concentration of oxidative stress parameters as a result of brucellosis [85]. The biomarkers of oxidative stress in brucellosis-positive cattle were significantly increased in the present study. The increased values of these biomarkers are suggestive of induction of oxidative stress and indicate that the increased process of oxidation in erythrocytes is responsible for the rapid generation of free radicals, ultimately leading to inefficient antioxidant capacity and breakdown of erythrocytes [72, 86]. It is further added as brucellosis renders low concentration of antioxidant enzymes; thus, oxidative enzymes (such as MDA, ceruloplasmin, NO, and Cu) increased [65]. Thus, increased oxidative stress leads to breakage of DNA, lipid peroxidation, and protein denaturation [64, 70, 87]; thus, total proteins and albumin were found to be lowered in brucellosis-infected cattle.

5. Conclusions

From the results, it was concluded that brucellosis is still prevailing in animals in Pakistan. Prevalence of cattle

brucellosis was recorded to be 11.75%, 10.7%, and 9.64% based on RBPT, ELISA, and PCR, respectively. The hematological parameters studied including erythrocyte counts, hemoglobin quantity, hematocrit, lymphocytes, and monocytes significantly ($P \leq 0.05$) reduced, whereas total leukocyte and neutrophils significantly increased in infected cases. The MDA and NO scavenging activity of erythrocyte increased significantly, while antioxidant enzymes (SOD, RGS, and CAT) reduced significantly. Total serum proteins and albumin also lowered significantly in brucellosis-infected cattle.

Abbreviations

ALB:	Albumin
CAT:	Catalase
ELISA:	Enzyme-linked immunosorbent assay
IgG:	Immunoglobulin G
IL-1:	Interleukin-1
MDA:	Malondialdehyde
MRT:	Milk ring test
NO:	Nitric oxide
PCR:	Polymerase chain reaction
RBPT:	Rose Bengal precipitation test
RGS:	Reduced glutathione
SOD:	Superoxide dismutase
TNF- α :	Tissue necrosis factor alpha.

Data Availability

All the data related to the study is mentioned in the manuscript.

Conflicts of Interest

The authors declare that there is no conflict of interest regarding the publication of this paper.

Authors' Contributions

Riaz Hussain planned, designed, and executed the study and collected the data. Riaz Hussain and Ahrar Khan analyzed the collected data. Riaz Hussain, Ahrar Khan, and Iahsham Khan interpreted the data. Riaz Hussain and Ahrar Khan prepared the early and final draft of the manuscript. Adil Jamal and Bahaaldeen Babiker Mohamed performed ELISA and PCR of brucellosis. All authors read and approved the final version of the manuscript.

Acknowledgments

This study was financially supported by an International Research Project "Brucellosis in Pakistan" funded by the Federal Foreign Office, Germany. All the authors are very thankful to Friedrich-Loeffler-Institut, Jena, Germany, for providing financial support. The authors are also thankful to Friedrich-Loeffler-Institut, Jena, Germany, for their technical and scientific support for successful completion of this study.

References

- [1] A. Shahzad, A. Khan, M. Z. Khan, and M. Saqib, "Seroprevalence and molecular investigations of brucellosis in camel of selected regions of Pakistan," *Thai Journal of Veterinary Medicine*, vol. 47, pp. 207–215, 2017.
- [2] W. Imtiaz, A. Khan, S. T. Gul et al., "Evaluation of DNA vaccine encoding BCSP₃₁ surface protein of *Brucella abortus* for protective immunity," *Microbial Pathogenesis*, vol. 125, pp. 514–520, 2018.
- [3] S. T. Gul, A. Khan, F. Rizvi, and I. Hussain, "Sero-prevalence of brucellosis in food animals in the Punjab, Pakistan," *Pakistan Veterinary Journal*, vol. 34, pp. 454–458, 2014.
- [4] A. Shahzad, D. Xiaoxia, A. Khan et al., "Patho-morphological valuation of acute infection of *Brucella melitensis* in goats," *Pakistan Veterinary Journal*, vol. 38, no. 4, pp. 341–346, 2018.
- [5] S. Ali, Q. Ali, F. Melzer et al., "Isolation and identification of bovine *Brucella* isolates from Pakistan by biochemical tests and PCR," *Tropical Animal Health and Production*, vol. 46, no. 1, pp. 73–78, 2014.
- [6] O. M. Radostits, C. C. Gay, K. W. Hinchcliff, and P. D. Constable, *Veterinary Medicine. A Textbook of the Diseases of Cattle, Horses, Sheep, Pigs and Goats*, Elsevier Saunders, 10 edition, 2017.
- [7] I. Hussain, M. I. Arshad, M. S. Mahmood, and M. Akhtar, "Seroprevalence of brucellosis in human, cattle, and buffalo populations in Pakistan," *Turkish Journal of Veterinary and Animal Sciences*, vol. 32, pp. 315–318, 2008.
- [8] L. B. Lopes, R. Nicolino, and J. P. A. Haddad, "Brucellosis - risk factors and prevalence: a review," *Open Veterinary Sciences journal*, vol. 4, no. 1, pp. 72–84, 2010.
- [9] N. Lapaque, I. Moriyon, E. Moreno, and J. P. Gorvel, "Brucella lipopolysaccharide acts as a virulence factor," *Current Opinions in Microbiology*, vol. 8, no. 1, pp. 60–66, 2005.
- [10] E. J. Young, "Brucella species," in *Mandell, Douglas and Bennett's Principles and Practice of Infectious Diseases*, G. L. Mandell, J. E. Bennett, and R. Dolin, Eds., pp. 2669–2674, Elsevier, Philadelphia, USA, 2005.
- [11] M. Asif, U. Waheed, M. Farooq, T. Ali, and Q. M. Khan, "Frequency of brucellosis in high risk human groups in Pakistan detected through polymerase chain reaction and its comparison with conventional slide agglutination test," *International Journal of Agriculture and Biology*, vol. 16, pp. 986–990, 2014.
- [12] T. Jamil, F. Melzer, M. Saqib et al., "Serological and molecular detection of bovine brucellosis at institutional livestock farms in Punjab, Pakistan," *International Journal of Environmental Research and Public Health*, vol. 17, no. 4, p. 1412, 2020.
- [13] R. Yousaf, I. Khan, W. Shehzad et al., "Seroprevalence and molecular detection of brucellosis in hospitalized patients in Lahore hospitals, Pakistan," *Infectious Disease Reports*, vol. 13, no. 1, pp. 166–172, 2021.
- [14] U. D. Khan, A. Khan, S. T. Gul, M. K. Saleemi, and X. X. Du, "Seroprevalence of brucellosis in cattle (*Bos taurus*) kept in peri urban areas of Pakistan," *Agrobiological Records*, vol. 1, pp. 6–10, 2020.
- [15] S. Ali, S. Akhter, I. Khan et al., "Molecular typing of *Brucella abortus* isolated from cattle in different districts of Pakistan based on Bruce-ladder-PCR and MLVA-16 assays," *Pakistan Veterinary Journal*, vol. 39, pp. 463–465, 2019.
- [16] R. Mahmood, U. Waheed, T. Ali et al., "Serological and nucleic acid based detection of brucellosis in livestock species and

- molecular characterization of *Brucella melitensis* strains isolated from Pakistan,” *International Journal of Agriculture and Biology*, vol. 18, no. 2, pp. 311–318, 2016.
- [17] S. Fatima, I. Khan, A. Nasir et al., “Serological, molecular detection and potential risk factors associated with camel brucellosis in Pakistan,” *Tropical Animal Health and Production*, vol. 48, no. 8, pp. 1711–1718, 2016.
- [18] T. Jamil, F. Melzer, I. Khan et al., “Serological and molecular investigation of *Brucella* species in dogs in Pakistan,” *Pathogens*, vol. 8, no. 4, 2019.
- [19] R. Ahmed and M. A. Munir, “Epidemiological investigations of brucellosis in horses, dogs, cats and poultry,” *Pakistan Veterinary Journal*, vol. 15, pp. 85–88, 1995.
- [20] S. T. Gul and A. Khan, “Epidemiology and epizootology of brucellosis: a review,” *Pakistan Veterinary Journal*, vol. 27, pp. 145–151, 2007.
- [21] S. Ali, Q. Ali, H. Neubauer et al., “Seroprevalence and risk factors associated with brucellosis as a professional hazard in Pakistan,” *Foodborne Pathogens and Disease*, vol. 10, no. 6, pp. 500–505, 2013.
- [22] S. T. Gul, A. Khan, M. Ahmad, and I. Hussain, “Seroprevalence of brucellosis and associated hematobiochemical changes in Pakistani horses,” *Pakistan Journal of Agricultural Sciences*, vol. 50, pp. 745–750, 2013.
- [23] A. Hussain, T. Jamil, A. M. Tareen et al., “Serological and molecular investigation of brucellosis in breeding equids in Pakistani Punjab,” *Pathogens*, vol. 9, no. 9, 2020.
- [24] M. Abubakar, M. Javed Arshed, M. Hussain, Ehtisham-ul-Haq, and Q. Ali, “Serological evidence of *Brucella abortus* prevalence in Punjab province, Pakistan—a cross-sectional study,” *Journal of veterinary medicine A, Physiology, pathology, clinical medicine*, vol. 57, no. 6, pp. 443–447, 2010.
- [25] M. Shafee, M. Rabbani, A. A. Sheikh, M. . Ahmad, and A. Razzaq, “Prevalence of bovine brucellosis in organized dairy farms, using milk ELISA, in Quetta City, Balochistan, Pakistan,” *Veterinary Medicine International*, vol. 2011, Article ID 358950, 3 pages, 2011.
- [26] M. Z. Saleem, R. Akhtar, A. Aslam et al., “Evidence of *Brucella abortus* in non-preferred caprine and ovine hosts by real-time PCR assay,” *Pakistan Journal of Zoology*, vol. 51, pp. 1187–1189, 2019.
- [27] D. V. Sotnikov, A. N. Berlina, A. V. Zherdev et al., “Immuno-chromatographic serodiagnosis of brucellosis in cattle using gold nanoparticles and quantum dots,” *International Journal of Veterinary Science*, vol. 8, pp. 28–34, 2019.
- [28] Y. R. Pandeya, D. D. Joshi, S. Dhakal et al., “Seroprevalence of brucellosis in different animal species of Kailali district, Nepal,” *International Journal of Infection and Microbiology*, vol. 2, no. 1, pp. 22–25, 2013.
- [29] M. Z. Khan and M. Zahoor, “An overview of brucellosis in cattle and humans, and its serological and molecular diagnosis in control strategies,” *Tropical Medicine and Infectious Disease*, vol. 3, no. 2, p. 65, 2018.
- [30] A. Shehzad, F. A. Rantam, W. Tyasningsih, and S. Rehman, “Prevalence of bovine and human brucellosis in Pakistan—a review,” *Advanced Animal and Veterinary Science*, vol. 9, no. 4, pp. 473–482, 2020.
- [31] A. Q. Khan, S. K. Haleem, M. Shafiq, N. A. Khan, and S. ur Rahman, “Seropositivity of brucellosis in human and livestock in Tribal-Kurram Agency of Pakistan indicates cross circulation,” *Thai Journal of Veterinary Medicine*, vol. 47, pp. 349–355, 2017.
- [32] S. T. Gul, A. Khan, M. Ahmad, F. Rizvi, A. Shahzad, and I. Hussain, “Epidemiology of brucellosis at different livestock farms in the Punjab, Pakistan,” *Pakistan Veterinary Journal*, vol. 35, pp. 309–314, 2015.
- [33] M. Asif, A. R. Awan, M. E. Babar, A. Ali, S. Firyal, and Q. M. Khan, “Development of genetic marker for molecular detection of *Brucella abortus*,” *Pakistan Journal of Zoology*, vol. 9, Suppl, pp. 267–271, 2009.
- [34] S. Arif, J. Heller, M. Hernandez-Jover, D. M. McGill, and P. C. Thomson, “Evaluation of three serological tests for diagnosis of bovine brucellosis in smallholder farms in Pakistan by estimating sensitivity and specificity using Bayesian latent class analysis,” *Preventive Veterinary Medicine*, vol. 149, pp. 21–28, 2018.
- [35] S. Arif, C. P. Thomson, M. Hernandez-Jover, D. M. McGill, H. M. Warriach, and J. Heller, “Knowledge, attitudes and practices (KAP) relating to brucellosis in smallholder dairy farmers in two provinces in Pakistan,” *PLoS ONE*, vol. 12, no. 3, article e0173365, 2017.
- [36] T. Ahmad, I. Khan, S. Razzaq, S. U. H. Khan, and R. Akhtar, “Prevalence of bovine brucellosis in Islamabad and Rawalpindi districts of Pakistan,” *Pakistan Journal of Zoology*, vol. 49, no. 3, pp. 1123–1126, 2017.
- [37] A. S. Baloch, A. Rasheed, R. Rind et al., “Seroprevalence of brucellosis in camels in Sindh, Pakistan,” *Pakistan Journal of Zoology*, vol. 49, pp. 367–369, 2016.
- [38] T. I. Khan, S. Ehtisham-ul-Haque, U. Waheed, I. Khan, M. Younus, and S. Ali, “Milk indirect-ELISA and milk ring test for screening of brucellosis in buffaloes, goats and bulk tank milk samples collected from two districts of Punjab, Pakistan,” *Pakistan Veterinary Journal*, vol. 38, no. 1, pp. 105–108, 2018.
- [39] A. Shahzad, *Molecular Characterization and Pathological Studies of Brucella Species in Naturally Infected Animals*, Ph.D. Thesis, Department of Pathology, University of Agriculture, Faisalabad, Pakistan, 2017.
- [40] S. Ali, A. Akbar, M. Shafee, B. Tahira, A. Muhammed, and N. Ullah, “Sero-epidemiological study of brucellosis in small ruminants and associated human beings in district Quetta, Balochistan,” *Pure and Applied Biology*, vol. 6, no. 3, pp. 797–804, 2017.
- [41] A. Khan, M. Shafee, N. Khan et al., “Incidence of brucellosis in aborted animals and occupationally exposed veterinary professionals of Bannu, Khyber Pakhtunkhwa, Pakistan,” *Thai Journal of Veterinary Medicine*, vol. 48, pp. 47–54, 2018.
- [42] P. M. Muñoz, C. M. Marín, D. Monreal et al., “Efficacy of several serological tests and antigens for diagnosis of bovine brucellosis in the presence of false-positive serological results due to *Yersinia enterocolitica* O:9,” *Clinical and Diagnostic Laboratory Immunology*, vol. 12, no. 1, pp. 141–151, 2005.
- [43] A. Agrawal, R. A. Sahel, and M. A. Bedaiwy, “Role of reactive oxygen species in the pathology of human reproduction,” *Fertility and Sterility*, vol. 79, no. 4, pp. 829–843, 2003.
- [44] L. Gomez, F. Alvarez, D. Betancur, and A. Onate, “Brucellosis vaccines based on the open reading frames from genomic island 3 of *Brucella abortus*,” *Vaccine*, vol. 36, no. 21, pp. 2928–2936, 2018.
- [45] V. Joshi, V. K. Gupta, A. G. Bhanuprakash, R. S. K. Mandal, U. Dimri, and Y. Ajith, “Haptoglobin and serum amyloid A as putative biomarker candidates of naturally occurring bovine respiratory disease in dairy calves,” *Microbial Pathogenesis*, vol. 116, pp. 33–37, 2018.

- [46] R. Hussain, Z. Guangbin, R. Z. Abbas et al., "Clostridium perfringens types A and D involved in peracute deaths in goats kept in Cholistan ecosystem during winter season," *Frontiers in Veterinary Science*, vol. 9, article 849856, 2022.
- [47] M. Nawaz, I. Khan, M. Shakeel et al., "Bovine and caprine brucellosis detected by milk indirect ELISA and milk ring test in Islamabad Capital Territory, Pakistan," *Pakistan Journal of Zoology*, vol. 53, no. 1, pp. 391–394, 2020.
- [48] A. Grewal, C. S. Ahuja, S. P. S. Singh, and K. C. Chaudhary, "Status of lipid peroxidation, some antioxidant enzymes and erythrocytic fragility of crossbred cattle naturally infected with *Theileria annulata*," *Veterinary Research Communications*, vol. 29, no. 5, pp. 387–394, 2005.
- [49] H. P. Misra and I. Fridovich, "Superoxide dismutase and peroxidase: a positive activity stain applicable to polyacrylamide gel electropherograms," *Archives of Biochemistry and Biophysics*, vol. 183, no. 2, pp. 511–515, 1977.
- [50] S. Asri-Rezaei and B. Dalir-Naghadeh, "Evaluation of antioxidant status and oxidative stress in cattle naturally infected with *Theileria annulata*," *Veterinary Parasitology*, vol. 142, no. 1–2, pp. 179–186, 2006.
- [51] L. C. Green, D. A. Wagner, J. Glogowski, P. L. Skipper, J. S. Wishnok, and S. R. Tannenbaum, "Analysis of nitrate, nitrite, and [¹⁵N]nitrate in biological fluids," *Analytical Biochemistry*, vol. 126, no. 1, pp. 131–138, 1982.
- [52] Statistical Analysis System, *SAS Statistical Software Version 9.1*, SAS Institute Inc, Cary, NC, USA, 2004.
- [53] A. Tijjani, A. Junaidu, M. Salihu et al., "Serological survey for brucella antibodies in donkeys of North-Eastern Nigeria," *Tropical Animal Health and Production*, vol. 49, no. 6, pp. 1211–1216, 2017.
- [54] F. Wadood, M. Ahmad, A. Khan, S. T. Gul, and N. Rehman, "Seroprevalence of brucellosis in horses in and around Faisalabad," *Pakistan Veterinary Journal*, vol. 29, pp. 196–198, 2009.
- [55] N. Mohamand, L. Gunaseelan, B. Sukumar, and K. Porteen, "Milk ring test for spot identification of *Brucella abortus* infection in single cow herds," *Journal of Advanced Veterinary and Animal Research*, vol. 1, no. 2, pp. 70–72, 2014.
- [56] F. U. Mohammed, S. Ibrahim, I. Ajogi, and B. J. Olaniyi, "Prevalence of bovine brucellosis and risk factors assessment in cattle herds in Jigawa state," *ISRN Veterinary Science*, vol. 2011, Article ID 132897, 4 pages, 2011.
- [57] I. Khan, S. Ali, R. Hussain et al., "Serosurvey and potential risk factors of brucellosis in dairy cattle in peri-urban production system in Punjab, Pakistan," *Pakistan Veterinary Journal*, vol. 41, pp. 459–462, 2021.
- [58] I. M. Rabah, M. A. Nossair, M. M. Elkamshishi, and E. Khalifa, "Serological and molecular epidemiological study on ruminant brucellosis in Matrouh Province, Egypt," *International Journal of Veterinary Science*, vol. 11, no. 1, pp. 82–90, 2022.
- [59] O. F. Kokoglu, S. Hosoglu, M. F. Geyik et al., "Clinical and laboratory features of brucellosis in two university hospitals in Southeast Turkey," *Tropical Doctor*, vol. 36, no. 1, pp. 49–51, 2006.
- [60] S. C. Olsen and M. V. Palmer, "Advancement of knowledge of *Brucella* over the past 50 years," *Veterinary Pathology*, vol. 51, no. 6, pp. 1076–1089, 2014.
- [61] N. Zanganeh, E. Siahpoushi, N. Kheiripour, S. Kazemi, M. T. Goodarzi, and M. Y. Alikhani, "Brucellosis causes alteration in trace elements and oxidative stress factors," *Biological Trace Element Research*, vol. 182, no. 2, pp. 204–208, 2018.
- [62] I. A. Cotgreave and R. C. Gerdes, "Recent trends in glutathione biochemistry – glutathione protein interactions: a molecular link between oxidative stress and proliferation," *Biochemical and Biophysical Research Communications*, vol. 242, no. 1, pp. 1–9, 1998.
- [63] N. Kataria, A. K. Kataria, R. Maan, and A. K. Gahlot, "Evaluation of oxidative stress in *Brucella* infected cows," *Journal of Stress Physiology and Biochemistry*, vol. 6, pp. 19–25, 2010.
- [64] H. Karsen, "Oxidative stress and brucellosis," in *Oxidative Stress in Microbial Diseases*, S. Chakraborti, T. Chakraborti, D. Chattopadhyay, and C. Shaha, Eds., pp. 315–327, Springer, Singapore, 2019.
- [65] R. Akram, A. Ghaffar, R. Hussain et al., "Hematological, serum biochemistry, histopathological and mutagenic impacts of triclosan on fish (bighead carp)," *Agrobiological Records*, vol. 7, pp. 18–28, 2021.
- [66] J. Q. Wang, R. Hussain, A. Ghaffar et al., "Clinicohematological, Mutagenic, and Oxidative Stress Induced by Pendimethalin in Freshwater Fish Bighead Carp (*Hypophthalmichthys nobilis*)," *Oxidative Medicine and Cellular Longevity*, vol. 2022, Article ID 2093822, 15 pages, 2022.
- [67] Y. Mahmood, R. Hussain, A. Ghaffar et al., "Acetochlor affects bighead carp (*Aristichthys nobilis*) by producing oxidative stress, lowering tissue proteins, and inducing genotoxicity," *BioMed Research International*, vol. 2022, Article ID 9140060, 12 pages, 2022.
- [68] H. H. Ahmed, N. E. S. El-Toukhey, S. S. Abd El-Rahman, and A. K. H. Hendawy, "Efficacy of melatonin against oxidative stress, DNA damage and histopathological changes induced by nicotine in liver and kidneys of male rats," *International Journal of Veterinary Science*, vol. 10, no. 1, pp. 31–36, 2021.
- [69] G. Jabeen, F. Manzoor, and M. Arshad, "Effect of cadmium exposure on hematological, nuclear and morphological alterations in erythrocyte of fresh water fish (*Labeo rohita*)," *Continental Veterinary Journal*, vol. 1, no. 1, pp. 20–24, 2021.
- [70] E. Birben, U. M. Sahiner, C. Sackesen, S. Erzurum, and O. Kalayci, "Oxidative stress and antioxidant defense," *World Allergy Organization Journal*, vol. 5, no. 1, pp. 9–19, 2012.
- [71] K. Serephanoglu, A. Taskin, H. Turan, F. E. Timurkaynak, H. Arslan, and O. Erel, "Evaluation of oxidative status in patients with brucellosis," *Brazilian Journal of Infectious Diseases*, vol. 13, no. 4, pp. 249–251, 2009.
- [72] A. Kumar, A. Rahal, and V. K. Gupta, "Oxidative stress, pathophysiology, and immunity in brucellosis," in *Oxidative Stress in Microbial Diseases*, pp. 365–378, Springer, Singapore.
- [73] N. Sriranganathan, S. M. Boyle, G. Schurig, and H. Misra, "Superoxide dismutases of virulent and avirulent strains of *Brucella abortus*," *Veterinary Microbiology*, vol. 26, no. 4, pp. 359–366, 1991.
- [74] F. Miao, "Hydroxytyrosol alleviates dextran sodium sulfate-induced colitis by inhibiting NLRP3 inflammasome activation and modulating gut microbiota *in vivo*," *Nutrition*, vol. 97, 2022.
- [75] M. McIntyre, D. F. Bohr, and A. F. Dominiczak, "Endothelial function in hypertension," *Hypertension*, vol. 34, no. 4, pp. 539–545, 1999.
- [76] G. N. Landis and J. Tower, "Superoxide dismutase evolution and life span regulation," *Mechanisms of Ageing and Development*, vol. 126, no. 3, pp. 365–379, 2005.
- [77] D. Armstrong, *Methods in Molecular Biology*, vol. 108, Humana Press, Toronto, 1998.

Retraction

Retracted: Apoptotic and Antioxidant Activity of Gold Nanoparticles Synthesized Using Marine Brown Seaweed: An In Vitro Study

BioMed Research International

Received 8 January 2024; Accepted 8 January 2024; Published 9 January 2024

Copyright © 2024 BioMed Research International. This is an open access article distributed under the Creative Commons Attribution License, which permits unrestricted use, distribution, and reproduction in any medium, provided the original work is properly cited.

This article has been retracted by Hindawi following an investigation undertaken by the publisher [1]. This investigation has uncovered evidence of one or more of the following indicators of systematic manipulation of the publication process:

- (1) Discrepancies in scope
- (2) Discrepancies in the description of the research reported
- (3) Discrepancies between the availability of data and the research described
- (4) Inappropriate citations
- (5) Incoherent, meaningless and/or irrelevant content included in the article
- (6) Manipulated or compromised peer review

The presence of these indicators undermines our confidence in the integrity of the article's content and we cannot, therefore, vouch for its reliability. Please note that this notice is intended solely to alert readers that the content of this article is unreliable. We have not investigated whether authors were aware of or involved in the systematic manipulation of the publication process.

Wiley and Hindawi regrets that the usual quality checks did not identify these issues before publication and have since put additional measures in place to safeguard research integrity.

We wish to credit our own Research Integrity and Research Publishing teams and anonymous and named

external researchers and research integrity experts for contributing to this investigation.

The corresponding author, as the representative of all authors, has been given the opportunity to register their agreement or disagreement to this retraction. We have kept a record of any response received.

References

- [1] S. Rajeshkumar, R. P. Parameswari, J. Jayapriya et al., "Apoptotic and Antioxidant Activity of Gold Nanoparticles Synthesized Using Marine Brown Seaweed: An In Vitro Study," *BioMed Research International*, vol. 2022, Article ID 5746761, 9 pages, 2022.

Research Article

Apoptotic and Antioxidant Activity of Gold Nanoparticles Synthesized Using Marine Brown Seaweed: An In Vitro Study

S. Rajeshkumar ¹, R. P. Parameswari ¹, J. Jayapriya,¹ M. Tharani,¹ Huma Ali,² Nada H. Aljarba,³ Saad Alkahtani,⁴ and Saud Alarifi⁴

¹Center for Transdisciplinary Research (CFTR), Nanobiomedicine Lab, Department of Pharmacology, Saveetha Dental College, Saveetha Institute of Medical and Technical Science, Saveetha University, Chennai, India

²Department of Chemistry, Maulana Azad National Institute of Technology, Bhopal, India

³Department of Biology, College of Science, Princess Nourah bint Abdulrahman University, P. O. Box 84428, Riyadh 11671, Saudi Arabia

⁴Department of Zoology, College of Science, King Saud University, P. O. Box 2455, Riyadh 11451, Saudi Arabia

Correspondence should be addressed to S. Rajeshkumar; rajeshkumars.sdc@saveetha.com

Received 6 June 2022; Revised 17 June 2022; Accepted 23 June 2022; Published 13 July 2022

Academic Editor: Hafiz Ishfaq Ahmad

Copyright © 2022 S. Rajeshkumar et al. This is an open access article distributed under the Creative Commons Attribution License, which permits unrestricted use, distribution, and reproduction in any medium, provided the original work is properly cited.

A major paradigm shift in the field of nanobiotechnology is the invention of an eco-friendly, economical, and green approach for synthesis of metal nanoparticles. In the present study, we have synthesized gold nanoparticles (AuNPs) using aqueous extracts of marine brown seaweed *Sargassum longifolium*. The synthesized nanoparticle was subjected to characterization using different techniques such as UV-Vis spectroscopy, Fourier transform infrared spectroscopy, atomic force microscope, scanning electron microscope, transmission electron microscope, and elemental dispersive X-ray diffraction. Further, the seaweed extract and the synthesized AuNPs were evaluated for its anticancer effect using MG-63 human osteosarcoma cells besides in vitro antioxidant effect. The formation of *S. longifolium*-mediated synthesis of gold nanoparticles was demonstrated by UV-Vis spectroscopy. Presence of elemental gold was confirmed by EDX analysis. TEM analysis demonstrated spherical morphology of the synthesized AuNPs and SEM analysis revealed the particle size to be in the range of 10-60 nm. The FTIR showed the presence of hydroxyl functional groups. The toxicity of *S. longifolium* extract and the synthesized AuNPs was tested using brine shrimp lethality assay at different concentrations with results showing both seaweed extract and AuNPs to be nontoxic. Both *S. longifolium* and AuNPs exhibited significant antioxidant activity by scavenging DPPH free radicals and H₂O₂ radicals. Significant antiproliferative effect was observed against MG-63 osteosarcoma cells. It was also shown that the seaweed extract and the AuNPs induced cytotoxicity in cell lines by mechanism of apoptosis. In conclusion, this study provided insight on AuNPs synthesized from *S. longifolium* as a potent antioxidant and anticancer agent.

1. Introduction

Nanotechnology has been defined as a field of study that integrates physics, chemistry, and biology principles to create new materials with unique features on a very small scale, referred to as the nanoscale (0–100 nm) [1]. It involves both research and technology, a new discipline of science and engineering [2]. Nanotechnology has pervaded practically every branch of science, allowing for the development of unique alternatives to many research tailbacks. Nanomedicine, a combination of nanotechnology and medicine offers various advantages over traditional treatment methods [3]. Metal nanoparticles have reinforced immense interest in the field of nanomedicine owing to their unique properties than their bulk counterpart [4]. However, the physicochemical methods adopted to produce these metal nanoparticles have intrinsic limits, which constitute a significant barrier to the science's maturity [5]. Therefore, development of eco-friendly technologies termed as “green approach” has found to be comparatively safe, nontoxic, inexpensive, and

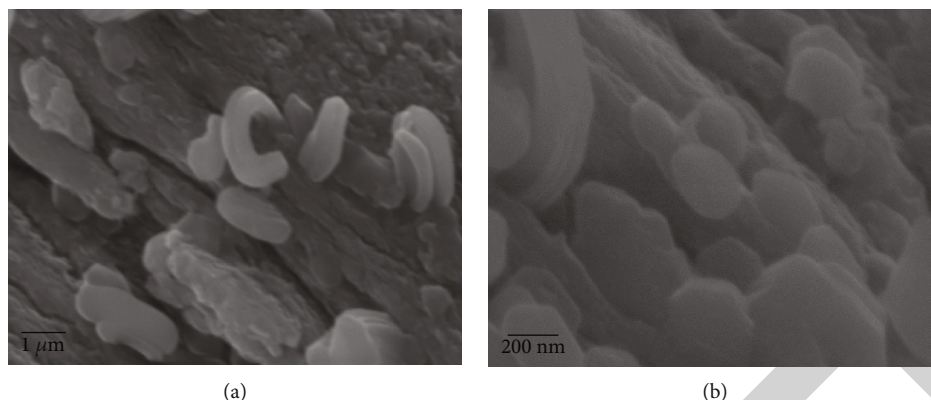


FIGURE 1: Representative SEM images of (a) *S. longifolium* and (b) its mediated gold nanoparticles.

biocompatible [6]. During chemical formulation, there are high chances of contamination. Unlike other methods, green synthesis produces a pure form of NPs [7].

Due to their biocompatibility, low toxicity, ease of surface functionalization, and optical and electronic qualities, gold nanoparticles (Au-NPs) have sparked considerable interest than any other metal nanoparticles and hence utilized for various biomedical applications [8, 9]. Gold nanoparticles own the history of being used for various applications right from colouring glass to treating complex mental illness [10]. Moreover, the diverse fascinating properties of AuNPs, viz., electronic, magnetic, optical, and catalytic properties, have made AuNPs a suitable candidate for use in bioimaging like X-ray computed tomography, drug or gene delivery, diagnostic, therapeutics, tissue engineering, and theranostics [11, 12]. Further, AuNPs are prevalently used in the field of cancer therapy [13]. Despite possessing significant advantages, use of AuNPs has its own limitation due to application of various hazardous chemical synthesis methods for preparation. Hence, green synthesis method using plants, microbes, seaweeds, and its respective bioactive metabolites is used to synthesize AuNPs [14].

About 80% of the world's biodiversity has been found in the marine ecosystem. Among the various marine sources, seaweeds have gained immense response in different fields of research owing to its unique properties like high biodiversity, living habitats, and specific living conditions [15]. Seaweeds are found prevalent in harsh marine environment which possess numerous bioactive metabolites with various activities [16, 17]. Brown seaweeds are predominantly brown due to the presence of the carotenoid fucoxanthin and the primary polysaccharides include alginates, laminarins, fucans, and cellulose [17].

Sargassum species are tropical and subtropical brown macroalgae of the shallow marine meadow [18]. They are nutritious and rich sources of bioactive compounds such as vitamins, carotenoids, dietary fibers, proteins, and minerals [19]. Also, many biologically active compounds like terpenoids, flavonoids, sterols, sulphated polysaccharides, polyphenols, sargaquinoic acids, sargachromenol, and pheophytine were isolated from different *Sargassum* species [20]. These isolated compounds exhibit diverse biological activities like analgesic, anti-inflammatory, anti-

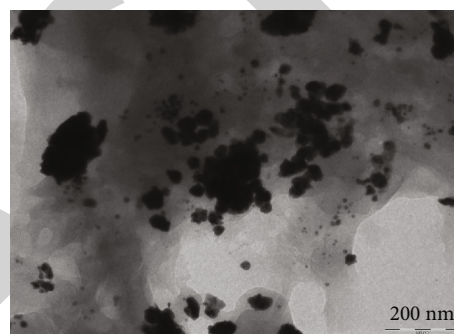


FIGURE 2: Representative TEM images of *S. longifolium* and *S. longifolium*-mediated gold nanoparticles (scale-200 nm).

oxidant, neuroprotective, antimicrobial, antitumor, fibrinolytic, immune-modulatory, anticoagulant, hepatoprotective, and antiviral activity. Hence, *Sargassum* species have great potential to be used in pharmaceutical and nutraceutical areas [21–23]. Several studies have exhibited the anticancer potential of *Sargassum* species studies against various tumour cells [24–27]. Similarly, AuNPs prepared using several other sources have been reported for its potent anticancer effect using liver cancer, lung cancer, and breast cancer cells [28–30]. Although many reports are available on the potential of *Sargassum* against various disorders, the green synthesized AuNPs mediated by the marine seaweed *Sargassum longifolium* have not been investigated. Therefore, in the present study, we synthesized *Sargassum longifolium*-mediated AuNPs and evaluated its antioxidant and anticancer effect.

2. Materials and Methods

2.1. Chemicals and Reagents. Gold (III) chloride trihydrate ($\text{HAuCl}_4 \cdot 3\text{H}_2\text{O}$), 2,2-diphenyl-1-picrylhydrazyl, hydrogen peroxide (H_2O_2), MTT (3-(4,5-dimethylthiazol-2-yl)-2,5-diphenyltetrazolium bromide), ethidium bromide, and acridine orange were purchased from Sigma Aldrich, USA. Dulbecco's minimum essential media (DMEM), fetal bovine serum (FBS), penicillin/streptomycin, Trypsin-EDTA, phosphate buffered saline (PBS), and dimethyl sulfoxide were

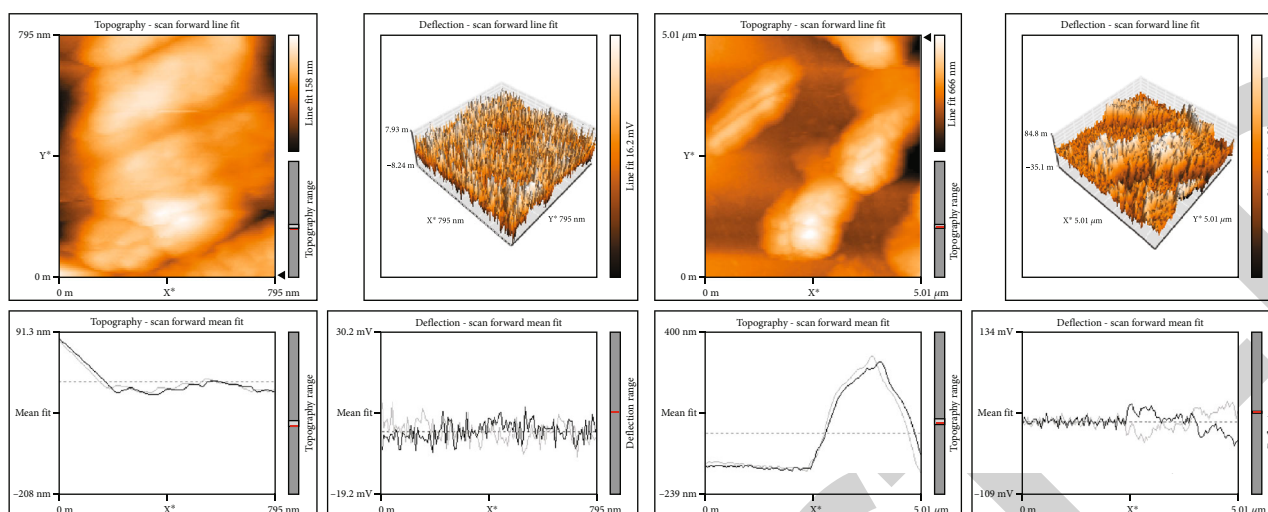


FIGURE 3: Representative AFM images of *S. longifolium*-mediated gold nanoparticle.

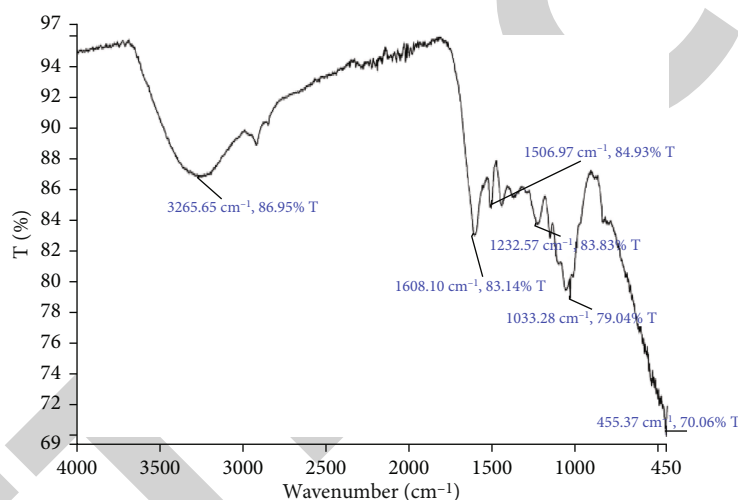


FIGURE 4: FTIR spectrum of *S. longifolium*-synthesized gold nanoparticles.

purchased from Gibco, USA. All other chemicals, reagents, and solvents used were of analytical grade and procured from Himedia, India.

2.2. Preparation of Extract. About 1 g of *S. longifolium* was mixed with 100 mL of double distilled H₂O, boiled for 5 min, and filtered through Whatman No. 1 filter paper. It was refrigerated at 4°C for further experimental purpose.

2.3. Synthesis of AuNPs. To prepare the gold nanoparticles, 80 mL of aqueous sea weed extract was mixed with 20 mL of AuCl₄ solution in a clean conical flask. The mixture was kept for stirring on a magnetic stirrer at room temperature. The change in the solution colour indicated the reduction of Au³⁺ ions in the solution, and the wavelength of which was measured at periodic intervals using UV-Vis spectrophotometer after the reaction reached saturation. Later on confirming the formation of AuNPs, the solution was centrifuged at 10,000 rpm for 15 min and pellet was collected for further analysis.

2.4. UV Visible Spectroscopy. The UV-Visible spectrum of the gold nanoparticles solution was recorded using double beam UV-Visible Spectrophotometer (UV-2450, Shimadzu). Optical density was taken from 360 to 650 nm (ranges increased 10 nm gradually) at different time points. Based on the OD values, the peak was identified and denoted as an optimum nanoparticles biosynthesis.

2.5. Microscopic Studies. A drop of sample was placed on carbon-coated copper grid, air dried at room temperatures, and stained with 2% uranyl acetate. The nanoparticle size measurement was done using transmission electron microscope (Hitachi, H-7500), and average nanoparticle size was considered as the size of the sample. The morphological characterizations of the *S. longifolium* were performed using SEM. To know the exact particle size and nanosize effect, the sample was characterized using atomic force microscope (AFM), which measures the atomic range of the particle.

2.6. FTIR. FTIR measurements demonstrate the presence of functional groups which can be liable for capping leading to

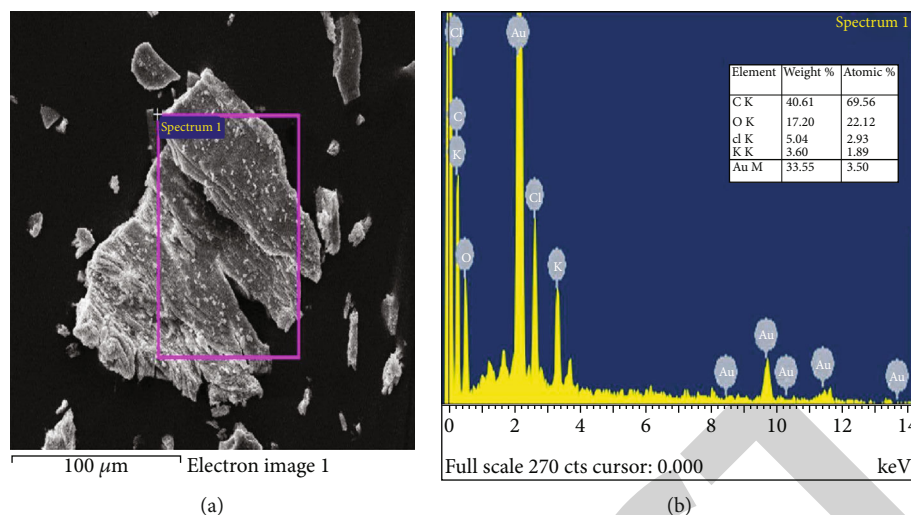


FIGURE 5: (a) EDX spectrum *S. longifolium*-mediated gold nanoparticle; (b) the elements, its weight %, and atomic %.

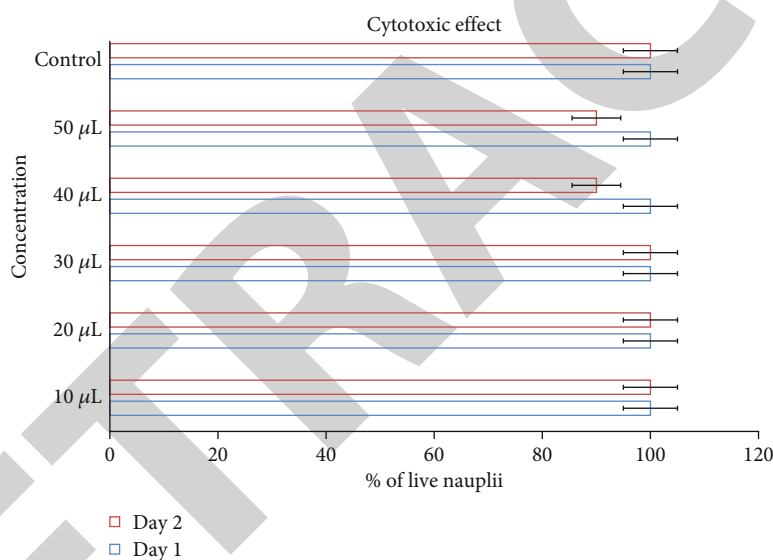


FIGURE 6: Effect of *S. longifolium* and its mediated gold nanoparticle represented as % of nauplii on day 1 and day 2.

proficient stabilization of the gold nanoparticles. The refined suspension containing the nanoparticles was completely dried and ground with KBr pellets and used for FTIR analysis. In order to obtain decent signal/noise ratio, 512 scans were verified to get appropriate results.

2.7. EDX. Energy dispersive X-ray spectroscopy is a technique used for determination of elemental analysis of *S. longifolium*. It can be used to basically determine the amount of AuNPs produced with a thin film of bacterial biomass.

3. Antioxidant Activities

3.1. DPPH Free-Radical Scavenging Assay. The free-radical scavenging activity of the biosynthesized gold chloride nanoparticles and the *S. longifolium* extract was evaluated by

DPPH free-radical scavenging assay. The seaweed extract, seaweed extract-mediated gold nanoparticles, and standard ascorbic acid were prepared at different concentrations of 2-10 μg/mL. 1 mL of different concentration seaweed extract, AuNPs, and standard to appropriately labelled test tubes. To the above test tubes, 1 ml of 0.1 mM DPPH prepared in methanol and 450 μL of 50 mM Tris HCl buffer (pH 7.4) were mixed and incubated in dark for 30 minutes. 1 mL of distilled water, 1 ml of DPPH, and 450 μL of 50 mM Tris HCl buffer served as control blank. The absorbance of the solution was measured at 517 nm. The percentage inhibition of free radical formation was determined from the following equation:

$$\% \text{inhibition} = \frac{\text{Absorbance of control} - \text{absorbance of test sample}}{\text{Absorbance of control}} \times 100. \quad (1)$$

3.2. Hydrogen Peroxide Scavenging Assay. The H_2O_2 radical scavenging activity was determined for the *S. longifolium* extract, AuNPs. Different volume ($10\ \mu\text{L}$ - $50\ \mu\text{L}$) of *S. longifolium* extract and AuNPs were added to appropriately labelled test tubes and incubated with $50\ \mu\text{L}$ of $5\ \text{mM}$ H_2O_2 . Ascorbic acid served as standard reference. Blank control consisted of $50\ \mu\text{L}$ of $5\ \text{mM}$ H_2O_2 devoid of the sample. The test tubes were allowed to incubate for 20 min at room temperature. The absorbance was measured at 610 nm. The percentage inhibition of H_2O_2 radical formation was determined from the following equation:

$$\% \text{inhibition} = \frac{\text{Absorbance of control} - \text{absorbance of test sample}}{\text{Absorbance of control}} \times 100. \quad (2)$$

3.3. Brine Shrimp Lethality Assay. 2 g of iodine free salt was weighed and dissolved in 200 mL of distilled water in which dried cysts were placed. The larvae (nauplii) were hatched after 36 h of incubation under conditions of strong ventilation and continuous illumination. The evaluation of cytotoxicity was carried out using nauplii of brine shrimp as follows: Briefly, 5 ml of water was filled in 6 well ELISA plates. Fresh suspensions of *S. longifolium* extract and AuNPs were prepared using the artificial sea water at 1-fold serial dilution between the range of $10\ \mu\text{L}$, $20\ \mu\text{L}$, $30\ \mu\text{L}$, $40\ \mu\text{L}$, and $50\ \mu\text{L}$. The different concentration seaweed extract and the synthesized AuNPs were added to the 6-well plates. To that 10 nauplii were slowly added to each well, and the plates were incubated for 48 h. After every 24 hours, the ELISA plates were observed for number of live nauplii's using stereoscopic microscope and the lethality was calculated using following formula: $\% \text{lethality} = (\text{number of dead nauplii}) / (\text{number of dead nauplii} + \text{number of live nauplii}) \times 100$.

3.4. Cell Culture. Human osteosarcoma cell line MG-63 was purchased from National Centre for Cell Sciences (NCCS), Pune with the passage number of 16. The cells were grown in Dulbecco's modified Eagle medium (DMEM) supplemented with 10% fetal bovine serum (FBS), 100 U/mL penicillin, and 100 U/ml of streptomycin at 37°C in 95% humidified air with 5% CO_2 . On reaching 80-90% confluency, the cells were trypsinized using 0.25% Trypsin-EDTA and plated for further assays.

3.5. Anticancer Activity-*MTT* Assay. The cytotoxic potential of the synthesized gold nanoparticles was assessed on human osteosarcoma cell lines, MG-63. Briefly, cells were grown in 96-well plates at a density of 5×10^4 cells/well. After 24 h of incubation, the cells were treated with different concentrations (1, 5, 10, 20, 40, and 80 ng/mL) of the seaweed extract and the synthesized gold nanoparticles. Cells which did not receive treatment with either seaweed extract or gold nanoparticles, were treated as controls. After 24 h of incubation, media was aspirated from all the wells and $50\ \mu\text{L}$ of MTT (3-(4,5-dimethylthiazol-2-yl)-2,5-diphenyltetrazolium bromide) was added at a concentration of 5 mg/mL prepared in PBS (phosphate buffered saline). After 4 h of MTT incubation, $150\ \mu\text{L}$ of DMSO (dimethyl

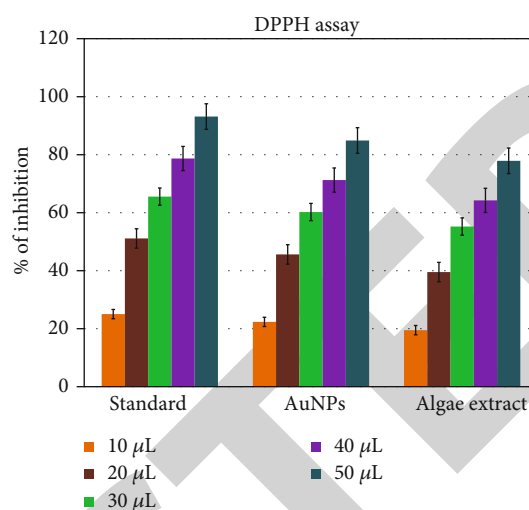


FIGURE 7: % inhibition of DPPH free radicals by AuNPs mediated from *S. longifolium* and *S. longifolium* extract. Results are expressed in terms of mean \pm SEM ($n = 3$).

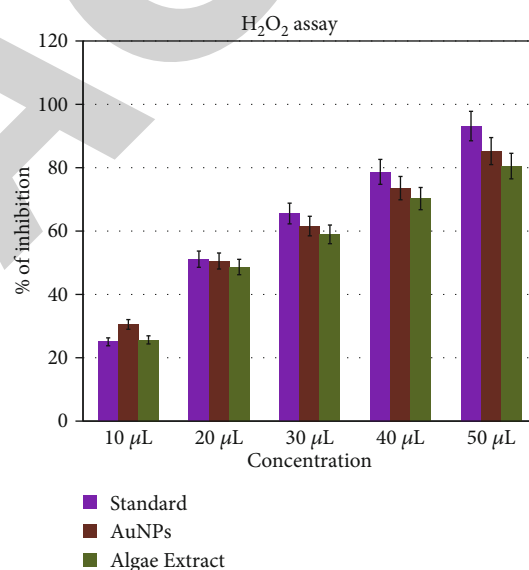


FIGURE 8: % inhibition of H_2O_2 free radicals by AuNPs mediated from *S. longifolium* and *S. longifolium* extract. Results are expressed in terms of mean \pm SEM ($n = 3$).

sulfoxide) was added to dissolve the purplish formazan product. Absorbance was read at 540 nm using Multimode reader (Perkin Elmer, USA). The % inhibition of cell proliferation was calculated using the following formula: $((\text{OD of control} - \text{OD of the test}) / \text{OD of the control}) * 100$.

3.6. Dual Ethidium Bromide/Acridine Orange (EtBr/AO) Staining Assay. AO/EtBr staining of MG-63 cells was performed as per Banda et al. [31]. MG-63 cells 4×10^5 /well were treated with two different concentrations of seaweed extract (16 and 32 ng/ml) and c (12 and 24 ng/mL) for 24 h. The concentrations for apoptosis assay were selected based on IC_{50} value. After 24 h, the media was aspirated. The cells were stained using AO/EtBr dual staining

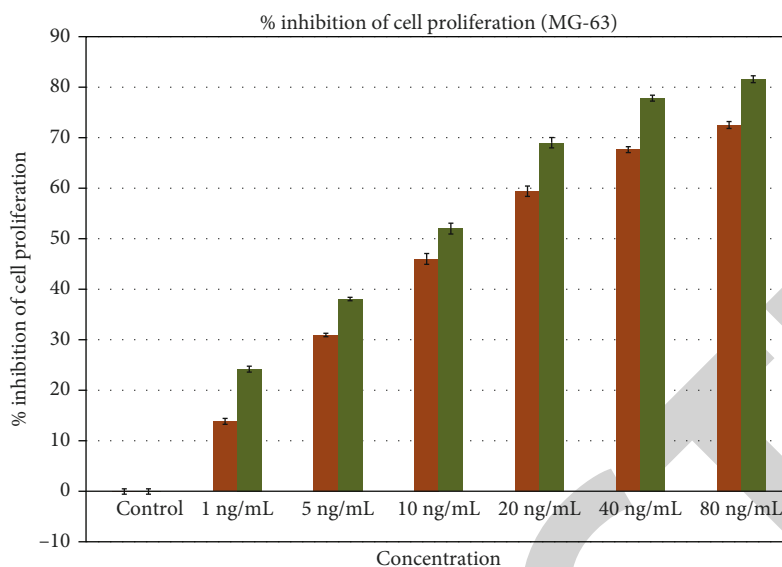


FIGURE 9: Representative graph demonstrating the antiproliferative effect of *S. longifolium* and its synthesized AuNPs determined by MTT assay. Results are expressed in terms of mean \pm SEM ($n = 3$).

solution prepared in PBS by incubating the cells with $5 \mu\text{L}$ of a mixture of AO/EtBr ($60 \mu\text{g}/\text{mL}$ (acridine orange)/ $100 \mu\text{g}/\text{mL}$ (ethidium bromide)) for 5 min in the dark after staining. The cells were immediately imaged in a fluorescence microscope (Nikon Eclipse E200, Tokyo, Japan).

4. Results and Discussion

4.1. Biosynthesis of AuNPs and UV-Vis Spectroscopy. Aqueous extract of *S. longifolium* was added into gold chloride solution. The formation of AuNPs was confirmed by the development of colour which is characteristic of AuNPs. The confirmation was done by recording the UV-Vis absorbance was at 350-650 nm which corroborated with the earlier published results [14, 32] in which the UV-Vis spectral analysis of AuNP absorbance was measured at 520-560 nm (27). They confirmed the peak around 540 nm and a broader peak between 700 and 800 nm.

4.2. Microscopic Analyses. The results of SEM and TEM revealed the size and shape of AuNPs, respectively (Figures 1 and 2). SEM analysis exhibited uniformly distributed AuNP which was found to be spherical in morphology with size ranging between 10 and 60 nm. Some of the AuNPs were seen aggregated. The separation between nanoparticles was observed from TEM image due to the presence of capping agent. The images of AFM showed the presence of AuNPs synthesized by *S. longifolium* (Figure 3). From the images, it is confirmed that a nanoplate structure was formed proving this method to be appropriate and successful for the synthesis of AuNPs [27].

4.3. FTIR. The functional groups of the *S. longifolium*-synthesized gold nanoparticles are shown in Figure 4. FTIR shows the characteristic peaks indicating the presence of different functional groups. A broad band observed at 3265 cm^{-1} was shown to be associated with C-H and O-H stretches from carboxylic acids and alcohols. The carboxylic

group assigned at 1232 cm^{-1} corresponds to C-O stretch, presence of amides, and N-H stretch at 1608 cm^{-1} . The analysis also revealed the presence of nitro groups N=O stretch at 1506 cm^{-1} . Other weak band also present at 455 cm^{-1} corresponds to alkyl halides.

4.4. EDX Analysis. EDX was performed to analyse the presence of various elements in the synthesized AuNPs. In Figures 5(a) and 5(b), a strong atomic signal from Au atom was observed with atomic % of 3.50% along with O atom 22.12%, C atom 69.56%, K atom 1.89%, and Cl atom 2.93%; there were no evident peaks for other elements or impurities [32].

4.5. Toxicological Evaluation of *S. Longifolium* Extract and Its Synthesized AuNPs. Figure 6 shows the brine shrimp lethality assay, and it is a preliminary and important screening tool to evaluate the toxicity of a drug. In the cytotoxic effect, the percentage of live nauplii was calculated. On day 1, the different concentrations of synthesized AuNPs as well as control showed 100% live nauplii. On the 2nd day except $40 \mu\text{L}$ and $50 \mu\text{L}$, other concentrations exhibited 100% survival which was in comparison to that of untreated control. Minimum lethality (20%) was observed in $40 \mu\text{L}$ and $50 \mu\text{L}$ AuNP-treated groups on day 2. From the results, the nontoxic nature of the synthesized AuNPs was inferred up to $30 \mu\text{L}$ towards brine shrimps [7].

4.6. DPPH Free-Radical Scavenging. The antioxidant activity of formulated AuNPs and the seaweed extract was estimated by evaluating the percentage inhibition of DPPH radicals (Figure 7). The DPPH radical scavenging activity of AuNPs was found to be directly proportional to the concentration of the seaweed extract and its synthesized AuNPs. The results exhibited significant inhibition of DPPH free radicals in a dose-dependent manner at 10, 20, 30, 40, and 50 mg/ml. AuNPs showed marked radical scavenging activity when compared to

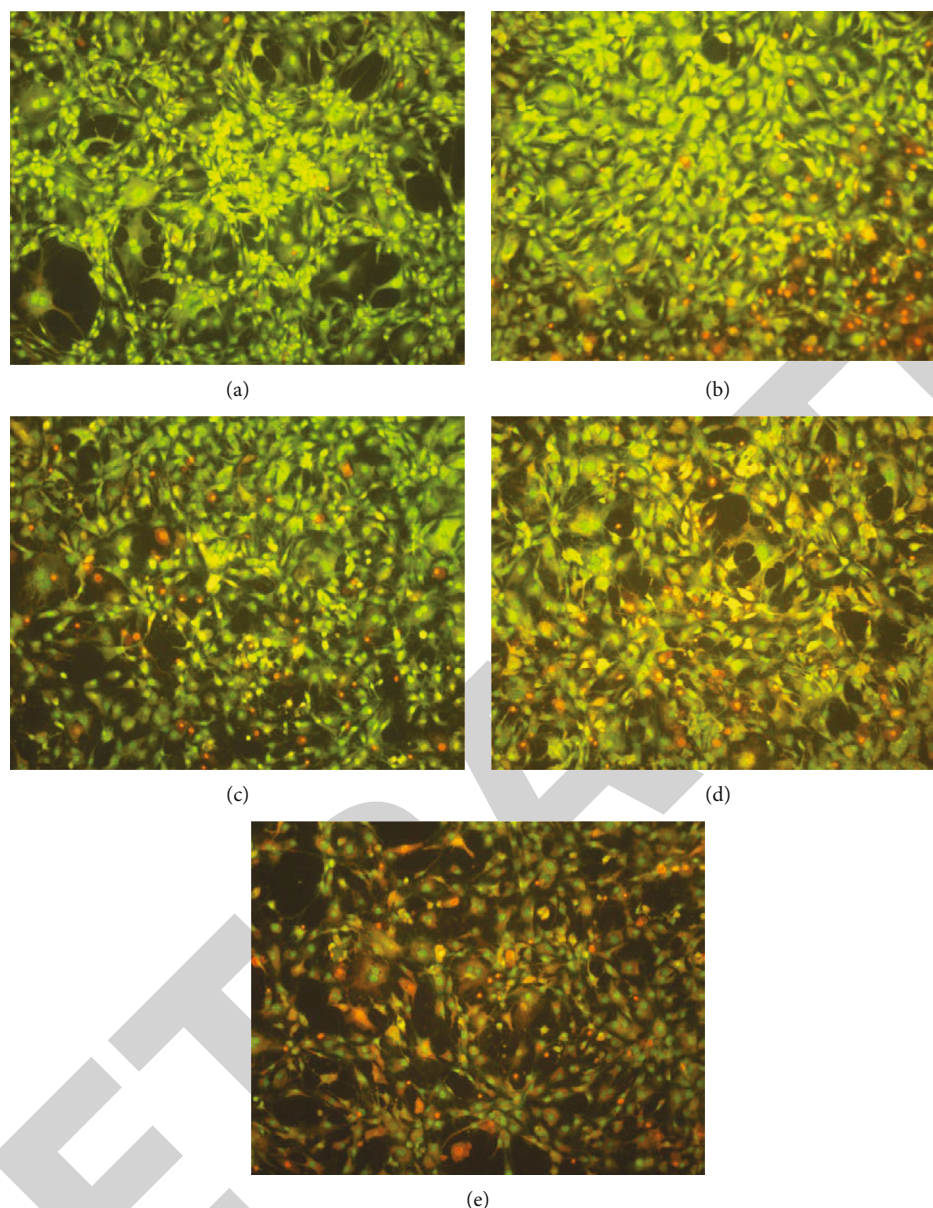


FIGURE 10: Induction of apoptosis by seaweed extract and its mediated synthesis AuNPs. (a) Untreated control; (b) seaweed extract 16 ng/ml; (c) seaweed extract 32 ng/ml; (d) AuNPs 12 ng/ml; (e) AuNPs 24 ng/ml. Magnification: 20x.

seaweed extract. The results revealed that the AuNPs were found to be more potent than the seaweed extract which was comparable with that of standard ascorbic acid [7].

4.7. H_2O_2 Radical Scavenging Activity. The H_2O_2 scavenging effect of *S. longifolium* extract and its mediated synthesis AuNPs was found to be dose-dependent (Figure 8). The free radical scavenging ability of the seaweed extract and the AuNPs was compared to standard ascorbic acid. AuNPs exhibited better scavenging effect than seaweed extract alone [5].

4.8. Anticancer Activity

4.8.1. Cytotoxicity Evaluation by MTT. The cytotoxicity activity of *S. longifolium* extract and its synthesized AuNPs was determined using MG-63 human osteosarcoma cells by

MTT assay (Figure 9). The results showed dose-dependent cytotoxic effect of both seaweed extract and AuNPs. A maximum inhibition of 72.5% was observed in seaweed extract whereas the AuNPs showed 81.5% inhibition at higher concentration of 80 ng/ml indicating that the seaweed-synthesized AuNPs is more potent than seaweed extract alone. The IC_{50} was found to be 32 ng/ml for seaweed extract and 23.58 ng/ml for AuNPs, respectively. Earlier published data have reported that AuNPs induce cytotoxicity by means of oxidative stress which results in production of reactive oxygen species thereby causing impairment in mitochondria function, ultimately resulting in cell death [33, 34].

4.8.2. Apoptosis Assay by EtBr/AO Dual Staining. MG-63 cells were treated with seaweed extract and AuNPs. After

24 h incubations, the cells were stained using EtBr/AO dual stain and the morphological changes were observed by examining under fluorescent microscope. Dual staining of the treated and control cells demonstrated induction of apoptosis by the seaweed extract and AuNPs. Viable cells emitted green fluorescence while early and late apoptotic cells appeared yellowish orange and orange in colour (Figure 10). Red fluorescence indicates necrosis. Previously published data has demonstrated that oxidative stress triggers apoptosis by activation of p38 MAPK pathway (34). In line with this, the present study findings have shown that the synthesized AuNPs might have induced apoptosis by oxidative stress-mediated pathway. However, further studies are needed to elucidate the mechanism of action.

5. Conclusion

In this present study, we have reported an eco-friendly method for green synthesis gold nanoparticle synthesized from marine seaweed *S. longifolium*. The results demonstrated the presence of elemental gold. Both seaweed extract and AuNPs exhibited significant free-radical scavenging activity indicating that they possess antioxidant effect. Also, the nontoxic nature of AuNPs was also confirmed by brine shrimp lethality assay. The cytotoxic and apoptotic effect of the AuNPs was also confirmed in MG-63 cell line which might be due to induction of oxidative stress in the MG-63 cells. However, in vivo and molecular studies are warranted in future to elucidate the exact mechanism of anticancer effect rendered by *S. longifolium*-mediated synthesized AuNPs.

Data Availability

The research data used to support the findings of this study are included within the article.

Conflicts of Interest

There is no conflict of interest.

Acknowledgments

The authors would like to thank Saveetha Dental College and Hospital, SIMATS for encouragement. This work was funded by the Princess Nourah bint Abdulrahman University Researchers Supporting Project number (PNURSP2022R62), Princess Nourah bint Abdulrahman University, Riyadh, Saudi Arabia and Researchers Supporting Project number (RSP-2021/26), King Saud University, Riyadh, Saudi Arabia.

References

- [1] S. Jadoun, R. Arif, N. K. Jangid, and R. K. Meena, "Green synthesis of nanoparticles using plant extracts: a review," *Environmental Chemistry Letters*, vol. 19, no. 1, pp. 355–374, 2021.
- [2] S. Rajeshkumar, "Synthesis of zinc oxide nanoparticles using algal formulation (*Padina tetrastratica* and *Turbinaria conoides*) and their antibacterial activity against fish pathogens research," *Journal of Biotechnology*, vol. 13, no. 9, pp. 15–19, 2018.
- [3] P. H. L. Tran, T. T. D. Tran, T. V. Vo, and B. J. Lee, "Promising iron oxide-based magnetic nanoparticles in biomedical engineering," *Archives of Pharmacal Research*, vol. 35, no. 12, pp. 2045–2061, 2012.
- [4] J. K. Patra, G. Das, L. F. Fraceto et al., "Nano based drug delivery systems: recent developments and future prospects," *Journal of Nanobiotechnology*, vol. 16, no. 1, p. 71, 2018.
- [5] R. Shanmugam, R. Subramaniam, S. G. Kathirason et al., "Curcumin-chitosan nanocomposite formulation containing *Pongamia pinnata*-mediated silver nanoparticles, wound pathogen control, and anti-inflammatory potential," *BioMed Research International*, vol. 2021, Article ID 3091587, 2021.
- [6] G. S. Dhillon, S. K. Brar, S. Kaur, and M. Verma, "Green approach for nanoparticle biosynthesis by fungi: current trends and applications," *Critical Reviews in Biotechnology*, vol. 32, no. 1, pp. 49–73, 2012.
- [7] S. Viswanathan, P. Thirunavukkarasu Palaniyandi, R. S. Kanaki et al., "Biogenic synthesis of gold nanoparticles using red seaweed *Champiaparvula* and its anti-oxidant and anticarcinogenic activity on lung cancer," *Particulate Science and Technology*, pp. 1–9, 2022.
- [8] N. E. Eleraky, A. Allam, S. B. Hassan, and M. M. Omar, "Nanomedicine fight against antibacterial resistance: an overview of the recent pharmaceutical innovations," *Pharmaceutics*, vol. 12, no. 2, p. 142, 2020.
- [9] H. Daraee, A. Eatemadi, E. Abbasi, S. Fekri Aval, M. Kouhi, and A. Akbarzadeh, "Application of gold nanoparticles in biomedical and drug delivery," *Artificial Cells, Nanomedicine, And Biotechnology*, vol. 44, no. 1, pp. 410–422, 2016.
- [10] M. C. Daniel and D. Astruc, "Gold nanoparticles: assembly, supramolecular chemistry, quantum-size-related properties, and applications toward biology, catalysis, and nanotechnology," *Chemical Reviews*, vol. 104, no. 1, pp. 293–346, 2004.
- [11] S. A. Bansal, V. Kumar, J. Karimi, A. P. Singh, and S. Kumar, "Role of gold nanoparticles in advanced biomedical applications," *Nanoscale Advances*, vol. 2, no. 9, pp. 3764–3787, 2020.
- [12] N. Elahi, M. Kamali, and M. H. Baghersad, "Recent biomedical applications of gold nanoparticles: a review," *Talanta*, vol. 184, pp. 537–556, 2018.
- [13] M. Fan, Y. Han, S. Gao et al., "Ultrasmall gold nanoparticles in cancer diagnosis and therapy," *Theranostics*, vol. 10, no. 11, pp. 4944–4957, 2020.
- [14] M. R. Priya and P. R. Iyer, "Antiproliferative effects on tumor cells of the synthesized gold nanoparticles against Hep2 liver cancer cell line," *Egypt Liver Journal*, vol. 10, no. 1, p. 15, 2020.
- [15] H. S. Auta, C. U. Emenike, and S. H. Fauziah, "Distribution and importance of microplastics in the marine environment: a review of the sources, fate, effects, and potential solutions," *Environment International*, vol. 1, no. 102, pp. 165–176, 2017.
- [16] I. Michalak and K. Chojnacka, "Algae as production systems of bioactive compounds," *Engineering in Life Sciences*, vol. 15, no. 2, pp. 160–176, 2015.
- [17] M. T. Ale and A. S. Meyer, "Fucoidans from brown seaweeds: an update on structures, extraction techniques and use of enzymes as tools for structural elucidation," *RSC Advances*, vol. 3, no. 22, pp. 8131–8141, 2013.
- [18] S. I. Shofia, K. Jayakumar, A. Mukherjee, and N. Chandrasekaran, "Efficiency of brown seaweed (*Sargassum longifolium*) polysaccharides encapsulated in nanoemulsion and nanostructured lipid carrier against colon cancer cell lines HCT 116," *RSC Advances*, vol. 8, no. 29, pp. 15973–15984, 2018.

Retraction

Retracted: Antioxidant and Anti-Inflammatory Activities of Coenzyme-Q10 and Piperine against Cyclophosphamide-Induced Cytotoxicity in HuH-7 Cells

BioMed Research International

Received 8 January 2024; Accepted 8 January 2024; Published 9 January 2024

Copyright © 2024 BioMed Research International. This is an open access article distributed under the Creative Commons Attribution License, which permits unrestricted use, distribution, and reproduction in any medium, provided the original work is properly cited.

This article has been retracted by Hindawi following an investigation undertaken by the publisher [1]. This investigation has uncovered evidence of one or more of the following indicators of systematic manipulation of the publication process:

- (1) Discrepancies in scope
- (2) Discrepancies in the description of the research reported
- (3) Discrepancies between the availability of data and the research described
- (4) Inappropriate citations
- (5) Incoherent, meaningless and/or irrelevant content included in the article
- (6) Manipulated or compromised peer review

The presence of these indicators undermines our confidence in the integrity of the article's content and we cannot, therefore, vouch for its reliability. Please note that this notice is intended solely to alert readers that the content of this article is unreliable. We have not investigated whether authors were aware of or involved in the systematic manipulation of the publication process.

Wiley and Hindawi regrets that the usual quality checks did not identify these issues before publication and have since put additional measures in place to safeguard research integrity.

We wish to credit our own Research Integrity and Research Publishing teams and anonymous and named external researchers and research integrity experts for contributing to this investigation.

The corresponding author, as the representative of all authors, has been given the opportunity to register their agreement or disagreement to this retraction. We have kept a record of any response received.

References

- [1] N. S. AL-Johani, M. Al-Zharani, N. H. Aljarba, N. M. Alhoshani, N. Alkeraishan, and S. Alkahtani, "Antioxidant and Anti-Inflammatory Activities of Coenzyme-Q10 and Piperine against Cyclophosphamide-Induced Cytotoxicity in HuH-7 Cells," *BioMed Research International*, vol. 2022, Article ID 8495159, 10 pages, 2022.

Research Article

Antioxidant and Anti-Inflammatory Activities of Coenzyme-Q10 and Piperine against Cyclophosphamide-Induced Cytotoxicity in HuH-7 Cells

Norah S. AL-Johani ¹, Mohammed Al-Zharani ², Nada H. Aljarba ³,
Norah M. Alhoshani ¹, Nora Alkeraishan ¹ and Saad Alkahtani ¹

¹Department of Zoology, College of Science, King Saud University, P. O. Box 2455, Riyadh 11451, Saudi Arabia

²Imam Mohammad Ibn Saud Islamic University (IMSIU), College of Science, Biology Department, Riyadh 11623, Saudi Arabia

³Department of Biology, College of Science, Princess Nourah Bint Abdulrahman University, P. O. Box 84428, Riyadh 11671, Saudi Arabia

Correspondence should be addressed to Saad Alkahtani; salkahtani@ksu.edu.sa

Received 20 May 2022; Accepted 30 June 2022; Published 13 July 2022

Academic Editor: Hafiz Ishfaq Ahmad

Copyright © 2022 Norah S. AL-Johani et al. This is an open access article distributed under the Creative Commons Attribution License, which permits unrestricted use, distribution, and reproduction in any medium, provided the original work is properly cited.

Cyclophosphamide (CP) alkylates DNA and RNA produce crosslinks that cause gene expression and protein synthesis inhibition to exert its anticancer effect. However, adverse effects of CP have restricted the CP application in cancer treatment. We investigate coenzyme-Q10 (Q10) and piperine (P) protective role on CP oxidant and inflammatory effect. HuH-7 cells were exposed to varying concentrations and combinations of Q10, P, and CP and evaluated intracellular ROS generation as well as inflammatory responses upon exposure. Our results showed Q10 and/or P suppressed both basal and CP-induced ROS generation without upsetting the balance in activities of SOD, catalase, and GSH levels. Analysis of proinflammatory cytokine gene expression showed that CP treatment alone only induced expression of *IL-6*. However, coexposure of the cells to both Q10 and CP caused significant suppression of basal *Cox-2* and *TNF- α* gene expression, while coexposure of the cells to CP and P with Co-Q10 suppressed basal *IL-1 β* gene expression. Q10 also suppressed CP-induced expression of *Cox-1*. P and CP suppressed basal expression of *IL-6* and *IL-12 β* , while P and Q10 suppressed CP-induced *IL-1 α* gene expression. Taken together, both Q10 and P seem to be inhibiting NF κ B pathway to suppress CP-mediated inflammation. In conclusion, Q10 and/or P induced suppression of ROS generation mediated by CP and also suppressed CP-induced inflammation by inhibiting expression of specific inflammatory cytokine.

1. Introduction

Several chemotherapeutic drugs used to treat different types of cancer diseases. Some of those drugs have been failed due to adverse effect exhibited by the drugs preventing their continued application in treating cancer patients. One such compound which is widely restricted is cyclophosphamide (CP). CP is an anticancer drug used in treatment of various solid tumors such as in the breast, lung, and prostate cancers, in addition to blood disorders like leukemia and lymphoma [1–4]. Unfortunately, adverse effects such as hepatotoxicity, nephrotoxicity, cardiotoxicity,

and severe immunotoxicity have restricted the use of CP in cancer treatment [5].

CP is an alkylating agent metabolized by cytochrome p450 (CYP450) liver enzyme to phosphoramidate and acrolein, in which alkylates DNA and RNA produce crosslinks that inhibit gene expression and protein synthesis [6]. Furthermore, CP metabolism results in generation of active carbonium ions, an electrophile that attack electron rich nucleic acids in DNA, RNA, and proteins causing DNA damage and producing reactive oxygen species (ROS) [7]. The ROS generated due to administration of CP further result in DNA damage and perturbation in

the oxidant-antioxidant balance in the cell, negatively affecting cellular homeostasis even in normal healthy cells.

One downstream effect of ROS generation is induction of inflammation. ROS generation induces activation of different transcription factors like $\text{NF}\kappa\beta$, which regulates expression of proinflammatory cytokines like interleukin 6 (IL-6) and tumor necrosis factor α (TNF- α) which subsequently result in activating cyclooxygenase-2 (COX-2) [8]. Interestingly, there are studies on chemotherapeutic agents such as CP inducing inflammation via ROS-induced activation of $\text{NF}\kappa\beta$ [9]. In addition, $\text{NF}\kappa\beta$ activation may also result in activation of additional transcription factors such as STAT-3 which in turn activates IL-6 expression creating sustained inflammatory response loop [10]. Girard et al. [11] showed in rat model that CP induced bladder inflammation through activation of JAK/STAT pathway involving expression of IL-6 and IL-6R α . Moschella et al. [12] also demonstrated in a mouse model that CP treatment resulted in expression of gene and protein belonging to IL-1 family members such as IL-1 β , IL-18, and interferon γ (IFN- γ).

In order to prevent or minimize the adverse effects of CP and its metabolite to improve it for therapy in cancer is to employ less toxic drugs. Natural antioxidant products are explored for therapeutic purposes because such perceived safety against normal healthy cells. Piperine (P) is an alkaloid that is found in black pepper (*Piper nigrum* L.). P is a pharmacologically active agent known to possess hepatoprotective, antioxidant, and immunomodulatory effects [13]. Similarly, coenzyme Q10 (Q10) is a naturally occurring compound in mammalian cells with repeating isoprene units that has been investigated for alleviating the toxicity of different compounds due to its antioxidant properties [14]. For instance, Q10 has been used to suppress cisplatin-mediated oxidative stress which induces inflammation, necrosis, and apoptosis in renal tissue via its antioxidant activities [15]. Similarly, Q10 has been used to alleviate toxicity of anthracycline, tamoxifen, and doxorubicin [16–18]. Here, we explored P and Q10 as protective agents against inflammation and oxidative stress induced by CP. We investigated CP cytotoxic effect alone and with Q10 and P in HuH-7 cell line and evaluate the oxidative stress, antioxidant levels, and inflammatory responses in HuH-7 cell line.

2. Methodology

2.1. Preparation of the Treatments. CP (MedChemExpress LLC, USA), P, and Q10 (BioPiperine®USA) were dissolved in DMSO to make 1 mg/1 ml.

2.2. MTT Assay. HuH-7 (ATCC, USA) were cultured in 70% DMEM supplemented with 30% FBS and 1% penicillin-streptomycin and incubated at 5% CO_2 and 37°C. Cell viability and proliferation were both determined using an MTT assay (Mosmann, 1983). Cells were cultured in 24-well plate after which they were incubated at above conditions for 24 h. The cells were exposed to predetermined concentrations of P, CP, Q10 alone, or combination of P and/or Q10 with CP for 48 h. MTT solution (100 μl) was added, and cells were returned to incubator for 4 h. Medium

was aspirated from the culture plate, and formed crystals were dispersed in isopropanol (1 ml/well) in 0.04 HCl followed by shaking at RT for 12 minutes to ensure complete solubilization. Afterwards, 100 μl of the media from each well was added into a 96-well plate for absorbance measurement at 540 nm (multimode Microplate Reader-Gen5™, Bio-Tek Cytation 5™, USA).

2.3. Lactate Dehydrogenase Assay (LDH Assay). Cell viability and membrane integrity were assessed by performing LDH assay kit (MAK066 Sigma-Aldrich, St Louis, USA). Briefly, the cells were seeded as above 100 μl of medium, then incubated under above conditions for 24 h. The media was aspirated, discarded, and then, replaced with 200 μl of new medium for each well. Cells were then exposed to 10 $\mu\text{g}/\text{ml}$ of CP, 12 $\mu\text{g}/\text{ml}$ P, 10 $\mu\text{g}/\text{ml}$ Q10, 12 $\mu\text{g}/\text{ml}$ of P + Q10, and combination of CP + P, CP + Q10, and CP + P + Q10 as in the individual concentrations for 48 h. Then, the supernatant (50 μl) was transferred to new 96-well plate followed by addition of 50 μl of the Master Reaction Mix to each well. The cells were mixed and incubated on a horizontal shaker for 3 min in the dark. The OD was measured at 450 nm using the spectrophotometer. The plate was reincubated, and OD was measured twice every 5 mins.

2.4. Oxidative Stress

2.4.1. Production of ROS. ROS production was evaluated by $\text{H}_2\text{DCF-DA}$ (Dikalov et al., 2007). ROS was assayed using the Cayman-ROS Detection Cell-Based Assay Kit following manufacturer's instruction. Briefly, the HuH-7 cells were seeded in black 96-well plate of 5×10^4 /well for 24 h under above incubation conditions. Cells were exposed to each treatment for 48 h as above, and then, the media was replaced with 100 μl of diluted $\text{H}_2\text{DCF-DA}$ dye solution, which was prepared by adding 1 μl of $\text{H}_2\text{DCF-DA}$ dye to 99 μl of MEME in the dark; the plates were returned to the incubator for 60 min. Absorbance analysis was done at excitation wavelengths of 480 and emission 530 nm in a microplate reader. To monitor the intracellular ROS under microscope, cells were seeded in 6-well plate and incubated for 24 h. After that cell were exposed as above for 48 h, then the medium was replaced with 1 ml diluted $\text{H}_2\text{DCF-DA}$ solution in the dark 1 h. The cells were washed in pre-warmed PBS for 3 times. Fluorescent images were taken by DMLB fluorescence microscope (Leica, Germany) and analyzed using the ImageJ software (version 1.51, NIH, Bethesda, MD, USA).

2.4.2. Catalase Activity. The assessment of CAT activity was achieved by catalase colorimetric Kit, K773-100, BioVision. Briefly, the HuH-7 cells seeded in 25 ml flask of 1×10^6 cells/ml culture media were incubated for 24 h. Treatments were applied as before. After incubation, cells were washed, and then, 1 ml cold assay buffer was added. Immediately, cells were scraped and vortexed for 2 min, followed by centrifuging at 12000 rpm at 4°C for 7 min. After this, samples were added/well, and the total volume was adjusted to 78 μl with assay buffer. To stop the reaction, 10 μl of stop solution was added, and then, 12 μl of fresh (1 mM H_2O_2)

was added to start the reaction. Cells were incubated for 30 min at 25°C, and 10 µl of stop solution was added to each sample well. The developer mix (50 µl) was added to each sample, mixed well, and incubated for 10 min at 25°C. OD was then measured at 570 nm.

2.4.3. Superoxide Dismutase (SOD). The assessment of SOD activity was conducted by SOD kit (Cayman Chemical, Michigan USA). The HuH-7 cells were seeded in 25 ml flask of 1×10^6 cells/well for 24 h. Treatments were done as above h. Cells were washed, and 1 ml cold SOD lysis buffer (pH 7.2) was added. Cells were collected and sonicated for 2 min, then centrifuged at 12000 rpm at 4°C for 8 min. Then, 500 µl of supernatant was transferred into new Eppendorf tubes, and 200 µl of radical detector was added, followed by adding 10 µl of each sample (cell lysates), and then, 20 µl of diluted xanthine oxidase was added. The cells were incubated at RT for 10 min. OD was measured at 460 nm (Synergy-H1; BioTek).

2.4.4. Glutathione (GSH). Evaluation of total glutathione (GSH) content was analysed using Glutathione assay kit (Cayman Chemical, Michigan USA). Briefly, the HuH-7 cells were cultivated in 25 ml flask for 24 h. After treatment 1 ml of cold buffer (0.4 M 2-(N-morpholino) ethanesulfonic acid, 0.1 M phosphate, and 2 mM EDTA, pH = 6) at 4°C was added to each flask. Cells were collected and sonicated for 2 min after which they were 2 centrifuged at 12000 rpm at 4°C for 8 min. Then, 500 µl of supernatant and 50 µl of sample (cell lysate from treated and control cells) were added to each well. A 150 µl of freshly prepared cocktail assay was added and mixed well by pipetting; plate was in the dark on an orbital shaker. OD was recorded at 405 nm (Synergy-H1; BioTek).

2.5. Gene Expression

2.5.1. RNA Extraction. Briefly, HuH-7 cells were cultured and exposed as before. After incubation, the cells were washed with cold PBS, and 2 ml of Trizol was added to each flask on ice for 5 min. 1 ml of cells was transferred into Eppendorf tubes (1 ml/tube) after which 200 µl of cold chloroform was added. Tubes were mixed and then centrifuged at 15000 rpm for 10 min at 4°C. Then, 500 µl of supernatant was added followed by addition of 500 µl iso-propanol alcohol to each tube, gently mixed, and incubated for 10 min on ice followed by centrifuged at 12000 rpm for 15 min at 4°C. Supernatant was discarded; 1 ml of cold absolute ethanol was added and gently mixed for 15 sec. Tubes were centrifuged at 10000 rpm for 5 min and 4°C, and the step was repeated. Supernatant was discarded, and tubes were allowed to dry for 15 min, and 30 µl of DEPC water was added. Concentration and purity of RNA were measured by Nanodrop 8000 (Thermo Fisher Scientific, USA).

2.5.2. Complementary DNA (cDNA) Synthesis. cDNA synthesis kit GoScript™ Reverse Transcriptase (CAT No A5003, Promega, USA) was carried out according to manufacturer instructions. Briefly, 0.5 µl Oligo (dT) and 0.5 µl random hexamer primer were added to a PCR tube. Total RNA and nuclease-free water were added up to 5 µl total volume. PCR tubes were placed in the thermal cycler (TECHNE, UK) at

70°C for 5 min. Afterwards, 15 µl of mater-mix was added to each sample and placed in thermal cycler. After cycle completion, 180 µl of nuclease-free water was added to each cDNA sample (total volume of each sample was 200 µl).

2.5.3. Quantification of mRNA Expression. Quantitative analysis of mRNA expression was performed by RT-PCR through PCR amplification (cDNA) in CFX96™ real-time system (BIO-RAD, USA) using KAPA SYBER FAST Universal qPCR Kit (Cat No. KK4600, KAPA BIOSYSTEM, USA). The RT-PCR data analysis was done using the relative gene expression (i.e., $\Delta\Delta Ct$) method, as described previously (Livak and Schmittgen, 2001).

2.6. Statistical Analysis. The SPSS software (ver.22; SPSS Inc., Chicago, IL, USA) was used to analyze the obtained data. Data were examined by using two-way ANOVA, followed by a post hoc LSD (least significant difference) test, and results were presented as average \pm SE, $p < 0.05$ were considered statistically significant.

3. Results

3.1. P and Q10 Exhibit Lower Cytotoxicity vs. CP. MTT assay was performed to determine the cytotoxicity of CP and impact of P and Q10 on CP's cytotoxicity, postexposure to the compounds. We observed dose-dependent decrease of cell survival for all the compounds. Both P and Q10 had similar impact on cell viability at 5 µg/ml compared to unexposed cells while CP significantly induced cell viability at 5 µg/ml compared to the control unexposed cells. Similarly, we found that coexposure of the HuH-7 resulted in less cytotoxic effect compared to CP (Table 1).

3.2. P and Q10 Enhance Permeabilisation of HuH-7 Cell Membrane. Findings from LDH assay indicated a significant loss of membrane integrity after exposure of the cells to all investigated compounds when compared to untreated cells after 48 h (Figure 1). However, combination of CP+P or CP+Q10 or CP with both P and Q10 significantly increased permeability of the cell membrane compared to CP. This indicates P/Q10 seems to enhance cell membrane permeabilisation effect of CP alone.

3.3. Induction of (ROS). A significant increase in ROS level posttreatment with CP compared with control unexposed cells ($p < 0.05$). Contrastingly, single exposure to either of P or Q10 alone or combination of both compounds resulted in significant suppression of ROS generation compared to control cells ($p < 0.05$). Furthermore, coexposure of the cells to either of CP+P, CP+Q10, and CP+P+ Q10 significantly suppressed ROS generation compared to exposure to CP alone (Figures 2(a) and 2(b)).

3.4. Catalase (CAT) Activity. Based on the suppressed ROS generation observed above, we proceeded to assess catalase activity in the cell postexposure to the compounds. Our findings showed significant reduction in CAT activity post-treatment with P, CP+Q10, and CP+P+Q10 was significantly reduced after 48 h ($*p < 0.05$, $**p < 0.01$) (Figure 3).

TABLE 1: Cell viability of HuH-7 cells after treatment with CP, PIP, CoQ-10, and PIP+CoQ-10 for 48 hrs as evaluated by MTT assay. Each value represents the mean \pm SE ($n = 3$) (* $p < 0.05$, ** $p < 0.01$, *** $p < 0.001$) compared with control.

Treatments	Concentrations ($\mu\text{g/ml}$)	Average	Viability (%)	IC50 ($\mu\text{g/ml}$)
Control	—	0.557 \pm 0.001	100	
CP	5	0.373 \pm 0.003	67.05**	10
	10	0.273 \pm 0.003	49.1***	
	15	0.175 \pm 0.004	31.5**	
	20	0.138 \pm 0.006	24.8***	
	25	0.093 \pm 0.002	16.6***	
PIP	5	0.523 \pm 0.12	93.9	16
	10	0.382 \pm 0.07	68.6	
	15	0.275 \pm 0.007	49.4**	
	20	0.231 \pm 0.02	41.5**	
	25	0.186 \pm 0.02	33.4*	
Q10	5	0.44 \pm 0.001	78.9	15
	10	0.368 \pm 0.01	66*	
	15	0.277 \pm 0.02	49.7*	
	20	0.206 \pm 0.01	37**	
	25	0.161 \pm 0.02	28.9*	
PIP+Q10	5	0.42 \pm 0.07	75.4	18
	10	0.387 \pm 0.04	69.4	
	15	0.338 \pm 0.05	60.7	
	20	0.258 \pm 0.05	46.4	
	25	0.231 \pm 0.05	41.4	

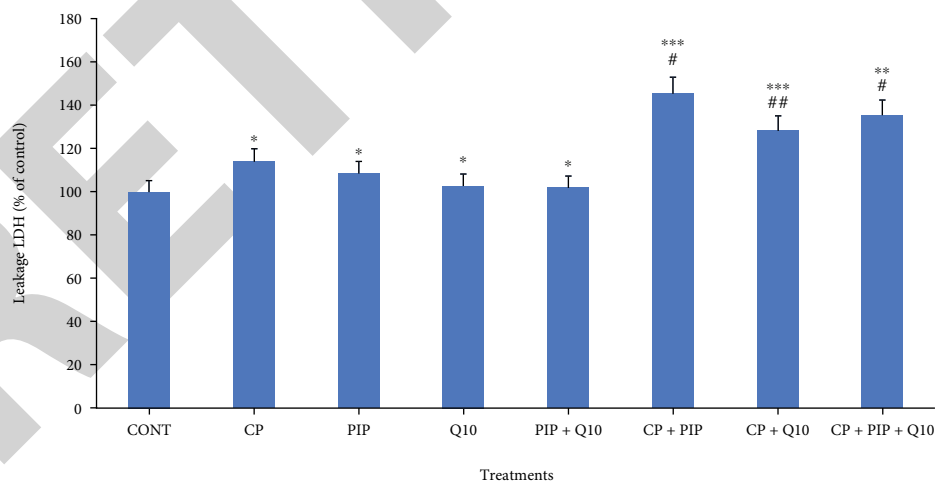


FIGURE 1: Effect of CP, PIP, and CoQ-10 on LDH % in HuH-7 cell lines when treated for 48 h (* $p < 0.05$, *** $p < 0.001$) compared to the control group (# $p < 0.05$, ## $p < 0.01$) compared with CP.

3.5. *Superoxide Dismutase (SOD)*. This enzyme catalyzes the conversion of superoxide radical into less-toxic hydrogen peroxides to help healthy cells actively fight oxidative stress. After treatment, a significant drop in activity of SOD due to CP exposure was observed compared to the control cells (** $p < 0.01$). In addition, reduction in SOD

activity was observed after treatment with other investigated compounds compared to control although these were not significant. Similarly, a nonsignificant increase in SOD activity was observed after treatment with CP+P, CP+Q10, and CP with both P and Q10 compared to CP alone (Figure 4).

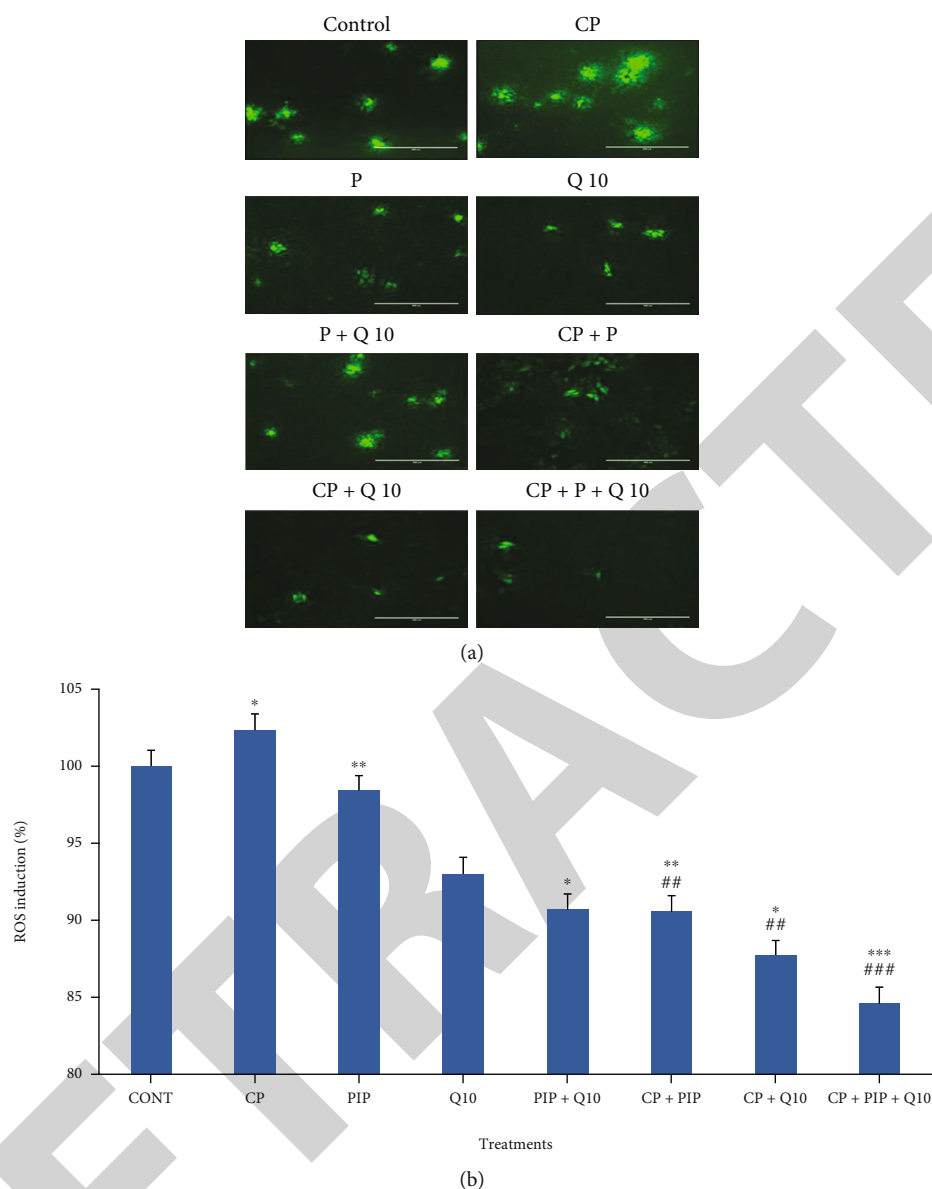


FIGURE 2: (a) The production of ROS in HuH-7 cells as stained with fluorescence dye (DCFH-DA) after treatments. Bar: 400 μm. (b) Induction of ROS levels in HuH-7 after treatment with CP, PIP, and CoQ-10 for 48 h. Each value represents the mean ± SE (n = 3) (*p < 0.05, **p < 0.01, ***p < 0.001) compared with control (#p < 0.05, ##p < 0.01, ###p < 0.001) compared with CP.

3.6. Glutathione (GSH). Glutathione (GSH) plays a crucial function in removal of many reactive species. HuH-7 cells were exposed to CP, P, Q10, and in combination with CP. Our result as shown in (Figure 5) indicated nonsignificant reduction in GSH level when exposed to CP, P, and Q10 but there was significant decrease in GSH level after treatment with combination of P+Q10 and combination of CP +P and CP+P+ Q10 compared to CP.

3.7. Gene Expression

3.7.1. Inflammatory Marker Genes at Transcriptional Level. Gene expression of *Cox-1* was found higher in cells exposed to CP alone. However, coexposure of the cells to CP and Q10 resulted in significant reduction in *Cox-1* gene

expression (#p < 0.05). We found that coexposure of the cells to CP and either of P or P+Q10 as well as single exposure to P alone resulted in considerable reduction of *Cox-1* expression (Figure 6). Assessment of *Cox-2* expression produced a contrasting finding to that of *Cox-1*. We found *Cox-2* expression after exposure to P or Q10 led to a significant increase in expression of *Cox-2* gene compared with untreated cells. Similarly, exposure to CP alone also considerably increased *Cox-2* gene expression. On the contrary, coexposure of the cells to CP and Q10 led to significant decrease of *Cox-2* expression compared to control cells (*p < 0.05). Furthermore, when CP was combined with P and/or Q10, *Cox-2* gene expression was maintained at the levels of the control unexposed cells (Figure 6).

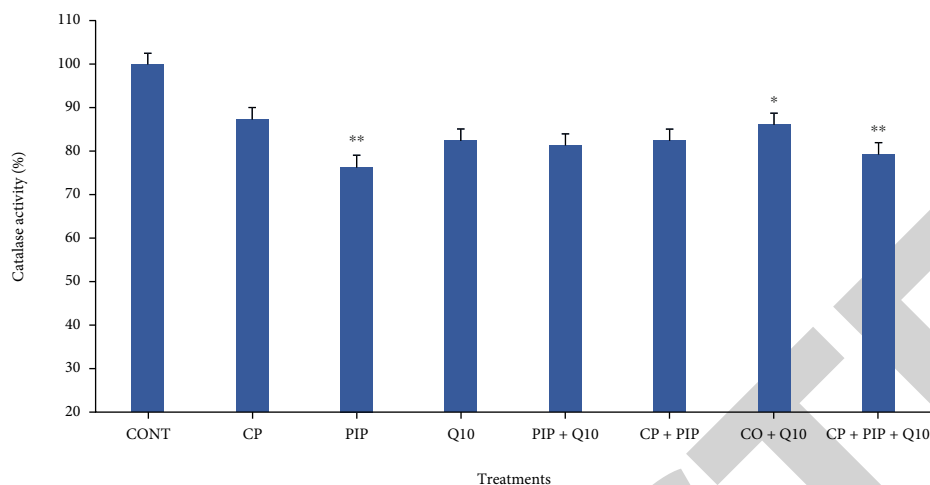


FIGURE 3: CAT levels in HuH-7 after treatment with CP, PIP, Q-10, and in combination of CP with each compound for 48 hr. Data present represents the mean \pm SE ($n = 3$) (* $p < 0.05$, ** $p < 0.01$) compared with untreated control.

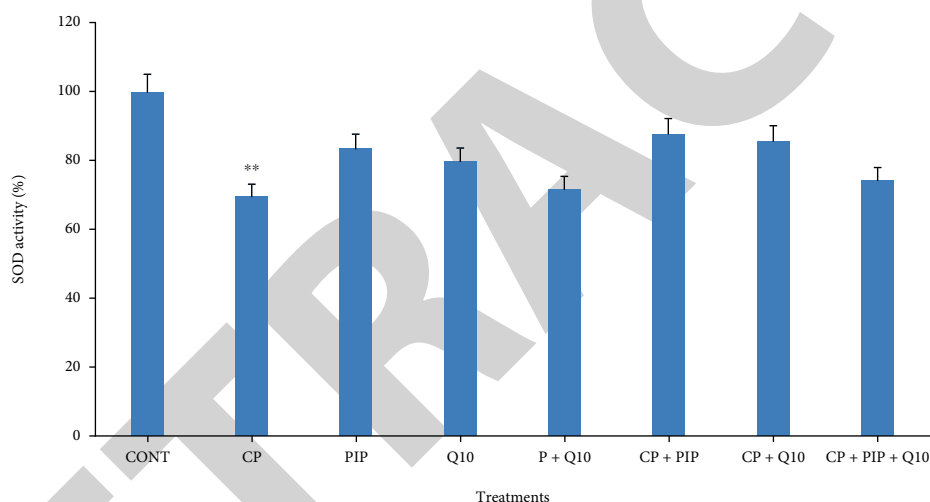


FIGURE 4: SOD levels in HuH-7 after treatment with CP, PIP, CoQ-10, and in combination of CP with each compound for 48 hr. Data present represents the mean \pm SE ($n = 3$) (* $p < 0.05$) compared with untreated control.

The expression of *TNF- α* was assessed in the HuH7-treated cells after 48 h. Current results indicated that expression of *TNF- α* was significantly upregulated after treatment with P, Q10, P+ Q10, CP+P, and CP+ Q10 compared to untreated cells (* $p < 0.05$, ** $p < 0.01$). Furthermore, when CP was combined with P and Q10, there was an insignificant downregulation of *TNF- α* expression compared to CP alone. The expression of *IFN- γ* was considerably increased after exposure to CP. However, a decrease in *IFN- γ* gene expression was observed after exposure to P alone or with Q10 and CP with P or with Q10. CP combination with P and Q10 resulted in similar levels of *IFN- γ* expression as in the control untreated cells. Assessment of *IL-1 α* expression showed that exposure to P alone or with CP and/or P+Q10 caused significant downregulation of *IL-1 α* expression compared to untreated control cells (* $p < 0.05$, ** $p < 0.01$, and *** $p < 0.001$). In addition, P alone or with Q10 led to significant reduction in *IL-1 α* expression compared to CP (# $p < 0.05$) (Figure 6). This suggests that coexposure of the

cells to P alone or with Q10 suppresses both basal and CP-mediated *IL-1 α* expression. Figure 6 shows the results obtained for *IL-1 β* expression. Upon exposure of the HuH-7 cells to P, P+Q10, and CP+ P+Q10, expression of *IL-1 β* was significantly downregulated when compared with the untreated cells (* $p < 0.05$, ** $p < 0.01$). Furthermore, considerable but not statistically significant downregulation of the gene expression was observed after cotreatments with CP +P, CP+Q10, and CP+P+Q10 compared to CP alone (Figure 6). This suggests that coexposure of the cells to P alone or with Q10 suppresses both basal and CP-mediated *IL-1 β* gene expression.

Analysis of *IL-6 β* expression after treatments of HuH-7 with CP, P, Q10, and P+ Q10 for 48 h indicated a significantly increased *IL-6 β* gene expression compared to untreated cells (** $p < 0.01$, *** $p < 0.001$). In contrast, treatments of the cells with CP+P, CP+Q10, and CP+P+ Q10 led to significantly decreased compared to CP (# $p < 0.05$, ## $p < 0.01$) (Figure 6). This finding indicates coexposure

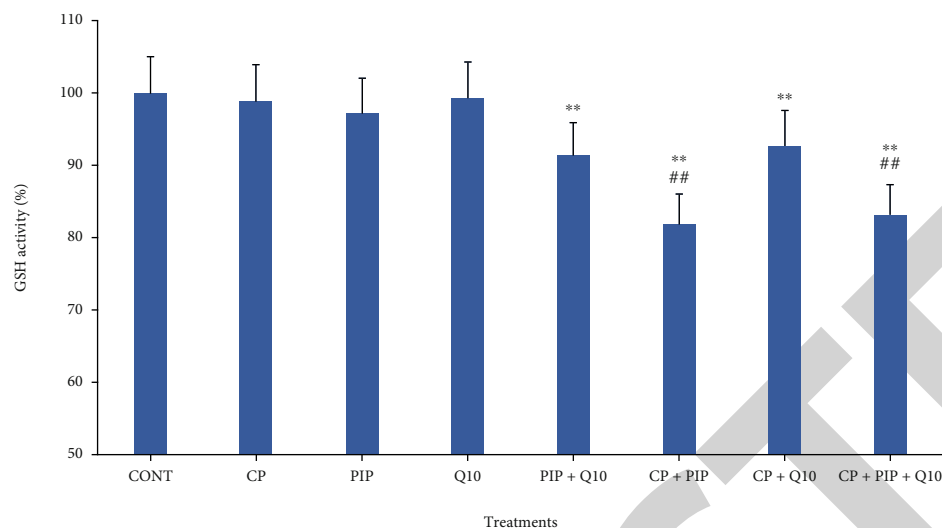


FIGURE 5: GSH levels in HuH-7 after treatment with CP, PIP, Q-10, and in combination of CP with each compound for 48 hr. Data present represents the mean \pm SE ($n = 3$) (** $p < 0.01$) compared with untreated control ($^{\#}p < 0.05$, $^{\#\#}p < 0.01$) compared with CP.

of the cells to P and/or Q10 suppresses both basal and CP-mediated *IL-6 β* gene expression. The obtained results from *IL-12 β* analysis showed that expression of *IL-12 β* was significantly downregulated by exposure of the cells to P, Q10, P+Q10, CP+P, and CP+P+Q10 compared to control cells (** $p < 0.01$, *** $p < 0.001$) (Figure 6). The expression of *IL-22* gene was unaffected by all the compounds alone or in combination except for CP+Q10 exposure.

4. Discussion

Some side effects hampering the application or administration of CP in cancer treatment includes associated oxidative stress and inflammation [19]. In this study, we evaluated the impact of two naturally occurring compounds, P and Q10, as protective agents that can mediate suppression of inflammation and oxidative stress induced by CP. One of the uses of CP is in treatment of liver cancer. The first step in the activation reaction of CP occurs in the liver microsomal oxidation system in a process that produces 4-hydroxy-CP, a cytotoxic metabolite that diffuses from liver cells into the plasma and then to other organs in the body. As such, we have selected the HuH-7 cell line, as a hepatocellular carcinoma model [20]. Findings from this study showed that HuH-7 cell treatment with CP significantly reduced cell viability with an IC₅₀ of 10 μ g/ml higher than the IC₅₀ of P and Q10 alone or in combination, indicating CP was more cytotoxic compared to P and Q10. This reiterates the cytotoxicity of CP as supported by previous studies in hepatocarcinoma cells [21–23]. One of the toxicity mechanism of CP is through generation of intracellular ROS, which causes oxidative stress. Investigation of ROS generation upon CP treatment showed that the HuH-7 cells underwent significant oxidative stress based on the increased ROS generation in comparison to the control untreated cells. The increased ROS generation by CP led to our assessment of some oxidative markers such as catalase, SOD, and GSH. We found that CP treatment caused reduction in SOD activities while cata-

lase activity and GSH levels were unaffected. This finding is supported by Germoush and Mahmoud [24], who showed CP induced suppression of SOD activity and GSH levels in a rat model. Oxidative stress within a cell is a measure of the balance between pro- and antioxidant activities. Increased ROS in a normal cell is followed by increased levels and activities of antioxidants such as catalase, SOD, and GSH to metabolize the ROS. SOD will convert ROS to H₂O₂ while catalase converts the H₂O₂ into oxygen and water [25]. However, inadequate levels or activities of these antioxidants that can cope with the generated ROS as observed in CP-treated cells result in detrimental oxidative stress [26, 27]. P and Q10 were both found to significantly suppress ROS generation alone or during coexposure. Similarly, we found P and Q10 suppressed CP-induced ROS generation in HuH-7 cells alone or when they are both coexposed with CP. This finding may be because of both P and Q10 antioxidant activities. P is initially oxidized to form a catechol that has an antioxidant activity that is known to be neuroprotective [28]. Q10 is an important electron acceptor during ATP synthesis, making it an important compound for normal cellular energy homeostasis. In addition, Q10 is effective against oxidation that results in modifications of organic and genetic materials. Q10 level often declines in some diseases correlated with increased ROS generation and activity and deficiency of Q10 results in decreased cell efficiency consequent upon respiratory chain dysfunction, which is characterized with insufficient production of high-energy compounds [29]. The finding in our study indicates that P and/or Q10 did not influence SOD activity while they suppressed catalase activity and GSH level. This finding shows that both P and Q10 maintained the antioxidant and prooxidant balance since ROS generation is suppressed requiring no activity of the antioxidant parameters.

Intracellular ROS can induce activation of cellular pathways mediating activities of redox sensitive transcription factors like nuclear factor- κ B (NF- κ B) which then activate expression of proinflammatory proteins like cox-2, IL-1 β ,

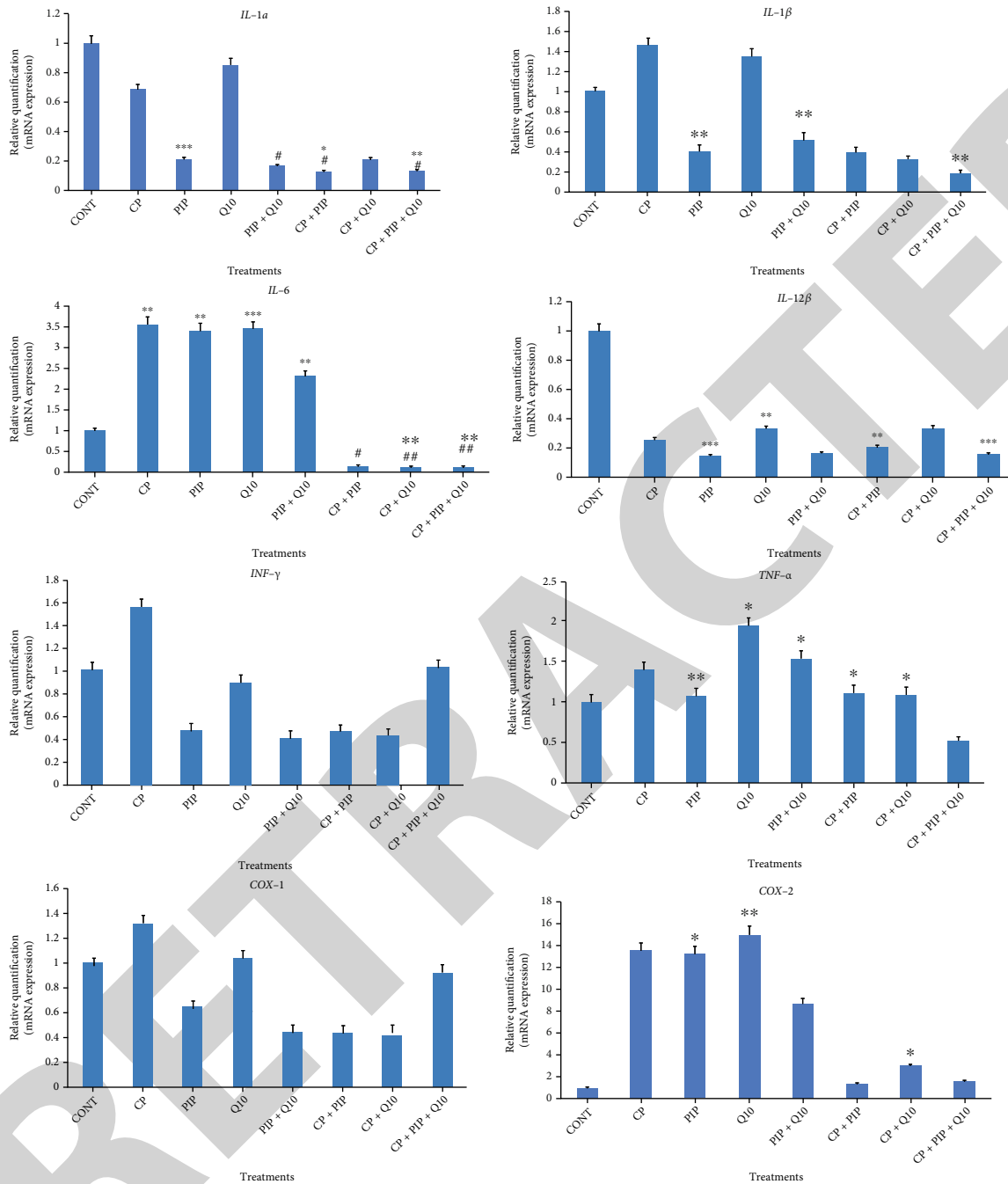


FIGURE 6: mRNA levels of inflammatory related genes in HuH7 cells after treatments for 48 h. Each value represents the mean \pm SE of three experiments. $n = 3$ (* $p < 0.05$, ** $p < 0.01$, *** $p < 0.001$) vs. control.

IL-6, and TNF- α [10, 30]. Induction of proinflammatory cytokines like Cox-2 can lead to increased levels of prostaglandin, resulting in recruitment of more inflammatory cells followed by and stimulation of inflammatory responses and generation of ROS [31]. Similarly, this sustained loop of inflammation is seen during induction of IL-6 β resulting from NF κ B activation. IL-6 β binds its receptor, IL-6R, which activates STAT-3, a transcription factor regulating transcription of NF κ B with further expression of IL-6 β [32].

We found that CP treatment alone did not induce gene expression of any of the proinflammatory cytokines we eval-

uated except for IL-6 β . However, coexposure of the HuH-7 cells to Q10 and CP caused significant suppression of basal Cox-2 and TNF- α gene expression while coexposure of the cells to CP and P with Co-Q10 suppressed basal IL-1 β gene expression. Q10 also suppressed CP-induced expression of Cox-1. Similarly, P and CP suppressed basal expression of IL-6 β and IL-12 β , while P and Q10 suppressed CP-induced expression of IL1- α . These findings suggest that anti-inflammatory effect Q10 and P of CP-mediated inflammation is due to inhibition of NF κ B pathway. NF κ B activation controls the regulation of myriads of inflammatory

proteins including the aforementioned proteins that were inhibited in this study [33]. These findings are in line with other studies that have investigated anti-inflammatory activities of natural compounds on CP. Mansour et al. [34] showed that genistein inhibited CP-induced *Cox-2* expression. Similarly, *Vernonia cinerea* was also reported to suppress CP-induced *TNF- α* gene expression in a mouse model [19]. Contrastingly, the anti-inflammatory roles of P and Q10 as illustrated in this study are supported by those of other studies. P has been shown to suppress protein expression of inflammatory proteins like *Cox-2*, IL-6, and IL-8 through suppression of ROS in HaCaT cells [31]. P also downregulates gene expression of IL-1 β in human osteoarthritis chondrocytes [35]. Also, IL-1 β -mediated expression of *Cox-2* gene and protein was abrogated. In a similar manner, there are studies showing anti-inflammatory activities of Q10, supporting our findings here on the impact of Q10 on CP-mediated inflammation. Q10 has been demonstrated to mediate its antiapoptotic and anti-inflammatory activities, via redox-dependent mechanisms. For instance, it has been shown that Q10 supplementation causes reduction in plasma levels of IL-6, *TNF- α* , and C-reactive protein (CRP) [36].

5. Conclusion

Our findings shows that Q10 and/or P induced suppression of ROS generation mediated by CP. We also found that Q10 and P suppressed CP-induced inflammation by inhibiting gene expression-specific inflammatory cytokine. This anti-inflammatory role of Q10 and P is likely linked to their antioxidant mechanism. Findings from this study thus show that Q10 and P may have protective effect on oxidant and inflammatory side effects of CP.

Data Availability

The data generated or analyzed in this article are available without request.

Conflicts of Interest

The authors declare no conflicts of interest associated with this manuscript.

Authors' Contributions

Norah S. AL-Johani and Mohammed Al-Zharani performed cytotoxicity assays. Norah M. Alhoshani and Nada H. Aljarba prepared and conducted gene expression. Nora Alkeraishan and Saad Alkahtani assessed the oxidative stress and antioxidant enzymes.

Acknowledgments

This work was funded by the Researchers Supporting Project Number RSP-2021/26, King Saud University, Riyadh, Saudi Arabia, and Princess Nourah Bint Abdulrahman University Researchers Supporting Project Number PNURSP2022R62, Princess Nourah Bint Abdulrahman University, Riyadh, Saudi Arabia.

References

- [1] T. Nelius, T. Klatter, W. de Riese, A. Haynes, and S. Filleur, "Clinical outcome of patients with docetaxel-resistant hormone-refractory prostate cancer treated with second-line cyclophosphamide-based metronomic chemotherapy," *Medical Oncology*, vol. 27, no. 2, pp. 363–367, 2010.
- [2] H. Cai, C. Wang, S. Shukla, and N. F. Steinmetz, "Cowpea mosaic virus immunotherapy combined with cyclophosphamide reduces breast cancer tumor burden and inhibits lung metastasis," *Adv Sci (Weinh)*, vol. 6, no. 16, p. 1802281, 2019.
- [3] M. Toriyama, E. Tagaya, T. Yamamoto, M. Kondo, Y. Nagashima, and J. Tamaoki, "Lung cancer development in the patient with granulomatosis with polyangiitis during long term treatment with cyclophosphamide: first documented case," *Respirol Case Rep*, vol. 6, no. 2, article e00284, 2018.
- [4] S. Jnaneshwari, M. Hemshekhar, M. S. Santhosh et al., "Crocin, a dietary colorant, mitigates cyclophosphamide-induced organ toxicity by modulating antioxidant status and inflammatory cytokines," *The Journal of Pharmacy and Pharmacology*, vol. 65, no. 4, pp. 604–614, 2013.
- [5] Y. Temel, S. Kucukler, S. Yildirim, C. Caglayan, and F. M. Kandemir, "Protective effect of chrysin on cyclophosphamide-induced hepatotoxicity and nephrotoxicity via the inhibition of oxidative stress, inflammation, and apoptosis," *Naunyn-Schmiedeberg's Archives of Pharmacology*, vol. 393, no. 3, pp. 325–337, 2020.
- [6] Q. Khurshid, A. J. Dar, M. A. Mirza et al., "Rituximab and cyclophosphamide based regimens for treatment of Waldenstrom Macroglobulemia, lessons from clinical literature: a systemic review," *Blood*, vol. 136, Supplement 1, pp. 10-11, 2020.
- [7] G. R. Mahrous, N. S. Elkholy, G. Safwat, and M. W. Shafaa, "Enhanced cytotoxic activity of beta carotene conjugated liposomes towards breast cancer cell line: comparative studies with cyclophosphamide," *Anti-Cancer Drugs*, vol. 33, no. 1, pp. e462–e476, 2022.
- [8] A. M. Uttra, Alamgeer, M. Shahzad, A. Shabbir, and S. Jahan, "Ephedra gerardiana aqueous ethanolic extract and fractions attenuate Freund complete adjuvant induced arthritis in Sprague Dawley rats by downregulating PGE2, COX2, IL-1 β , IL-6, *TNF- α* , NF- κ B and upregulating IL-4 and IL-10," *Journal of Ethnopharmacology*, vol. 224, pp. 482–496, 2018.
- [9] S. Reuter, S. C. Gupta, M. M. Chaturvedi, and B. B. Aggarwal, "Oxidative stress, inflammation, and cancer: how are they linked?," *Free Radical Biology and Medicine*, vol. 49, no. 11, pp. 1603–1616, 2010.
- [10] A. Yusuf and A. Casey, "Surface modification of silver nanoparticle (AgNP) by liposomal encapsulation mitigates AgNP-induced inflammation," *Toxicology In Vitro*, vol. 61, article 104641, 2019.
- [11] B. M. Girard, B. P. Cheppudira, S. E. Malley, K. C. Schutz, V. May, and M. A. Vizzard, "Increased expression of interleukin-6 family members and receptors in urinary bladder with cyclophosphamide-induced bladder inflammation in female rats," *Frontiers in Neuroscience*, vol. 5, p. 20, 2011.
- [12] F. Moschella, M. Valentini, E. Aricò et al., "Unraveling cancer chemoimmunotherapy mechanisms by gene and protein expression profiling of responses to cyclophosphamide," *Cancer Research*, vol. 71, no. 10, pp. 3528–3539, 2011.
- [13] V. P. Viswanadha, V. Dhivya, N. M. Beeraka et al., "The protective effect of piperine against isoproterenol-induced

Retraction

Retracted: Betamethasone Dipropionate Derivatization, Biotransformation, Molecular Docking, and ADME Analysis as Glucocorticoid Receptor

BioMed Research International

Received 8 January 2024; Accepted 8 January 2024; Published 9 January 2024

Copyright © 2024 BioMed Research International. This is an open access article distributed under the Creative Commons Attribution License, which permits unrestricted use, distribution, and reproduction in any medium, provided the original work is properly cited.

This article has been retracted by Hindawi following an investigation undertaken by the publisher [1]. This investigation has uncovered evidence of one or more of the following indicators of systematic manipulation of the publication process:

- (1) Discrepancies in scope
- (2) Discrepancies in the description of the research reported
- (3) Discrepancies between the availability of data and the research described
- (4) Inappropriate citations
- (5) Incoherent, meaningless and/or irrelevant content included in the article
- (6) Manipulated or compromised peer review

The presence of these indicators undermines our confidence in the integrity of the article's content and we cannot, therefore, vouch for its reliability. Please note that this notice is intended solely to alert readers that the content of this article is unreliable. We have not investigated whether authors were aware of or involved in the systematic manipulation of the publication process.

Wiley and Hindawi regrets that the usual quality checks did not identify these issues before publication and have since put additional measures in place to safeguard research integrity.

We wish to credit our own Research Integrity and Research Publishing teams and anonymous and named external researchers and research integrity experts for contributing to this investigation.

The corresponding author, as the representative of all authors, has been given the opportunity to register their agreement or disagreement to this retraction. We have kept a record of any response received.

References

- [1] S. Rashid, S. Anjum, A. Ahmad et al., "Betamethasone Dipropionate Derivatization, Biotransformation, Molecular Docking, and ADME Analysis as Glucocorticoid Receptor," *BioMed Research International*, vol. 2022, Article ID 6865472, 9 pages, 2022.

Research Article

Betamethasone Dipropionate Derivatization, Biotransformation, Molecular Docking, and ADME Analysis as Glucocorticoid Receptor

Sana Rashid ¹, Shazia Anjum ^{1,2}, Aqeel Ahmad ³, Raziya Nadeem ⁴,
Maqsood Ahmed ⁵, Syed Adnan Ali Shah ^{6,7}, Muhammad Abdullah ⁸, Komal Zia ⁹,
and Zaheer Ul-haq ⁹

¹Institute of Chemistry, The Islamia University of Bahawalpur, Bahawalpur 63100, Pakistan

²H.E.J. Research Institute of Chemistry, International Center for Chemical and Biological Sciences, University of Karachi, Karachi 75270, Pakistan

³University of Chinese Academy of Science (UCAS), Beijing, China

⁴Department of Chemistry, University of Agriculture, Faisalabad, Pakistan

⁵Material Chemistry Lab, Institute of Chemistry, The Islamia University of Bahawalpur, Bahawalpur 63100, Pakistan

⁶Faculty of Pharmacy, Atta-ur-Rahman Institute for Natural Products Discovery, Universiti Teknologi MARA, Cawangan Selangor Kampus Puncak Alam, 42300 Bandar Puncak Alam, Selangor D. E, Malaysia

⁷Atta-ur-Rahman Institute for Natural Product Discovery (AuRIns), Universiti Teknologi MARA Cawangan Selangor Kampus Puncak Alam, 2300 Bandar Puncak Alam, Selangor, Malaysia

⁸Cholistan Institute of Desert Studies, The Islamia University of Bahawalpur, Bahawalpur 63100, Pakistan

⁹Dr. Panjwani Center for Molecular Medicine and Drug Research, International Center for Chemical and Biological Sciences, University of Karachi, Karachi 75270, Pakistan

Correspondence should be addressed to Shazia Anjum; shazia.anjum@iub.edu.pk and Aqeel Ahmad; aqeel@igsnr.ac.cn

Received 25 April 2022; Accepted 14 June 2022; Published 6 July 2022

Academic Editor: Dr Muhammad Hamid

Copyright © 2022 Sana Rashid et al. This is an open access article distributed under the Creative Commons Attribution License, which permits unrestricted use, distribution, and reproduction in any medium, provided the original work is properly cited.

Betamethasone is an important glucocorticoids (GCs), frequently used to cure allergies (such as asthma and angioedema), Crohn's disease, skin diseases (such as dermatitis and psoriasis), systemic lupus erythematosus, rheumatic disorders, and leukemia. Present investigation deals to find potential agonist of glucocorticoid receptors after biotransformation of betamethasone dipropionate (1) and to carry out the molecular docking and ADME analyses. Biotransformation of 1 was carried out with *Launaea capitata* (dandy) roots and *Musa acuminata* (banana) leaves. *M. acuminata* furnished low-cost value-added products such as Sananone dipropionate (2) in 5% yields. Further, biocatalysis of Sananone dipropionate (2) with *M. acuminata* gave Sananone propionate (3) and Sananone (4) in 12% and 7% yields, respectively. However, Sananone (4) was obtained in 37% yields from *Launaea capitata*. Compound 5 was obtained in 11% yield after β -elimination of propionic acid at C-17 during oxidation of compound 1. The structure elucidation of new compounds 2-5 was accomplished through combined use of X-ray diffraction and NMR (1D and 2D) studies. In addition to this, molecular docking and ADME analyses of all transformed products of 1 were also done. Compounds 1-5 showed -12.53 to -10.11 kcal/mol potential binding affinity with glucocorticoid receptor (GR) and good ADME profile. Moreover, all the compounds showed good oral bioavailability with the octanol/water partition coefficient in the range of 2.23 to 3.65, which indicated that compounds 1-5 were in significant agreement with the given criteria to be considered as drug-like.

1. Introduction

Glucocorticoids (GCs), a group of steroid hormones, regulate various metabolic and homeostatic functions including growth, apoptosis, developmental behavior, and inflammation that are necessary for life [1]. GCs are one of the most frequently prescribed medications worldwide. They mediate their signals by specific receptor protein, namely, glucocorticoid receptor (GR). The GR is a transcription factor classified within the nuclear receptor (NR) superfamily and consists of three conserved domains: an N-terminal transactivation domain, a central DNA-binding domain (DBD), and a C-terminal ligand-binding domain (LBD) [2]. Prednisolone, dexamethasone, and corticosteroid analogs are used to treat diverse medical conditions associated with GR. However, these medications are associated with a number of side effects [3, 4]. Thus, identification of potential ligands against GR, which may decrease the off-target effects, is of great interest.

The breadth of biocatalyzed reactions covers the syntheses of myriad of compounds that otherwise possess major challenges in organic syntheses. Biocatalysis proves a low-cost chemical process that is environmentally friendly as well. It avoids high temperature, use of organic solvents, and toxic chemicals to achieve target compounds. However, in present era, there has been rising demand for safer chemical methods that furnish diversity of compounds. Consequently, biocatalytic methods that are alternate of historical chemical processes provide surety about green environment and decrease the cost of final products [5]. Biotransformation is replacement of toxic chemicals by the enzymatic ability of an organism that can lead towards variety of reactions at inactivated position [6].

Several interesting biotransformations of small molecules using different fruits and vegetables have reported in literature [7–10] but no such method is reported for the steroidal compounds. Steroidal compounds have large assortment in clinical applications with diversified functions—they are second biggest class of present-day drugs [11]. Steroidal compounds are captivating substrates for biotransformations because of their inactivated carbons and immense biological activities that make chemical alterations complex. The most common class of steroids is glucocorticoids that comprise betamethasone, methylprednisolone, dexamethasone, and prednisolone. Betamethasone dipropionate is a synthetic glucocorticoid and widely used for the skin problems [12]. Bioconversion or biotransformation of steroids by microorganisms can be a single reaction or tandem reactions [13]. Hydroxylation of steroids has been done using bacteria and fungi [14].

Therefore, present study deals with biocatalyzed transformation of relatively bigger molecules such as betamethasone dipropionate (1) and its derivative (2). *Musa acuminata* (banana) leaves and *Launaea capitata* roots were used to get low-cost value-added products of betamethasone. To best of our knowledge, this is the first study of using plants for the biotransformation of tetracyclic steroidal skeleton and herein molecular docking studies were also carried out using GR crystal structure to determine the potency of

all the biotransformed products of betamethasone dipropionate as potential drug.

2. Materials and Methods

2.1. General Experimental Procedures. IR spectra were measured using Bruker Tensor 27 FT-IR spectrometer and Agilent Technologies FTIR-ATR. NMR spectra were obtained on a Bruker-AM-500 spectrometer. X-ray diffraction technique was done with Bruker D8 Venture diffractometer having PHOTON II detector. The Thermo Scientific Vanquish Horizon UHPLC was linked to LCMS (Thermo Scientific Orbitrap FusionTM TribridTM) to get the mass spectra. The UHPLC-LCMS elution was done using gradient of 0.1% formic acid in H₂O (A) and 0.1% formic acid in acetonitrile. All compounds were purified through column chromatography using silica gel (200–400 mesh, Sigma Aldrich). Thin-layer chromatography (TLC) was carried on Silica Gel (60 F₂₅₄) Alumina sheets from Merck.

Betamethasone dipropionate was obtained from Lahore Drug Testing Laboratory as a generous gift, while fresh *M. acuminata* (banana) leaves and roots of *L. capitata* were collected from Cholistan Institute of Desert Studies, The Islamia University of Bahawalpur and identified by a taxonomist, Dr. Muhammad Abdullah. Crystallographic data for compounds 2, 3, and 5 have been deposited with the Cambridge Crystallographic Data Centre as the supplementary publication no. 2072132, 2072126, and 2072133, respectively. Copies of the data can be obtained, free of charge, on application to CCDC, 12 Union Road, Cambridge CB2 1EZ, UK (fax: +44-1223-336033; -mail: deposit@ccdc.cam.ac.uk).

2.2. Biotransformation of 1 and 2. The fresh plant material (*M. acuminata* leaves and *L. capitata* roots) was thoroughly washed with distilled water and dried at room temperature. The leaves were cut into approximately 1 cm² pieces. Consequently, the leaves (25 g) were transferred to the conical flask containing 150 ml of 0.2 M phosphate buffer (pH 7.0); and then, the solution of substrates (100 mg) in 2 ml of MeOH was added into the reaction flask. The reaction mixture was placed on orbital shaker (500 rpm) at room temperature (35°C) for 72 h. Parallel control experiments were conducted which included leaves, 0.2 M phosphate buffer, and MeOH without samples 1 and 2. The reaction products were obtained by simple filtration of reaction mixture, followed by extraction with ethyl acetate (3 × 150 ml). The combined organic extracts were dried at room temperature. The crude reaction mixture was separated by silica gel column chromatography eluting with a Hexane-EtOAc gradient to afford compounds 2-4.

2.3. Spectral Data. *Sananone dipropionate* (2): white crystals or greenish crystalline solid. IR (KBr, cm⁻¹): 3019, 2366, 1732, 1635, 1214, and 741. ¹H-NMR (500 MHz, CDCl₃): Table 1 and ¹³C-NMR (125 MHz, CDCl₃): Table 1.

Sananone propionate (3): white solid. ¹H-NMR (500 MHz, CDCl₃): Table 1 and ¹³C-NMR (125 MHz, CDCl₃): Table 1

TABLE 1: The ^1H NMR (500 MHz) and ^{13}C NMR (125 MHz) data of compounds 2–5.

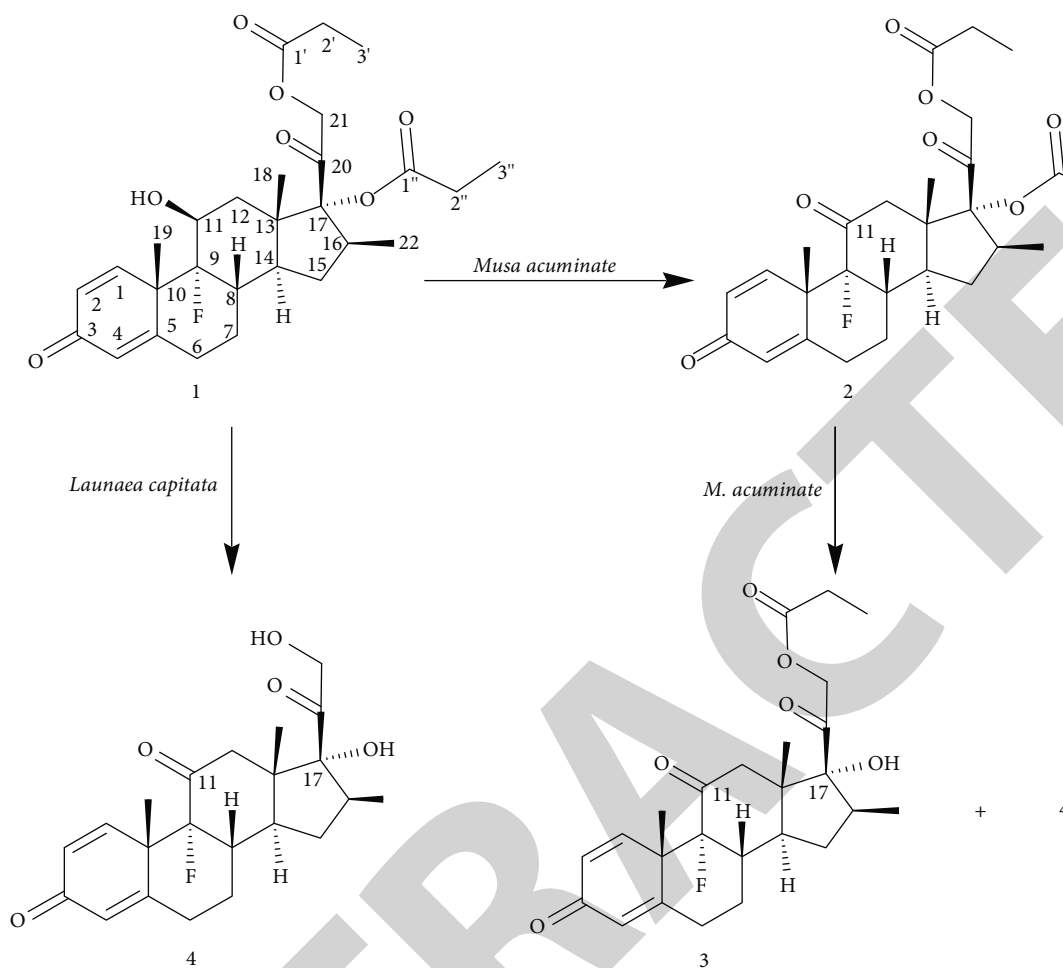
No.	δ_H (mult., J in Hz)	δ_C , type	δ_H (mult., J in Hz)	δ_C , type	δ_H (mult., J in Hz)	δ_C , type	δ_H (mult., J in Hz)	δ , type
1	7.43 d (16.4)	151.2 CH	7.56 m	153.3 CH	7.54 d (10.3)	153.0 CH	7.51 d (10.3)	151.6 CH
2	6.32 d (16.5)	129.8 CH	6.25 dd (2.0, 10.3)	128.4 CH	6.26 dd (2.0, 7.6)	128.5 CH	6.30 d (10.3)	129.6 CH
3		186.0 CO		186.0 CO		187.0 CO		186.0 CO
4	6.19 s	126.7 CH	6.18 s	125.2 CH	6.18 s	125.2 CH	6.18 s	126.8 CH
5		162.7 C		166.6 C		166.6 C		162.7 C
6	2.48 m 1.92 m	34.7 CH ₂	2.31 m 2.27 m	37.9 CH ₂	2.01 m	46.7 CH	2.61 m 2.51 m	31.3 CH ₂
7	2.02 m 1.21 m	28.2 CH ₂	2.00 m 1.70 m	29.5 CH ₂	2.03 m 1.68 m	26.9 CH	1.86 m 1.74 m	24.8 CH ₂
8	2.30 m	51.0 CH	2.60 m	42.5 CH	2.62 m	42.6 CH	2.40 m	47.4 CH
9		99.6 (J = 183.2 Hz, CF)		100.2 (J = 182.4 Hz, CF)		100.2 (J = 183.2 Hz, CF)		98.8 (J = 183.6 Hz, CF)
10		46.2 C		-		38.0 C		46.3 C
11		204.1 (J = 27 Hz, CO)		205.9 (J = 26.9 Hz, CO)		205.9 (J = 27.1 Hz, CO)		204.1 (J = 27.4 Hz, CO)
12	2.63 d (11.9) 2.33 m	47.4 CH ₂	-	-	2.74 td (5.0, 10.0, 20.0) 2.50 d (19.5)	67.8 CH ₂	3.03 d (0.9) 2.81 m	50.7 CH ₂
13		38.2 C	-	-		37.9 C	-	35.5 C
14	1.73 m	43.9 CH	1.27 m	-	1.30 m	52.0 CH	1.27 m	-
15	0.87 m	21.5 CH ₂	0.9 m	-	2.15 m 1.23 m	33.7 CH ₂	2.33 m	37.7 CH ₂
16	3.43 m	47.2 CH	-	-	2.31 m	46.8 CH	-	142.9 C
17		93.6 C		87.3 C		87.3 C	-	153.5 C
18	0.77 s	14.7 CH ₃	0.88 s	14.2 CH ₃	0.91 s	14.5 CH ₃	0.99 s	17.2 CH ₃
19	1.26 s	31.9 CH ₃	1.59 s	20.6 CH ₃	1.59 s	20.6 CH ₃	1.54 s	21.4 CH ₃
20		198.3 CO		205.9 CO		211.5 CO		192.2 CO
21	4.74 d (16.4) 4.36 d (16.5)	67.6 CH ₂	4.96 m 4.92 m	69.2 CH ₂	4.50 d (19.5) 4.38 d (19.5)	87.3 CH ₂	4.96 d (16.0) 4.92 d (25.5)	68.2 CH ₂
22	1.36 d (7.3)	19.0 CH ₃	1.11 d (7.4)	18.3 CH ₃	1.12 d (7.3)	18.4 CH ₃	2.14 s	19.1 CH ₃
1'		174.6 CO		173.9 CO				174.0 CO
2'	2.47 q (11.4)	27.0 CH ₂	2.47 m	26.6 CH ₂			2.50 q (15.1)	27.1 CH ₂
3'	1.20 m	8.86 CH ₃	1.18 t (10.0)	8.0 CH ₃			1.20 t (9.8)	10.8 CH ₃
1''		173.9 CO						
2''	2.47 q (11.4)	27.0 CH ₂						
3''	1.20 m	8.86 CH ₃						

Sananone (4): white crystals or white solid. IR (cm⁻¹): 3504,3260,1722,1707, 1660, 1599, 1066, and 899. ^1H -NMR (500 MHz, CDCl₃): Table 1 and ^{13}C -NMR (125 MHz, CDCl₃): Table 1

Sana-16,17-enone propionate (5): white crystals or solid. IR (cm⁻¹): 1725, 1743, 1658, 1625, 1602, and 886. ^1H -NMR (500 MHz, CDCl₃): Table 1 and ^{13}C -NMR (125 MHz, CDCl₃): Table 1

2.4. Molecular Docking. In the present study, molecular docking studies were carried out for the biotransformed products

of betamethasone dipropionate using the crystal structure of glucocorticoid receptor (GR). All the compounds were sketched in ChemBioDraw Ultra 14.0 [15]. Compounds were further corrected and protonated using Structure Preparation module of MOE v.2019. Crystal structure of GR in complex with dexamethasone, an agonist and a coactivator motif derived from the transcriptional intermediary factor 2, was retrieved from Protein Data Bank under the accession code 1M2Z [16]. All the water molecules were deleted since; no conserved water molecules were reported. The crystal structure was subjected to geometry correction using structure



SCHEME 1: Biotransformation of compounds 1 and 2.

preparation module of MOE v.2019. Further hydrogens were placed, and ionization states were assigned followed by energy minimization using Amber10: EHT force field. Atomic coordinates of cognate ligand were selected to define the docking grid, and all the biotransformed products of betamethasone dipropionate were docked into the define grid using Induce Fit protocol. The docked poses were placed using Triangular Matcher placement method while the resulting poses were scored using London dG and GBVI/WSA dG as scoring and rescoring functions, respectively. Highest ranked poses were visually analyzed using the Chimera software [17].

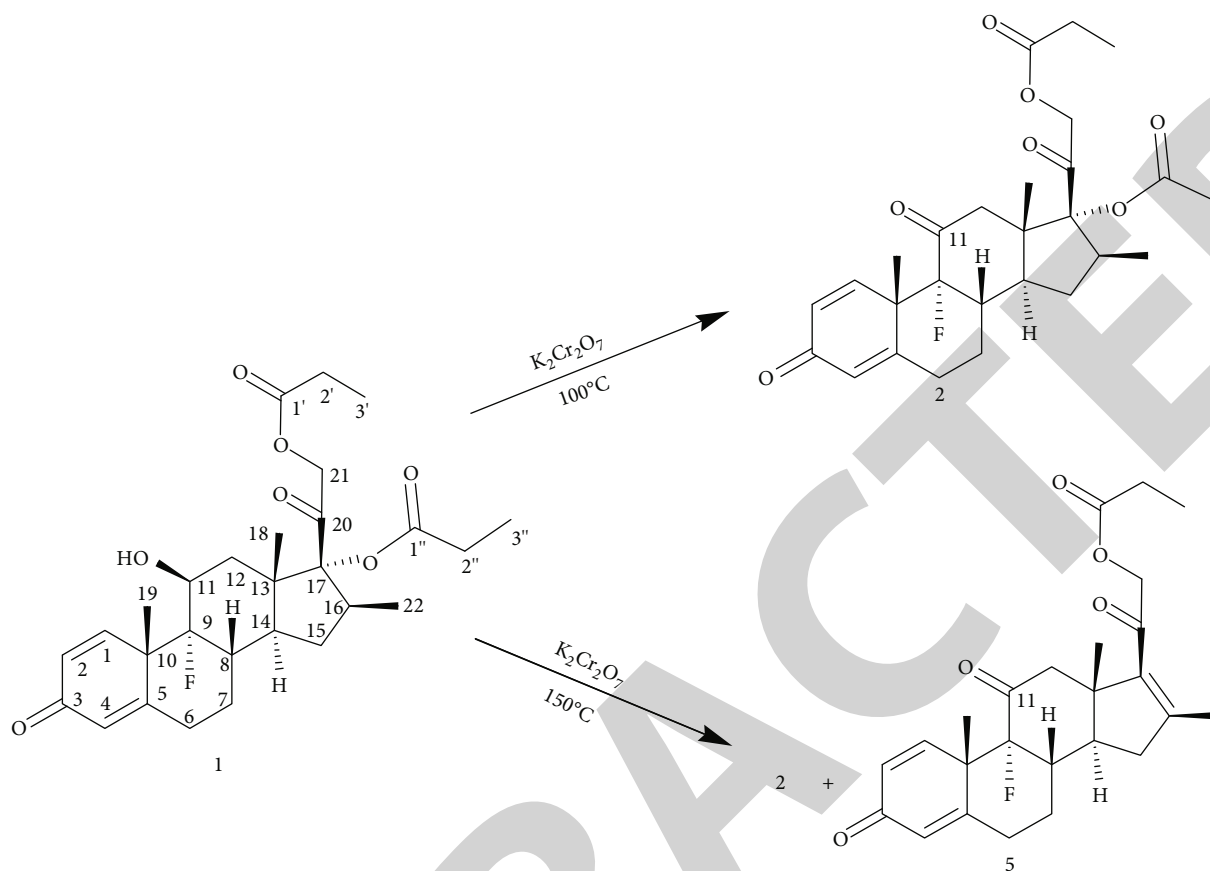
2.5. In Silico ADME Analysis. For the assessment of physico-chemical, pharmacokinetics, drug-likeness, and medicinal chemistry friendliness properties of biotransformed products of betamethasone dipropionate, SwissADME (<http://www.swissadme.ch/>), an online webserver, was used. SMILES notation of all the compounds was subjected to submission webpage of SwissADME for the estimation of afore-said properties.

3. Results and Discussion

Present study is one of its own kind in which medicinally important betamethasone dipropionate (1) was subjected

to biocatalyzed transformation using *Musa acuminata* (banana) leaves to get low cost and value-added products 2-4 (Scheme 1). The structure conformity of oxidized product 2 was also done through its chemical synthesis (Scheme 2) using $K_2Cr_2O_7$ in equimolar ratio as per standard procedure in good yields (69%). However, compound 5 was obtained in 11% yield after β -elimination of propionic acid at C-17 during oxidation of compound 1 using 2.0 equivalents of $K_2Cr_2O_7$ along with desired compound 2 in 56% yields (Scheme 2).

M. acuminata treated biotransformation of betamethasone dipropionate (1) resulted oxidized product Sananone dipropionate (2) in 5% yields. Compound 2 was again biotransformed with *M. acuminata* that led the formation of Sananone propionate (3) in 12% with respect to starting material along with a hydrolyzed and oxidized compound, Sananone 4 in 7% yield. Compound 3 was obtained with compound 4 in 3:1 ratios in the 1H -NMR. Interestingly, compound 4 was also obtained from betamethasone dipropionate (1) after biotransformation with *Launaea capitata* roots in 37% yield (Scheme 1). The structures of new biotransformed compounds 2-4 and a synthetic compound 5 were established by combined use of IR and NMR (1D and 2D) and finally confirmed through X-ray diffraction studies.



SCHEME 2: Synthetic oxidation of compound 1.

Sananone dipropionate (2) was obtained in the form of white crystalline solid. Its molecular formula was determined by LC-MS m/z 503.2453 [$M^+ + 1$] as $C_{28}H_{35}FO_7$ (Supplemental Figure S1). In IR spectrum, a stretching at 1732 cm^{-1} indicated the oxidation of C-11 hydroxyl group (Supplemental Figure S2). The ^{13}C -NMR spectrum exhibited 05 methyls, 07 methylenes, 06 methines, and 10 quaternary carbons (Supplemental Figure S4). There were characteristic peaks of five carbonyl carbons, suggesting that OH group attached to C-11 in compound 1 was oxidized into keto group that appeared as a doublet at δ_C 204.1 ($J = 27\text{ Hz}$) due to ^{13}C -F coupling (Table 1). The two geminal proton doublets at δ_H 2.63 (1H, d, $J = 11.9\text{ Hz}$) and a multiplet at δ_H 2.33 (1H, m) were linked to C-11 (carbonyl group) in HMBC (Supplemental Figure S6). The COSY spectrum showed six isolated spin systems in the respective compound (Supplemental Figure S7). The rest of the skeleton remained intact (Table 1) as the absolute structures of Sananone dipropionate (2) were confirmed by its single-crystal X-ray diffraction studies (Supplemental Table S1).

Sananone propionate (3) was isolated as white solid. The molecular formula was determined by LC-MS m/z 447.2187 [$M^+ + 1$] as $C_{25}H_{31}FO_6$ (Supplemental Figure S8). The IR spectrum showed a stretching at 1730 cm^{-1} for C=O group and a broad peak $3190\text{--}3400\text{ cm}^{-1}$ for -OH group (Supplemental Figure S9). All of the spectral features were

similar to compound 2 except for the absence of one ethyl group as one propionate group was hydrolyzed, as indicated by LC-MS analysis. Further, the ^{13}C -NMR spectrum revealed the presence of 04 methyls (CH_3), 06 methylenes (CH_2), 06 methines (CH), and 9 quaternary carbon (C) signals (Supplemental Figure S10). The COSY spectrum also showed four isolated spin systems in the respective compound (Supplemental Figure S13). These information suggested that in biotransformed compound, Sananone propionate (3) has only one propionate group and rest of the Sananone dipropionate (2) skeleton remained intact (Table 1).

Sananone (4) was obtained as a white solid and later crystallized into a white crystalline form. Its molecular formula was determined by LC-MS m/z 390.1919 as $C_{22}H_{27}FO_5$ (Supplemental Figure S14). In IR spectrum, a stretching at 1722 cm^{-1} indicated the oxidation of C-11 hydroxyl group. Two stretching at 3504 and 3260 cm^{-1} indicated the presence of hydroxyl group (Supplemental Figure S15). In the ^1H -NMR spectrum of the compound, absence of two ethyl groups in the side chain revealed the presence of completely hydrolyzed product (Supplemental Figure S16). The presence of -OH group at C-21 and C-17 was also confirmed through a broad stretching band of $3504\text{--}3260\text{ cm}^{-1}$ in the IR spectrum. There appeared the same sort of three deshielded protons in the ^1H -NMR as of compound 2. The ^{13}C -NMR spectrum revealed three

TABLE 2: In silico ADME assessment and binding affinities of biotransformed products of betamethasone dipropionate.

Compounds	Binding affinity kcal/mol	Mol. weight g/mol	HBA	HBD	TPSA Å ²	Log P	GI absorption	BBB	P-gp substrate	Lipinski violations
1	-10.94	504.59	8	1	106.97	3.36	High	No	Yes	1
2	-10.11	502.57	8	8	103.81	3.11	High	No	Yes	1
3	-11.16	444.49	7	1	97.74	2.64	High	No	Yes	0
4	-12.53	390.45	6	2	91.67	2.23	High	No	Yes	0
5	-11.37	372.43	5	1	71.44	3.65	High	Yes	Yes	0

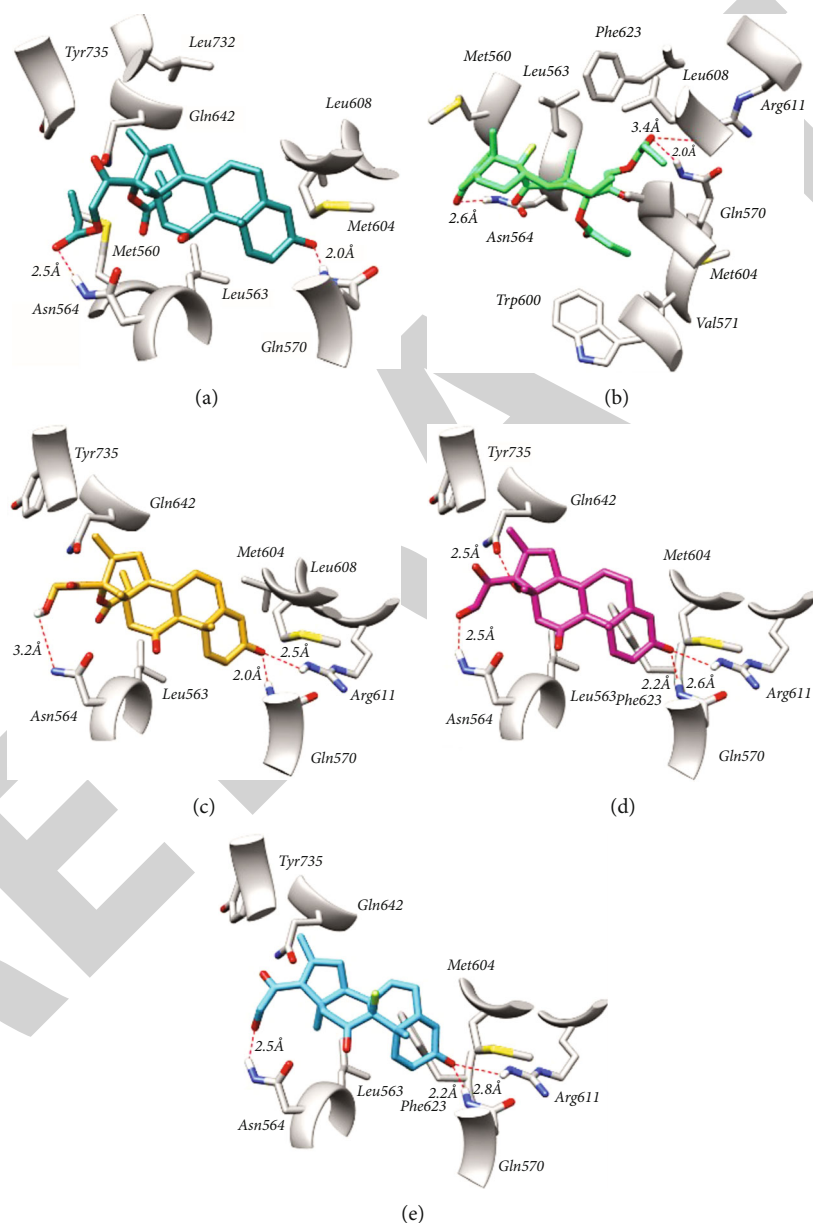


FIGURE 1: Binding pose of (a) betamethasone dipropionate (1), its biotransformed products (b) 2, (c) 3, and (d) 4, and (e) synthetic derivative 5 in the ligand binding domain of glucocorticoid receptor (PDB 1M2Z).

methyls (CH₃), five methylenes (CH₂), six methines (CH), and eight quaternary carbon signals (C) (Supplemental Figure S17). The COSY spectrum showed four isolated

spin systems in the respective compound (Supplemental Figure S20). All ID and 2D NMR spectral information supported complete hydrolysis of starting material 2.

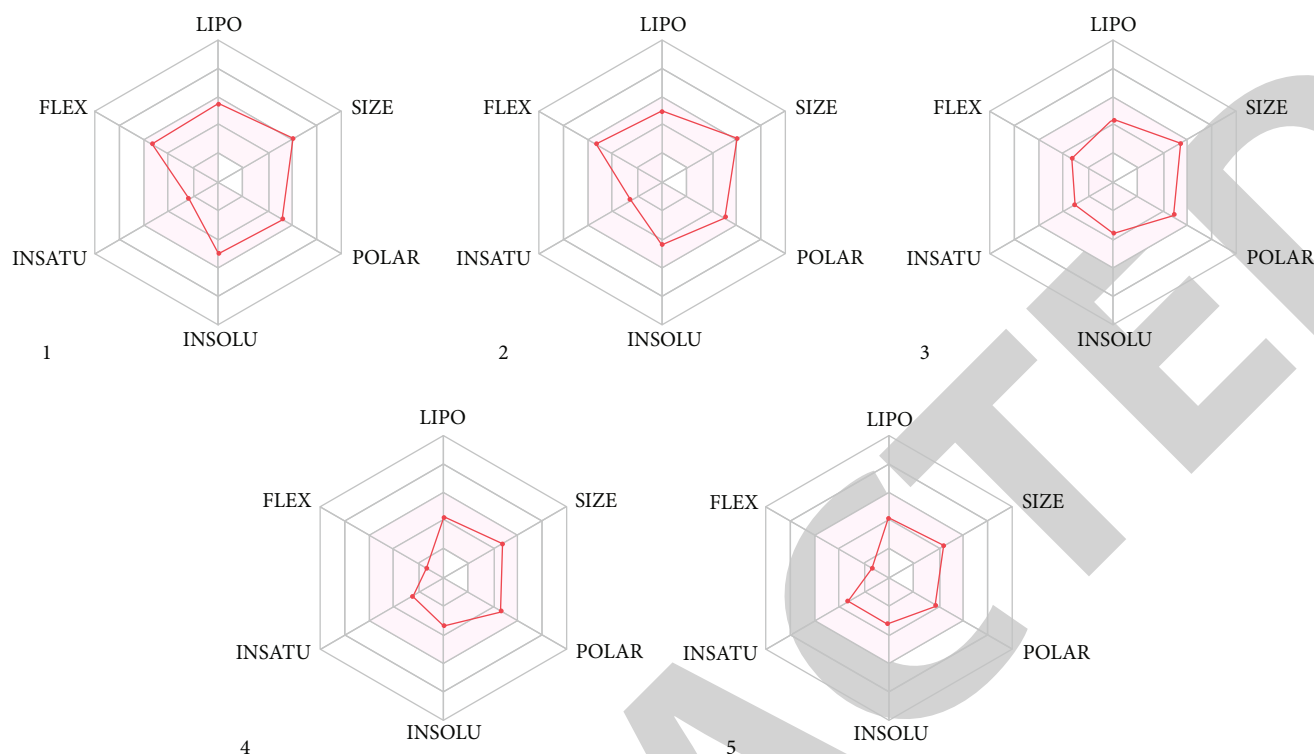


FIGURE 2: Oral bioavailability radar of betamethasone dipropionate (1), its biotransformed products 2, 3, and 4, and synthetic derivative 5. The pink area represents the optimal range for six physicochemical properties.

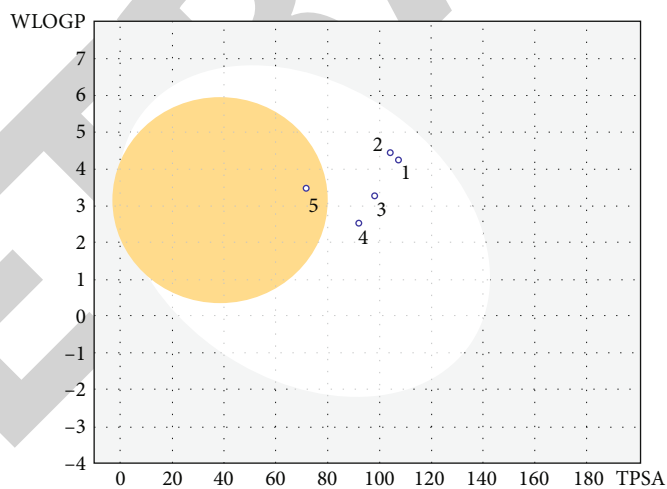


FIGURE 3: The boiled-egg model of betamethasone dipropionate (1), its biotransformed products 2, 3, and 4, and synthetic derivative 5. Yellow egg's yolk like and white region represent the optimal area for blood brain permeation and gastrointestinal absorption, respectively.

Finally, the absolute structure of compound 4 was also determined through XRD (Supplemental Table S2).

Sana-16,17-enone propionate (5) is a synthetic product that was formed during oxidation of betamethasone dipropionate (1). Its molecular formula was determined by LC-MS m/z 428.2078 as $C_{25}H_{29}FO_5$ (Supplemental Figure S21). In IR spectrum, a stretching at 1725 cm^{-1} indicated the oxidation of C-11 hydroxyl group and a single stretching at 1743 cm^{-1} indicated the presence of single propionate group (Supplemental Figure S22). The $^1\text{H-NMR}$

(Supplemental Figure S23) and $^{13}\text{C-NMR}$ spectra (Supplemental Figure S24) of the compound 5 were very much similar to parent compound 2. The only difference observed was the presence of a singlet of three protons at δ 2.14 indicated that methyl group attached to C-16 (δ_C 142.9) that indicated the β -elimination of propionic acid compound to form a double bond between C-16 and C-17 (Table 1). The $^{13}\text{C-NMR}$ data revealed that there were 04 methyls, 06 methylenes, 05 methines, and 10 quaternary carbon atoms (Table 1). In 2D-NMR, COSY relationships

showed five spin systems in the respective compound (Supplemental Figure S28). Finally, the absolute structure of compound 5 was determined through XRD (Supplemental Table S3).

3.1. Molecular Docking. All compounds 1-5 reside well in the ligand binding domain of GR with the binding affinity in the range of -12.53 to -10.11 kcal/mol (Table 2). The docked pose of compound 1 demonstrated a number of significant noncovalent interactions in the LBD of GR (Figure 1(a)). Carbonyl group at C-3 establishes a hydrogen bond with Gln570 while hydroxyl group at C-11 mediates hydrogen bond contact with Asn564. Similarly, methyl groups of compound 1 observed to mediate significant alkyl-alkyl and π -alkyl interactions with Met560, Leu563, Met604, Leu608, Gln642, Leu732, Tyr735, and Thr739. Compound 2 showed different pose in the LBD of GR in comparison of other compounds (Figure 1(b)). Carbonyl group at C-3 establishes a hydrogen bond Asn564 while carbonyl group of ester mediates hydrogen bonds with Gln570 and Arg611. Further, anchorage was provided by significant hydrophobic interactions with the crucial residues of LBD of GR including, Met560, Leu563, Val571, Trp600, Met604, Ala605, Leu608, and Phe623. Similarly, the docked pose of compound 3 demonstrated the three hydrogen bonds and a network of hydrophobic interactions in the LBD of GR (Figure 1(c)). Terminal hydroxyl group mediates hydrogen bond with Asn564 while carbonyl at C-3 mediates hydrogen bonds with Gln570 and Arg611. Moreover, few hydrophobic interactions were also observed with Leu563, Met604, Leu608, Gln642, and Tyr735. Likewise, the docked pose of compound 4 in the LBD of GR demonstrated a network of significant interactions with the highest binding affinity of -12.53 kcal/mol (Figure 1(d)). Both the hydroxyl groups of compound 4 establishes hydrogen bonds with Asn564 and Gln642 while carbonyl at C-3 establish two hydrogen bonds with Gln570 and Arg611. Moreover, substantial alkyl-alkyl interactions were observed with Leu563, Met604, Phe623, and Tyr735. Compound 5 also showed the similar type of interactions like compound 4 except a hydrogen bond with Gln642 was missing (Figure 1(e)). A hydrogen bond was observed between hydroxyl group and Asn564 while two hydrogen bonds were observed between carbonyl at C-3 and Gln570 and Arg611. Similarly, hydrophobic interactions were observed with Leu563, Met604, Phe623, and Tyr735. Taken together, the results demonstrated that all the biotransformed products of betamethasone dipropionate accommodated well in the ligand binding domain of GR which pronounce the potencies of these compounds.

3.2. ADME Analysis. Many potential compounds fail in late stage of drug development process because of poor pharmacokinetics and toxicity. In earlier process of drug discovery, computational predictions of pharmacokinetics and toxicity of compounds are alternatives to experimental techniques to reduce the last-stage failure of drug development process. Therefore, *in silico* assessment of physicochemical, pharmacokinetics, drug-likeness, and medicinal chemistry friendliness properties of betamethasone dipropionate analogs was

achieved by SwissADME, and obtained values are summarized in Table 2. Bioavailability radar was plotted for prediction of oral bioavailability which presents the six physicochemical properties including lipophilicity, size, polarity, solubility, flexibility, and saturation. It was evident from Figure 2 all the compounds displayed physicochemical properties in the acceptable range. Similarly, for the predictions of human gastrointestinal (GI) absorption, blood brain permeation, and permeability of p-glycoprotein, boiled-egg model was generated (Figure 3). All the compounds showed high GI absorption and permeability of p-glycoprotein while only compound 5 showed blood brain permeation.

4. Conclusion

Present study dealt with plant-based biocatalyzed transformation of relatively bigger molecules for the first time. *M. acuminata* leaves transformed betamethasone dipropionate (1) into an oxidized compound Sananone dipropionate (2) that further transformed to furnish completely hydrolyzed compounds Sananone propionate (3) and a Sananone (4). In addition to this, *L. capitata* roots reacted with compound 1 to exclusively yield compound 4. The structures of all new biotransformed compounds 2-4 and a synthetic compound, Sana-16,17-enone propionate (5), were determined through combined use of IR, NMR (1D and 2D), and X-ray diffraction studies. Further, molecular docking studies revealed that all the biotransformed compounds reside well in the ligand binding domain of glucocorticoid receptor. Taken together, betamethasone dipropionate analogs can be further optimized and developed as lead compounds against GR.

Data Availability

The Supplementary Information file has been deposited to the journal website.

Conflicts of Interest

The authors declare no conflict of interest.

Acknowledgments

One of us (Shazia Anjum) acknowledges the supporting role of the Higher Education Commission, Islamabad, Pakistan, under National Research Program for Universities grant nos. 3985 and 11786.

Supplementary Materials

Supplemental Figure S1: LC-MS analysis of compound 2. Supplemental Figure S2: IR spectrum of compound 2. Supplemental Figure S3: ^1H NMR spectrum of compound 2 (400 MHz, CD_3OD). Supplemental Figure S4: ^{13}C NMR of compound 2 (100 MHz, CD_3OD). Supplemental Figure S5: HSQC spectrum of compound 2 (CD_3OD). Supplemental Figure S6: HMBC spectrum of compound 2 (CD_3OD). Supplemental Figure S7: ^1H - ^1H COSY spectrum of 2 (CD_3OD). Supplemental Figure S8: LC-MS analysis of compound 3. Supplemental Figure S9: ^1H NMR spectrum of compound

Retraction

Retracted: Antidiabetic Effect of *Tamarindus indica* and *Momordica charantia* and Downregulation of TET-1 Gene Expression by Saroglitazar in Glucose Feed Adipocytes and Their Involvement in the Type 2 Diabetes-Associated Inflammation *In Vitro*

BioMed Research International

Received 8 January 2024; Accepted 8 January 2024; Published 9 January 2024

Copyright © 2024 BioMed Research International. This is an open access article distributed under the Creative Commons Attribution License, which permits unrestricted use, distribution, and reproduction in any medium, provided the original work is properly cited.

This article has been retracted by Hindawi following an investigation undertaken by the publisher [1]. This investigation has uncovered evidence of one or more of the following indicators of systematic manipulation of the publication process:

- (1) Discrepancies in scope
- (2) Discrepancies in the description of the research reported
- (3) Discrepancies between the availability of data and the research described
- (4) Inappropriate citations
- (5) Incoherent, meaningless and/or irrelevant content included in the article
- (6) Manipulated or compromised peer review

The presence of these indicators undermines our confidence in the integrity of the article's content and we cannot, therefore, vouch for its reliability. Please note that this notice is intended solely to alert readers that the content of this article is unreliable. We have not investigated whether authors were aware of or involved in the systematic manipulation of the publication process.

Wiley and Hindawi regrets that the usual quality checks did not identify these issues before publication and have since put additional measures in place to safeguard research integrity.

We wish to credit our own Research Integrity and Research Publishing teams and anonymous and named external researchers and research integrity experts for contributing to this investigation.

The corresponding author, as the representative of all authors, has been given the opportunity to register their agreement or disagreement to this retraction. We have kept a record of any response received.

References

- [1] M. Saxena, S. V. Prabhu, M. Mohseen et al., "Antidiabetic Effect of *Tamarindus indica* and *Momordica charantia* and Downregulation of TET-1 Gene Expression by Saroglitazar in Glucose Feed Adipocytes and Their Involvement in the Type 2 Diabetes-Associated Inflammation *In Vitro*," *BioMed Research International*, vol. 2022, Article ID 9565136, 10 pages, 2022.

Research Article

Antidiabetic Effect of *Tamarindus indica* and *Momordica charantia* and Downregulation of TET-1 Gene Expression by Saroglitazar in Glucose Feed Adipocytes and Their Involvement in the Type 2 Diabetes-Associated Inflammation *In Vitro*

Madhukar Saxena ^{1,2}, S. Venkatesa Prabhu,³ M. Mohseen ², Amit Kumar Pal,² Saud Alarifi,⁴ Neelam Gautam,⁵ and Hemalatha Palanivel ⁶

¹Department of Biotechnology, Babasaheb Bhimrao Ambedkar University, Lucknow 226025, India

²Department of Toxicology and Pharmacology, Institute for Industrial Research & Toxicology, UPSIDC, Ghaziabad 201302, India

³Center of Excellence for Bioprocess and Biotechnology, Department of Chemical Engineering, College of Biological and Chemical Engineering, Addis Ababa Science and Technology University, Addis Ababa, Ethiopia

⁴Department of Zoology, College of Science, King Saud University, PO Box 2455, Riyadh 11451, Saudi Arabia

⁵Department of Biological Sciences, Sungkyunkwan University, Jangan-Gu, Suwon, 16419 Gyeonggi-Do, Republic of Korea

⁶Center of Excellence for Bioprocess and Biotechnology, Department of Biotechnology, College of Biological and Chemical Engineering, Addis Ababa Science and Technology University, Addis Ababa, Ethiopia

Correspondence should be addressed to Hemalatha Palanivel; hemalatha.palanivel@aastu.edu.et

Received 10 May 2022; Accepted 26 May 2022; Published 4 July 2022

Academic Editor: Hafiz Ishfaq Ahmad

Copyright © 2022 Madhukar Saxena et al. This is an open access article distributed under the Creative Commons Attribution License, which permits unrestricted use, distribution, and reproduction in any medium, provided the original work is properly cited.

To date, there is no satisfactory and effective therapy available to cure type 2 diabetes mellitus (T2DM). This present work is focused on plant extracts and the effect of saroglitazar and TET genes on oxidative stress and inflammation in vitro adipocytes. Aqueous extracts of *Tamarindus indica* and *Momordica charantia* seed have shown potent antidiabetic activity that decreases glucose levels in diabetic adipocytes. After seven and fourteen days, the sugar level in the blood was significantly reduced when plant extracts were supplemented. Lipid profiles including total cholesterol (TC), triglyceride (TGL), high-density lipoprotein (HDL), low-density lipoprotein (LDL), and very low-density lipoprotein (VLDL) showed a highly significant change as expected in adipocytes treated with glucose compared with controlled adipocytes ($P < 0.001$). Gene expression of catalase, superoxide dismutase (SOD1, SOD2), and glutathione peroxidase (GPx) are changed twice, thrice, and quadruplet, respectively. The level of interleukin-1 (IL1) and tumor necrosis factor- α (TNF- α) was restored but the interleukin-6 (IL6) and ten-eleven-translocation-1 (TET1) were completely knocked down by the use of saroglitazar. In comparison with the diabetic group, this supplementation significantly increased glycogen content and glucose-6-phosphate dehydrogenase activity. In the extract supplemented group, glucose-6-phosphatase, glucose-oxidizing enzyme, and glucose-phosphorylating enzyme activities were significantly reduced. After seven days of extract supplementation, these parameters were not resettled to a controlled level; however, after 14 days of supplementation, all parameters were restored to the control level. In addition to altering gene expression, TET enzymes may contribute to altered adiposity and its metabolic consequences. The purpose of this study is to examine new ideas and approaches for treating obesity, T2DM, and other associated metabolic disorders.

1. Introduction

Diabetes especially type 2 diabetes mellitus (T2DM) is holding its position under five around the globe for decades and is a leading cause of death after cardiac disease and cancer. T2DM is a chronic metabolic and inflammatory state mainly related to obesity as well as increased oxidative stress. Obesity is nowadays represented to become a global health issue because it somehow becomes a cause of many chronic diseases and thereby also severely affecting expectancy of life and also suppressing quality of life [1]. As with the current lifestyle, adaptation leads to the stimulus of many metabolic disorders associated with lifestyles such as type 2 diabetes mellitus (T2DM), dyslipidemia, hyperuricemia, and nonalcoholic steatohepatitis (NASH) is becoming prevalent worldwide. It is very common in T2DM patients of showing a high level of dyslipidemia. T2DM is a disease due to alteration in the metabolism of carbohydrates or low levels of blood insulin [2]. In the present scenario of medicine, it is not possible to cure the onset of T2DM with a satisfactory and effective therapy or medicine. However, insulin therapy has many lacunae, like insulin resistance, anorexia nervosa, brain atrophy, and fatty liver after chronic therapy and treatment [3, 4]. Many studies that have been conducted previously have shown clearly that T2DM suffering individuals are likely to have a very high triglyceride ratio and a major characteristic to prove the condition of diabetic dyslipidemia is decreased level of high-density lipoprotein cholesterol (HDL) [5]. Due to such fluctuations in the level of lipid has been a kick start for severe chronic conditions as nonalcoholic fatty liver disease (NAFLD) that with itself has continued to deteriorate health conditions by starting much other liver affecting diseases as fatty liver (NAFL) to chronic fibrosis and cirrhosis and later causes NASH. Furthermore, many case studies have shown that severe and uncontrolled NASH will lead to an increase in the patients of cirrhosis and has been an alarming condition to perform liver transplantation to protect patients from hepatocellular carcinoma (HCC). Many models have been designed for future predictions of major setbacks of NAFLD as by analyzing many dynamic models, it is predicted that if it will be left untreated, then the current fatal conditions of end-stage liver disease by NAFLD will just be doubled and lead to an epidemic till 2030 [6]. Besides all this, great progress is observed in the clinical trials to reveal and identify many drivers involved in the initiation and pathogenesis of life-threatening such metabolic diseases and disorders. However, during such analysis, an exponential rise is reached in clinical trials that all are involved in a search of potential therapeutic targets and crucial targeted drugs for urgent medical needs and helpful approaches which do not meet appropriately. Many challenges came across and found unfulfilled medical needs that resulted in a condition where still no potent therapeutic drug or potential target can lead for approval or use and diseases remain untreated [6]. A survey conducted by World Health Organization (WHO) in the year 2016 showed some statistics that reveals some shocking results about the population, approximately 13% of people were obese and 39% of people were overweight in the survey. It has been suggested to do many lifestyle changes that involve focusing priority on physical

activity and daily intake of proper nutrition can become a major tool to manage and treat obesity. The major functional food having monounsaturated fatty acids (MUFAs) and polyunsaturated fatty acids (PUFAs) is the major risk for the development of obesity and T2DM-associated complications [7]. During research on the cause of NAFLD, one major name came in focus that is ten-eleven translocation (TET) methylcytosine dioxygenase protein that is a DNA cytosine oxygenase that is majorly involved in the catalysis of 5-methyl cytosine to produce a 5-hydroxymethylcytosine in a manner-dependent regulation that occurs on α -ketoglutarate and Fe^{2+} . However, herbal drugs generally showed nontoxic effects for the treatment against different diseases as reported from animal studies [8, 9], while it is not clear in humans whether herbal drugs are toxic or nontoxic [10]. Traditional medicine *Tamarindus indica* Linn. was used for the management of diabetes mellitus [11]. *Tamarindus indica* Linn. (Caesalpiniaceae family) is a tree-type dicotyledonous plant and it is widely available throughout India. *Momordica charantia* (bitter melon) *Momordica charantia* (Cucurbitaceae family) is one of the most common vegetables in the tropical region, particularly in India [12, 13]. It is supposed to be used as herbal medicine and has anti-inflammatory activity, antioxidant activity, antiviral activity, anticancer activity, antibacterial activity, and antidiabetic activity [14, 15]. Many studies have been conducted on TET-1 and its correlation with the oxidized derivatives that showed that it is known to regulate and affect many biological processes which are named tumorigenesis, gene transcription, and embryonic development. A missense mutation in TET-1 and TET-2 is in close association with the pathogenesis of NAFLD and T2DM [16].

Our goal is to analyze the chemical basis of the aqueous extracts of seeds from *Tamarindus indica* and *Momordica charantia* to determine whether these extracts are an effective treatment for insulin-dependent diabetes mellitus or type 1 diabetes mellitus (T1DM) and to identify the enzyme activities related to glucose levels altered by these extracts in adipocytes derived from Wharton's Jelly Mesenchymal Stem Cells. We also aimed to find the expression and close relation or effect of saroglitazar and TET genes on oxidative stress and inflammation on *in vitro* adipocytes concerning the used extracts.

2. Material and Method

2.1. Plant Material. Seeds of *Tamarindus indica* and *Momordica charantia* were collected from district Bulandshahr, Hapur, and Ghaziabad, and the material was identified by a taxonomist.

2.2. Preparation of Aqueous Extract of Seed of *Tamarindus indica* and *Momordica charantia*. We dried the seeds of *Momordica charantia* and *Tamarindus indica* in an incubator for two days at 40°C, ground them in an electric grinder, and then powdered them. In a Soxhlet apparatus, 50 g powder was extracted in 500 ml of distilled water for 18 h. Aqueous extracts were obtained. They were dried under reduced pressure and lyophilized.

2.3. Adipocytes and Saroglitazar Treatment. Wharton's Jelly Mesenchymal Stem Cells (Himedia) were cultured for 0-48 h in DMEM (Dulbecco's modified Eagle's medium)/Ham's F12 (1:1) media supplemented with 10% FCS (fetal calf serum) having antibiotics and normal glucose level (5 mM). The cell line proliferated in the medium containing DMEM/F-12 medium (1:1, v/v), HEPES, FBS/FCS, and antibiotics and upon the addition of insulin transferrin selenium (ITS), sodium bicarbonate, biotin, and pantothenate begin the differentiation phase. These cells were maintained and at ~7 days, abundant lipid droplets were accumulated in the cell which was checked by using lipophilic/fatty acid soluble dye, the Oil Red O staining. Cultured cells were then fixed in a 10% formaldehyde solution in PBS (phosphate buffer saline) for 5 min at RT (room temperature) followed by washing with 60% isopropanol. The cells were then stained with Oil Red O solution in 60% isopropanol for 10 min, then wash the cells with 10 ml water at least four times. Stained cells were then immediately viewed under phase contrast inverted microscope and images were captured using an inbuilt mounted digital camera. High glucose concentration (20 mM) was used to mimic the state of diabetes adipocytes and co-cultured cells were harvested for the treatment of saroglitazar (10 μ M) (ChemScene) for about 24 hours.

2.4. Induction of Diabetes Mellitus and Selection of Dose. 20 mM glucose is used to induce the diabetes model in adipocytes derived from Wharton's Jelly Mesenchymal Stem Cells (Himedia). Supplementation with *Tamarindus indica* and *Momordica charantia* was dose-dependently selected. Using this dose as a threshold dose, the experiment was continued. In all groups, the basal glucose level was measured before supplementation with *Tamarindus indica* and *Momordica charantia* extract.

2.5. Experimental Designs

- (i) Control group (7 days): Adipocytes derived from Wharton's Jelly Mesenchymal Stem Cells (Himedia) without any glucose treatment
- (ii) Diabetic group (7 days): Adipocytes derived from Wharton's Jelly Mesenchymal Stem Cells (Himedia) with 20 mM glucose treatment
- (iii) *Tamarindus indica* supplement group (7 days): Adipocytes derived from Wharton's Jelly Mesenchymal Stem Cells (Himedia) with 20 mM glucose and aqueous seed extract of *Tamarindus indica* at the dose of 80 mg/0.5 ml distilled water
- (iv) *Momordica charantia* supplement group (7 days): Adipocytes derived from Wharton's Jelly Mesenchymal Stem Cells (Himedia) with 20 mM glucose and aqueous seed extract of *Momordica charantia* at the dose of 100 mg/0.5 ml distilled water
- (v) *Tamarindus indica* supplement group (14 days): Adipocytes derived from Wharton's Jelly Mesenchymal Stem Cells (Himedia) with 20 mM glucose

and aqueous seed extract of *Tamarindus indica* at the dose of 80 mg/0.5 ml distilled water

- (vi) *Momordica charantia* supplement group (14 days): Adipocytes derived from Wharton's Jelly Mesenchymal Stem Cells (Himedia) with 20 mM glucose and aqueous seed extract of *Momordica charantia* at the dose of 100 mg/0.5 ml distilled water

On the 7th and 14th days of the experiment, all the wells of each group have been analyzed to perform the analysis.

2.6. Testing of Glucose Level. For all groups, we measured glucose load after seven days and 14 days of aqueous extract of seed of *Tamarindus indica* and *Momordica charantia* supplementation. A single-touch glucometer was used to measure glucose levels in the secretome collected from the wells [17]. Results are expressed in milligrams per deciliter of blood (mg/dl).

2.7. Biochemical Testing of Enzyme Activities and Glycogen Content

2.7.1. Assay of Glucose-6-Phosphate Dehydrogenase Activity. In accordance with [18] protocol, liver glucose-6-phosphate dehydrogenase activity was measured. This method uses the cell secretome. Assays were performed using 0.3 ml of 1 M Tris chloride buffer (pH 7.5), 0.3 ml of 2.5×10^{-2} M glucose-6-phosphate, 0.1 ml of 2×10^{-3} M NADP, 0.3 ml of 0.2 M $MgCl_2$, and 0.3 ml of secretome. At 340 nm, the rate of change in absorbency was measured. In enzyme activity, one unit is defined as the quantity that catalyzes the reduction of one micromolar amount of NADP per minute.

2.7.2. Assay of Glucose-6-Phosphatase. A standard protocol was followed to determine the liver glucose-6-phosphatase activity [19]. We used the secretome of the cells. 0.1 ml of 0.1 M glucose-6-phosphate solution and 0.3 ml of 0.05 M maleic acid buffer (pH 6.5) were mixed in a calibrated centrifuge tube and brought to 37°C in the water bath for 15 minutes. After stopping the reaction with 1 ml of 10% TCA, the reaction was chilled on ice and centrifuged at 3000 g for 10 minutes. An optical density of 340 nm was determined. The enzyme activity was expressed as milligrams of inorganic phosphate liberated per gram of sample.

2.7.3. Glutamate Oxaloacetate Transaminase (GOT) and Glutamate Pyruvate Transaminase (GPT). The secretome of the cells was used. Transasia Bio-Medicals Ltd. (Sikkim, India) supplied the kit for measuring liver and kidney GOT and GPT, and the enzyme activities were measured following the standard protocol [20]. Each enzyme activity was expressed as a unit per milligram of sample.

2.7.4. Biochemical Assay of Glycogen Level. Based on the standard method [21], glycogen content was determined. Cell secretomes were used. The secretome was diluted with distilled water and 5 ml of 52% perchloric acid. 20 minutes were spent at 0°C for extraction. A 15-minute centrifugation at 8000 g collected the supernatant from the collected

material. We transferred 0.2 ml of the supernatant into a graduated test tube, and 1.0 ml of distilled water was added to make the volume 1.0 ml. A graded standard was prepared using 0.1, 0.2, 0.4, 0.6, 0.8, and 1.0 ml of working standard solution, and all the standards were made up to 1.0 ml with distilled water. The anthrone reagent was added to all test tubes in 4.0 ml. Test tubes were placed in boiling water for 10 minutes. Using a bioanalyzer, the intensity of the green to dark green color of the solution was measured at 630 nm after they cooled at room temperature. A standard glucose solution was used to prepare a standard curve for measuring glycogen. In micrograms of glucose per milligram of tissue, glycogen was measured.

2.7.5. Biochemical Assays. Biochemical analysis was done using adipocytes which were centrifuged at 300 g for 2 minutes. The estimation of total cholesterol (TC) was done using ferric chloride-acetic acid reagents which were gently mixed and centrifuged at 3354xg for 10 min. at 4°C followed by supernatant incubation in conc. H₂SO₄ 50~60°C for 10 minutes. The estimation of high-density lipoprotein (HDL) was done by using phosphotungstate reagent and magnesium chloride (MgCl₂). The mixture is centrifuged similarly as that for TC and supernatant was mixed with ferric chloride-acetic acid reagent and 0.033 N sulfuric acid followed by incubation. The absorbances were recorded at 560 nm at room temperature (RT). Triglycerides (TGL) were also measured in adipocytes with n-heptane, isopropanol, sulfuric acid (0.08 N H₂SO₄), potassium hydroxide (6.25 mol/L), sodium metaperiodate, and acetylacetone. A 425 nm absorbance measurement was taken after 20 minutes of incubation at 70°C. We calculated LDL (low-density lipoprotein cholesterol) and VLDL (very low-density lipoprotein cholesterol) using known formulas [LDL=TC - (TGL/5) + HDL] and VLDL (TC - (LDL + HDL)]. Readings were checked randomly using Inoline kits (Merck) in a double-beam UV-vis spectrophotometer. A triplicate of each reading was recorded.

2.7.6. RNA Isolation, cDNA Synthesis, and Quantitative PCR (qPCR). Total RNA was extracted from cultured adipocytes by GeneJET RNA Purification kit (Thermo Scientific, India) followed by cDNA amplification using random hexamer primers (Verso cDNA synthesis kit (Thermo Scientific, India)). Gene expression of mRNA was performed by DyNAmo ColorFlash SYBR-Green qPCR kit (Thermo Scientific, India). Relative quantification was done between all the groups. Quantification was performed with an SYBR-Green real-time PCR assay of target gene mRNA which was expressed relative to the housekeeping gene mRNA. Amplification was performed with PCR master mix-containing target primers (Table 1), DNA polymerase, SYBR-Green I, 5 mM MgCl₂, and dNTP mix including dUTP and PCR buffer in duplicates. The amplification cycle starts with an initial denaturation at 95°C for 7 min, followed by 40 PCR cycles each consisting of 95°C for 10 sec, 60°C for 30 sec, and 74°C for 60 sec. Relative gene expression was calculated.

3. Statistical Analysis

One-way ANOVA followed by a multiple two-tailed “t” test was used for statistical analysis of the collected data and was calculated using GraphPad. Differences were considered significant at $P < 0.05$.

4. Results

4.1. Glucose Level. In Table 2, we show the glucose levels in all groups before and after extract treatment. The level of glucose was significantly elevated after 24h of 20 mM glucose induction compared with the control level. Supplementing with aqueous seed extracts of *Tamarindus indica* and *Momordica charantia* for 7 and 14 days, glucose levels were not significantly different from the control level (Table 2).

4.2. Glycogen Level. *Tamarindus indica* and *Momordica charantia* aqueous seed extracts were supplemented to the diabetic-induced wells for seven days, resulting in an increased glycogen level in comparison to a diabetic group; however, this parameter did not return to the control level (Figure 1). After 14 days of this supplementation, the above-mentioned parameter was reset to the control level (Figure 1).

4.3. Glucose-6-Phosphate Dehydrogenase Activity. When the aqueous extract of seed of *Tamarindus indica* and *Momordica charantia* was supplemented for 7 days, glucose-6-phosphate dehydrogenase activity was elevated in comparison to a diabetic group, but this parameter did not return to the control level (Figure 2). A resettlement to a control level (Figure 2) was achieved after 14 days of supplementation.

4.4. Glucose-6-Phosphatase Activity. In an experiment with aqueous extracts of seeds of *Tamarindus indica* and *Momordica charantia* supplementation for seven days, liver glucose-6-phosphatase activity increased significantly in comparison to a diabetic group, but this parameter did not return to control levels (Figure 3). Within 14 days of this supplementation, the above-mentioned parameter returned to the control level (Figure 3).

4.5. GOT and GPT Activities. In 20 mM glucose-induced diabetic wells, GPT and GT activities were significantly elevated in comparison with the control group (Table 3). With the aqueous extract of seeds of *Tamarindus indica* and *Momordica charantia* supplementation for 7 days, GOT and GPT activities showed a significant reduction in the diabetic group, but these parameters did not return to control levels (Table 3). These parameters were reestablished to control levels after 14 days of supplementation (Table 3).

4.6. Gene Expression Profiling. Figure 2 shows the mean \pm standard deviation of lipid profile estimation in vitro adipocytes in control, glucose-treated, and after the treatment of saroglitazar (10 μ M). Lipid profiles including TC, TGL, HDL, LDL, and VLDL showed a highly significant change as expected in adipocytes treated with glucose when

TABLE 1: Primer pair sequences used for real-time PCR reactions.

Gene	Forward primer(5'-3')	Reverse primer(5'-3')
β -Actin	ACGGGGTCACCCACACTGTGC	CTAGAAGCATTTCGCGGTGGACGATG
Catalase	TAGCCTTCGACCCAAGCAA	CGATGGCGGTGAGTGTC
SOD1	ACTCTCAGGAGACCATTGCATCA	TCCTGTCTTTGTACTTTCTTCATTTC
SOD2	CACATCAACGCGCAGATCAT	CCAACGCCTCCTGGTACTTC
GPx	GCAACCAGTTTGGGCATCA	AGCATGAAGTTGGGCTCGAA
IL1 β	TGAAGCTGATGGCCCTAAACA	GTAGTGGTGGTTCGGAGATTTCG
TNF α	TCAACCCCGAGTGACAAG	TTGGCCAGGAGGGCATT
IL6	CCTGACCCAACCACAAATGC	CCTTAAAGCTGCGCAGAATGA
TET1	AGGTCCAGGGCCAAATAACT	AGAAGGTGCCAGGTCAGAGA

TABLE 2: Effect of aqueous seed extract of *Tamarindus indica* and *Momordica charantia* after 7 days and 14 days of treatment on glucose level in diabetic adipocytes (mean \pm S.E.M.).

Group	Glucose level (mg/dl)			
	At the time of grouping 0 day	Days of supplements		
		7 days	14 days	
Control adipocytes	87.4 \pm 7.8	88.2 \pm 8.6	84.3 \pm 7.4	84.2 \pm 7.6
Diabetic adipocytes	85.4 \pm 8.1	352.3 \pm 11.2***	336.4 \pm 10.8***	328.8 \pm 10.6***
<i>Tamarindus indica</i> supp.	86.1 \pm 10.2	365.9 \pm 11.9***	121.4 \pm 9.2	88.2 \pm 12.4
<i>Momordica charantia</i> supp.	86.8 \pm 9.7	371.2 \pm 13.5***	130.8 \pm 8.4	87.6 \pm 9.8

ANOVA followed by multiple two-tailed *t*-tests. In each vertical column, mean with an asterisk (***) differs significantly from control or diabetic adipocytes ($P < 0.05$).

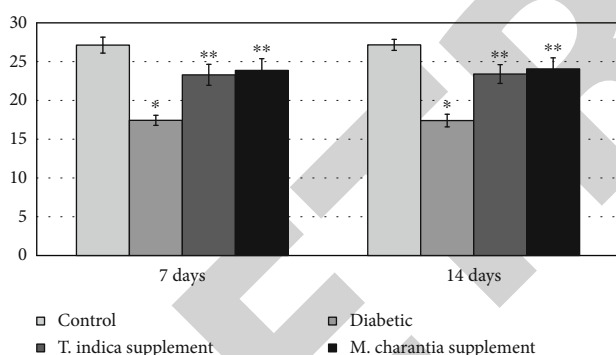


FIGURE 1: Effect of aqueous seed extract of *Tamarindus indica* and *Momordica charantia* supplementation on glycogen level in diabetic adipocytes. Data are expressed as mean S.D., by multiple two-tailed *t*-tests. (*) indicates that means differed from one another as well as from controls ($P > 0.05$). Nonasterisk figures do not differ significantly from one another in each vertical column ($P > 0.05$) within the same duration of treatment.

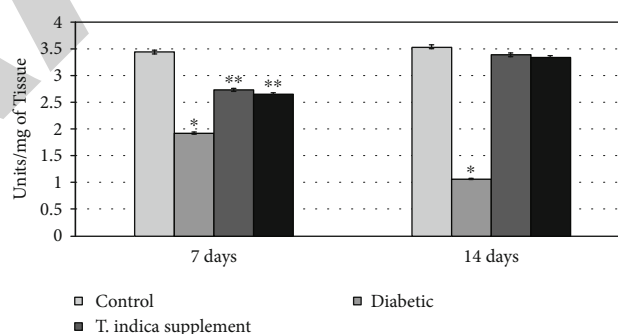


FIGURE 2: Effect of aqueous seed extract of *Tamarindus indica* and *Momordica charantia* on glucose-6-phosphate dehydrogenase activity in diabetic adipocytes. Data are expressed as mean S.D., by multiple two-tailed *t*-tests. (*) indicates that means differed from one another as well as from controls ($P > 0.05$). Nonasterisk figures do not differ significantly from one another in each vertical column ($P > 0.05$) within the same duration of treatment.

compared with controlled adipocytes ($P < 0.001$). However, after the treatment of diabetic mimicked adipocytes, i.e., glucose-treated adipocytes with saroglitazar, we found that TGL and VLDL showed significant association ($P < 0.005$) (Figure 4). It is a fact that PPAR α is involved in lipid metabolism and is the major transcription factor for lipids. This is supported by our results that the lipid TGL and VLDL showed significant association with the saroglitazar. Cultured adipocytes were firstly treated with high glucose concentration followed by saroglitazar drug (10 μ M) for

24 hours. The high glucose caused a diabetic state by which the inflammation is increased which was then significantly normalized by treatment of saroglitazar (Figure 5). During the estimation of gene expression of catalase, we found that it almost doubled while in the estimation of superoxide dismutase, i.e., SOD1 and SOD2, it was found to be around 3 folds. However, during the estimation of glutathione peroxidase (GPx), the activity was around four folds as compared to controlled adipocytes (Figure 5). The increased inflammation caused due to glucose load was found to be restored by the use of saroglitazar. The level of IL1 beta is restored

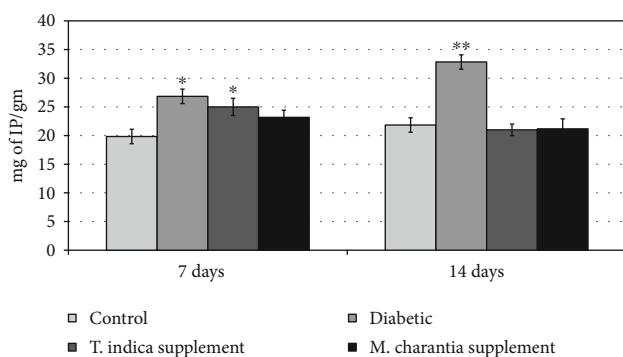


FIGURE 3: Effect of aqueous seed extract of *Tamarindus indica* and *Momordica charantia* on glucose-6-phosphatase activity in diabetic adipocytes. Data are expressed as mean S.D., by multiple two-tailed *t*-tests. (*) indicates that means differed from one another as well as from controls ($P > 0.05$). Nonasterisk figures do not differ significantly from one another in each vertical column ($P > 0.05$) within the same duration of treatment.

to half the load of inflammation in glucose-treated adipocytes with the use of saroglitazar, i.e., highly significant ($P < 0.001$) (Figure 5). However, TNF gene expression was also reduced but not as much as that of IL-1 beta and also showed a highly significant association ($P < 0.001$) (Figure 5). Similarly, the pleiotropic inflammatory marker IL-6 was severally reduced and showed a highly significant association ($P < 0.001$) (Figure 5). Moreover, a new gene TET-1 was also analyzed to find the association of saroglitazar effect on adipocytes. Interestingly, it was found that the TET expression was significantly regulated by the use of saroglitazar ($P < 0.001$) (Figure 5). This clarifies that when the glucose load is increased in adipocytes, the cell is more susceptible to inflammation and may cause many metabolic abnormalities. As per our results on reactive oxygen metabolites, we found that the level of it is increased rapidly. The adipocytes are now sluggish to respond against any behavior in this state. This happens due to enhanced inflammation in the cell. However, after the treatment with saroglitazar drug, the rate of inflammation is reduced significantly (Figure 5).

5. Discussion

The purpose of this report is to demonstrate the antidiabetic effects of aqueous extracts of seeds from *Tamarindus indica* and *Momordica charantia* for the management of insulin-dependent diabetes mellitus or type 1 diabetes mellitus (T1DM) and to investigate the enzyme actions associated with glucose levels modified by the extracts in adipocytes derived from Wharton's Jelly Mesenchymal Stem Cells. As well, we examined the expression and close relation of the saroglitazar gene with the TET gene on oxidative stress and inflammation in the presence of aqueous extract from seeds of *Tamarindus indica* and *Momordica charantia*. Supplementation of aqueous extract from *Tamarindus indica* and *Momordica charantia* results in a significant decrease in glucose levels in diabetic adipocytes as compared to controls, further suggesting antidiabetic action of these extracts.

A variety of mechanisms may be involved in the hypoglycemic action of extracts of known hypoglycemic plants. *Tamarindus indica* and *Momordica charantia* are two herbal hypoglycemic plants whose extracts are not fully understood. Moreover, it has not been reported what is the exact mechanism and principle behind their hypoglycemic effects and their regulation of blood glucose levels. Insulin plays a major role in glucose production in the muscle and liver. Studies have found that streptozotocin-induced diabetic rats have reduced hepatic and skeletal muscle glycogen stores [22]. A similar observation was made in the present study in our *in vitro* model. It is possible that the decreased glycogen content in diabetics is due to lack of insulin and inactivation of glycogen synthase. Upon supplementation with aqueous extracts of *Tamarindus indica* seeds and *Momordica charantia* seeds for 7 and 14 days, glycogen levels were significantly elevated. Therefore, the extract's antidiabetic action is due to an improvement in glycogen synthesis. G-6-PDH (glucose-6-phosphate dehydrogenase) is a key enzyme in maintaining normal blood sugar levels [23]. Streptozotocin-induced type I diabetes is also caused by a reduction of G-6-PDH activity in the liver, which prevents glucose from being absorbed through PPP (Pentose Phosphate Pathway), since this enzyme activity is regulated by insulin [24]. The seed extracts of *Tamarindus indica* and *Momordica charantia* significantly enhanced this enzyme activity and supported its other possible method of antidiabetic action. In the liver and kidney, glucose-6-phosphatase plays an important role in maintaining glucose homeostasis [25]. In addition, we attempted to understand the biochemical and antidiabetic mechanisms of the action of these seed extracts. Therefore, we have measured the activity of glucose-6-phosphatase (G-6-P), which is responsible for maintaining glucose homeostasis. According to previous studies [26], G-6-P activity was increased in diabetic adipocytes. In diabetic adipocytes, these extracts significantly restored G-6-P activity compared to the control, and this points to another possible mechanism of its antidiabetic activity. These results are supported by other previous studies [26]. Ghosh and Suryawanshi [27] found that diabetic adipocytes have an elevated activity of glutamic pyruvic transaminase (GPT) and glutamic oxaloacetic transaminase (GOT). Diabetes is characterized by elevated levels in both GOT and GPT activities that are responsible for gluconeogenesis and ketogenesis [28]. GOT and GPT activities were restored to normal levels after supplementation with *Tamarindus indica* and *Momordica charantia* extracts and support the hypothesis that *Tamarindus indica* and *Momordica charantia* have antidiabetic properties. Using these results pieces of information, it might be revealed that the extracts of seeds from *Tamarindus indica* and *Momordica charantia* may contain some specific biomolecules that could stimulate or sensitize the insulin receptors or β -cells in the Islets of Langerhans. Additionally, diabetic adipocytes can improve the metabolism of carbohydrates and restore normal glucose levels. Obesity and type 2 diabetes are chronic metabolic disorders characterized by insulin resistance, inflammation, and oxidative stress. The situation has been managed and the ideal cellular state nurtured with a variety of drugs.

TABLE 3: In streptozotocin-induced diabetic male albino rats with liver and kidney GOT and GPT activities, aqueous seed extracts of *Tamarindus indica* and *Momordica charantia* (mean \pm S.D.) were compared to their aqueous seed extracts after 7 days and 14 days.

Group	GOT (unit/ml)	GPT (unit/ml)
Control (7 days)	14.6 \pm 0.5	11.7 \pm 0.6
Diabetic (7 days)	23.2 \pm 0.6*	20.0 \pm 0.9*
<i>Tamarindus indica</i> supplement (7 days)	19.1 \pm 0.6**	17.0 \pm 0.6**
<i>Momordica charantia</i> supplement (7 days)	19.4 \pm 0.5**	17.2 \pm 0.5**
Control (14 days)	14.1 \pm 0.6	12.3 \pm 0.8
Diabetic (14 days)	26.4 \pm 0.5*	23.4 \pm 0.4*
<i>Tamarindus indica</i> supplement (14 days)	14.2 \pm 0.4	12.1 \pm 0.3
<i>Momordica charantia</i> supplement (14 days)	14.6 \pm 0.5	12.5 \pm 0.6

ANOVA followed by multiple two-tailed *t*-tests. Within each vertical column, (*) indicates that means differed from one another as well as from controls ($P > 0.05$). Nonasterisk figures do not differ significantly from one another in each vertical column ($P > 0.05$) within the same duration of treatment.

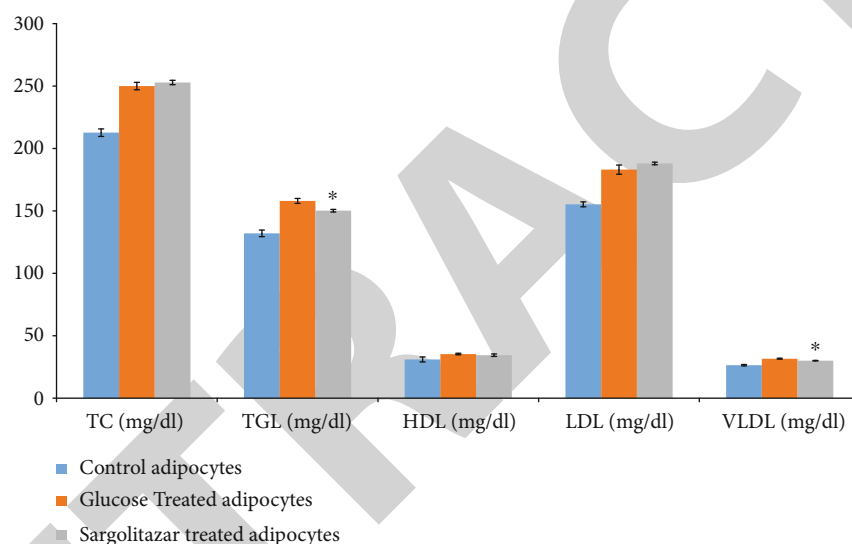


FIGURE 4: Mean \pm standard deviation of lipid profile in controlled adipocytes, glucose-fed adipocytes, and saroglitazar-treated adipocytes. TC: total cholesterol; TGL: triglycerides; HDL: high-density lipoproteins; LDL: low-density lipoproteins; VLDL: very low-density lipoproteins. ** showed a significant association and *** showed a highly significant association when compared with glucose-treated adipocytes and control adipocytes, respectively. The *P* values were calculated using one-way ANOVA.

The major regulating sites are PPAR α and PPAR γ receptors; surprisingly, saroglitazar promises to regulate these metabolic disturbances especially in liver-associated disease. The mechanism of it is that the binding of PPAR α with peroxisome proliferator response element (PPRE) and this location is found upstream of target genes named ACOX1 and CPT1A play a major role in fatty acid oxidation. In a NAFLD model, it is observed that there is a very slight amount of PPAR α present that is confirmed by measuring mRNA and protein level of PPAR α and is confirmed by comparing with the control group. To confirm that it is possible for PPAR α regulation by TET-1-mediated hydroxymethylation, it is necessary to confirm first that PPAR α is regulated by an impact of methylation. After performing treatment with various kinds of DNA methyltransferase inhibitors, a slight increase is observed in the level of mRNA of PPAR α . This concluded hydroxymethylation rate is lowered after inhibition of TET-1 [16]. TET-1 overexpression

plasmid can help to reduce the accumulation or gathering of intracellular TG by early transfection in mice [16]. As the abnormal level of insulin activity in the body can result in hyperglycemia in the body along with many other severe changes that result in NASH and major cardiovascular disease, major fluctuations observed in the increase in protein oxidation, lipid peroxidation, production of reactive oxygen species in mitochondria at a very excess level [29] currently there is an all-important need for the upshot of essential and significant drug or determining the particular target of NAFLD to the ultimate eradication of it [5]. In many mice models of NASH, visceral fat can be a major base for measurement or assessment of obesity [30]. The major exploring fact about saroglitazar is that it can act as a PPAR- α/γ agonist. This theory is confirmed and escorted by the results that are observed in this study all correlated with target genes of both PPAR- α (ACOX1, CPT1A) and PPAR- γ (CD36, UCP2) as their crucial involvement is evidence

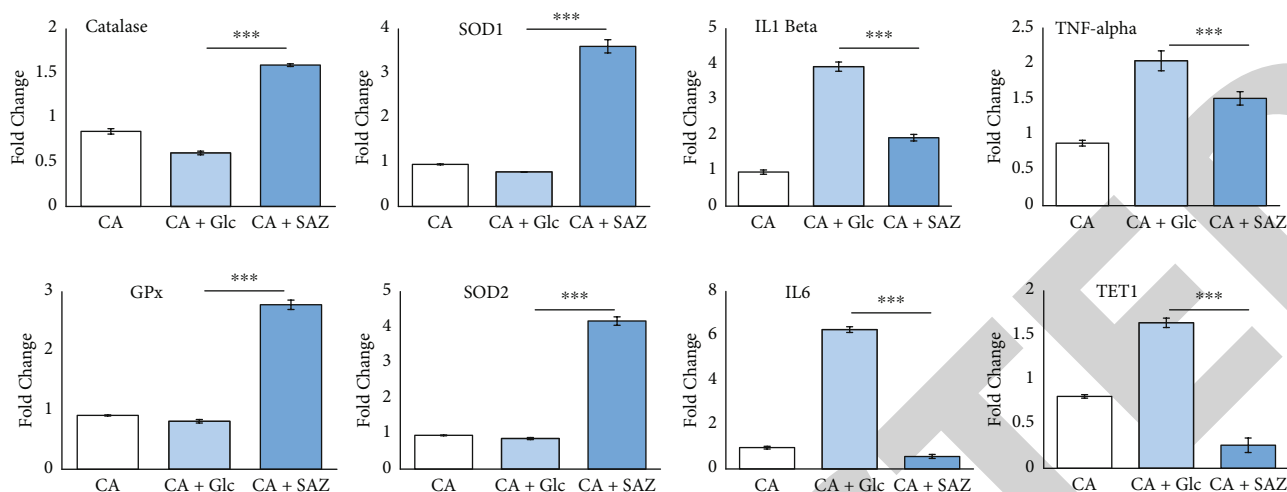


FIGURE 5: The relative mRNA expression in response to saroglitazar drug in catalase, SOD1, SOD2, GPx, IL1 Beta, IL-6, TNF, and TET1 gene. CA: control adipocytes; CA+Glc: glucose-fed adipocytes; CA+SAZ: saroglitazar-treated adipocytes. ** showed a significant association and *** showed a highly significant association when compared with glucose-treated adipocytes and control adipocytes, respectively. The *P* values were calculated using one-way ANOVA.

supported by previous reports. It also confirmed that this can prove the therapeutic ability of saroglitazar in the cure or medication of NASH [16]. However, menaquinone (MK-7) is also an important factor that is confirmed to lower glycemic indices rate but lipid accumulation cannot be controlled using MK-7 supplementation [31]. Saroglitazar has no such side effects or toxicity levels as it has been previously given to many diabetic patients to control the abnormal rate of dyslipidemia [6]. As much literature confirmed about the Indian population suffering from such metabolic-associated diseases is due to their genetic background and many dietary and environmental factors are responsible for this, can be evidenced by published previous literature [32, 33]. Very unexplored fascinations revealed about saroglitazar are notable such as it has the crucial ability of histological benefits and advantage as compared with that of pioglitazone either of having same effects they both generated over the cure of insulin resistance markers called or known as HOMA-IR. While in the context of pioglitazone it has two enantiomers existed named as R and S types, R enantiomer has a major effect generated on the hepatic insulin signaling pathway. Besides this, pioglitazone is a PPAR- γ agonist and the major role it plays is to work as a positive control in case it has no negative effect because saroglitazar is still needed to go under the phase of human trials [16]. Moreover, *in vitro* model of NAFLD is shown to decrease the production or function of TET-1, and it is an important hydroxymethylase that serves to play a superior role in development and tumor formation. Pathogenesis of NAFLD is known to be activated by a series of the process known as DNA methylation, has the epigenetic background. Still, the TET-1 role is not well studied in the case of NAFLD, but TET-1 plays a major role in the PPAR α expression in the methylated PPAR α promoter region and it has great involvement in the expression of enzymes potentially in the regulation of fatty acid β -oxidation, hence inhibiting triglyceride deposition in the liver, as lack of TET-1 can cause tri-

glyceride accumulation in the liver as well as in adipocytes [16]. Our study deals with the effect of saroglitazar (is a dual peroxisome proliferator-activated receptor (PPAR) agonist), with the association of the TET-1 gene with other inflammatory molecules, is regulated by the use of saroglitazar performed *in vitro* adipocytes and manage the normal state of the cell by regulating the lipid metabolism. Several studies suggest that TET enzymes alter gene expression in synergy with epigenetic changes, remaining important contributors to adiposity and its metabolic consequences. This study will explore new approaches to treating obesity, type 2 diabetes, and other metabolic disorders. The TET-1 regulation in diabetic adipocytes is well regulated by the seed extract of *Tamarindus indica* and *Momordica charantia* supplementation. In conclusion, our study results suggest that the supplementation of seed extract of *Tamarindus indica* and *Momordica charantia* may have beneficial effects on the regulation of diabetes and that will hold the new antidiabetic drugs hope as therapeutic medications. However, furthermore, studies are required to unfold a clear view of these extracts.

Data Availability

On reasonable request, the corresponding author will provide access to the data sets used and analyzed during the current study.

Conflicts of Interest

There are no competing interests between the authors.

Acknowledgments

This research work was funded by the Researchers Supporting Project number RSP-2021/27, King Saud University, Riyadh, Saudi Arabia.

References

- [1] R. Gupta, P. Kumar, N. Fahmi et al., "Endocrine disruption and obesity: a current review on environmental obesogens," *Current Research in Green and Sustainable Chemistry*, vol. 3, article 100009, 2020.
- [2] M. Saxena and M. Banerjee, "Diabetes: history, prevalence, insulin action and associated genes," *Journal of Applied Biosciences*, vol. 34, pp. 139–151, 2008.
- [3] G. Piedrola, E. Novo, F. Escobar, and R. Garcia-Robles, "White blood cell count and insulin resistance in patients with coronary artery disease," *Annual Endocrinology*, vol. 62, no. 1, pp. 7–10, 2001.
- [4] J. A. Yaryura-Tobias, A. Pinto, and F. Neziroglu, "Anorexia nervosa, diabetes mellitus, brain atrophy, and fatty liver," *International Journal of Etiological Disorders*, vol. 30, no. 3, pp. 350–353, 2001.
- [5] M. Ma, H. Liu, J. Yu et al., "Triglyceride is independently correlated with insulin resistance and islet beta cell function: a study in population with different glucose and lipid metabolism states," *Lipids in Health and Disease*, vol. 19, no. 1, p. 121, 2020.
- [6] M. Banerjee and M. Saxena, "Genetic polymorphisms of cytokine genes in type 2 diabetes mellitus," *World Journal of Diabetes*, vol. 5, no. 4, pp. 493–504, 2014.
- [7] M. Moszak, A. Zawada, A. Juchacz, M. Grzymislawski, and P. Bogdański, "Comparison of the effect of rapeseed oil or amaranth seed oil supplementation on weight loss, body composition, and changes in the metabolic profile of obese patients following 3-week body mass reduction program: a randomized clinical trial," *Lipids in Health and Disease*, vol. 19, no. 1, p. 143, 2020.
- [8] B. S. Geetha, C. M. Biju, and K. T. Augusti, "Hypoglycemic effects of leucodelphinidin derivative isolated from *Ficus bengalensis* (Linn.)," *Indian Journal of Pharmacology*, vol. 38, pp. 220–222, 1994.
- [9] B. K. Rao, P. R. Sudarshan, M. D. Rajasekhar, N. Nagaraju, and C. A. Rao, "Antidiabetic activity of *Terminalia pallida* fruit in alloxan induced diabetic rats," *Journal of Ethnopharmacology*, vol. 85, no. 1, pp. 169–172, 2003.
- [10] V. Vats, J. K. Grover, and S. S. Rathi, "Evaluation of anti-hyperglycemic and hypoglycemic effect of *Trigonella foenum-graecum* Linn, *Ocimum sanctum* Linn and *Pterocarpus marsupium* Linn in normal and alloxanized diabetic rats," *Journal of Ethnopharmacology*, vol. 79, no. 1, pp. 95–100, 2002.
- [11] S. R. Iyer, "Tamarindus indica Linn," in *Indian Medicinal Plants*, vol. V, P. K. Warrier, V. P. K. Nambiar, and C. R. Kutty, Eds., pp. 235–236, Orient Longman Limited, Madras, 1995.
- [12] W. L. Li, H. C. Zheng, J. Bukuru, and N. De Kimpe, "Natural medicines used in the traditional Chinese medical system for therapy of diabetes mellitus," *Journal of Ethnopharmacology*, vol. 92, no. 1, pp. 1–21, 2004.
- [13] S. S. Rathi, J. K. Grover, and V. Vats, "The effect of *Momordica charantia* and *Mucuna pruriens* in experimental diabetes and their effect on key metabolic enzymes involved in carbohydrate metabolism," *Phytotherapy Research*, vol. 16, no. 3, pp. 236–243, 2002.
- [14] R. Maiti, D. Jana, U. K. Das, and D. Ghosh, "Antidiabetic effect of aqueous extract of seed of *Tamarindus indica* in streptozotocin-induced diabetic rats," *Journal of Ethnopharmacology*, vol. 92, no. 1, pp. 85–91, 2004.
- [15] F. Saeed, M. Afzaal, B. Niaz et al., "Bitter melon (*Momordica charantia*): a natural healthy vegetable," *International Journal of Food Properties*, vol. 21, no. 1, pp. 1270–1290, 2018.
- [16] J. Wang, Y. Zhang, Q. Zhuo et al., "TET1 promotes fatty acid oxidation and inhibits NAFLD progression by hydroxymethylation of PPAR α promoter," *Nutrition & Metabolism*, vol. 17, no. 1, p. 46, 2020.
- [17] S. H. Atkin, A. Dasmahapatra, M. A. Jaker, M. I. Chorost, and S. Reddy, "Fingerstick glucose determination in shock," *Annual International Medicine*, vol. 114, no. 12, pp. 1020–1024, 1991.
- [18] R. G. Langdon, "Glucose-6-phosphate dehydrogenase from erythrocytes," in *Methods in Enzymology*, vol. 9, W. A. Wood, Ed., pp. 126–131, Academic press, New York, 1966.
- [19] M. A. Swanson, "Glucose-6-phosphatase from liver," in *Methods in Enzymology*, vol. 2, S. P. Colowick and N. O. Kaplan, Eds., pp. 541–543, Academic press, New York, 1955.
- [20] R. J. Henry, M. Chiamori, O. J. Golub, and S. Berkman, "Revised spectrophotometric methods for the determination of glutamic-oxalacetic transaminase, glutamic-pyruvic transaminase, and lactic acid dehydrogenase," *American Journal of Clinical Pathology*, vol. 34, no. 4, pp. 381–398, 1960.
- [21] S. Sadasivam and A. Manickam, "Carbohydrates," in *Methods in Biochemistry*, S. Sadasivam and A. Manickam, Eds., pp. 11–12, New Age International Pvt. Ltd, New Delhi, 1996.
- [22] J. K. Grover, V. Vats, and S. Yadav, "Effect of feeding aqueous extract of *Pterocarpus marsupium* on glycogen content of tissues and the key enzymes of carbohydrate metabolism," *Molecular and Cellular Biochemistry*, vol. 241, no. 1/2, pp. 53–59, 2002.
- [23] P. A. Mayes, "The pentose phosphate pathway and other pathway of hexose metabolism," in *Herper's Biochemistry*, R. K. Murray, D. K. Granner, and V. W. Mayes, Eds., pp. 219–237, McGraw-Hill, USA, 2000.
- [24] N. H. Ugochukwu and N. E. Babady, "Antihyperglycemic effect of aqueous and ethanolic extracts of *Gongronema latifolium* leaves on glucose and glycogen metabolism in livers of normal and streptozotocin-induced diabetic rats," *Life Science*, vol. 73, no. 15, pp. 1925–1938, 2003.
- [25] J. M. Berg, J. L. Tymoczko, and L. Stryer, "Glycolysis and gluconeogenesis," in *Biochemistry*, J. M. Berg, J. L. Tymoczko, and L. Stryer, Eds., pp. 433–474, W.H. Freeman and Co., New York, NY, 2006.
- [26] D. Gupta, J. Raju, and N. Z. Baquer, "Modulation of some gluconeogenic enzyme activities in diabetic rat liver and kidney: effect of antidiabetic compounds," *Indian Journal of Experimental Biology*, vol. 37, no. 2, pp. 196–199, 1999.
- [27] S. Ghosh and S. A. Suryawanshi, "Effect of *Vinca rosea* extracts in treatment of alloxan diabetes in male albino rats," *Indian Journal of Experimental Biology*, vol. 39, no. 8, pp. 748–759, 2001.
- [28] P. Felig, E. Marliss, J. Ohman, and J. F. Cahill, "Plasma amino acid levels in diabetic ketoacidosis," *Diabetes*, vol. 19, no. 10, pp. 727–729, 1970.
- [29] D. P. Kumar, R. Caffrey, J. Marioneaux et al., "The PPAR α/γ agonist saroglitazar improves insulin resistance and steatohepatitis in a diet induced animal model of nonalcoholic fatty liver disease," *Scientific Reports*, vol. 10, no. 1, p. 9330, 2020.
- [30] D. Statovci, M. Aguilera, J. MacSharry, and S. Melgar, "The impact of Western diet and nutrients on the microbiota and immune response at mucosal interfaces," *Frontiers in Immunology*, vol. 8, p. 838, 2017.

Retraction

Retracted: The Impact of Seeding Density and Nitrogen Rates on Forage Yield and Quality of *Avena sativa* L

BioMed Research International

Received 8 January 2024; Accepted 8 January 2024; Published 13 January 2024

Copyright © 2024 BioMed Research International. This is an open access article distributed under the Creative Commons Attribution License, which permits unrestricted use, distribution, and reproduction in any medium, provided the original work is properly cited.

This article has been retracted by Hindawi following an investigation undertaken by the publisher [1]. This investigation has uncovered evidence of one or more of the following indicators of systematic manipulation of the publication process:

- (1) Discrepancies in scope
- (2) Discrepancies in the description of the research reported
- (3) Discrepancies between the availability of data and the research described
- (4) Inappropriate citations
- (5) Incoherent, meaningless and/or irrelevant content included in the article
- (6) Manipulated or compromised peer review

The presence of these indicators undermines our confidence in the integrity of the article's content and we cannot, therefore, vouch for its reliability. Please note that this notice is intended solely to alert readers that the content of this article is unreliable. We have not investigated whether authors were aware of or involved in the systematic manipulation of the publication process.

Wiley and Hindawi regrets that the usual quality checks did not identify these issues before publication and have since put additional measures in place to safeguard research integrity.

We wish to credit our own Research Integrity and Research Publishing teams and anonymous and named external researchers and research integrity experts for contributing to this investigation.

The corresponding author, as the representative of all authors, has been given the opportunity to register their agreement or disagreement to this retraction. We have kept a record of any response received.

References

- [1] A. Kanwal, D. Zubair, R. M. u. Rehman et al., "The Impact of Seeding Density and Nitrogen Rates on Forage Yield and Quality of *Avena sativa* L," *BioMed Research International*, vol. 2022, Article ID 8238634, 9 pages, 2022.

Research Article

The Impact of Seeding Density and Nitrogen Rates on Forage Yield and Quality of *Avena sativa* L

Aroosa Kanwal,¹ Dawood Zubair,² Rao Mehboob ur Rehman,³ Muhammad Ibrahim,⁴ Muhammad Amjad Bashir ,⁵ Muhammad Mudassar Maqbool,⁴ Muhammad Imran,⁶ Ubaid ur Rehman,^{4,7} Omaima Nasif,⁸ and Mohammad Javed Ansari⁹

¹Rural Health Center, Bhekhro More District, Mandi Bahauddin, Punjab, Pakistan

²ER Medical Officer at Iqra Medical Complex, Johar Town Lahore, Pakistan

³Hamdard College of Medicine and Dentistry, Hamdard University, Karachi, Pakistan

⁴Department of Agronomy Faculty of Agricultural Sciences, Ghazi University, Dera Ghazi Khan Punjab, Pakistan

⁵Department of Plant Protection Faculty of Agricultural Sciences, Ghazi University, Dera Ghazi Khan Punjab, Pakistan

⁶Department of Soil and Environmental Sciences, MNS University of Agriculture, Multan Punjab, Pakistan

⁷United States Department of Agriculture, Washington DC, USA

⁸Department of Physiology, College of Medicine, King Khalid University Hospital, King Saud University, Medical City, PO Box 2925, Riyadh 11461, Saudi Arabia

⁹Department of Botany, Hindu College Moradabad (Mahatma Jyotiba Phule Rohilkhand University Bareilly), India

Correspondence should be addressed to Muhammad Amjad Bashir; abashir@gudgk.edu.pk

Received 22 April 2022; Accepted 16 May 2022; Published 30 June 2022

Academic Editor: Dr Muhammad Hamid

Copyright © 2022 Aroosa Kanwal et al. This is an open access article distributed under the Creative Commons Attribution License, which permits unrestricted use, distribution, and reproduction in any medium, provided the original work is properly cited.

Green forage is an excellent feed source for livestock. It is an integral part of livestock production to accomplish the demands for butter, milk, and other derivatives for human utilization. Livestock contributes 11.39% towards the gross domestic product of Pakistan and 58.33% in agricultural farming. Livestock face shortage or insufficient supply of green fodder during the winter season, which ultimately reduces milk yield. Oat (*Avena sativa* L.) is a major forage crop in the winter season; however, several biotic and abiotic factors negatively affect its yields. Low soil fertility, particularly nitrogen deficiency, is regarded as one of the few reasons responsible for the low forage yield of oat. Low organic matter content in the soil, suboptimal agronomic practices, and harsh climatic conditions are the other major reasons for low oat yield. Seed rate and different nitrogen rates significantly alter green forage yield and quality of oat. This study assessed the impact of different seeding densities and nitrogen (N) doses on the forage yield of oat. Three seeding densities (70, 80, and 90 kg ha⁻¹) and five N doses (0, 40, 80, 120, and 160 kg ha⁻¹) were included in the study. The interactive effect of seeding density and N doses significantly altered green forage yield and quality attributes of oat. The highest green forage yield (54.67 t ha⁻¹) was noted for the interaction among 90 kg seed rate ha⁻¹ and 160 kg N ha⁻¹. Similarly, the highest germination count (140 m⁻²), number of tillers (5.97 m⁻²), plant height (122.97 cm), number of leaves per plant (24.50 m⁻²), leaf area per tiller (123.18 cm²), fresh weight (5.47 kg m⁻²), dry weight (1692 g m⁻²), dry matter yield (20.90 t ha⁻¹), crude protein (10.54%), crude fiber (31.62%), and total ash (9.39%) were recorded for the interactive effect of 90 kg seed rate ha⁻¹ and 160 kg N ha⁻¹. Economic analysis revealed that interaction between 90 kg seed rate ha⁻¹ with 120 and 160 kg N ha⁻¹ was superior to others with higher benefit: cost ratio and net economic returns. It is recommended that the oat seed rate of forage oat crop must be kept at 90 kg ha⁻¹ and it should be supplied 120 kg N ha⁻¹ for higher yield, better quality, and more economic returns.

1. Introduction

Green forage is a valuable and the cheapest source of energy and provides excellent feed for livestock. A sustainable supply of green forage is a major constraint in livestock production to achieve the requirements for milk, butter, and other milk derivatives for human consumption [1]. Livestock contributes 58.33% towards agriculture and 11.39% towards the gross domestic product of Pakistan during 2016-2017 [2]. Livestock is usually underfed in Pakistan, which results in a low animal population. Imbalanced and low soil fertility, low organic matter content, and nitrogen deficiency are the major factors responsible for the low forage yield globally [3].

Oat is locally known as “jai” or “jodar” in Pakistan and belongs to the family Poaceae. Pakistan is facing a 52-54% deficiency in the domestic fodder requirements [4]. Globally, oat is grown for grain, green forage, and fodder for livestock. It is the most important and cheapest source of cereal fodder crops grown during the winter season throughout Pakistan under rain-fed and irrigated conditions. Oat fodder is nutritious, palatable, and succulent. The nutritive value of oat fodder can be increased by combining it with legumes, like alfalfa, Persian clover, berseem, and pea [5]. It contains high amounts of minerals, including phosphorus and iron, fat, vitamin B₁, and protein. Oat is a high-yielding crop in temperate climates and exhibits low tolerance to waterlogging [1]. Oat grains are a rich nutritive feed for dairy cows, sheep, horses, and young breeding animals [6]. Oat forage contains 30.44% crude fiber, 9.3% crude protein, 3.56% fat, and 0.27% phosphorus. It can be directly grazed to feed animals before seed setting and can be grown for grain purposes [7]. Its good quality grains and leaves are a rich source of carotene and carbohydrates. Oat requires 16-32°C temperature and 400 mm rainfall during the growing season for optimum growth and development [8].

Grains and leaves of forage oat are a rich source of carotene and carbohydrates [7]. The forage yield of oat in Pakistan is too low than other countries. The main reasons for low forage production are changing climate, low soil fertility, unavailability of high-yielding varieties, socioeconomic factors, shortage of irrigation water, poor seeding techniques, and mismanagement of fertilizer application [9].

Genus *Avena* consists of seventy species. *Avena byzantina* and *Avena sativa* are mainly cultivated for green forage and fodder purposes. There is a dire need to improve the forage yield of oat, which can be achieved by adopting improved agronomic practices [8]. Oat ranks 6th as a cereal crop worldwide after wheat, maize, rice, barley, and sorghum. Oat is a multicut fodder crop and achieves maximum green fodder yield with appropriate management. It should be harvested at 50% flower blooming [10].

Sowing fodder crops with optimum seed rate is important to get sufficient plant population, which ultimately contributes towards high forage production. Plant population has a direct impact on forage yield and quality. Low and high plant population reduces the yield and quality of forages; thus, seeding density must be kept optimum. The seed rate of legumes could be decreased when these are sown in a

TABLE 1: Analysis of variance of different seeding rates, nitrogen doses, and their interactions on germination count, plant height, number of tillers per plant, leaf area per tiller, and fresh and dry biomass of oat.

SOV	DF	SS	MS	P value
<i>Germination count</i>				
Seed rate (S)	2	6932.5	3466.25	0.0000**
Nitrogen doses (N)	4	994.2	248.56	0.0852NS
S × N	8	1168.6	146.08	0.2640NS
<i>Plant height</i>				
Seed rate (S)	2	359.69	179.85	0.0028*
Nitrogen doses (N)	4	4829.57	1207.39	0.0000**
S × N	8	569.46	71.18	0.0173*
<i>Number of tillers</i>				
Seed rate (S)	2	9.9613	4.98067	0.0000**
Nitrogen doses (N)	4	25.3444	6.33611	0.0000**
S × N	8	2.5542	0.31928	0.00136*
<i>Leaf area per tiller</i>				
Seed rate (S)	2	1570.23	785.114	0.0000**
Nitrogen doses (N)	4	2863.32	715.831	0.0000**
S × N	8	883.81	110.476	0.0235*
<i>Fresh weight</i>				
Seed rate (S)	2	3.4964	1.74822	0.0000*
Nitrogen doses (N)	4	32.3658	8.09144	0.0000**
S × N	8	0.1969	0.02461	0.0240*
<i>Dry weight</i>				
Seed rate (S)	2	287097	143548	0.0008*
Nitrogen doses (N)	4	7122222	1780555	0.0000**
S × N	8	534114	66764	0.0016*

SOV: source of variation, DF: degree of freedom, SS: sum of squares, MS: mean squares, *: significant, NS: nonsignificant.

mixture with other fodders [11, 12] The use of low or high seed rate exerts negative impacts on forage yield and quality [13]. A lower seed rate increases plant height, while a high seed rate reduces plant height due to less space, antagonism for light, and other resources [14]. The plant height of forage crops decreases with increasing seeding rate, which indicates competition for light [14].

Kakol et al. [15] recorded the highest green forage yield of oat with a 100 kg ha⁻¹ seed rate compared to 125 kg ha⁻¹, while the quality of forage remained unaffected. Jan and Jan [16] have also reported a nonsignificant impact of seed rates on green and dry forage yields of oat. Abate and Wegi [13] concluded that optimum seed rate and fertilizer level have a significant effect on green forage yield of oat and dry matter production.

Nitrogen (N) is a compulsory part of protein and a physiologically important compound that improves the growth and development of crop plants [17]. Nitrogen plays a vital role in crop production [18–20]. It is an essential ingredient of plant cell constituents like green pigments, amino acids,

TABLE 2: Interactive effect of seed rate and nitrogen level on germination count, plant height, numbers of leaves, and leaf area per tiller of forage oat.

Treatments	Germination count (m ⁻²)	Plant height (cm)	Number of leaves (m ⁻²)	Leaf area per tiller (cm ²)	Fresh weight (kg m ⁻²)	Dry weight (g m ⁻²)
<i>Seed rate (S)</i>						
S ₁	108.42 C	104.45 B	20.180 B	110.08 B	3.8267 C	897.7 B
S ₂	125.19 B	108.1 AB	20.780 B	118.32 A	4.2200 B	845.3 B
S ₃	138.77 A	111.37 A	22.060 A	100.02 C	4.5067 A	1034.7 A
LSD	3.8	1.8	0.32	2.33	0.34	45.13
<i>Nitrogen doses (N)</i>						
N ₁	119.93 NS	92.51 D	19.667 D	107.00 B	2.7889 E	457.6 C
N ₂	118.64	103.48 C	17.756 E	117.81 A	3.7444 D	468.1 C
N ₃	123.08	105.32 C	20.956 C	121.95 A	4.3333 C	1008.9 B
N ₄	128.47	116.71 B	22.756 B	94.91 de	4.9556 B	1342.0 A
N ₅	130.61	121.90 A	23.900 A	96.54 de	5.1000 A	1353.0 A
LSD 0.05	4.91	2.33	0.42	90.54 e	0.44	58.26
<i>S × N</i>						
S ₁ N ₁	109.97 NS	94.43 g	17.50 g	115.91 ab	2.47 k	403.0 e
S ₁ N ₂	103.23	94.37 g	17.67 fg	121.61 a	3.23 h	459.7 e
S ₁ N ₃	101.70	96.33 fg	20.63 d	102.15 cd	4.03 fg	962.7 cd
S ₁ N ₄	115.97	115.70 abc	22.20 c	104.71 cd	4.63 d	1317.3 b
S ₁ N ₅	111.23	121.40 ab	22.90 bc	104.58 cd	4.77 d	1346.0 b
S ₂ N ₁	111.2	91.37 g	17.43 g	115.78 ab	2.87 j	494.0 e
S ₂ N ₂	114.53	104.50 ef	19.10 ef	123.18 a	3.90 g	470.7 e
S ₂ N ₃	129.13	106.30 de	20.03 de	107.38 bc	4.33 e	1167.3 bc
S ₂ N ₄	131.23	115.57 abc	23.03 abc	121.54 a	4.93 c	1016.7 cd
S ₂ N ₅	139.87	122.97 a	24.30 ab	119.88 a	5.07 c	1348.3 b
S ₃ N ₁	138.33	91.73 g	18.33 fg	121.74 a	3.03 i	475.7 e
S ₃ N ₂	138.17	111.57 cde	22.23 c	121.08 a	4.10 f	474.0 e
S ₃ N ₃	138.4	113.33 bcd	22.20 c	10.65	4.63 d	896.7 d
S ₃ N ₄	138.2	118.87 abc	23.03 abc	110.77	5.30 b	1692.0 a
S ₃ N ₅	140.73	121.33 ab	24.50 a		5.47 a	1364.7 b
LSD 0.05	17.44	8.29	1.48		0.16	206.7
Mean	124.13	107.98	21		4.18	19.32

Here, S₁ = 70 kg ha⁻¹, S₂ = 80 kg ha⁻¹, S₃ = 90 kg ha⁻¹, N₁ = 0 kg ha⁻¹, N₂ = 40 kg ha⁻¹, N₃ = 80 kg ha⁻¹, N₄ = 120 kg ha⁻¹, and N₅ = 160 kg ha⁻¹. Means sharing similar letters within a column are statistically nonsignificant.

enzymes, and nucleic acids. Plants uptake N in dissolved form and partition it into different organs. Nitrogen exerts significant impacts on tillering, stem elongation, heading, cell division, booting, and grain filling. Nitrogen also affects crop morphology [21]. It is the most deficient nutrient in soils, thus required in heavy amounts for cereal and fodder crops [22]. Several factors including soil pH, moisture contents, and temperature significantly affect N losses [23]. However, the application of optimum dose is important to fetch high yield and quality [16]. Higher N application improves forage yield. Green fodder yield of oat was significantly affected by 80 kg N ha⁻¹, and it was higher than control, 40 and 120 kg ha⁻¹ [24]. However, the optimum N dose significantly varies among locations and agroclimatic conditions. Therefore, it is mandatory to optimize the N application dose and seed rate for high forage production.

It was hypothesized that increasing the N dose will significantly differ the forage yield and quality. Similarly, different seed rates would have a significant impact on forage yield and quality of oat. The results will help to optimize seed rate and N doses for oat fodder production in agroclimatic conditions of Dera Ghazi Khan, Pakistan.

2. Materials and Methods

2.1. Experimental Site. The current field study to optimize seed rate and N application rate for oat were conducted at a research farm, Ghazi University, Dera Ghazi Khan, Pakistan, during the winter season, 2015-2016.

2.2. Experimental Details. The experiment was conducted on a fallow field, which was leveled, and fallow cultivation was

TABLE 3: Analysis of variance of different seeding rates, nitrogen doses, and their interactions on forage and dry matter yields, crude fiber, crude protein, and total ash of forage oat.

SOV	DF	SS	MS	P value
<i>Forage yield</i>				
Seed rate (S)	2	338.71	169.356	0.0000**
Nitrogen doses (N)	4	3213.35	803.338	0.0000**
S × N	8	28.89	3.612	0.0151*
<i>Dry matter yield</i>				
Seed rate (S)	2	3.7773	1.8887	0.0008*
Nitrogen doses (N)	4	83.3142	20.8286	0.0000**
S × N	8	4.2604	0.5326	0.0268*
<i>Crude protein</i>				
Seed rate (S)	2	1.2379	0.6189	0.0304*
Nitrogen doses (N)	4	72.2770	18.0692	0.0000**
S × N	8	6.8236	0.8529	0.0003*
<i>Crude fiber</i>				
Seed rate (S)	2	53.324	26.6618	0.0037*
Nitrogen doses (N)	4	226.558	56.6395	0.0000**
S × N	8	97.847	12.2309	0.0111*
<i>Total ash</i>				
Seed rate (S)	2	9.3352	4.66760	0.0000**
Nitrogen doses (N)	4	11.2192	2.80480	0.0000**
S × N	8	4.8808	0.61010	0.0029*

SOV: source of variation, DF: degree of freedom, SS: sum of squares, MS: mean squares, *: significant, NS: nonsignificant.

done. Thereafter, presocking irrigation of 10 cm was applied, and the field was cultivated two times with the help of a cultivator followed by planking when the soil attained a workable moisture regime. The approved oat cultivar for forage production (S-2000) was used in the experiment. Three seed rates, i.e., 70, 80, and 90 kg ha⁻¹, and five N levels (0, 40, 80, 120, and 160 kg ha⁻¹) were included in the study. Seeds were sown in 30 cm-apart rows with the help of a single-row hand drill, and each experimental unit consisted of six lines. The crop was sown during the 2nd week of December 2015. Urea and single super phosphate (SSP) were used as the source of nitrogen and phosphorus, respectively. The whole amount of recommended phosphorus rate (80 kg ha⁻¹) was applied as a basal dose, while N was applied in two splits according to the treatments. The first split of N was applied at the time of sowing, whereas the second split was given with the first irrigation. Three irrigations were given during the entire growth period of the crop. The crop was harvested manually at a ground level with the help of a sickle date.

2.3. Data Collection. Standard procedures were used for data collection which were kept uniform for all treatments. Data relating to germination count (m⁻²), plant height (cm), number of leaves (per plant), number of tillers (m⁻²), leaf area per tiller (cm²), fresh weight (kg m⁻²), dry weight (g m⁻²), green forage yield (tha⁻¹), and dry matter yield (tha⁻¹) were col-

lected. For seed germination, experimental plots were visited daily until the last seed emerged. The number of seeds germinated on the final day of the count was regarded as germination count. The heights of five randomly selected plants from each experimental unit were measured and averaged. The number of tillers from five randomly selected plants in each experimental unit was counted and averaged. The destructive sampling method was used for the determination of fresh and dry biomass. A 1 m² area was harvested and weighed to record fresh forage yield. The harvested sample was dried in an oven at 70°C, and then the dry yield was measured. This yield was then converted to tha⁻¹ by a unitary method. Crude protein (%), crude fiber (%), and total ash (%) were determined by burning a predefined quantity of the plants.

2.4. Economic Analysis. Economics analysis was conducted to determine the economic feasibility of applied treatments. Total and gross incomes were calculated from the total yield of the forage oat. Then the total cost of production was calculated by adding total fixed and total variable costs. Benefit-cost was determined by dividing the gross income by the total cost according to the procedures devised by CIMMYT (1988).

$$\text{Benefit - cost ratio} = \frac{\text{Net income}}{\text{Total expenditure}} \quad (1)$$

2.5. Statistical Analysis. The collected data of all parameters were analyzed by Fisher's analysis of the variance technique, and the LSD test at a 0.05 probability level was applied to compare the significance of treatment means [25].

3. Results

3.1. Germination Count (m⁻²). The germination count of forage oat was significantly affected by different seed rates, while the main effects of the N level were nonsignificant (Table 1). Similarly, the interactive effect of the seed rate and N level was also nonsignificant. The highest germination count was recorded for S₃ (138.77 m⁻²), whereas the lowest plant population (108.42 m⁻²) was noted for S₁ (Table 2). The higher germination count is directly linked to a higher seed rate used.

3.2. Morphological Attributes. The individual and interactive effects of seed rate and N doses significantly altered plant height, number of leaves per plant, leaf area per tiller, and fresh and dry weight (Table 1). The highest plants were observed for S₂N₅ (122.97 cm), which was statistically at par with S₁N₅, S₃N₅, S₃N₄, and S₁N₄. The lowest plant height was observed for S₂N₁ (91.37 cm), S₁N₂ (94.37 cm), S₁N₁ (94.43 cm), and S₁N₃ (96.33 cm). The increase in N unit increased plant height (Table 2).

More number of leaves of forage oat were noted for S₃N₅ (24.50 m⁻²), which was statistically similar to S₂N₅, S₃N₄, and S₂N₄. The lowest numbers of leaves per plant were recorded for S₂N₁, which was statistically similar to S₁N₁, S₁N₂, and S₃N₁ (Table 2).

TABLE 4: Interactive effect of seed rate and nitrogen level on green forage yield, dry matter yield, crude protein, crude fiber, and total ash of forage oat.

Treatments	Green forage yield (t ha ⁻¹)	Dry matter yield (t ha ⁻¹)	Crude protein (%)	Crude fiber (%)	Total ash (%)
<i>Seed rate (S)</i>					
S ₁	38.827 C	19.07 B	8.87 A	27.28 B	7.58 C
S ₂	42.717 B	19.16 B	8.52 A	27.10 B	7.91 B
S ₃	45.517 A	19.73 A	8.88 B	29.49 A	8.67 A
LSD 0.05	0.4	0.16	0.14	0.72	0.14
<i>Nitrogen doses (N)</i>					
N ₁	28.389 E	17.17 D	6.98 E	24.75 C	7.14 C
N ₂	37.978 D	18.57 C	7.82 D	26.76 B	7.93 B
N ₃	43.983 C	19.40 B	8.72 C	27.36 B	8.30 AB
N ₄	50.170 B	20.64 A	9.86 B	29.88 A	8.44 A
N ₅	51.249 A	20.87 A	10.42 A	31.03 A	8.48 A
LSD 0.05	0.51	0.21	0.19	0.92	0.18
<i>S × N</i>					
S ₁ N ₁	25.833 i	16.60 d	7.45 ef	24.55 d	6.57 e
S ₁ N ₂	32.600 g	18.07 c	8.23 d	24.71d	7.02 e
S ₁ N ₃	41.033 ef	19.33 b	8.41 d	27.75 bcd	8.00 cd
S ₁ N ₄	46.667 c	20.57 a	9.80 bc	29.32 abc	7.88 cd
S ₁ N ₅	48.000 c	20.80 a	10.45 ab	30.05 ab	8.45 bc
S ₂ N ₁	29.000 h	16.70 d	5.94 g	20.55 e	6.78 e
S ₂ N ₂	39.667 f	18.23 c	7.22 f	26.22 cd	7.79 d
S ₂ N ₃	43.917 d	19.43 b	9.27 c	27.15 bcd	8.45 bc
S ₂ N ₄	49.923 b	20.63 a	9.93 abc	30.15 ab	8.05 cd
S ₂ N ₅	51.080 b	20.80 a	10.28 ab	31.42 a	8.49 bc
S ₃ N ₁	30.333 h	18.20 c	7.54 ef	29.15 abc	8.05 cd
S ₃ N ₂	41.667 e	19.37 b	8.00 de	29.35 abc	8.99 ab
S ₃ N ₃	47.000 c	19.43 b	8.49 d	27.18 bcd	8.45 bc
S ₃ N ₄	53.920 a	20.90 a	9.85 bc	30.15 ab	9.39 a
S ₃ N ₅	54.667 a	20.73 a	10.54 a	31.62 a	8.49 bc
LSD 0.05	1.84	0.75	0.66	3.29	0.65
Mean	42.35	19.32	8.76	27.95	8.06

Here, S₁ = 70 kg ha⁻¹, S₂ = 80 kg ha⁻¹, S₃ = 90 kg ha⁻¹, N₁ = 0 kg ha⁻¹, N₂ = 40 kg ha⁻¹, N₃ = 80 kg ha⁻¹, N₄ = 120 kg ha⁻¹, and N₅ = 160 kg ha⁻¹. Means sharing similar letters within a column are statistically nonsignificant.

The highest leaf area was recorded for S₂N₅, which was statistically similar to S₃N₄, S₁N₅, S₃N₂, and S₃N₅. The lowest leaf area was observed for S₁N₁, and it was closely related to S₁N₂ and S₁N₃ (Table 2).

3.3. Yield and Quality Attributes. The individual and interactive effects of seed rate and N doses significantly affected forage yield, dry matter yield, crude fiber, crude protein, and total ash in forage oat (Table 3). Overall, these parameters were increased with increasing seed rate and N levels. The highest green forage yield was noted for S₃N₅, which was similar to S₃N₄, S₂N₅, and S₂N₄ (Table 4). The lowest green forage yield was produced by S₁N₁, and it was statistically similar to S₂N₁ and S₃N₁. Kakol et al. (2003) reported that oat plants positively respond to seed rate and N, which improve their growth and forage production. Shukla and Lal (1998) recorded significant differences among 80 and

60 kg phosphors for green forage yield. The highest dry matter yield was observed for S₁N₄, whereas S₁N₁ recorded the lowest dry matter yield (Table 4).

Variation in seed rate and N level significantly affected the crude fiber percentage. The highest crude fiber percentage was observed for S₃N₅, while S₂N₁ resulted in the lowest crude fiber percentage (Table 4).

3.4. Economic Analysis. The interactive effect of seed rate and N doses has a significant impact on variable costs (Table 5) and economics (Table 6). The highest net income and benefit-cost ratio was recorded for S₃N₄, whereas S₁N₁ recorded the lowest net income and benefit-cost ratio, although increasing N doses improved all traits and the highest dose proved superior in this regard. However, the economic analysis revealed that applying higher N doses is not an economic option. Although the highest N dose, i.e.,

TABLE 5: Fixed and variable costs of production for forage oat.

Operation/input	No. of operations/ha	Rate per unit (PKR)	Cost per unit (PKR)
<i>Land preparation</i>			
Ploughing	2	2000 ha ⁻¹	4000 ha ⁻¹
Planking	1	1500 ha ⁻¹	1500 ha ⁻¹
<i>Sowing</i>			
Seed/sowing	*	*	*
Drill sowing		2500 ha ⁻¹	2500 ha ⁻¹
<i>Irrigation</i>			
Irrigation charges	3 irrigations	1000	3000
Labor cost for irrigation	1 man for 3 times	500 per day	1500
<i>Fertilizer</i>			
Nitrogen from urea	*	*	*
Phosphorus from single super phosphate	80 kg	111 kg ⁻¹	8888
Plant protection measures		Weeding	1000
<i>Harvesting</i>			
Labor charges for harvesting	7 men	500 per men	3500
Land rent	6 months	30250 ha ⁻¹	15125
Total fixed cost			41013

*: variable cost of seed, *: variable cost of nitrogen.

TABLE 6: Economics analysis for different seed rates and nitrogen doses used to produce forage oat.

Treatments	Gross income (PKR ha ⁻¹)	Total cost (PKR ha ⁻¹)	Net income (PKR ha ⁻¹)	Benefit : cost ratio
S ₁ N ₁	51666	45213	6453	1.14
S ₁ N ₂	65200	48253	16947	1.35
S ₁ N ₃	82066	51293	30773	1.60
S ₁ N ₄	93334	54333	39001	1.72
S ₁ N ₅	96000	57373	38627	1.67
S ₂ N ₁	58000	45813	12187	1.27
S ₂ N ₂	79334	48853	30481	1.62
S ₂ N ₃	87834	51893	35941	1.69
S ₂ N ₄	99846	54933	44913	1.82
S ₂ N ₅	102160	57973	44187	1.76
S ₃ N ₁	60666	46413	14253	1.31
S ₃ N ₂	83334	49453	33881	1.69
S ₃ N ₃	94000	52493	41507	1.79
S ₃ N ₄	107840	55533	52307	1.94
S ₃ N ₅	109334	58573	50761	1.87

1 USD = 160 PKR. Here, S₁ = 70 kg ha⁻¹, S₂ = 80 kg ha⁻¹, S₃ = 90 kg ha⁻¹, N₁ = 0 kg ha⁻¹, N₂ = 40 kg ha⁻¹, N₃ = 80 kg ha⁻¹, N₄ = 120 kg ha⁻¹, and N₅ = 160 kg ha⁻¹.

N₅, also recorded a higher net income and benefit-cost ratio than other N doses, N₄ recorded the highest net income and benefit-cost ratio (Table 6).

4. Discussion

The higher germination count is directly linked to a higher seed rate used. These results are similar to [26] who recorded the highest number of plants of forage maize with a higher seeding density. The nonsignificant effect of N doses on ger-

mination of forage oat is also reported by Shukla and Lal [27] who also reported nonsignificant results of oat germination percentage when grown with organic or inorganic sources of fertilizers. This might be due to the contribution of N in the growth of oat plants. Zahid et al. [28] concluded that plant height was increased with increasing N doses and farmyard manure. Irfan et al. [29] found a significant difference in the plant height of oat, and these results are also in line with others. Another concluded that the plant height of oat was significantly altered by the split application of N

and potassium. One of them recorded significantly higher plant height (119.58 cm) in forage oat by the application of 80 kg N ha⁻¹.

The higher number of leaves per plant can be owed to the contribution of N in vegetative growth. Similar findings have been reported by Ahmad et al. [30]. Irfan et al. [29] reported higher and lower numbers of leaves of forage oat with the highest and the lowest N application.

The highest number of tillers m⁻² was counted for S₃N₅, which was similar to S₃N₄, S₂N₅, S₃N₃, and S₃N₂. The lowest number of tillers per plant in forage oat was observed for S₁N₁, which was statistically similar to S₂N₁, S₃N₁, and S₁N₂ (Table 2). Metwally et al. [31] concluded that the application of 100 kg ha⁻¹ N significantly enhanced the tillering capacity of forage oat. Jehangir et al. [32] reported that the number of tillers significantly increased with increasing the fertility status of the soil. These results are in line with Ahmad et al. [30] who concluded that 150 kg ha⁻¹ N and 60 kg ha⁻¹ phosphorus produces the highest leaf area of (128 cm²) in forage oat. Jiwang et al. [33] reported that increasing the fertilizer level increases the leaf area. Khandaker and Islam [34] recorded the highest leaf area of forage oat with 120 kg ha⁻¹ N. Tanha [35] observed the highest leaf area in forage maize with 200 kg ha⁻¹ N application.

Fresh and dry weights significantly increased with the increasing seed rate and N level. The highest fresh weight was observed for S₃N₅, which was close to S₃N₄. The lowest fresh weight was observed for S₁N₁. Sharma and Bhunia [36] studied the response of organic and inorganic sources of N and concluded that the inorganic N source produced the highest fresh weight per tiller. Singh et al. [37] reported that the application of farmyard manure significantly increased the fodder yield in maize. Wheed et al. [38] reported that a higher N level increased green forage yield.

Orloff et al. [39] recorded the highest dry fodder yield with 136 kg ha⁻¹ N application.

Crude protein percentage is an important quality parameter, which determined the quality of forage crops. Application of N from lower to higher levels significantly increased crude protein contents; however, crude protein beyond a certain range reduced the forage quality and increases succulence. The highest crude protein was observed for S₂N₅, whereas S₂N₁ resulted in the lowest crude protein. Kumar et al. [40] observed that 80 kg ha⁻¹ N resulted in the maximum crude protein yield and observed a maximum crude protein yield with 120 kg N ha⁻¹. Kumar et al. [41] observed that the application of N up to 80 kg per hectare enhanced the crude protein yield, and a further increase in N decreased the crude protein yield. Khan et al. [42] concluded that crude protein quality may be affected by N application as it is an essential part of protein, chlorophyll, and protoplast. Farooq et al. [43] also reported similar results. These results are in line with [44] who observed higher crude fiber with 150 kg ha⁻¹ N application.

The highest ash percentage was recorded for S₃N₄, and the lowest was observed for S₁N₁ (Table 4). These results are in line with Alajmi et al. [45] who observed a maximum ash percentage with 150 kg ha⁻¹ N application. Saleh et al.

[46] also concluded similar results and reported that increasing N application significantly increased the ash content in forage maize.

5. Conclusion

The results revealed that seed rate and nitrogen doses significantly altered the yield and forage quality of forage oat. It is concluded that forage oat crops should be grown with a seed rate of 90 kg ha⁻¹ and supplemented with 120 kg ha⁻¹ of nitrogen for higher yield, better quality, and more economic returns.

Data Availability

All data is available in the manuscript.

Conflicts of Interest

The authors declare that they have no conflicts of interest.

Acknowledgments

This project was supported by the Researchers Supporting Project number RSP-2022/257, King Saud University, Riyadh, Saudi Arabia.

References

- [1] M. F. Iqbal, M. A. Sufyan, M. M. Aziz, I. A. Zahid, Q. Ghani, and S. Aslam, "Efficacy of nitrogen on green fodder yield and quality of oat (*Avena sativa* L.)," *The Journal of Animal and Plant Sciences (Pakistan)*, vol. 19, no. 2, pp. 82–84.b, 2009.
- [2] H. Karar, M. Amjad Bashir, R. Atalla Alajmi et al., "Farmers' knowledge, perception and management of mango mealy bug, *Drosicha mangiferae* Green (Hemiptera: Monophlebidae), on *Mangifera indica* in Punjab, Pakistan," *Saudi Journal of Biological Sciences*, vol. 28, no. 7, pp. 3936–3942, 2021.
- [3] S. J. Ulysses, *Fertilizers and Soil Fertility*, Reston Publishing Co, Reston, Virginia, 2nd edition, 1982.
- [4] B. Bhatti, "Fodder production in rainfed areas of Punjab," in *Fodder Production in Pakistan*, pp. 113–114, PARC. P, 1992.
- [5] E. F. Thomson, S. Rihawi, and N. Nersoyan, "Nutritive value and yields of some forage legumes and barley harvested as immature herbage, hay and straw in northwest Syria," *Experimental Agriculture*, vol. 26, no. 1, pp. 49–56, 1990.
- [6] A. Hussain, S. Khan, M. U. Mufti, and A. Bakhsh, "Introduction and use of oats cultivars in Pakistan," in *Proceedings of 5th TAPAFON (Temperate Asia Pasture and Fodder Network) meeting/conference held at Renewable Natural Resources Research Center*, pp. 159–166, Bajo (Wangdue-Bhutan), 2002.
- [7] A. R. Chaudhry, *Crop production*, Nation book foundation Islamabad, 1994.
- [8] M. B. Bhatti, A. Hussain, and D. Mohammad, "Fodder production potential of different oat cultivars under two cut system," *Pakistan Journal of Agricultural Research*, vol. 13, pp. 184–190, 2002.
- [9] M. Ibrahim, "Determining forage production potential of maize sown as a mixture with different legumes under different nitrogen applications. Ph. D. Thesis, Dept. of Agron., Univ. of Agric., Faisalabad, Pakistan".

- [10] A. Alipatra, C. K. Kundu, M. K. Mandal, H. Banerjee, and P. Bandopadhyay, "Yields and quality improvement in fodder oats (*Avena sativa* L.) through split application of fertilizer and cutting management," *Journal of Crop and Weed*, vol. 9, no. 2, pp. 193–195, 2013.
- [11] A. Basit, M. Farhan, W. D. Mo et al., "Enhancement of resistance by poultry manure and plant hormones (salicylic acid & citric acid) against tobacco mosaic virus," *Saudi Journal of Biological Sciences*, vol. 28, no. 6, pp. 3526–3533, 2021.
- [12] H. Karar, M. Amjad Bashir, A. Khaliq, M. Jaffar Ali, R. Atalla Alajmi, and D. M. Metwally, "Stink bug *Agonoscelis* spp. (Heteroptera: Pentatomidae) - An emerging threat for seed production in alfalfa crop (*Medicago sativa* L.) and their successful management," *Saudi Journal of Biological Sciences*, vol. 28, no. 6, pp. 3477–3482, 2021.
- [13] D. Abate and T. Wegi, "Determination of optimum seed and fertilizer rate for fodder oat in Bale Highland Southeastern Ethiopia," *International Journal of Soil and Crop Sciences*, vol. 2, no. 7, pp. 73–76, 2014.
- [14] B. S. Reddy, *Physiological Studies on Oat (Avena sativa) Varieties under Two Cutting Regimes*, M. Sc. (Agri.) Thesis, Govind Ballabh Pant University of Agriculture and Technology, Pantnagar, 1976.
- [15] N. B. Kakol, S. C. Alagundagi, and S. V. Hosamani, "Effect of seed rate and nitrogen levels on forage yield and quality of oat," *Indian Journal of Animal Nutrition*, vol. 20, no. 2, pp. 149–154, 2003.
- [16] T. Jan and M. T. Jan, "Effect of sowing dates and seed rates on the forage yields of oats," *Sarhad Journal of Agriculture (Pakistan)*, vol. 10, no. 5, pp. 473–476, 1994.
- [17] S. K. Das, K. L. Sharma, N. Sharma, and K. Srinivas, "Soil fertility management and fertilizer use," in *Sustainable Development of Dry Land Agriculture in Ind*, R. P. Singh, Ed., pp. 95–117, Scientific Publishers, Jodhpur, India, 1995.
- [18] R. A. Olson and D. J. Sander, "Corn production," in *Corn and Corn Improvement*, G. F. Sprague and J. W. Dudley, Eds., pp. 639–686, American Society of Agronomy/Crop Sci. Society of America/Soil Sci. Society of America, Madison, 2015.
- [19] F. Zapata and O. V. Cleenput, "Recovery of ¹⁵N-labelled fertilizer by sugar beet/spring wheat and winter rye/sugar beet cropping sequences," *Fertilizer Research*, vol. 8, no. 3, pp. 269–278, 1986.
- [20] M. Worku, B. E. Friesen, O. A. Diallob, and W. J. Horst, "Nitrogen uptake and utilization in contrasting nitrogen efficient tropical maize hybrids," *Crop Science*, vol. 47, no. 2, pp. 519–528, 2007.
- [21] R. A. K. Amanullah and S. K. Khalil, "plant density and nitrogen Effects on Maize phenology and Grain yield," *Journal of Plant Nutrition*, vol. 32, no. 2, pp. 246–260, 2009.
- [22] J. L. Havlin, J. D. Beaton, S. L. Tisdale, and W. L. Nelson, *Soil Fertility and Fertilizers: An Introduction to Nutrient Management*, Pearson Education Inc., India, 6th edition, 1999.
- [23] B. Malakar, S. Mondal, P. Bandopadhyay, and C. K. Kundu, "Response of forage oat to nitrogen and phosphorous fertilizer in the new alluvial zone of West Bengal," *Journal of crop and weed*, vol. 5, no. 2, pp. 36–38, 2009.
- [24] N. Ratan, U. N. Singhand, and H. C. Pandey, "Yield and quality of oat as influenced by nitrogen and varieties in Bundelkhand region U. P. India," *Agricultural Science Research Journal*, vol. 6, no. 1, pp. 27–30, 2016.
- [25] R. Singh, B. R. Sood, V. K. Sharma, N. S. Rana, and R. Singh, "Effect of cutting management and nitrogen on forage and seed yields of oat (*Avena sativa* L.)," *Indian Journal of Agronomy*, vol. 43, no. 2, pp. 362–366, 1998.
- [26] M. Ayub, R. Ahmad, M. A. Nadeem, and R. M. A. Khan, "Effect of different levels of nitrogen and seed rates on growth, yield and quality of maize fodder," *Pakistan Journal of Agricultural Sciences*, vol. 40, pp. 140–143, 2003.
- [27] N. P. Shukla and M. Lal, "Response of oat (*Avena sativa* L.) to nitrogen in relation to moisture conservation techniques under restricted irrigations," *Indian Journal of Agronomy*, vol. 39, no. 2, pp. 229–232, 1994.
- [28] M. S. Zahid, Z. A. Gurmani, M. Imran, and M. Bashir, "Effect of fertilizer dose on yield and yield components of fodder oat under rainfed condition of pothwar region," *J. Agric*, vol. 43, no. 3, 2005.
- [29] M. Irfan, M. Ansar, A. Sher, A. Wasaya, and A. Sattar, "Improving forage yield and morphology of oat varieties through various row spacing and nitrogen application," *JAPS: Journal of Animal & Plant Sciences*, vol. 26, no. 6, pp. 1718–1724, 2016.
- [30] A. H. Ahmad, A. Wahid, F. Khalid, N. Fiaz, and M. S. I. Zamir, "Impact of organic and inorganic sources of nitrogen and phosphorus fertilizers on growth, yield and quality of forage oat (*Avena sativa* L.)," *Cercetari Agronomic in Moldova*, vol. 44, no. 3, 2011.
- [31] D. M. Metwally, S. A. Albasyouni, I. A. H. Barakat et al., "Prevalence rate and molecular characteristics of *Oestrus ovis* L. (Diptera, Oestridae) in sheep and goats from Riyadh, Saudi Arabia," *Animals*, vol. 11, no. 3, p. 689, 2021.
- [32] I. A. Jehangir, M. H. Khan, F. Rasool et al., "Effect of sowing dates, fertility levels and cutting managements on growth, yield and quality of oats (*Avena sativa* L.)," *African Journal of Agricultural Research*, vol. 8, no. 7, pp. 648–651, 2013.
- [33] Z. Jiwang, H. Changhao, W. Kongjun, D. Shuting, and L. Peng, "Effects of plant density on forage nutritive value of whole plant corn," *Agricultural Sciences in China*, vol. 3, no. 11, pp. 842–848, 2004.
- [34] Z. H. Khandaker and M. M. Islam, "Effect of nitrogen fertilization and stage of maturity on yield and quality of fodder maize," *Bangladesh Journal of Animal Science (Bangladesh)*, vol. 7, no. 1-2, pp. 47–53, 1988.
- [35] I. Y. Tanha, *Yield and Quality Response Od Forage Maize as Affected by Different Nitrogen Levels and Seeding Rates*, M. Sc. Thesis, Dept. Agron. Univ. Agric, Faisalabad, Pakistan, 2009.
- [36] S. K. Sharma and S. K. Bhunia, "Response of oat to cutting management, method of sowing and nitrogen," *Indian Journal of Agronomy*, vol. 46, no. 3, pp. 563–567, 2001.
- [37] V. Singh, J. S. Khokar, Y. P. Joshi, and S. S. Verma, "Effect of nitrogen, seed rates and methods of sowing on forage oat (*Avena sativa* L.)," *Forage Research*, vol. 15, no. 1, pp. 29–32, 1989.
- [38] A. Wheed, W. Ahmad, M. A. Shehzad, and M. Shahid, "Nitrogen and phosphorous impact on forage oat (*Avena sativa* L.) growth, yield and its quality attributes," *Pakistan Journal of Agricultural Sciences*, vol. 49, no. 4, pp. 473–479, 2012.
- [39] E. Johansson, M. L. Prieto-Linde, and J. Ö. Jönsson, "Effects of wheat cultivar and nitrogen application on storage protein composition and breadmaking quality," *Cereal Chemistry Journal*, vol. 78, no. 1, pp. 19–25, 2001.

Retraction

Retracted: Synergistic Effect of Conventional Medicinal Herbs against Different Pharmacological Activity

BioMed Research International

Received 8 January 2024; Accepted 8 January 2024; Published 9 January 2024

Copyright © 2024 BioMed Research International. This is an open access article distributed under the Creative Commons Attribution License, which permits unrestricted use, distribution, and reproduction in any medium, provided the original work is properly cited.

This article has been retracted by Hindawi following an investigation undertaken by the publisher [1]. This investigation has uncovered evidence of one or more of the following indicators of systematic manipulation of the publication process:

- (1) Discrepancies in scope
- (2) Discrepancies in the description of the research reported
- (3) Discrepancies between the availability of data and the research described
- (4) Inappropriate citations
- (5) Incoherent, meaningless and/or irrelevant content included in the article
- (6) Manipulated or compromised peer review

The presence of these indicators undermines our confidence in the integrity of the article's content and we cannot, therefore, vouch for its reliability. Please note that this notice is intended solely to alert readers that the content of this article is unreliable. We have not investigated whether authors were aware of or involved in the systematic manipulation of the publication process.

Wiley and Hindawi regrets that the usual quality checks did not identify these issues before publication and have since put additional measures in place to safeguard research integrity.

We wish to credit our own Research Integrity and Research Publishing teams and anonymous and named external researchers and research integrity experts for contributing to this investigation.

The corresponding author, as the representative of all authors, has been given the opportunity to register their agreement or disagreement to this retraction. We have kept a record of any response received.

References

- [1] H. Ali, D. Ali, B. O. Almutairi et al., "Synergistic Effect of Conventional Medicinal Herbs against Different Pharmacological Activity," *BioMed Research International*, vol. 2022, Article ID 7337261, 7 pages, 2022.

Research Article

Synergistic Effect of Conventional Medicinal Herbs against Different Pharmacological Activity

Huma Ali ¹, Daoud Ali,² Bader O. Almutairi,² Gokhlesh Kumar,³
Gizachew Assefa Karga ⁴, Chandran Masi ⁵ and Venkatesa Prabhu Sundramurthy ⁶

¹Department of Chemistry Maulana Azad National Institute of Technology, Bhopal, India

²Department of Zoology, College of Science, King Saud University, P.O. Box 2455, Riyadh 11451, Saudi Arabia

³Clinical Division of Fish Medicine, University of Veterinary Medicine Vienna, 1210 Vienna, Austria

⁴Addis Ababa Science and Technology University, Addis Ababa, Ethiopia

⁵Bioprocess and Biotechnology, Center of Excellence, Addis Ababa Science and Technology University, P.O. Box 16417, Addis Ababa, Ethiopia

⁶Department of Chemical Engineering, College of Biological and Chemical Engineering, Addis Ababa Science and Technology University, P.O. Box 16417, Addis Ababa, Ethiopia

Correspondence should be addressed to Gizachew Assefa Karga; gizachew.assefa@aastu.edu.et

Received 26 May 2022; Accepted 17 June 2022; Published 29 June 2022

Academic Editor: Hafiz Ishfaq Ahmad

Copyright © 2022 Huma Ali et al. This is an open access article distributed under the Creative Commons Attribution License, which permits unrestricted use, distribution, and reproduction in any medium, provided the original work is properly cited.

Triticum aestivum (Family: Poaceae), *Ocimum sanctum* (Family: Lamiaceae), and *Tinospora cordifolia* (Family: Menispermaceae) are commonly known as wheatgrass, tulsi, and giloy, respectively, which are the plants used as medicines for the treatment of various diseases. All three medicinal plants possess phenolic compounds with other important chemical constituents such as polysaccharides, aliphatic compounds, and alkaloids. The extract of these plants has been prepared and investigated for antioxidant, total phenolic content, total flavonoid content, and antimicrobial study in order to discover potential sources for new pharmaceutical formulations. To determine the antioxidant activity, a free radical scavenging assay for 2,2-diphenyl-1-picrylhydrazyl (DPPH) and hydrogen peroxide was performed using ascorbic acid as the standard. The R^2 value of the prepared extract was found to be 0.9964 and 0.990 in DPPH and hydrogen peroxide scavenging activity, respectively. The phenolic and flavonoid content was found to be 87.50 $\mu\text{l/ml}$ and 58.00 $\mu\text{l/ml}$, respectively. The diffusion method was used to screen the antimicrobial activity of the prepared extract sample against various microorganisms. This extract showed better results for antioxidant and antimicrobial activity.

1. Introduction

Multidrug therapy is a useful method that focuses on inhibiting or destroying harmful agents (such as cancer cells or infections) as well as activating human body defense or healing mechanisms. It is the result of the progressive abandonment of the previously held dogma of monodrug therapy; for decades, pharmacological research was predicated on the discovery of a single active principle [1]. In terms of phytotherapy research, traditional Chinese medicine, Ayurveda,

and traditional Western phytomedicines have just recently begun to be scientifically validated and valued. Furthermore, over the last 20 years, the use of conventional drugs in combination with complementary and alternative medicine (CAM) has increased worldwide, including not just homeopathy, naturopathy, chiropractic, and energy medicine but also ethnopharmacology and phytotherapy [2]. Many diseases now have a complicated aetiology that could be treated more effectively with a drug combination strategy rather than a single administration. In Western countries,

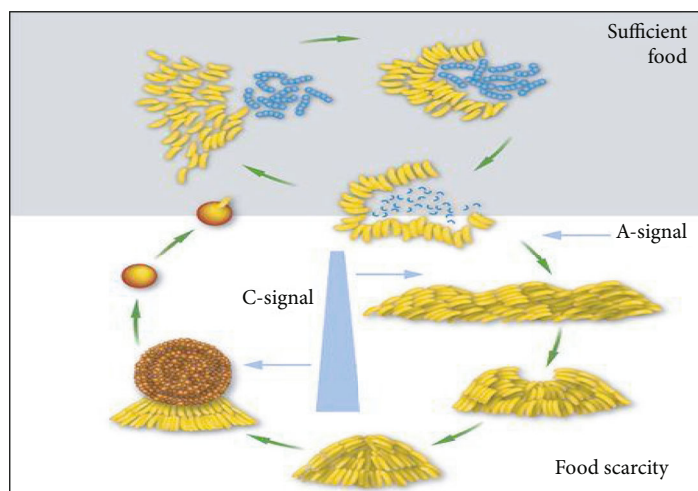


FIGURE 1: *Myxococcus xanthus*: synergy by cooperation.

efficient multidrug therapy is routinely used to treat multifactorial or complicated disorders (e.g., cancer, hypertension, metabolic and inflammatory diseases, acquired immune deficiency syndrome (AIDS), and infections) [3].

Synergistic effects are the combined effects of at least two drugs that have a greater influence than either of them could have had individually. It is what happens when chemical substances or biological structures interact, resulting in a larger overall effect than the sum of their separate effects. Skin damage caused by combining tobacco smoke and UV radiation is more noticeable than tobacco smoke alone or UV radiation alone, as an example of synergistic effects. The liver is harmed by both carbon tetrachloride and ethanol (ethyl liquor) [4]. When used combined, they cause more serious liver damage than the sum of their individual effects on the liver. Barbiturate medications can have more harmful effects on the central nervous system (CNS) when combined with general anaesthetics, alcohol (acute consumption), narcotic analgesic (pain reliever), and other sedative-hypnotic agents (by causing CNS depression), when doctors use ampicillin and gentamicin to treat bacterial heart infections. This is done because the two antimicrobials target different parts of the bacteria, and combining them destroys the microscopic organisms faster, allowing for speedier recovery. Another example of synergism is the treatment of cancer. Chemotherapy and radiation therapy are often administered to cancer patients. They work to halt cancer cell proliferation by focusing on distinct aspects of the replicating process [5].

Social insects are an example of synergy in ecology since they have diverse responsibilities and classes in their colony. Chemical signals picked up by their antennae are the primary means by which they communicate with one another. *Colobopsis explodens*, for example, exhibits an intriguing trait known as autothysis. While wrapped around their victim, these ants will spontaneously erupt (thus the name). This suicidal gesture is a desperate attempt to protect their nest. Soldier termites will rupture their bodies to function as a roadblock to tunnels, preventing invaders from entering their nest, which is known as autothysis [6, 7].

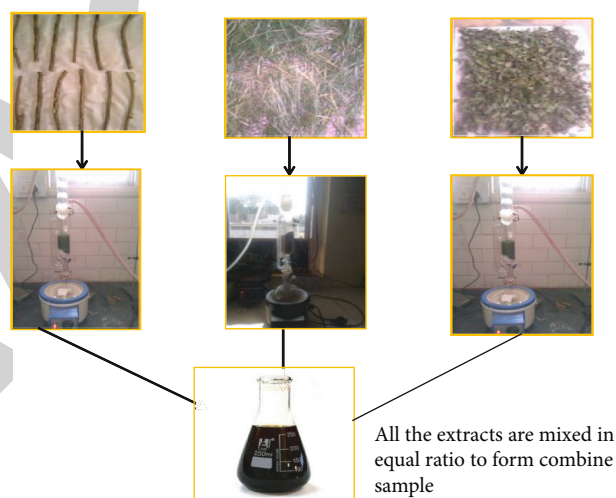


FIGURE 2: Flowchart showing preparation of combined sample of extract.

Myxococcus xanthus, a predatory myxobacterial species, exhibits cooperative behaviour that leads to synergism. *M. xanthus* is a bacterium that feeds on other bacteria in the soil. Through the soil, they create a cooperative hunting group (colony). As they come into contact with bacteria and feed on it, they emit digestive enzymes. They can feed a much larger prey and generate considerably more digestive enzymes in colonies than they do individually, which has the disadvantage of being distributed through the soil [8, 9] (Figure 1).

Pest synergy is defined as the presence of two or more parasites in the same host. As an example, the presence of two different types of parasitic worms would result in synergistic negative effects that are significantly bigger than the impacts of each individual parasitic worm. As a result, the impact is proportional to the density. Even in infection, this is visible. The host that harbours pathogenic bacteria or viruses may or may not produce symptoms of infection, as the impact of the pathogens' presence is determined by the size or population density of the pathogens [10].

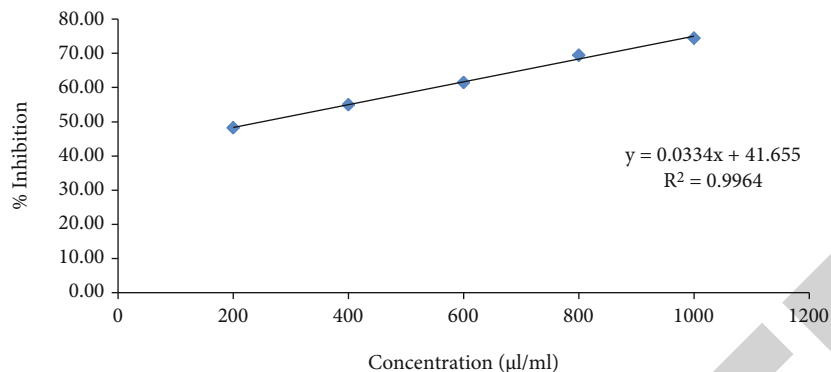


FIGURE 3: Effect of ascorbic acid for antioxidant activity using DPPH as free radical scavenging agent.

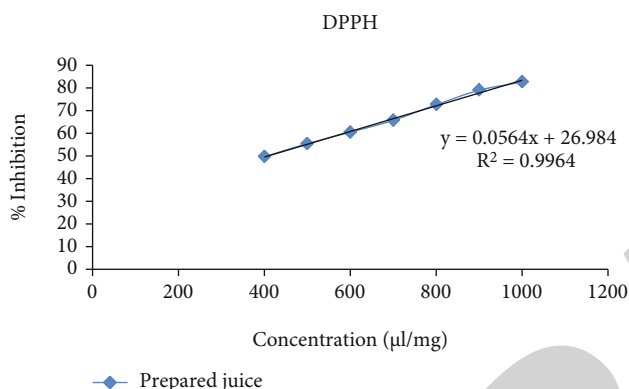


FIGURE 4: Effect of prepared extract sample for antioxidant activity using DPPH as free radical scavenging agent.

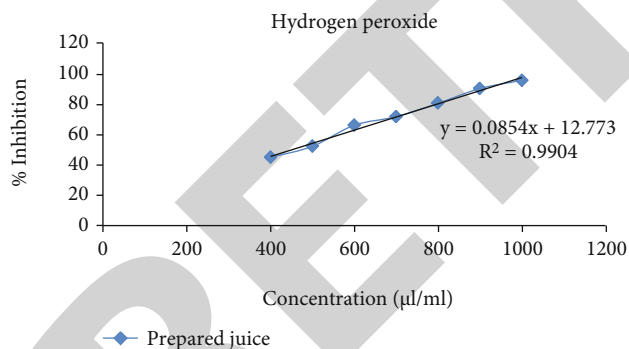


FIGURE 5: Effect of prepared extract sample for antioxidant activity using H₂O₂ as free radical scavenging agent.

TABLE 1: Effect of ascorbic acid for antioxidant activity using DPPH as free radical scavenging agent.

% inhibition	Intercept (C)	Slope (M)	IC ₅₀ (µl/ml)
50	41.655	0.033	253.03

Since ancient times, we have used plants as major sources of medicines and antidotes. Compounds derived from plants (i.e., phytochemicals) are an enormous interest of researchers as natural alternatives to synthetic or chemical-based compounds [11]. The Indian System of Medicine is based on the use of plant extracts to treat various

TABLE 2: Effect of prepared extract sample for antioxidant activity using DPPH as free radical scavenging agent.

% inhibition	Intercept (C)	Slope (M)	IC ₅₀ (µg/ml)
50	26.984	0.0564	435.91

TABLE 3: Effect of prepared extract sample for antioxidant activity using H₂O₂ as free radical scavenging agent.

% inhibition	Intercept (C)	Slope (M)	IC ₅₀ (µg/ml)
50	12.773	0.0854	408.08

diseases. The Indian subcontinent features a diverse flora and fauna in a relatively small geographic region due to topography, altitude, and climate changes [12]. It therefore also contains an impressive amount of medicinal plants. Over 3000 plant species have medicinal properties in India. Most of the wild varieties found here are rich in medicinal properties like antibacterial, antiviral, antihelminthic, anticancer, sedative, laxative, cardiotoxic, and diuretic. According to the World Health Organization (WHO), any plant that possesses therapeutic (curative) properties or exerts a beneficial pharmacological (relating to drugs) effect on the animal body is called a medicinal plant [13].

It has now been discovered that the pharmacological activity (i.e., drug-like activity) of a plant is because they can naturally synthesize secondary metabolites (small organic molecules which are unnecessary for their growth, development, or reproduction), like oils, glycosides, vitamins, alkaloids, and tannins. Metabolite plants produce a vast range of organic substances that can be divided into two categories: primary and secondary metabolites. Primary metabolites, unlike secondary metabolites, play a direct role in normal growth, development, and reproduction. Ethanol, lactic acid, and some amino acids are all examples of primary metabolites. Secondary metabolites have complex structures and extraordinary concentrations in their cells [14]. They are unique to a specific species. They are identified by highly specific actions within or outside the cells. They are often produced as by-products of primary metabolism, perhaps to deal with excess metabolic compounds and play an important role in plant defense. Thousands of plants worldwide are used to cure various diseases, like cancer and

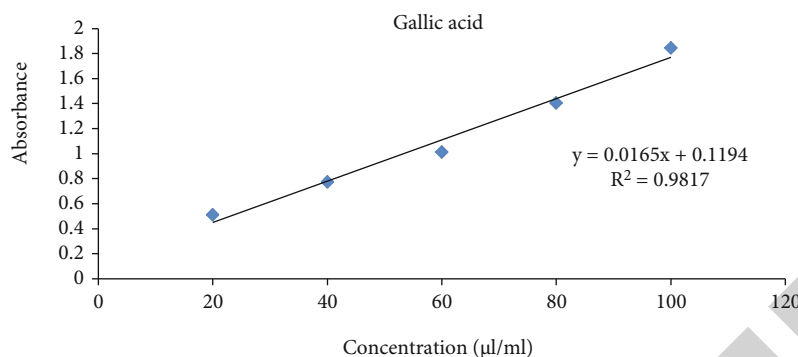


FIGURE 6: Standard curve of gallic acid.

TABLE 4: Total phenolic content of prepared extract sample.

Extract sample ($\mu\text{l/ml}$)	Absorbance	Gallic acid equivalent ($\mu\text{l/ml}$)
1000	1.51	87.50

many chronic diseases, including cardiovascular diseases (diseases related to the heart and circulatory system). Traditional medicinal plants contain antiviral properties and are used to treat viral infections in both animals and humans [15].

2. Materials and Methods

2.1. Plant Material and Preparation of Combined Sample of Extract. 25 g grass of *Triticum aestivum* (Poaceae), 15 g stem of *Tinospora cordifolia* (Menispermaceae), and 10 g of leaves of *Ocimum sanctum* (Labiatae) were collected from a botanical garden of Bhopal, Madhya Pradesh, India, and authenticated. Plant materials were washed, dried, powdered, and then extracted by using solvent methanol and acetone in the ratio of 70:30, ethyl acetate and acetone, respectively, for 24 hours. 50 ml of each extract was mixed to form a combined sample of extract (Figure 2).

2.2. Chemicals. Sigma Chemical Co. provided the 2,2-diphenyl-1-picrylhydrazyl (DPPH), Folin-Ciocalteu reagent, ascorbic acid and gallic acid, and sodium nitrite (L-AA) (St. Louis, MO, USA). Other chemical reagents were available commercially and were of analytical quality.

2.3. Screening of Antioxidant Activity of Combined Sample of Extract

2.3.1. 2,2-Diphenyl-2-picryl-hydrazyl (DPPH) Radical Scavenging Assay. The delocalization of the extra electron above the molecule as a whole distinguishes the DPPH molecule as an established free radical. The molecules then do not dimerise, as they would with mainly more free radicals. The deep violet colour owes to delocalization in ethanol solution, which is characterised by an absorption band at about 517 nm [16].

Different concentrations of combined sample of extract were arranged for DPPH radical scavenging activity. The

dilutions (400 to 1000 l/ml) were then varied with 0.5 ml DPPH solution and incubated for 30 minutes in the dark at room temperature. Using the formula below, the % inhibition test was calculated. Using distilled water as a blank, absorbance was measured at 517 nm [17, 18].

$$\% \text{inhibition of DPPH radical} = \frac{\text{Control} - (\text{sample with DPPH} - \text{sample without DPPH})}{\text{Control}} \times 100. \quad (1)$$

2.3.2. Hydrogen Peroxide Radical Scavenging (H_2O_2) Assay. Certain variations were used to test the ability of combined sample of extract to scavenge hydrogen peroxide. At varying concentrations of aq. arranged extract (400 to 1000 l/ml), 0.5 ml of hydrogen peroxide solution made in phosphate buffer saline with a pH of 7.4 was added. After 10 minutes, the absorbance was measured at 230 nm against a blank solution containing phosphate buffer but no hydrogen peroxide. For background subtraction, a single blank sample was used for each concentration. The absorbance of hydrogen peroxide without the extract sample was measured at 230 nm as a control. The following formula was used to compute the % inhibitory activity. As a standard, gallic acid (10-100 g/ml) was used [19].

$$\% \text{inhibition of } \text{H}_2\text{O}_2 \text{ radical} = \frac{\text{Control} - (\text{sample with } \text{H}_2\text{O}_2 - \text{sample without } \text{H}_2\text{O}_2)}{\text{Control}} \times 100. \quad (2)$$

2.3.3. Total Flavonoid Content (TFC). Flavonoids can scavenge virtually all known ROS depending on their structure [20]. TFC was performed using a 1 l/ml extract concentration and rutin as a reference. The absorbance of a mixture was measured at 510 nm versus produced water as a blank using the method of Zou et al. [21].

2.3.4. Total Phenolic Content (TPC). The total phenolic content of the combined sample of extract was determined using the Folin-Ciocalteu reagent, as described by McDonald et al. As a control, gallic acid was utilised [22].

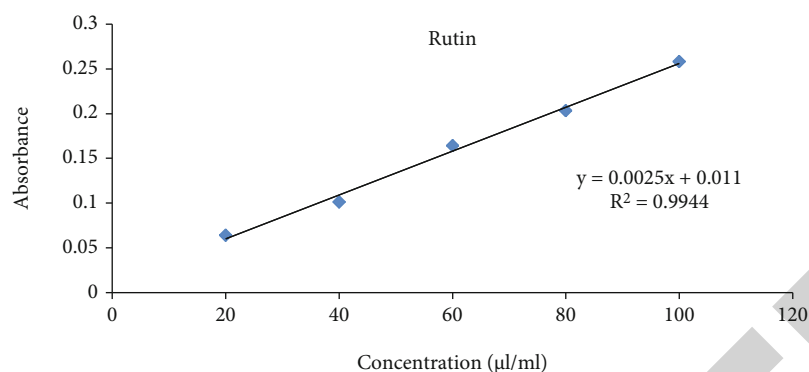


FIGURE 7: Standard curve of rutin.

TABLE 5: Total flavonoid content of the prepared extract.

Extract (µl/ml)	Absorbance	Rutin equivalent (µl/ml)
1000	0.156	58.00

2.4. Screening of Antimicrobial Activity of Combined Sample of Extract

2.4.1. Test Microorganisms. The bacterial strains *Escherichia coli* (MTCC No. 1698), *Proteus* (MTCC No. 658), *Staphylococcus aureus* (MTCC No. 9886), *Staphylococcus cohnii* (MTCC No. 10219), and *Klebsiella pneumoniae* (MTCC No. 3040) were selected based on their scientific and medicinal importance. All the strains were purchased from the Institute of Microbial Technology, Chandigarh, and used for evaluating antimicrobial activity.

2.4.2. Growth Media Preparation. Nutrient agar for bacterial strains was prepared according to the following standard procedure.

2.4.3. Nutrient Agar

(1) **Purpose.** Nutrient agar is a nutrient agar that can be used to grow a wide range of nonfastidious bacteria. It was created in response to a demand for a standardized media for the study of water and wastewater, dairy products, and diverse meals.

(2) **Method for Preparation.** In 250 ml filtered water, dissolve 6 g of the powder. Boil for 1 minute with frequent agitation to completely dissolve the powder. Autoclave for 15 minutes at 121°C. Cool to 45-50 degrees Celsius. Fill sterile 20 ml glass universal tubes with 15-20 ml of the supplied media. Allow thirty minutes for the tubes to freeze before resting them leaning at 30-60°C to achieve the slope effects. The sterility of the media was confirmed by incubating it at 37°C for 24 hours and then storing it at 40°C for up to two weeks.

Composition of nutrient agar media used was as follows:

- (i) Peptone: 5 g/l
- (ii) Beef extract: 1.50 g/l

(iii) Yeast extract: 1.50 g/l

(iv) Sodium chloride: 5.0 g/l

(v) Distilled water: 1000 ml

2.4.4. Determination of Antimicrobial Activity. The nutrient agar media was sterilised by autoclaving for 15 minutes at 121°C and 15 pounds of pressure. Petri dishes were filled with sterile media. A 5 mm diameter cork bearer was used to bore the cemented plates. The antimicrobial experiments were conducted on plates having wells. Antibacterial activity of 0.1 ml of the above produced combined sample of extract at varied concentrations of 7%, 5%, 3%, and 1% was tested against Gram-positive *S. aureus* and *S. cohnii* and Gram-negative *E. coli*, *Proteus*, and *K. pneumoniae*. The well diffusion method [23] was used to demonstrate this.

The streak plate method was used to inoculate the prepared culture plates with several bacteria strains. With a 6 mm cork borer, wells were drilled into the medium surface. Using a sterile syringe, the various samples were poured into the well. For bacterial activity, the plates were incubated at 37°C for 24 hours. Each concentration of the several samples was put to the test against a different microbe. The zone of inhibition was estimated by adding the well diameter to the diameter of the inhibition zone around the well (in mm). The average values of the readings were calculated in four separate fixed directions.

3. Results

3.1. Antioxidant Activity. Line of regression was found to be $y = 0.0564x + 26.984$ (3) and $y = 0.0854x + 12.773$ (4) which revealed IC₅₀ to be 435.91 and 408.08 µl/ml in the above prepared extract sample for 1,1-diphenyl-2-picryl-hydrazyl (DPPH) radical and hydrogen peroxide (H₂O₂) scavenging assay, respectively. It was observed that inhibition of DPPH and H₂O₂ was increasing continuously. Thus, from 400 µl/ml to 1000 µl/ml, the R² value was found to be 0.9964 and 0.9904, respectively, which could be considered as the best fit one. Degradation of H₂O₂ showed the decline in absorbance of H₂O₂ radical at 230 nm caused by reaction between antioxidants present in the prepared extract and free radical (Figures 3–5 and Tables 1–3).

TABLE 6: Zone of inhibition at different concentrations of prepared extract sample against different microorganism.

Conc.	Prepared extract sample Zone of inhibition mm in diameter (mean \pm SD)				
	<i>Escherichia coli</i>	<i>Proteus</i>	<i>Staphylococcus aureus</i>	<i>Staphylococcus cohnii</i>	<i>Klebsiella pneumoniae</i>
7%	16.54 \pm 0.32	21.54 \pm 0.35	20.78 \pm 0.49	19.38 \pm 0.21	22.45 \pm 0.26
5%	16.09 \pm 0.21	19.87 \pm 0.28	19.45 \pm 0.43	18.76 \pm 0.32	21.65 \pm 0.87
3%	15.67 \pm 0.60	18.98 \pm 0.19	18.23 \pm 0.62	17.91 \pm 0.76	19.98 \pm 0.54
1%	14.12 \pm 0.98	18.03 \pm 0.16	17.11 \pm 1.45	17.01 \pm 2.43	18.54 \pm 0.89

The total phenols were expressed as $\mu\text{l/ml}$ gallic acid equivalent using the standard curve equation: $y = 0.016x + 0.119$, $R^2 = 0.981$ (5). Figure 6 shows the variation of mean absorbance with concentration of gallic acid. Table 4 shows the contents of total phenols that were measured by Folin-Ciocalteu reagent in terms of gallic acid equivalent. The phenolic content was found to be 87.500 $\mu\text{l/ml}$.

The total flavonoids were expressed as $\mu\text{g/mg}$ rutin equivalent using the standard curve equation: $y = 0.002x + 0.011$, $R^2 = 0.994$ (6). Figure 7 shows the variation of mean absorbance with concentration of rutin. Table 5 shows the contents of flavonoid in terms of rutin equivalent that was found to be 58.00 $\mu\text{l/ml}$.

3.2. Antimicrobial Activity. The zone of inhibition obtained in the present study was mentioned in mean \pm SD. The antibacterial activity of the prepared extract sample of different concentration was analyzed against different bacterial strains. The better activity was observed in this combined sample of extract against different microorganism (Table 6).

4. Discussion

1,1-Diphenyl-2-picrylhydrazyl (DPPH), is a type of established organic radical. The DPPH oxidative assay is used worldwide in the quantification of antioxidant activity. The ability of natural reagents to scavenge the DPPH radical can be stated as its extent of antioxidation capability [24]. The colour of an alcoholic solution of DPPH is deep purple, with an absorption peak at 517 nm that fades when the radical scavenger is present in the immediate system and when the odd electron of the nitrogen in DPPH is paired [25]. The produced extract was tested for linear inhibition of DPPH in the concentration range of 400-1000 g/ml in this study.

Several oxidase enzymes and activated phagocytes produce hydrogen peroxide *in vivo*, and it is known to have a role in the death of diverse tissues. There is growing evidence that hydrogen peroxide can operate as a messenger molecule in the creation and activation of numerous inflammatory mediators, either directly or indirectly via its reduction product, OH $^-$ [26]. When a scavenger is treated with H $_2$ O $_2$, the loss of H $_2$ O $_2$ can be evaluated using a peroxidase test method. The prepared combined sample of extract was evaluated in this study to see if it had considerable hydrogen peroxide scavenging capability.

Phenolic compounds are a group of antioxidant agents which acts as free radical terminators. Estimation of the total

phenolic content revealed that the prepared extract possesses good total phenolic and flavonoid content. Total phenol content was estimated on the basis of gallic acid. Results are mentioned as gallic acid equivalent (GAE). Total flavonoid was expressed in rutin equivalent (RE). Prepared extract showed positive results against all microorganisms. These findings are due to the synergistic effect of individual extract of *Triticum aestivum*, *Ocimum sanctum*, and *Tinospora cordifolia*.

5. Conclusion

According to the findings of this study, the above-mentioned combined sample of extract has the potential to be used as medication because it contains antioxidant and antimicrobial properties. To fully validate the established claim, additional knowledge of contemporary pharmaceutical techniques such as extraction and separation of active chemical constituents is required. In order to determine its position in medical claims, additional, well-controlled double-blind trial exams are required to reconsider the efficacy and side effects.

Data Availability

The original contributions presented in the study are included in the article; further inquiries can be directed to the corresponding author.

Conflicts of Interest

The authors declare that they have no conflicts of interest.

Authors' Contributions

HA and DA were responsible for conceptualization; HA was responsible for data curation; HA and DA were responsible for formal analysis; BOA was responsible for funding acquisition; HA and DA were responsible for investigation; HA and DA were responsible for methodology; HA and BOA were responsible for project administration; DA, GK, CM, VPS, and GAK were responsible for software; HA and DA were responsible for supervision; HA was responsible for validation; HA was responsible for writing—original draft; DA, GK, CM, VPS, BOA, and GAK were responsible for writing—review and editing.

Retraction

Retracted: Nutrigenomic Interventions to Address Metabolic Stress and Related Disorders in Transition Cows

BioMed Research International

Received 8 January 2024; Accepted 8 January 2024; Published 9 January 2024

Copyright © 2024 BioMed Research International. This is an open access article distributed under the Creative Commons Attribution License, which permits unrestricted use, distribution, and reproduction in any medium, provided the original work is properly cited.

This article has been retracted by Hindawi, as publisher, following an investigation undertaken by the publisher [1]. This investigation has uncovered evidence of systematic manipulation of the publication and peer-review process. We cannot, therefore, vouch for the reliability or integrity of this article.

Please note that this notice is intended solely to alert readers that the peer-review process of this article has been compromised.

Wiley and Hindawi regret that the usual quality checks did not identify these issues before publication and have since put additional measures in place to safeguard research integrity.

We wish to credit our Research Integrity and Research Publishing teams and anonymous and named external researchers and research integrity experts for contributing to this investigation.

The corresponding author, as the representative of all authors, has been given the opportunity to register their agreement or disagreement to this retraction. We have kept a record of any response received.

References

- [1] F.-u. Hassan, A. Nadeem, M. Javed et al., “Nutrigenomic Interventions to Address Metabolic Stress and Related Disorders in Transition Cows,” *BioMed Research International*, vol. 2022, Article ID 2295017, 17 pages, 2022.

Review Article

Nutrigenomic Interventions to Address Metabolic Stress and Related Disorders in Transition Cows

Faiz-ul Hassan ¹, Asif Nadeem ², Maryam Javed ³, Muhammad Saif-ur-Rehman,¹
Muhammad Aasif Shahzad,⁴ Jahanzaib Azhar,² and Borhan Shokrollahi ⁵

¹Institute of Animal and Dairy Sciences, University of Agriculture, Faisalabad, Pakistan

²Department of Biotechnology, Virtual University of Pakistan, Lahore, Pakistan

³Institute of Biochemistry & Biotechnology, University of Veterinary and Animal Sciences, Lahore, Pakistan

⁴Hillandale Farms, Gettysburg Lp., 3910 Oxford Road Gettysburg, PA 17325, USA

⁵Department of Animal Science, Sanandaj Branch, Islamic Azad University, Sanandaj, Iran

Correspondence should be addressed to Borhan Shokrollahi; borhansh@iausdj.ac.ir

Received 6 April 2022; Accepted 23 May 2022; Published 11 June 2022

Academic Editor: Faheem Ahmed Khan

Copyright © 2022 Faiz-ul Hassan et al. This is an open access article distributed under the Creative Commons Attribution License, which permits unrestricted use, distribution, and reproduction in any medium, provided the original work is properly cited.

For dairy cattle, the period involving a shift from late pregnancy to early lactation termed transition or periparturient is an excruciating phase. Health-related disorders are likely to happen in this time frame. Timely postpartum and metabolic adjustments to this new physical state demands correct management strategies to fulfill the cow's needs for a successful transition to this phase. Among the management strategies, one of the most researched methods for managing transition-related stress is nutritional supplementation. Dietary components directly or indirectly affect the expression of various genes that are believed to be involved in various stress-related responses during this phase. Nutrigenomics, an interdisciplinary approach that combines nutritional science with omics technologies, opens new avenues for studying the genome's complicated interactions with food. This revolutionary technique emphasizes the importance of food-gene interactions on various physiological and metabolic mechanisms. In animal sciences, nutrigenomics aims to promote the welfare of livestock animals and enhance their commercially important qualities through nutritional interventions. To this end, an increasing volume of research shows that nutritional supplementation can be effectively used to manage the metabolic stress dairy cows undergo during the transition period. These nutritional supplements, including polyunsaturated fatty acids, vitamins, dietary amino acids, and phytochemicals, have been shown to modulate energy homeostasis through different pathways, leading to addressing metabolic issues in transition cows.

1. Introduction

In dairy cattle, transition period is known to be a critical physiological stage because majority of the diseases related to infections and metabolism are likely to happen during this phase [1, 2]. The transition period involves several biological changes that involve various complex biochemical interactions. These alterations take place in a series of reactions that starts three weeks prior to calving, lasting an estimated duration of three to four weeks following parturition [3].

The transition period in cows can be one of the most detrimental phases in terms of their overall well-being and productivity [4]. During the transition phase, cows face

severe metabolic challenges requiring high energy and nutrient intake. This is because the production of colostrum and milk in cows during lactation requires higher than normal amount of nutrients and energy. Conversely, it is also generally observed that cows' feed intake during transition periods is reduced. There can be different reasons for lower feed intake in dairy cattle during the transition period including environmental factors, physiological changes, level of production, feed digestibility, feed processing, and consistency of ration ingredients, but the main factors observed for decreased feed intake are effects on rumen capacity [5], heat stress [6], and hepatic oxidation [7]. Transition dairy cows are reported to have a large volume of fetus during the last

3 weeks of gestation, affecting the rumen capacity and adaptation, leading to decreased feed intake. The high energy requirements coupled with less intake of feed create negative energy balance (NEB) and nutrient deprivation [8]. Moreover, the lower feed intake is usually associated with reduced appetite in cows during the transition phase, which is believed to be caused by various molecular mechanisms, including acute inflammation. In response to inflammation in the transition phase, the body produces more inflammatory mediators, including complement proteins, cytokines, and eicosanoids. These molecules form a complex network and regulate different systemic responses, including reduced appetite and enhanced heart rate [9]. The NEB also invigorates metabolic changes that can be detrimental to cow's health, like increased accumulation of body fat such as non-esterified fatty acids (NEFA). The higher storage of body fat causes the accumulation of beta-hydroxybutyric acid (BHBA) in the blood. Such nutritional responses can be considered a normal process. However, cows generally fail to adapt to such metabolic changes during the transition period, causing an increase in the rate of metabolic and infectious diseases that influence cows' reproductive and productive capability [8].

The inefficient transition from the pregnancy stage to lactation frequently brings about the loss of 4.5 to 9 kilograms of milk compared to peak production times [10], that is, equivalent to 907 to 1814 kilograms of untapped milk production from each cow [8]. Regardless of huge advances in comprehension of transition cow biology, there is still a high occurrence of diseases related to infection and metabolism that has been accounted as occurring after the early lactation phase [11, 12]. The frequency of metabolic diseases in transition cows such as fatty liver, ketosis, and milk fever accounted from 7.8 to 16.8%, infections of mammary gland such as udder edema and mastitis accounted from 2.8 to 12.6%, and reproductive diseases such as retained placenta and dystocia accounted from 6.7 to 19.2% in high milk-producing cows [13, 14]. Hence, a delicate transition is crucial for managing health-related disorders and improving productivity of cows during transition period. Therefore, managing stress that occurs during the transition period is important for the animals' wellbeing and for maintaining their maximum productivity.

2. Risk of Metabolic Disorders during the Transition Period

Specific desirable outcomes are required for a cattle farm's successful and profitable operation, including the successful adaptation of cows to metabolic challenges during the transition phase with minimum or no disease rate, no culls, and good reproductive performance. However, the truth frequently contrasts incredibly. Poor side effects of the production process are self-evident. The expression "production disease" was generally viewed as incorporating the important metabolic issues such as ketosis, hypocalcemia, and hypomagnesemia of dairy cows. More diseases like metritis, laminitis, and abomasum have been incorporated into this term [15]. With the development and expansion of the dairy

industry worldwide, the sensitivity of diagnostic methods used for identifying cattle diseases has also improved. Despite improvements in diagnostic methods and better farm management practices, dairy farms still continuously face high rates of metabolic disorders that negatively impact dairy cows' health, reproduction, and productivity [16, 17]. Extensive research has addressed the correlations between cows' metabolism with various periparturient diseases, physiological adaptations, and nutritional requirements in the transition phase. According to a study by LeBlanc (2013), 30 to 50% of dairy cows during calving are influenced by some metabolic and infectious disorders that significantly affect dairy production. Frequency rates of compiled periparturient disease are listed in Table 1. However, contrary to the scientific evidence, research by Van and Sniffen (2014) reported that most dairy farmers still believe that the metabolic disorders affecting dairy cattle have no substantial effect on the milk production performance and cows can maintain their milk production capacities even in the presence of metabolic disorders.

As opposed to the extensive informational collections on the performance attributes of dairy cows, the testing of metabolic diseases is usually confined to information from single scientific examinations. In contrast to clinical infections, subclinical metabolic illnesses are much harder to distinguish as they require extra screening tests, and getting a whole image is not generally conceivable. This refers not exclusively to the seriousness of subclinical diseases but also to the impacts these metabolic disease may have on the risk of getting infectious and fertility disorders. Previously, equivalently not many examinations have been done to explore connections over an expanded range of medical conditions with reference to the production of milk. For instance, in the case of subclinical ketosis, hyperketonemia has been reported in the initial two months of lactation, which went broadly from 8.9% to 34% in different investigations [19, 20]. It would not be helpful to compare the current incidence rate of diseases to those from past years as records are unreliable. Moreover, higher quantity milk-yielding cows than their mates in herds are not consequently at higher risk of getting disorders [21]. As indicated by Mulligan and Doherty [15], the concept that high-yielding cows consequently have elevated levels of production disorders is probably erroneous as the speculation that lower-yielding dairy animals experience the lower levels of diseases related to production.

Drackley [1] reported in his study that unnecessary the NEB in times of early lactation leads to uncontrolled lipid metabolism that paves the way for numerous health complications in dairy cows. These metabolic changes increase the chances of hypocalcemia, ketosis, hepatic lipidosis, and other metritis and mastitis like infectious diseases [22–24]. However, considerable variation in the concentration of plasma of substrate during diurnal and in subsequent days in early lactation has been observed. For instance, the concentration of plasma BHBA is considered the indicator for developing ketosis in cows, contrasting broadly as does the higher concentration of plasma estimated in dairy animals that do not develop clinical ketosis in the initial six weeks lactation [25]. Variation in metabolites and hormone concentration in the

TABLE 1: Compiled periparturient prevalence of metabolic disorders from various published studies according to [18].

Diseases name	Median incidence risk (%)	Range of incidence risk (%)
Hypocalcemia	6.5	0.3-22
Metritis	10.1	2-37
Subclinical metritis	53	37-74
Lameness	7	1.8-30
Retained fetal membranes	8.6	1.3-39.2
Subclinical hypocalcemia	2.2	8-54
Clinical mastitis	14.2	1.7-54.6
Subclinical mastitis	30	15-60
Ketosis	4.8	1.3-18.3
Retained fetal membranes	8.6	1.3-39.2

period of postpartum vary remarkably among animals held under comparable and exceptionally normalized conditions provided in the research farm, demonstrating that the ability to adapt to metabolic pressure fluctuates impressively between individual cows [26].

Sordillo and Raphael [27] reported the potential associations between dysfunctional inflammation responses and the mobilization of fat that may be associated with increased mortality and morbidity in the phase of transition. On the other hand, an effective inflammatory response eliminates the invading microbe, returns tissues back to normal morphology and function, and reestablishes the homeostasis of the immune system. This causes various aspects of cows' immune systems to be undermined around the hour of calving, particularly affecting inflammatory responses [28]. Sordillo and Raphael [27] presumed in their study that an adequate response of inflammation is required for the ideal clearance of pathogen because; during the state of transition in cows, swift return to immune homeostasis is generally lost. Suppression of the immune system is observed to be a common phenomenon in the periparturient dairy cows which has been connected to the poor status of metabolism and NEB [29, 30]. Immunoresistant genes are observed to be upregulated in the cows that suffer NEB [31], while the genes involved in acquired immune responses are downregulated [32]. Huzzey et al. [33] reported that cows suffering from severe metritis ate less than healthy cows during the half-month preceding the clinical indications of metritis [33]. Less food intake is related to expanded NEFA concentration that may directly [34] or indirectly [35] play a role in hampering the function of neutrophils. Both higher pathogen challenges and metabolic need force the cattle to regularly experience the significant oxidative pressure in early lactation [36] and also confer a proinflammatory response that destabilizes the defense mechanism [37]. Metabolic pressure is a significant fundamental factor in the progress of diseases in transition cows, which occurs when cows fail to adjust physiologically to higher requirements of nutrients during parturition and early lactation [37]. The cumulative impact of oxidative stress, impaired nutrient metabolism,

and impaired inflammatory response can shape destructive input loops that worsen the metabolic stress and induce health complications [19].

The role of such pathways that are associated with inflammation in the processes of adaptation is not yet wholly comprehended. Farney et al. [38] recommend that in some cases, insulin resistance induced by inflammation is an adaptive phenomenon instead of a pathological one, and that successful adaptation requires some level of inflammation. The increased number of analytes related to inflammation and stress during the periparturient phase is related to a lower yield of milk and while impaired reproductive ability is related to the later phase of lactation [39]. The overexpression of reactive oxygen species is an essential factor of an impaired inflammatory response leading to oxidative stress [40]. Conversely, free radicals play a fundamental role in physiological phenomena, but their excessive or imbalanced production plays a vital role in disease pathogenesis. Oxidative stress has been distinguished as a connection between inflammation and nutrient metabolism during the phase of transition [37].

Numerous investigations have revealed the close relationship between fertility disorders and NEB [41–44]. A large number of locomotive problems increase the duration of NEB in transition cows [45]. Essential drivers and the confounding components which add to the advancement of metabolic diseases are complex and differ impressively from farm to farm. These variables are identified as feeding regimes and convoluted by different administration problems. Regardless of the normal production of milk, a few farms do well, while others fail notably in decreasing clinical and subclinical issues. Vastly unique nourishment and executive programs produce great or poor success in corresponding to metabolic problems [1].

3. Strategies to Alleviate Biological Stress during the Transition Period

The transition period in cows is characterized by dietary, hormonal, metabolic, and immunological variations, causing various infections and metabolic illnesses. The continuous NEB state in dairy cows during the transition period necessitates higher energy intake than from ingested food [46]. It reduces glucose levels in blood and the mobilization of biological reserves to supply extra energy, resulting in metabolic imbalances and immune suppression [47–50]. Therefore, improving the energy balance in the transition period of dairy cows can significantly lower the prevalence of diseases associated with this period. Several methods have been proposed to achieve this purpose, including routine monitoring of the health status of cows during pregnancy and lactation, improving husbandry practices, nutritional supplementation, and optimal feeding. However, nutritional supplementation has received the most attention during last few years [51, 52]. In the upcoming sections, we will describe the metabolic changes cows face during the transition period and how nutritional supplementation can help minimize the destructive effects of metabolic changes during this period.

3.1. Metabolic and Physiological Adaptations from Gestation to Lactation. Previous studies have extensively demonstrated the traditional homeorhetic, physiological, and metabolic adaptations that cows go through from late gestation to early lactating [24, 53–55]. All these adaptations have been summed up in the current review related to the consequent fertilization period. Amidst the late gestation and primal lactation, certain changes in the endocrine and neuroendocrine system cause alteration in the nutrient segregation from fetal maturation up until the milk synthesis [54]. During the non-lactation period, the higher quantity of insulin and leptin is associated with the balance of energy, in comparison to the late lactating period [56]. These hormones are involved in and are responsive towards energy storage inside the adipose tissues. Fetal calf and placenta require more nutrients throughout the last month of gestation [57]. It is necessary for cows to provide their fetus with the required nutrients through diet, though dry matter intake (DMI) should be reduced up to 10-30% from the early nonlactating period [58]. However, stressors and severely limited DMI can cause NEB ahead of delivery; yet, the chances are much reduced as compared to what happens following parturition. Near parturition, the release of growth hormone (GH) depends on required nutrients [59]. In response to prepartum reduction in insulin concentration, milk production, and GH mobilized nutrients, fats storage primarily in adipose tissues is affected [60]. Noticeable reduction in important hepatic GH receptor (GHR-1A) causes acute reduction in the secretion of insulin-like growth factor 1 (IGF-1). Consequently, feedback suppression of the secretion of GH via IGF-1 is prevented due to the uncoupling of somatotrophic mechanism, that maintains the elevated quantities of GH [60].

3.1.1. Lipid Metabolism. The prolific reduction in insulin and increased GH directs the adipose tissues to mobilize the triacylglycerols (TAG) reservoir. In adipocytes, repeated esterification of NEFA is reduced because of the complete inhibition of lipogenesis. The significant antilipolysis effect on the fatty tissues get also that are removed due to the reduced concentration of insulin. GH increases the sensibility and the response towards catecholamines present in the fatty tissues, causing enhanced lipolysis of triacylglycerols [24, 53, 61]. Additionally, several components including interleukin-1 (IL-1), interleukin-6 (IL-6), and cytokines, i.e., tumor necrosis factor- α (TNF α) are secreted as a responsive action to stress, infection, and trauma which increases NEFA and TAG concentrations in the blood and heart [62]. Thus, stress inducers and poor management of the nutrients reduce DMI, enhancing the mobility of TAG and NEFA instantly after calving. During NEB, upon restricted glucose supply, ketogenesis is increased which causes ketosis [53]. Excessive uptake of fatty acids, with their oxidation into the ketone entities or CO₂, gets reconverted to triacyl glycerides. Ruminant animals cannot efficiently export hepatic triacyl glycerides—low density lipoproteins which consequently leads to the accumulation of fatty liver.

3.1.2. Glucose and Protein Metabolism. Dairy cows meet their glucose demand by relying on propionate hepatic glu-

coneogenesis. After calving, limited DMI limits the availability of propionate; therefore, increased conversion of amino acids mainly, alanine and glutamine, and glycerol from the diet or skeletal muscle and glycerol from mobilized adipose TAG assists glucose synthesis. Increased gluconeogenesis in liver tissue around and after calving aids in the sustainable supply of glucose to the mammary gland to prevent hypoglycemia [24]. In dairy cows, the estimation of plasma concentrations of 3-methyl-histidine during the first week after calving related with prepartum values revealed increased mobilization of limited proteins, reserved primarily in the form of skeletal muscle protein [63]. Even before calving or before the initiation of fat mobilization, loss of muscle mass might begin [63]. Different disorders like ketosis and other periportal diseases which reduce fertility rate are linked to the deficient stock of metabolizable proteins; therefore, it is essential to maintain maternal protein reserves for long-term health, productivity, and reproduction [25, 57, 61, 64],

3.1.3. Immune System Function. During the transition phase, the ability of the immune system to encounter infectious challenges get suppressed, which likely increases the incidence rate for environmental mastitis as well as the high incidence of metritis, more specifically around calving [54, 65]. Retained placenta has also been associated with failure of the immune system to identify the placenta as a foreign tissue [66]. Reasons for the declined immune functioning are not clear yet. Both vitamins A and E, as well as trace minerals (selenium, copper, zinc), boost immune functions. Cows show a significant decline in body condition score (BCS) and high chances of sickness when stressed either by nutrition or environmental factors. Negative energy balances or an inadequate supply of metabolizable protein could also be a serious contributing factor to impairment of the immune functions [54, 65, 67, 68] found impaired and insufficient neutrophils content (reserve glucose as fuel for neutrophil functions) with reduced glycogen in early postpartum cows.

3.1.4. Calcium Metabolism. The calcium concentrations abruptly drop in blood due to high demand required and with sudden onset of milk synthesis at calving, leading to milk fever. Subclinical hypocalcemia is more prevalent, with over 40% of cows entering the second or higher lactation getting affected [69]. This leads to disorders like displaced abomasum and ketosis by decreasing smooth muscle function essential to normal function of the digestive tract [70], reducing DMI, and also making animal immunocompromised [71]. Before the digestive tract improves the required calcium absorption, calcium must be attained from bone resorption. A negative dietary cation-anion difference (DCAD) triggers metabolic acidosis to facilitate calcium mobilization from bones, whereas a high potassium and positive DCAD inhibit this mobilization [70, 72]. Meanwhile, magnesium is found to be regulating bone resorption [70]. Nutritional intervention to start at least 14 days before calving effectively prevents hypocalcemia [53].

DeGaris et al. [73] reported that the optimal consumption of calcium in cows in diet before calving improved

pregnancy rates in two of three commercial herds and cow's impregnation rates at 6 weeks and 21 weeks after the start of the insemination period.

3.2. Nutrient-Gene-Metabolism Nexus Associated with Metabolic Adaptation in Transition Cows. Under the same circumstances and production level, variation in the accomplishment of adaptation early in lactation among cows revealed that these modifications may possess a genetic baseline [74, 75]. Different genes, metabolites, and main pathways in the plasma came to be earlier established that they have critical role in controlling the endocrine and metabolic adaptations in dairy cows [76, 77]. Nevertheless, these genes and metabolic processes may express at a specific time in the candidate [74]. For instance, a few genes which change the glucose level may be expressed at the start of lactation and a few others that change the affluence of NEFA, for instance, are expressed 4 weeks before or after 13 weeks of calving. Analyzing, pinpointing the genes, and regulating processes are significant biological roles during particular physiological conditions of dairy cattle that can assist in recognizing the DNA variants that influence milk production and, consequently, fertility [78].

The starting phase of lactation in dairy cows goes hand in hand with increased milk production. These adaptations are involved in metabolic regulation in peripheral tissues (comprising adipose tissues, mammary gland, kidney, and the skeleton muscles) and liver and are further involved in movement of body reservoirs and hyper lipid metabolism [79]. Mapping based on genes and identification of pathways revealed that three processes (steroid hormone biosynthesis, ether lipid metabolism, and glycerophospholipid metabolism) cooperatively influence the amount of β -hydroxybutyric acid, nonesterified fatty acids, and glucose in cows during transition interval. The main genes presumed to control the energy metabolism in different tissues include ACACA, PPARA, FASN, PCK1, FBP2, ACSL1, FABP3, PPARGC1A, AGPAT6, ACOX1, LPIN1, ACSL, CPT I, and CPT II [76, 80–84]. These genes influence the absorption of fatty acids mostly in the liver and mammary glands, oxidation of mitochondrial and peroxisomal fatty acids in the liver, ketone body metabolism, and cholesterol metabolism (in the liver) during the early stages of lactation in dairy cattle [85] (Figure 1). Therefore, alteration in the expression of these genes results in metabolic disruption in transition intervals in dairy cows.

For instance, ketosis is one of the primary metabolic diseases during transition intervals in dairy cows. Zhou et al. studied the changes in gene expression and genes linked with ketosis in Holstein cows. The RNA-seq process was utilized for analyzing the gene expression, from which a total of 27,233 genes were quantified with four billion premium reads. Consequently, the researchers realized that 75, along with four differentially expressed genes (DEGs) among sick and control dairy cows at postpartum and prepartum, subsequently, show that sick and control cows possess the same gene expression sequence at prepartum. However, there were 95 DEGs among postpartum and prepartum sick cows, which revealed depressed variations of the gene expression

in the transition interval compared to healthy cows (428 DEGs). Functional examination shows that DEGs linked with ketosis were the fundamental reason for biological stress response, ion homeostasis, amino acids metabolism, energy signaling, and disease-related processes [86].

In another examination, Laguna et al. [87] examined the expression of genes that encode for the enzymes and different processes linked with the metabolism of lipids and carbohydrates of 2 genetic classes of dairy cows in the transition phase. Examination of the expression of cytosolic phosphoenolpyruvate carboxykinase (*PEPCK-C*), glucose-6-phosphatase (*G6PC*), β -hydroxybutyrate dehydrogenase-2 (*BDH2*), methylmalonyl-CoA mutase (*MUT*), carnitine palmitoyltransferase-2 (*CPT2*), acetyl-CoA carboxylase (*ACC*), glucose transporter-2 (*SLC2A2*), 3-hydroxy-3-methylglutaryl-CoA reductase (*HMGCR*), and the transcription factor peroxisome proliferator-activated receptor α (*PPARA*) was directed, and a comparison was established between Holstein and F1 Holstein-Gir cows. The results revealed that the expression of *PEPCK-C*, *G6PC*, *ACC*, *BDH2*, *CPT2*, *SLC2A2*, *HMGCR*, and *PPARA* genes was not different among the genetic group excluding the *PEPCK-C*. Furthermore, no association between genetic groups and the experimental period was examined. In both dairy cows, *PEPCK-C* and *G6PC* gene expression was not prominent and decreased compared to the gene expression with 21 and 36 DIM and increased in d 51 postpartum. The expression of *MUT* was not the same among 2 studied groups and showed a noticeable increase after d 36 postpartum, whereas mRNA level of *HMGCR* likely to increase when compared d 21 and 36 to d 51 postpartum. The expression of *MUT* gene was not the same among 2 studied groups and showed a notable increase after d 36 postpartum, whereas mRNA level of *HMGCR* was likely to increase when compared d 21 and 36 to d 51 postpartum. Moreover, glucose levels were also not the same between the two groups and were sufficiently higher in the plasma of F1 Holstein-Gir cows compared to Holstein cows. However, no significant difference in glucose level was observed within each group during the analysis period. β -Hydroxybutyrate and NEFA concentrations were not different in both genetic groups but showed a high level from prepartum to d 6 and 21 postpartum [87]. The altered expressions of these different genes in liver are linked with metabolic stress in transition dairy cows.

3.3. Nutritional Interventions to Modify Gene Expression during the Transition Period

3.3.1. Nutritional Supplementation. Nutritional interventions for dairy cows during the transition period are primarily intended to ameliorate the effects of metabolic changes indicated above. Many nutrients have been reported to induce metabolic adaptations and regulate NEB by controlling the expression of many genes in different signaling pathways (Table 2) (Figure 2). The most significant effects have been observed by polyunsaturated fatty acids (PUFAs). Mammals can produce all types of fatty acids necessary to carry out normal physiologic functions, excluding PUFAs, especially from omega-3 and omega-6 families known as essential

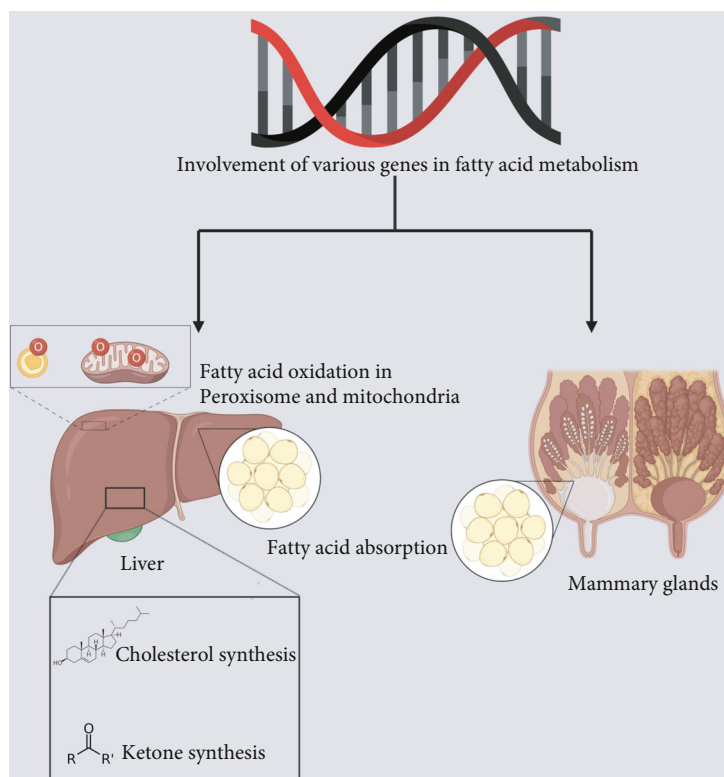


FIGURE 1: Phenotypic effects of various genes involved in fatty acid metabolism.

TABLE 2: Regulation altered gene expression through nutrients in transition cows.

Nutrients	Effect on gene expression regulation and on various traits	References
Rumen protected methionine (RPM)	Enhance the expression of ABCG2 and GHR genes during lactation Improved milk production and butterfat content	[93, 94]
Rumen protected choline (RPC)	(1) Regulate the expression of genes for acetylcholine and acetylcholine receptor (2) Enhanced the expression of FA transport protein 5 and carnitine transporter SLC22A5 in the liver (3) Reduce lipolysis of adipose tissues, thereby treats fatty liver	[95, 96]
Calcium supplementation	Treatment of hypocalcaemia, improving leukocyte function, improvement in impregnation and pregnancy rates, and management of transition period related stress	[73, 97, 98]
Yeast supplements	Regulate the expression of inflammation-related genes in dairy cows during transition period. Increase DMI content through increasing availability of fiber content	[99–101]
Polyunsaturated fatty acids (PUFAs)	Control the altered expression of many key genes (TLR2, PPAR) and transcription factors (NF- κ B) implicated in metabolic stress Also exerts immune modulation effects to control inflammatory processes	[96, 102]
n-3 PUFA	Inhibit the expression of adhesion molecules involved in inflammation Essential for the central nervous system (CNS) and reproductive system development and thereby improves embryo survival	[95, 103–105]
n-6 PUFA	Enhance mRNA levels of estrogen receptor 1 and oxytocin receptor and decrease insulin growth factor levels	[106]
Conjugated linolenic acid	Upregulate the transcription of many genes, including insulin signaling, TLR4, inflammatory cytokines, and protein kinases for metabolic adaptation	[107]
Long chain fatty acids (LCFAs)	Improvement in adjusting to the transition period stress and milk and milk fat yield	[108]

fatty acids. During the transition phase in cows, the concentration of PUFA lessens sufficiently in every part of the body compared to the mid-lactation cows [36, 88], whereas

the proportion of different saturated fatty acids (SFAs) is elevated. The fundamental source of omega-3 fatty acids in ruminants is forage, specifically for grazing cattle, as a

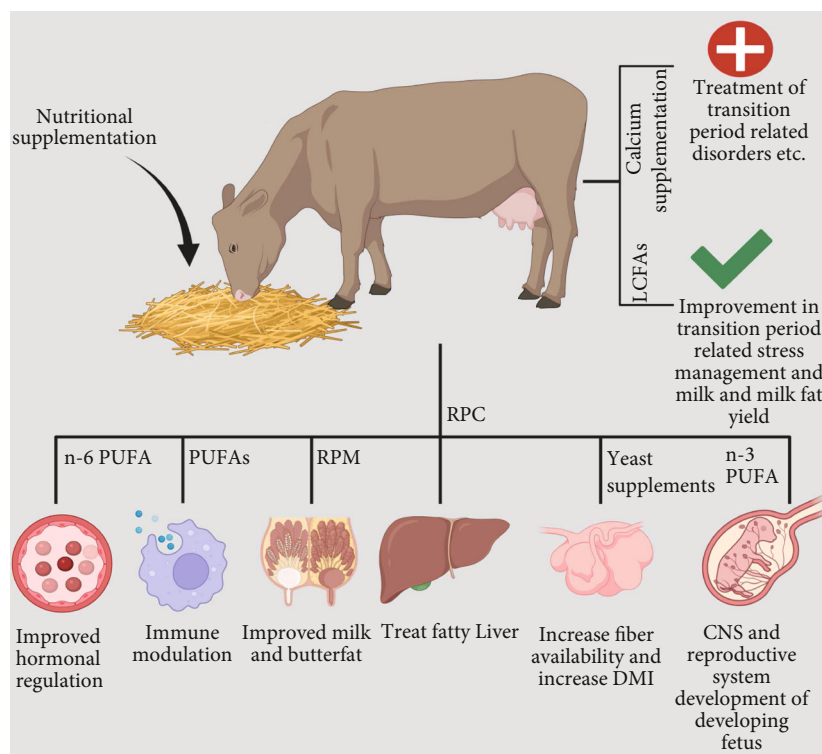


FIGURE 2: Effects of different nutritional elements on dairy cows' health, productivity, and reproductive ability. In the figure, the effects of individual nutritional compounds are shown. In reality, each compound can affect several organs and physiological functions. Moreover, each trait can be shared by various compounds.

huge amount of alpha α -linolenic acid (ALA) is found in forage galactolipids. A supplemental source of the n-3 PUFA in dairy cows' diets includes docosahexaenoic acids (DHA) and eicosapentaenoic (EPA) from fish oil and ALA from flaxseed [89].

On the other hand, n-6 PUFA is present in various other feeds, including sunflower, soybean, cottonseeds, and corn, and their ingestion increases sufficiently during and after calving. Supplementing requisite PUFAs (as rumen-protected mainly) directly influences the immune cells by modulating the expression of various transcription factors exerting pro- or anti-inflammatory activities. All n-3 PUFAs downregulate the expression of adhesion molecules intricate in inflammatory interactions between leukocytes and endothelial cells [90]. Linoleic acid and specifically its isomers cis-9, trans-11 and trans-10, and cis-12 were linked with peroxisome proliferation activated receptors (PPAR)- γ , while long-chain n-3 (EPA and DHA) was linked with toll-like receptors- (TLRs-) 2 and 4, PPARs, and sterol reaction element-binding protein family [91, 92]. All these genes play a major role in controlling NF- κ B that orchestrates the synthesis of proinflammatory cytokines in both immune and nonimmune cells. The absence of n-3 and n-6 PUFAs in the postpartum interval can cause uncontrolled inflammation. Besides fatty acids, other vital nutrients profoundly impact cow's health, productivity, and reproduction. An extended list of nutrients and their effects is shown in Table 1 and Figure 2.

3.3.2. Nutrients as Metabolic Modifiers

(1) *Water*. The nutrient that has the primary daily requirement for most life forms is water, and it is 56-81% of BW. Milk contains 85-88% water. For milk production, water is predicted to be 4:1 (water: milk) by McCandless and Gaessler (1919). Water required for 1 kg of milk is 2.0-2.7 kg [109]. Loss of water in the body occurs through urine, faeces, sweating, and expiration. The quality of water is defined by many aspects such as organoleptic qualities, physicochemical properties, mineral content, and presence of toxic chemicals and bacteria [109].

As environmental temperature increases, intake of water also increases [110]. Water helps to conserve body temperature via evaporation. Dairy farms situated in the hot areas have fitted cooling systems that use the mechanism of evaporative cooling to maintain the cow's core body temperature. Water deprivation is more deadly than starvation. Rumen water kinetics was integrated to demonstrate rumen VFA kinetics [111]. Rumen osmolality increases after feeding. Water from the body moves into the rumen to decrease the osmotic pressure of the rumen. The passage rate of water and feed particles increases with the rumen's osmolality. Buffering effect of bicarbonate salts is less due to less time spent in the rumen.

Due to the strong positive relationship between water and solid feed intake, greater water intake can lead to greater

feed consumption, rumen stability, and regulation of rumen pH. A recent study showed the positive effect of drinking warm water on rumen functionality in beef cattle [112]. Drinking warm water reduced the time during which the ruminal pH was below pH 5.8 or 5.5, and the time during which the temperature was lower than 37 or 39°C. It has been reported that the rumen temperature and pH are correlated with the gene expression in rumen epithelium (RE). Rumen acidosis caused by low pH in rumen might alter the expression of genes and cytokine expression in RE [113]. Water helps to maintain the rumen pH so that it can act to modify the expression of genes and cytokine concentration in RE. Thus, water is an essential metabolic modifier in transition dairy cows.

(2) *Protein and Amino Acids*. In a dairy ration, the costliest ingredient is protein supplements. For an ideal economy, the effective use of protein supplements must also consider the utilization of this important nutrient by bacterial communities present in an animal. Virtanen was presented Nobel Prize on his development of a fodder preservation method. Later, he verified that cows could produce in a single lactation 4,200 kg of milk on a protein free ration [114].

Proteins are made up of 20 amino acids (AAs) for maintenance and production. Out of 20 AAs, ten are non-essential (NEAA), and ten are essential amino acids (EAA). NEAA are those which body can synthesize on its own, while (EAA) are those that the body cannot synthesize and must be provided in the feed to meet the body's requirement.

Protein in meals from the whole oilseeds is soluble in the rumen. Rumen bacteria degrade the protein to ammonia, which gets assimilated into microbial protein. Microbial protein is highly digestible, but a net loss of nitrogen occurs from them. Rumen degradation decreases, and rumen bypass increases of oilseed meals and whole oilseeds by heat and chemical methods [115–117]. The extent of rumen bypass and total tract digestibility depends on the temperature and total time when supplements are exposed. Due to overheating of meals and seeds, a reaction occurs between reducing sugars and AAs, resulting in decreased protein degradation in the rumen and digestibility in the small intestine. This whole reaction is called the Maillard reaction. Cows fed recombinant bST and rumen-bypass protein that have increased milk yield [118]. Rumen cellulolytic bacteria cellulolytic require ammonia which they degrade to produce essential proteins for their growth. The more fermentable energy, the more the growth rate of rumen bacteria. Satter and Slyter [119] studied that when ammonia concentration exceeds 5 mg/100 mL, ammonia overflow occurs from continuous cultures. Satter and Roffler [120] studied that when NPN sources are added to the ration beyond 12 to 13% of CP, milk production does not increase. These experiments started a discussion among nutritionists, and new ideas were evolved on how to create rumen bypass protein supplements [120, 121]. Chalupa [122] studied that protein from the ration must escape rumen degradation and reach the small intestine for increased milk production. Applying

heat to protein meals and whole seeds increases rumen undegradable protein [123].

Rumen bacteria destroy the trypsin inhibitor and other compounds that are present in the whole soybeans. Soybeans should be processed to destroy these compounds when given to young calves to avoid these. Reddy et al. [124] fed calves from birth to 10 weeks of age. The whole soybeans were heated at a temperature 99 to 163°C. And they found that the most significant gain occurred when soybeans were roasted at 143 to 146°C for 30 min. Protein meals treated with formaldehyde had increased rumen bypass protein [125] but milk production was notably lacking in most experiments. Formaldehyde is cancer-causing in nature. The FDA prohibited feeding formaldehyde-treated feeds to livestock.

The most limiting essential amino acids in dairy cows are lysine and methionine. Two conditions must be considered: grams of absorbable AA per 100 g and Lys: Met ratio. Lysine comprises of 16.3 of lean tissue and 16.0 of milk proteins, while Met 5.1 of lean tissue and 5.5 of milk proteins [109]. The lysine requirement for maximum use by tissue is 7.2 g/100 g and for Met is 3.2 g/100 g of absorbed AA [109]. Methionine has a half-life of almost 2.4 h [126]. Supplementation of methionine increased milk protein and weight of milk protein [127]. Vyas and Erdman [128] determined that when both Lys and Met approached requirements, the marginal efficiency of use Lys and Met decreased.

From nutrigenomic perspective, EAA are reported to increase milk yield and milk protein synthesis via regulation of different genes. Methionine supplementation is shown to be associated with high milk yield via increased expression of β -casein [129]. Valine, leucine, and histidine are also reported to increase the milk yield in dairy cows via increase in casein and β -casein mRNA abundance [129, 130]. Enhanced methionine supplementation during the periparturient period is reported to increase dry matter intake and milk yield in dairy cows. Liang et al. studied the nutrigenomic potential of methionine supplementation in Holstein cows during their periparturient period [131]. They reported that enhanced methionine supply led to greater overall mRNA abundance of Gln (SLC38A1), small zwitterionic α -AA (SLC36A1), Glu (SLC1A1), and neutral AA (SLC1A5) transporters. Moreover, abundance of AKT1, RPS6KB1, and EIF4EBP1 was also upregulated in response to methionine. Furthermore, the increased supply of methionine upregulated the expression of peroxisome proliferator-activated receptor-gamma, mTOR, and fatty acid synthase.

During the transition period, dairy cows experience inflammation and oxidative stress. Methionine supply can profoundly alter these biological processes in transition dairy cows via fine-tuning of oxidative stress-related genes, inflammatory cytokines, improved liver function, and glutathione metabolism. Methionine is also studied to upregulate PPAR α through DNA methylation during the transition period in cows and is considered a suitable mechanism to explain consistent improvement in the performance of a dairy cow [132]. Arginine and glutamine are also known to mediate metabolic stress via modulation of PPARs [84]. In addition, plasma levels of cysteine are reported to decrease

around parturition in dairy cows, and studies suggested that cysteine supply helps lower the oxidative stress and expression of proinflammatory cytokines, which are hallmarks of stressful conditions in cows [133]. Hence, amino acids and proteins have much nutrigenomic potential and can be utilized as metabolic modifiers in transition dairy cows.

(3) *Lipids*. Lipids contain fatty acids that are absorbed in the small intestine and then enter the lymphatic system where they are transported to the liver. An enzyme lipase acts on the lipids and releases glycerol and fatty acids which are then used by tissues as an energy source even by the brain, in severe NEB. In the tissues, fatty acids are hydrolyzed to 2- and 4-carbon and enter the Krebs cycle to produce ATP. It may result in ketosis if excessive oxidation occurs. Fatty liver may result from incomplete utilization of fatty acids. In a positive energy balance, adipose tissue absorbs the acetate and butyrate and converts into storage form as triglyceride. Among fatty acids, the main source of energy for the cows are long-chain fatty acids. These fatty acids are given to the cows via oil seeds, animal-vegetable blends, or ruminal inert fat. In the rumen, the unsaturated fatty acids are converted into C18:0 and C18:1. Rate of fermentation and extent of fermentation decrease by unsaturated fatty acids. When given dietary fat, it was found that the milk response was curvilinear with 16% of ME from fat equals to 600 to 700 g or 3% added fat. Forages and grain contain an average of 3 to 4% fat. One should remember that the diet's total fat should not exceed 7% of total DM [134]. Fatty acids that are long chained and unsaturated are toxic to rumen bacteria. To overcome this effect, biohydrogenation of UFA is done. To avoid the increase of fat solubility in the rumen, rumen-protected fats are used, e.g., calcium soaps and amides.

Sutton [135] gave an intriguing tale from Eckles at the University of Missouri, who kept in touch with Powell in 1927: "as far as anyone is concerned, this or some other investigation in the nation has not as of late directed experiments to decide whether feed would influence the composition of milk. It is looked on as a very unsettled inquiry." Powell [136] later gave proof that actual qualities of roughage, did truth be told, influence rumen fermentation with a significant impact on milk fat percent. That trait of forage was depicted as "physically effective fiber." Chewing, saliva secretion, and rumen pH are affected by this forage quality [137].

In another study, the impact of diet on intermediary metabolism and fat content of milk was surveyed. The following three hypotheses were examined: (1) decreased acetate production in the rumen, (2) insufficiency of BHB in the mammary gland, and (3) endocrine variables. Amount of forage, forage: concentrate ratio, carbohydrate fractions of the concentrate, lipids, and meal frequency were found to be the variables influencing milk fat composition [135]. Beitz and Davis [138] compared 3 diets for milk fat: (1) control diet, (2) high grain ration, and (3) diet containing cod liver oil. The researchers found that the grain intake and milk fat quantity differed between the three groups. Milk fat percent averaged 3.21, 2.16, and 1.77 for the 3 rations, respec-

tively. High-grain diet had increased rumen propionate. Fish oil and high-grain diets had lower milk fatty acids, and all double bonds stated were in the cis position. Earlier, Davis and Brown [139] and later Bauman et al. [140] also observed that an increase in trans 18:1 in milk fat was associated with decreased milk fat percent.

Increased C18:1, C18:2, and C18:3 in milk are due to oil from plant sources. Unsaturated fats of the plant have double bonds in the cis position at each 3-carbon unit starting at carbon-9 from the C end. Fish and plant oils cause a significant decrease in milk fat % and change the fatty acid composition of milk fat [141]. The substance of C20:5n-3 and C22:6n-3 is improved by fish oil [142, 143].

Unsaturated fats are harmful to rumen bacteria. Rumen bacteria utilize metabolic hydrogen to detoxify UFA. This effect by bacteria to UFA results in an increment of milk fat [144]. Cows fed with an animal-vegetable blend of fat, coconut oil, safflower oil, flaxseed, and monensin in a diet had increased trans C18:1 [145, 146]. Medium-chain fatty acids were decreased in all diets. Total protozoal numbers and ruminal NDF digestion were decreased in a coconut oil feed [146]. Fatty acids less than C16 were reduced, and trans C18:1 and trans-10 and cis-12 CLA in milk fat were increased when monensin was fed [147]. Cows fed with low fiber and unsaturated fat had lower milk fat % and milk yield, around 30% and 35% as compared to high forage ration and saturated fat [148]. Cows showed increased trans-10 C18 UFA in milk and decreased milk and fat yields when fed with low fiber and unsaturated fat compared to high forage rations. Baumgard et al. [149] recognized trans-10, and cis-12 isomer is produced in rumen and a potent inhibitor of de novo milk fat synthesis. Two isomers that also inhibit milk fat synthesis are cis-10, trans-12 and trans-9, and cis-11, and these are CLA isomers.

Supplementing fat to increase the energy or caloric density in the diet of lactating dairy cows has a long history. Dietary long-chain fatty acids (LCFA) have prominent nutrigenomic effects on several components of different organs in dairy cows during their transition period. In an in vivo study, the supplementation of saturated lipids to dairy cows showed higher expression of lipogenic genes in mammary tissue resulting in higher milk yield [150]. In another study, greater expression of lipogenic genes was observed in mid-lactation dairy cows when they were supplemented with a mixture of oil [151]. However, the nutrigenomic effects of saturated LCFA were not prominent. In contrast, in a recent experiment, Schmitt et al. observed the increased expression of nuclear receptor coactivators, lipogenic genes, and related transcription factors when cows were supplemented with high saturated LCFA diet for 30 days [152]. Furthermore, in the same experiment, Akbar et al. investigated the hepatic expression, and the results uncovered the strong nutrigenomic effect of saturated LCFA supplementation prepartum and larger nutrigenomic effect of fish oil supplementation postpartum [153]. Interestingly, overall supplementation of lipid diet resulted in low expression of CPT1A, FGF21, and ACOX1 but the expression of PPAR α is reported to be upregulated by lipid diet. This data seems to indicate that supplementation of lipids might be

advantageous in liver parturition which can further manage the metabolic stress in transition dairy cows.

Among the short-chain fatty acids (SCFA), butyrate exerts nutrigenomic effects in dairy cows. Butyrate is reported to induce an immune response and cell cycle arrest in dairy cows and goats [154]. The nutrigenomic effects of butyrate are evident in ruminal papillae of dairy cows by modulating the expression of genes related to lipogenesis and glycolysis [155]. The effects of propionate are also observed on free fatty acid receptor 3 (FFAR3) in transition dairy cows. Lemor et al. have studied the effects of propionate, and they reported the increased expression of FFAR3 and adiponectin genes from pregnancy to lactation in bovine adipose tissue which can regulate the lipid metabolism, energy expenditure, and insulin sensitivity [156].

Recent studies in cows and rodents have shown the importance of lipids in regulating gene expression in mammary tissues and the liver. For example, dietary lipids regulate lipogenesis through interaction with several transcription factors, including PPARs and sterol-regulatory element binding protein (SREBP) [157, 158]. Polyunsaturated fatty acids (PUFA) are the main FA that act at the level of nucleus in connection with these transcription factors to regulate the expression of different lipogenic genes. PUFA reduces SREBP-1a and 1c by accelerating the decay of *SREBP-1c* mRNA, therefore lowering their hepatic content to regulate lipid metabolism and FA oxidation [159]. PUFA and eicosanoids are also shown to bind directly with PPAR α , controlling gene expression and metabolic networks to enhance milk yield. Thus, insight into the nutrigenomic potential of lipids highlighted their importance as metabolic modifiers in transition dairy cows.

(4) *Minerals*. Minerals and micronutrients are considered to fulfill various functions such as regulating body water balance, building bones, immunomodulation, and influencing muscle functions for optimal functioning of dairy animals and acquisition of their products [160]. In particular, the ability of minerals to regulate the expression of gene products through modulation of transcription and translation is now being recognized. The deficiency of certain nutrients is evident in dairy cows during their transition period. Bone contains 98% of total body calcium, and the other 2% is extracellular fluid. The concentration of calcium in the blood is around 9 to 10 mg/100 mL, and it is regulated by a hormone called parathyroid hormone (PTH). Release of PTH depends upon the blood calcium level. When calcium in the blood is low, PTH release increases the mobilization of Ca from bone to maintain the concentration to calcium to normal. 1,25-Dihydroxycholecalciferols regulate calcium absorption, and it is derived from vitamin D. Bones become less responsive to calcium release with age. As blood calcium declines, cows become subclinical, partial, or full paralysis with recumbency occurs at a calcium level of ≤ 5 to 6 mg/100 mL. With the increase in calving and low calcium levels, the risk of parturient paresis (milk fever) increases. Minerals have been identified to reduce the severity of parturient paresis when supplemented to transition cows in their diet [161]. These include the amount and ratio of Ca and P,

administration of vitamin D per os or by injection, and manipulating alkalinity in diets.

Magnesium oxide (MgO) is a source of elemental magnesium (Mg), and it is absorbed by ruminal epithelium. Particle size MgO affects the rate of solubility in rumen [162]. Rumen fluid solubility ranges from 25 to 75% in a pH of 5.5 to 6.5 [163]. When pH increases beyond 6.5, the solubility of ruminal fluid decreases. Mg absorption (% of intake) is about 26% but it ranges from 9.9 to 73.9%. Forages are rich in potassium (K), and K decreases the Mg absorption; so, with forages, the high Mg concentration must be also be given to an animal. Grass tetany occurs in the spring in cows by grazing on rapidly growing grass with a high K concentration [164]. Lactating cows fed with a positive dietary cation-anion difference (DCAD) rations have increased DMI and milk fat in a curvilinear response [165]. Magnesium has numerous roles in the immune system functioning that can exert nutrigenomic effect in dairy cows. In experimental animals, Mg deficiency is correlated with altered proinflammatory status in which systemic IL-6 increases and increase in correlates of oxidative stress. In a trial, dietary Mg supplementation improves the metabolic profile by regulating the metabolic and inflammatory biomarkers, including decreased C-peptide concentrations, TNF- α concentration, and increased calcium and leptin levels. Moreover, certain genes linked to metabolic and inflammatory pathways, including C1q and tumor necrosis factor-related protein 9 (C1QTNF9), were downregulated [166]. Mg has been also shown to interact with miRNA machinery. Mg interacts with RNA-induced silencing complex (RISC) being an Mg²⁺-dependent protein and involved in binding of specific miRNAs to argonaute protein for cleavage of miRNA targets to control the gene expression. Therefore, Mg supplementation can improve the miRNA profile in dairy cows during their dry-off period for metabolic adaptation.

Many feedstuffs are deficient in selenium because the soils are low in selenium. One of the diseases due to deficiency of selenium in sheep is white muscle disease. Selenium is a cofactor of the enzyme glutathione peroxidase [167]. According to FDA, diets should be supplemented with selenium with a concentration up to 0.3 mg/kg [109]. Selenium deficiency in diet is associated with oxidative stress and autoimmunity [168]. Oxidative stress and autoimmunity are the hallmarks of disease conditions in transition dairy cows. In cows, the roles of selenium include participation in the cattle farms' antioxidant defense. Selenium supplementation may reduce the incidence of metritis and ovarian cysts during the postpartum period. Selenium has been reported to regulate the levels of proinflammatory cytokines and burden of free radicals in the body by downregulating the expression of IL-6, TNF- α and NF κ B at the RNA level [169]. Furthermore, dietary supplementation of selenium can also potentially affect thyroid hormone metabolism and redox-active proteins to improve the immune response of dairy cows [170]. In rodents, selenium-enriched probiotics have also been reported to improve lipid metabolism, histopathological lesions, and antioxidative status via upregulation of PPAR α

[171]. In this context, dietary supplementation of minerals or trace elements can be good for metabolic modification in transition dairy cows.

3.4. Nutrigenomic Perspectives: Challenges and Opportunities.

The notion that dietary elements interact with the cellular environments at the molecular level to alter biological activities has transformed nutritional science [172]. Nutrients, in such respect, are more than simply cellular fuel and building blocks; they are also molecular messages sensed by the sensors of cells that cause a shift in the biology of cells; hence, nutritional components are active biomolecular compounds [173]. Dietary components can also have nutrigenomic impacts without bioactive, such as dietary calorie restriction [174]. It is possible to fine-tune an organism's diet since dietary substances can interact with the genome, especially transcription regulators. Such methods have paved a path for developing a relatively recent area of science called nutrigenomics, which is defined as studying the effect of nutrients on gene expression in an organism [175]. In the ever-changing world of nutrition science of animals, nutrigenomics research aids in understanding how nutrient-gene interaction occurs that ultimately affects productivity and reproduction. The use of nutrigenomics in the animal nutrition provides many benefits, including improved animal productivity, fertility, feed efficiency, and immune functions. Transcriptomics and metabolomics are two potential nutrigenomic tools for understanding the molecular processes occurring in a genome obtaining nutritional cues and reacting to them via unique metabolic reactions in an organism. The nutritional requirements for an organism's upkeep and growth vary depending on its genetic variability, allowing nutrigenomic-based selection to be used to produce animals with superior traits for improved feed efficiency. It is especially important during the transition period and in the first few months of lactation as animals in this time period are more vulnerable to nutritional deficiencies [176]. We have highlighted a number of nutritional intervention strategies that can improve the performance and productivity of dairy cattle during the transition period. One example of such a nutrient is LCFA, the presence of which in the diet induces the expression of genes in the mammary gland that induces higher production of milk and milk fats in lactating cows and improves the management of stress during the transition period [108].

Though the research in nutrigenomics in animal nutrition has interesting potential implications in promoting animal well-being and productivity, this research area requires an extensive amount of research. Each animal species contains around thirty thousand to forty thousand genes, and their interaction with innumerable metabolites or nutritional elements cannot be ascertained within a short period of time and with limited resources. Though the sequencing techniques related to omics have improved over the years, it is still not feasible to find interaction of every known metabolite with each gene in a particular species [176, 177]. Future research in the development of more cost-effective and robust omics approaches is required to integrate nutrigenomics research to promote animal health and their productivity. Moreover, most of the nutrigenomic research

been done on the beneficial effects of nutrients on animals' health. The nutrients' toxic and potentially detrimental effects should also be investigated in detail. A detailed investigation of the nutrigenomic effects of the nutrients will help farmers formulate better feed formulations and curtail the use of antibiotics, the resistance against which is becoming an alarming situation around the world [178, 179].

4. Conclusions

The transitional period can be challenging for farmers and cattle alike. To sustain health of animals and attain projected production results, a smooth transition from late pregnancy to early lactation is required. In the transition period, implementing optimum management methods for dairy cows can significantly enhance their metabolic and immunological health, leading to increased cow wellbeing, health, and productivity. The scientific data support the usage of nutritional supplements in the periparturient period to improve metabolic and immunological responses while also reducing the production of biochemical signals that cause inflammation, immune dysfunction, and metabolic adaptation impairments. The nutritional research from dairy cattle generally demonstrates that the existing approaches for developing diets for dairy cattle are blind regarding the nutrigenomic impacts of dietary components, which, by modifying the animal's metabolism, are expected to modify its various metabolic pathways. The knowledge acquired from nutrigenomics research can better understand the genes and biochemical pathways influenced by dietary components and the impact such nutritional supplementation can have on the modulation of these molecular species. It is expected that the inclusion of nutrigenomics research in the diet formulation of dairy cows during metabolically challenging times like the transition period can help in planning more rational dietary plans that produce optimal results. Thus far, the potential of nutrigenomic research appears promising; nevertheless, the operational applicability of nutrigenomics in animal nutrition has not been implemented as of now. This is partially due to the intricacy of the biological systems under study and the further need to improve the technologies used for studying them. For this reason, we do not believe that practical nutrigenomic-based dietary formulations will be accessible very soon. More fundamental research is required before valuable applications may be developed.

Conflicts of Interest

The authors declare that they have no conflict of interest.

Authors' Contributions

Faiz-ul Hassan and Asif Nadeem contributed equally to this work.

References

- [1] J. K. Drackley, "Biology of dairy cows during the transition period: the final frontier?," *Journal of Dairy Science*, vol. 82, no. 11, pp. 2259–2273, 1999.

- [2] R. Van Saun, "Indicators of dairy cow transition risks: metabolic profiling revisited," *Tierärztliche Praxis. Ausgabe G, Grosstiere/nutztiere*, vol. 44, no. 2, pp. 118–126, 2016.
- [3] O. B. Pascottini, J. L. Leroy, and G. Opsomer, "Metabolic stress in the transition period of dairy cows: focusing on the prepartum period," *Animals*, vol. 10, no. 8, p. 1419, 2020.
- [4] W. Butler, "Nutritional effects on resumption of ovarian cyclicity and conception rate in postpartum dairy cows," *Publication*, vol. 26, no. 1, pp. 133–145, 2001.
- [5] C. K. Reynolds, B. Dürst, B. Lupoli, D. J. Humphries, and D. E. Beever, "Visceral tissue mass and rumen volume in dairy cows during the transition from late gestation to early lactation," *Journal of Dairy Science*, vol. 87, no. 4, pp. 961–971, 2004.
- [6] S. Tao and G. E. Dahl, "Invited review: heat stress effects during late gestation on dry cows and their calves," *Journal of Dairy Science*, vol. 96, no. 7, pp. 4079–4093, 2013.
- [7] M. S. Allen and B. J. Bradford, "Control of eating by hepatic oxidation of fatty acids. A note of caution," *Appetite*, vol. 53, no. 2, pp. 272–273, 2009.
- [8] P. R. Wankhade, A. Manimaran, A. Kumaresan et al., "Metabolic and immunological changes in transition dairy cows: a review," *Veterinary world*, vol. 10, no. 11, p. 1367, 2017.
- [9] B. Bradford, K. Yuan, J. Farney, L. Mamedova, and A. Carpenter, "Invited review: inflammation during the transition to lactation: new adventures with an old flame," *Journal of Dairy Science*, vol. 98, no. 10, pp. 6631–6650, 2015.
- [10] R. Wallace, G. McCoy, T. Overton, and J. Clark, "Effect of adverse health events on dry matter consumption, milk production, and body weight loss of dairy cows during early lactation," *Journal of Dairy Science*, vol. 79, Supplement 1, p. 205, 1996.
- [11] T. Rukkwamsuk, T. Kruip, and T. Wensing, "Relationship between overfeeding and overconditioning in the dry period and the problems of high producing dairy cows during the postparturient period," *Veterinary Quarterly*, vol. 21, no. 3, pp. 71–77, 1999.
- [12] B. N. Ametaj, A. Hosseini, J. F. Odhiambo et al., "Application of acute phase proteins for monitoring inflammatory states in cattle," in *Acute Phase Proteins as Early non-specific Biomarkers of Human and Veterinary Diseases*, pp. 299–354, InTech, Rijeka, Croatia, 2011.
- [13] M. T. Correa, C. R. Curtis, H. N. Erb, J. M. Scarlett, and R. D. Smith, "An ecological analysis of risk factors for postpartum disorders of Holstein-Friesian cows from thirty-two New York farms," *Journal of Dairy Science*, vol. 73, no. 6, pp. 1515–1524, 1990.
- [14] E. Jordan and R. Fourdraine, "Characterization of the management practices of the top milk producing herds in the country," *Journal of Dairy Science*, vol. 76, no. 10, pp. 3247–3256, 1993.
- [15] F. Mulligan and M. Doherty, "Production diseases of the transition cow," *The Veterinary Journal*, vol. 176, no. 1, pp. 3–9, 2008.
- [16] W. Knaus, "Dairy cows trapped between performance demands and adaptability," *Journal of the Science of Food and Agriculture*, vol. 89, no. 7, pp. 1107–1114, 2009.
- [17] W. Rauw, E. Kanis, E. Noordhuizen-Stassen, and F. Grommers, "Undesirable side effects of selection for high production efficiency in farm animals: a review," *Livestock Production Science*, vol. 56, no. 1, pp. 15–33, 1998.
- [18] R. S. Van and C. J. Sniffen, "transition cow nutrition and feeding management for disease prevention," *the veterinary clinics of North America*, *Food animal practice*, vol. 30, no. 3, pp. 689–719, 2014.
- [19] A. Sundrum, "Metabolic disorders in the transition period indicate that the dairy cows' ability to adapt is overstressed," *Animals*, vol. 5, no. 4, pp. 978–1020, 2015.
- [20] L. Andersson and U. Emanuelson, "An epidemiological study of hyperketonaemia in Swedish dairy cows; determinants and the relation to fertility," *Preventive Veterinary Medicine*, vol. 3, no. 5, pp. 449–462, 1985.
- [21] H. N. Erb, "Interrelationships among production and clinical disease in dairy cattle: a review," *The Canadian Veterinary Journal*, vol. 28, no. 6, p. 326, 1987.
- [22] P. Melendez, M. Marin, J. Robles, C. Rios, M. Duchens, and L. Archbald, "Relationship between serum nonesterified fatty acids at calving and the incidence of periparturient diseases in Holstein dairy cows," *Theriogenology*, vol. 72, no. 6, pp. 826–833, 2009.
- [23] P. Ospina, D. Nydam, T. Stokol, and T. Overton, "Evaluation of nonesterified fatty acids and β -hydroxybutyrate in transition dairy cattle in the northeastern United States: critical thresholds for prediction of clinical diseases," *Journal of Dairy Science*, vol. 93, no. 2, pp. 546–554, 2010.
- [24] J. K. Drackley, H. M. Dann, N. Douglas et al., "Physiological and pathological adaptations in dairy cows that may increase susceptibility to periparturient diseases and disorders," *Italian Journal of Animal Science*, vol. 4, no. 4, pp. 323–344, 2005.
- [25] S. Van der Drift, R. Jorritsma, J. Schonewille, H. Knijn, and J. Stegeman, "Routine detection of hyperketonemia in dairy cows using Fourier transform infrared spectroscopy analysis of β -hydroxybutyrate and acetone in milk in combination with test-day information," *Journal of Dairy Science*, vol. 95, no. 9, pp. 4886–4898, 2012.
- [26] S. Kessel, M. Stroehl, H. Meyer et al., "Individual variability in physiological adaptation to metabolic stress during early lactation in dairy cows kept under equal conditions," *Journal of Animal Science*, vol. 86, no. 11, pp. 2903–2912, 2008.
- [27] L. M. Sordillo and W. Raphael, "Significance of metabolic stress, lipid mobilization, and inflammation on transition cow disorders," *Veterinary Clinics: Food Animal Practice*, vol. 29, no. 2, pp. 267–278, 2013.
- [28] S. L. Aitken, C. M. Corl, and L. M. Sordillo, "Immunopathology of mastitis: insights into disease recognition and resolution," *Journal of Mammary Gland Biology and Neoplasia*, vol. 16, no. 4, pp. 291–304, 2011.
- [29] G. Esposito, P. C. Irons, E. C. Webb, and A. Chapwanya, "Interactions between negative energy balance, metabolic diseases, uterine health and immune response in transition dairy cows," *Animal Reproduction Science*, vol. 144, no. 3–4, pp. 60–71, 2014.
- [30] M. Loisel, C. Ster, B. Talbot et al., "Impact of postpartum milking frequency on the immune system and the blood metabolite concentration of dairy cows," *Journal of Dairy Science*, vol. 92, no. 5, pp. 1900–1912, 2009.
- [31] D. C. Wathes, Z. Cheng, W. Chowdhury et al., "Negative energy balance alters global gene expression and immune responses in the uterus of postpartum dairy cows," *Physiological Genomics*, vol. 39, no. 1, pp. 1–13, 2009.
- [32] K. M. Moyes, J. K. Drackley, D. E. Morin et al., "Mammary gene expression profiles during an intramammary challenge

- reveal potential mechanisms linking negative energy balance with impaired immune response,” *Physiological Genomics*, vol. 41, no. 2, pp. 161–170, 2010.
- [33] J. Huzzey, D. Veira, D. Weary, and M. Von Keyserlingk, “Prepartum behavior and dry matter intake identify dairy cows at risk for metritis,” *Journal of Dairy Science*, vol. 90, no. 7, pp. 3220–3233, 2007.
- [34] C. Ster, M.-C. Loisel, and P. Lacasse, “Effect of postcalving serum nonesterified fatty acids concentration on the functionality of bovine immune cells,” *Journal of Dairy Science*, vol. 95, no. 2, pp. 708–717, 2012.
- [35] D. Hammon, I. Evjen, T. Dhiman, J. Goff, and J. Walters, “Neutrophil function and energy status in Holstein cows with uterine health disorders,” *Veterinary Immunology and Immunopathology*, vol. 113, no. 1-2, pp. 21–29, 2006.
- [36] L. M. Sordillo, G. Contreras, and S. L. Aitken, “Metabolic factors affecting the inflammatory response of periparturient dairy cows,” *Animal Health Research Reviews*, vol. 10, no. 1, p. 53, 2009.
- [37] L. Sordillo and V. Mavangira, “The nexus between nutrient metabolism, oxidative stress and inflammation in transition cows,” *Animal Production Science*, vol. 54, no. 9, pp. 1204–1214, 2014.
- [38] J. K. Farney, L. K. Mamedova, J. F. Coetzee et al., “Anti-inflammatory salicylate treatment alters the metabolic adaptations to lactation in dairy cattle,” *American Journal of Physiology-Regulatory, Integrative and Comparative Physiology*, vol. 305, no. 2, pp. R110–R117, 2013.
- [39] J. M. Huzzey, S. Mann, D. V. Nydam, R. J. Grant, and T. R. Overton, “Associations of peripartum markers of stress and inflammation with milk yield and reproductive performance in Holstein dairy cows,” *Preventive Veterinary Medicine*, vol. 120, no. 3-4, pp. 291–297, 2015.
- [40] A. Abuelo, J. Hernández, J. L. Benedito, and C. Castillo, “The importance of the oxidative status of dairy cattle in the periparturient period: revisiting antioxidant supplementation,” *Journal of Animal Physiology and Animal Nutrition*, vol. 99, no. 6, pp. 1003–1016, 2015.
- [41] V. Taylor, D. Beever, and D. Wathes, “Physiological adaptations to milk production that affect the fertility of high yielding dairy cows,” *BSAP Occasional Publication*, vol. 29, pp. 37–71, 2004.
- [42] D. E. Beever, “The impact of controlled nutrition during the dry period on dairy cow health, fertility and performance,” *Animal Reproduction Science*, vol. 96, no. 3-4, pp. 212–226, 2006.
- [43] J. Robinson, C. Ashworth, J. Rooke, L. Mitchell, and T. McEvoy, “Nutrition and fertility in ruminant livestock,” *Animal Feed Science and Technology*, vol. 126, no. 3-4, pp. 259–276, 2006.
- [44] J. Leroy, T. Vanholder, A. Van Kneusel, I. Garcia-Ispuerto, and P. Bols, “Nutrient prioritization in dairy cows early postpartum: mismatch between metabolism and fertility?,” *Reproduction in Domestic Animals*, vol. 43, pp. 96–103, 2008.
- [45] B. Collard, P. Boettcher, J. Dekkers, D. Petitclerc, and L. Schaeffer, “Relationships between energy balance and health traits of dairy cattle in early lactation,” *Journal of Dairy Science*, vol. 83, no. 11, pp. 2683–2690, 2000.
- [46] D. E. Bauman and W. B. Currie, “Partitioning of nutrients during pregnancy and lactation: a review of mechanisms involving homeostasis and homeorhesis,” *Journal of Dairy Science*, vol. 63, no. 9, pp. 1514–1529, 1980.
- [47] S. LeBlanc, K. Leslie, and T. Duffield, “Metabolic predictors of displaced abomasum in dairy cattle,” *Journal of Dairy Science*, vol. 88, no. 1, pp. 159–170, 2005.
- [48] S. LeBlanc, “Managing critical periods—transition dairy cows,” in *Book of Abstracts, 15th Conference on Production Diseases in Farm Animals*, pp. 62–65, 2013.
- [49] A. Busato, D. Faissler, U. Küpfer, and J. Blum, “Body condition scores in dairy cows: associations with metabolic and endocrine changes in healthy dairy cows,” *Journal of Veterinary Medicine Series A*, vol. 49, no. 9, pp. 455–460, 2002.
- [50] B. Nonnecke, K. Kimura, J. Goff, and M. Kehrl Jr., “Effects of the mammary gland on functional capacities of blood mononuclear leukocyte populations from periparturient cows,” *Journal of Dairy Science*, vol. 86, no. 7, pp. 2359–2368, 2003.
- [51] L. S. Caixeta and B. O. Omontese, “Monitoring and improving the metabolic health of dairy cows during the transition period,” *Animals*, vol. 11, no. 2, p. 352, 2021.
- [52] P. Lacasse, N. Vanacker, S. Ollier, and C. Ster, “Innovative dairy cow management to improve resistance to metabolic and infectious diseases during the transition period,” *Research in Veterinary Science*, vol. 116, pp. 40–46, 2018.
- [53] J. K. Drackley, T. R. Overton, and G. N. Douglas, “Adaptations of glucose and long-chain fatty acid metabolism in liver of dairy cows during the periparturient period,” *Journal of Dairy Science*, vol. 84, pp. E100–E112, 2001.
- [54] K. L. Ingvarstsen, “Feeding-and management-related diseases in the transition cow: physiological adaptations around calving and strategies to reduce feeding-related diseases,” *Animal Feed Science and Technology*, vol. 126, no. 3-4, pp. 175–213, 2006.
- [55] J. Loor, “Genomics of metabolic adaptations in the periparturient cow,” *Animal: an international journal of animal bioscience*, vol. 4, no. 7, p. 1110, 2010.
- [56] N. Janovick, Y. Boisclair, and J. Drackley, “Prepartum dietary energy intake affects metabolism and health during the periparturient period in primiparous and multiparous Holstein cows¹,” *Journal of Dairy Science*, vol. 94, no. 3, pp. 1385–1400, 2011.
- [57] A. W. Bell, W. S. Burhans, and T. R. Overton, “Protein nutrition in late pregnancy, maternal protein reserves and lactation performance in dairy cows,” *Proceedings of the Nutrition Society*, vol. 59, no. 1, pp. 119–126, 2000.
- [58] J. Drackley and F. Cardoso, “Prepartum and postpartum nutritional management to optimize fertility in high-yielding dairy cows in confined TMR systems,” *Animal*, vol. 8, no. s1, pp. 5–14, 2014.
- [59] D. Grum, J. K. Drackley, R. Younker, D. LaCount, and J. Veenhuizen, “Nutrition during the dry period and hepatic lipid metabolism of periparturient dairy cows,” *Journal of Dairy Science*, vol. 79, no. 10, pp. 1850–1864, 1996.
- [60] M. Lucy, “Regulation of ovarian follicular growth by somatotropin and insulin-like growth factors in cattle¹,” *Journal of Dairy Science*, vol. 83, no. 7, pp. 1635–1647, 2000.
- [61] J. Roche, A. Bell, T. Overton, and J. J. Loor, “Nutritional management of the transition cow in the 21st century—a paradigm shift in thinking,” *Animal Production Science*, vol. 53, no. 9, pp. 1000–1023, 2013.
- [62] G. A. Contreras and L. M. Sordillo, “Lipid mobilization and inflammatory responses during the transition period of dairy

- cows," *Comparative Immunology, Microbiology and Infectious Diseases*, vol. 34, no. 3, pp. 281–289, 2011.
- [63] S. Van der Drift, M. Houweling, J. Schonewille, A. Tielens, and R. Jorritsma, "Protein and fat mobilization and associations with serum β -hydroxybutyrate concentrations in dairy cows," *Journal of Dairy Science*, vol. 95, no. 9, pp. 4911–4920, 2012.
- [64] I. J. Lean, R. Van Saun, and P. J. DeGaris, "Energy and protein nutrition management of transition dairy cows," *Veterinary Clinics: Food Animal Practice*, vol. 29, no. 2, pp. 337–366, 2013.
- [65] K. Moyes, J. K. Drackley, J. Salak-Johnson, D. Morin, J. Hope, and J. J. Loor, "Dietary-induced negative energy balance has minimal effects on innate immunity during a *Streptococcus uberis* mastitis challenge in dairy cows during midlactation," *Journal of Dairy Science*, vol. 92, no. 9, pp. 4301–4316, 2009.
- [66] K. Kimura, J. P. Goff, M. E. Kehrl Jr., and T. A. Reinhardt, "Decreased neutrophil function as a cause of retained placenta in dairy cattle," *Journal of Dairy Science*, vol. 85, no. 3, pp. 544–550, 2002.
- [67] J. G. Houdijk, N. S. Jessop, and I. Kyriazakis, "Nutrient partitioning between reproductive and immune functions in animals," *Proceedings of the Nutrition Society*, vol. 60, no. 4, pp. 515–525, 2001.
- [68] K. Galvão, M. Flaminio, S. Brittin et al., "Association between uterine disease and indicators of neutrophil and systemic energy status in lactating Holstein cows," *Journal of Dairy Science*, vol. 93, no. 7, pp. 2926–2937, 2010.
- [69] T. A. Reinhardt, J. D. Lippolis, B. J. McCluskey, J. P. Goff, and R. L. Horst, "Prevalence of subclinical hypocalcemia in dairy herds," *The Veterinary Journal*, vol. 188, no. 1, pp. 122–124, 2011.
- [70] J. Goff, R. Horst, T. Reinhardt, and D. Buxton, "Preventing Milk Fever in Dairy Cattle," in *Proceedings of the Tri-State Dairy Nutrition Conference*, pp. 41–55, Indiana, 1997.
- [71] K. Kimura, T. Reinhardt, and J. Goff, "Parturition and hypocalcemia blunts calcium signals in immune cells of dairy cattle," *Journal of Dairy Science*, vol. 89, no. 7, pp. 2588–2595, 2006.
- [72] I. J. Lean, R. Van Saun, and P. J. DeGaris, "Mineral and antioxidant management of transition dairy cows," *Veterinary Clinics: Food Animal Practice*, vol. 29, no. 2, pp. 367–386, 2013.
- [73] P. DeGaris, I. Lean, A. Rabiee, and C. Heuer, "Effects of increasing days of exposure to prepartum transition diets on reproduction and health in dairy cows," *Australian Veterinary Journal*, vol. 88, no. 3, pp. 84–92, 2010.
- [74] N.-T. Ha, J. J. Gross, A. van Dorland et al., "Gene-based mapping and pathway analysis of metabolic traits in dairy cows," *PLoS One*, vol. 10, no. 3, p. e0122325, 2015.
- [75] E. Kessler, J. J. Gross, R. Bruckmaier, and C. Albrecht, "Cholesterol metabolism, transport, and hepatic regulation in dairy cows during transition and early lactation," *Journal of Dairy Science*, vol. 97, no. 9, pp. 5481–5490, 2014.
- [76] M. Bionaz and J. J. Loor, "ACSL1, AGPAT6, FABP3, LPIN1, and SLC27A6 are the most abundant isoforms in bovine mammary tissue and their expression is affected by stage of lactation," *The Journal of Nutrition*, vol. 138, no. 6, pp. 1019–1024, 2008.
- [77] H. Dann and J. Drackley, "Carnitine palmitoyltransferase I in liver of periparturient dairy cows: effects of prepartum intake, postpartum induction of ketosis, and periparturient disorders," *Journal of Dairy Science*, vol. 88, no. 11, pp. 3851–3859, 2005.
- [78] W. Snelling, R. Cushman, J. Keele et al., "Breeding and genetics symposium: networks and pathways to guide genomic selection—," *Journal of Animal Science*, vol. 91, no. 2, pp. 537–552, 2013.
- [79] R. Weikard, T. Goldammer, R. M. Brunner, and C. Kuehn, "Tissue-specific mRNA expression patterns reveal a coordinated metabolic response associated with genetic selection for milk production in cows," *Physiological Genomics*, vol. 44, no. 14, pp. 728–739, 2012.
- [80] M. Baik, B. Etchebarne, J. Bong, and M. VandeHaar, "Gene expression profiling of liver and mammary tissues of lactating dairy cows," *Asian-Australasian Journal of Animal Sciences*, vol. 22, no. 6, pp. 871–884, 2009.
- [81] A. Chmurzyńska, "The multigene family of fatty acid-binding proteins (FABPs): function, structure and polymorphism," *Journal of Applied Genetics*, vol. 47, no. 1, pp. 39–48, 2006.
- [82] J. J. Loor, R. E. Everts, M. Bionaz et al., "Nutrition-induced ketosis alters metabolic and signaling gene networks in liver of periparturient dairy cows," *Physiological Genomics*, vol. 32, no. 1, pp. 105–116, 2007.
- [83] M. C. Rudolph, J. L. McManaman, T. Phang et al., "Metabolic regulation in the lactating mammary gland: a lipid synthesizing machine," *Physiological Genomics*, vol. 28, no. 3, pp. 323–336, 2007.
- [84] F.-U. Hassan, A. Nadeem, Z. Li et al., "Role of peroxisome proliferator-activated receptors (PPARs) in energy homeostasis of dairy animals: exploiting their modulation through nutrigenomic interventions," *International Journal of Molecular Sciences*, vol. 22, no. 22, p. 12463, 2021.
- [85] G. Schlegel, J. Keller, F. Hirche et al., "Expression of genes involved in hepatic carnitine synthesis and uptake in dairy cows in the transition period and at different stages of lactation," *BMC Veterinary Research*, vol. 8, no. 1, pp. 1–12, 2012.
- [86] Z.-L. Wu, S.-Y. Chen, C. Qin et al., "Clinical ketosis-associated alteration of gene expression in Holstein cows," *Genes*, vol. 11, no. 2, p. 219, 2020.
- [87] J. Laguna, M. Cardoso, J. Lima et al., "Expression of hepatic genes related to energy metabolism during the transition period of Holstein and F1 Holstein-Gir cows," *Journal of Dairy Science*, vol. 100, no. 12, pp. 9861–9870, 2017.
- [88] G. Douglas, T. Overton, H. Bateman II, H. Dann, and J. Drackley, "Prepartal plane of nutrition, regardless of dietary energy source, affects periparturient metabolism and dry matter intake in Holstein cows," *Journal of Dairy Science*, vol. 89, no. 6, pp. 2141–2157, 2006.
- [89] U. Moallem, "Invited review: roles of dietary n-3 fatty acids in performance, milk fat composition, and reproductive and immune systems in dairy cattle," *Journal of Dairy Science*, vol. 101, no. 10, pp. 8641–8661, 2018.
- [90] M. Lessard, N. Gagnon, D. Godson, and H. Petit, "Influence of parturition and diets enriched in n-3 or n-6 polyunsaturated fatty acids on immune response of dairy cows during the transition period," *Journal of Dairy Science*, vol. 87, no. 7, pp. 2197–2210, 2004.
- [91] J. Y. Lee, L. Zhao, and D. H. Hwang, "Modulation of pattern recognition receptor-mediated inflammation and risk of chronic diseases by dietary fatty acids," *Nutrition Reviews*, vol. 68, no. 1, pp. 38–61, 2010.

- [92] D. Scalia, N. Lacetera, U. Bernabucci, K. Demeyere, L. Duchateau, and C. Burvenich, "In vitro effects of nonesterified fatty acids on bovine neutrophils oxidative burst and viability," *Journal of Dairy Science*, vol. 89, no. 1, pp. 147–154, 2006.
- [93] M. Alim, Y. Xie, Y. Fan et al., "Genetic effects of ABCG2 polymorphism on milk production traits in the Chinese Holstein cattle," *Journal of Applied Animal Research*, vol. 41, no. 3, pp. 333–338, 2013.
- [94] Z. Zhou, M. Vailati-Riboni, D. N. Luchini, and J. J. Loor, "Methionine and choline supply during the periparturient period alter plasma amino acid and one-carbon metabolism profiles to various Extents: potential role in hepatic metabolism and antioxidant status," *Nutrients*, vol. 9, no. 1, 2017.
- [95] R. Goselink, J. Van Baal, H. Widjaja et al., "Effect of rumen-protected choline supplementation on liver and adipose gene expression during the transition period in dairy cattle," *Journal of Dairy Science*, vol. 96, no. 2, pp. 1102–1116, 2013.
- [96] V. Lopreiato, M. Mezzetti, L. Cattaneo, G. Ferronato, A. Minuti, and E. Trevisi, "Role of nutraceuticals during the transition period of dairy cows: a review," *Journal of Animal Science and Biotechnology*, vol. 11, no. 1, pp. 1–18, 2020.
- [97] L. Reitsma, T. Batchelder, E. Davis, V. Machado, R. Neves, and M. Ballou, "Effects of oral calcium bolus supplementation on intracellular polymorphonuclear leukocyte calcium levels and functionality in primiparous and multiparous dairy cows," *Journal of Dairy Science*, vol. 103, no. 12, pp. 11876–11888, 2020.
- [98] B. Leno, R. Neves, I. Louge et al., "Differential effects of a single dose of oral calcium based on postpartum plasma calcium concentration in Holstein cows," *Journal of Dairy Science*, vol. 101, no. 4, pp. 3285–3302, 2018.
- [99] E. Trevisi, N. Jahan, G. Bertoni, A. Ferrari, and A. Minuti, "Pro-inflammatory cytokine profile in dairy cows: consequences for new lactation," *Italian Journal of Animal Science*, vol. 14, no. 3, p. 3862, 2015.
- [100] H. Dann, J. Drackley, G. McCoy, M. Hutjens, and J. Garrett, "Effects of yeast culture (*Saccharomyces cerevisiae*) on prepartum intake and postpartum intake and milk production of Jersey cows¹," *Journal of Dairy Science*, vol. 83, no. 1, pp. 123–127, 2000.
- [101] P. Williams, C. Tait, G. Innes, and C. Newbold, "Effects of the inclusion of yeast culture (*Saccharomyces cerevisiae* plus growth medium) in the diet of dairy cows on milk yield and forage degradation and fermentation patterns in the rumen of steers," *Journal of Animal Science*, vol. 69, no. 7, pp. 3016–3026, 1991.
- [102] M. Bionaz, S. Chen, M. J. Khan, and J. J. Loor, "Functional role of PPARs in ruminants: potential targets for fine-tuning metabolism during growth and lactation," *PPAR Research*, vol. 2013, 28 pages, 2013.
- [103] W. Stoffel, B. Holz, B. Jenke et al., "Δ6-desaturase (FADS2) deficiency unveils the role of ω3-and ω6-polyunsaturated fatty acids," *The EMBO Journal*, vol. 27, no. 17, pp. 2281–2292, 2008.
- [104] B. Koletzko, E. Larque, and H. Demmelmair, "Placental transfer of long-chain polyunsaturated fatty acids (LC-PUFA)," *Journal of Perinatal Medicine*, vol. 35, no. s1, pp. S5–S11, 2007.
- [105] S. M. Innis, "Dietary omega 3 fatty acids and the developing brain," *Brain Research*, vol. 1237, pp. 35–43, 2008.
- [106] L. Greco, J. N. Neto, A. Pedrico et al., "Effects of altering the ratio of dietary n-6 to n-3 fatty acids on spontaneous luteolysis in lactating dairy cows," *Journal of Dairy Science*, vol. 101, no. 11, pp. 10536–10556, 2018.
- [107] N. Qin, A.-R. Bayat, E. Trevisi et al., "Dietary supplement of conjugated linoleic acids or polyunsaturated fatty acids suppressed the mobilization of body fat reserves in dairy cows at early lactation through different pathways," *Journal of Dairy Science*, vol. 101, no. 9, pp. 7954–7970, 2018.
- [108] J. Lofton, J. Linn, J. Drackley, T. Jenkins, C. Soderholm, and A. Kertz, "Invited review: palmitic and stearic acid metabolism in lactating dairy cows," *Journal of Dairy Science*, vol. 97, no. 8, pp. 4661–4674, 2014.
- [109] N. R. Council, *Nutrient requirements of dairy cattle: 2001*, National Academies Press, 2001.
- [110] H. Khelil-Arfa, P. Faverdin, and A. Boudon, "Effect of ambient temperature and sodium bicarbonate supplementation on water and electrolyte balances in dry and lactating Holstein cows," *Journal of Dairy Science*, vol. 97, no. 4, pp. 2305–2318, 2014.
- [111] J. Argyle and R. Baldwin, "Modeling of rumen water kinetics and effects of rumen pH changes," *Journal of Dairy Science*, vol. 71, no. 5, pp. 1178–1188, 1988.
- [112] S. Grossi, L. Rossi, M. Dell'Anno, S. Biffani, and C. A. Sgoifo Rossi, "Effects of heated drinking water on the growth performance and rumen functionality of fattening Charolaise beef cattle in winter," *Animals*, vol. 11, no. 8, p. 2218, 2021.
- [113] Y.-H. Kim, N. Toji, K. Kizaki, K. Takemura, S. Kushibiki, and S. Sato, "Effects of ruminal pH on gene expression in the rumen epithelium, peripheral blood mononuclear cell subpopulations, and blood metabolites from Holstein calves during weaning transition," *The Journal of Veterinary Medical Science*, vol. 81, no. 6, pp. 808–816, 2019.
- [114] A. I. Virtanen, "Milk production of cows on protein-free feed," *Science*, vol. 153, no. 3744, pp. 1603–1614, 1966.
- [115] D. Schingoethe, D. Casper, C. Yang, D. Illg, J. Sommerfeldt, and C. Mueller, "Lactational response to soybean meal, heated soybean meal, and extruded soybeans with ruminally protected methionine," *Journal of Dairy Science*, vol. 71, no. 1, pp. 173–180, 1988.
- [116] T. Scott, D. Combs, and R. Grummer, "Effects of roasting, extrusion, and particle size on the feeding value of soybeans for dairy cows," *Journal of Dairy Science*, vol. 74, no. 8, pp. 2555–2562, 1991.
- [117] R. R. Grummer, M. L. Luck, and J. A. Barmore, "Lactational performance of dairy cows fed raw soybeans, with or without animal by-product proteins, or roasted soybeans," *Journal of Dairy Science*, vol. 77, no. 5, pp. 1354–1359, 1994.
- [118] R. McGuffey, H. Green, and R. Basson, "Lactation response of dairy cows receiving bovine somatotropin and fed rations varying in crude protein and undegradable intake protein," *Journal of Dairy Science*, vol. 73, no. 9, pp. 2437–2443, 1990.
- [119] L. Satter and L. Slyter, "Effect of ammonia concentration on rumen microbial protein production in vitro," *British Journal of Nutrition*, vol. 32, no. 2, pp. 199–208, 1974.
- [120] L. Satter and R. Roffler, "Nitrogen requirement and utilization in dairy cattle," *Journal of Dairy Science*, vol. 58, no. 8, pp. 1219–1237, 1975.
- [121] R. Roffler and L. Satter, "Relationship between ruminal ammonia and nonprotein nitrogen utilization by ruminants. I. Development of a model for predicting nonprotein

- nitrogen utilization by cattle," *Journal of Dairy Science*, vol. 58, no. 12, pp. 1880–1888, 1975.
- [122] W. Chalupa, "Rumen bypass and protection of proteins and amino acids," *Journal of Dairy Science*, vol. 58, no. 8, pp. 1198–1218, 1975.
- [123] S. Mabeesh, A. Arieli, I. Bruckental, S. Zamwell, and H. Tagari, "Effect of type of protein supplementation on duodenal amino acid flow and absorption in lactating dairy cows," *Journal of Dairy Science*, vol. 79, no. 10, pp. 1792–1801, 1996.
- [124] P. Reddy, J. Morrill, and L. Bates, "Effect of roasting temperatures on soybean utilization by young dairy calves," *Journal of Dairy Science*, vol. 76, no. 5, pp. 1387–1393, 1993.
- [125] J. Spears, J. Clark, and E. Hatfield, "Nitrogen utilization and ruminal fermentation in steers fed soybean meal treated with formaldehyde," *Journal of Animal Science*, vol. 60, no. 4, pp. 1072–1080, 1985.
- [126] R. Emery, "Disappearance of methionine from the rumen," *Journal of Dairy Science*, vol. 54, no. 7, pp. 1090–1091, 1971.
- [127] L. Armentano, S. Bertics, and G. Ducharme, "Response of lactating cows to methionine or methionine plus lysine added to high protein diets based on alfalfa and heated soybeans," *Journal of Dairy Science*, vol. 80, no. 6, pp. 1194–1199, 1997.
- [128] D. Vyas and R. Erdman, "Meta-analysis of milk protein yield responses to lysine and methionine supplementation," *Journal of Dairy Science*, vol. 92, no. 10, pp. 5011–5018, 2009.
- [129] H. Gao, S. Zhao, N. Zheng et al., "Combination of histidine, lysine, methionine, and leucine promotes β -casein synthesis via the mechanistic target of rapamycin signaling pathway in bovine mammary epithelial cells," *Journal of Dairy Science*, vol. 100, no. 9, pp. 7696–7709, 2017.
- [130] Y. Zhou, Z. Zhou, J. Peng, and J. Loor, "Methionine and valine activate the mammalian target of rapamycin complex 1 pathway through heterodimeric amino acid taste receptor (TAS1R1/TAS1R3) and intracellular Ca^{2+} in bovine mammary epithelial cells," *Journal of Dairy Science*, vol. 101, no. 12, pp. 11354–11363, 2018.
- [131] Y. Liang, F. Batistel, C. Parys, and J. Loor, "Methionine supply during the periparturient period enhances insulin signaling, amino acid transporters, and mechanistic target of rapamycin pathway proteins in adipose tissue of Holstein cows," *Journal of Dairy Science*, vol. 102, no. 5, pp. 4403–4414, 2019.
- [132] J. S. Osorio, "Amino acid balancing and its role on metabolism, inflammation, and oxidative stress: future molecular implications," in *29th Annual Florida Ruminant Nutrition Symposium, University of Florida*, pp. 19–37, Gainesville, FL, United States, 2018.
- [133] D. N. Coleman, V. Lopreiato, A. Alharthi, and J. J. Loor, "Amino acids and the regulation of oxidative stress and immune function in dairy cattle," *Journal of Animal Science*, vol. 98, Supplement_1, pp. S175–S193, 2020.
- [134] D. Palmquist and T. Jenkins, "Fat in lactation rations1, 2: review," *Journal of Dairy Science*, vol. 63, no. 1, pp. 1–14, 1980.
- [135] J. Sutton, "Altering milk composition by feeding," *Journal of Dairy Science*, vol. 72, no. 10, pp. 2801–2814, 1989.
- [136] E. Powell, "Some relations of the roughage intake to the composition of milk," *Journal of Dairy Science*, vol. 22, p. 453, 1939.
- [137] M. S. Allen, "Relationship between fermentation acid production in the rumen and the requirement for physically effective fiber," *Journal of Dairy Science*, vol. 80, no. 7, pp. 1447–1462, 1997.
- [138] D. Beitz and C. Davis, "Relationship of certain milk fat depressing diets to changes in the proportions of the volatile fatty acids produced in the rumen," *Journal of Dairy Science*, vol. 47, no. 11, pp. 1213–1216, 1964.
- [139] C. Davis and R. Brown, *Low-fat milk syndrome*, Low-fat milk syndrome, 1970.
- [140] D. Bauman, I. Mather, R. Wall, and A. Lock, "Major advances associated with the biosynthesis of milk," *Journal of Dairy Science*, vol. 89, no. 4, pp. 1235–1243, 2006.
- [141] Y. Chilliard, C. Martin, J. Rouel, and M. Doreau, "Milk fatty acids in dairy cows fed whole crude linseed, extruded linseed, or linseed oil, and their relationship with methane output¹," *Journal of Dairy Science*, vol. 92, no. 10, pp. 5199–5211, 2009.
- [142] P. Kairenius, A. Ärölä, H. Leskinen et al., "Dietary fish oil supplements depress milk fat yield and alter milk fatty acid composition in lactating cows fed grass silage-based diets," *Journal of Dairy Science*, vol. 98, no. 8, pp. 5653–5671, 2015.
- [143] K. J. Shingfield, C. K. Reynolds, G. Hervás, J. M. Griinari, A. S. Grandison, and D. E. Beever, "Examination of the persistency of milk fatty acid composition responses to fish oil and sunflower oil in the diet of dairy cows," *Journal of Dairy Science*, vol. 89, no. 2, pp. 714–732, 2006.
- [144] J. Kennelly, B. Robinson, and G. Khorasani, "Influence of carbohydrate source and buffer on rumen fermentation characteristics, milk yield, and milk composition in early-lactation Holstein cows," *Journal of Dairy Science*, vol. 82, no. 11, pp. 2486–2496, 1999.
- [145] J. Bell, J. Griinari, and J. Kennelly, "Effect of safflower oil, flaxseed oil, monensin, and vitamin E on concentration of conjugated linoleic acid in bovine milk fat," *Journal of Dairy Science*, vol. 89, no. 2, pp. 733–748, 2006.
- [146] C. Reveneau, S. Karnati, E. Oelker, and J. Firkins, "Interaction of unsaturated fat or coconut oil with monensin in lactating dairy cows fed 12 times daily. I. Protozoal abundance, nutrient digestibility, and microbial protein flow to the omasum," *Journal of Dairy Science*, vol. 95, no. 4, pp. 2046–2060, 2012.
- [147] M. He, K. Perfield, H. Green, and L. Armentano, "Effect of dietary fat blend enriched in oleic or linoleic acid and monensin supplementation on dairy cattle performance, milk fatty acid profiles, and milk fat depression," *Journal of Dairy Science*, vol. 95, no. 3, pp. 1447–1461, 2012.
- [148] J. Griinari, D. Dwyer, M. McGuire, D. Bauman, D. Palmquist, and K. Nurmela, "Trans-octadecenoic acids and milk fat depression in lactating dairy cows," *Journal of Dairy Science*, vol. 81, no. 5, pp. 1251–1261, 1998.
- [149] L. H. Baumgard, B. A. Corl, D. A. Dwyer, A. Sæbø, and D. E. Bauman, "Identification of the conjugated linoleic acid isomer that inhibits milk fat synthesis," *American Journal of Physiology-Regulatory, Integrative and Comparative Physiology*, vol. 278, no. 1, pp. R179–R184, 2000.
- [150] G. Invernizzi, B. Thering, M. Bionaz, G. Savoini, and J. J. Loor, "Metabolic and signalling pathway alterations in mammary gland of cows fed saturated or unsaturated fat," *Energy and protein metabolism and nutrition*, vol. 127, p. 73, 2010.
- [151] B. Thering, D. Graugnard, P. Piantoni, and J. Loor, "Adipose tissue lipogenic gene networks due to lipid feeding and milk

Retraction

Retracted: Pathological, Histological, and Molecular Based Investigations Confirm Novel *Mycobacterium bovis* Infection in *Boselaphus tragocamelus*

BioMed Research International

Received 8 January 2024; Accepted 8 January 2024; Published 9 January 2024

Copyright © 2024 BioMed Research International. This is an open access article distributed under the Creative Commons Attribution License, which permits unrestricted use, distribution, and reproduction in any medium, provided the original work is properly cited.

This article has been retracted by Hindawi following an investigation undertaken by the publisher [1]. This investigation has uncovered evidence of one or more of the following indicators of systematic manipulation of the publication process:

- (1) Discrepancies in scope
- (2) Discrepancies in the description of the research reported
- (3) Discrepancies between the availability of data and the research described
- (4) Inappropriate citations
- (5) Incoherent, meaningless and/or irrelevant content included in the article
- (6) Manipulated or compromised peer review

The presence of these indicators undermines our confidence in the integrity of the article's content and we cannot, therefore, vouch for its reliability. Please note that this notice is intended solely to alert readers that the content of this article is unreliable. We have not investigated whether authors were aware of or involved in the systematic manipulation of the publication process.

Wiley and Hindawi regrets that the usual quality checks did not identify these issues before publication and have since put additional measures in place to safeguard research integrity.

We wish to credit our own Research Integrity and Research Publishing teams and anonymous and named external researchers and research integrity experts for contributing to this investigation.

The corresponding author, as the representative of all authors, has been given the opportunity to register their agreement or disagreement to this retraction. We have kept a record of any response received.

References

- [1] R. Hussain, A. Jamal, Z. Ahmed et al., "Pathological, Histological, and Molecular Based Investigations Confirm Novel *Mycobacterium bovis* Infection in *Boselaphus tragocamelus*," *BioMed Research International*, vol. 2022, Article ID 7601463, 9 pages, 2022.

Research Article

Pathological, Histological, and Molecular Based Investigations Confirm Novel *Mycobacterium bovis* Infection in *Boselaphus tragocamelus*

Riaz Hussain ¹, Adil Jamal ², Zulfiqar Ahmed,³ Bahaeldeen Babiker Mohamed ⁴,
Abu Baker Siddique ⁵, Iahtasham Khan ⁶, Muhammad Khalid Mansoor,⁷ Xiaoxia Du ⁸,
and Ahrar Khan ^{8,9}

¹Department of Pathology, Faculty of Veterinary and Animal Sciences, The Islamia University of Bahawalpur, 63100, Pakistan

²Sciences and Research, College of Nursing, Umm Al Qura University, 715 Makkah, Saudi Arabia

³Department of Food Science and Technology, Faculty of Agriculture and Environment, The Islamia University of Bahawalpur, 63100, Pakistan

⁴Institute of Environment Natural Resources, The National Centre of Research, Khartoum, Sudan

⁵Department of Microbiology, Government College University, Faisalabad 38000, Pakistan

⁶Section of Epidemiology and Public Health, University of Veterinary and Animal Sciences, Lahore, Sub-Campus Jhang, Pakistan

⁷Department of Microbiology, Faculty of Veterinary and Animal Sciences, The Islamia University of Bahawalpur-63100, Pakistan

⁸Shandong Vocational Animal Science and Veterinary College, Weifang 261061, China

⁹Faculty of Veterinary Science, University of Agriculture, Faisalabad 38040, Pakistan

Correspondence should be addressed to Riaz Hussain; dr.riaz.hussain@iub.edu.pk
and Bahaeldeen Babiker Mohamed; bahaeldeen.elhag@ncr.gov.sd

Received 14 April 2022; Revised 1 May 2022; Accepted 19 May 2022; Published 2 June 2022

Academic Editor: Faheem Ahmed Khan

Copyright © 2022 Riaz Hussain et al. This is an open access article distributed under the Creative Commons Attribution License, which permits unrestricted use, distribution, and reproduction in any medium, provided the original work is properly cited.

Mycobacterium bovis (*M. bovis*) being the main cause of animal tuberculosis is a complex infectious agent and can be a cause of zoonotic tuberculosis zoonosis in public health. To date, the uncommon infection in public health due to *M. bovis* still is a great challenge to both veterinary and medical professions and requires a careful diagnosis and confirmation of the bacterium. Therefore, this study for the first time reports the clinical, gross, histopathological, and molecular based confirmation of *M. bovis* infection in wildlife animals (nilgai). Prior to death, the morbid animal showed severe pneumonic ailments like moist cough, thick nasal exudates, and dyspnoea. At necropsy, enlargement of mandibular cervical and mesenteric lymph nodes was observed. Different macroscopic lesions such as congestion and hyperaemia, creamy white and catarrhal exudates in trachea, consolidation, grey and red hepatisation of lungs, and micro- and macrogranulomatous tubercles containing caseous materials in lungs were observed. The heart of morbid animal showed congestions, myocarditis, and a copious amount of straw-colored fluid in the pericardial sac. At the microscopic level, lungs indicated granulomatous inflammatory response, presence of multinucleated giant cells, fibrosis, and punctuation of alveoli with chronic inflammatory cells. Histopathological examination of various sections of the heart of the infected animal showed chronic inflammatory response consisting of chronic inflammatory cells like monocyte, lymphocytes, and fibroblasts along with noncalcified eosinophilic materials. At the molecular level, *M. bovis* infection was confirmed in various tissues like the heart, lungs, cervical, and mesenteric lymph nodes in morbid animals. In conclusion, based on our results, it can be suggested that more molecular based epidemiological studies are crucial to know the exact cause of pulmonary and cervical tuberculosis in wild animals.

1. Introduction

The majority of newly emerging human diseases are caused by zoonotic diseases. Furthermore, 71% of newly emerging diseases are either derived from wildlife or have an epidemiologically significant animal host [1]. Many of the diseases that infect domestic animals can also infect wild animals, and transmission between domestic animals and wildlife can occur in both directions. The primary occurrence, however, was frequently the spread of disease from domestic animals to wildlife. *Mycobacterium bovis*, the causal agent of tuberculosis in cattle and most other mammals, wild or domestic, is one such pathogen [2]. Importantly, it has a wide spectrum of hosts including humans [3].

Mycobacterium tuberculosis of the family Mycobacteriaceae is Gram-positive and rod-shaped and causes tuberculosis in mammals. *Mycobacterium bovis* (bovine tuberculosis), *M. caprae* (caprine tuberculosis), *M. pinnipedii*, *M. orygis*, and *M. microti* are reported in animals [4]. *Mycobacterium caprae*, *M. pinnipedii*, and *M. orygis* are classified as subspecies of *M. bovis*. Two other organisms, *M. tuberculosis* and *M. africanum*, are found in humans but infect animals infrequently [4]. A few countries (for example, Australia, Iceland, Greenland, Singapore, several European countries, and Israel) are completely free of *M. bovis*, although infected cattle herds are now rare in Europe, Canada, United States, New Zealand, and other countries.

The majority of data on zoonotic mycobacteria transmission is evidenced by investigations on *M. bovis* [4]. Depending on the areas, where it has localized, the causal organism may be identified in respiratory secretions, exudates/secretions from lesions (e.g., draining lymph nodes, certain skin lesions), urine, feces, milk, vaginal discharge, and semen. *Mycobacterium bovis* is more likely to be transferred when the respiratory system gets infected and during the late stages of the disease with widespread lesions [4]. The extent to which an infected host brings itself or its excretions into close contact with other vulnerable hosts, including members of the same species, is determined by host ecology and behaviour [5].

Prevalence alludes not only to the quantity of diseased animals in a given community but also to their geographic and temporal distribution [5]. Multiple species are epidemiologically linked in several countries with suspected or confirmed *M. bovis* wildlife animals, which may involve multiple hosts and different transmission routes [6]. In Pakistan, different species of livestock animals including large ruminants (camel, cattle, and buffaloes) and small ruminants (sheep and goat) are particularly kept for milk and meat purposes [7–10]. These animals are usually and mainly reared under tropical and subtropical conditions in the country. Epidemiological studies in Pakistan have reported the prevalence of contagious and zoonotic bacteria [11–17], parasites [18], and viral diseases [19]. Among various zoonotic diseases, tuberculosis due to *M. bovis* is a fatal problem for dairy and wild animals [20–22]. *Mycobacterium bovis* infection causes huge economic losses in terms of reduced milk yield, increased cost of treatment and control strategies, cul-

ling of infected animals, and limiting the international trade of dairy animals and their products [23].

Studies have indicated that in several developing countries, *M. bovis* acts as an endemic threat [24, 25] and has been reported in free-ranging carnivores and wild animals [26, 27]. Earlier studies have reported a 5.75% prevalence of *M. bovis* infection in cattle and buffalo while 4% in humans [28, 29]. Recently, in Pakistan, 5.88% of *M. bovis* infection has been recorded in different districts of Paktunkhwa [23]. Higher prevalence of *M. bovis* infection in buffaloes (8.48%) reared at various livestock farms [30] and in cattle (11.71%) of different private farms has been recorded [31]. Several studies in Pakistan have determined an increased prevalence *M. bovis* infection such as 12.72% [32], 11.3% [33], 10.6% [34], 7.47% [35], and 9.6% in dairy animals [36]. A lower prevalence (2.2–3%) of *M. bovis* infection in buffaloes kept at different locations in Punjab has also been documented [30, 37]. Previously, scanty information could be found regarding the prevalence of bovine tuberculosis in different zoo animals including Bovidae and Cervidae [38].

The exact mechanisms of spread and transmission of *M. bovis* to wildlife animals still remain unclear. However, the wild animals may get these infections directly via close contact with scavengers or indirectly through contamination of the environment or ingestion of infected products. Few reports are available about bovine tuberculosis in wild animals kept at various zoological parks and different zoos in Pakistan [19].

Tuberculosis is commonly diagnosed by isolating the organism from the sputum, milk, feces, and other bodily fluids [39]. Tuberculosis is commonly detected using direct smear microscopy with the fluorescent acid-fast staining technique and Ziehl-(ZN) Neelsen's staining of clinical samples [39]. Although culturing on selective media provides a confirmed *Mycobacterium* diagnosis, the main disadvantage of this approach is the slow bacterial growth [40]. Using polymerase chain reaction (PCR) amplification of the *Mycobacterium* DNA, it is possible to make a rapid diagnosis of *Mycobacterium* from clinical samples. PCR is a more precise and reliable method for rapid diagnosis, with substantially higher sensitivity and specificity than bacterial culture [40]. It is necessary to comprehend the involvement of wildlife in the epidemiology of *M. bovis* infection.

This study is aimed at studying necropsy lesions and histopathological findings of tuberculosis due to *M. bovis* in nilgai. *Mycobacterium bovis* detection was further confirmed using PCR. Regular livestock and wildlife screening will help prevent *M. bovis* transmission to other animals.

2. Materials and Methods

2.1. Ethical statement. The technical and ethical committee constituted by the Department of Pathology, Faculty of Veterinary and Animal Sciences, the Islamia University of Bahawalpur, Pakistan, approved the protocol of the postmortem study of nilgai.

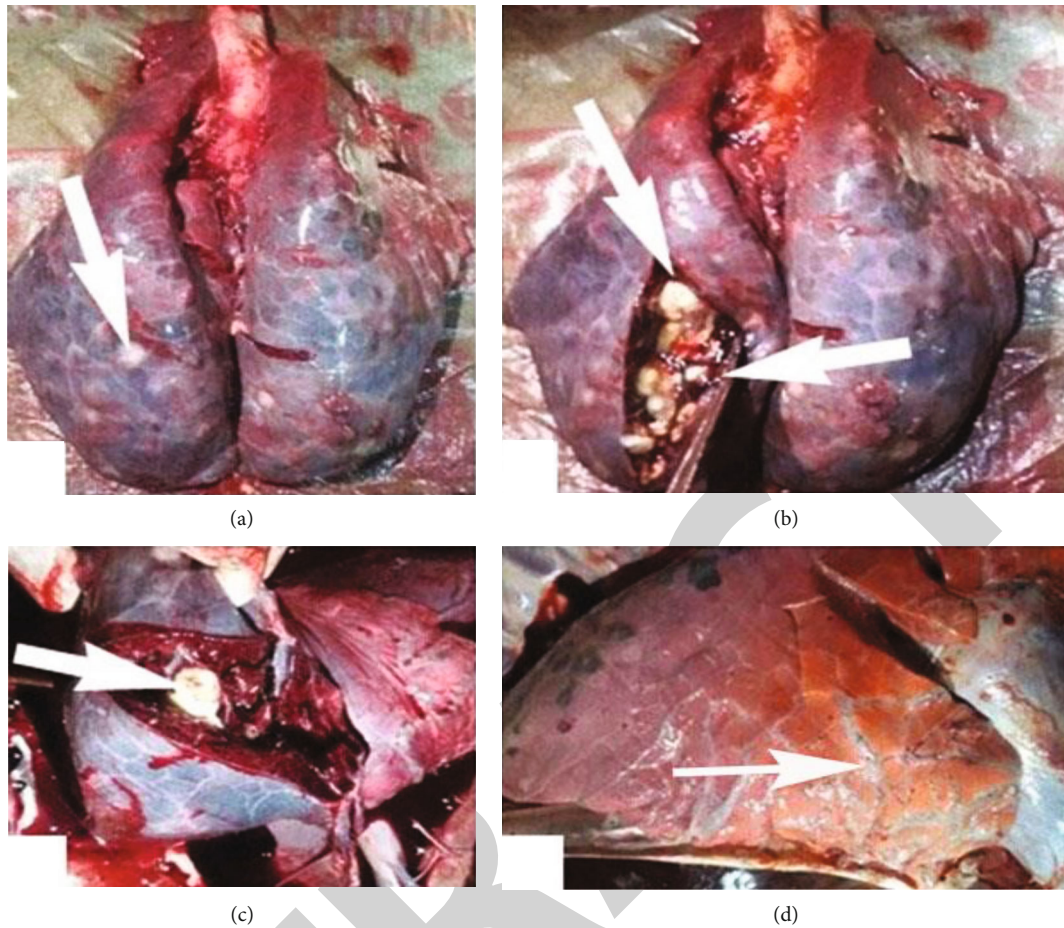


FIGURE 1: Photograph lungs of Nilgai showing (a) multifocal tubercles and red hepatisation, (b, c) cut sections exhibiting creamy white exudates, and (d) severe emphysema in the lungs of nilgai that died from *M. bovis* infection.

2.2. Study Location and Animals. The current study included two animals that suddenly died at Bahawalpur Zoo, Punjab, Pakistan. Both the animals were kept together under tropical and subtropical environmental conditions. History from the concerned veterinarian and curator of the zoo revealed that a male nilgai become sick and exhibited different clinical signs like anorexia, being reluctant to move, depression, dyspnea, lethargy, disorientation, and coughing while the female died without any signs of respiratory infections and exhibited increased watery fluid from mouth and disorientation. These animals were offered seasonal green fodder and grain (0.5 kg) daily. In one case, the persistent cough was a prominent clinical sign observed early in the morning and during the late evening. In spite of extensive care, management practices, and treatment therapy, the animals died. The necropsy was performed after half an hour of death to determine the possible cause of death.

2.3. Necropsy and Histopathological Investigation. Prior to complete skinning and abdominal opening, the nilgai were carefully observed for external lesions. The nilgai were quite normal and had fair body conditions. At necropsy, the external examination showed severe congested nasal passages and thick nasal discharge before skinning in the male while enlarged and swollen cervical and mandibular lymph nodes

in the female. After thorough and complete external observation, the dead animals were dissected and opened to know any internal lesions.

2.4. Sample Collection and Histopathology Studies. The visceral organs showing abnormal lesions such as the lungs and heart were removed and immediately fixed in 10% neutral buffered formalin solutions for histological changes [10]. For histopathological observations, various tissues from the lungs and heart were embedded in paraffin wax, and about 5 μ m-thick sections were stained with haematoxylin and eosin (H&E) stains [41].

2.5. Genetic Analysis. For bacilli confirmation, different tissue samples having lesions, e.g., the lungs, heart, mesenteric, and cervical lymph nodes, were used for bacterial DNA extraction and confirmation of suspected cause [42]. Genomic DNA was extracted from samples using the GeneJET Genomic DNA Extraction kit (Cat# K0721, Thermo Scientific™, USA) following the manufacturer's guidelines. The gene-specific primer targeting the JB21 and JB22 genes (sense JB21; 5'-TCGTCCGCTGATGCAAGTGC-3', anti-sense JB22; 5'-CGTCCGCTGACCTCAAGAAG-3') was used for the genomic amplification of *M. bovis* in samples [43]. The PCR was performed in a thermocycler (Bio-Rad,

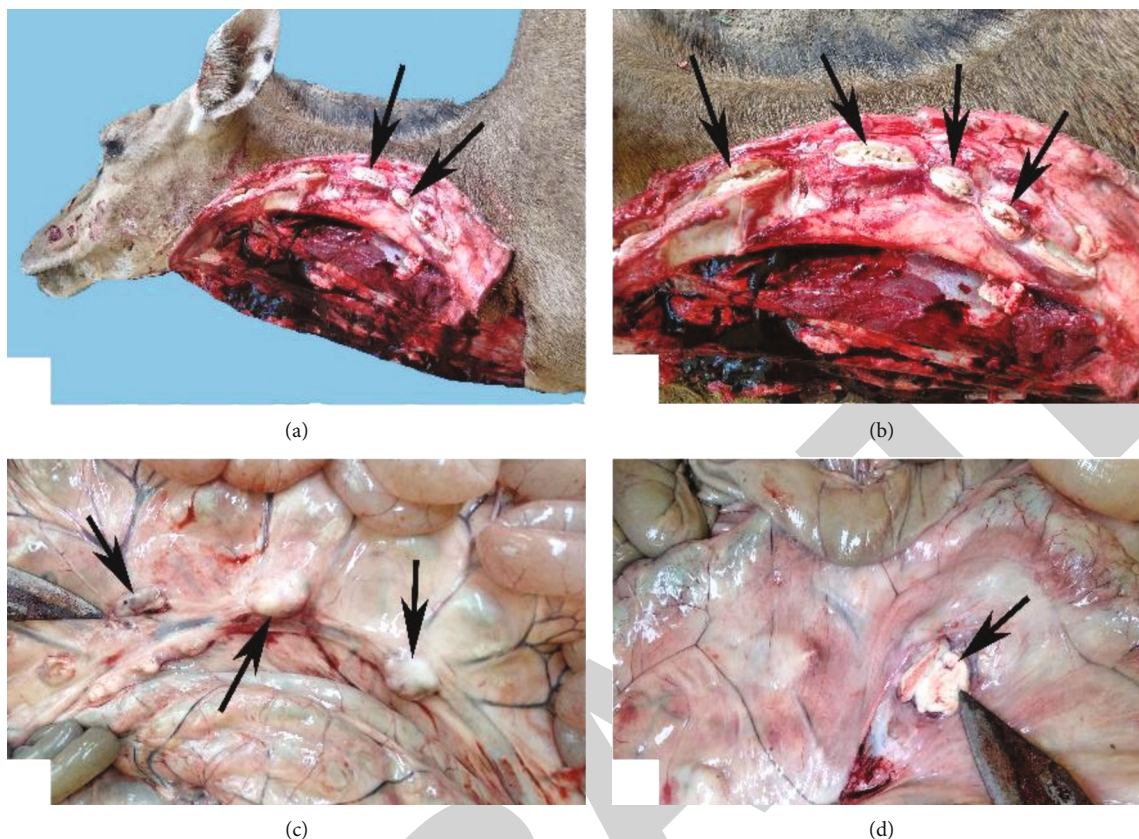


FIGURE 2: Necropsy of Nilgai showing (a, b) caseated exudate and calcified lymph nodes in opened neck region (arrows) and (c, d) enlarged, caseated exudate, and calcified mesenteric lymph nodes (arrows).

T100 Thermal Cycler, USA) using the master mixture (Cat # 0171, Invitrogen, USA). The PCR product was run on 1% agarose gel for electrophoreses and visualized through the Gel Documentation System (GelDoc Go System, Bio-Rad, USA).

3. Results and Discussion

3.1. Disease Onset (Signs and Symptoms). In wildlife, particularly ungulates and free-ranging species, the diagnosis of *M. bovis* infection mainly involves culturing of an infectious microbial agent, postmortem lesions, and tissue studies [21]. It has been determined that wild animals can get the infection by preys or scavenged carcasses and disseminate the infection to other animals. Therefore, continuous monitoring and diagnosis of *M. bovis* are crucial to controlling its spread in wildlife, domestic animals, and public health. The morbid nilgai exhibited different nonspecific clinical signs like cough, dyspnoea, and thick nasal exudates prior to death. Previously, no clinical signs of tuberculosis including cough have been observed in experimentally induced captive wild animals [44]. Tuberculosis in wild animals is frequently diagnosed at necropsy after natural death, with no prior suspicion of tuberculosis. Gross lesions may be substantial, covering whole organs in one or both cavities; nevertheless, the anatomical sites of the lesions, the level of pathological involvement, and the nature of nodular struc-

tures with some conjunctiva necrosis are frequently present before unthriftiness is often obvious [45].

3.2. Disease Progression and Development. During necropsy, our study reported severely congested trachea with creamy white catarrhal exudate. The lungs exhibited small granulomatous tubercles, severe consolidation, and grey and red hepatisation, and cut sections showed a creamy white caseous material (Figure 1). At necropsy, enlarged mandibular, cervical, and mesenteric lymph nodes are packed with caseated and calcified exudate (Figure 2). So far, no published report is available about these lesions in nilgai due to *M. bovis* infection. Lesions in cervids, thoracic cavities, and lymph nodes may be purulent, while others may be dry, depending on where they are located in the animal's body [46, 47]. However, few studies have observed similar pneumonic lesions due to *M. bovis* infection in wild animals [48]. Oryx, nilgai, and stable antelope tumors are strikingly similar to those found in other Bovidae species. There is no evidence of connective tissue involvement in the nodular areas of caseation and epithelioid cells [49]. However, *M. bovis* infection has also been detected in lymph nodes of buffaloes [50], mesenteric lymph nodes [51], and cervical lymphadenitis [52].

3.3. Histopathology. At a microscopic level, the lungs indicated congestion, emphysema, infiltration of chronic inflammatory cells, granulomatous inflammation, multinucleated

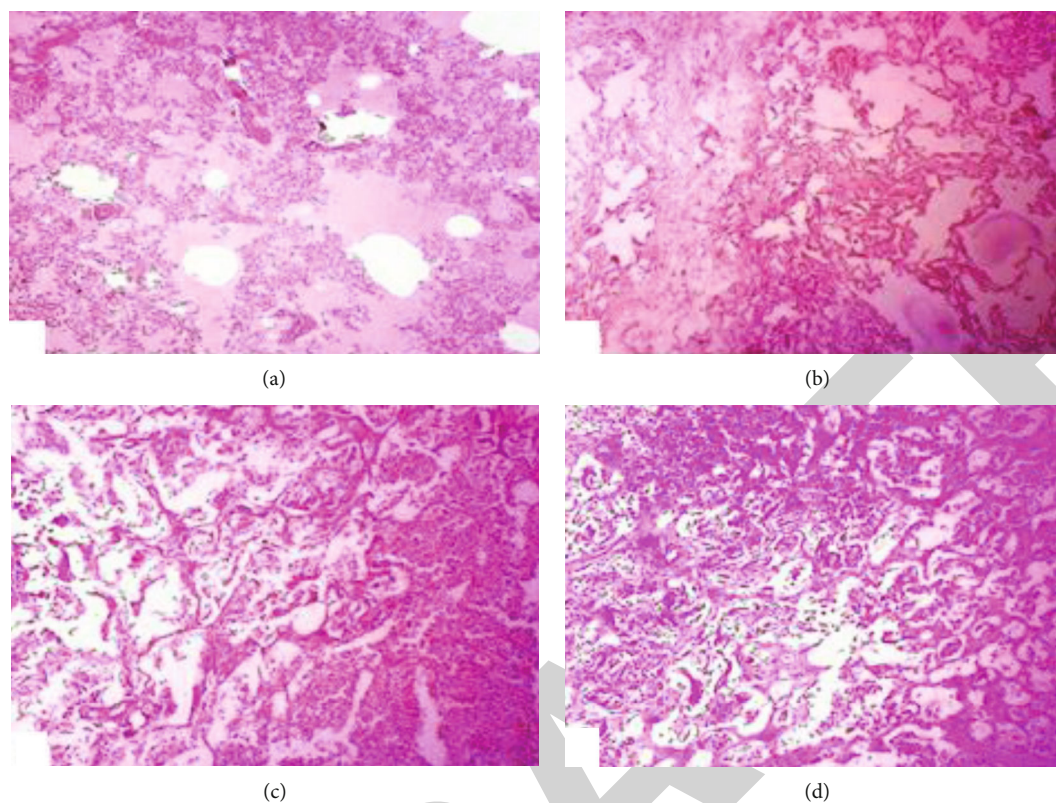


FIGURE 3: Photomicrograph of the lungs of nilgai of tuberculosis showing (a) severe edema, congestion, small foci of abscess, (b) fibrosis, ruptured interalveolar septa, hyperplasia of pneumocyte, (c) micronodules, chronic inflammatory cells in alveolar spaces and obliteration of alveoli, and (d) extensive exudate containing fibroblast, macrophage, monocytes, and thick interlobular septa (H&E; 200X).

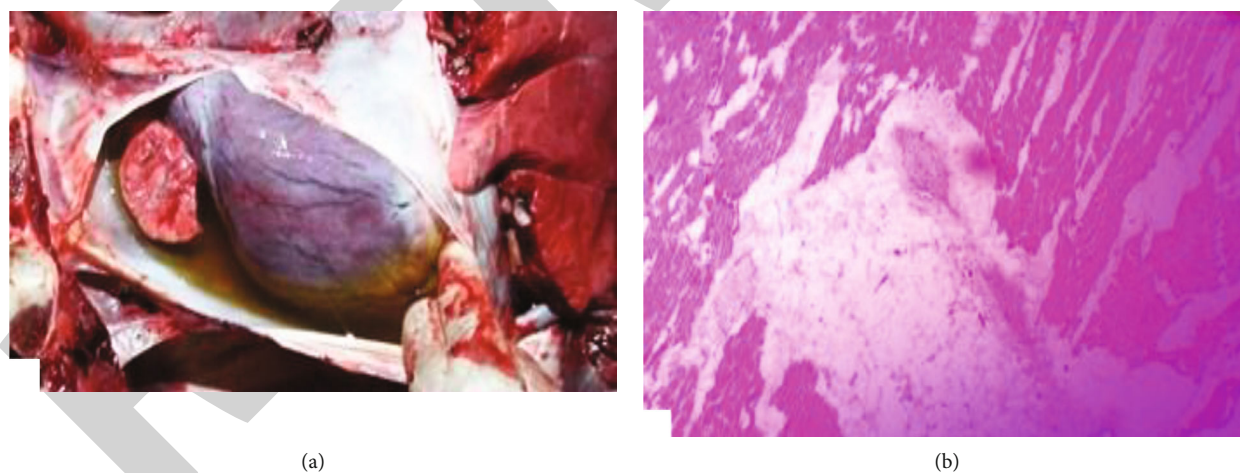


FIGURE 4: Photograph of the heart of Nilgai showing (a) congestion and presence of straw-colored fluid in the cardiac cavity and (b) severe inflammatory exudates, fibrosis, and calcified material surrounded by chronic inflammatory cells and immature tubercles in the heart of nilgai that died from *M. bovis* infection. (H&E; 400X).

giant cells, fibrosis, and alveoli punctuated with chronic inflammatory cells (Figure 3). Our observations regarding different microscopic lesions in lungs of nilgai, similar lesions due to bovine tuberculosis, including lymphohistiocytic inflammatory and necrotic debris in bears [21], granulomatous lesions comprising caseation surrounded by plasma cells epithelioid, lymphocytes, multinucleated giant

cells, and fibrous capsule in rhinoceros and dairy cattle have been investigated earlier [11, 44, 53, 54]. Furthermore, similar histopathological lesions due to experimental infection induced by *M. bovis* in the lungs of deer and cattle have been observed previously [55]. In our findings, the heart of nilgai was extensively enlarged, hyperaemic, and dark in color with a huge amount of straw-colored fluid in the pericardial sac

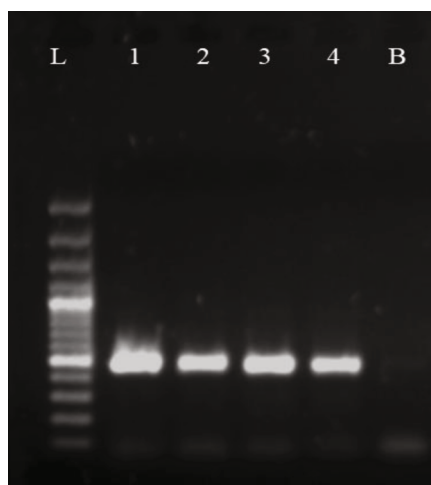


FIGURE 5: Confirmation of *Mycobacterium bovis* by PCR (500 bp). Lane L shows DNA ladder (100 bp), lanes 1-4 show PCR positive samples, and lane B with no band shows negative control.

(Figure 4). The Histopathological observation of heart sections showed a caseous material in lamellar arrangement, immature and mature tubercles, infiltration of mononuclear cells, micronodules, and calcified exudates surrounded by fronts of monocytes, fibroblast, macrophage, and fibrocyte (Figure 4). Moreover, heart tissues showed the presence of few neutrophils, eosinophilic noncellular oedematous and homogeneous fluid. No report is available about the different lesions in heart of infected animals due to tuberculosis. Previously, chronic microscopic lesions in the kidneys, liver, and lungs of nilgai that died from bovine tuberculosis have also been observed [56]. The heart lesions observed in Nilgai due to *M. bovis* might be the due release of nucleases and proteases in multiple chronic inflammatory cells comprising macrophages, epithelioid cells, plasma cells, and neutrophils resulting to liquefaction [57]. However, similar pathological lesions in the liver of infected animals have been observed [11]. Therefore, the prevalence of *M. bovis* infection in wild animals and the increasing frequency of the infectious agent draw huge attention for its regular screening not only in domestic animals but also in wildlife in captivity.

3.4. Molecular Confirmation. Genotype approaches have been beneficial in epidemiological investigations to determine the source of infection [58–60]. PCR assays are the most promising alternative method for tuberculosis detection with regard to specificity and sensitivity [61, 62]. In a range of biological samples, such as tissue, blood, and nasal exudates, PCR techniques have been successfully used to diagnose *M. bovis* [63, 64]. Our study reported the JB21 and JB22 amplified regions of the *Mycobacterium* genome (Figure 5). Similar genetic analyses have been shown to be very effective in detecting *M. bovis* DNA isolates from blood samples, with 100% accuracy when compared to the traditional microbiological method [65, 66]. In line with the global effort to halt the tuberculosis disease outbreak, it is critical to determine the true burden of zoonotic tuberculosis, particularly in the low- and middle-income countries,

where cattle-control programs may be marginal or nonexistent. The epidemiology of tuberculosis can be better understood by combining traditional disease-tracing investigation with molecular typing, which can reveal the role played by various hosts in the spread of disease infection.

4. Conclusion and Future Perspective

In recent years, the frequency of tuberculosis in zoo animals has grown, which may be related to the closer confinement of several wild species in one location. The ease and regularity with which organisms transmit from animal to human attract increasing attention to zoonotic relevance. In this regard, there is an urgent need for ongoing research into this disease in both captive and free-roaming wild animals. Only one isolate from nilgai was analyzed in this study, but a more detailed study with a larger sample size would be preferable to improve the transmission routes and the pathology of *M. bovis*. It is also critical to investigate the incidence of *M. bovis* in other animals in developing countries like Pakistan.

Data Availability

All the data relevant to this study is mentioned in the manuscript. There is no supplementary data.

Conflicts of Interest

The authors declare no conflict of interest.

Authors' Contributions

RH is responsible for the conception, monitoring, necropsy, and clinical examination; RH, AK, and XD are involved in histopathology studies; ZA, ABS, MKM, and IK are responsible for the early draft of the manuscript; AJ is responsible for the genetic analysis and manuscript critical revision; BBM is responsible for the logical interpretation of results with reported findings.

Acknowledgments

All authors are thankful to the Department of Pathology, Faculty of Veterinary and Animal Sciences, Department of Pathology, Faculty of Veterinary Science, University of Agriculture, Faisalabad 38040, Pakistan, for providing lab facilities to carry out histopathological studies and molecular confirmation smoothly and successfully.

References

- [1] K. E. Jones, N. G. Patel, M. A. Levy et al., "Global trends in emerging infectious diseases," *Nature*, vol. 451, no. 7181, pp. 990–993, 2008.
- [2] A. Dobson and J. Foufopoulos, "Emerging infectious pathogens of wildlife," *Phil Trans R Soc Lond B*, vol. 356, no. 1411, pp. 1001–1012, 2001.

- [3] J. M. Grange, "Mycobacterium bovis infection in human beings," *Tuberculosis (Edinburgh, Scotland)*, vol. 81, no. 1-2, pp. 71-77, 2001.
- [4] The Center for Food Security and Public Health (CFSPH) Institute for International Cooperation in Animal Biologics, Iowa State University, College of Veterinary Medicine, Zoonotic Tuberculosis in Mammals, including Bovine and Caprine Tuberculosis, 2003-2019, https://www.cfsph.iastate.edu/Factsheets/pdfs/bovine_tuberculosis.pdf.
- [5] R. J. Delahay, C. L. Cheeseman, and R. S. Clifton-Hadley, "Wildlife disease reservoirs: the epidemiology of *Mycobacterium bovis* infection in the European badger (*Meles meles*) and other British mammals," *Tuberculosis (Edinburgh, Scotland)*, vol. 81, no. 1-2, pp. 43-49, 2001.
- [6] P. Caley and J. Hone, "Assessing the host disease status of wildlife and the implications for disease control: *Mycobacterium bovis* infection in feral ferrets," *Journal of Applied Ecology*, vol. 42, no. 4, pp. 708-719, 2005.
- [7] F. Ali, R. Hussain, A. Qayyum, S. T. Gul, Z. Iqbal, and M. F. Hassan, "Milk somatic cell counts and some hemato-biochemical changes in sub-clinical mastitic dromedary she-camels (*Camelus dromedarius*)," *Pakistan Veterinary Journal*, vol. 36, no. 4, pp. 405-408, 2016.
- [8] H. M. Ali, A. S. Qureshi, R. Hussain et al., "Effects of natural environment on reproductive histo-morphometric dynamics of female dromedary camel," *Animal Reproduction Science*, vol. 181, pp. 30-40, 2017.
- [9] R. Hussain, A. Khan, Jahanzaib et al., "Clinico-hematological and oxidative stress status in Nili Ravi buffaloes infected with *Trypanosoma evansi*," *Microbial Pathogenesis*, vol. 123, pp. 126-131, 2018.
- [10] R. Hussain, F. Mahmood, B. Aslam et al., "Investigation of different serotypes of FMDV in vaccinated buffaloes (*Bubalus bubalis*) in southern areas of Punjab province, Pakistan," *Pakistan Veterinary Journal*, vol. 40, no. 1, pp. 118-122, 2019.
- [11] M. A. Haque, H. Quan, Z. Zuo, A. Khan, N. Siddique, and C. He, "Pathogenicity of feed-borne *Bacillus cereus* and its implication on food safety," *Agrobiological Records*, vol. 3, pp. 1-16, 2021.
- [12] F. Mahmood, A. Khan, R. Hussain et al., "Patho-bacteriological investigation of an outbreak of *Mycoplasma bovis* infection in calves - emerging stealth assault," *Microbial Pathogenesis*, vol. 107, pp. 404-408, 2017.
- [13] R. Hussain, F. Mahmood, H. M. Ali, and A. B. Siddique, "Bacterial, PCR and clinico-pathological diagnosis of naturally occurring pneumonic pasteuriosis (mannheimiosis) during subtropical climate in sheep," *Microbial Pathogenesis*, vol. 112, pp. 176-181, 2017.
- [14] R. Hussain, F. Mahmood, A. Khan, and K. Mehmood, "Prevalence and pathology of bovine coccidiosis in Faisalabad district," *Pakistan, Thai Journal of Veterinary Medicine*, vol. 47, no. 3, pp. 401-406, 2017.
- [15] R. Hussain, M. T. Javed, I. Khan et al., "Pathological and clinical investigations of an outbreak of Blackleg disease due to *C. chauvoei* in cattle in Punjab, Pakistan," *Journal of Infection in Developing Countries*, vol. 13, no. 9, pp. 786-793, 2019.
- [16] U. D. Khan, A. Khan, S. T. Gul, and M. K. Saleem, "Seroprevalence of brucellosis in cattle (*Bos taurus*) kept in peri urban areas of Pakistan," *Agrobiological Records*, vol. 1, pp. 6-10, 2020.
- [17] M. Q. U. H. Faraz, M. T. Javed, I. Javed et al., "Association of tuberculosis with TLR-9 gene polymorphism and C-reactive protein levels in blood of humans and animals," *Pakistan Veterinary Journal*, vol. 41, no. 2, pp. 254-258, 2021.
- [18] R. Hussain, A. Khan, R. Z. Abbas et al., "Clinico-hematological and biochemical studies on naturally infected camels with trypanosomiasis," *Pakistan Journal of Zoology*, vol. 48, no. 2, pp. 311-316, 2016.
- [19] J. Abbas, S. Azam, and A. Bhutta, "Molecular, pharmacological, and biochemical approaches: The latest panacea for emerging viral diseases," *Continental Veterinary Journal*, vol. 1, pp. 9-19, 2021.
- [20] E. Butler Rachel, A. A. Smith, T. A. Mendum et al., "*Mycobacterium bovis* uses the ESX-1 Type VII secretion system to escape predation by the soil-dwelling amoeba *Dictyostelium discoideum*," *The ISME Journal*, vol. 14, no. 4, pp. 919-930, 2020.
- [21] R. Fico, A. Mariacher, A. Franco et al., "Systemic tuberculosis by *Mycobacterium bovis* in a free-ranging Marsican brown bear (*Ursus arctos marsicanus*): a case report," *BMC Veterinary Research*, vol. 15, no. 1, Article ID.152, 2019.
- [22] E. A. Nasr, R. E. Fawzy, G. S. Marian, A. M. Abbas, and E. Khalifa, "Using of gamma interferon γ -IFN and multiplex PCR (m-PCR) for detection of bovine tuberculosis in dairy herds in Egypt," *International Journal of Veterinary Science*, vol. 10, no. 3, pp. 229-233, 2021.
- [23] A. Ullah, U. S. Khattak, S. Ayaz et al., "Bovine tuberculosis (bTB): prevalence and associated risk factors in large ruminants in the Central Zone of Khyber Pakhtunkhwa, Pakistan," *Pakistan Journal of Zoology*, vol. 51, no. 1, pp. 127-133, 2018.
- [24] S. Ali, I. A. Khan, M. S. Mian, and W. Raana, "Detection of mycobacteria from milk of cattle and buffaloes at government livestock farms," *Pakistan Journal of Agricultural Sciences*, vol. 42, pp. 11-12, 2005.
- [25] A. U. Rehman, S. E. U. Haque, M. T. Javed et al., "Monitoring the health status and herd-level risk factors of tuberculosis in water buffalo (*Bubalus bubalis*) dairy farms in Pakistan," *Pakistan Veterinary Journal*, vol. 41, no. 4, pp. 552-556, 2021.
- [26] R. L. Higgitt, O. L. Van Schalkwyk, L. M. De Klerk-Lorist et al., "*Mycobacterium bovis* infection in African wild dogs, Kruger National Park, South Africa," *Emerging Infectious Diseases*, vol. 25, no. 7, pp. 1425-1427, 2019.
- [27] A. Muwonge, F. Egbe, M. Bronsvort, D. B. Areda, T. Hlokwe, and A. Michel, "Molecular epidemiology of *Mycobacterium bovis* in Africa," *Tuberculosis in animals: An African perspective*, A. Dibaba, N. Kriek, and C. Thoen, Eds., pp. 127-169, 2019.
- [28] I. Khattak, M. H. Mushtaq, M. U. D. Ahmad, M. S. Khan, M. Chaudhry, and U. Sadique, "Risk factors associated with *Mycobacterium bovis* skin positivity in cattle and buffalo in Peshawar, Pakistan," *Pakistan. Tropical Animal Health and Production*, vol. 48, no. 3, pp. 479-485, 2016.
- [29] I. Khattak, M. H. Mushtaq, S. Ayaz et al., "Incidence and drug resistance of zoonotic *Mycobacterium bovis* infection in Peshawar, Pakistan," *Advances in Experimental Medicine and Biology*, vol. 1057, pp. 111-126, 2018.
- [30] M. T. Javed, A. F. Farooqi, and R. U. Khan, "Epidemiological basis of bovine tuberculosis in buffaloes," *Pakistan Journal of Zoology*, vol. 9, pp. 417-420, 2009.

- [31] M. A. Ghumman, A. W. Manzoor, S. Naz, R. Ahmad, and R. Ahmad, "Prevalence of tuberculosis in cattle and buffalo at various livestock farms in Punjab," *International Journal of Veterinary Medicine: Research and Reports*, vol. 2013, pp. 1–4, 2013.
- [32] I. A. Khan and A. Khan, "Prevalence and risk factors of bovine tuberculosis in Nili Ravi buffaloes in the Punjab, Pakistan," *Italian Journal of Animal Science*, vol. 6, no. sup2, pp. 817–820, 2007.
- [33] M. T. Javed, L. Ahmad, F. Felizianib et al., "Analysis of some of the epidemiological risk factors affecting the prevalence of tuberculosis in buffalo at seven livestock farms in Punjab Pakistan," *Asian Biomedicine*, vol. 6, no. 1, pp. 35–42, 2012.
- [34] I. A. Khan, A. Khan, A. Mubarak, and S. Ali, "Factors affecting prevalence of bovine tuberculosis in Nili-Ravi buffaloes," *Pakistan Veterinary Journal*, vol. 28, no. 4, pp. 155–158, 2008.
- [35] F. Mahmood, A. Khan, R. Hussain, and I. A. Khan, "Molecular based epidemiology of bovine pulmonary tuberculosis - a mortal foe," *Pakistan Veterinary Journal*, vol. 34, no. 2, pp. 185–188, 2014.
- [36] N. Mumtaz, Z. I. Chaudhry, N. Mahmood, and A. R. Shakoori, "Reliability of PCR for detection of bovine tuberculosis in Pakistan," *Pakistan Journal of Zoology*, vol. 40, no. 5, pp. 347–351, 2008.
- [37] M. T. Javed, A. L. Shahid, F. A. Farooqi et al., "Risk factors associated with the presence of positive reactions in the SCCIT test in water buffalo around two cities in Punjab, Pakistan," *Acta Tropica*, vol. 115, no. 3, pp. 242–247, 2010.
- [38] A. L. Shahid, M. Tariq Javed, M. Nisar Khan, and M. Cagiola, "Prevalence of bovine tuberculosis in zoo animals in Pakistan," *Iranian Journal of Veterinary Research, Shiraz University*, vol. 13, no. 1, pp. 58–63, 2012.
- [39] F. Attig, S. A. Barth, M. Kohlbach et al., "Unusual manifestation of a *Mycobacterium bovis* SB0950 infection in a domestic cat," *Journal of Comparative Pathology*, vol. 172, pp. 1–4, 2019.
- [40] H. H. Ramadan, A. H. N. El-Gohary, and A. A. Mohamed, "Detection of *Mycobacterium bovis* and *Mycobacterium tuberculosis* from clinical samples by conventional and molecular techniques in Egypt," *Global Veterinaria*, vol. 9, no. 6, pp. 648–654, 2012.
- [41] S. A. Khaliq, M. Mohiuddin, M. Habib et al., "Clinico-hematobiochemical and molecular diagnostic investigations of Peste des petits ruminants in goats," *Pakistan Veterinary Journal*, vol. 40, no. 3, pp. 313–318, 2020.
- [42] H. M. Ramadan, N. A. Taha, and H. H. Ahmed, "Melatonin improves blood biochemical parameters and DNA integrity in the liver and kidney of hyperthyroid male rats," *International Journal of Veterinary Science*, vol. 9, no. 4, pp. 511–516, 2020.
- [43] D. Kidane, J. O. Olobo, A. Habte et al., "Identification of the causative organism of tuberculous lymphadenitis in Ethiopia by PCR," *Journal of Clinical Microbiology*, vol. 40, no. 11, pp. 4230–4234, 2002.
- [44] A. L. Michel, E. P. Lane, L.-M. de Klerk-Lorist et al., "Experimental *Mycobacterium bovis* infection in three white rhinoceroses (*Ceratotherium simum*): susceptibility, clinical and anatomical pathology," *PLoS One*, vol. 12, no. 7, article e0179943, 2017.
- [45] C. O. Thoen, T. Schliesser, and B. Kormendy, "Tuberculosis in captive wild animals," in *Mycobacterium bovis infection in animals and humans*, C. O. Thoen, J. H. Steele, and M. J. Glisendorf, Eds., pp. 18–33, Blackwell Publishing, Ames, Iowa, 2nd edition, 1995.
- [46] D. J. O. Brien, S. M. Schmitt, S. D. Fitzgerald, D. E. Berry, and G. J. Hickling, "Managing the wildlife reservoir of *Mycobacterium bovis*: The Michigan, USA, experience," *Veterinary Microbiology*, vol. 112, no. 2–4, pp. 313–323, 2006.
- [47] M. V. Palmer, D. L. Whipple, J. B. Payeur et al., "Naturally occurring tuberculosis in white-tailed deer," *Journal of the American Veterinary Medical Association*, vol. 216, no. 12, pp. 1921–1924, 2000.
- [48] I. W. Espie, T. M. Hlokwé, N. C. G. Pittius et al., "Pulmonary infection due to *Mycobacterium bovis* in a black rhinoceros (*Diceros bicornis minor*) in South Africa," *Journal of Wildlife Diseases*, vol. 45, no. 4, pp. 1187–1193, 2009.
- [49] C. O. Thoen, P. A. LoBue, D. A. Enarson, J. B. Kaneene, and I. N. de Knator, "Tuberculosis: a re-emerging disease in animals and humans," *Veterinaria Italiana*, vol. 45, no. 1, pp. 135–181, 2009.
- [50] S. Amin, M. A. Khan, H. A. Hashmi, M. S. Khan, I. Ahmad, and M. A. Bhatti, "Detection of buffalo tuberculosis by using short thermal test and isolation of causal organisms from lymph nodes," *Buffalo Journal*, vol. 8, pp. 83–87, 1992.
- [51] A. Muwonge, T. B. Johansen, E. Vigdis et al., "Mycobacterium bovis infections in slaughter pigs in Mubende district, Uganda: a public health concern," *BMC Veterinary Research*, vol. 8, no. 1, article 168, p. 168, 2012.
- [52] G. J. Fennelly, "Mycobacterium bovis versus Mycobacterium tuberculosis as a cause of acute cervical lymphadenitis without pulmonary disease," *The Pediatric Infectious Disease Journal*, vol. 23, no. 6, pp. 590–591.
- [53] H. R. Bermudez, E. T. Renteria, B. G. Medina et al., "Correlation between histopathological, bacteriological and PCR diagnosis of bovine tuberculosis," *Journal of Animal and Veterinary Advances*, vol. 9, no. 15, pp. 2082–2084, 2010.
- [54] H. Ozturk-Gurgen, B. Rieseberg, M. Leipzig-Rudolph, R. K. Straubinger, and W. Hermanns, "Morphology of naturally-occurring tuberculosis in cattle caused by *Mycobacterium caprae*," *Journal of Comparative Pathology*, vol. 174, pp. 120–139, 2020.
- [55] J. E. Shitaye, B. Getahun, T. Alemayehu et al., "A prevalence study of bovine tuberculosis by using abattoir meat inspection and tuberculin skin testing data, histopathological and IS6110PCR examination of tissues with tuberculous lesions in cattle in Ethiopia," *Veterinárni Medicina*, vol. 51, no. 11, pp. 512–522, 2012.
- [56] R. Verma, A. K. Sharma, S. Ramane, A. Kidangam, T. Mandal, and H. Verma, "Generalized tuberculosis in Nilgai (*Boselaphus tragocamelus*) caused by *Mycobacterium fortuitum*," *Indian Journal of Veterinary Pathology*, vol. 36, no. 1, pp. 33–36, 2012.
- [57] I. M. Orme and R. J. Basaraba, "The formation of the granuloma in tuberculosis infection," *Seminars in Immunology*, vol. 26, no. 6, pp. 601–609, 2014.
- [58] F. Suazo Milian and V. Banda-Ruiz, "Genotyping of *Mycobacterium bovis* by geographic location within Mexico," *Arriaga-Diaz, Genotyping of Mycobacterium bovis by geographic location within Mexico, Preventive Veterinary Medicine*, vol. 55, no. 4, pp. 255–264, 2002.
- [59] A. Parra, P. Fernnandez-Llario, A. Tato et al., "Epidemiology of *Mycobacterium bovis* infections of pigs and wild boars

Retraction

Retracted: Histopathological Investigations and Molecular Confirmation Reveal *Mycobacterium bovis* in One-Horned Rhinoceros (*Rhinoceros unicornis*)

BioMed Research International

Received 8 January 2024; Accepted 8 January 2024; Published 9 January 2024

Copyright © 2024 BioMed Research International. This is an open access article distributed under the Creative Commons Attribution License, which permits unrestricted use, distribution, and reproduction in any medium, provided the original work is properly cited.

This article has been retracted by Hindawi following an investigation undertaken by the publisher [1]. This investigation has uncovered evidence of one or more of the following indicators of systematic manipulation of the publication process:

- (1) Discrepancies in scope
- (2) Discrepancies in the description of the research reported
- (3) Discrepancies between the availability of data and the research described
- (4) Inappropriate citations
- (5) Incoherent, meaningless and/or irrelevant content included in the article
- (6) Manipulated or compromised peer review

The presence of these indicators undermines our confidence in the integrity of the article's content and we cannot, therefore, vouch for its reliability. Please note that this notice is intended solely to alert readers that the content of this article is unreliable. We have not investigated whether authors were aware of or involved in the systematic manipulation of the publication process.

Wiley and Hindawi regrets that the usual quality checks did not identify these issues before publication and have since put additional measures in place to safeguard research integrity.

We wish to credit our own Research Integrity and Research Publishing teams and anonymous and named

external researchers and research integrity experts for contributing to this investigation.

The corresponding author, as the representative of all authors, has been given the opportunity to register their agreement or disagreement to this retraction. We have kept a record of any response received.

References

- [1] A. B. Siddique, R. Hussain, A. Jamal et al., "Histopathological Investigations and Molecular Confirmation Reveal *Mycobacterium bovis* in One-Horned Rhinoceros (*Rhinoceros unicornis*)," *BioMed Research International*, vol. 2022, Article ID 5816986, 7 pages, 2022.

Research Article

Histopathological Investigations and Molecular Confirmation Reveal *Mycobacterium bovis* in One-Horned Rhinoceros (*Rhinoceros unicornis*)

Abu Baker Siddique ¹, Riaz Hussain ², Adil Jamal ³, Md. Belal Hossain ⁴,
Zulfiqar Ahmad,⁵ Muhammad Khalid Mansoor,⁶ Iahtasham Khan,⁷ Kainat Zahra,⁸
and Ahrar Khan ^{9,10}

¹Department of Microbiology, Government College University, Faisalabad, Pakistan

²Department of Pathology, Faculty of Veterinary and Animal Sciences, The Islamia University of Bahawalpur, 63100, Pakistan

³Sciences and Research, College of Nursing, Umm Al Qura University, 715 Makkah, Saudi Arabia

⁴Department of Plant Pathology, Faculty of Agriculture, Sher-e-Bangla Agricultural University, Sher-e-Bangla Nagar, Dhaka 1207, Bangladesh

⁵Department of Food Science and Technology, Faculty of Agriculture and Environment, Baghdad-UI-Jadeed Campus, The Islamia University of Bahawalpur-63100, Pakistan

⁶Department of Microbiology, Faculty of Veterinary and Animal Sciences, The Islamia University of Bahawalpur, 63100, Pakistan

⁷Section of Epidemiology and Public Health, University of Veterinary and Animal Sciences, Lahore, Sub-Campus Jhang, Pakistan

⁸Institute of Biochemistry and Biotechnology, University of Veterinary and Animal Sciences, Lahore, Pakistan

⁹Shandong Vocational Animal Sciences and Veterinary College, Weifang 261061, China

¹⁰Faculty of Veterinary Science, University of Agriculture, Faisalabad, Pakistan

Correspondence should be addressed to Riaz Hussain; dr.riaz.hussain@iub.edu.pk
and Md. Belal Hossain; dr.mbhossain@sau.edu.bd

Received 9 April 2022; Accepted 27 April 2022; Published 18 May 2022

Academic Editor: Faheem Ahmed Khan

Copyright © 2022 Abu Baker Siddique et al. This is an open access article distributed under the Creative Commons Attribution License, which permits unrestricted use, distribution, and reproduction in any medium, provided the original work is properly cited.

Mycobacterium bovis causes tuberculosis in dairy and wild animals. Presence of tuberculosis in animals poses a threat not only to their herd mates but also for public. No reports are available about the clinical, pathological, and molecular investigation of naturally occurring tuberculosis (TB) due to *M. bovis* in one-horned rhinoceros. One-horned female rhinoceros (*Rhinoceros unicornis*) at the age of 41 years died in a public park in Pakistan. Postmortem and other investigations were carried out to know the cause of death. The present study describes necropsy, histopathology, and molecular-based confirmation of TB in a captive female rhinoceros that died of this infection. Clinically, the rhinoceros showed nonspecific clinical signs including anorexia, lethargy, dyspnoea, coughing, and sudden death. At necropsy, the trachea exhibited mild congestion and contained catarrhal exudate at the bronchial bifurcation. Macroscopic examination revealed characteristic tubercles on all parenchymatous organs. The lungs showed consolidation, grey hepatization, and contained granulomatous lesions packed with cheesy exudate. Histopathological examination showed severe pneumonic changes in the form of granulomatous inflammation consisting of lymphocytes, multinucleated giant cells, caseous materials, and mineralized foci surrounded by a fibrous capsule. PCR amplicon of 500 bp confirmed the presence of *M. bovis* in multiple hepatic and pulmonary tissue samples, as well as in uterine exudates. It was concluded that the presence of tuberculosis in rhinoceros may pose potential transmission risk to other animals and the application of practical tools to determine TB status in the rhinoceros is crucial.

1. Introduction

Tuberculosis (TB) produced by *Mycobacterium tuberculosis* is an infectious and chronic debilitating illness that affects humans, domestic animals, and wild animals worldwide [1]. *M. tuberculosis* is the most important pathogen causing human tuberculosis, whereas *Mycobacterium bovis* is the most important pathogen causing bovine tuberculosis (BTB) and has a high potential to infect humans and other animals due to its wide host range [2]. Because of its occurrence in numerous animal species and their products, which are utilized for human consumption, this disease is of significant economic and public health importance [3]. Several developed countries have recently reduced or eliminated BTB from their cattle populations, but significant pockets of infection remain in developing countries of world in wildlife [4]. Several investigations regarding have been reported in large and small ruminants in Pakistan [5].

Transmission of *M. bovis* to public health mainly occurs through inhalation, consumption of untreated milk/raw milk, aerosols inhalation of the pathogen from morbid animals at the time of close contact, and shedding of bacteria by infected animal for the environmental contamination [6]. The exact transmission of the infectious agent to wildlife animals is still not clear. The acquisition of infected animals, herd size, poor husbandry, and sanitary procedures is the key routes of disease transfer into herds. Furthermore, animal herds with a stronger tendency to roam play an important role in disease transmission [6]. However, different studies have reported that the infected dairy animals and wild animals secrete *M. bovis* in their faeces and urine, as bacilli have been detected in naturally contaminated environmental samples such as soil and faeces [7].

M. bovis has proven to infect multiple hosts within the wildlife community [8]. Data on human tuberculosis due to *M. bovis* is poorly documented [9]. Different studies have reported various risk factors with tuberculosis in cattle and buffaloes kept at various livestock farms [9]. Specific data on bovine tuberculosis in Pakistan's wild animals are scarce except few reports in zoo animals [10]. *M. tuberculosis* and *M. bovis* have been found in black rhinoceros confined in zoos or under semi-intensive management [11]. Despite the presence of *M. bovis* in livestock and other wildlife species in Pakistan with rhinoceros populations, no instances of tuberculosis have been observed in rhinos.

TB is often diagnosed by isolating the organism from sputum, milk, faeces, and other body fluids [12]. The usual methods for diagnosing tuberculosis include direct smear microscopy using the fluorescent acid-fast staining technique and Ziehl-(ZN) Neelsen's staining of clinical samples [12]. Although cultivation on selective media offers a confirmed diagnosis of *Mycobacterium* but the primary disadvantage of this method is the slow bacterial growth [13]. Rapid diagnosis of *Mycobacterium* from clinical samples is possible using polymerase chain reaction (PCR) amplification of the *Mycobacterial* DNA. PCR is a more precise and reliable approach for quick diagnosis with much more sensitivity and specificity comparable to bacterial culture [13].

Our study aimed to study necropsy lesions followed by histopathological findings of tuberculosis due to *M. bovis* in a captive female rhinoceros. *M. bovis* detection was further confirmed based on molecular approach using PCR. Regular livestock and wildlife screening will help to prevent *M. bovis* transmission to other animals.

2. Materials and Methods

2.1. Ethical Statement. The technical and ethical committee constituted by Department of Pathology, Faculty of Veterinary and Animal Sciences, The Islamia University of Bahawalpur, Pakistan, approved the protocol of the postmortem study of one-horned rhinoceros.

2.2. Study Area and Sample. South Punjab region had tropical and subtropical climatic conditions with hot and humid summer and cold winter. In this region, lack of intensive animal health monitoring facilities, nutrition, water sources, and unavailability of sufficient seasonal fodder are the main limitations for the livestock and various other animals. Near the zoological park where the rhinoceros was kept, the region is mainly dominated by nomadic and sedentary system where the animals are routinely migrated for fodder and water which may cause spread of infectious agents from one location to other during common grazing and drinking.

At that time, these animals were transported on the recommendations of the governor of Punjab to district Bahawalpur and were kept at Lal Suhanra National Park Punjab province. The administrator of the park built a trench-cum-lake where these animals were kept. The rhinoceros were daily monitored for any obvious clinical ailments. According to the administration of the Park and history from the caretakers, female rhinoceros was feed green seasonal fodder (90 kg), bread (5 kg), and mixed grains (4 kg), daily. According to the administrator of park, the female might have died because of excessive bleeding that had weakened her. The veterinary assistants of the park noted animal stillbirth in rhinoceros. Animal became sick, showing nonspecific signs such as depression, anorexia, lethargy, disorientation, dyspnoea, and coughing. Despite treatment, the rhinoceros died asymptotically in December 2019.

2.3. Necropsy Examination. The necropsy was performed soon after death. Before complete skinning, the animal was carefully examined for external lesions. The rhinoceros was average and fair in body condition. However, congested nasal mucosa, pale mucous membrane, and bloody discharge from the vagina were observed. Afterward, a complete postmortem examination was performed [14].

2.4. Sample Collection and Histopathological Analysis. Morbid tissues exhibiting lesions, including lungs and liver, were collected and fixed in 10% neutral buffered formalin for microscopic investigation. Tissues were embedded in paraffin wax, and sections of about 4-5 μm thick were cut [15]

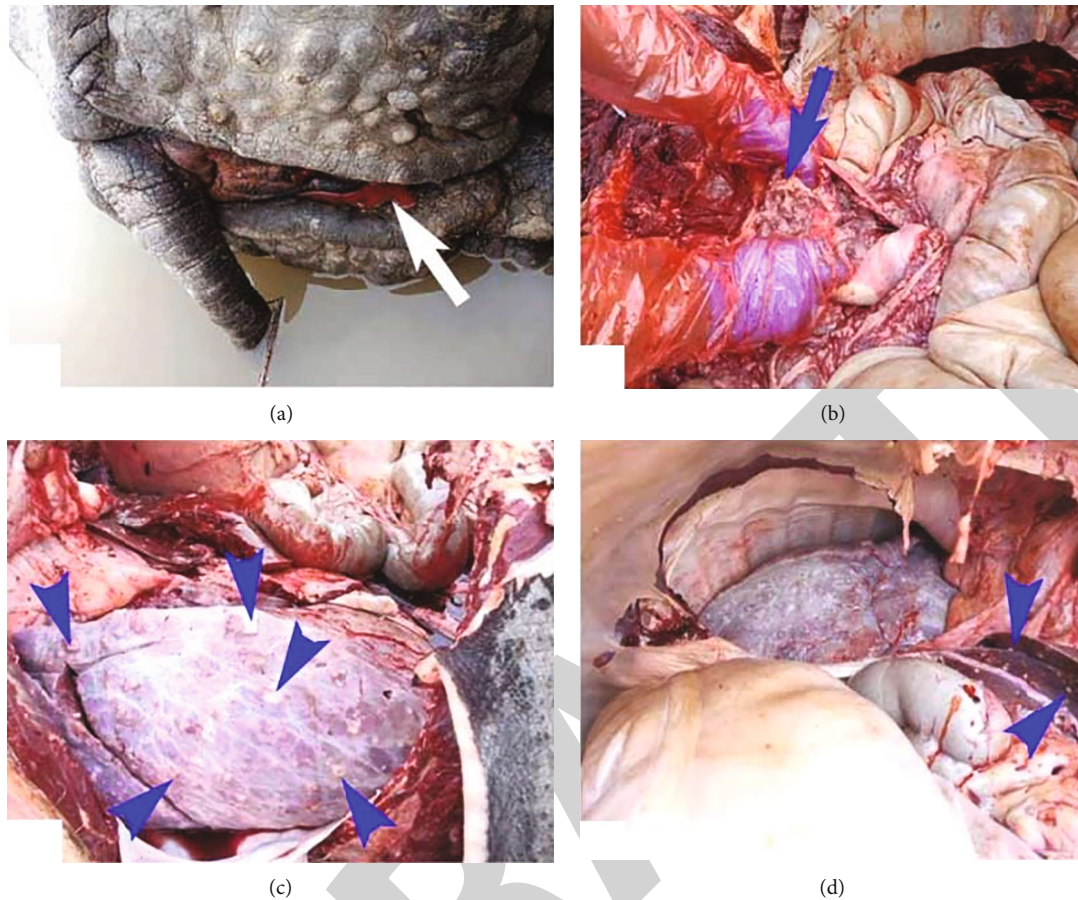


FIGURE 1: Photographs of one-horned female rhinoceros died of *M. bovis* infection. (a) Showing blood mixed exudate coming out of the vagina (white arrow), (b) uterine pus mixed with tissue debris (blue arrow), (c) small multifocal tubercular lesions (arrowheads) containing creamy white exudate in the lungs, and (d) small multifocal tubercular lesions (arrowheads) on the parietal surface of liver (arrowheads).

and stained with hematoxylin and eosin stain for histopathological examination.

2.5. Genomic DNA Extraction and Molecular Detection. For bacilli detection and confirmation, various tissue samples having lesions, e.g., liver, lungs, and uterine pus were used for bacterial DNA extraction and confirmation of suspected cause. Genomic DNA was extracted from samples using GeneJET Genomic DNA Extraction kit (Thermo Scientific, USA). The species-specific primer targeting the JB21 and JB22 genes (forward JB21; 5'-TCGTCCGCTGATGCAAGTGC-3', reverse JB22; 5'-CGTCCGCTGACCTCAAGAAG-3') were used for the confirmation of samples [16]. The amplification conditions were set as initial denaturation at 95°C for 4 min followed by 30 cycles of denaturation at 94°C for 1 min, annealing at 55°C for 30 s, and primer extension at 72°C for 1 min, with a final extension at 72°C for 10 min. The amplification was performed using PCR master mixture (2X) (Cat # 0171, Invitrogen, USA) and thermocycler (T 100 Thermal cycler, BioRad, USA). The PCR product was run on 1% agarose gel for

electrophoreses and visualized through gel documentation system (Gel Doc XR+ System, BioRad, USA).

3. Results

In the present study, at necropsy, the external examination showed that the female rhinoceros was normal and had fair body condition. The carcass exhibited congested nasal mucosa, pale mucous membrane, and bloody discharge from the vagina (Figure 1(a)). The head, skin, eyes, mouth, ears, and rectum appeared normal. After skinning, the abdominal cavity exhibited moderate hyperaemia of serosal membranes and mild peritonitis. The small and large intestines showed moderated ballooning and appeared empty. The external surfaces of the rectum appeared hyperaemic. The spleen was moderately hyperaemic. The reproductive organs showed severe inflammatory changes, including metritis and pyometra. The inner surfaces of the uterus were thick and contained pus mixed with tissue debris (Figure 1(b)).

The trachea showed mild congestion and contained catarrhal exudates at the bifurcation junction. The thoracic

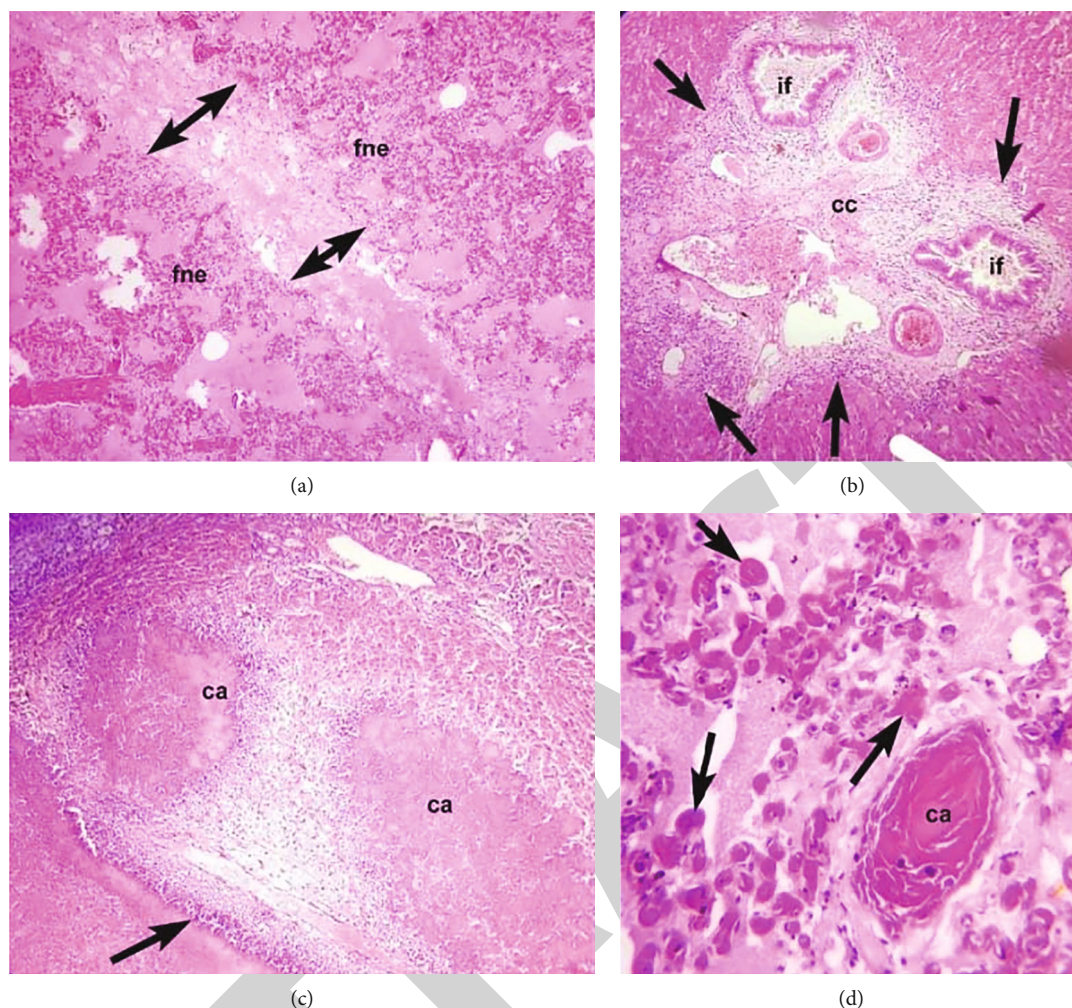


FIGURE 2: Photomicrographs of lungs of one-horned female rhinoceros died of *M. bovis* infection showing (a) thickened alveolar septa (double-sided arrows), and alveoli filled with fibrino-necrotic edema (fne) fluid along with massive infiltration of inflammatory cells, (b) micronodules with minimum calcified exudate surrounded by fronts of fibroblasts, fibrocytes, monocytes, macrophages (arrows), multinucleated giant cells, and calcified centre (cc) along with inflammatory cells infiltration in bronchioles (if), (c) two calcified (ca) tubercle nodules surrounded by fronts of fibroblasts, fibrocytes, monocytes, macrophages (arrows), and (d) calcified (ca) centre. H & E; magnification: (a)–(c) 100X; (d) -400X.

cavity showed moderate pleural adhesions. The lungs exhibited grey hepatization, consolidation, and granulomatous lesions. Lesions in the lungs were small multifocal tubercular lesions containing creamy white caseous material exudate (Figure 1(c)). The liver was found consolidated, hyperaemic, dark in color, enlarged, and had tuberculous nodules packed with caseous material (Figure 1(d)).

Histopathological examination of lungs exhibited fibrino-necrotic edema, thickening of interlobular septa with infiltration of chronic inflammatory cells, and ruptured interalveolar septa (Figure 2(a)). Fibrosis, hyperplasia of pneumocytes, the punctuation of mononuclear cells, and multinucleated giant cells in alveolar spaces obliterating the adjacent alveoli were also seen (Figure 2(b)). Extensive micro and macrotubercular nodules with exudate surrounded by fibroblast fronts, fibrocytes, monocytes, macrophages, and caseous and calcified material were seen in the lamellar arrangement (Figures 2(b)–2(d)). Multiple granulomatous foci contain fibrosis, bacilli,

and lymphohistiocytic inflammatory cells (Figure 3(a)). Histopathological observation of liver sections showed immature and mature tubercles, heavily infiltrated with inflammatory cells in portal triad areas. Perivascular cuffing of lymphocytes, monocyte, and fibroblasts was seen. Numerous small blood-filled angiomatic cysts were observed. Bilateral granulomatous inflammation and bronchial exudate were the consistent findings in infected lungs. The PCR (500pb) confirmed *M. bovis* in samples collected from the liver, lungs, and uterine pus (Figure 3(b)). We did not observe lesions in mesenteric lymph nodes in this case. Therefore, mesenteric lymph nodes were not obtained.

4. Discussion

Tuberculosis is a highly contagious zoonotic disease transmitted to wild animals in captivity in close contact with free-ranging animals [17]. Wild animals are susceptible

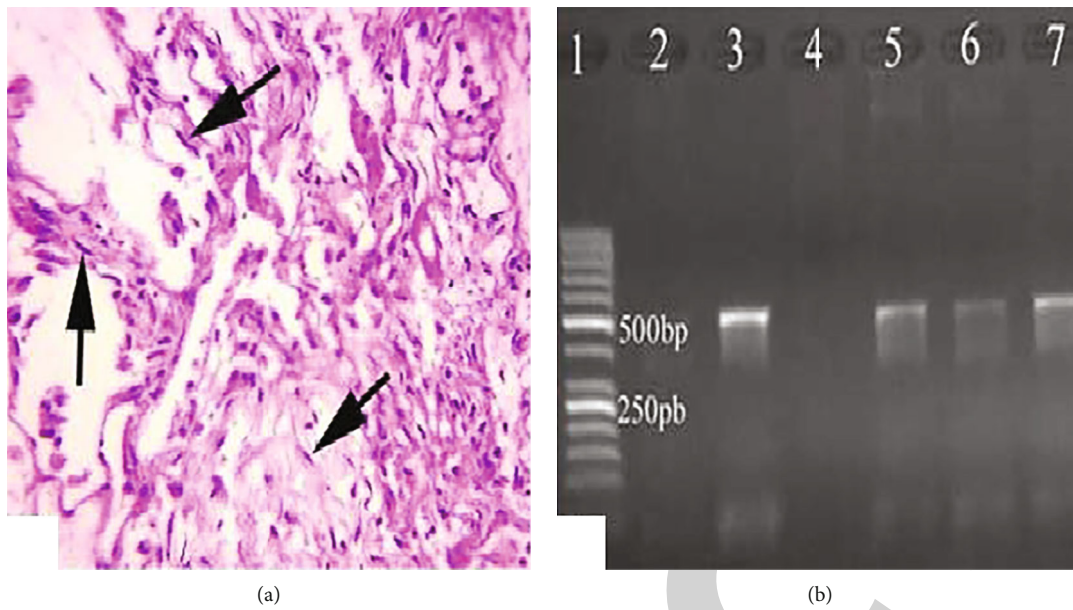


FIGURE 3: Photomicrograph of lung tissues of rhinoceros died of *M. bovis* infection showing (a) extensive fibrosis, presence of bacilli (arrows), and hyperplasia of pneumocytes. H & E; 400X. (b) Confirmation of *Mycobacterium bovis* by PCR (500 bp) from lungs (5), liver (6), and uterine pus (7). Lane 1 shows DNA marker (50 bp), lane 3 positive samples and lane 2 and 4 show negative control.

to tuberculosis and can act as reservoirs, maintain the infectious agents, and continued the spill over of the disease via scavenged carcasses or by prey. In the present study, we reported the *M. bovis* based mortality in rhinoceros in southern Punjab region, Bahawalpur, Pakistan. The researchers discovered tuberculous lesions in rhinoceros, which was consistent with prior investigations in other animals [18, 19, 20, 21] but rarely reported than other findings [23, 24]. The prevalence of TB varies from country to country, or even within a country [22]. This variation might be linked to the type of animal production system [23, 24] and animal breed [25]. Tuberculous lesions have also been seen in parenchymatous organs of slaughtered animals [12] and in an adult female Marsican brown bear died due to *M. bovis* infection [26].

The diagnosis of TB in wild animals mainly relies on necropsy lesions, histopathology, and the bacterial culturing. The changes and distribution of lesions caused by *M. bovis* mainly depend upon the possible route of infection. Very few information is available about the gross and microscopic lesions due to *M. bovis* in captive individuals' rhinoceroses [27, 28] and very rare in free-ranging wild animals. Similar pulmonary lesions have been seen in a semicaptive black rhinoceros due to natural infection with *M. bovis* [29]. However, no characteristic lesions have been observed in rhinoceros experimentally infected with *M. bovis* [27].

Bilateral granulomatous inflammation and bronchial exudate were the consistent findings in infected lungs in the present case. It is speculated that in *M. bovis*, infected lungs caseated tissues liquefy due to the liberation of nucleases and proteases from macrophages [7]. Lungs of dairy cattle infected with *M. bovis* showed frequent classical lesions of tuberculosis, such as granuloma comprising caseation/mineralization surrounded by epithelioid, multi-

nucleated giant cells, fibrous capsule, plasma cells, and lymphocytes [7, 12]. Similarly, granulomatous inflammation composed of mixed inflammatory cells, multinucleated giant cells, fibrous nodules, and mineralized centers has been observed in the lungs of experimentally induced *M. bovis* infection in rhinoceros [27]. No report is available in the accessible published literature about the presence of blood-filled cysts in the liver of rhinoceroses due to *M. bovis* infection. However, it has been observed in the liver of crossbred cows suffered from chronic tuberculosis [7].

PCR assays are the most promising alternative tool for the quick and specific detection of tuberculosis [30, 31, 32]. PCR techniques have been effectively utilized to diagnose bovine tuberculosis in a variety of naturally infected organic samples, including tissue, blood, and nasal exudates [32, 33]. The most widely used method is based on primers that amplify parts of the DNA. JB21/JB22 has been shown to be extremely accurate at identifying *M. bovis* DNA isolates from blood samples, with 100 percent concordance with the traditional microbiological approach [34]. Studies reported in past also employed a multiplex-PCR to detect a single 500 bp product in *M. bovis* while MTB produced a single 185 bp product, with or without an additional 500 bp product [35, 36].

5. Conclusion and Future Perspective

The present study supports the historical assumption that *M. bovis* could establish itself in a rhinoceros population and other wildlife but remain underestimated and unrecognized for decades. TB in rhinoceros within a given reserve or facility is a potential risk for human infection, either visitors or workers. Thus, the application of effective tools to

determine the tuberculosis status in the rhinoceros is crucial. An organized approach to disease management shared between wildlife and cattle needs to be identified as a key requirement in national and international zoological parks. Integrating these components allows for adaptive disease management and may be the most effective way to manage *M. bovis*. A large-scale study is required to determine *M. bovis* prevalence in the zoological parks of Pakistan and rest of countries.

Data Availability

All the data relevant to this study is mentioned in the manuscript. There is no any supplementary data.

Conflicts of Interest

The authors declare no conflict of interest.

Acknowledgments

All authors are thankful to the Department of Pathology, Faculty of Veterinary and Animal Sciences, Department of Pathology, Faculty of Veterinary Science, University of Agriculture, Faisalabad 38040, Pakistan, for providing lab facilities to carry out histopathological studies and molecular confirmation smoothly and successfully.

References

- [1] M. A. Ghumman, A. W. Manzoor, S. Naz, R. Ahmad, and R. Ahmad, "Prevalence of tuberculosis in cattle and buffalo at various livestock farms in Punjab. International Journal of Veterinary Medicine: Research and Reports," *Int J Vet Med*, vol. 2013, pp. 242–247, 2013.
- [2] I. A. Khan and A. Khan, "Prevalence and risk factors of bovine tuberculosis in Nili Ravi buffaloes in the Punjab, Pakistan," *Italian Journal of Animal Science*, vol. 6, no. sup 2, pp. 817–820, 2007.
- [3] R. Tschopp, A. Aseffa, E. Schelling et al., "Bovine tuberculosis at the wildlife-livestock-human interface in Hamer Woreda, South Omo, Southern Ethiopia," *PLoS One*, vol. 5, no. 8, article e12205, 2010.
- [4] *OIE, OIE-listed Diseases, Infections and infestations. office international desepizootics*, World Organization for Animal Health, Paris, France, 2017, <http://www.oie.int>.
- [5] A. Basit, M. Hussain, M. Shahid et al., "Occurrence and risk factors associated with mycobacterium tuberculosis and mycobacterium bovis in milk samples from north east of Pakistan," *Pakistan Veterinary Journal*, vol. 38, no. 2, pp. 199–203, 2018.
- [6] P. R. Sichewo, C. V. Kelen, S. Thys, and A. L. Michel, "Risk practices for bovine tuberculosis transmission to cattle and livestock farming communities living at a wildlife-livestock-human interface in northern Kwa Zulu Natal, South Africa," *PLoS Neglected Tropical Diseases*, vol. 14, no. 3, article e0007618, 2020.
- [7] F. Mahmood, A. Khan, R. Hussain, and I. A. Khan, "Molecular based epidemiology of bovine pulmonary tuberculosis – a mortal foe," *Pakistan Veterinary Journal*, vol. 34, no. 2, pp. 185–188, 2014.
- [8] C. Richomme, E. Réveillaud, J. L. Moyon et al., "Mycobacterium bovis infection in red foxes in four animal tuberculosis endemic areas in France," *Microorganisms*, vol. 8, no. 7, p. 1070, 2020.
- [9] I. Khattak, M. H. Mushtaq, M. U. D. Ahmad, M. S. Khan, and J. Haider, "Zoonotic tuberculosis in occupationally exposed groups in Pakistan," *Occupational Medicine (Lond)*, vol. 66, no. 5, pp. 371–376, 2016.
- [10] R. Akhtar, M. Sadiqa, M. Tipu et al., "Use of molecular probes for presumptive diagnosis of tuberculosis associated with Mycobacterium tuberculosis and Mycobacterium bovis infection in antelopes in Pakistan," *Pakistan Veterinary Journal*, vol. 39, no. 2, pp. 316–319, 2019.
- [11] M. Miller, A. Michel, P. van Helden, and P. Buss, "Tuberculosis in rhinoceros: an underrecognized threat?," *Transboundary and Emerging Diseases*, vol. 64, no. 4, pp. 1071–1078, 2017.
- [12] J. E. Shitaye, B. Getahun, T. Alemayehu et al., "A prevalence study of bovine tuberculosis by using abattoir meat inspection and tuberculin skin testing data, histopathological and IS6110 PCR examination of tissues with tuberculous lesions in cattle in Ethiopia," *Veterinárni Medicína*, vol. 51, no. 11, pp. 512–522, 2012.
- [13] H. H. Ramadan, A. H. N. El-Gohary, and A. A. Mohamed, "Detection of Mycobacterium bovis and Mycobacterium tuberculosis from clinical samples by conventional and molecular techniques in Egypt," *Global Veterinaria*, vol. 9, no. 6, pp. 648–654, 2012.
- [14] Q. Mujahid, A. Khan, M. F. Qadir et al., "Allethrin induced toxicopathological alterations in adult male albino rats," *Agro-biological Records*, vol. 5, pp. 8–14, 2021.
- [15] S. A. Khaliq, M. Mohiuddin, M. Habib et al., "Clinico-hematobiochemical and molecular diagnostic investigations of peste des petits ruminants in goats," *Pakistan Veterinary Journal*, vol. 40, no. 3, pp. 313–318, 2020.
- [16] D. Kidane, J. O. Olobo, A. Habte et al., "Identification of the causative organism of tuberculous lymphadenitis in Ethiopia by PCR," *Journal of Clinical Microbiology*, vol. 40, no. 11, pp. 4230–4234, 2002.
- [17] S. Songthammanuphap, S. Puthong, C. Pongma et al., "Detection of Mycobacterium tuberculosis complex infection in Asian elephants (*Elephas maximus*) using an interferon-gamma release assay in a captive elephant herd," *Scientific Reports*, vol. 10, article 14551, 2020.
- [18] G. Ameni, F. Desta, and R. Firdessa, "Molecular typing of Mycobacterium bovis isolated from tuberculosis lesions of cattle in north eastern Ethiopia," *Veterinary Record*, vol. 167, no. 4, pp. 138–141, 2010.
- [19] Y. Tekle, G. Mamo, G. Ameni, and F. Mulugeta, "Assessment of bovine tuberculosis like lesions and its risk factors in cattle slaughtered at Hawassa University and municipal Abattoirs, Southern Ethiopia," *Journal of Veterinary Science and Medicine*, vol. 5, no. 2, pp. 1–9, 2017.
- [20] B. Demelash, F. Inangolet, J. Oloya et al., "Prevalence of bovine tuberculosis in Ethiopian slaughter cattle based on post-mortem examination," *Tropical Animal Health and Production*, vol. 41, no. 5, pp. 755–765, 2009.
- [21] B. Nemomsa, G. Gebrezgabiher, T. Birhanu, H. Tadelles, G. Tadesse, and B. Getachew, "Epidemiology of bovine tuberculosis in Butajira, southern Ethiopia: a cross-sectional abattoir-based study," *African Journal of Microbiology Research*, vol. 8, no. 33, pp. 3112–3117, 2014.

Retraction

Retracted: Cigarette Smoke Regulates the Expression of EYA4 via Alternation of DNA Methylation Status

BioMed Research International

Received 8 January 2024; Accepted 8 January 2024; Published 9 January 2024

Copyright © 2024 BioMed Research International. This is an open access article distributed under the Creative Commons Attribution License, which permits unrestricted use, distribution, and reproduction in any medium, provided the original work is properly cited.

This article has been retracted by Hindawi following an investigation undertaken by the publisher [1]. This investigation has uncovered evidence of one or more of the following indicators of systematic manipulation of the publication process:

- (1) Discrepancies in scope
- (2) Discrepancies in the description of the research reported
- (3) Discrepancies between the availability of data and the research described
- (4) Inappropriate citations
- (5) Incoherent, meaningless and/or irrelevant content included in the article
- (6) Manipulated or compromised peer review

The presence of these indicators undermines our confidence in the integrity of the article's content and we cannot, therefore, vouch for its reliability. Please note that this notice is intended solely to alert readers that the content of this article is unreliable. We have not investigated whether authors were aware of or involved in the systematic manipulation of the publication process.

Wiley and Hindawi regrets that the usual quality checks did not identify these issues before publication and have since put additional measures in place to safeguard research integrity.

We wish to credit our own Research Integrity and Research Publishing teams and anonymous and named external researchers and research integrity experts for contributing to this investigation.

The corresponding author, as the representative of all authors, has been given the opportunity to register their agreement or disagreement to this retraction. We have kept a record of any response received.

References

- [1] B. O. Almutairi, M. H. Almutairi, A. F. Alrefaei, D. Ali, S. Alkahtani, and S. Alarifi, "Cigarette Smoke Regulates the Expression of EYA4 via Alternation of DNA Methylation Status," *BioMed Research International*, vol. 2022, Article ID 5032172, 7 pages, 2022.

Research Article

Cigarette Smoke Regulates the Expression of EYA4 via Alternation of DNA Methylation Status

Bader O. Almutairi , **Mikhlid H. Almutairi**, **Abdulwahed F. Alrefaei**, **Daoud Ali**, **Saad Alkahtani** , and **Saud Alarifi** 

Department of Zoology, College of Science, King Saud University, P.O. Box: 2455, 11451 Riyadh, Saudi Arabia

Correspondence should be addressed to Bader O. Almutairi; bomotairi@ksu.edu.sa

Received 7 April 2022; Accepted 28 April 2022; Published 14 May 2022

Academic Editor: Hafiz Ishfaq Ahmad

Copyright © 2022 Bader O. Almutairi et al. This is an open access article distributed under the Creative Commons Attribution License, which permits unrestricted use, distribution, and reproduction in any medium, provided the original work is properly cited.

Cigarette SMOKE (CS) considerably contributes to causing some diseases such as cancer, and it has a role in the alternation of gene expression through several mechanisms including epigenetics modification, particularly DNA methylation. *EYA4* is one of the genes, that whose expression has been dysregulated in lung, colon, bladder, and breast cancer, leading to tumor progression. The alternation of DNA methylation levels has been implicated in regulating the expression of the *EYA4* gene. Thus, in this study, we have shown the effect of CS on the DNA methylation level of the *EYA4* promoter region as well as the methylation level on *EYA4* expression. To determine the level of DNA methylation on the promoter region of the *EYA4* gene, we have employed the bisulfite conversion treatment followed by the Sanger Sequence for 100 DNA samples taken from Saudi people (50 smokers and 50 nonsmokers). We found that 26% of DNA extracted from smoker samples is methylated, while there was no methylation identified in nonsmoker samples. Also, using the demethylating agents such as AZA on LoVo and Caco-2 cancer cell lines causes induction of transcription level of *EYA4*, implying the possible mechanism of DNA methylation in the upregulation of *EYA4*. These findings suggest the possible mechanism of CS in controlling the expression of *EYA4* via changing the status of DNA methylation.

1. Introduction

Cigarette smoke (CS) is the most prevalent cause of death and disease in the world [1]. CS may negatively affect nearly all organs of the body, accelerate the process of organ aging, and consequently lead to various disease, such as cardiovascular diseases [1], chronic obstructive pulmonary disease [2], and cancers [3]. Clinical studies have illustrated that CS can trigger several aging-related changes, from cell phenotype to gene expression and epigenetic regulation, in the respiratory system [4], as well as the ability to induce oxidative damage, inflammation, immune changes, genetic alterations [5], and single-nucleotide polymorphism (SNP) alternations [6]. Thus, understanding the mechanism of smoking and its contribution of causing chronic illness is a crucial for the discovery of therapeutic targets [7]. Few studies have been conducted on epigenetic mechanisms including DNA methylation, showing a possible role of CS in regulation of DNA

methylation [8] that could lead to remarkable changes in gene transcription, resulting in diseases development [9–11].

Epigenetics, including DNA methylation, has been implicated in causing several diseases such as neuroblastoma [12], breast cancer [13], colon cancer [14], and liver cancer [14], via silencing tumor suppressor genes [15] and inducing oncogenes [12]. Recent studies have shown that the alternation of DNA methylation is a leading cause of colon cancer and being considered as biomarkers [16]. It is noteworthy that several environmental factors can negatively affect the epigenetic mechanisms including DNA methylation [8], especially CS, air pollution, and dietary changes [8].

One of the specific genes which has been regulated by alternation of DNA methylation is *EYA4* [17, 18], and it belongs to eyes absent gene family (EYA), playing a major role in the mediation of DNA repair, cell apoptosis, angiogenesis, and tumor growth [19, 20]. EYA protein harbors different domains, including transcriptional activation,

protein tyrosine phosphate, and threonine phosphate, and its conserved C-terminal domain carrying 270 amino acids, while less likely conserved N-terminal having a vary amino acids between 266 and 320 [21]. Translational level of EYA, particularly protein-protein interaction domain involves in the binding site of SIX and DACH protein [22]. Interestingly, disruption of *EYA4* expression was implied to contribute to cancer progression including lung cancer [23], hepatocellular carcinoma [24], breast cancer [25], esophageal squamous cell carcinoma [17], and bladder cancer [26]. Also, it is reported that CS could dysregulate *EYA4* expression [27]. Therefore, in the current study, we have investigated the effect of CS on DNA methylation level in nonsmoker and smoker Saudi adults as well as the contribution of DNA methylation in regulating *EYA4* expression.

2. Materials and Methods

2.1. Ethical Approval. The ethical approval of this study was obtained from the Research Ethics Committee of the College of Applied Medical Sciences at King Saud University in Riyadh, Saudi Arabia (Reference No. CAMS 13/3536).

2.2. Collection of Blood Samples. We have collected blood samples from 100 healthy Saudi adults of which 50 people are smokers and other 50 nonsmokers (Table 1), from the Blood Donation Center at King Saud medical city (Riyadh, Saudi Arabia) between September 2018 and December 2019.

2.3. DNA Extraction, Bisulfite Conversion, and Sanger Sequence. The lymphocyte genomic DNA was extracted with PureLink® Genomic DNA Mini Kit (Invitrogen) [28] and 500 ng was treated with EZ DNA methylation-Gold™ kit (Zymo Research) [12]. *EYA4* forward AGGGGATGTTT TGTTTTTATTAGAG and reverse TAAAAATTCTCTCA ACTCAAACCTCC were amplified using end point PCR, PCR condition: 5 minutes at 95°C; followed by 37 cycles, 94°C for 30 seconds, and then 30 seconds at 60°C and 30 seconds at 72°C, respectively. Having terminated the amplification with a 10 minutes at 72°C, followed by sanger sequencing via MacroGen Inc. (Seoul, Republic of Korea).

2.4. Cells and 5-Aza-2'-Deoxycytidine Treatment. The LoVo and Caco-2 were obtained from American Type Culture Collection (ATCC), USA. Cells were grown in DMEM (Sigma) media containing 10% FBS and 10000 U/ml antibiotic and then kept at 37°C in 5% CO₂ incubator. LoVo and Caco-2 were treated with 1 μM 5-aza-2'-deoxycytidine (Sigma) for 72 hours, and a medium was replaced every 24 hours. Control cultures had an equal volumes of drug solvent (DMSO) [12].

2.5. RNA Extraction, cDNA Synthesis, and RT-PCR. Total RNA was extracted with a QIAzol Lysis reagent (Qiagen), and GoScript™ Reverse Transcriptase (Promega) was applied to synthesis cDNA; gene-specific primers of *EYA4* forward ATAACACAGCCGATGGCACA and reverse TCCTGG TTGGTTAGTCAGTCC were used for QPCR (GoTaq® qPCR; Promega) on Prime Q real-time PCR machine (Techine), normalizing the amount of target gene to the

TABLE 1: Clinical and demographic data of the study participants.

Variable	Smokers	Nonsmokers
Number	50	50
Age (years), median ± SD	31.75 ± 2.84	29.8 ± 3.5
Age (years)		
≤30 years	31 (62%)	18 (36%)
>30 years	19 (38%)	32 (64%)
Years of smoking		
≤12 years	26 (52%)	—
>12 years	24 (48%)	—

house keeping gene *GAPDH* forward AATGGGCAGCC GTTAGGAAA and reverse AAAAGCATCACCCGGA GGAG [29]. PCR conditions are as follows: one cycle at 95°C for 15 minutes, followed by 36 cycles of 95°C for 30 seconds, then 30 seconds at 58°C and 30 seconds at 72°C, terminating the incubation by 1 cycle of 95°C for 1 minute, 58°C for 30 seconds, and 95°C for 30 seconds successively. The $2^{-\Delta\Delta Ct}$ method was applied to define the relative mRNA expression.

2.6. Statistical Analysis. Statistical analysis was performed using SPSS software Ver.22 (SPSS Inc., Chicago, USA). Data were examined using Student's *t*-test, and results were presented as average ± SD. Paired *t*-test were being considered statistically significant at **p* < 0.05; ***p* < 0.005.

3. Results

3.1. Clinical Data of the Participants. In this study, there was no significant difference in the age of participants (average age nonsmokers = 29.85 years old and smokers = 31.75 years old) (Table 1). Smoker participants consume a minimum of 10 cigarettes a day for a minimum of 7 years.

3.2. EYA4 Promoter Is Enriched with CpG Islands, and Its Expression Is Downregulated in Colon Cancer. We designed our assay on *EYA4* promoter region which is enriched with CpG island (on human genome build NCBI36/Hg18 (UCSC genome browser; <http://genome.ucsc.edu>) (Figure 1(a)). Also, we have noticed that the expression of *EYA4* is decreased in number of colon cancer sets: GSE8672, GSE4554, GSE2150, and GSE37892 compared to different set of normal tissues GSE3526 and GSE7307 that are appeared in R2 genomic analysis and visualization platform (<https://hgserver1.amc.nl/cgi-bin/r2/main.cgi>) (Figure 1(b)). These data suggested the possible relation between DNA methylation and regulation of *EYA4* expression.

3.3. EYA4 Amplification in Bisulfite Genomic DNA Extracted from Smoker and Nonsmoker Adults. Genomic DNA was extracted from participants and was treated with bisulfite conversion, followed by PCR amplification. The expression of *EYA4* was detected in all samples (Figure 2). Then, PCR products were dispatched for Sanger sequence to see the alternation of DNA methylation level.

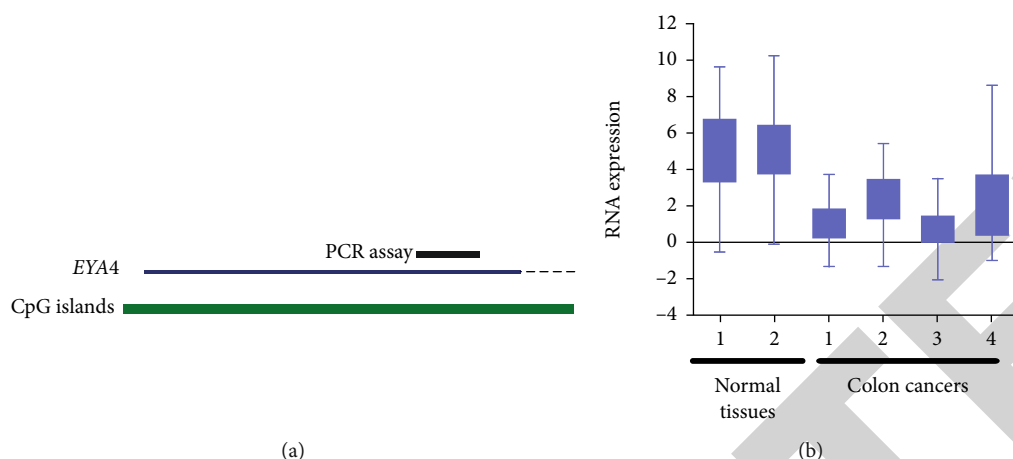


FIGURE 1: Location of *EYA4* assay and RNA expression in normal tissues and colon cancer. (a) USCS genome browser (<https://genome.ucsc.edu>) indicates the place of amplicon on the *EYA4* promoter and the distribution of CpG island on the promoter region of *EYA4*. (b) Box blot shows the expression of *EYA4* in normal tissues (1: GSE3526 contains 353 samples and 2: GSE7307 contains 504 samples) and in colon cancers (1: GSE8671 contains 32 samples, 2: GSE4554 contains 84 samples, 3: GSE21510 contains 148 samples, and 4: GSE37892 contains 130 samples) taken from R2 online public data (<https://hgserver1.amc.nl/cgi-bin/r2/main.cgi>).

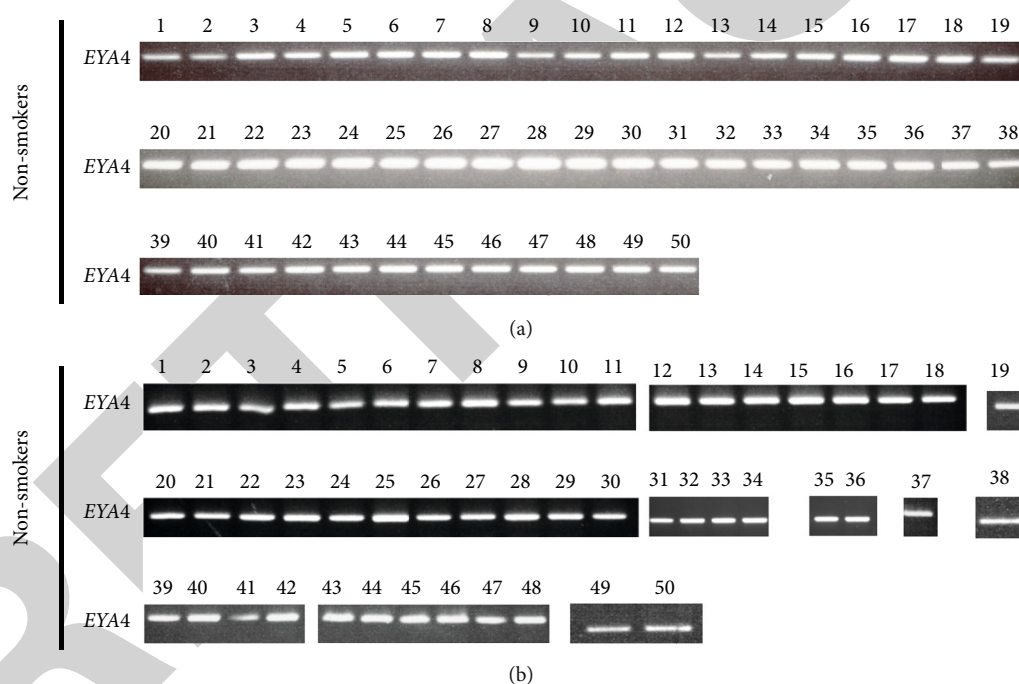


FIGURE 2: 2% agarose gel of PCR product shows the amplification of *EYA4* gene in lymphocyte genomic DNA extracted from nonsmokers and smokers. Followed by treatment with bisulfite conversion in nonsmoker and smoker adults. 1 to 50 indicates the samples number. (a) *EYA4* bands after being amplified by PCR in 50 samples of nonsmokers. (b) *EYA4* bands after being amplified by PCR in 50 samples of smokers.

3.4. *EYA4* Methylation in Nonsmoker and Smoker Adults. Interestingly, Sanger sequence data has shown that there is no methylation on *EYA4* promoter in all nonsmoker samples (Figure 3(a)), However, 26% of smokers harbored methylated promoter of *EYA4* (Figure 3(b)). The level of DNA methylation was significantly increased in smokers compared to nonsmokers (Figure 3(c)). Our results indicated that CS causes a noticeable change in DNA methylation. Therefore, the effect

of DNA methylation on the regulation of the *EYA4* expression was investigated in colon cancer cell lines.

3.5. 5-Aza-2'-Deoxycytidine Induces *EYA4* Expression. Colon cancer cell lines LoVo and Caco-2 were treated with 1 μ M 5-Aza-CdR for 72 hours, and the expression of *EYA4* was significantly upregulated in LoVo (Figure 4(a)) and Caco-2 (Figure 4(b)) compared to cells treated with DMSO.

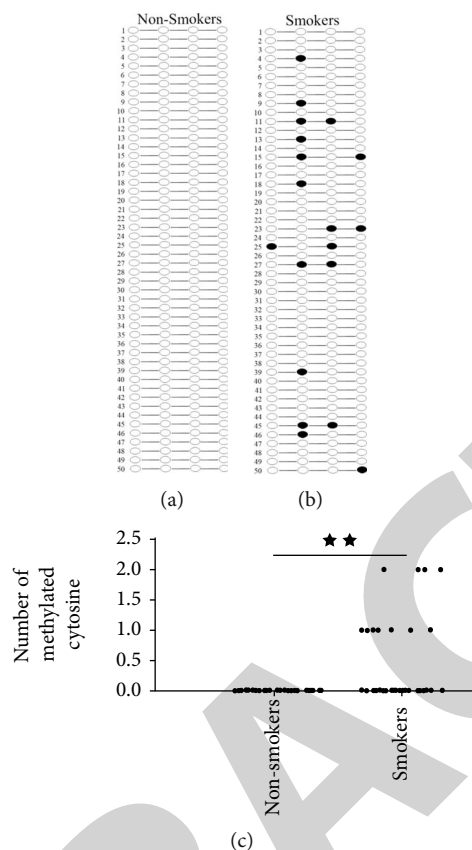


FIGURE 3: *EYA4* methylation level in nonsmoker and smoker samples. (a) Lollipop diagram displays the methylation level of 4 CpG islands that located on the *EYA4* promoter in DNA extracted from nonsmokers ($n = 50$). White lollipop indicates unmethylated cytosine, black lollipop indicates methylated cytosine, and there was no methylation observed. (b) Lollipop diagram displays the methylation level of 4 CpG islands that located on the *EYA4* promoter in DNA extracted from nonsmokers ($n = 50$). White lollipop indicates unmethylated cytosine, black lollipop indicates methylated cytosine, and methylated cytosine was detected in 26% of tested samples. (c) Box blot shows the number of methylated cytosine in nonsmoker and smoker adults. $**p < 0.01$, two samples t -test.

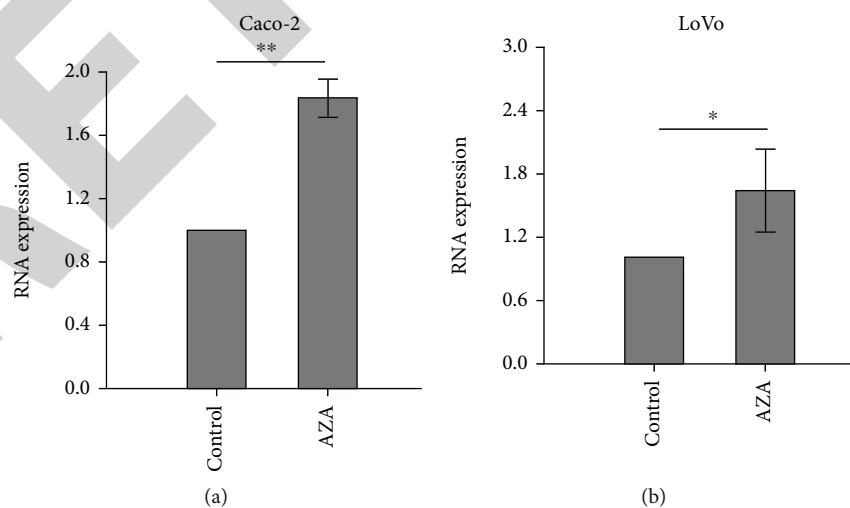


FIGURE 4: The effects of 5-Aza-CdR on *EYA4* RNA expression in colon cancer cells. (a) RNA expression of *EYA4* in Caco-2 cell lines after being treated with DMSO (control) and with $1 \mu\text{M}$ 5-Aza-CdR (AZA) for 72 hours and media was replaced every 24 hours. (b) RNA expression of *EYA4* in LoVo cell lines after being treated with DMSO (control) and with $1 \mu\text{M}$ 5-Aza-CdR (AZA) for 72 hours and media was replaced every 24 h. Mean \pm SD of three experiments, $*p < 0.05$, $**p < 0.005$, paired sample t -test.

Taken together, our results suggested that CS could epigenetically regulate the expression of *EYA4* through the alternation of DNA methylation.

4. Discussion

In this paper, we have examined the effect of CS on the regulation of DNA methylation as well as the involvement of DNA methylation in controlling the expression *EYA4* gene. The expression of *EYA4* gene is important in cell proliferation, migration, and angiogenesis [21]. *EYA4* promoter is covered with CpG island, and alternation of DNA methylation was observed in tumor samples compared to normal samples [17, 30]. Additionally, abnormality of *EYA4* expression has been mentioned to contribute to cancer progression for instance, colon cancer [31], glioma [32], lung cancer [23], and bladder cancer [26]. Also, downregulation of its expression was defined in different sets of colon cancers, suggesting its role in inhibiting tumor development [31]. A recent study by Deger et al. revealed the role of *EYA4* methylation in predicting the favourable outcomes of colorectal liver metastasis patients as the level of DNA methylation has comparably decreased in blood samples taken from patients after and before treatments [33].

Interestingly, our result showed for the first time among Saudi population, no methylation of *EYA4* was appeared in nonsmokers, whereas 26% of smoker samples were methylated and these differences are significant. Our finding is in line with that found in Zhu et al. [34] in DNA methylation of cigarette smoking of the Chinese population. Also, other researchers have reported that DNA methylation is associated with cigarette smoking [34–37], and changing the methylation in one CpG could induce gene expression [38]. Thus, due to the involvement of CS in alteration of DNA methylation status [39, 40], and in hampering the expression of *EYA4* in lung tissues taken from smokers compared to nonsmokers [27] as well as the impact of DNA methylation in depleting *EYA4* expression in oral [41] and colon cancer [31], we suggest that CS could have a role in changing the methylation status of *EYA4* in Saudi population.

CS is implicated in inducing hypermethylation mechanism via increasing the expression of DNA methyl transferase enzymes (DNMTs) [42, 43]. The possible mechanism could be through DNA damage on *DNMT3b* which occurs as a result of the existences of carcinogens content in CS including arsenic, formaldehyde, and nitrosamines [44], leading to a transition from C to T that is located on the promoter 149bp away from the transcription start site; it was revealed that nonsmokers harbor *DNMT3b*-149 CT genotype while smokers contain *DNMT3b*-149 TT genotype [42]. Consequently, an increase of *DNMT3b* activity is observed, causing an establishment of de novo methylation of CpG on some tumor suppressor genes [45].

A few studies have shown the dysregulation of DNA methylation in colon cancer including *EYA4*, which was hypermethylated and treatment with demethylating agents caused induction of its expression [46]. In agreement with Kim et al. [31] and Moon et al. [47], we have restored the

expression of *EYA4* after treating the Caco-2 and LoVo colon cancer cells with 1 μ M 5-Aza-CdR for 72 hours, this implies the possible mechanism of involvement of DNA methylation in hampering the expression of *EYA4* [31], which could accelerate colon cancer formation [31].

The consequence of the existence of *EYA4* expression conceivably blocks the development of colon cancer [31], through the downregulation of MYCBP [48] via dephosphorylating β -catenin [49]. Therefore, the depletion of *EYA4* expression has been detected in colorectal cancer, possibly due to hypermethylated promoter [31]. Overall, our result indicates the deleterious impacts of CS on the alternation of the level of DNA methylation in *EYA4* promoter, presumably resulting in *EYA4* inhibition.

Data Availability

The original contributions presented in the study are included in the article; further inquiries can be directed to the corresponding author.

Conflicts of Interest

The authors declare that they have no conflicts of interest.

Authors' Contributions

BA is responsible for the conceptualization; BA and MHA for data curation; BA, MHA, DA, AFA, SA, and SuA for formal analysis; BA for funding acquisition; BA for investigation and methodology; BA and DA for project administration; BA for software and supervision; BA and SA for validation; BA and DA for writing—original draft and writing—review and editing.

Acknowledgments

The authors express their sincere appreciation to the Researchers Supporting Project Number (RSP-2022R414), King Saud University, Riyadh, Saudi Arabia.

References

- [1] J. Lee, V. Taneja, and R. Vassallo, "Cigarette smoking and inflammation: cellular and molecular mechanisms," *Journal of Dental Research*, vol. 91, no. 2, pp. 142–149, 2012.
- [2] S. T. Lugg, A. Scott, D. Parekh, B. Naidu, and D. R. Thickett, "Cigarette smoke exposure and alveolar macrophages: mechanisms for lung disease," *Thorax*, vol. 77, no. 1, pp. 94–101, 2022.
- [3] H. Scherubl, "Smoking tobacco and cancer risk," *Deutsche Medizinische Wochenschrift*, vol. 146, no. 6, pp. 412–417, 2021.
- [4] X. Wu, Q. Huang, R. Javed, J. Zhong, H. Gao, and H. Liang, "Effect of tobacco smoking on the epigenetic age of human respiratory organs," *Clinical Epigenetics*, vol. 11, no. 1, p. 183, 2019.
- [5] A. W. Caliri, S. Tommasi, and A. Besaratinia, "Relationships among smoking, oxidative stress, inflammation, macromolecular damage, and cancer," *Mutation Research-Reviews in Mutation Research*, vol. 787, p. 108365, 2021.

- [6] M. H. Almutairi, B. O. Almutairi, T. M. Alrubie et al., "Association between tobacco substance usage and a missense mutation in the tumor suppressor gene P53 in the Saudi Arabian population," *PLoS One*, vol. 16, no. 1, 2021.
- [7] W. Qiu, E. Wan, J. Morrow et al., "The impact of genetic variation and cigarette smoke on DNA methylation in current and former smokers from the COPDGene study," *Epigenetics*, vol. 10, no. 11, pp. 1064–1073, 2015.
- [8] X. Gao, M. Jia, Y. Zhang, L. P. Breitling, and H. Brenner, "DNA methylation changes of whole blood cells in response to active smoking exposure in adults: a systematic review of DNA methylation studies," *Clinical Epigenetics*, vol. 7, no. 1, p. 113, 2015.
- [9] C. G. Howe, M. Zhou, X. Wang et al., "Associations between maternal tobacco smoke exposure and the cord blood CD4+ DNA methylome," *Environmental Health Perspectives*, vol. 127, no. 4, p. 047009, 2019.
- [10] D. Fragou, E. Pakkidi, M. Aschner, V. Samanidou, and L. Kovatsi, "Smoking and DNA methylation: correlation of methylation with smoking behavior and association with diseases and fetus development following prenatal exposure," *Food and Chemical Toxicology*, vol. 129, pp. 312–327, 2019.
- [11] X. Gao, Y. Zhang, L. P. Breitling, and H. Brenner, "Tobacco smoking and methylation of genes related to lung cancer development," *Oncotarget*, vol. 7, no. 37, pp. 59017–59028, 2016.
- [12] B. Almutairi, J. Charlet, A. R. Dallosso et al., "Epigenetic deregulation of GATA3 in neuroblastoma is associated with increased GATA3 protein expression and with poor outcomes," *Scientific Reports*, vol. 9, no. 1, p. 18934, 2019.
- [13] P. J. Ho, R. Dorajoo, I. Ivanković et al., "DNA methylation and breast cancer-associated variants," *Breast Cancer Research and Treatment*, vol. 188, no. 3, pp. 713–727, 2021.
- [14] X. Hao, H. Luo, M. Krawczyk et al., "DNA methylation markers for diagnosis and prognosis of common cancers," *Proceedings of the National Academy of Sciences of the United States of America*, vol. 114, no. 28, pp. 7414–7419, 2017.
- [15] Y. Liang, Q. Lu, W. Li et al., "Reactivation of tumour suppressor in breast cancer by enhancer switching through NamiRNA network," *Nucleic Acids Research*, vol. 49, no. 15, pp. 8556–8572, 2021.
- [16] G. Jung, E. Hernández-Illán, L. Moreira, F. Balaguer, and A. Goel, "Epigenetics of colorectal cancer: biomarker and therapeutic potential," *Nature Reviews. Gastroenterology & Hepatology*, vol. 17, no. 2, pp. 111–130, 2020.
- [17] M. Luo, Y. Li, X. Shi et al., "Aberrant methylation of EYA4 promotes epithelial-mesenchymal transition in esophageal squamous cell carcinoma," *Cancer Science*, vol. 109, no. 6, pp. 1811–1824, 2018.
- [18] L. Barault, A. Amatu, G. Siravegna et al., "Discovery of methylated circulating DNA biomarkers for comprehensive non-invasive monitoring of treatment response in metastatic colorectal cancer," *Gut*, vol. 67, no. 11, pp. 1995–2005, 2018.
- [19] Y. Liu, N. Han, S. Zhou et al., "The DACH/EYA/SIX gene network and its role in tumor initiation and progression," *International Journal of Cancer*, vol. 138, no. 5, pp. 1067–1075, 2016.
- [20] Y. Wang, E. Tadjuidje, R. N. Pandey et al., "The eyes absent proteins in developmental and pathological angiogenesis," *The American Journal of Pathology*, vol. 186, no. 3, pp. 568–578, 2016.
- [21] E. Tadjuidje and R. S. Hegde, "The eyes absent proteins in development and disease," *Cellular and Molecular Life Sciences*, vol. 70, no. 11, pp. 1897–1913, 2013.
- [22] X. Zheng, Q. Liu, M. Yi, S. Qin, and K. Wu, "The regulation of cytokine signaling by retinal determination gene network pathway in cancer," *Oncotargets and Therapy*, vol. 11, pp. 6479–6487, 2018.
- [23] I. M. Wilson, E. A. Vucic, K. S. S. Enfield et al., "_EYA4_ is inactivated biallelically at a high frequency in sporadic lung cancer and is associated with familial lung cancer risk," *Oncogene*, vol. 33, no. 36, pp. 4464–4473, 2014.
- [24] S. J. Mo, X. Hou, X. Y. Hao et al., "EYA4 inhibits hepatocellular carcinoma growth and invasion by suppressing NF- κ B-dependent RAPI transactivation," *Cancer Commun (Lond)*, vol. 38, no. 1, p. 9, 2018.
- [25] K. Conway, S. N. Edmiston, R. May et al., "DNA methylation profiling in the Carolina Breast Cancer Study defines cancer subclasses differing in clinicopathologic characteristics and survival," *Breast Cancer Research*, vol. 16, no. 5, p. 450, 2014.
- [26] W. Dong, J. Bi, H. Liu et al., "Circular RNA ACVR2A suppresses bladder cancer cells proliferation and metastasis through miR-626/EYA4 axis," *Molecular Cancer*, vol. 18, no. 1, p. 95, 2019.
- [27] G. Pintarelli, S. Noci, D. Maspero et al., "Cigarette smoke alters the transcriptome of non-involved lung tissue in lung adenocarcinoma patients," *Scientific Reports*, vol. 9, no. 1, p. 13039, 2019.
- [28] M. Almutairi, A. Mohammad Alhadeq, R. Almeer, M. Almutairi, M. Alzahrani, and A. Semlali, "Effect of the thymine-DNA glycosylase rs4135050 variant on Saudi smoker population," *Molecular Genetics & Genomic Medicine*, vol. 7, no. 4, article e00590, 2019.
- [29] J. D. Combes, G. Grelier, M. Laversanne et al., "Contribution of cell culture, RNA extraction, and reverse transcription to the measurement error in quantitative reverse transcription polymerase chain reaction-based gene expression quantification," *Analytical Biochemistry*, vol. 393, no. 1, pp. 29–35, 2009.
- [30] X. Hou, J. X. Peng, X. Y. Hao et al., "DNA methylation profiling identifies EYA4 gene as a prognostic molecular marker in hepatocellular carcinoma," *Annals of Surgical Oncology*, vol. 21, no. 12, pp. 3891–3899, 2014.
- [31] S. J. Kim, C. H. Tae, S. N. Hong et al., "EYA4Acts as a new tumor suppressor gene in colorectal cancer," *Molecular Carcinogenesis*, vol. 54, no. 12, pp. 1748–1757, 2015.
- [32] Z. Li, R. Qiu, X. Qiu, and T. Tian, "EYA4 promotes cell proliferation through downregulation of p27Kip1 in glioma," *Cellular Physiology and Biochemistry*, vol. 49, no. 5, pp. 1856–1869, 2018.
- [33] T. Deger, R. G. Boers, V. de Weerd et al., "High-throughput and affordable genome-wide methylation profiling of circulating cell-free DNA by methylated DNA sequencing (MeD-seq) of LpnPI digested fragments," *Clinical Epigenetics*, vol. 13, no. 1, p. 196, 2021.
- [34] X. Zhu, J. Li, S. Deng et al., "Genome-wide analysis of DNA methylation and cigarette smoking in a Chinese population," *Environmental Health Perspectives*, vol. 124, no. 7, pp. 966–973, 2016.
- [35] Y. V. Sun, A. K. Smith, K. N. Conneely et al., "Epigenomic association analysis identifies smoking-related DNA methylation sites in African Americans," *Human Genetics*, vol. 132, no. 9, pp. 1027–1037, 2013.

Retraction

Retracted: Toxicological Effects of Sewage Water on Chick Embryonic Development

BioMed Research International

Received 8 January 2024; Accepted 8 January 2024; Published 9 January 2024

Copyright © 2024 BioMed Research International. This is an open access article distributed under the Creative Commons Attribution License, which permits unrestricted use, distribution, and reproduction in any medium, provided the original work is properly cited.

This article has been retracted by Hindawi following an investigation undertaken by the publisher [1]. This investigation has uncovered evidence of one or more of the following indicators of systematic manipulation of the publication process:

- (1) Discrepancies in scope
- (2) Discrepancies in the description of the research reported
- (3) Discrepancies between the availability of data and the research described
- (4) Inappropriate citations
- (5) Incoherent, meaningless and/or irrelevant content included in the article
- (6) Manipulated or compromised peer review

The presence of these indicators undermines our confidence in the integrity of the article's content and we cannot, therefore, vouch for its reliability. Please note that this notice is intended solely to alert readers that the content of this article is unreliable. We have not investigated whether authors were aware of or involved in the systematic manipulation of the publication process.

Wiley and Hindawi regrets that the usual quality checks did not identify these issues before publication and have since put additional measures in place to safeguard research integrity.

We wish to credit our own Research Integrity and Research Publishing teams and anonymous and named external researchers and research integrity experts for contributing to this investigation.


The corresponding author, as the representative of all authors, has been given the opportunity to register their agreement or disagreement to this retraction. We have kept a record of any response received.

References

- [1] S. Khan, H. M. N. Baqa, H. Mahmood et al., "Toxicological Effects of Sewage Water on Chick Embryonic Development," *BioMed Research International*, vol. 2022, Article ID 6859798, 7 pages, 2022.

Research Article

Toxicological Effects of Sewage Water on Chick Embryonic Development

Sana Khan,¹ Hafiz Muhammad Noman Baqa,² Hamas Mahmood,³ Muhammad Farooq,¹ Khizar Samiullah,¹ Riffat Yasin,⁴ Muhammad Amjad Bashir ,⁵ Abdur Rahman,^{6,7} Tahir Mehmood,⁸ Sagheer Atta,^{5,9} and Afrah Fahad Alkhuriji¹⁰

¹Department of Zoology Faculty of Sciences Ghazi University Dera Ghazi Khan Punjab, Pakistan

²Hospital Bahawalnagar Punjab, Pakistan

³Hospital Kallurkot Bhakkar Punjab, Pakistan

⁴Faculty of Veterinary and Animal Sciences, MNSUA, Multan, Pakistan

⁵Department of Plant Protection Faculty of Agricultural Sciences Ghazi University Dera Ghazi Khan Punjab, Pakistan

⁶Department of Animal Sciences, University of Veterinary and Animal Sciences, Jhang, Pakistan

⁷Department of Animal Nutrition, Afyon Kocatepe University, Turkey

⁸Centre for Applied Molecular Biology (CAMB), University of the Punjab, Lahore-53700, Punjab, Pakistan

⁹United States Department of Agriculture, Washington DC, USA

¹⁰Zoology Department College of Sciences, King Saud University, Riyadh, Saudi Arabia

Correspondence should be addressed to Muhammad Amjad Bashir; abashir@gudgk.edu.pk

Received 8 April 2022; Accepted 18 April 2022; Published 12 May 2022

Academic Editor: Faheem Ahmed Khan

Copyright © 2022 Sana Khan et al. This is an open access article distributed under the Creative Commons Attribution License, which permits unrestricted use, distribution, and reproduction in any medium, provided the original work is properly cited.

For toxicity research, a total of 100 fertilized nonincubated eggs were used for this study. There were two trials in this experiment which were further divided into 2 phases based on a different days of sewage water treatment and observation days. In each trial, 50 eggs were used and divided into 5 groups. Group A, B, and C were treated with three different concentrations of pure and diluted sewage water (100%, 70%, and 30%), respectively. Control group D was given 0.3 ml saline solution (0.9% NaCl) and group E was uninjected. Different parameters such as the embryo's body weight, body length, forelimb length, hindlimb length, and head diameter were determined. In trial 1, eggs were treated with sewage water on 7th day of incubation and opened on 8th day (phase I) and 9th day (phase II). When the trial 1 (phase I) findings were compared to the control groups, it was observed that body weight, body length, forelimb length, and hindlimb length were highly statistically significant differences ($p < 0.01$), but the head diameter was not significant ($p > 0.05$). Phase II result showed embryo's head diameter was a highly statistically significant difference ($p < 0.01$), whereas forelimb length was significant ($p < 0.05$), and body weight, body length, and hindlimb length were nonsignificant ($p > 0.05$). In trial 2, eggs were treated with sewage water on 14th day of incubation and opened on 15th day (phase I) and 16th day (phase II). Results of 15th day showed a highly statistically significant ($p < 0.01$) difference in hindlimb length, while body weight, body length, forelimb length, and head diameter were nonsignificant ($p > 0.05$). Phase II of trial 2 showed that on 16th day, body weight, body length, forelimb length, hindlimb length, and head diameter showed a nonsignificant ($p > 0.05$) difference between experimental and control groups. Embryos were observed to be deforming on the 9th day (after 48 hours of exposure to sewage water). Other phases showed no signs of deformation. Except on 8th day of incubation, dose-related mortalities were present in experimental groups, while the control group showed no mortality.

1. Introduction

Sewage water, also known as domestic wastewater, is a form of waste water. It is made up of a community of individuals. It is identified by its appearance, organic and inorganic compounds, toxic elements, and the nature of pathogens like bacteria and viruses for example hepatitis A, enteroviruses, protozoa, and parasitic helminths (WHO and UNICEF, [1]). A large proportion of it is made up of greywater (from showers, bathtubs, pools, dishwashers, and cloth washers), black water comes from toilets, along with the human waste washed away, soaps and detergents, and toilet papers (Jackson and Ord, [2]). Untreated sewage water is generated in large quantities across the world, leading to widespread water pollution, particularly in low-income countries. According to UNDP and UN-Habitat figures, 90 percent of all waste water is released untreated into the environment (Corcoran et al., [3]).

With population growth, urbanization, and better living standards, the amount of wastewater produced by domestic, industrial, and commercial sources has increased (Qadir et al., [4]). Sewage water also contains pharmaceutical contaminants that are persistent in the environment. Sewage has also been examined to ascertain the relative rates of prescription and illicit drug use among city residents (Castiglioni et al., [5]). It is also possible to infer general socioeconomic demographics (Choi et al., [6]). However, sewage water can contain biological hazards such as bacteria, viruses, and protozoa, as well as chemical hazards, primarily heavy metals (Hussain et al., [7]). Nowadays, a large amount of untreated sewage/industrial water is being discharged into surface bodies for disposal. It has been indicated that long-term exposure to Cd (heavy metal) in food and water leads to abnormalities in embryonic development (Lone et al., [8]).

Because of a scarcity of water and chemical fertilizer application in many developing countries, using sewage water to irrigate agricultural land is common practice with a long background (Zhang et al., [9]). Many domestic and wild animal species, including other forms of human waste, can use greywater supplies if they are available, raising the risk of pathogen fallout and chemical contamination. This is especially significant in dryland areas where greywater can attract water-dependent animals in an area where groundwater is scarce. Animals consuming greywater infected with animal microbes can promote the transmission of antibiotic-resistant microbes from humans to animals, directly leading to the resistant bacteria in the setting (Alexander and Godrej, [10]). The absence of effective sanitation for human beings is a huge issue. An estimated 4.5 billion cannot get access to appropriate sanitation or do not have access to it at all (WHO and UNICEF, [1]).

Chickens are the most common domestic animal and the primary source of animal protein among domesticated animals (Wang et al., [11]). The chicken model organism has also shown great promise in terms of studying environmental contaminants and chemotherapeutics (Rodriguez et al., [12]). Avian eggs are often used as a bioindicator in environmental pollutant testing systems, and infected eggs can be used to determine the risk of lipophilic environmental pollutants. For more than twenty years, the chicken embryo

has been used as a model system for embryology and developmental biology (Stern et al., [13]).

In the present study, the effects of sewage water on the embryonic development of chicks were evaluated. Different parameters such as body weight, body length, forelimb length, hindlimb length, and head diameter were measured. Embryos were also evaluated for normal development. And the mortality rate of developing embryos was also observed.

2. Material and Methods

The experiment was performed at Ghazi University's Zoology departmental lab in DG Khan, Punjab, Pakistan. The study was fundamental and experimental. Toxicological effects of sewage water were evaluated in chick embryos in this study. The eggs were purchased from Govt. Poultry Farm Bahawalpur, Punjab, Pakistan. Different concentrations of sewage water were given to experimental groups and compared to control groups. The shells of all the eggs were sterilized with 70% ethanol. With an egg driller, a tiny hole was created in the shell of each egg excepting uninjected eggs. With the small injector, a single dose of each concentration was injected into the air sac of each egg. The hole was sealed with paraffin wax after sewage water had been administered. To ensure the continuity of the embryos, eggs were put in the incubator with the sharp ends pointing down. Eggs were accessible at the times needed. The incubator was maintained at a steady temperature of $37.8^{\circ}\text{C} \pm 0.2^{\circ}\text{C}$ with a humidity of 60-70%. During the incubation cycle, the eggs were automatically rolled at a 45-degree angle to the vertical axis every 2 hours.

2.1. Sewage Water Sample Locality. The noncentralized treated sewage water was obtained from Bhutta Colony Dera Ghazi Khan. Dera Ghazi Khan is a district in Pakistan's Punjab province. This sample was collected from house holding tanks.

2.2. Sewage Water Sample Analysis. The physical, chemical, and bacteriological properties of sewage water samples were examined at the Laboratory of Pakistan Council of Research in Water Resources (PCRWR) Water Quality Laboratory, Dera Ghazi Khan Punjab, Pakistan.

2.2.1. Physical and Chemical Analyses. Total dissolved solids, electrical conductivity, turbidity, and pH of the water were examined as significant physical parameters in the physical analysis. In chemical analysis, essential chemical parameters such as carbonates, bicarbonates, chloride, calcium, sodium, and potassium were examined. These physicochemical parameters were examined by different methods and instruments as described in Table 1. With the help of this analysis, the following results were obtained from the sewage water sample as shown in Table 2. According to the results of these physical and chemical parameters, it was concluded that sewage water contains various concentrations of contaminants that cause adverse effects on human health and the environment.

2.2.2. Bacteriological Analysis. Total coliform, fecal coliform, and *E. coli* were studied in the raw form (100%) of sewage water in this sort of examination. Table 3 displays their results

TABLE 1: Methods/instruments for physical and chemical parameter analysis.

Sr. no.	Parameters	Analysis methods/instruments
1.	pH	pH meter
2.	Electrical conductivity	Conductivity method, electrical conductivity meter
3.	Turbidity	Turbidity meter/nephelometer
4.	Color	Sensory test
5.	Carbonates	Titration (standard solution of strong acid)
6.	Bicarbonates	Titration (standard solution of strong acid)
7.	Alkalinity	Titration (standard solution of strong acid)
8.	Calcium	Calcium meters
9.	Chloride	Titration (silver nitrate solution)
10.	Fluoride	Fluoride electrode method (water+zirconyl xylenol orange complex reagent)
11.	Hardness	Titration (standard solution of strong acid)
12.	Magnesium	EDTA (ethylenediaminetetraacetic acid)
13.	Sodium	Flame photometer
14.	Nitrate	Visible spectrophotometer
15.	Potassium	Flame photometer
16.	Sulfate	Titration (barium chloride)
17.	TDS	TDS meter

TABLE 2: Results of physicochemical parameter analysis.

Sr. no.	Physicochemical parameters	Results
1.	Appearance	Turbid
2.	Color	Greyish
3.	Odor	Foul
4.	Bicarbonate (mg/l)	165
5.	Alkalinity (mmol/l)	3.3
6.	Calcium (mg/l)	426
7.	Carbonate	Nil
8.	Chloride (mg/l)	208
9.	Conductivity	7560
10.	Turbidity	225
11.	Fluoride (mg/l)	3.65
12.	Hardness (mg/l)	1425
13.	Magnesium (mg/l)	87.48
14.	Nitrate	0.95
15.	pH	8.25
16.	Potassium (mg/l)	22
17.	Sodium (mg/l)	680
18.	Sulfate (mg/l)	3685
19.	TDS (mg/l)	4536

TABLE 3: Results of bacteriological analysis.

Sr. no.	Parameters	Results
1.	Total coli form	210
2.	Fecal coli form	112
3.	E. Coli	75

2.3. *Experimental Design.* A total of 100 fertilized nonincubated eggs (*Gallus gallus domesticus*) were used for this study. There were two trials in this experiment based on different days of sewage water administration. In each trial, 50 eggs were used and divided into 5 groups A, B, C, D, and E. In experimental groups, A = 100% sewage water, B = 70% sewage water, and C = 30% sewage water (0.3 ml dose) were given. Control group D was treated with 0.3 ml saline solution (0.9% NaCl) and E remained uninjected. Each trial was further divided into 2 phases based on different observation days.

(i) Trial no. 1

For this trial, 50 fertilized eggs were used. These eggs were divided into five groups, each with five eggs. The trial was divided into 2 phases:

- (i) Phase I: this phase included a total of 25 fertilized eggs. On the 7th day of incubation, sewage water was inserted. On the eighth day of incubation, these eggs were determined to be sacrificed (after 24 hours of injection)
- (ii) Phase II: a total of 25 fertilized eggs were used for this phase. Sewage water was injected on 7th day of incubation. These eggs were determined to sacrifice on the 9th-day of incubation (after 48 hours of injection)

(ii) Trial no. 2

50 fertilized eggs were used for the second trial. These eggs were divided into 5 groups. Trial 2 was separated into two phases:

- (i) Phase I: this phase requires a total of 25 fertilized eggs. Sewage water was given on 14th day of incubation. These eggs opened on 15th day of incubation (after 24 hours of injection)
- (ii) Phase II: a total of 25 fertilized eggs were required for this phase. Sewage water was injected on 14th day of incubation. These eggs were determined to sacrifice on the 16th-day of incubation (after 48 hours of injection)

2.4. *Parameters Studied in Trials 1 and 2.* On observing days, the eggs were opened, and the outer shells were scratched up to expose the embryo. The embryos were removed from the albumin using a spoon and put on a petri dish and evaluated their different parameters.

Different parameters were studied:

- (i) Body length (mm), forelimb length (mm), hindlimb length (mm), and head diameter (mm) were measured on observation days by using a scale. The embryos' body weight (g) was determined by using a digital electronic balance (model no. FA2204)
- (ii) Embryos were observed to find the effect of sewage water on the embryonic development of chicks
- (iii) The mortality rate was evaluated on different observation days. Mortality percentage (%) was calculated by using the following formula:

$$\text{Mortality percentage (\%)} = \frac{\text{Dead embryos}}{\text{Total number of embryos}} \times 100 \quad (1)$$

2.5. *Statistical Analysis.* Using SPSS version 20.0, the data were statistically analyzed. All of the data was given as group mean \pm SE, and one-way ANOVA was used to compare the results to the control. For post hoc analysis, Duncan's multiple range test was used. When the difference between the control and experimental groups was less than 0.05, it was considered significant. If $p < 0.01$, it was considered highly significant.

3. Results

3.1. *Trial No. 1.* Trial 1 was divided into 2 phases based on different observation days. Sewage water was given on 7th day of incubation. And eggs were opened after 24 hours of sewage water insertion in phase I and after 48 hours in phase II.

In phase I, the finding of body weight, body length, forelimb length, and hindlimb length according to the effects of sewage water demonstrated a highly statistically significant difference ($p < 0.05$), but head diameter showed nonsignificance ($p > 0.05$) between the experimental and control groups. All these parameters were raised in group E which was the control group, while reduced in experimental groups. Table 4 depicts the sewage water effect on these parameters.

Phase II findings showed that the impact of various concentrations of sewage water on 9th day embryo's head diameter was a highly statistically significant difference ($p < 0.01$), while forelimb length was significant ($p < 0.05$). Body weight, body length, and hindlimb length showed nonsignificance ($p > 0.05$) between the experimental and control groups as represented in Table 4.

3.2. *Trial No. 2.* Trial 2 was divided into 2 phases based on different observation days. On the 14th day of incubation, sewage water was administered. And eggs were opened after 24 hours of sewage water insertion in phase I and after 48 hours in phase II.

In phase I, Table 5 displays the mean \pm SE values of various sewage water treatments in comparison to control groups. Hindlimb length revealed a highly statistically significant ($p < 0.01$) difference between the experimental and control groups, while body weight, body length, forelimb length, and head diameter showed nonsignificance ($p > 0.05$).

On 16th day after 48 hours of sewage water administration (phase II), body weight, body length, forelimb length, hindlimb length, and head diameter showed a nonsignificant difference ($p > 0.05$) between the experimental and control groups. These parameters were increased in the control groups, and head diameter increased in group A, while these values decreased in the experimental groups as depicted in Table 5.

3.3. *Effect of Sewage Water on Chick Embryos on Different Observation Days.* Figure 1 displays the development of various body parts after being exposed to sewage water treatments and compared to control groups. Embryos exhibited normal development in phase I of trial 1; however, deformation of body parts of chick embryos in experimental groups (A, B and C) was detected on the 9th day after 48 hours of sewage water treatment in phase II, as compared to control groups that showed normally developed body parts.

In trial 2, sewage water was given on 14th day of incubation; after 24 hours (phase I) and 48 hours (phase II) of administration, embryos were evaluated for normal development. In both phases, embryos showed no abnormality.

3.4. *Mortality Percentage (%) on Different Observation Days.* Mortality percentage (%) in different experimental and control groups has been given in Figure 2. There was no mortality in 8th day old chick embryos treated with sewage water on 7th day. While in others, mortalities were increased with increasing concentration of sewage water. Control groups did not show any mortality.

4. Discussion

The main purpose of this study was to determine the toxicological effects of sewage water on the embryonic development of chicks. A total of 100 fertilized nonincubated eggs (*G. gallus domesticus*) were used for this study. There were two trials in this experiment. Each trial was further divided into 2 phases. In each trial, 50 eggs were used and divided into 5 groups. Groups A, B, and C were treated with three

TABLE 4: Different parameter's mean \pm standard error of chick embryos given sewage water on 7th day of incubation.

Parameters	Trial 1	Observation days	Experimental groups			Control groups		p value
			A	B	C	D	E	
Body weight (g)	Phase I	8 th day	0.37 \pm 0.07 ^b	0.69 \pm 0.34 ^b	0.42 \pm 0.05 ^b	1.43 \pm 0.16 ^a	1.74 \pm 0.03 ^a	0.01**
	Phase II	9 th day	1.42 \pm 0.06	1.22 \pm 0.08	1.47 \pm 0.03	1.28 \pm 0.11	1.16 \pm 0.09	0.14
Body length (mm)	Phase I	8 th day	24.00 \pm 1.58 ^b	21.60 \pm 1.16 ^b	22.00 \pm 1.14 ^b	33.00 \pm 2.19 ^a	33.40 \pm 1.07 ^a	0.01**
	Phase II	9 th day	31.00 \pm 1.52	30.75 \pm 1.10	32.50 \pm 1.04	31.40 \pm 1.07	31.20 \pm 0.58	0.80
Forelimb length (mm)	Phase I	8 th day	5.60 \pm 0.87 ^{ab}	3.60 \pm 0.81 ^b	4.00 \pm 0.70 ^b	6.40 \pm 0.748 ^a	7.20 \pm 0.37 ^a	0.01**
	Phase 2	9 th day	6.33 \pm 0.33 ^b	7.75 \pm 0.47 ^{ab}	7.62 \pm 0.68 ^{ab}	9.40 \pm 0.92 ^a	9.40 \pm 0.24 ^a	0.02*
Hindlimb length (mm)	Phase I	8 th day	9.00 \pm 0.83 ^b	5.80 \pm 0.73 ^c	8.00 \pm 1.04 ^{bc}	10.00 \pm 1.0 ^{ab}	12.00 \pm 0.70 ^a	0.01**
	Phase II	9 th day	12.00 \pm 1.52	11.00 \pm 0.70	13.25 \pm 1.54	14.00 \pm 1.73	13.60 \pm 0.60	0.49
Head diameter (mm)	Phase I	8 th day	4.60 \pm 0.24	3.40 \pm 0.67	3.40 \pm 0.50	4.60 \pm 0.67	5.40 \pm 0.40	0.06
	Phase II	9 th day	3.66 \pm 0.33 ^b	7.00 \pm 0.40 ^a	7.00 \pm 0.70 ^a	6.60 \pm 0.40 ^a	7.00 \pm 0.31 ^a	0.01**

^{a, b, c}Values with a different superscript in row differ significantly (* $p < 0.05$, ** $p < 0.01$).

TABLE 5: Different parameter's mean \pm standard error of chick embryos given sewage water on 14th day of incubation.

Parameters	Trial 2	Observation days	Experimental groups			Control groups		p value
			A	B	C	D	E	
Body weight (g)	Phase I	15 th day	8.67 \pm 1.14	9.56 \pm 0.99	11.05 \pm 0.37	11.27 \pm 0.36	10.87 \pm 0.18	0.10
	Phase II	16 th day	15.58 \pm 1.23	15.07 \pm 2.14	14.80 \pm 0.63	21.93 \pm 5.32	18.28 \pm 2.26	0.32
Body length (mm)	Phase I	15 th day	6.15 \pm 0.33	6.26 \pm 0.32	6.75 \pm 0.10	6.35 \pm 0.26	6.38 \pm 0.11	0.56
	Phase II	16 th day	7.66 \pm 0.35	6.85 \pm 0.59	6.77 \pm 0.15	7.73 \pm 0.37	7.60 \pm 0.32	0.29
Forelimb length (mm)	Phase I	15 th day	2.10 \pm 0.24	2.54 \pm 0.17	2.17 \pm 0.21	1.92 \pm 0.09	2.44 \pm 0.12	0.12
	Phase II	16 th day	2.96 \pm 0.03	2.60 \pm 0.23	2.80 \pm 0.12	3.10 \pm 0.20	2.96 \pm 0.24	0.42
Hindlimb length (mm)	Phase I	15 th day	2.62 \pm 0.11 ^b	2.98 \pm 0.03 ^a	3.20 \pm 0.07 ^a	3.17 \pm 0.16 ^a	3.14 \pm 0.07 ^a	0.01**
	Phase II	16 th day	4.00 \pm 0.05	3.45 \pm 0.55	4.07 \pm 0.11	4.43 \pm 0.34	4.56 \pm 0.12	0.20
Head diameter (mm)	Phase I	15 th day	2.10 \pm 0.62	2.54 \pm 0.50	2.17 \pm 0.75	1.92 \pm 0.47	2.44 \pm 0.37	0.13
	Phase II	16 th day	8.66 \pm 0.88	8.25 \pm 1.03	8.00 \pm 0.91	8.50 \pm 1.89	8.16 \pm 0.83	0.99

^{a, b, c}Values with different superscripts in row differ significantly (* $p < 0.05$, ** $p < 0.01$).

different concentrations of sewage water (100%, 70%, and 30%) and compared to controls (saline solution given 0.9% NaCl and uninjected group). Different parameters such as body weight, body length, hindlimb length, forelimb length, and head diameter were evaluated on the 8th, 9th, 15th, and 16th days.

When examined, sewage water included total coli, fecal coli, and E. coli. Hughes and Thompson (2004) had also found that total coliforms (which include *Enterobacteriaceae* and fecal coliforms) are the most common bacteria and are used as indications of sewage pollution.

Greywater (from showers, bathtubs, pools, dishwashers, and clothes washers) makes up a major amount of sewage water, as does black water (from toilets, along with the human waste washed away, soaps and detergents and toilet papers). Greywater, according to Jackson and Ord, is water that is of poor significance than potable water (drinking water) but of greater value than black water (Jackson and Ord, [2]). In the current investigation, the sewage water analyzed was grey and had a foul smell.

When sewage water was examined in the current study, it included nitrate 0.95 mg/l and sodium 680 mg/l, which affected the body weight of chick embryos in trials 1 and 2, except in phase II of trial 1, in which its value decreased in control group E. This work was supported by the work of (Mohamadi et al., [14]) who found that adding nitrate sodium to the air sac of fertilized chicken eggs did not affect the production, hatching, or survival of one-day chicks. However, it promotes hypoxia, diminishes overall antioxidant capacity, and increases malondialdehyde in the body, resulting in a reduction in freshly chick weight. Grizzle et al. [15] had found that water quality in broiler farms has a negative impact on broiler performance, which is negatively associated with body weight and immune resistance.

In the present study, body length decreased in chick embryos in the sewage water-treated groups when compared with the control groups. The present study was in corroboration with the findings of (Bhanot and Hundal, [16]) that conducted an experiment on fish *Labeo rohita* and found a decrease in total body length in the sewage water-treated groups in comparison with the control. The present study



FIGURE 1: Effect of sewage water in different sewage water-treated groups (groups A-C) and control groups (groups D and E): (a) chick embryos on 8th day given sewage water on 7th day of incubation, (b) chick embryos on 9th day administered sewage water on 7th incubation day, (c) chick embryos on 15th incubation day given sewage water on 14th day of incubation, and (d) Chick embryos on 16th day injected sewage water on 14th day of incubation.

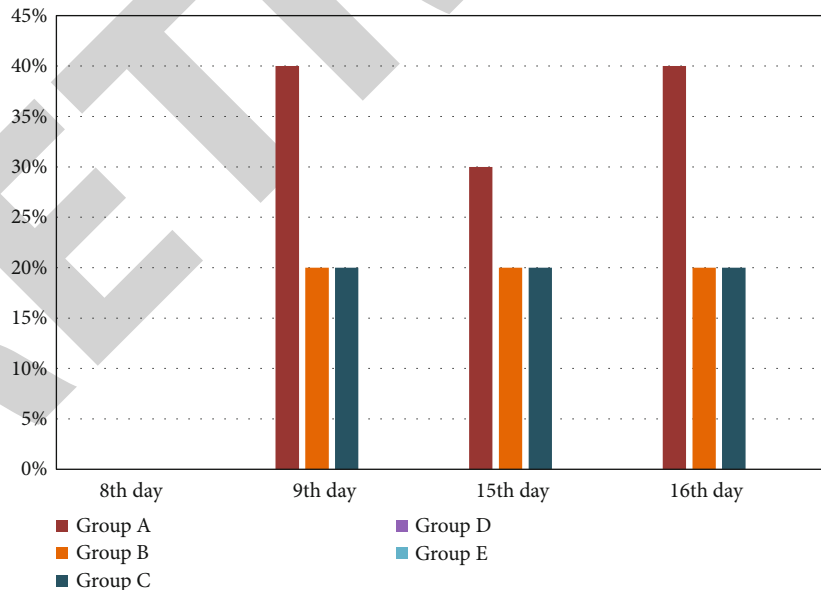


FIGURE 2: Mortality percentage (%) in different sewage water-treated groups and control groups on different observation days.

was also consistent with (Sultana et al., [17])’s findings who had also observed a decrease in the morphometric parameters, such as total body length and standard length of the fish *Labeo rohita* which was inhabiting industrial wastewater contaminated water of river Ravi, Pakistan.

Mortalities had occurred in all experimental groups except on the 8th day of incubation (phase I of trial 1). After 24 hours of sewage water treatment, there was less mortality that occurred in chick embryos. The dose-dependent mortality rate was present in the current investigation, and the